Facultad de Ciencias

Departamento de Biología Molecular

Estudio de los requerimientos para la entrada del virus de la fiebre aftosa en cultivos celulares y caracterización del ácido valproico como compuesto antiviral

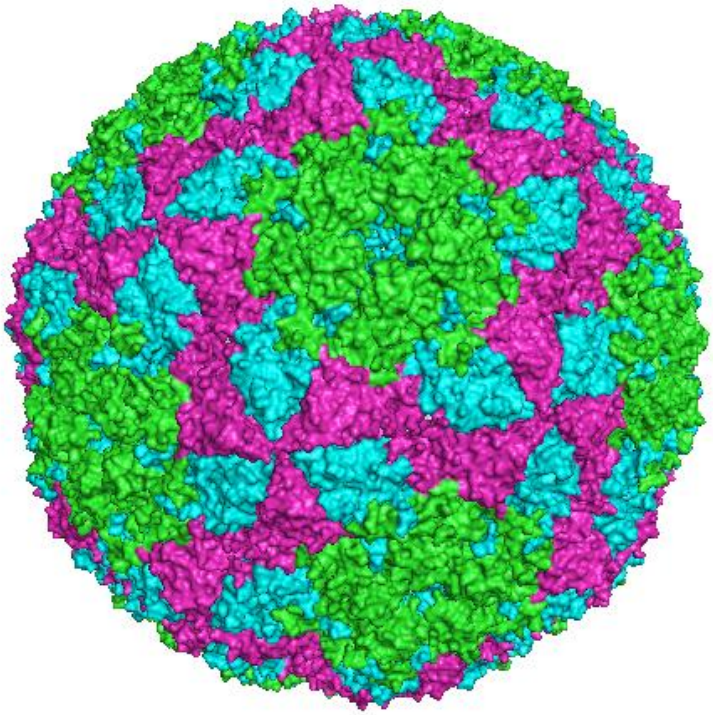

Tesis Doctoral

Ángela Vázquez Calvo

Madrid, 2012

Facultad de Ciencias

Departamento de Biología Molecular

Estudio de los requerimientos para la entrada del virus de la fiebre aftosa en cultivos celulares y caracterización del ácido valproico como compuesto antiviral

Ángela Vázquez Calvo, Licenciada en Biología

Directores de Tesis: Francisco Sobrino Castelló y Miguel Ángel Martín Acebes

Memoria presentada por la Licenciada en Biología Ángela Vázquez Calvo para optar al grado de Doctor en Ciencias por la Universidad Autónoma de Madrid.

Madrid, Septiembre 2012

El trabajo presentado en esta Tesis Doctoral ha sido realizado en el Centro de Biología Molecular "Severo Ochoa", bajo la dirección del Dr. Francisco Sobrino Castelló y el Dr. Miguel Ángel Martín Acebes, y financiado por una beca predoctoral de la Junta de Ampliación de Estudios (JAE) del CSIC. Durante esta Tesis Doctoral se realizó una estancia de 96 días en "The Scripps Research Institute" (La Jolla, California) en el laboratorio del Dr. Juan Carlos de la Torre financiada por la beca predoctoral JAE del CSIC.

A mi familia

Agradecimientos

En primer lugar quiero agradecer a la Dra. Rosario Armas Portela (Charo) la posibilidad que me brindó de hacer el proyecto fin de carrera en el laboratorio del Dr. Francisco Sobrino (Pachi), iniciando así mi camino en el mundo de la ciencia. Sin ella, nada de esto hubiera sido posible. Por otro lado, quiero dar las gracias a mis directores de Tesis, Pachi y Miguel Ángel, por darme la oportunidad de trabajar con ellos, por su confianza y apoyo.

También quiero agradecer al Dr. Juan Carlos de la Torre por aceptar que realizara una estancia corta en su laboratorio en *The Scripps Research Institute* (La Jolla, California) y hacer que me sintiera como en casa. A su grupo (Beatrice, Himangi, Nhi y Shuzo) por ser tan amables y hacer de mi estancia una experiencia inolvidable.

A mi tutor académico, el Dr. Iván Ventoso, por sus comentarios para mejorar la Tesis.

No me puedo olvidar de todos aquellos que han contribuido con materiales indispensables para la realización de esta Tesis Doctoral, los Dres. : Miguel Ángel Alonso, Tamas Balla, Esther Blanco, Belén Borrego, Emiliana Brocchi, Luis Carrasco, Ángel L. Carrascosa, Juan Carlos de la Torre, Esteban Domingo, Cristina Escarmis, José Antonio Esteban, C. A Hartley, Juan Carlos Saiz, Ignacio Sandoval e Iván Ventoso.

A mis compañeros y excompañeros de laboratorio: Miguel Ángel, que además de director y maestro es un amigo y ha estado apoyándome en todo momento; Mónica, por ser como una hermana más y mi compañera de escritura; Flavia, por tener siempre una sonrisa; Miguel R. por sus consejos; Yuri, por todas sus ayudas informáticas; Marga, por esas conversaciones tan enriquecedoras; Belén Borrego, por abrirnos siempre las puertas en el CISA; Maite, por ser como es incluso en la distancia; Mari, por darnos ese toque argentino; Raúl, por su amabilidad; María, por su perseverancia, y Mónica G. por su sinceridad. También a aquellos que han pasado fugazmente por el laboratorio pero nos han dejado experiencias inolvidables: Susan, Jacob, Marianne, Marina, Brian y Carlos.

Al Dr. Mauricio G. Mateu y su laboratorio, en especial a la Dra. Verónica Rincón que en las colaboraciones hizo más llevadero los protocolos tan largos. A todos los integrantes del grupo del Dr. Juan Carlos Saiz (Ana, Estela, Nereida y él) por hacer que los experimentos en el CISA sean mucho más amenos y a Nuria de la Losa por su ayuda en los experimentos *in vivo* presentados en la Tesis.

Al servicio de cultivos, lavado y esterilización por hacernos el trabajo mucho más fácil, en especial a Mª Angeles, Alfonso, Anunciación y Mercedes. Al servicio de microscopía óptica y confocal (Carlos, Mª Angeles, Maite y Vero) y, al servicio de microscopía electrónica (en especial a Maite y Milagros) por su asistencia técnica, la resolución de dudas y ser siempre tan amables con los usuarios.

A los amigos y compañeros de otros laboratorios, en especial a Desi, Ana O., Elena, Esther y Bruno.

A los compañeros y excompañeros de cultivos que hacen y han hecho que el trabajo en el sótano fuera muy agradable: Ana I., Isabel, Celia, Nacho, Vero, Héctor, Mila, Alicia, Pablo, Verónica R., Rebeca, Carola, Patricia, Pepa y Mónica H.

A Luis, que ha sabido apoyarme en los momentos difíciles y está siempre conmigo. A mis padres (Manuel y Teresa), hermanos (Ana, Bego, Petra y Miguel) y mis sobrinitos (Claudia, Aldo, Nora y Paula) por hacer que las comidas del domingo sean uno de los mejores momentos de la semana.

Abreviaturas

293T	Línea celular derivada de riñón humanas
AcM	Anticuerpo monoclonal
AcP	Anticuerpo policlonal
AF	Alexa Fluor
AN	Apertura numérica
ANOVA	Análisis de la varianza
AP	Proteína adaptadora (*adaptor protein*)
ATPasa	Adenosin trifosfatasa
AVP	Ácido valproico (*Valproic acid, VPA*)
BHK-21	Línea celular derivada de riñón de hamster (*Baby hamster kidney 21*)
BSA	Albumina de suero bovino
BSL-3	Laboratorio de bioseguridad 3
c.p.m	Cuentas por minuto
CAT	Cloroanfelicol transferasa
cDNA	DNA copia
CFP	Proteína fluorescente cian (*cyan fluorescent protein)*
Da	Dalton
DACH	Deacetilasas de histonas
DAG	Diacilglicerol
DAPI	4'-6 diamidina-fenilindol
DEAE	Dietilaminoetil
DEPC	Dietilpirocarbonato
DIC	Contraste de fases interdiferencial
DMEM	Medio Eagle modificado por Dulbeco (*Dulbecco's modified Eagle medium*)
DMSO	Dimetilsulfóxido
DN	Dominante negativo
DNA	Ácido desoxirribonucleico
dsRNA	RNA de doble cadena
DTT	Ditiotreitol
E.coli	*Escherichia coli*
EDTA	Ácido etilén diamino tetraacético
eGFP	Proteína verde fluorescente mejorada (*enhanced green fluorescent protein*)
EGTA	Ácido etilén glicol tetracético
eIF-4G	Factor de iniciación de traducción eucariótico *gamma* 4
ELISA	*Enzyme-linked immunosorbent assay*
ESCRT	*Endosomal sorting complex required for transport*
EVB	Enterovirus bovino (*bovine enterovirus, BEV*)
FA	Fiebre aftosa
FKBP	*FK506 binding protein*
FRB	*FKBP rapamycin binding domain*

G	Glicoproteína de VEV
g	Valor de aceleración de la gravedad
G3PDH	Gliceraldehído-3-fosfato
GAK	Ciclina G asociada a quinasa
GED	Dominio efector de GTPasa
GFP	Proteína fluorescente verde (*Green fluorescent protein*)
GP	Glicoproteína de VCML
GPI	Glicosil fosfatidil inositol
GTP	Guanosin trifosfato
GTPasa	Guanosin trifosfatasa
h	Hora
HEPES	Ácido 4-(2-hidroxietil)-1-piperazina etanosulfónico
HS	Heparán sulfato
Hsc70	*Heat schok cognate protein*
I3P	Inositol-3-fosfato
ICTV	Comité Internacional de Taxonomía de Virus
IC_{50}	Valor de la concetración de un fármaco que produce una inhibición del 50%
Ig	Inmunoglobulina
IRES	Sitio de entrada interna del ribosoma (*Internal ribosome entry site*)
Kb	Kilobase
kDa	Kilodalton
L	Proteína *large* de VEV
LB	Medio de cultivo Luria-Bertani
LD_{50}	Dosis letal 50
M	Proteína de la matriz de VEV
m.d.i.	Multiplicidad de infección
MG	Minigenoma
min	Minuto
MOPS	3-morfolino-1-propanosulfonato
mTOR	*Mammalian target of rapamycin*
MuLV	Virus de la leucemia murina
N	Nucleoproteína de VEV
NP	Nucleoproteína de VCML
OIE	Organización Mundial de Sanidad Animal
ORF	Fase abierta de lectura (*open reading frame*)
P	Fosfoproteína de VEV
p.i.	Post-infección
p.t.	Post-transfección
PBS	Tampón fosfato salino
PBTG	PBS conteniendo 1% BSA; 0,1% Tritón-X 100 y 1 M glicina
PCR	Reacción en cadena de la polimerasa
PDB	Banco de datos de proteínas (*Protein Data Bank*)

PDI	Proteína disulfuro isomerasa
PH	Dominio de homología a plecstrina (*Pleckstrin homology*)
$pH_{50}D$	Valor de pH que ocasiona una disociación a pentámeros de la cápsida del 50% de los viriones totales
$pH_{50}I$	Valor de pH que ocasiona una reducción de la infectividad viral del 50%
PI	Fosfatidilinositol
PI(3)P	Fosfatidilinositol-3-fosfato
$PI(3,5)P_2$	Fosfatidilinositol-3,5-bisfosfato
PI(4)P	Fosfatidilinositol-4-fosfato
$PI(4,5)P_2$	Fosfatidilinositol-4,5-bisfosfato
PI4P5K	Fosfatidilinositol 4-fosfato 5-quinasa
PLC	Fosfolipasa C (*phospholipase C*)
PM	Membrana plasmática
PMSF	Fenilmetilsulfonifluoruro
poliA	Poliadenilato
poliC	Polirribocitidilato
PRD	Dominio rico en prolina/arginina
PV	Poliovirus
PVDF	Polivinildifluorido
Rab	*Ras-related proteins in brain*
RFP	Proteína fluorescente roja (*Red fluorescent protein*)
RNA	Ácido ribonucléico
rRNA	Ácido ribonucléico ribosómico
RT	Transcipción inversa (*retrotranscription*)
s	Segundo
S	Svedberg
SDS	Dodecil sulfato sódico
SFB	Suero fetal bovino
SI	Índice de selectividad (*Selectivity index*)
siRNA	RNA de interferencia corto (*short interference RNA*)
SV40	Virus del simio 40
t.a.	Temperatura ambiente
TAE	Tampón tris-acetato sódico-EDTA
TBS	Tampón tris salino
TC_{50}	Valor de la concetración de un fármaco que produce una mortalidad celular del 50%
TF	Transferrina
TNE	Tampón tris-NaCl-EDTA
Tris	Tris-hidroximetil-aminometano
TSA	Tricostatina A
UFF	Unidad formadora de foco
UFP	Unidad formadora de placa
UTR	Región no codificante (*Untranslated región*)

UV	Ultravioleta
V-ATPasa	ATPasa vacuolares
VBS	Virus del bosque de Semliki (*Semliki forest virus, SFV*)
VCML	Virus de la coriomeningitis linfocitaria (*Lymphocytic choriomeningitis virus, LCMV*)
VEMC	Virus de la encefalomiocarditis (*Encephalomyocarditis virus, EMCV*)
Vero	Células epiteliales de riñón de mono verde africano
VEV	Virus de la estomatitis vesicular (*Vesicular stomatitis virus, VSV*)
VFA	Virus de la fiebre aftosa (*Foot-and-mouth disease virus, FMDV*)
VLP	Partículas virales vacías (*Viral like particle*)
VNO	Virus del Nilo occidental (*West Nile virus, WNV*)
VPPA	Virus de la peste porcina africana (*African swine fever virus, ASFV*)
VREA	Virus de la renitis equina A (*Equine rhinitis A virus, ERAV*)
VSIN	Virus Sindbis (*Sindvis virus, SINV*)
VUSU	Virus Usutu (*Usutu virus, USUV*)
VVAC	Virus vaccinia (*Vaccinia virus, VACV*)

Códigos de una y tres letras para los aminoácidos

Alanina	Ala, A	Leucina	Leu, L
Arginina	Arg, R	Lisina	Lys, K
Ácido aspártico	Asp, D	Metionina	Met, M
Asparagina	Asn, N	Fenilalanina	Phe, F
Cisteína	Cys, C	Prolina	Pro, P
Ácido glutámico	Glu, E	Serina	Ser, S
Glicina	Gly, G	Tirosina	Tyr, Y
Glutamina	Gln, Q	Treonina	Thr, T
Histidina	His, H	Triptófano	Trp, W
Isoleucina	Ile, I	Valina	Val, V

Índice

Índice

Resumen en inglés (*Summary*)

1. Resumen en inglés (*Summary*)

Foot-and-mouth disease virus (FMDV) is a small non-enveloped virus belonging to the *Picornaviridae* family (*Aphthovirus* genus). The FMDV genome, which consists of a positive RNA strand, is enclosed inside an icosahedral capsid built up with 60 copies of each of the four structural proteins (VP1 to VP4). FMDV initiates infection of cultured cells via binding of different α_v integrins and then is internalized by clathrin-mediated endocytosis. The current model suggests that uncoating should mainly take place inside early endosomes, since FMDV particles disassembly at pHs around 6.5, which is consistent with pH values inside early endosomes (6.1 to 6.8).

The expression of a dominant negative form of dynamin protein, involved in the vesicle scission during clathrin-mediated endocytosis, inhibited the internalization and infection of FMDV (C-S8c1 and MARLS isolates) and of the rhabdovirus vesicular stomatitis virus (VSV), a model virus for clathrin-mediated endocytosis. Alterations in the plasma membrane level of $PI(4,5)P_2$ (a phospholipid with an important role in clathrin-mediated endocytosis) using ionomycin, 1-butanol or an inducible system, revealed that VSV as well as FMDV C-S8c1 displayed a high dependence on $PI(4,5)P_2$ for internalization. Interestingly MARLS, a FMDV variant that uses receptors other than integrins for cell entry, was less sensitive to $PI(4,5)P_2$ depletion.

The role of cellular Rab GTPases that govern traffic between different endosome populations was also analyzed. Changes on viral receptor specificity between C-S8c1 and MARLS did not alter Rab5 requirement for infection. However, a correlation between uncoating pH and requirement of Rab5 for infection was observed. A FMDV mutant with higher uncoating pH threshold was less sensitive to inhibition of Rab5 function, whereas another mutant with higher acidic requirements was more sensitive to inhibition of Rab5 function. On the contrary, an opposite correlation was found between uncoating pH and dependence of Rab function upon expression of dominant negative forms of Rab7 or 11. In addition, modulation of uncoating pH also reduced FMDV virulence in suckling mice. These results are consistent with FMDV uncoating occurring inside early endosomes and indicate that displacements from optimum pH for uncoating reduce viral fitness *in vivo*.

Two biological clones resistant to NH_4Cl (drug that raise endosomal pH) and with an enhanced sensitivity to acidic pH were isolated from biological samples of natural host (pigs) infected with C-S8c1. A single amino acid substitution VP3 A116V was responsible of the phenotype exhibited by the mutant that exhibited higher resistance to NH_4Cl. Replacement VP3 A116V was located close to substitution previously found in cell culture isolated NH_4Cl resistant mutants, indicating that the structure of the β-E sheet from VP3 is important for capsid stability.

When the effect of valproic acid (VPA) on the infection of cultured cells by different viruses was analyzed, it was observed that this drug drastically inhibited multiplication of all the enveloped viruses tested, including VSV and the zoonotic lymphocytic choriomeningitis virus (LCMV) and West Nile virus (WNV). VPA reduced VSV and LCMV infection yield without causing a major blockage of either viral RNA or protein synthesis. In contrast, VPA drastically abolished WNV RNA and protein synthesis, indicating that this drug can interfere the viral cycle at different steps of enveloped virus infection. Thus, VPA can contribute to an understanding of the crucial steps of viral maturation and to the development of future strategies against infections associated with enveloped viruses.

Introducción

2. Introducción

2.1 Etapas tempranas de la infección viral

Los virus son patógenos muy importantes que pueden infectar humanos, animales o plantas. A pesar de su gran diversidad, dependen de la célula hospedadora para completar su ciclo replicativo. El contacto inicial de la partícula viral con la célula se produce a través de moléculas de superficie de la célula susceptible de ser infectada (adsorción). Los virus animales utilizan como receptores moléculas de diversa naturaleza, entre las cuales se encuentran moléculas de adhesión celular, azúcares, lípidos y componentes de la matriz extracelular (Baranowski y col., 2001; Grove y col., 2011; Marsh y col., 2006). Las moléculas de la superficie de la partícula viral encargadas de interaccionar con el receptor mimetizan la estructura de ligandos celulares de tal manera que, al unirse al receptor, pueden desencadenar una compleja cascada de fenómenos de transducción de señales que induce el ensamblaje de la maquinaria endocítica celular y la internalización de la partícula viral unida a su receptor (Mercer y col., 2010). Posteriormente, el material genético debe ser introducido dentro de la célula hospedadora (penetración). En la mayoría de los casos, como parásitos intracelulares obligados, los virus animales entran en la célula mediante endocitosis y explotan distintas alternativas para penetrar en el citosol (Tsai, 2007).

2.2 Rutas de internalización explotadas por virus

La membrana plasmática de la célula no es un entorno de composición homogénea, sino que contiene microdominios lipídicos, como los denominados balsas lipídicas (*lipid-rafts*) (Chamberlain, 2004), o los acúmulos (*clusters*) de fosfatidilinositol-4,5-bisfosfato [$PI(4,5)P_2$] (Kwiatkowska, 2010), que se han asociado a distintos procesos endocíticos (Antonescu y col., 2011; Chinnapen y col., 2007; De Matteis y col., 2004; James y col., 2008b; Martín-Belmonte y col., 2003; Rollason y col., 2007; Stoddart y col., 2002; Zoncu y col., 2007). Endocitosis es el término empleado para referirse a la internalización de sustancias de distinta naturaleza (complejos receptor-ligando, lípidos, proteínas de membrana, nutrientes, virus, etc.), como consecuencia de la invaginación de la membrana plasmática y de la formación de vesículas (Huotari y col., 2011; Silverstein y col., 1977). Se pueden distinguir una gran variedad de rutas de internalización que se agrupan en función de la maquinaria celular

utilizada: endocitosis dependiente de clatrina (caracterizada por que las vesículas se encuentran revestidas con una proteína denominada clatrina) (McMahon y col., 2011; Pearse, 1976), endocitosis independiente de clatrina, macropinocitosis, y otras rutas alternativas cuyos componentes no han sido aún bien identificados (Marsh y col., 2006) (Fig. 1). Dentro de las independientes de clatrina se incluyen rutas de diverso tipo, siendo la de las caveolas la mejor caracterizada (Reeves y col., 2012).

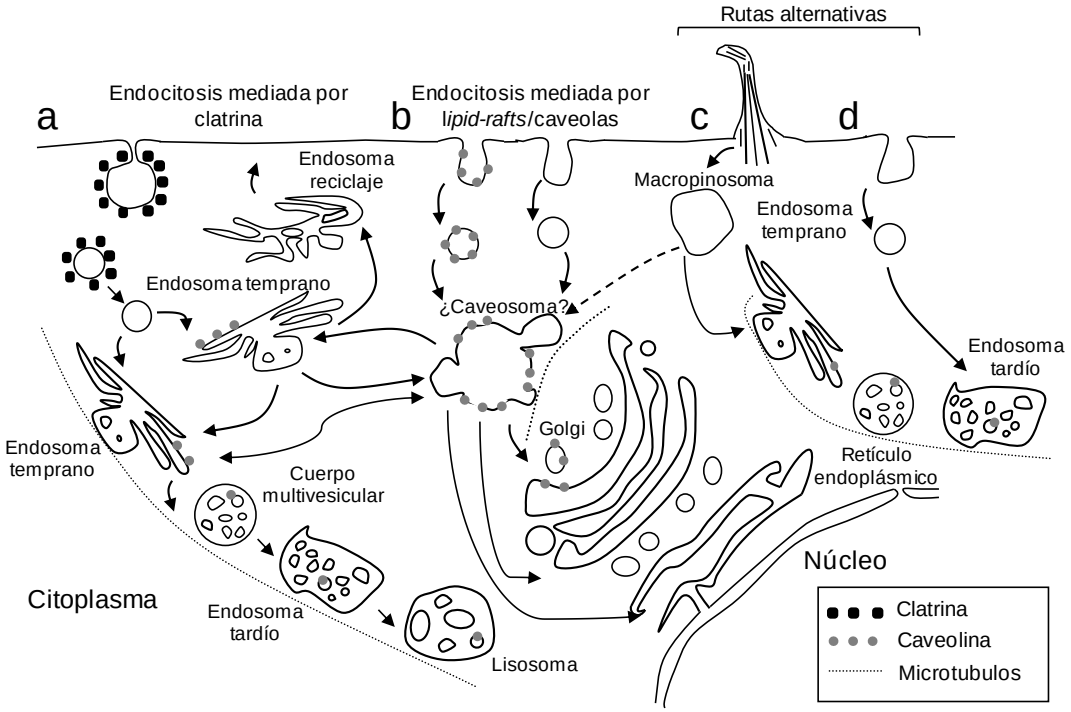

Figura 1. Principales rutas de internalización utilizadas por virus. Modificado de Martín-Acebes, 2009. (a) Endocitosis mediada por vesículas revestidas de clatrina. (b) Endocitosis mediada por *lipid-rafts*/caveolas. (c) Macropinocitosis (d) Rutas alternativas, como la empleada por el virus de la coriomeningitis linfocitaria (VCML).

2.2.1 Endocitosis mediada por clatrina

La endocitosis mediada por clatrina es la vía endocítica en la que la célula recluta material desde la superficie usando vesículas revestidas de clatrina (Fig. 1a). La unidad de ensamblaje de la clatrina se denomina trisquelión (Fig. 2b) y está formado por tres cadenas pesadas (~ 190 kDa), cada una de ellas asociada a una cadena ligera (~ 25 kDa) (Fotin y col., 2004; Kirchhausen y col., 1981; Ungewickell y col., 1981). Las patas de diferentes trisqueliones se intercalan entre sí formando una jaula poliédrica que recubre la vesícula endocítica (Fig. 2c), dando como resultado la polimerización de la clatrina. Este proceso está regulado por la actuación de distintas proteínas que, generalmente, presentan varios dominios de unión que median la interacción entre

proteínas, o entre proteínas y lípidos, de forma que estas interacciones espacio-temporales constituyen sus bases moleculares. En este proceso, el $PI(4,5)P_2$ tiene un papel muy importante en la formación de las vesículas revestidas de clatrina por su interacción con distintas proteínas implicadas (Antonescu y col., 2011; De Matteis y col., 2004; James y col., 2008a; Zoncu y col., 2007). Considerando el número de virus que utilizan esta ruta, parece que ésta fuera la forma de endocitosis más explotada por los virus para entrar en la célula (Mercer y col., 2010).

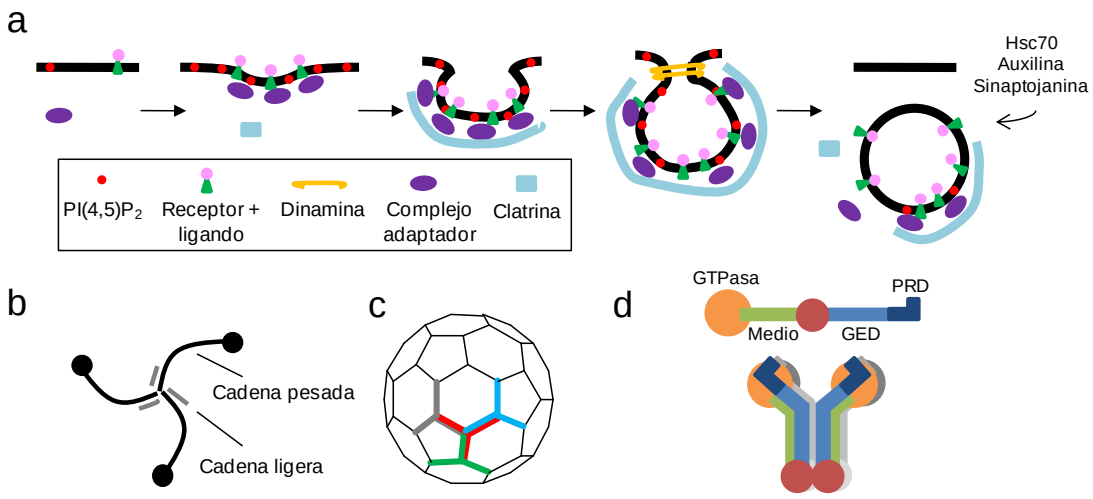

Figura 2. Endocitosis mediada por clatrina. (a) Formación de la vesícula revestida de clatrina. Modificado de Schmid y col., 2007. (b) Trisquelión de clatrina formado por tres cadenas ligeras (representadas en gris) y tres cadenas pesadas (representadas en negro). (c) Vesícula revestida de clatrina. En rojo, verde, azul y gris están destacados distintos trisqueliones de clatrina. (d) Arriba, esquema de la dinamina con sus distintos dominios: GTPasa, medio, GED y PRD. Abajo, tetrámero de dinamina.

El proceso inicial de la formación de la vesícula de clatrina (Fig. 2a) viene mediado por la actuación de distintas proteínas adaptadoras (como pueden ser AP-2, AP-180 y epsina 15) que son movilizadas hacia la membrana plasmática por medio de su unión a motivos proteicos situados en la región citoplasmática de los receptores y al $PI(4,5)P_2$ localizado en la membrana plasmática (Antonescu y col., 2011; Henne y col., 2010; Honing y col., 2005; McMahon y col., 2011; Ohno y col., 1995). A continuación, se produce el ensamblaje del revestimiento de clatrina que junto con el $PI(4,5)P_2$ estabiliza la curvatura de la membrana plasmática que dará lugar a la vesícula (Antonescu y col., 2011). Posteriormente, se produce la escisión de la vesícula revestida de clatrina, proceso que depende de la actividad de una proteína denominada dinamina (Loerke y col., 2009; Takei y col., 1995; Takei y col., 2005). Esta proteína es una GTPasa que contiene varios dominios, incluyendo, un dominio GTPasa, un dominio de

unión a $PI(4,5)P_2$ del tipo de homología a plecstrina (PH), un dominio efector de GTPasa (GED) y un dominio rico en prolina/arginina (PRD) que le permite la unión a otras proteínas (Schmid y col., 2011; Takei y col., 2005) (Fig. 2d). La dinamina se encuentra formando tetrámeros en solución y polimeriza para formar anillos alrededor del cuello de la vesícula en formación (Takei y col., 1995) (Fig. 2d). Mediante la hidrólisis de GTP la dinamina produce la constricción de la membrana plasmática hasta dar lugar a la escisión de la vesícula, siendo esta actividad GTPasa estimulada por la interacción de su dominio PH con el $PI(4,5)P_2$ localizado en la membrana (Zheng y col., 1996). Finalmente, la vesícula revestida de clatrina pierde rápidamente su revestimiento por acción de la proteína Hsc70 y su cofactor, auxilina −o ciclina G asociada a quinasa (GAK) en los tejidos no neuronales− (Reider y col., 2009; Robinson, 2004). En este proceso también es importante el papel de la fosfatasa sinaptojanina, que por un lado actúa facilitando el reclutamiento de la auxilina (Massol y col., 2006) y, por otro, dando lugar a fosfatidilinositol-4-fosfato [PI(4)P] a partir del $PI(4,5)P_2$ de membrana (Cremona y col., 1999). Se considera que el cambio de composición de los fosfolípidos de membrana provoca la pérdida de la afinidad de las proteínas adaptadoras con la membrana, lo que ayudaría a desestabilizar la estructura del ensamblaje de clatrina. El desensamblaje del revestimiento de clatrina permite a la vesícula continuar su viaje y fusionar con un endosoma temprano (ver apartado 2.3).

2.2.2 Endocitosis mediada por *lipid-raft*

Los *lipid-raft* son dominios con un alto contenido en colesterol, glicoesfingolípidos (GPI) y proteínas ancladas a GPI, proteínas modificadas con grupos mirístico y palmítico, y proteínas transmembrana (Jacobson y col., 2007). Los *lipid-raft* se han asociado con distintos mecanismos de endocitosis independientes de clatrina (Chinnapen y col., 2007; Reeves y col., 2012; Rollason y col., 2007; Stoddart y col., 2002) que aprovechan algunos virus para poder ser internalizados en la célula (Mercer y col., 2010; Pelkmans y col., 2005; Thorley y col., 2010). Entre los mecanismos endocíticos responsables de internalizar *lipid-rafts* podemos distinguir dos tipos: el de las caveolas y la endocitosis mediada por *lipid*-rafts no caveolas (Fig. 1b). Ambas rutas pueden considerarse variantes de una ruta común más amplia denominada *lipid-raft*/caveola (Le y col., 2003; Marsh y col., 2006; Nabi y col., 2003).

Las caveolas constituyen una especialización dentro de la endocitosis mediada por *lipid-raft* caracterizada por la presencia de una proteína denominada caveolina

(Parton y col., 2007; Rothberg y col., 1992) (Fig. 1b). La endocitosis dependiente de caveolina requiere la formación de una invaginación denominada caveola como consecuencia de la oligomerización de la caveolina y de su asociación con microdominios ricos en colesterol (Bauer y col., 2006). La fisión de la caveola desde la membrana plasmática puede ser dependiente de dinamina (del Pozo y col., 2005; Henley y col., 1998; Oh y col., 1998; Pelkmans y col., 2002; Pietiainen y col., 2004) o independiente de ésta (Mayor y col., 2007; Welling y col., 2010). Inicialmente se propuso que las caveolas internalizadas fusionaban con un orgánulo intracelular denominado caveosoma (Pelkmans y col., 2001) que, a diferencia de los endosomas, estaba asociado con pH neutro (Pelkmans y col., 2004; Pelkmans y col., 2001; Pelkmans y col., 2002). Sin embargo, el concepto de caveosoma como un orgánulo independiente está siendo cuestionado ya que estudios recientes indican que el caveosoma es una especialización de un compartimento endosomal tardío (y por tanto con pH ácido interno), modificado por la acumulación de caveolina (Engel y col., 2011; Hayer y col., 2010; Parton y col., 2010). Desde los caveosomas, los ligandos son distribuidos hacia el Golgi, la membrana plasmática, el retículo endoplasmico y los endosomas tempranos. Las caveolas internalizadas también pueden fusionar con endosomas tempranos directamente (Pelkmans y col., 2004). Ejemplos de virus internalizados mediante caveolas son el Coxsackievirus B3 (Coyne y col., 2007) y el virus del simio 40 (SV40) (Engel y col., 2011; Pelkmans y col., 2001), entre otros.

Por otro lado, la internalización vía *lipid-rafts* puede también ser independiente de caveolina (Fig. 1b). Por ejemplo, el SV40 es capaz de entrar también en células que no expresan caveolina de manera dependiente de *lipid/rafts* (Damm y col., 2005).

2.2.3 Macropinocitosis y otras rutas alternativas

Existen otras rutas que no están clasificadas dentro de las categorías descritas anteriormente. Una de ellas es la macropinocitosis (Fig. 1c), que consiste en una protusión de la membrana plasmática con participación del citoesqueleto de actina, que acaba originando una vacuola donde se internaliza la carga (Swanson, 2008). Este es un proceso activado por las células para internalizar grandes cantidades de fluidos y otras sustancias (Mayor y col., 2007), que se ha asociado a la internalización de diversos virus, como el virus Vaccinia (Mercer y col., 2009) o el citomegalovirus humano (Haspot y col., 2012). Por otro lado, se han descrito otras rutas diferentes asociadas con la internalización de distintos virus, como por ejemplo, la ruta que sigue el virus de la

coriomeningitis linfocitaria (VCML), que es internalizado de forma independiente de clatrina y de *lipid-rafts*, y transportado a endosomas tardíos sin pasar por endosomas tempranos (Quirin y col., 2008; Rojek y col., 2008) (Fig. 1d); o la ruta que sigue poliovirus (PV), que es independiente de clatrina, caveolina y flotillina, pero dependiente de actina y de quinasas de tirosina (Brandenburg y col., 2007).

2.3 Tráfico viral a través del sistema endosomal

Las células eucarióticas se caracterizan por tener un núcleo diferenciado y por un sistema complejo de endomembranas que da lugar a una gran compartimentalización. Los orgánulos celulares que comprenden la vía secretora y endocítica (el retículo endoplasmático, el aparato de Golgi, los endosomas y los lisosomas) no son estáticos, puesto que las moléculas endocitadas o las que entran en la ruta secretora están continuamente empaquetándose en pequeñas vesículas que se escinden de un compartimento para dirigirse a otro. Esto es lo que se conoce como tráfico de membranas o tráfico vesicular. Esta Tesis Doctoral se ha centrado en el estudio de la interacción viral con la vía endocítica, y en concreto, con los denominados endosomas, que son orgánulos tubulovesiculares encargados de transportar la carga que acaba de ser introducida mediante endocitosis (Huotari y col., 2011; Jovic y col., 2010). Los endosomas se clasifican en distintos tipos: tempranos, de reciclaje y tardíos (Fig. 1). Los endosomas tempranos son los encargados de recibir las vesículas procedentes de procesos endocíticos y actúan como los principales organizadores de las distintas cargas internalizadas (Huotari y col., 2011; Jovic y col., 2010). A su vez, se pueden diferenciar poblaciones de endosomas tempranos en función de su motilidad mediada por microtúbulos y de su velocidad de progresión hacia endosomas tardíos (Lakadamyali y col., 2006). Gran parte del material endocitado es reciclado hacia la membrana plasmática a través de los endosomas de reciclaje o es degradado en los endosomas tardíos y lisosomas (Huotari y col., 2011; Jovic y col., 2010).

2.3.1 Control del tráfico endosomal mediado por proteínas Rab

La membrana endosomal está formada por un mosaico de subdominios con diferente contenido de lípidos y proteínas (De Matteis y col., 2004; Gruenberg, 2001; Stenmark, 2009). Además, estos orgánulos están en constante maduración, transformación, fusión y fisión; lo que hace difícil la diferenciación entre ellos (Huotari y col., 2011).

Tabla I. Ejemplos de virus que utilizan distintas proteínas Rab en etapas tempranas de la infección.

Virus	Proteína Rab[a]	Tipo de endosoma	Referencia
Arenaviridae			
Virus Junín	Rab5 Rab7	Tempranos Tardíos	(Martínez y col., 2009)
Virus Pichindé	Rab5 Rab7	Tempranos Tardios	(Vela y col., 2008)
Bunyaviridae			
Virus de La Crosse	Rab5	Tempranos	(Hollidge y col., 2012)
Virus de Uukuniemi	Rab5	Tempranos	(Lozach y col., 2010)
Dicistroviridae			
Virus del síndrome de Taura	Rab7	Tardíos	(Ongvarrasopone y col., 2011)
Flaviviridae			
Virus dengue	Rab5	Tempranos	(Krishnan y col., 2007)
Virus del Nilo Occidental	Rab5	Tempranos	(Krishnan y col., 2007)
Orthomyxoviridae			
Virus de la gripe	Rab5 Rab7	Tempranos Tardíos	(Sieczkarski y col., 2003)
Parvoviridae			
Virus de la panleucopenia	Rab5 Rab7	Tempranos Tardíos	(Harbison y col., 2009)
Parvovirus canino	Rab5 Rab7	Tempranos Tardíos	(Harbison y col., 2009)
Picornaviridae			
Coxsackievirus B3	Rab5 Rab34	Tempranos Macropinosoma	(Coyne y col., 2007)
Ecovirus 7	Rab7	Tardíos	(Kim y col., 2012)
Virus de la fiebre aftosa	Rab5	Tempranos	(Johns y col., 2009)
Polyomaviridae			
Virus JC	Rab5	Tempranos	(Querbes y col., 2006)
Retroviridae			
Virus de la inmunodeficiencia humana-1	Rab5 Rab7	Tempranos Tardíos	(Vidricaire y col., 2005)
Reoviridae			
Reovirus aviar	Rab5	Tempranos	(Huang y col., 2011)
Rhabdoviridae			
Virus de la estomatitis vesicular	Rab5	Tempranos	(Sieczkarski y col., 2003)
Togaviridae			
Virus del bosque de Semliki	Rab5 Rab7	Tempranos Tardíos	(Vonderheit y col., 2005)
Virus chikungunya	Rab5	Tempranos	(Bernard y col., 2010)
Virus de la encefalitis equina venezolana	Rab5 Rab7	Tempranos Tardíos	(Colpitts y col., 2007)

[a] Los estudios se realizaron utilizando plásmidos que expresaban una forma dominante negativa de la proteína Rab o por medio de siRNA.

A pesar de esto, las proteínas Rab (que reciben su nombre de *ras-related in brain*) son los principales marcadores e identificadores de la vía endocítica. Estas proteínas constituyen una gran familia de GTPasas pequeñas (21-30 kD) (Yang, 2002), que se encuentran activas cuando están unidas a GTP e inactivas cuando se encuentran unidas a GDP, controlando el tráfico entre las diferentes poblaciones de endosomas por medio de interacciones espacio-temporales con distintas proteínas efectoras y lípidos

(Jordens y col., 2005; Rink y col., 2005; Stein y col., 2003; Stenmark, 2009). Las proteínas efectoras de Rab se unen preferentemente a la forma activa de Rab, es decir, a aquella que se encuentra unida a GTP (Stenmark, 2009). Una característica de la familia de las proteínas Rab es la distinta localización intracelular de sus miembros. De esta manera, los endosomas tempranos se pueden identificar y definir por la presencia de la proteína Rab5 (Barbieri y col., 1996; Bucci y col., 1992; Bucci y col., 1994; Gorvel y col., 1991; Rink y col., 2005), los endosomas de reciclaje por la de la proteína Rab11 (Green y col., 1997; Ren y col., 1998; Ullrich y col., 1996; Wilcke y col., 2000) y los endosomas tardíos por la presencia de la proteína Rab7 (Bucci y col., 2000; Feng y col., 1995; Meresse y col., 1995; Press y col., 1998; Vitelli y col., 1997) (Fig. 3). El tráfico entre diferentes poblaciones endosomales se produce por un reemplazo progresivo de unas proteínas Rab por otras (Bucci y col., 2000; Poteryaev y col., 2011; Rink y col., 2005).

En los últimos años se vienen utilizando principalmente versiones dominantes negativas de estas proteínas incapaces de unirse a GTP para analizar su importancia en la infección de distintos virus. Empleando esta aproximación se han identificado diferentes proteínas Rab involucradas en las etapas tempranas de la infección viral (Tabla I).

2.3.2 Maduración de los endosomas

Existen varios eventos importantes en el proceso de maduración de los endosomas tempranos a endosomas tardíos (Fig. 3). Por una parte, el reemplazamiento de la proteína Rab5 por la proteína Rab7 es un paso esencial para la maduración de los endosomas tempranos a endosomas tardíos y en el transporte de la carga hacia los lisosomas para su degradación (Poteryaev y col., 2010; Rink y col., 2005). Por otra parte, la conversión de fosfatidilinositol-3-fosfato [PI(3)P] a fosfatidilinositol-3,5-bisfosfato [$PI(3,5)P_2$] contribuye a la identidad de los endosomas tempranos y tardíos respectivamente, lo que hace posible el reclutamiento de distintas proteínas por medio de sus dominios de unión a PI (Vicinanza y col., 2008) dando lugar a una diferenciación funcional progresiva. Asímismo, la aparición de vesículas intraluminales da origen a los denominados cuerpos multivesiculares y permite la organización de la carga que va a ser degradada en los lisosomas (Huotari y col., 2011). Finalmente, la acidificación progresiva del interior de los endosomas constituye un paso importante en el proceso de maduración de éstos, y puede actuar como sensor de la localización de la carga

endocitada (Huotari y col., 2011). Los endosomas tempranos tienen un rango de pH entre 6,8–6,1; los endosomas tardíos de 6,0-4,8 y los lisosomas de alrededor de 4,5 (Huotari y col., 2011; Maxfield y col., 1987). La regulación del pH en el lumen viene dada por la concentración de ATPasas vacuolares (V-ATPasas) en la membrana de los endosomas que bombean protones hacia el lumen del endosoma produciendo la acidificación de éstos (Huotari y col., 2011; Marshansky y col., 2008). Esta acidificación es aprovechada por muchos virus como mecanismo desencadenante de la liberación del genoma viral al interior de la célula (Le Blanc y col., 2005; Marsh y col., 2006; Pelkmans y col., 2003; Smith y col., 2004).

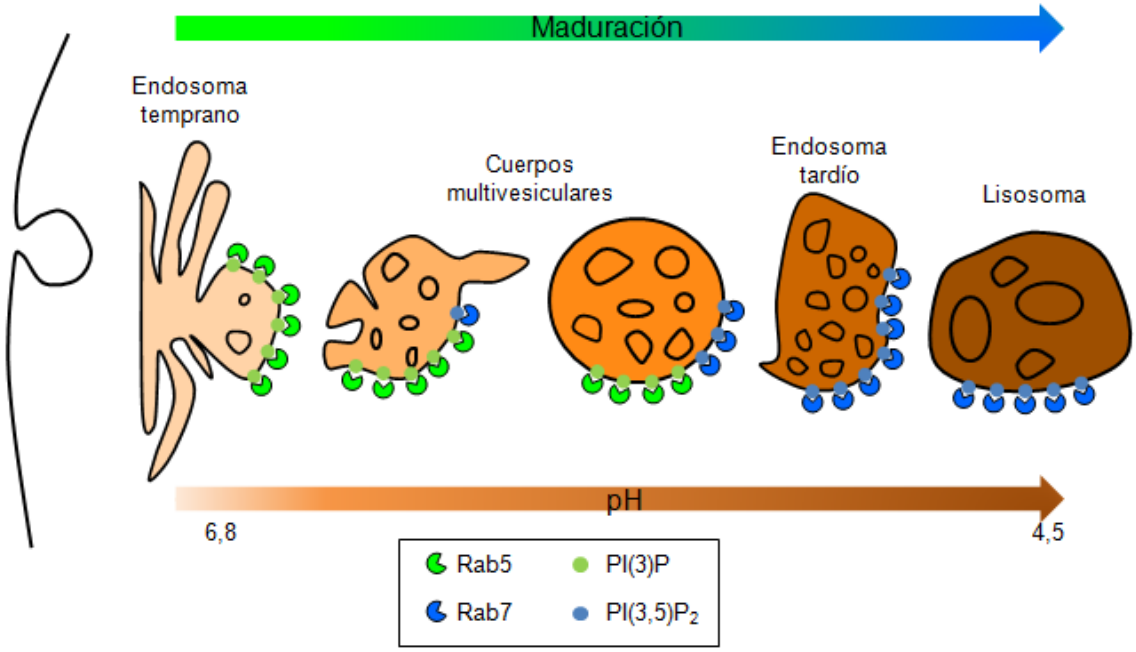

Figura 3. Maduración endosomal. Esquema del progreso de la maduración de un endosoma temprano a endosoma tardío caracterizado por: (i) reemplazamiento de la proteína Rab5 a Rab7, (ii) conversión del PI(3)P a $PI(3,5)P_2$, (iii) aumento de las vesículas internas, y (iv) acidificación del interior. Modificado de Huotari y col., 2011.

2.3.3 Mecanismos de liberación del genoma viral

Los virus han desarrollado distintas estrategias para asegurar que la liberación de su material genético ocurre en el compartimento celular adecuado para dar lugar a una infección productiva. Los lugares donde se producen estos procesos de penetración son variados e incluyen endosomas tempranos, endosomas de reciclaje, endosomas tardíos, el retículo endoplásmico (Lozach y col., 2011) y el núcleo (Greber y col., 2005; Whittaker y col., 1998). En el caso de los virus con envoltura, la estrategia general consiste en la fusión entre la membrana viral y la membrana plasmática o la membrana

de un compartimento intracelular determinado. Este proceso está mediado por proteínas virales que se denominan proteínas de fusión (Harrison, 2008; Puri y col., 2002; Teissier y col., 2007). La actividad de estas proteínas de fusión puede ser dependiente de pH, de forma que la acidificación progresiva en el interior de los endosomas puede activar el proceso de fusión dando lugar a la liberación de la nucleocapsida viral (Gaudin y col., 1999; Luo, 2012; Plemper, 2011). Recientemente se ha visto que también es importante el contenido lipídico de la membrana celular donde se va a producir el proceso de fusión (Roth y col., 2011; Zaitseva y col., 2010). En el caso de los virus sin envoltura, las estrategias más comunes están basadas en la alteración de la partícula viral y en la exposición de residuos hidrofóbicos (Tsai, 2007) o en cambios conformacionales inducidos por pH ácido (Konecsni y col., 2009). Para los virus cuya penetración se produce a partir de la acidificación endosomal, este proceso puede producirse por una disrupción de la membrana del endosoma, provocando la salida de todo su contenido, o por la formación de un poro en la membrana endosomal (Chandran y col., 2002; Danthi y col., 2003; FitzGerald y col., 1983; Knipe y col., 1997; Prchla y col., 1994; Prchla y col., 1995; Schober y col., 1998).

2.4 Papel de los lípidos en la infección viral

Dentro de los factores requeridos por los virus, los lípidos tienen un papel importante en las infecciones virales, tanto en los virus con envoltura como en los que carecen de ella (Alvisi y col., 2011; Heaton y col., 2011; Lorizate y col., 2011; Stapleford y col., 2010). Además de utilizar los lípidos que se encuentran de forma natural en la célula, los virus pueden inducir cambios en el metabolismo global de las células infectadas de forma que alteren el metabolismo de lípidos para facilitar la producción viral (Blackham y col., 2010; Diamond y col., 2011; Heaton y col., 2010b; 2011; Munger y col., 2008; Perera y col., 2012; Rodgers y col., 2009; Targett-Adams y col., 2010). En algunos casos, estas alteraciones permiten la reorganización de las membranas intracelulares de la célula hospedadora, dando lugar a un entorno adecuado para la replicación viral (den Boon y col., 2010; Miller y col., 2008). En este sentido, la modulación del metabolismo de diferentes lípidos está comenzando a ser considerado como una nueva estrategia antiviral factible (Bassendine y col., 2011; Munger y col., 2008). Durante esta Tesis Doctoral se ha evaluado el potencial antiviral del ácido valproico (AVP), un ácido graso de cadena corta usado comúnmente para el tratamiento de enfermedades neurológicas (Bruni y col., 1979; Terbach y col., 2009), cuyo

mecanismo de acción incluye, entre otros, la alteración del metabolismo de diversos lípidos (Shaltiel y col., 2004; Tokuoka y col., 2008; Xu y col., 2007).

2.5 La fiebre aftosa

2.5.1 La enfermedad de la fiebre aftosa: el virus de la fiebre aftosa

La fiebre aftosa (FA) es la enfermedad de mayor importancia para la Sanidad Animal Mundial, lo que la convierte en una enfermedad infecciosa de declaración obligatoria a la Organización Mundial de Sanidad Animal (OIE). El agente etiológico de esta enfermedad, el virus de la fiebre aftosa (VFA), es probablemente el patógeno animal más transmisible (Pereira, 1981). La FA produce una enfermedad vesicular sistémica aguda que afecta a animales de pezuña hendida (artiodáctilos), entre los que se encuentran la vaca, el cerdo, la oveja y la cabra, caracterizada por la aparición de lesiones cutáneas (aftas) principalmente en las zonas de la boca y patas. A pesar de la baja mortalidad con la que cursa, su gran transmisibilidad y los costes directos e indirectos que ocasiona provocan importantes pérdidas económicas (Sobrino y col., 2001).

El VFA está clasificado por el Comité Internacional de Taxonomía de Virus (ICTV) dentro del orden *Picornavirales* en la familia *Picornaviridae* y constituye la especie tipo dentro del género *Aphthovirus* (ICTV, 2009). La partícula viral contiene una molécula de RNA de cadena simple y polaridad positiva, con una pequeña proteína viral (VPg) unida covalentemente al extremo 5', englobada en una cápsida proteica de simetría icosaédrica (Sobrino y col., 2001). La cápsida tiene un diámetro de 28-30 nm y está formada por 60 copias de cada una de las proteínas estructurales (VP1-VP4) (Acharya y col., 1989; Lea y col., 1994a).

2.5.2 Organización genómica

El material genético de VFA está compuesto por una única molécula de RNA de polaridad positiva de unos 8,2 kb. En el caso del aislado de VFA empleado en esta Tesis Doctoral (C-S8c1) (ver apartado 4.2), la longitud de su RNA es de 8115 nt, sin contar los tramos homopoliméricos de polirribocitidilato (poliC) y poliadenilato (poliA), que son heterogéneos en longitud (Escarmis y col., 1996; Escarmis y col., 1992; Toja y col., 1999). El genoma consta de una única fase abierta de lectura (ORF) flanqueada por dos regiones no codificantes altamente estructuradas, denominadas 5' *untranslated región*

(UTR) y 3' UTR, involucradas en la replicación y traducción virales (Bigeriego y col., 1999; Saiz y col., 2001) (Fig. 4).

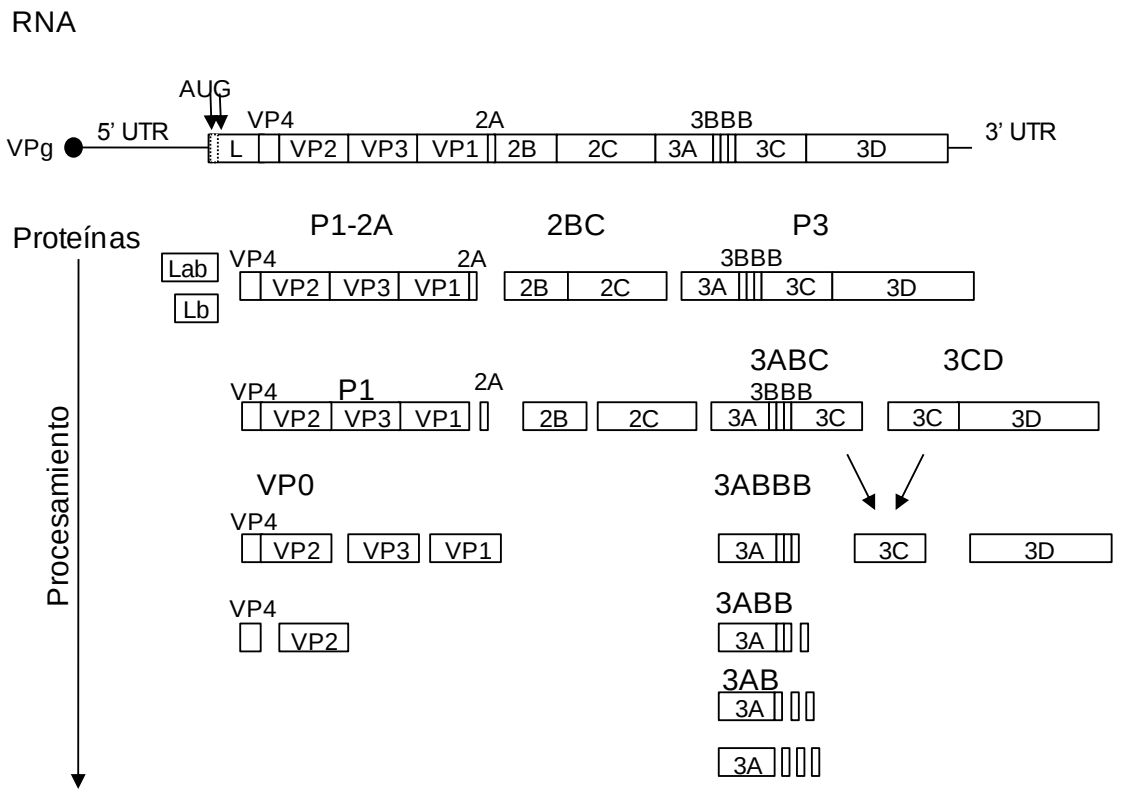

Figura 4. Organización genómica de VFA y procesamiento proteolítico de la poliproteína viral. Arriba: representación esquemática de la molécula de RNA de VFA, indicando la localizacion del marco de lectura abierta (representado por cajas), flanqueado por las regiones no codificantes (UTR) 5' y 3', con la proteína 3B (VPg) covalentemente unida en el extremo 5'. Abajo: representación esquemática del procesamiento proteólitico de la poliproteína para dar lugar a los diferentes precursores y proteínas maduras. Modificado de Martín-Acebes, 2009.

La traducción de la ORF se realiza mediante un mecanismo de iniciación interna independiente de CAP, mediado por un elemento IRES (Belsham y col., 1990; Kuhn y col., 1990), sintetizándose una única poliproteína que es procesada para dar lugar a las distintas proteínas virales (Belsham, 1993). La ORF se divide en cuatro regiones: L, P1-2A, P2 y P3. L codifica dos proteínas solapadas (Lab y Lb) con actividad proteasa encargadas de cortar el eIF-4G, factor implicado en la formación del complejo ribosómico de unión al CAP, lo que produce la inhibición de la síntesis de proteínas de la célula infectada (Devaney y col., 1988). La región P1-2A codifica las proteínas de la cápsida (VP1, VP2, VP3 y VP4) (Domingo y col., 2002) y el péptido 2A, que cataliza en *cis* la excisión de P1-2A de 2B (Ryan y col., 1991). Las regiones P2 y P3 codifican

varios precursores proteicos y un total de 6 proteínas no estructurales maduras (2B, 2C, 3A, 3B o VPg, 3C y 3D) implicadas en la replicación del RNA viral (Porter, 1993).

2.5.3 Proteínas estructurales

La cápsida de VFA está formada por 60 copias de cada una de las proteínas estructurales VP1 (1C), VP2 (1B), VP3 (1D) y VP4 (1A). Se ha resuelto mediante cristalografía de rayos X la estructura tridimensional a nivel atómico de la cápsida de diferentes serotipos de VFA (Acharya y col., 1989; Curry y col., 1996; Curry y col., 1997; Fry y col., 1999; Fry y col., 2005). La cápsida tiene simetría icosaédrica y un diámetro de unos 30 nm. Las proteínas VP1, VP2 y VP3 (~ 23 – 24 kDa) constituyen la superficie externa de la cápsida y comparten una estructura en barril β compuesta por 8 cadenas antiparalelas conectadas entre sí por bucles. La proteína VP4 (~ 9 kDa) se localiza en la cara interna de la cápsida y está unida en su extremo N-terminal a un residuo de ácido merístico (Belsham y col., 1991). La proteína VP4 madura resulta del procesamiento proteolítico del precursor VP0 en VP2 + VP4 (Fig. 4), lo que se produce una vez ensamblada la cápsida (Knipe y col., 1997).

La primera unidad de ensamblaje de la cápsida la constituye el protómero biológico (Fig. 5a), formado por una copia de cada una de las cuatro proteínas estructurales. Cinco protómeros se ensamblan dando lugar a un pentámero (Fig. 5b). Las subunidades pentaméricas constituyen los intermedios de ensamblaje y desensamblaje de la cápsida de VFA. Doce pentámeros se asocian y forman la cápsida (Fig. 5c). En las interfases interpentaméricas existen residuos que participan en puentes de hidrógeno y puentes salinos entre las distintas subunidades que son importantes para la estabilidad de la cápsida (Mateo y col., 2003). Las cápsidas de VFA son extremadamente sensibles a pH ácido (Brown, 1972; Newman y col., 1973), siendo su valor de disociación a pentámeros cercano a los valores de pH neutro (Acharya y col., 1989; Martín-Acebes y col., 2011c; van Vlijmen y col., 1998). La sensibilidad a pH ácido está implicada en el mecanismo de desencapsidación que utiliza el VFA (Baxt, 1987; Carrillo y col., 1985; Carrillo y col., 1984; Martín-Acebes, 2009), habiéndose asociado a la presencia de residuos de His que se localizan cerca de las interfaces pentaméricas (Acharya y col., 1989; van Vlijmen y col., 1998). Así, las cargas positivas producidas por la protonación de estos residuos de His (pk 6,8 en solución) a pH ácido pueden inducir el desensablaje de la cápsida. De acuerdo con esta hipótesis, los residuos His 142 y 145 de VP3 en el VFA tipo A, que corresponde a las His 140 y 143 en VP3

de C-S8c1, constituyen residuos claves para este proceso (Curry y col., 1995; Ellard y col., 1999; van Vlijmen y col., 1998).

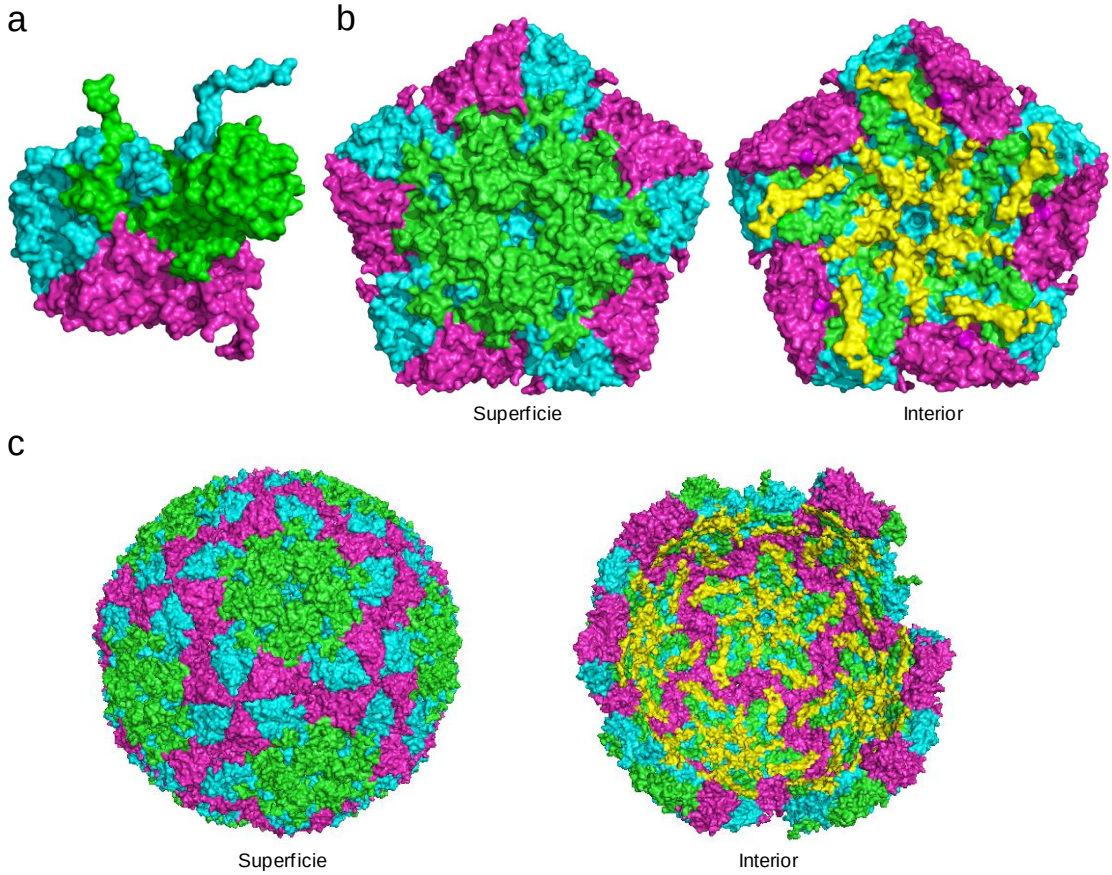

Figura 5. Representación tridimensional de la estructura de la cápsida de VFA y de los intermediarios de ensamblaje. La estructura se basa en las coordenadas atómicas de la cápsida del aislado C-S8c1 (Lea y col., 1994b). La representación se realizó con el programa PyMol. Código de colores: VP1 En verde, VP2 en magenta, VP3 en cian y VP4 en amarillo (a) Vista de superficie del protómero biológico. (b) Vista de una subunidad pentamérica. Izquierda: vista de superficie. Derecha: vista de la cara interna. (c) Vista de la cápsida. Izquierda: vista de superficie de la cápsida completa. Izquierda: vista interna.

La superficie de la partícula viral no es lisa ya que muchos de los bucles que conectan las láminas β entre sí y las propias láminas β sobresalen de la cápsida. Entre ellos destaca el bucle G-H de la proteína VP1, comprendido entre las posiciones 138 a 150 (Lea y col., 1994b). Se trata de un bucle largo y flexible en cuya posición central (posiciones 141-143) se localiza un triplete Arg, Gly, Asp (RGD) altamente conservado, que mimetiza la secuencia de interacción de algunos ligandos celulares con moléculas de la familia de las integrinas (Pierschbacher y col., 1984a; b; Takada y col., 2007). Mediante ensayos de competición con péptidos conteniendo el motivo RGD se ha

demostrado el papel funcional de este motivo como ligando viral de unión a receptores celulares (Baxt y col., 1990; Fox y col., 1989; Mateu y col., 1996).

Las integrinas constituyen el receptor utilizado por los aislados naturales del VFA para infectar hospedadores naturales (McKenna y col., 1995; Monaghan y col., 2005; Nuñez y col., 2007). Hasta el momento se han descrito 5 integrinas capaces de interaccionar con el VFA, aunque dentro de estas, el papel funcional de la integrina $\alpha_5\beta_1$ no ha sido demostrado, y sólo las integrinas $\alpha_v\beta_1$, $\alpha_v\beta_3$, $\alpha_v\beta_6$ y $\alpha_v\beta_8$, pueden actuar como receptor para la entrada del virus en células en cultivo (Jackson y col., 2004; Jackson y col., 2002; Jackson y col., 2000; Neff y col., 1998). Por otro lado, el VFA es capaz de entrar en las células utilizando rutas independientes de integrinas. Por ejemplo, el virus acomplejado con anticuerpos puede ser internalizado en células que expresan el receptor Fc (Baxt y col., 1995; Mason y col., 1993; Mason y col., 1994). Además, virus adaptados a cultivos celulares pueden entrar en las células vía heparán sulfato (HS), un glucosaminoglicano de superficie (Fry y col., 1999; Jackson y col., 1996). También se han descrito variantes que pueden utilizar como receptores otras moléculas que no son integrinas ni HS (Baranowski y col., 2000; Baranowski y col., 1998; Zhao y col., 2003).

Las protuberancias de la cápsida constituyen sitios antigénicos reconocidos por linfocitos B para inducir anticuerpos frente al virus (Domingo y col., 1999). La variabilidad de secuencia dentro de estas regiones ha llevado a la identificación de siete serotipos; los euroasíaticos A, O, C y Asia 1; y los sudafricanos SAT1, SAT2 y SAT3 (Domingo, 1990). La clasificación en diferentes serotipos obedece a criterios funcionales agrupando, en cada caso, a aquellos virus capaces de inducir protección cruzada en animales (Saiz y col., 2002) y dentro de los cuales existen múltiples variantes virales. El bucle G-H de la proteína VP1 constituye un sitio antigénico principal compuesto por diferentes epítopos solapantes, denominado sitio A (Mateu y col., 1990). Otros sitios antigénicos son los denominados sitio C, que se localiza en el extremo C-terminal de VP1 y es continuo e independiente del sitio A en C-S8c1 pero no en VFA de serotipo O (Parry y col., 1990), y el sitio D, que es discontinuo y comprende residuos de VP1, VP2 y VP3 (Lea y col., 1994b).

2.5.4 Interacción con la célula hospedadora

Las células epiteliales constituyen el blanco principal del VFA; *in vivo* la replicación inicial tiene lugar en el epitelio de la faringe (Jackson y col., 2004). A pesar de ello la mayoría de los datos sobre las interacciones del VFA con las células

hospedadores se han obtenido mediante estudios realizados en cultivos de líneas celulares susceptibles. En estos sistemas, el virus inicia la infección por unión a alguno de los cuatro miembros del subgrupo α_v perteneciente a la familia de las integrinas (Ruiz-Sáenz y col., 2009) (ver apartado 2.5.3). Tras esta interacción, la entrada del virus en la célula tiene lugar mediante un mecanismo de endocitosis mediada por vesículas recubiertas de clatrina (Berryman y col., 2005; Martín-Acebes y col., 2007; O'Donnell y col., 2005), seguido por el paso a través de compartimentos endosomales. En el caso de un variante de VFA que utiliza HS como receptor se ha descrito que su entrada en la célula está mediada por un mecanismo de endocitosis dependiente de caveolas (O'Donnell y col., 2008).

La liberación del genoma viral es un proceso dependiente de la acidificación endosomal, debido a que gran variedad de agentes que bloquean la acidificación de los endosomas, como bases débiles e ionóforos, inhiben la infección de VFA (Baxt, 1987; Carrillo y col., 1985; Carrillo y col., 1984; Martín-Acebes y col., 2010). Por otro lado, se ha descrito que las partículas de VFA internalizadas colocalizan con marcadores de endosomas tempranos y de reciclaje, pero no con marcadores de endosomas tardíos o lisosomas (Berryman y col., 2005; O'Donnell y col., 2008; O'Donnell y col., 2005). Además, recientemente se ha observado que el VFA de tipo O requiere la GTPasa Rab5, localizada en los endosomas tempranos, para dar lugar a una infección productiva (Johns y col., 2009). Estos datos, junto con el valor de pH (6,56 - 6,65) de disociación de la cápsida (Curry y col., 1995; Martín-Acebes y col., 2010), sugieren que la desencapsidación de VFA tendría lugar dentro de estos compartimentos. Durante el desensamblaje de la cápsida en subunidades pentaméricas, la proteína VP4 es liberada, habiéndose propuesto que esta proteína podría contribuir a la permeabilización de la membrana endosomal, permitiendo la penetración del RNA viral al citoplasma (Knipe y col., 1997), de una manera similar a lo descrito para otros picornavirus (Davis y col., 2008).

El RNA viral actúa como mensajero y es traducido de manera independiente de CAP dando lugar al conjunto de proteínas virales (ver apartado 2.5.2). A partir de un intermedio replicativo poco caracterizado se sintetiza RNA de polaridad negativa y, a partir de éste, RNA de polaridad positiva. La expresión de las proteínas virales provoca reorganizaciones en la célula hospedadora, que incluyen el aumento del número de las vesículas citoplasmáticas. Aunque el origen preciso de las membranas celulares no ha sido determinado todavía, éstas podrían provenir del retículo endoplásmico y/o del

complejo de Golgi (Knox y col., 2005; Martín-Acebes y col., 2008; Monaghan y col., 2004). La traducción y la replicación de los picornavirus se producen asociadas a la superficie de estas vesículas (Bienz y col., 1987). El ciclo viral transcurre en el citoplasma, aunque se ha observado que determinadas proteínas pueden translocarse al núcleo (de Los Santos y col., 2007; García-Briones y col., 2006).

2.5.5 Variabilidad y dinámica de cuasiespecie

El VFA se caracteriza por presentar una elevada variabilidad genética (Domingo y col., 2003; Domingo, 1990) y las poblaciones de VFA, al igual que las de los virus RNA, son distribuciones dinámicas complejas de mutantes relacionados entre sí, denominadas cuasiespecies virales (Domingo y col., 2006). Dentro de las cuasiespecies existe un equilibrio entre una alta tasa de mutación, inherente a la replicación del RNA y una continúa competición reflejada en el mantenimiento de la eficacia biológica (*fitness*). Esta estructura confiere una gran flexibilidad adaptativa a los virus RNA (Domingo y col., 1997). Para el VFA, existen distintos ejemplos de cambios fenotípicos notables derivados de cambios genéticos mínimos, incluyendo mutaciones puntuales, como la adquisición de resistencia a anticuerpos monoclonales (Lea y col., 1994b), fármacos (Ferrer-Orta y col., 2010; Sierra y col., 2007), vacunas peptídicas (Taboga y col., 1997), cambios en rango de hospedador (Nuñez y col., 2001), o alteraciones de las propiedades físico-químicas de la cápsida como estabilidad frente a pH (Martín-Acebes, 2009) o temperatura (Mateo y col., 2007a) .

2.6 El virus de la estomatitis vesicular

La estomatitis vesicular es una enfermedad viral que afecta a numerosas especies animales, entre ellas caballos, vacas, cerdos e incluso humanos (Letchworth y col., 1999; Rodríguez, 2002). El agente etiológico de esta enfermedad es el virus de la estomatitis vesicular (VEV), incluído en la familia *Rhabdoviridae*, dentro del género *Vesiculovirus*, siendo la especie tipo el VEV Indiana (ICTV, 2009). Los viriones tienen forma de bala, con un tamaño en torno a 180 nm de longitud y 80 nm de diámetro. Poseen una envoltura lipídica que recubre una nucleocápsida proteica interna donde se localiza el material genético viral, compuesto por una molécula simple de RNA de polaridad negativa y 11 kb de tamaño (Fig. 6a). El genoma codifica cinco proteínas principales: nucleoproteína (N), fosfoproteína (P), proteína de la matriz (M), glicoproteína (G), y proteína *large* (L) (Fig. 6b). La proteína G es transmembrana y se

localiza en la envoltura del virion. La proteína M forma parte de la nucleocápsida y tiene distintos papeles en el proceso de replicación. La proteína N se encuentra asociada al RNA viral, y las proteínas L y P catalizan la replicación del RNA viral (Albertini y col., 2008; Letchworth y col., 1999; Lichty y col., 2004).

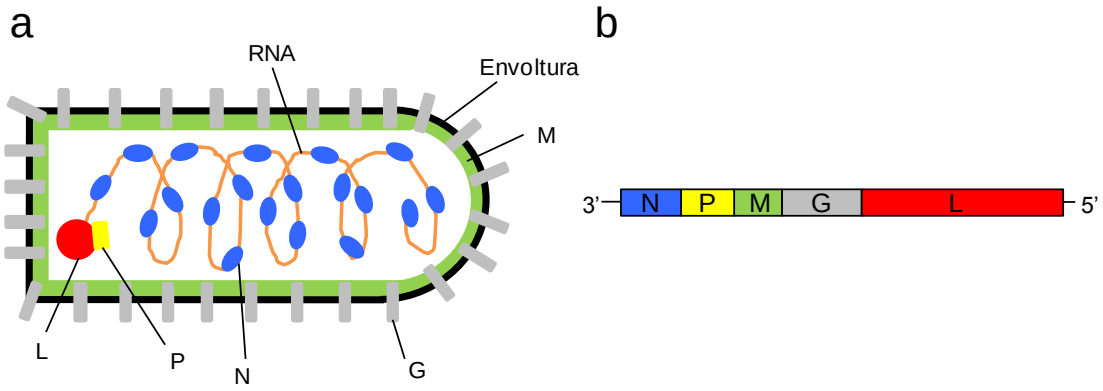

Figura 6. **Partícula de VEV y organización genómica del virus.** Modificado de Martín-Acebes, 2009. (a) Representación esquemática de una partícula de VEV. En marrón la molécula de RNA, en verde la proteína de la matriz (M), en gris la glicoproteína (G), en azul la nucleoproteína (N). La proteína L y la P incluidas en el virión, se indican en rojo y amarillo, respectivamente. (b) Organizción genómica del RNA de polaridad negativa de VEV. Las regiones que codifican las distintas proteínas virales se indican como cajas con diferentes colores.

El VEV utiliza como receptores celulares lípidos cargados negativamente, como la fosfatidilserina (Carneiro y col., 2006; Schlegel y col., 1983). El contacto del virus con la célula se produce a través de la proteína G. El VEV es internalizado en la célula mediante endocitosis mediada por clatrina, siendo uno de los modelos clásicos para el estudio de la internalización de virus mediante esta ruta (Matlin y col., 1982; Simpson y col., 1969; Sun y col., 2005; Superti y col., 1987). La vesícula con el virus internalizado llega a los endosomas tempranos de forma dependiente de Rab5 (Sieczkarski y col., 2003) y sigue la vía endosomal hacia los endosomas tardíos, por lo que la liberación del material genético debe producirse en los cuerpos multivesiculares o en los endosomas tardíos. Este proceso parece deberse a un cambio conformacional en la proteína G, provocado por el entorno ácido de estos compartimentos, que da lugar a la fusión de la envoltura viral con las membranas endosomales (Roche y col., 2008; Roche y col., 2006; Roche y col., 2007). La liberación del genoma viral se produce en dos pasos, primero se fusiona la membrana viral con la vesícula interna de un cuerpo multivesicular y, después, esta vesícula interna se fusiona con la membrana de un endosoma tardío dando lugar a la liberación de la nucleocapsida (Le Blanc y col., 2005). Posteriormente tiene lugar la síntesis de proteínas virales y la replicación del material

genético. Los viriones maduros se ensamblan en la membrana plasmática y salen de la célula por un proceso de gemación (de Silva y col., 1990; Oda y col., 1990).

2.7 El virus de la coriomeningitis linfocitaria

El virus de la coriomeningitis linfocitaria (VCML), perteneciente a la familia *Arenaviridae* dentro del género *Arenavirus* (ICTV, 2009), afecta principalmente a roedores, aunque también es un patógeno humano con importancia clínica en infecciones congénitas y en individuos inmunosuprimidos (Borrow y col., 2010). Como ocurre en otros arenavirus, su partícula viral es pleiomórfica con un tamaño medio de 86 ± 21 nm de diámetro, aunque normalmente presenta morfología esférica.

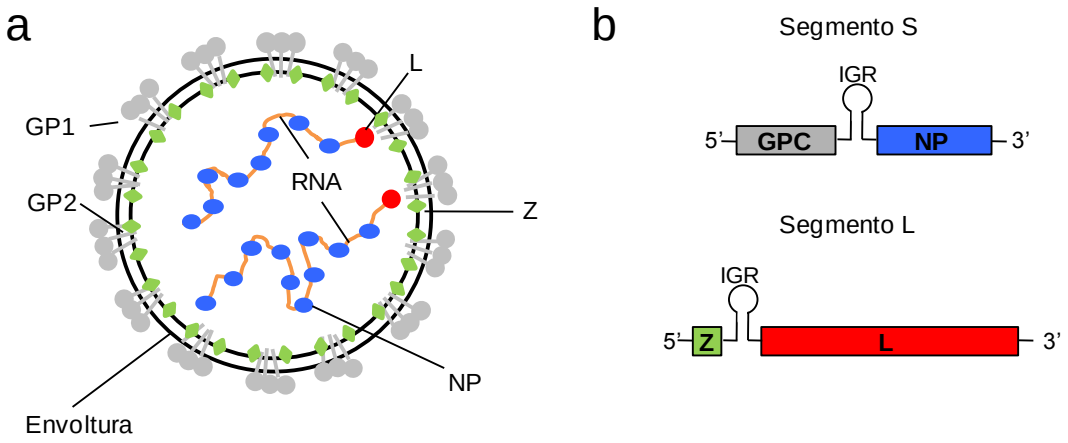

Figura 7. Partícula de VCML y organización genómica del virus. (a) Representación esquemática de una partícula de VCML. En rojo la polimerasa L, en azul la NP, en verde la proteína de la matriz Z, en gris los trimeros de GP1 y GP2. La envoltura lipídica del virión se representa en negro. Modificado de Lee y col., 2010. (b) Representación esquemática de la organización genómica del virus. Cada segmento de RNA codifica para dos proteínas con orientación opuesta y separadas por una región intergénica (IGR). El segmento S codifica para las proteínas estructurales: la nucleoproteína (NP) y las glicoproteínas (GPC). El segmento L codifica para las proteínas no estructurales: la polimerasa viral (L) y la proteína Z.

La partícula viral posee una envoltura lipídica con proyecciones en la superficie que recubre una nucleocápsida proteica interna donde se localiza el material genético y ribosomas (Murphy y col., 1975; Neuman y col., 2005) (Fig.7a). El genoma viral consta de dos segmentos de RNA de cadena sencilla y polaridad negativa. Cada segmento de RNA codifica dos proteínas en orientación opuesta y separadas por una región intergénica (Auperin y col., 1982; Auperin y col., 1984; Wilson y col., 1991) (Fig. 7b). El segmento más grande se denomina segmento *large* (L, 7,2 kb) y codifica la RNA polimerasa o proteína L, y la proteína Z, que es el homólogo de la proteína de la matriz (M) encontrada en muchos virus con envoltura de RNA de polaridad negativa. El

segmento *small* o segmento S (3,5 kb) codifica la nucleproteína (NP) y el precursor de la glicoproteína (GP), que es procesada para dar lugar a las proteínas GP1 y GP2 (Emonet y col., 2011). GP1 es la proteína viral asociada a la unión con el receptor celular (Buchmeier, 2007), mientras que GP2 es una proteína transmembrana que actúa como una proteína de fusión (Eschli y col., 2006; Igonet y col., 2011). Trimeros de las proteínas GP1/GP2 constituyen las espículas que decoran la superficie viral y median la entrada a la célula vía endocitosis mediada por receptor (Buchmeier, 2007; Kunz, 2009) (Fig. 7a). Las proteínas L y NP son los factores mínimos actuando en *trans* requeridos para la replicación del RNA viral y para la expresión de las proteínas virales (Lee y col., 2000), mientras que la producción de partículas virales infecciosas también requiere las proteínas GP1, GP2 y Z (Lee y col., 2002).

El VCML usa como receptor celular el α-distroglicano y entra en la célula hospedadora mediante un mecanismo de endocitosis independiente de clatrina, caveolina, dinamina y actina (Quirin y col., 2008). Una vez ha sido internalizado dentro la célula, el virus es liberado en los cuerpos multivesiculares de forma independiente de Rab5 y requiere un transporte activo, a través de los microtúbulos, hacia los endosomas tardíos (Pasqual y col., 2011). Debido al entorno ácido del endosoma tardío la proteína GP2 sufre un cambio conformacional que le permite dar lugar a la fusión de la membrana viral con la membrana endosomal para producir la liberación del genoma viral (Igonet y col., 2011). La replicación de VCML se produce en el citoplasma de la célula infectada y la gemación de la progenie viral tiene lugar mayoritariamente en la membrana plasmática (Buchmeier, 2007).

2.8 El virus del Nilo occidental

El virus del Nilo occidental (VNO) pertenece a la familia *Flaviviridae* dentro del género *Flavivirus* (ICTV, 2009). Este virus se mantiene en la naturaleza mediante un ciclo de transmisión entre aves y mosquitos ornitofílicos que actúan como vector. El virus puede, esporádicamente, infectar a caballos y humanos, pudiendo causar la enfermedad denominada fiebre del Nilo Occidental, cuyos síntomas incluyen fiebre, meningitis, encefalitis y parálisis muscular (Beasley, 2005; Brinton, 2002). La partícula viral tiene morfología icosaédrica y un tamaño de unos 50 nm de diámetro (Fig. 8a). La partícula posee una envoltura lipídica que recubre una nucleocápsida proteica interna donde se localiza el material genético viral, compuesto por una molécula simple de RNA de polaridad positiva (11 kb) (Mukhopadhyay y col., 2003). El RNA viral codifica

una única poliproteína que será procesada para dar lugar a tres proteínas estructurales (C, prM y E) y siete no estructurales (NS1, 2A, 2B, 3, 4A, 4B y 5) (Brinton, 2002) (Fig. 8b).

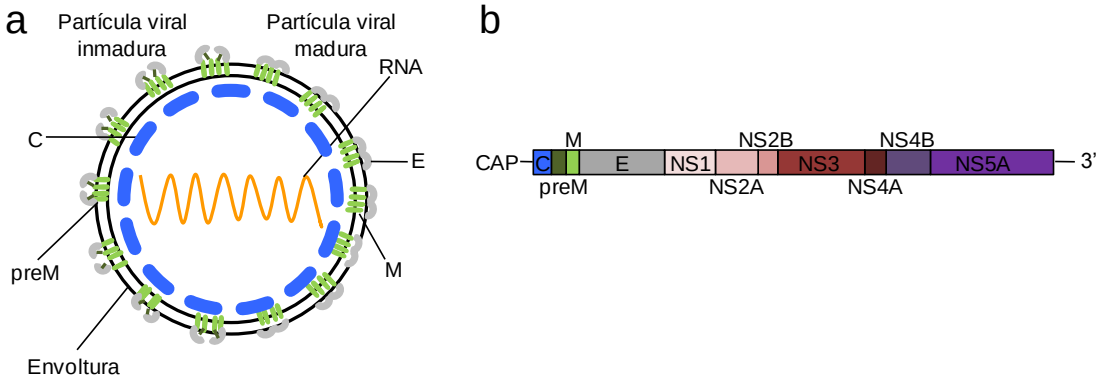

Figura 8. Partícula de VNO y organización genómica del virus. (a) Representación esquemática de una partícula de VNO. En marrón la molécula de RNA, en verde la proteína de la matriz (M y preM), en gris la glicoproteína (E), en azul la proteína de la cápsida (C). Modificado de De Filette y col., 2012. (b) Organización genómica del RNA de polaridad positiva de VNO. Las regiones que codifican las distintas proteínas virales se indican como cajas con diferentes colores.

La infección por VNO comienza por la unión con sus receptores celulares: glicosaminoglicanos, lectinas de tipo c o integrinas $\alpha_v\beta_3$ (Chu y col., 2004; Davis y col., 2006; Lee y col., 2004; Medigeshi y col., 2008). El virus es internalizado en la célula mediante un mecanismo de endocitosis mediada por vesículas revestidas de clatrina y dirigido hacia los compartimentos endosomales (Chu y col., 2006; Chu y col., 2004). El entorno ácido de los endosomas origina la fusión de la membrana viral con la membrana endosomal, mediada por la proteína E, lo que conlleva la liberación de la nucleocápsida (Martín-Acebes y col., 2011b). La replicación del virus y su ensamblaje tienen lugar en el retículo endoplásmico (Gillespie y col., 2010). Las partículas virales maduran a lo largo de la ruta secretora y son finalmente liberadas al medio (Brinton, 2002).

Objetivos

3. Objetivos

Los objetivos de esta Tesis Doctoral han sido:

1. Caracterizar el papel del $PI(4,5)P_2$ de la membrana plasmática y una de sus proteínas efectoras, la dinamina, en la internalización de VFA y VEV, para lo que se ha empleado la línea celular BHK-21.

2. Analizar el papel funcional de las GTPasas Rab5, Rab7 y Rab11 implicadas en el tráfico entre diferentes poblaciones endosomales en la infección de VFA, utilizando diferentes mutantes de este virus con distinto pH de desencapsidación.

3. Aislar y caracterizar mutantes de VFA resistentes a inhibidores de la acidificación endosomal (NH_4Cl) a partir de muestras biológicas procedentes de hospedadores naturales infectados (cerdos).

4. Estudiar el efecto del AVP en la infección de distintos virus con y sin envoltura lipídica.

Materiales y métodos

4. Materiales y métodos

4.1 Cultivo de células eucarióticas

Las líneas celulares empleadas fueron:

▪ BHK-21: fibroblastos de riñón de hámster sirio dorado (*Mesocricetus auratus*) (Stoker y col., 1964) procedentes de la ATCC.

▪ Vero: células de riñón de mono verde africano (*Cercopithecus aethiops*) (Rhim JS, 1967), amablemente cedidas por A. L. Carrascosa (CBMSO).

▪ 293T: células de riñón humanas (*Homo sapiens*) (DuBridge y col., 1987).

Todas las líneas celulares se crecieron en medio Eagle modificado por Dulbecco (DMEM) (Gibco), suplementado con 100 U/ml de penicilina (Sigma), 100 µg/ml de estreptomicina (Sigma), 2 mM L-glutamina (Gibco) y 5% suero fetal bovino (SFB); a 37º C en una atmósfera con 7% CO_2 y 98% humedad.

Las células fueron almacenadas en nitrógeno líquido tras un proceso de congelación lenta en una mezcla de 90% SFB y 10% DMSO (Sigma). Para su descongelación se introdujeron en un baño a 37º C, se centrifugaron a 250 × g durante 5 min y se distribuyeron en placas de cultivo celular en medio completo con 10% SFB. Cuando las células alcanzaron la confluencia, éstas se despegaron de las placas utilizando una mezcla de 0,05 mg/ml de tripsina (Difco) y 0,016% EDTA (Merck) y se sembraron en placas nuevas a la dilución deseada (pase).

4.2 Virus

En esta Tesis Doctoral se han utilizado distintos variantes de VFA que se enumeran a continuación:

• C-S8c1: derivado del aislado natural C_1-Sta. Pau España 70 por triple purificación de placa (clonaje biológico). Este aislado es representativo del subtipo europeo (C_1) del serotipo C de VFA (Sobrino y col., 1983).

• C-S8c1p213MARLS (denominado MARLS a lo largo de esta Tesis Doctoral): mutante de escape al anticuerpo monoclonal SD6 dirigido frente al bucle G-H de la proteína VP1 de la cápsida de VFA (Mateu y col., 1990). Este virus fue seleccionado a partir de la población C-S8c1p213 (C-S8c1 pasado 213 veces en células BHK-21) (Charpentier y col., 1996) y fue amablemente cedido por E. Domingo (CBMSO). Las mutaciones seleccionadas en MARLS con respecto al virus C-S8c1 parental, han sido descritas previamente (Baranowski y col., 1998).

• C-S8c1c2 (denominado c2 a lo largo de esta Tesis Doctoral): mutante con resistencia incrementada a NH_4Cl obtenido previamente en el laboratorio mediante clonaje biológico en presencia de 25 mM NH_4Cl a partir de la población del virus C-S8c1 (Martín-Acebes y col., 2010). Este mutante presenta las sustituciones de nucleótido C2903T y A3346G que codifica el cambio de aminoácido VP3 A118V y VP1 N47D, respectivamente.

• C-S8c1m6 (denominado m6 a lo largo de esta Tesis Doctoral): mutante con resistencia incrementada a pH 6 obtenido previamente en el laboratorio tras el tratamiento de la población de virus C-S8c1 con pH 6 y posterior clonaje biológico (Martín-Acebes y col., 2011c). Este mutante presenta la sustitución de nucleótido A3256G que codifica el cambio de aminoácido VP1 N17D.

Distintas variantes de VCML que se enumeran a continuación:

• VCML Arm (Martín y col., 2008) fue amablemente cedido por V. Martín (CISA-INIA) y E. Domingo (CBMSO).

• r3-VCML-GFP: virus trisegmentado (1S + 2L) recombinante de VCML (r3-VCML) (Fig. 9), en el que a cada segmento S se le ha remplazado el correspondiente ORF viral por el ORF de GFP, de tal forma que GP y NP se localizan en un segmento S diferente (Emonet y col., 2009). Este virus fue utilizado durante una estancia en el laboratorio de J. C. de la Torre (*The Scripps Research Institute*, La Jolla, California).

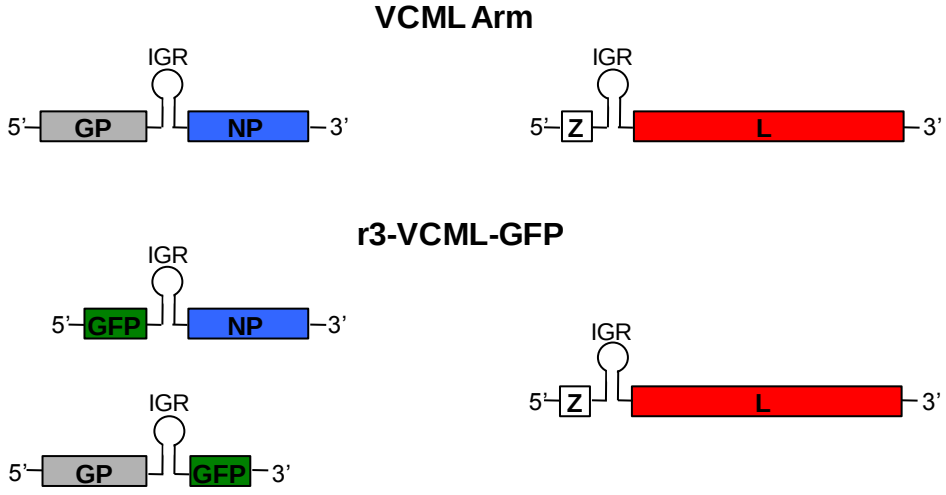

Figura 9. Representación esquemática de los genomas de VCML Arm y r3-VCML-GFP. A la izquierda están representados los segmentos S, a la derecha el segmento L. Cada segmento de RNA codifica dos proteínas con orientación opuesta y separadas por una región intergénica (IGR). En VCML Arm, el segmento S codifica las proteínas estructurales: la nucleoproteína (NP) y las glicoproteínas (GP); el segmento L codifica las proteínas no estructurales: la polimerasa viral (L) y la proteína Z. En el caso de r3-VCML-GFP, hay dos segmentos S, uno de ellos codifica las proteínas GFP y NP; el otro las proteínas GP y GFP.

Los restantes virus utilizados en esta Tesis Doctoral se enumeran en la Tabla II.

Tabla II. Otros virus utilizados

Familia	Virus[a]	Referencia
Asfaviridae	Virus de la peste porcina africana (VPPA) BA71V[1]	(Enjuanes y col., 1976)
Flaviviridae	Virus del Nilo Occidental (VNO) NY99[2]	(Lanciotti y col., 1999)
	Virus Usutu (VUSU) SAAR-1776[2]	(Buckley y col., 2003)
Picornaviridae	Enterovirus bovino (EVB)[2]	(Jiménez-Clavero y col., 2005)
	Virus de la encelafomiocarditis (VEMC)	(Rosas y col., 2008)
	Virus de la rinitis equina A (VREA)[3]	(Li y col., 1996)
Poxviridae	Virus vaccinia *Western Reserve* (VVAC)[4]	(Blasco y col., 1992)
Rhabdoviridae	Virus de la estomatitis vesicular (VEV) Indiana[5]	(de la Torre y col., 1985)
Togaviridae	Virus del bosque de Semliki (VBS)[6]	(Ventoso y col., 2006)
	Virus Sindbis (VSIN)[7]	(Ventoso y col., 2006)

[a] En los casos en que se empleó una cepa determinada del virus, ésta se indica.
[1] Amablemente cedido por C. Hurtado y A. L. Carrascosa (CBMSO).
[2] Amablemente cedido por J. C. Saiz (INIA).
[3] Amablemente cedido por C. A. Hartley (*Asia-Pacific Centre for Animal Health*, Universidad de Melbourne, Australia).
[4] Amablemente cedido por R. Blasco (INIA).
[5] Amablemente cedido por M. Dávila y E. Domingo (CBMSO).
[6] Amablemente cedido por I. Ventoso (CBMSO).
[7] Amablemente cedido por P. Moral y L. Carrasco (CBMSO).

4.3 Muestras biológicas

Se empleó líquido vesicular procedente de cerdos inmunizados 3 veces con 400 µg de la vacuna DNA pCMV-BTT y posteriormente desafiados con 10^4 unidades formadoras de placas (UFP) de VFA C-S8c1 (Ganges y col., 2011). Las muestras se recogieron de lesiones vesiculares procedentes del morro de los cerdos 3 días post-infección (p.i.). Estos animales se denominan como cerdo 5 y cerdo 6, manteniendo la numeración del estudio previo (Ganges y col., 2011). Estas muestras fueron amablemente cedidas por B. Borrego (CISA-INIA).

4.4 Clones infecciosos

Los clones infecciosos que expresan el genoma completo del VFA utilizados fueron:

▪ pMT28: codifica el RNA genómico del aislado C-S8c1 (García-Arriaza y col., 2004), que fue amablemente cedido por C. Escarmís (CBMSO). La numeración de los nucleótidos del genoma de VFA contenido en este plásmido utilizada en esta Tesis Doctoral corresponde a la descrita para C-S8c1 por Toja y col., 1999 (Número de acceso a GenBank: AJ33357).

▪ pMT28-VP3 116V: derivado del clon infeccioso pMT28, contiene la sustitución de nucleótido C2897T que codifica el cambio de aminoácido VP3 A116V (ver apartado 4.26).

▪ pMT28-VP1 17D: derivado del clon infeccioso pMT28, contiene la sustitución del nucleótido A3256G que codifica el cambio de aminoácido VP1 N17D (Martín-Acebes y col., 2011c).

4.5 Infecciones virales

4.5.1 Infección en medio líquido

Las monocapas celulares fueron lavadas dos veces con DMEM e infectadas con la multiplicidad de infección (m.d.i.) – definida como UFP/célula – elegida. Durante la primera hora de infección, o primera hora y media en el caso de VCML, las placas fueron agitadas cada 15 min. Transcurrido este tiempo, el inóculo fue retirado y se añadió medio fresco con SFB al 5%, considerándose este momento como tiempo 0 p.i. En todos los casos, las infecciones se realizaron a 37º C. En los ensayos realizados para analizar la internalización de viriones, las células se infectaron con una m.d.i. de 70 UFP/célula y se incubaron con los virus durante 25 min.

4.5.2 Infección en medio semisólido: titulación de virus

Para titular la producción viral total (virus en sobrenadante más virus intracelular), las placas conteniendo las células infectadas fueron congeladas y descongeladas tres veces para asegurar la rotura de las membranas celulares y la liberación al medio del virus intracelular. La titulación de virus extracelular se llevo a cabo a partir de sobrenadante de células infectadas.

La titulación de los diferentes virus se realizó infectando por duplicado monocapas de células BHK-21 (en el caso de VFA, VEMC, EVB, VEV, VBS, VSIN y VVAC) o Vero (en el caso de VREA, VCML, VNO, VUSU y VPPA), crecidas en placas de 6 o 12 (en el caso de VPPA) pocillos. Para ello, se realizaron diluciones seriadas de las suspensiones virales con las que se infectaron monocapas al 80-90% de confluencia, tal y como se describe en el apartado anterior. Tras la primera hora de infección se retiró el inoculo y se añadió medio semisólido [0,5% agar noble (Difco), 1% SFB y 0,045 mg/ml DEAE-dextrano en DMEM]. En el caso de VCML, el inoculo se retiró tras la primera hora y media, añadiéndose posteriormente medio semisólido (0,3% agar, 1% SFB y 0,045 mg/ml DEAE-dextrano en DMEM). Para el VNO y

VUSU, tras retirar el inóculo se añadió medio semisólido conteniendo 1% agarosa de bajo punto de fusión (Pronadisa, Laboratorios Conda) y 2% SFB. Las placas fueron incubadas a 37º C durante 24 h (VFA, VEMC y VEV), 48 h (VEVC, EVB, VREA, VBS y VSIN), 72 h (VNO, VUSU y VVAC) o 1 semana (VCML y VPPA). Transcurrido este tiempo las células se fijaron con una solución de 2% formaldehído durante 15 min, excepto para VNO y VUSU con los que se utilizó una solución de 4% formaldehido durante 1h. A continuación, se retiró el medio semisólido y las placas se tiñeron con 0,02% cristal violeta en 10% etanol y 2% paraformaldehído. Las placas fueron lavadas con agua para retirar el exceso de cristal violeta y se dejaron secar al aire. Una vez secas se contaron las UFP formadas.

Durante la estancia realizada en el laboratorio de J. C. de la Torre (The Scripps Research Institute) se utilizó un método de titulación de VCML alternativo basado en la inmunodetección de antígenos virales (Véase apartado 4.18.3).

4.6 Purificación de partículas virales

4.6.1 Concentración de partículas de VEV

Se realizó de acuerdo a una modificación del protocolo previamente descrito por Hackett y col., 1967. Para ello, células BHK-21 crecidas en botellas de 175 cm^2 de superficie fueron infectadas en medio líquido con VEV a una m.d.i. de 70 UFP/célula. A las 7 h p.i. se recogió el sobrenadante de 4 botellas que fue sometido a un ciclo de congelación-descongelación, tras lo que se centrifugó a 2.200 × g durante 5 min a 4º C para eliminar restos celulares. A continuación, se realizó un segundo clarificado más intensivo a 6.000 × g durante 10 min a 4º C en un rotor SS34 y una centrifuga Sorvall RC-5 (Du Pont Instruments). Finalmente, las partículas virales se sedimentaron a 30.000 × g durante 90 min a 4º C, utilizando una ultracentrifuga Optima L-100 XP (Beckman Coulter) y el rotor AH627. El precipitado se resuspendió en 100 µl de TNE y fue almacenado a 4º C hasta su utilización.

4.6.2 Concentración de partículas de VCML

Se utilizó una modificación del protocolo previamente descrito por Rodrigo y col., 2011. Para ello, se emplearon células BHK-21 crecidas en botellas de 175 cm^2 de superficie que fueron infectadas en medio líquido con VCML a una m.d.i. de 1 UFP/célula. A las 24 h p.i. se recogió el sobrenadante de 4 botellas, que se centrifugó a 2.200 × g durante 10 min a 4º C para eliminar restos celulares. Seguidamente, se realizó

un segundo clarificado a 13.000 × g (30 min a 4º C) en un rotor SS34 y una centrifuga Sorvall RC-5. Finalmente, las partículas virales fueron centrifugadas a través de un colchón de 20% sacarosa en PBS (150.000 × g, durante 2.5 h 4º C), utilizando una ultracentrifuga Optima L-100 XP y el rotor TST.41. Las partículas virales fueron resuspendidas en 40 µl de PBS y almacenadas a 4º C hasta su utilización.

4.6.3 Marcaje radiactivo y purificación de partículas de VFA

Este protocolo se realizó en colaboración con V. Rincón y M. G. Mateu (CBMSO). Para el marcaje con ^{35}S, se infectaron en medio líquido (ver apartado 4.5.1) 4 botellas de 175 cm^2 (Nunc) de células BHK-21 con una m.d.i. > 1. A las 3 h p.i. se retiró el medio y se incubaron las células 1 h en DMEM sin Met ni Cys suplementado con 5% SFB. A continuación, se añadió 1,87 mCi de la mezcla radiactiva de L-(^{35}S) Met/Cys (Redivue Pro-mix, Amersham). La infección prosiguió hasta la aparición de efecto citopático completo y los sobrenadantes se recogieron y almacenaron a -70º C.

La purificación de los viriones se realizó empleando el método descrito por Díez y col., 1990. El sobrenadante de la infección fue centrifugado 10 min a 690 × g y, a continuación, 20 min a 9.700 × g en un rotor SS34 y una centrifuga Sorvall RC-5. Los viriones fueron parcialmente purificados mediante ultracentrifugación en un colchón de sacarosa al 20% en TNE durante 2,5 h en un rotor AH627 a 112.400 × g utilizando una ultracentrifuga Optima L-100 XP. El sedimento resultante fue resuspendido en TNE, cargado en un gradiente lineal de sacarosa (7,5 al 30%) en TNE y centrifugado durante 1 h a 242.800 × g en un rotor SW40. Se recogieron fracciones de 0,5 ml y la radiactividad incorporada a los viriones en cada fracción se determinó utilizando un contador de centelleo (1219 *Rackbeta*, Wallac). Las fracciones que contenían viriones (coeficiente de sedimentación 140S) fueron recuperadas y sometidas a diálisis extensiva frente a PBS (utilizando membranas de Dialysis Tubing-Visking, MWCO 12-14.000 Da, Medicell Internacional) para eliminar los restos de sacarosa. Los viriones marcados radiactivamente fueron almacenados a 4º C hasta su posterior uso (veáse apartado 4.9.1).

4.7 Ensayos de letalidad de VFA en ratón lactante

Para ensayar la virulencia *in vivo* del VFA C-S8c1 y de los mutantes c2 y m6 se emplearon ratones lactantes (cepa *Swiss*, Harlam) de 7 días de edad. Éstos animales

fueron inoculados intraperitonealmente con distintas dosis de virus (10^2, 10^3, 10^4 o 10^6 UFP/ratón) resuspendido en PBS en un volumen total de 100 µl. Cada grupo constaba de 10 ó 11 ratones. Como control de buena praxis se inoculó un grupo de ratones con PBS. Los animales muertos se contabilizaron hasta los 9 días tras la inoculación, tiempo al que se realizó la eutanasia de los ratones supervivientes. Estos experimentos se realizaron en un box de seguridad biológica de nivel 3 (BSL-3) del CISA-INIA, con la aprobación del Comité de Ética de Experimentación Animal del INIA (Número de permiso: CBS 2008/016).

4.8 Aislamiento de mutantes con resistencia a NH_4Cl procedentes de lesiones vesiculares de animales infectados con VFA

Los mutantes de VFA resistentes a NH_4Cl fueron seleccionados mediante clonaje biológico en presencia de 25 mM NH_4Cl (Martín-Acebes y col., 2010). Para ello, se infectaron células BHK-21 con diluciones seriadas de una población viral procedente de lesiones vesiculares de cerdos infectados con el aislado C-S8c1 de VFA (apartado 4.3). Tras la primera hora de infección, se retiró el inóculo viral y se añadió medio semisólido suplementado con 25 mM NH_4Cl y 25 mM HEPES pH 7,4. A las 30 h de infección se aislaron placas de lisis denominadas como (av1, av2, av3, av4, av5 y av6) que se reinocularon en medio líquido con NH_4Cl.

4.9 Determinación de la sensibilidad diferencial a pH ácido

4.9.1 Ensayo de disociación

La sensibilidad diferencial a pH ácido de los viriones de VFA recuperados a partir de los clones infecciosos pMT28 (C-S8c1) y pMT28-VP1 17D, se determinó mediante una modificación del método descrito por Knipe y col., 1997. Para ello, se mezcalron 100 µl de VFA marcado radiactivamente y purificado (apartado 4.6.3) con 300 µl de tampón salino fosfato (50 mM $NaPO_4$ y 140 mM NaCl) de distinto pH (desde 7,5 hasta 6,0). Tras una incubación de 30 min a temperatura ambiente (t.a.), el pH fue neutralizado añadiendo 100 µl de tampón Tris 1 M pH 7,6. Para determinar la integridad del virus tras el tratamiento con distintos pH, las muestras fueron cargadas en un gradiente lineal de sacarosa del 7,5 al 45% en tampón TNE, centrifugadas en el rotor SW40 a 41.500 × g durante 18 h y fraccionadas en alícuotas de 0,5 ml. Para cada tratamiento se obtuvo el perfil de radiactividad en función del coeficiente de

sedimentación, determinando la radiactividad presente en cada una de las fracciones mediante contaje de centelleo.

4.9.2 Ensayo de inactivación

La sensibilidad a la inactivación por pH ácido de los viriones de VFA se determinó tratando 2-4 × 10^6 UFP de cada virus (en 10 µl) con 300 µl de tampón salino fosfato de distintos pH, tal y como se indica en el apartado anterior. El pH de las muestras fue neutralizado añadiendo 100 µl de tampón Tris 1 M pH 7,6. A continuación, las muestras fueron inoculadas en monocapas de células BHK-21. Transcurridas 24 h de infección en medio semisólido se determinó el número de UFP desarrolladas.

4.10 Experimentos de competición viral

La misma cantidad de UFP de los virus recuperados a partir de los clones infecciosos pMT28 (C-S8c1) y pMT28-VP3 116V se mezclaron para infectar células BHK-21 [m.d.i. inicial de 1 UFP/célula (0,05 para cada virus)] crecidas en placas de 35 mm de diámetro tratadas o no con 25 mM NH_4Cl (ver apartado 4.16). Tras la primera hora de infección se retiró el inóculo y se añadió medio nuevo conteniendo o no 25 mM NH_4Cl. Cuando se observó efecto citopático completo se recogieron los virus. Posteriormente, las células BHK-21, tratadas o no con 25 mM NH_4Cl, fueron infectadas con 200 µl de la suspensión viral recuperada previamente y se procedió de la misma manera. El ciclo infección y recolección de los virus se repitió hasta 10 veces por triplicado en presencia o ausencia de NH_4Cl. Finalmente se extrajo el RNA viral (apartado 4.21.1) de los virus recuperados de diferentes pases, y el cDNA que codifica para la proteína VP3 fue sintetizado y secuenciado (apartado 4.22). La proporción de los genomas que competían fue estimada a partir de los cromatogramas como la relación del área integrada correspondiente a cada nucleótido en la posición de la mutación puntual (C2897T) (Mateo y col., 2007b).

4.11 Plásmidos

Los plásmidos utilizados durante esta Tesis Doctoral, excepto los correspondientes a los clones infecciosos (ver apartado 4.4), se enumeran en la Tabla III.

Tabla III. Plásmidos utilizados

Nombre	Proteína expresada	Referencia
PH-PLC-eGFP[1]	Dominio PH de la proteína fosfolipasa C fusionado a GFP	(Arendt y col., 2010)
PM-FRB-CFP[2]	Dominio FRB de la proteína mTOR fusionado a CFP	(Varnai y col., 2006)
mRFP-FKBP-dom5ptasa[2]	Dominio FKBP fusionado con el dominio catalítico de la proteína 5 fosfatasa y RFP	(Varnai y col., 2006)
eGFP	Proteína verde fluorescente mejorada	Clontech
Dinamina DN[3]	Dominante negativo de dinamina	(Damke y col., 1994)
Rab5 WT[1]	Forma nativa de Rab5	(Gerges y col., 2005)
Rab5 DN[1]	Dominante negativo de Rab5	(Gerges y col., 2005)
Rab7 WT[1]	Forma nativa de Rab7	(Gerges y col., 2005)
Rab7 DN[1]	Dominante negativo de Rab7	(Gerges y col., 2005)
Rab11 WT[1]	Forma nativa de Rab11	(Gerges y col., 2005)
Rab11 DN[1]	Dominante negativo de Rab11	(Gerges y col., 2005)
Pol I MG-CAT[4]	Cloroanfenicol acetiltransferasa	(Lee y col., 2000)
pCAGGS-NP[4]	Nucleoproteína de VCML	(Lee y col., 2000)
pCAGGS-L[4]	Polimerasa de VCML	(Lee y col., 2000)
Z-Flag[4]	Proteína Z de VCML fusionada a FLAG	(Urata y col., 2012)

[1] Cedido por J. A. Esteban (CBMSO).

[2] Cedido por T. Balla (*National Institute of Health*, Bethesda, Maryland).

[3] Cedido por M. A. Alonso (CBMSO).

[4] Cedido por J. C. de la Torre (*The Scripps Research Institute*, La Jolla, California).

4.12 Transfección de células eucariotas

4.12.1 Transfección de DNA con Lipofectamina

Se emplearon monocapas subconfluentes de células que fueron transfectadas con el plásmido de interés, utilizando Lipofectamina Plus o Lipofectamina 2000 (Invitrogen) y siguiendo las instrucciones del fabricante.

4.12.2 Electroporación de DNA

Las células BHK-21 crecidas en placas de 100 mm de diámetro se lavaron con PBS (4º C), se despegaron de las placas y se resuspendieron en DMEM completo suplementado con 5% SFB. A continuación, se centrifugaron a 250 × g durante 5 min y se resuspendieron de nuevo en DMEM completo suplementado con 5% SFB. Las células (1-10 × 10^5) resuspendidas en 100 µl de medio, se colocaron en cubetas de electroporación de 0,2 cm (Bio Rad) en presencia de 20 µg del plásmido de interés y se les aplicó un pulso de 25 ms a 140 V y 25 µF, usando para ello el electroporador Gene Pulser XCell™ (Bio Rad). Una vez transfectadas las células se dispusieron sobre cubreobjetos (Menzel-Glässer, Thermo Scientific) colocados en placas de 24 pocillos.

4.12.3 Transfección con Lipofectina de RNA viral

Las monocapas subconfluentes de células BHK-21 (70% de confluencia), crecidas en placas de cultivo de tejido de 35 mm de diámetro, fueron transfectadas con 1 µg de RNA utilizando Lipofectina (Invitrogen) de acuerdo con las instrucciones del fabricante. El virus recuperado [48 h post-transfección (p.t.)] fue amplificado mediante un pase en células BHK-21. La identidad de la región P1 del virus recuperado de las transfecciones fue comprobada mediante extracción del RNA y secuenciación del mismo. Para más detalle véase apartado 4.21.

4.13 Disminución inducible de los niveles de $PI(4,5)P_2$ de la membrana plasmática

Este método está basado en la propiedad de la rapamicina de inducir la heterodimerización del dominio de unión a rapamicina de mTOR (FRB) y FKBP12 en mamíferos. El plásmido PM-FRB-CFP codifica el dominio FRB de mTOR de mamíferos fusionado con la proteína fluorescente cian (CFP), el cual, una vez expresado, se localiza en la membrana plasmática. Por otra parte, el plásmido mRFP-FKBP-dom5ptasa codifica el dominio FKBP12 de mamíferos fusionado con el dominio catalítico de la proteína de tipo IV 5-fosfatasa y la proteína fluorescente monomérica roja (mRFP), el cual una vez expresado, se localiza en el citoplasma (Varnai y col., 2006).

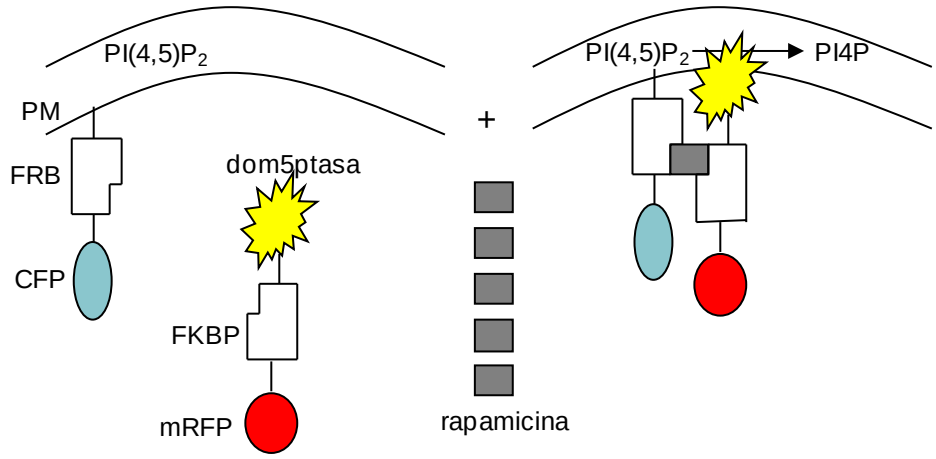

Figura 10. Esquema de funcionamiento del sistema inducible para disminuir los nivels de $PI(4,5)P_2$ de la membrana plasmática. La heterodimerización del fragmento FRB con FKBP después de añadir rapamicina provoca el reclutamiento del dominio catalítico de la enzima 5-fosfatasa de tipo IV a la membrana plasmática, con la consecuente desfosforilación del $PI(4,5)P_2$.

Para disminuir los niveles de $PI(4,5)P_2$ de la membrana plasmática se cotransfectaron ambos plásmidos en células BHK-21. A las 24 h p.t. las células se

incubaron durante 10 min con 10 nM rapamicina para producir el reclutamiento del dominio catalítico de la 5-fosfatasa a la membrana plasmática, dando como resultado la conversión de PI(4,5)P_2 a PI4P (Fig. 10), de acuerdo a lo descrito (Varnai y col., 2006).

4.14 Ensayo con un minigenoma de VCML

Este ensayo consiste en un sistema de genética reversa que permite el análisis de señales o factores actuando en *cis* o *trans* involucrados en la transcripción y replicación de VCML (Lee y col., 2000). La coexpresión del minigenoma (MG) del segmento S de VCML con las proteínas L y NP del virus permite la síntesis de RNA mediada por L (Fig. 11). Para ello, se emplearon células BHK-21 crecidas en placas de 12 pocillos (3×10^5 células/pocillo) que fueron cotransfectadas con 0,2 µg de pCAGGS-NP, 0,3 µg de pCAGGS-L y 0,25 µg de pol I MG-CAT usando Lipofectamina 2000 (apartado 4.12.1).

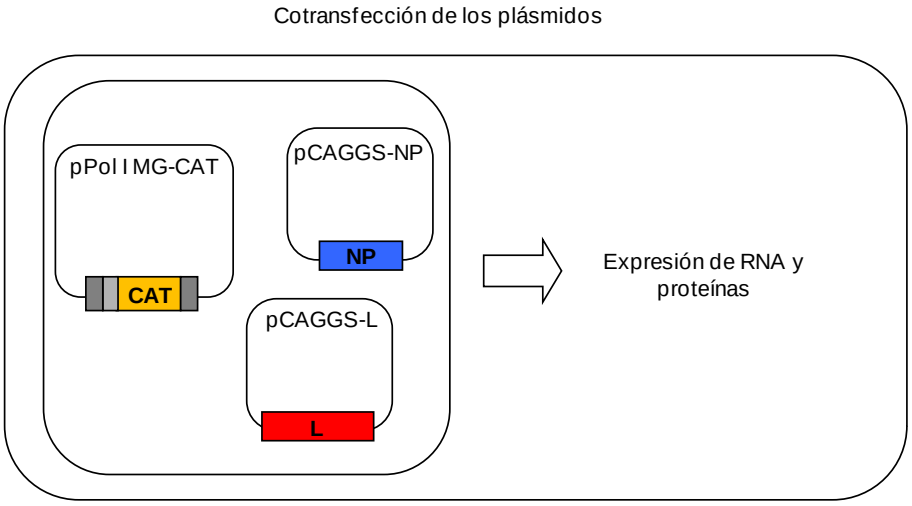

Figura 11. Diagrama esquemático del funcionamiento del MG de VCML. El minigenoma del segmento S de VCML consiste en un plásmido que codifica para el gen reportero CAT flanqueado en la zona 5' por la región UTR de la misma orientación del segmento S y la región IGR y en la zona 3' por la región UTR de la misma orientación del segmento S, denominándose como Pol I MG-CAT. La coexpresión intracelular del MG con las proteínas L (pCAGGS-L) y NP (pCAGGS-NP) del VCML permite la síntesis de RNA del gen CAT mediada por la polimerasa viral (L).

A las 5 h p.t. el medio fue reemplazado por otro conteniendo 2% SFB y distintas concentraciones de AVP (0, 2, 5 o 10 mM). A las 48 p.t. se prepararon lisados celulares utilizando el tampón de lisis del kit comercial CAT ELISA (Roche). Para cargar la misma concentración de proteínas, ésta fue determinada previamente para cada muestra mediante el método de Bradford (Bradford, 1976). Finalmente, se determinaron los niveles de proteína CAT por medio del kit comercial CAT ELISA. Los resultados obtenidos fueron normalizados con respecto al control negativo, que consistió en células

transfectadas con pCAGGS-NP y pol I MG-CAT en ausencia del plásmido que expresa la polimerasa L.

4.15 Ensayo de gemación (*budding*) mediado por la proteína Z de VCML

En este ensayo se emplearon células 293T (5×10^5 células) que fueron transfectadas utilizando Lipofectamina 2000 y 0,1 μg de Z-Flag (Ortiz-Riano y col., 2011) al mismo tiempo que se sembraban en un pocillo de placas de 24 pocillos. A las 16 h p.t. se retiró el medio, las células se lavaron dos veces con PBS y se les añadió medio nuevo conteniendo 2% SFB y distintas concentraciones de AVP (0, 2, 5 y 10 mM). Transcurridas 24 h se recuperó el medio de cultivo para recolectar las partículas de virus vacías (VLPs) producidas. Primero se eliminaron los restos celulares por medio de una centrifugación (1.500 × g, 5 min a 4º C) y después se sedimentarion las VLPs por ultracentrifugación (100.000 × g, 30 min a 4º C) a través de un colchón de 20% sacarosa en PBS (Pérez y col., 2003). Las células recuperadas fueron resuspendidas en tampón de lisis (1% NP-40, 50 mM Tris-HCl [pH 8,0], 62,5 mM EDTA, 0,4% deoxicolato de sodio), mientras que las VLP fueron resuspendidas en PBS. Las muestras fueron analizadas mediante *Western blot* (ver apartado 4.18.4.1).

4.16 Tratamientos farmacológicos

Las monocapas celulares fueron lavadas dos veces con DMEM y tratadas con el mismo medio sin suero con los diferentes fármacos indicados en la Tabla IV.

Las células se preincubaron 16 h con tricostatina A (TSA) (Disolvente: DMSO, concentración de uso: 400 nM); 1 h con monensina (DMSO, 10 μM) y nigericina (DMSO, 10 μM); 30 min con ionomicina (DMSO, 5 μM), 10 min con ácido valproico (AVP) (DMEM, 0,01-400 mM); 5 min con 1-butanol (DMEM, 1.5%) o 2-butanol (DMEM, 1,5%); en todos los casos el fármaco se mantuvo durante todo el período de infección. Para el tratamiento con NH_4Cl (H_2O, 25 mM) las células fueron preincubadas 1 h con el medio conteniendo NH_4Cl y suplementado con 25 mM HEPES pH 7,4, manteniendo el fármaco durante toda la infección.

Las concentraciones de los fármacos empleadas no tuvieron efectos significativos sobre la viabilidad celular [estimada mediante tinción vital con azul Tripán (Sigma) y observación de las células en campo claro]. En todos los casos, las células control se trataron de la misma manera, utilizando el mismo volumen del disolvente empleado con cada fármaco.

Tabla IV. Relación de fármacos utilizados

Compuesto	Efecto	Referencia	Compañía
Ionomicina	Retira $PI(4,5)P_2$ de la membrana plasmática por activación de la fosfolipasa C	(Zoncu y col., 2007)	Sigma
1-butanol	Inhibe la síntesis de $PI(4,5)P_2$ debido a la formación de fosfatidilalcoholes	(Boucrot y col., 2006)	Merck
2-butanol	Utilizado como control negativo del 1-butanol porque no induce la formación de fosfatidilalcoholes	(Boucrot y col., 2006)	Merck
AVP	Cambios en el metabolismo de lípidos de membrana, inhibición HDAC, entre otros	(Shaltiel y col., 2004; Tokuoka y col., 2008; Venkataramani y col., 2010; Wittenburg y col., 2010; Xu y col., 2007)	Sigma
NH_4Cl	Neutraliza el pH ácido dentro de endosomas/lisosomas	(Ohkuma y col., 1978)	Merck
Monensina + nigericina	Neutraliza el pH ácido dentro de endosomas/lisosomas	(Pelkmans y col., 2001)	Sigma

4.17 Evaluación del efecto de los tratamientos farmacológicos

4.17.1 Efecto de los fármacos sobre el $PI(4,5)P_2$ de la membrana plasmática

El dominio PH es el dominio de unión a los fosfoinositoles más caracterizado (Gao y col., 2009). La proteína fosfolipasa C (PLC) tiene un dominio PH por el cual se une al $PI(4,5)P_2$ de la membrana plasmática para hidrolizar éste en diacilglicerol (DAG) e inositol trifosfato (I3P). Para detectar el $PI(4,5)P_2$ de la membrana plasmática se transfectaron células BHK-21 con 1 µg de un plásmido que expresa el dominio PH de la PLC acoplado a la proteína fluorescente verde (GFP) (Adjobo-Hermans y col., 2008).

Para evaluar el efecto de la ionomicina, el 1-butanol y el 2-butanol sobre el $PI(4,5)P_2$, se transfectaron células BHK-21 con el plásmido PH-PLC-GFP, tal y como se ha descrito previamente. A las 24 h p.t. las células fueron tratadas con estos fármacos (ver apartado 4.16). Tras dos lavados con PBS, las células se fijaron en 4% paraformaldehído en PBS. La fluorescencia debida a aldehídos libres fue eliminada mediante la incubación con 1 M glicina en PBS durante 15 min a t.a. A continuación, las preparaciones fueron observadas con un microscopio de fluorescencia confocal (apartado 4.19.2) y las imágenes se tomaron utilizando las mismas condiciones de adquisición para las células control y las tratadas con los inhibidores farmacológicos.

4.17.2 Evaluación del efecto de los fármacos sobre la internalización de transferrina

Para evaluar el efecto de la ionomicina, el 1-butanol y el 2-butanol, se empleó un trazador de la ruta de endocitosis mediada por clatrina: la transferrina (TF) (Rodal y

col., 1999). Para ello, células crecidas sobre cubreobjetos, tratadas con los fármacos mencionadas anteriormente, fueron incubadas 5 min a 37º C con 10 μg/ml de TF acoplada a Alexa Fluor (AF) 488 (Molecular Probes, Invitrogen) en DMEM con 0,5% albúmina de suero bovino (BSA) y manteniendo la concentración del inhibidor. A continuación, las células se lavaron dos veces con 0,2 M ácido acético y 0,2 M NaCl y posteriormente con 150 mM $CaCl_2$ para eliminar la TF extracelular (Lukacs y col., 1997; Martín-Acebes y col., 2007). Tras dos lavados con PBS, las células se fijaron en 4% paraformaldehído en PBS. La fluorescencia debida a aldehídos libres fue eliminada mediante la incubación con 1 M glicina en PBS (ver apartado 4.17.1). Las imágenes se tomaron en las mismas condiciones para las células control y las tratadas con los inhibidores farmacológicos.

4.17.3 Evaluación del efecto de los fármacos sobre la internalización de viriones.

Para evaluar el efecto de la ionomicina, el 1-butanol y el 2-butanol sobre la internalización de viriones, se emplearon células crecidas sobre cubreobjetos que fueron lavadas dos veces con DMEM. Tras el tratamiento con los distintas fármacos, las células fueron infectadas tal y como se describe en el apartado 4.5.1.

4.17.4 Evaluación del efecto de los fármacos sobre la producción viral

Para analizar el efecto del fármaco sobre la producción viral, tras la primera hora de infección (adsorción) el inóculo viral fue retirado y se añadió DMEM con SFB 5% manteniendo el fármaco. Cuando los fármacos se aplicaron p.i., para determinar sus posibles efectos sobre la replicación viral, estos se añadieron 2,5 h p.i. y se mantuvieron hasta el final de la infección.

4.18 Inmunodetecciones

4.18.1 Anticuerpos

La relación de anticuerpos primarios empleados frente a los diferentes virus y proteínas celulares se muestra en la Tabla V.

Los anticuerpos secundarios anti-Ig de ratón o de conejo acoplados a AF 488, 555, 568 o 647 empleados en las inmunofluorescencias fueron adquiridos en Molecular Probes (Invitrogen). Los anticuerpos secundarios anti-Ig de ratón o conejo acoplados a peroxidasa empleados en los ensayos de *Western blot*, se adquirieron en GE Healthcare.

El anticuerpo secundario anti-Ig de cobaya acoplado a peroxidasa empleado en el *dot blot*, se adquirió en Sigma.

Tabla V. Relación de anticuerpos primarios utilizados

Anticuerpo	Antígeno	Tipo[a]	Origen
5C4 (VFA)[1]	Sitio D VFA	AcM	(Lea y col., 1994b)
SD6	Sitio A VFA	AcM	(Mateu y col., 1990)
163	3A VFA	AcP	(Rosas y col., 2008)
I1[2]	Glicoproteína del VEV	AcM	(Lefrancois y col., 1982)
3.67G	Glicoproteína E de VNO	AcM	Millipore
1.1.3[3]	Nucleoproteína del VCML	AcM	(Sullivan y col., 2011)
Suero hiperinmune[4]	VEV Indiana	AcP	
196	Tubulina βII	AcP	(Armas-Portela y col., 1999)
AC-15	Actina β	AcM	Sigma
I-19	Actina	AcP	Santa Cruz
25H8[5]	Gp74 (*cis*-Golgi)	AcM	(Alcalde y col., 1994)
1D3	Proteína disulfuro isomerasa (PDI)	AcM	Stressgene
Anti-acetil-histona H3	Histona H3 acetilada	AcP	Upstate
Anti-caveolina	Caveolina 1	AcM	BD Transduction Laboratorios
Anti-Flag	Flag	AcP	Cayman

[a] AcM: anticuerpo monoclonal. AcP: anticuerpo policlonal.
[1] Cedido por E. Brocchi (*IZSLER*, Italia).
[2] Cedido por M. Dávila y E. Domingo (CBMSO).
[3] Cedido por J. C. de la Torre (*The Scripps Research Institute*, California).
[4] Suero hiperinmune de cobaya cedido por Esther Blanco (CISA-INIA).
[5] Cedido por I. V. Sandoval (CBMSO).

4.18.2 Inmunofluorescencia indirecta

Las células crecidas sobre cubreobjetos de vidrio fueron lavadas con PBS y fijadas en 4% paraformaldehído en PBS durante 15 min a t.a. En el caso de la tinción de *cis*-Golgi, las células se fijaron con metanol frío (-20º C) durante 10 min. Después de tres lavados con PBS las células fueron bloqueadas y permeabilizadas con PBTG (PBS conteniendo 1% BSA; 0,1% Tritón-X 100 y 1 M glicina) 15 min. Después se incubaron con los anticuerpos primarios correspondientes diluídos en 1% BSA en PBS durante 1 h en cámara húmeda a t.a. Tras tres lavados con PBS, se incubaron con los anticuerpos secundarios adecuados diluidos en 1% BSA en PBS durante 30 min en las condiciones anteriores. Cuando se realizaron tinciones de los filamentos de actina, se utilizó faloidina acoplada a AF 488 (Molecular Probes, Invitrogen), que fue incubada junto con los anticuerpos secundarios. Tras tres lavados con PBS los núcleos fueron teñidos durante 5 min mediante incubación con 1 μg/ml de DAPI (4'-6 diamidina-fenilindol) para microscopia de fluorescencia convencional, o con TO-PRO-3 (Invitrogen), para microscopia de fluorescencia confocal. Finalmente, los cubreobjetos se lavaron tres veces con PBS y se montaron sobre portaobjetos de vidrio (Menzel-Glässer, Termo

Scientific) utilizando Fluoromont G (Southern Biotechnology Assoc., Inc.) como medio de montaje. Las preparaciones se guardaron en oscuridad a 4º C hasta ser observadas al microscopio.

4.18.3 Titulación de VCML mediante inmunodetección

Alternativamente a la titulación viral descrita en el apartado 4.5.2, para el caso del VCML también se realizó una titulación por medio de inmunodetección, determinándose las unidades formadoras de foco/ml (UFF/ml) presentes en las muestras. Para ello, se utilizaron diluciones seriadas del virus para infectar en medio líquido monocapas de células Vero crecidas en placas de 96 pocillos. A las 20 h p.i., las células fueron fijadas usando 4% paraformaldehído en PBS, permeabilizadas y bloqueadas por tratamiento con 0,3% Triton X-100, 3% BSA en PBS. Para la detección de las UFF se empleó como anticuerpo primario el AcM 1.1.3 (anti NP) y como anticuerpo secundario un anti-ratón marcado con AF 568 (Molecular Probes). El número de UFF se determinó por observación con un microscopio de fluorescencia convencional. En el caso del virus r3-VCML-GFP se procedió de la misma manera, contabilizando tras la fijación el número de focos que expresaban GFP.

4.18.4 Transferencia e inmunodetección de proteínas

4.18.4.1 *Western blot*

Las células fueron lisadas en hielo con tampón de lisis NP-40 (20 mM HEPES pH 7,4, 10 mM EGTA, 2,5 mM $MgCl_2$, 1% NP-40), suplementado con 1 mM fenilmetilsulfonifluoruro (PMSF) y con un cocktail inhibidor de proteasas (Roche). Las células fueron posteriormente fueron recogidas con un barredor, sonicadas 3 min y mezcladas con tampón de carga de Laemmli (Laemmli, 1970). En el ensayo de *budding* mediado por la proteína Z (apartado 4.15) las células fueron lisadas en un tampón compuesto de 50 mM Tris-HCl (pH 8,0), 62,5 mM EDTA, 0,4% deoxicolato de sodio y 1% NP-40. Para cargar la misma concentración de proteínas, ésta fue determinada previamente para cada muestra mediante el método de Bradford (Bradford, 1976). Las proteínas se separaron electroforéticamente en condiciones desnaturalizantes en presencia de dodecil sulfato sódico (SDS). Para este fin, se utilizaron geles discontinuos de poliacrilamida compuestos por un gel concentrador con 5% poliacrilamida (BioRad), seguido por un gel separador con 10% o 16% poliacrilamida. Posteriormente, las proteínas fueron transferidas a una membrana de nitrocelulosa (Protran, Whatman) o de

polivinildifluorido (PVDF) (Protran, Whatman) previamente incubada con metanol. La membrana de nitrocelulosa se bloqueó con 3% leche desnatada (Sveltesse) en PBS durante 45 min. A continuación, la membrana se lavó con PBS-Tween (0,5% Tween 20 en PBS) (3 veces, 5 min) y se incubó con el anticuerpo primario diluido en 1% BSA en PBS durante la noche a 4º C. Tras tres lavados de 10 min con PBS-Tween la membrana se incubó con los anticuerpos secundarios apropiados acoplados a peroxidasa durante 1 h. Finalmente la membrana fue lavada de nuevo tres veces con PBS-Tween (10 min) y revelada utilizando un kit de detección quimioluminiscente (Perkin Elmer) en una película de autorradiografía (Agfa) o utilizando el equipo Image Quant LAS 4000 (GE Healthcare). En el caso de la membrana de PVDF se procedió igual a lo previamente descrito pero utilizando TBS en lugar de PBS.

4.18.4.2 *Dot blot*

Para detectar las proteínas de VEV mediante *dot blot* se crecieron células BHK-21 en botellas de 175 cm^2 de superficie, tratadas o no con 50 mM AVP, que fueron infectadas en medio líquido con una m.d.i. de 70 UFP/célula. A 0 y 7 h p.i. se recogió sobrenadante y el virus se inactivó por incubación a 70º C durante 30 min. Las muestras fueron cargadas en una membrana de nitrocelulosa, que posteriormente fue bloqueada con 3% leche desnatada en PBS durante 45 min y lavada 3 veces con PBS-Tween (0,5% Tween 20 en PBS) durante 5 min. La membrana se incubó con un suero hiperinmune de cobaya frente a VEV Indiana diluído en 1% BSA en PBS durante toda la noche a 4º C. Por último, la membrana se lavó con PBS-Tween, se incubó con un anticuerpo secundario acoplado a peroxidasa, revelándose como se ha descrito en el apartado anterior.

4.19 Microscopía óptica

4.19.1 Microscopía de fluorescencia convencional

Para la observación de las muestras se empleó un microscopio de epifluorescencia BX61 (Olympus)-objetivos 60×/AN 1.25, 100×/AN 1.3- equipado con los filtros de excitación adecuados y una cámara digital DP70 (Olympus). Para la adquisición de imágenes se utilizó el software DPController 1.1.1.65 (Olympus). Alternativamente, se empleó un microscopio Axioskop (Zeiss) equipado con un objetivo Plan-Neofluar 63× (AN 1.25) acoplado a una cámara digital Coolsnap FX

monocroma (Roper Scientific), utilizando el programa RS Image 1.9.2 (Roper Scientific). En ambos casos las imágenes fueron procesadas con Adobe Photoshop 7.0 (Adobe Systems Inc.).

4.19.2 Microscopía de fluorescencia confocal

Para la observación de las muestras con esta técnica se utilizó un microscopio de barrido láser confocal LSM510 o, alternativamente, un microscopio LSM510 META acoplado a un microscopio invertido Axiovert200 (Zeiss) (objetivo Plan-Apochromat 63×/AN 1.4). Las imágenes fueron adquiridas con el software Zeiss LSM510 4.4 Sp2 (Zeiss) y procesadas utilizando los programas LSM Image Browser 4.2.0.121 (Zeiss) y Adobe Photoshop 7.0 (Adobe Systems Inc.).

4.20 Microscopía electrónica de transmisión

4.20.1 Microscopía electrónica en células infectadas

Las células BHK-21 crecidas en placas de cultivo de tejidos de 100 mm de diámetro fueron procesadas siguiendo el protocolo convencional de inclusión en resina epoxi (Renau, 1998). Una vez transcurrido el periodo de infección deseado, las células fueron lavadas tres veces (5 min) con tampón Sörensen y fijadas durante 1 h a t.a. en 4% paraformaldehído y 2% glutaraldehído en tampón Sörensen. Tras tres lavados con el mismo tampón, las células fueron raspadas de la placa y postfijadas con 1% tetróxido de osmio y 1% ferrocianuro potásico a 4º C durante 1 h. A continuación se lavaron tres veces con agua bidestilada y se trataron con 0,15% ácido tánico en tampón fosfato 0,1 M pH 7,4 durante 1 min. Las células fueron lavadas con el mismo tampón y con agua bidestilada, y teñidas con 2% acetato de uranilo durante 1 h a t.a. Después de tres lavados con agua bidestilada, las muestras fueron deshidratadas en una serie creciente de disoluciones de etanol (50%, 75%, 90%, 95%, y tres veces en etanol al 100% durante 5-10 min cada una) e incluídas en la resina epoxi TAAB 812 (TAAB *Laboratories*). Para ello, primero se infiltraron en una mezcla de resina:etanol 1:2 (1 h a t.a.), después 1:1 (1 h a t.a.), y a continuación en resina 100% (toda la noche a 4º C), seguido de un nuevo cambio de resina 100% (2 h). Las muestras fueron encapsuladas y polimerizadas durante 48 h a 60º C. Los cortes transparentes a los electrones (70-80 nm de grosor) fueron realizados con un microtomo Ultracut E (Leica) y montados en rejillas de cobre perforadas recubiertas de colodión y sombreados con carbono (G200, Gilder). Para la observación de las muestras se utilizó un microscopio electrónico de transmisión Jeol

JEM-1010 (Jeol) operado a un voltaje de aceleración de 80 kV y equipado con una cámara digital Bioscan 792 (Gatan). Para la adquisición de imágenes se empleó el programa DigitalMicrograph (Gatan). Alternativamente se utilizó el mismo microscopio en las mismas condiciones equipado con una cámara digital TemCam-F416 (TVIPS). En este caso, para la adquisición de las imágenes se empleó el programa EM-MENU4 (TVIPS). Las imágenes fueron procesadas utilizando los programas ImageJ (http://rsbweb.nih.gov/ij/) y Adobe Photoshop 7.0.

4.20.2 Tinción negativa de partículas virales

La tinción negativa de las partículas de VEV o VCML se realizó de acuerdo a lo descrito (García-Arriaza y col., 2004). Para ello, una gota de la muestra fijada con 2% glutaraldehído durante 30 min fue adsorbida a la cara ionizada de una rejilla durante 3 min. A continuación la muestra se tiñó con 2% acetato de uranilo durante 50 s. Por último la muestra fue secada al aire y observada al microscopio electrónico.

4.20.3 Cuantificación de partículas de VCML por microscopía electrónica

La determinación de la concentración de las partículas de VCML presentes en poblaciones virales purificadas (apartado 4.6.2) se realizó mediante microscopía electrónica cuantitativa utilizando esferas de látex de una concentración conocida (Agar Scientific Ltd, $1{,}05 \times 10^2$ esferas de látex/ml) y 120 nm de diámetro, las cuales pueden distinguirse fácilmente de las partículas virales al microscopio electrónico. De esta manera, poblaciones virales purificadas se mezclaron con una cantidad conocida de esferas de látex, procesándose las preparaciones mediante el método de tinción negativa descrito en el apartado anterior.

Puesto que la concentración de esferas de látex es conocida ($1{,}05 \times 10^2$ esferas de látex/ml), este método permite calcular el número de partículas virales presente en la suspensión viral original. Este proceso se realizó a partir de dos purificaciones independientes de VCML.

4.21 Extracción de RNA vírico

4.21.1 Extracción de RNA vírico procedente de células infectadas

El RNA de VFA y VEV fue extraído a partir de 100 µl de sobrenadante de cultivo infectado utilizando TRI Reagent (Sigma) de acuerdo a las instrucciones del

fabricante. El RNA se resuspendió en 15 µl de H_2O tratada con dietilpirocarbonato (DEPC) y fue almacenado a -70º C hasta su utilización.

El RNA del VNO fue extraído utilizando el kit comercial NucleoSpin viral RNA isolation (Macherey-Nagel) siguiendo las instrucciones del fabricante.

En el caso del RNA de VCML, éste fue extraído directamente de las monocapas de células infectadas. Para ello, tras retirar el medio de cultivo, las monocapas de células BHK-21 crecidas en placas de 24 pocillos e infectadas en las condiciones deseadas se lavaron dos veces con PBS, y se añadió 500 µl de TRI Reagent por pocillo (Molecular Research Center, Inc.), continuando la extracción de acuerdo a las instrucciones del fabricante. El RNA recuperado fue resuspendido en 20 µl de formazol (Sigma), calentado durante 5 min a 65º C para disolverlo correctamente y almacenado a -70º C hasta su utilización.

4.21.2 Extracción de RNA vírico procedente de ratones lactantes infectados

El RNA de VFA procedente de ratón lactante infectado fue extraído a partir de 200 µl de macerado tisular (tejido cerebral y muscular de las extremidades posteriores) resuspendido en PBS utilizando 1000 µl de TRI Reagent y siguiendo las indicaciones del fabricante.

4.22 Amplificación y secuenciación de ácidos nucleicos

4.22.1 Obtención de cDNA y su amplificación por RT-PCR

El DNA complementario al molde de RNA (cDNA) fue sintetizado utilizando la transcriptasa inversa MuLV (Roche) del virus de la leucemia de Moloney de ratón. El cDNA fue amplificado mediante PCR utilizando la DNA polimerasa BioTaq (Bioline) en combinación con un 20% de la polimerasa pfu (Biotools), que presenta actividad correctora de errores. Para la amplificación completa de la región P1 del genoma de VFA se realizaron dos reacciones de PCR solapantes, utilizando como molde el cDNA sintetizado. En la primera se emplearon los cebadores 991s y 2310a. En la segunda reacción se emplearon los cebadores SB5 y 3946a. En la Tabla VI se indican los cebadores utilizados, la posición y la secuencia nucleotídica de éstos. El tamaño y pureza de los fragmentos de DNA amplificados se determinó por electroforesis en gel de agarosa (1%) (Pronadisa, Laboratorios Conda) en tampón TAE (Tris-acetato sódico-EDTA) y tinción con bromuro de etidio.

Tabla VI. Oligonucleótidos cebadores utilizados para la amplificación del RNA que codifica la cápsida del VFA.

Región[a]	Cebador	Orientación[b]	Posición[c]	Secuencia
5' UTR VFA	961s	s	961	AAGCGCTCGGTTTAAAAAGC
VP4 VFA	SB5	s	1804	ACCTCTACACACACAACCAACACC
VP2 VFA	2310a	a	2310	GTACTTTTCCCTGTCACTGATGTC
VP3 VFA	VP3-HSF	s	2895	CGCGAAAGCTCGGTACATGGTGGCG
VP3 VFA	VP3-HSR	a	3200	CTAGCGTCCACAGGTAGCCGGAGC
2B VFA	3946a	a	3946	GCATCTGGTTAATTGTCTCCACC

[a] Región genómica de VFA a la que corresponde el oligonucleótido.
[b] Orientación del oligonucleótido iniciador: s significa sentido (de la misma polaridad que el RNA genómico de VFA); a significa antisentido (de la polaridad complementaria al RNA genómico de VFA).
[c] Posición en el genoma de VFA de acuerdo a lo descrito (Toja y col., 1999) del nucleótido en el extremo 5' del oligonucleótido (acceso GenBank: AJ133357).

4.22.2 Purificación y cuantificación de productos de PCR

El exceso de cebadores en las muestras amplificadas como se describe en el apartado anterior fue eliminado utilizando el kit comercial Wizard® SV Gel and PCR Clean-Up System (Promega), siguiendo las instrucciones del fabricante. La cuantificación de DNA se realizó mediante espectrofotometría UV utilizando un espectrofotómetro Nanodrop ND-1000 (Nanodrop).

4.22.3 Secuenciación de DNA

El DNA amplificado fue secuenciado en la Unidad de Genómica de Parque Científico de Madrid, utilizando un secuenciador multicapilar ABI Prism 3100, 3700 o 3730 (Aplied Biosystems). Para ello se emplearon los cebadores adecuados (Tabla VI) y el kit Big De Terminador Cycle Sequencing (Abi Prism, Perkin Elmer). Las secuencias fueron determinadas a partir de al menos dos reacciones de secuenciación independientes.

4.23 Detección de RNA de VEV

Para la detección de RNA viral de VEV se realizó una modificación de la RT-PCR previamente descrita por (Nuñez y col., 1998). Las muestras de RNA viral total (intracelular y extracelular) fueron diluidas de forma seriada en agua tratada con DEPC para realizar una RT-PCR semicuantitativa. El cDNA fue sintetizado y amplificado por RT-PCR tal y como se describe en el apartado 4.22.1. El RNA mensajero de la deshidrogenasa gliceraldehído-3-fosfato (G3PDH) se empleó como control interno del contenido de RNA celular. Los productos de PCR fueron analizados mediante

electroforesis de las muestras en un gel de agarosa (2%) y tinción con bromuro de etidio. En la Tabla VII se indican los cebadores utilizados, la posición y la secuencia nucleotídica de éstos.

Tabla VII. Oligonucleótidos cebadores utilizados para la detección de RNA de VEV.

Región[a]	Cebador	Orientación[b]	Posición	Secuencia
L VEV	IS	s	6211[c]	GGTGTTGCAGACTATGTTGGAC
L VEV	IA	a	6550[c]	GGTGGTTATTCCATTTTTCG
G3PDH[d]	aei 021	s	-	AAGTTGTCATGGATGACCTTGGCCA
G3PDH[d]	aei 025	a	-	CATCACCATCTTCCAGGAGCGAG

[a] Región genómica de VEV a la que corresponde el oligonucleótido.
[b] Orientación del oligonucleótido iniciador: s significa sentido (de la misma polaridad que el RNA genómico de VEV); a significa antisentido (de la polaridad complementaria al RNA genómico de VEV).
[c] Posición en el genoma de VEV de acuerdo a lo descrito (Novella y col., 2010) del nucleótido en el extremo 5' del oligonucleótido (acceso GenBank: EU849003).
[d] Oligonucleótidos utilizados para amplificar el RNA mensajero de G3PDH.

4.24 Detección de RNA de VNO

Este protocolo se realizó en colaboración con M. A. Martín y J. C. Saiz (INIA). El RNA de VNO se cuantificó mediante una RT-PCR cuantitativa a tiempo real con sonda TaqMan, según lo descrito (Lanciotti y col., 2000). Para el ensayo se combinó el RNA con los oligonucleótidos y la sonda marcada en el extremo 5' con el fluoróforo FAM y en el extremo 3' con el *quencher* TAMRA (Eurogentec), utilizando el kit TaqMan One Step RT-PCR Master Mix Reagents kit (Aplied Biosystems). Las muestras se amplificaron en el equipo Rotor-Gene 3000 (Corbett) de acuerdo al protocolo para RT-PCR con sonda TaqMan recomendado por el fabricante.

Tabla VIII. Oligonucleótidos cebadores y sonda utilizados en la RT-PCR cuantitativa a tiempo real de RNA de VNO

Región[a]	Cebador	Orientación[b]	Posición[c]	Secuencia
3'UTR	1F	s	10668	CAGACCACGCTACGGCG
3'UTR	1R	a	10770	CTAGGGCCGCGTGGG
3'UTR	Sonda	a	10691	TCTGCGGAGAGTGCAGTCTGCGAT

[a] Región genómica de VNO a la que corresponde el oligonucleótido.
[b] Orientación del oligonucleótido iniciador: s significa sentido (de la misma polaridad que el RNA genómico de VNO); a significa antisentido (de la polaridad complementaria al RNA genómico de VNO).
[c] Posición en el genoma de VNO de acuerdo a lo descrito (Lanciotti y col., 1999) del nucleótido en el extremo 5' del oligonucleótido (acceso GenBank: AF196835.2).

La cuantificación del número de copias de RNA se determinó como equivalentes genómicos extrapolando los valores de fluorescencia emitida durante la amplificación sobre una curva estándar realizada en paralelo a partir de diluciones seriadas de RNA

extraído de muestras previamente tituladas. Las características de los cebadores y sonda utilizados se indican en la Tabla VIII.

4.25 Detección del RNA que codifica la proteína NP de VCML por *Northern blot*

La detección de RNA viral de VCML por *Northern blot* se realizó según lo descrito (Cornu y col., 2001). El RNA presente en las muestras celulares se separaró en base a su tamaño por medio de una electroforesis en gel de agarosa (1,2%) conteniendo 6,6% formaldehído en tampón MOPS (3-morfolino-1-propanosulfonato). Una vez resuelto el gel, éste se lavó dos veces con H_2O tratada con DEPC (30º C, 10 min) y una vez más con tampón $NaPO_4$ (10 mM pH 6,8) (30º C, 10 min). Posteriormente, el RNA fue transferido a una membrana de nitrocelulosa (Protran, Whatman). A continuación, se realizó un *UV-crosslinking* a la membrana, se lavó con H_2O tratada con DEPC durante 10 min a t.a. y se tiñó con azul de metileno, para comprobar que la transferencia del RNA ribosómico se había realizado correctamente. Después, la membrana se lavó con 1% SDS en H_2O tratada con DEPC durante 10 min, repitiendo este paso hasta que las bandas teñidas de RNA ribosómico dejaron de observarse.

Tabla IX. Oligonucleótidos cebadores utilizados para producir la sonda frente al RNA de la proteína NP de VCML

Región[a]	Cebador	Orientación[b]	Posición[c]	Secuencia
NP	ArmNP *probe* F	a	549	GGCCAAACAGTCACAGACTCCG
NP	ArmNP *probe* R	s	885	GGATGTTTTCATAAGGGTTCCTG

[a] Región genómica de VCML a la que corresponde el oligonucleótido.

[b] Orientación del oligonucleótido iniciador: s significa sentido (de la misma polaridad que el RNA genómico de VCML); a significa antisentido (de la polaridad complementaria al RNA genómico de VCML).

[c] Posición en el genoma de VCML de acuerdo a lo descrito (Salvato y col., 1988) del nucleótido en el extremo 5' del oligonucleótido (acceso GenBank: M20869.1).

Finalmente, la membrana se incubó con una sonda de DNA frente a la NP de VCML marcada radiactivamente con α-^{32}P-dCTP. Para sintetizar dicha sonda, se realizó una RT-PCR utilizando los cebadores indicados en la Tabla IX, se purificó el producto de ésta reacción (apartado 4.21.2) que se marcó radiactivamente empleando el Decaprime kit (Ambion). Las bandas de RNA se detectaron mediante autoradiografía.

4.26 Clonaje molecular

El clon infeccioso pMT28-VP3 116V derivado de pMT28 (apartado 4.4), y los sitios de restricción empleados para su clonaje están esquematizados en la Fig. 12. Para este clonaje, la región correspondiente del cDNA obtenido mediante transcripción inversa a partir del RNA del virus av1 (apartado 4.8), fue amplificada mediante PCR utilizando los cebadores SB5 y 3946a (Tabla VI). El DNA obtenido fue purificado y digerido con las enzimas de restricción *Sfi*I y *Arv*II (New England Biolabs). El plásmido pMT28 fue digerido con estas mismas enzimas, purificado de gel y ligado con el inserto (relación plásmido:inserto de 1:3) utilizando la ligasa de DNA del bacteriófago T4 (Promega), de acuerdo a las instrucciones del fabricante.

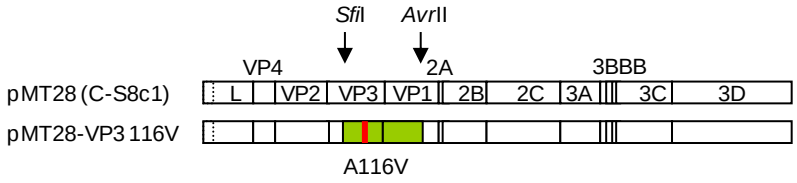

Figura 12. Representación esquemática de la región codificante contenida en el clon infeccioso de VFA construido. La posición de las dianas de las enzimas de restricción utilizadas en la construcción del clon infeccioso se indica con flechas. En verde se representa el fragmento de cDNA procedente del virus resistente a NH_4Cl av1 utilizado en la construcción del clon infeccioso. La barra roja indica la posición del cambio de aminoácido con respecto al pMT28.

Con el producto de la ligación se transformaron bacterias competentes *E. coli* DH5α (Inoue y col., 1990), preparadas en el Servicio de Fermentación del CBMSO. Las bacterias fueron sembradas en placas de agar con medio LB (Luria, 1957) suplementado con 100 µg/ml de ampicilina (Boheringer Mangheim). Las colonias de bacterias capaces de crecer fueron inoculadas y propagadas en medio líquido (LB con 50 µg/ml de ampicilina). El plásmido resultante de la amplificación en *E. coli* fue purificado con el *Plasmid Maxi Kit* (Quiagen), siguiendo las instrucciones del fabricante. La secuencia nucleotídica de la región del plásmido que codifica las proteínas de la cápsida de VFA fue confirmada mediante secuenciación de DNA (apartado 4.22).

4.27 Transcripción *in vitro* de plásmidos

Se empleó como molde DNA de los diferentes clones infecciosos (apartado 4.4), que fue linearizado mediante digestión con la enzima de restricción *Nde*I (New England Biolabs). El RNA fue transcrito a partir de 100 ng del molde linearizado utilizando la RNA polimerasa del bacteriófago SP6 (New England Biolabs). El DNA molde fue

eliminado por digestión con la nucleasa de DNA RQ1 libre de nucleasas de RNA (Promega). La cantidad y pureza del RNA sintetizado se determinó mediante electroforesis en gel de agarosa, tinción con bromuro de etidio y espectrofotometría UV, utilizando un espectrofotómetro Nanodrop ND-1000 (Nanodrop).

4.28 Métodos estadísticos y análisis de datos

Los valores representados en las gráficas corresponden a la media de los datos ± el valor de la desviación estándar de las muestras. Los datos fueron sometidos a análisis de la varianza (ANOVA) usando la distribución *F* de Fisher-Snedecor y aplicando la corrección de Bonferroni al test de la *t* de Student en el caso de las comparaciones múltiples. Para ello se empleó el programa informático estadístico SPSS versión 19 (SPSS). En los casos en los que se requería el test de la Chi^2 para analizar los datos se utilizó el programa informático estadístico Graph Pad Prism. Las diferencias fueron consideradas estadísticamente significativas cuando el *p*-valor calculado fue menor de 0,05 y se indican mediante un asterisco (*) en las gráficas.

4.29 Análisis estructural de cápsidas víricas y modelado molecular

Para el análisis estructural de la cápsida de VFA se utilizaron las coordenadas atómicas depositas en el banco de datos *Protein Data Bank* (PDB) para el virus C-S8c1 (Lea y col., 1994b). Para localizar los residuos de aminoácidos mutados en la estructura de la cápsida se utilizó el programa Pymol (DeLano Scientific, Inc.).

4.30 Disoluciones y tampones

MOPS: 3-morfolino-1-propanosulfonato 140 mM pH 7 en H_2O DEPC.

PBS: 1,5 mM KH_2PO_4, 8,1 mM Na_2HPO_4, 137 mM NaCl, 2,7 mM KCl.

PBTG: PBS conteniendo 1% BSA; 0,1% Tritón-X 100 y 1 M glicina

Tripsina-EDTA: 0,5 mg/ml tripsina (Difco), 0,016% EDTA, 0,0015% rojo fenol, 1,12 mM glucosa, disueltos en PBS.

Tampón TAE: 40 mM tris-acetato sódico pH 8, 1 mM EDTA.

Tampón de carga de Laemmli: 60mM Tris-Cl pH 6,8; 2% SDS, 10% glicerol, 5% β-mercaptoetanol, 0,01% azul de bromofenol.

Tampón electroforesis de proteínas: 192 mM glicina, 25 mM Tris, 0,1% SDS.

Tampón transferencia de proteínas: 192 mM glicina, 25 mM Tris, 20% metanol.

Tampón TNE: 50 mM Tris-HCl pH 7,5, 5mM EDTA, 100 mM NaCl.

Tampón Sörensen: cacodilato sódico 100 mM pH 7,4

TBS: 50 mM Tris-HCl pH 7,4, 150 Mm NaCl

Resultados

5. Resultados

5.1 Papel del PI(4,5)P_2 en la internalización del VFA en cultivos celulares

5.1.1 El VFA requiere dinamina para ser internalizado en células BHK-21

El PI(4,5)P_2 está implicado en varios procesos celulares debido a su capacidad para unirse a distintas proteínas efectoras (Abe y col., 2008; De Matteis y col., 2004; Erlmann y col., 2009; Johnson y col., 2008; Szentpetery y col., 2009; Varnai y col., 2006; Zoncu y col., 2007). Una de estas proteínas es la dinamina, una GTPasa implicada en la fisión de la vesícula endocítica (Loerke y col., 2009; Takei y col., 2005). Puesto que se ha descrito que el VFA utiliza la ruta de endocitosis mediada por clatrina para ser internalizado en la célula (Berryman y col., 2005; Martín-Acebes y col., 2007; O'Donnell y col., 2005), se analizó el efecto de la expresión de una forma dominante negativa (DN) de la dinamina deficiente en unión a GTP y su posterior hidrólisis (Damke y col., 1994) en la entrada de VFA (C-S8c1). En el estudio se incluyó VEV, modelo de endocitosis viral vía clatrina (Cureton y col., 2009; Sun y col., 2005), y VFA MARLS, variante de C-S8c1 que puede utilizar distintos receptores para ser internalizado en la célula (Baranowski y col., 2000). Las células BHK-21 transfectadas con los plásmidos eGFP o dinamina DN fusionada a GFP fueron infectadas tal y como se describe en el apartado 4.5.1. A continuación se contabilizó el número de células que habían internalizado los viriones mediante el uso de microscopía confocal. En la situación control, células transfectadas con eGFP, el porcentaje de células con viriones internalizados fue similar para VEV (76%), C-S8c1 (74%) y MARLS (79%); mientras que en células que expresaban la dinamina DN se observó una reducción significativa del número de éstas, siendo los porcentajes de células con viriones internalizados de 9% (VEV), 12% (C-S8c1) y 11% (MARLS) (Fig. 13a). Estos resultados indican que los tres virus estudiados requieren dinamina para entrar en la célula. También se observó una reducción significativa del porcentaje de células transfectadas e infectadas con C-S8c1, MARLS o VEV (Fig. 13b), indicando que los tres virus necesitan dinamina para dar lugar a una infección productiva.

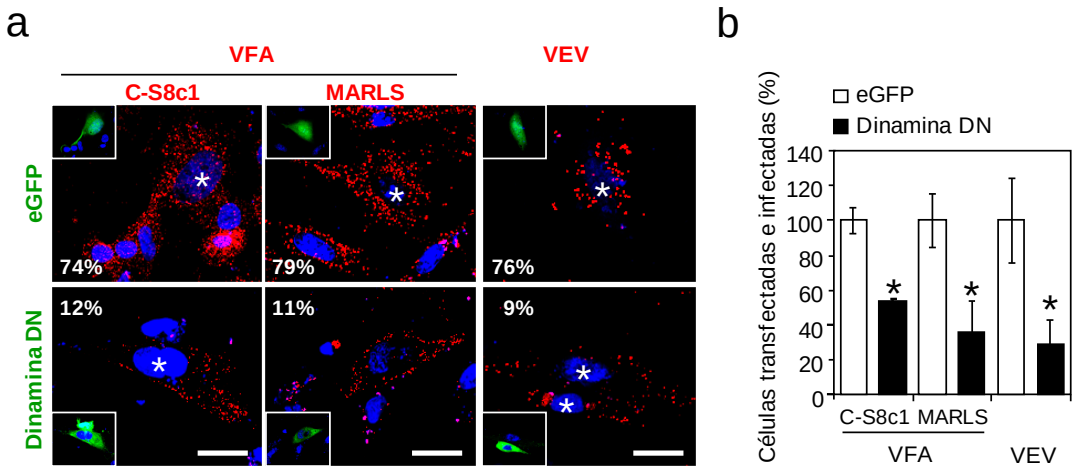

Figura 13. Requerimiento funcional de dinamina en la infección de VFA y VEV. (a) Células BHK-21 transfectadas con el plásmido eGFP o una versión que codifica un DN de la dinamina fusionada a GFP (Dinamina DN) utilizando Lipofectamina Plus. A las 24 h p.t., las células fueron infectadas con diferentes variantes de VFA (C-S8c1 y MARLS) o con VEV (m.d.i. de 70 UFP/célula). Tras 25 min de infección las células se fijaron y procesaron para inmunofluorescencia utilizando el anticuerpo 5C4 para detectar los viriones de VFA y el anticuerpo I1 para los viriones de VEV. El anticuerpo secundario estaba acoplado a AF 555. Los núcleos fueron teñidos con TO-PRO-3. Se indica el porcentaje de células transfectadas con viriones internalizados (n = 100). Las células transfectadas están indicadas con un asterisco (*). Barra: 10 µm. (b) Células BHK-21 electroporadas con los plásmidos eGFP o Dinamina DN e infectadas con el virus correspondiente a las 24 h p.t. (m.d.i. 1 UFP/célula). Las células fueron fijadas y procesadas para inmunofluorescencia a las 7 h p.i., tal y como se ha descrito en (a). En la gráfica se representa el porcentaje de células transfectadas e infectadas normalizado respecto al valor obtenido en las células expresando eGFP (control) (n = 500).

5.1.2 Efecto de la retirada del PI(4,5)P_2 de la membrana plasmática en la internalización de VFA y VEV

Se ha descrito que el tratamiento con ionomicina reduce los niveles de PI(4,5)P_2 de la membrana plasmática por activación de la fosfolipasa C (Zoncu y col., 2007). Cuando se trataron con este fármaco células BHK-21 transfectadas con un plásmido que expresa la proteína de fusión PH-GFP – que permite detectar de manera indirecta el PI(4,5)P_2 (Szentpetery y col., 2009) – (Fig. 14a), se observó una redistribución de la señal correspondiente a PI(4,5)P_2 desde la membrana plasmática al citosol. Este resultado confirma que el tratamiento con ionomicina reduce la cantidad de este fosfolípido en la membrana plasmática de células BHK-21. Además, la ionomicina provocó una reducción de la internalización de TF, ligando modelo que utiliza la ruta dependiente de clatrina (Miller y col., 1991) (Fig. 14b).

Puesto que estos resultados apoyaban que la ionomicina afectaba a la endocitosis dependiente de clatrina, se estudió el efecto de este fármaco sobre la internalización de C-S8c1, MARLS y VEV. Para ello, se emplearon células BHK-21 que fueron tratadas

con ionomicina e incubadas con los distintos virus, determinándose posteriormente la proporción de células que habían internalizado los viriones por medio de inmunofluorescencia. El análisis de las muestras por microscopía confocal indicó que el tratamiento con ionomicina provocaba una reducción similar de la internalización de partículas de VEV y C-S8c1 de aproximadamente el 90%; mientras que en el caso de MARLS la reducción fue en torno al 40% (Fig. 14c). Estos resultados indican que C-S8c1 y VEV requieren la presencia de $PI(4,5)P_2$ en la membrana plasmática para poder ser internalizados en mayor medida que MARLS.

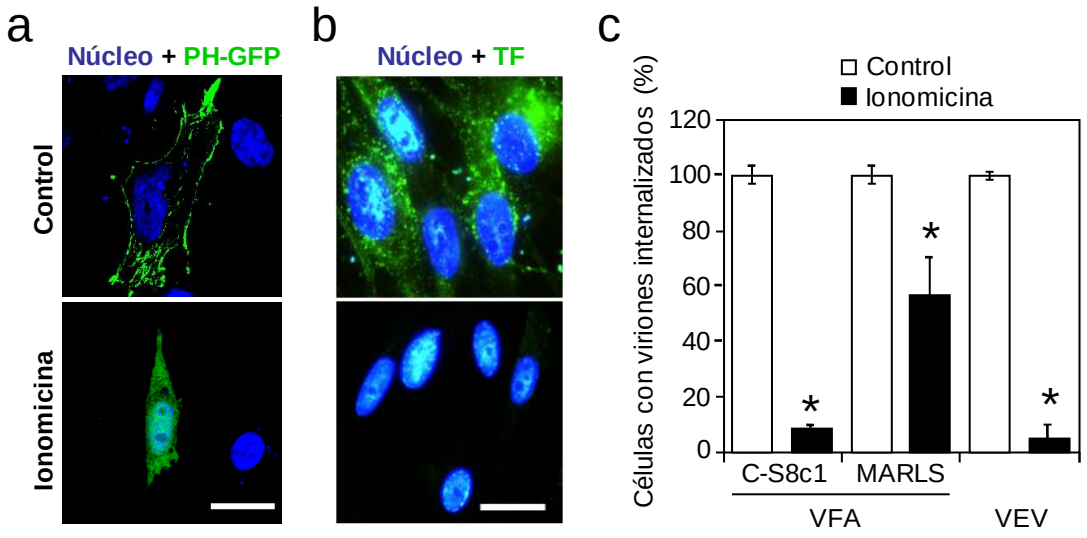

Figura 14. Efecto de la ionomicina en la internalización de VFA y VEV. (a) Visualización de la retirada de $PI(4,5)P_2$ de la membrana plasmática. Células BHK-21 fueron transfectadas con el plásmido PH-PLC-eGFP (PH-GFP) utilizando Lipofectamina Plus. A las 24 h p.t. se trataron con ionomicina 5 µM durante 30 min. Las células se fijaron y se procesaron para la observación en el microscopio confocal y los núcleos fueron teñidos con TO-PRO-3. Barra: 10 µm. (b) El tratamiento con ionomicina inhibe la endocitosis dependiente de clatrina. Células BHK-21 tratadas como en (a) fueron incubadas con TF acoplada a AF 488 fijadas y procesadas para la observación en el microscopio. Los núcleos se tiñeron con DAPI. Barra: 10 µm. (c) Reducción de la capacidad de las células para internalizar viriones deVFA (C-S8c1 y MARLS) y de VEV tras el tratamiento con ionomicina. Células tratadas con ionomicina como en (a) se infectaron con el virus correspondiente (m.d.i. de 70 UFP/célula) durante 25 min, se fijaron y se procesaron para inmunofluorescencia utilizando el anticuerpo 5C4 para detectar los viriones de VFA y el anticuerpo I1 para detectar los viriones de VEV. El anticuerpo secundario utilizado estaba acoplado a AF 555. En la gráfica se muestra el porcentaje de células que tenían viriones internalizados normalizado respecto al valor obtenido en la situación control (n = 500).

5.1.3 Efecto de la inhibición de la síntesis del $PI(4,5)P_2$ en la internalización de VFA y VEV

Los alcoholes primarios, como el 1-butanol, inducen a la fosfolipasa D a generar fosfatidilalcoholes en lugar de ácidos fosfatídicos, lo que conlleva una menor activación de la fosfatidilinositol 4-fosfato 5-quinasa (PI4P5K) y, por lo tanto, la inhibición de la

síntesis de PI(4,5)P_2 (Boucrot y col., 2006). Este efecto no ocurre en presencia de alcoholes secundarios, como el 2-butanol. El tratamiento con 1-butanol o 2-butanol no afectó a la distribución celular de la proteína de fusión PH-PLC-eGFP, que detecta de forma indirecta PI(4,5)P_2, confirmando que ninguno de estos compuestos produce una disminución significativa del contenido de PI(4,5)P_2 de la membrana plasmática (Fig. 15a).

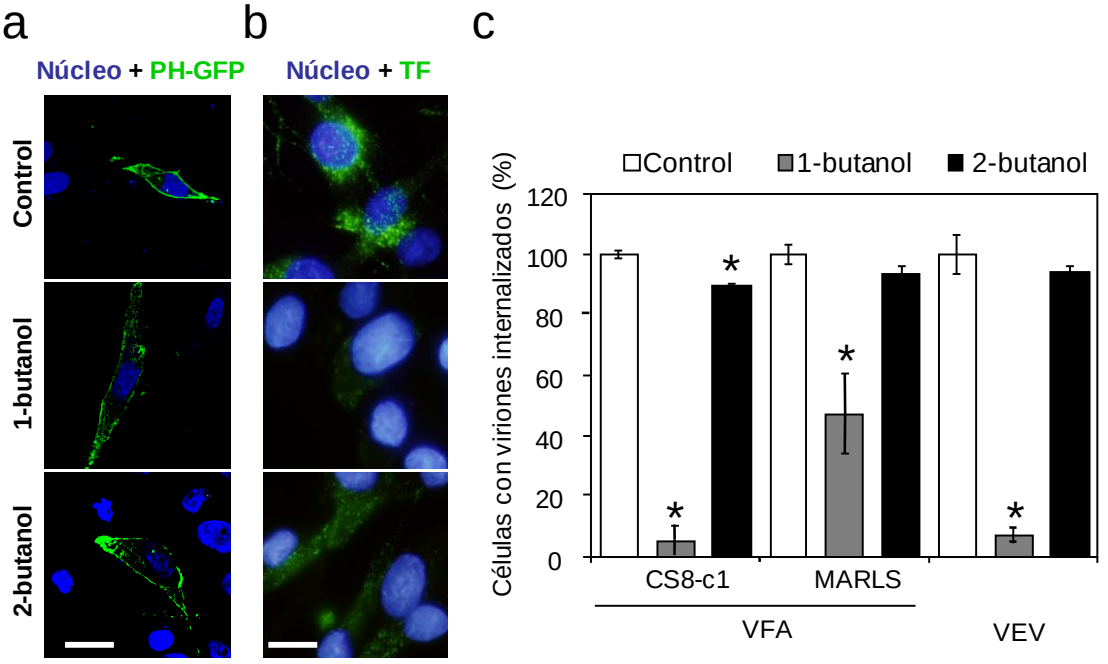

Figura 15. Efecto de la inhibición de la síntesis de PI(4,5)P_2 en la internalización de VFA y VEV. (a) Las células BHK-21 fueron transfectadas con el plásmido PH-PLC-eGFP (PH-GFP) utilizando Lipofectamina Plus. A las 24 h p.t. las células fueron tratadas con 1,5% de 1-butanol ó 2-butanol durante 10 min, fijadas y procesadas para su observación en el microscopio confocal. Los núcleos se tiñeron con TO-PRO-3. Barra: 10 µm. (b) El tratamiento con 1-butanol inhibe la endocitosis dependiente de clatrina. Células BHK-21 tratadas como en (a) fueron incubadas con TF acoplada a AF 488 fijadas y procesadas para la observación en el microscopio. En azul se muestra la tinción de los núcleos con DAPI. Barra: 10 µm. (c) Reducción de la capacidad de las células para internalizar VFA y VEV tras el tratamiento con 1-butanol. Células tratadas con 1-butanol como en (a) se infectaron con el virus correspondiente (m.d.i. de 70 UFP/célula) durante 25 min. A continuación, las células se fijaron y se procesaron para inmunofluorescencia utilizando los anticuerpos 5C4 para detectar viriones de VFA e I1 para detectar viriones de VEV. El anticuerpo secundario utilizado estaba acoplado a AF 555. En la gráfica se muestra el porcentaje de células que presentaron viriones internalizados normalizado respecto al valor obtenido en la situación control (n = 500).

Sin embargo, el tratamiento con 1-butanol inhibió la internalización de TF con respecto a las células no tratadas y a las tratadas con 2-butanol (Fig. 15b), confirmando su efecto sobre la ruta de endocitosis mediada por vesículas revestidas de clatrina. Cuando se analizó el efecto en la entrada viral, el tratamiento con 1-butanol resultó en

una reducción de la internalización de C-S8c1 y VEV de aproximadamente el 90%. Por otro lado, sólo se observó una reducción del 50% en el caso de MARLS. Para poder descartar que otros efectos que el alcohol pudiera tener sobre las células afectase a la internalización de los virus, se utilizó 2-butanol, que no provoca la inhibición de la síntesis de $PI(4,5)P_2$ (Boucrot y col., 2006), el cual afectó sólo ligeramente a la internalización de TF (Fig. 15b). El tratamiento con 2-butanol produjo en todos los casos una reducción de sólo un 10% en la internalización de viriones (Fig. 15c). En conjunto estos resultados indican que C-S8c1 y VEV requieren específicamente la síntesis de $PI(4,5)P_2$ para ser internalizados en mayor medida que MARLS.

5.1.4 Efecto en la internalización de VFA y VEV de la reducción del contenido de $PI(4,5)P_2$ de la membrana plasmática mediante un sistema inducible

Dado que los resultados obtenidos tras el tratamiento con ionomicina y 1-butanol indicaban que VFA y VEV requerían la presencia de $PI(4,5)P_2$ en la membrana plasmática para poder ser internalizados, se estudió el efecto de la retirada de este fosfolípido por medio de un sistema inducible descrito en el apartado 4.13. Este sistema consiste en la cotransfección de los plásmidos PM-FRB-CFP (localizado en la membrana plasmática) y mRFP-FKBP-dom5ptasa (localizado en el citosol). Cuando se añade rapamicina se induce la heterodimerización de los dominios FRB y FKBP, de tal manera que el dominio proteico dom5ptasa pasa a localizarse en la membrana plasmática donde produce la hidrólisis del $PI(4,5)P_2$ (Varnai y col., 2006). En primer lugar se validó este sistema en células BHK-21, comprobando que producía una redistribución de la señal correspondiente a $PI(4,5)P_2$ (detectado mediante la proteína de fusión PH-GFP) desde la membrana plasmática al citosol (Fig. 16a). Cuando las células BHK-21 transfectadas con estos plásmidos fueron infectadas con los virus estudiados tras la adición de la rapamicina, se observó una reducción estadísticamente significativa en el número de células que habían internalizado partículas de VEV y C-S8c1 con respecto al control sin rapamicina, siendo los valores de inhibición en torno al 73% ($P = 0,0001$) y 77% ($P = 0,0001$), respectivamente. En el caso de MARLS la reducción observada (13%) no fue estadísticamente significativa (Fig. 16b).

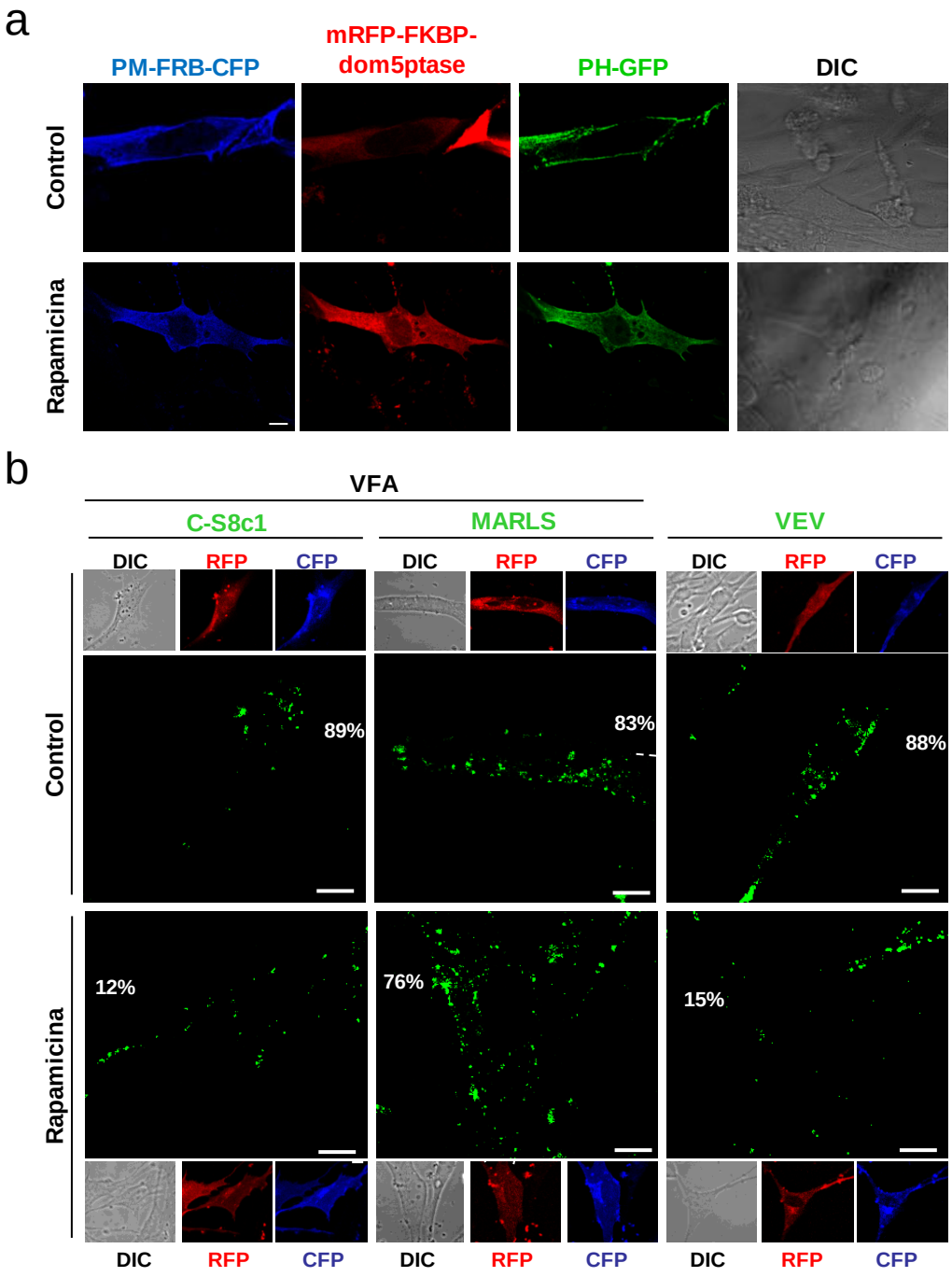

Figura 16. La retirada de PI(4,5)P_2 de forma inducible inhibe la internalización de C-S8c1 y VEV. (a) El sistema inducible empleado produce la retirada del PI(4,5)P_2 de la membrana plasmática en células BHK-21. Las células BHK-21 crecidas sobre cubreobjetos fueron cotransfectadas con los plásmidos PM-FRB-CFP, mRFP-FKBP-dom5ptasa y PH-PLC-eGFP (PH-GFP), utilizando Lipofectamina Plus. A las 24 h p.t., las células fueron incubadas durante 10 min con rapamicina a una concentración de 10 nM o con DMSO (control). A continuación, las células se fijaron y procesaron para su observación en el microscopio confocal. (b) Las células BHK-21 crecidas sobre cubreobjetos fueron cotransfectadas con los plásmidos PM-FRB-CFP (CFP) y mRFP-FKBP-dom5ptasa (RFP) y tratadas con rapamicina como en (a). Las células fueron infectadas con una m.d.i. de 70 UFP/célula en presencia de rapamicina (25 min de incubación), fijadas y procesadas para inmunofluorescencia. Los viriones de VFA y los de VEV fueron detectados con los anticuerpos 5C4 e I1, respectivamente, en combinación con un anticuerpo secundario acoplado a AF 647. Se indica el porcentaje de células cotransfectadas que han internalizado partículas virales (n = 100). Barra: 10 µm. Contraste de fases interdiferencial (DIC).

El efecto de la inhibición no fue consecuencia del uso de la rapamicina, puesto que no se observaron diferencias en la internalización de viriones entre las células control no transfectadas y las células no transfectadas tratadas con rapamicina. Estos resultados confirman que C-S8c1 y VEV requieren la presencia de $PI(4,5)P_2$ en la membrana plasmática para ser internalizados, siendo esta dependencia menor para MARLS.

5.2 Estudio del requerimiento de la acidificación endosomal en distintos variantes del VFA

5.2.1 El tratamiento con pH ácido induce la disociación de la cápsida de VFA

El tratamiento con pH ácido produce la reducción de la infectividad de VFA (Martín-Acebes y col., 2010). Para determinar si esta reducción está causada directamente por la disociación en pentámeros de la cápsida, el virus recuperado del clon infeccioso pMT28 (C-S8c1) y un mutante de éste con resistencia incrementada al tratamiento con pH ácido, pMT28-VP1 17D (Martín-Acebes, 2009), fueron crecidos en células BHK-21 en condiciones de marcaje metabólico con ^{35}S y purificados a través de un gradiente de sacarosa (apartado 4.6.3). En estos experimentos se observó para ambos virus un único pico de radiactividad, que correspondía a los viriones con un coeficiente de sedimentación de 140S (datos no mostrados). A continuación, los viriones purificados fueron incubados con diferentes pH durante 30 min y su integridad fue determinada mediante ultracentrifugación, tal y como se describe en el apartado 4.9.1. Los resultados mostraron que el mutante VP1 17D era más resistente que el virus parental C-S8c1 a la disociación a pentámeros de la cápsida inducida por tratamiento con pH ácido (Fig. 17a), siendo el valor de pH_{50} para la disociación ($pH_{50}D$, definido como el valor de pH que ocasiona una disociación a pentámeros de la cápsida del 50% de los viriones totales) de 6,3 y 6,6, respectivamente (Fig. 17b). Estos valores son similares a los descritos previamente para los ensayos de inactivación de la infectividad de estos virus, siendo los valores de pH_{50} de inactivación ($pH_{50}I$, definido como el valor de pH que ocasiona una reducción de la infectividad del 50%) de 6,2 para VP1 17D y de 6,6 para C-S8c1(Martín-Acebes y col., 2011c). Los resultados obtenidos muestran una correspondencia entre la inactivación por pH ácido y la disociación de la cápsida de VFA.

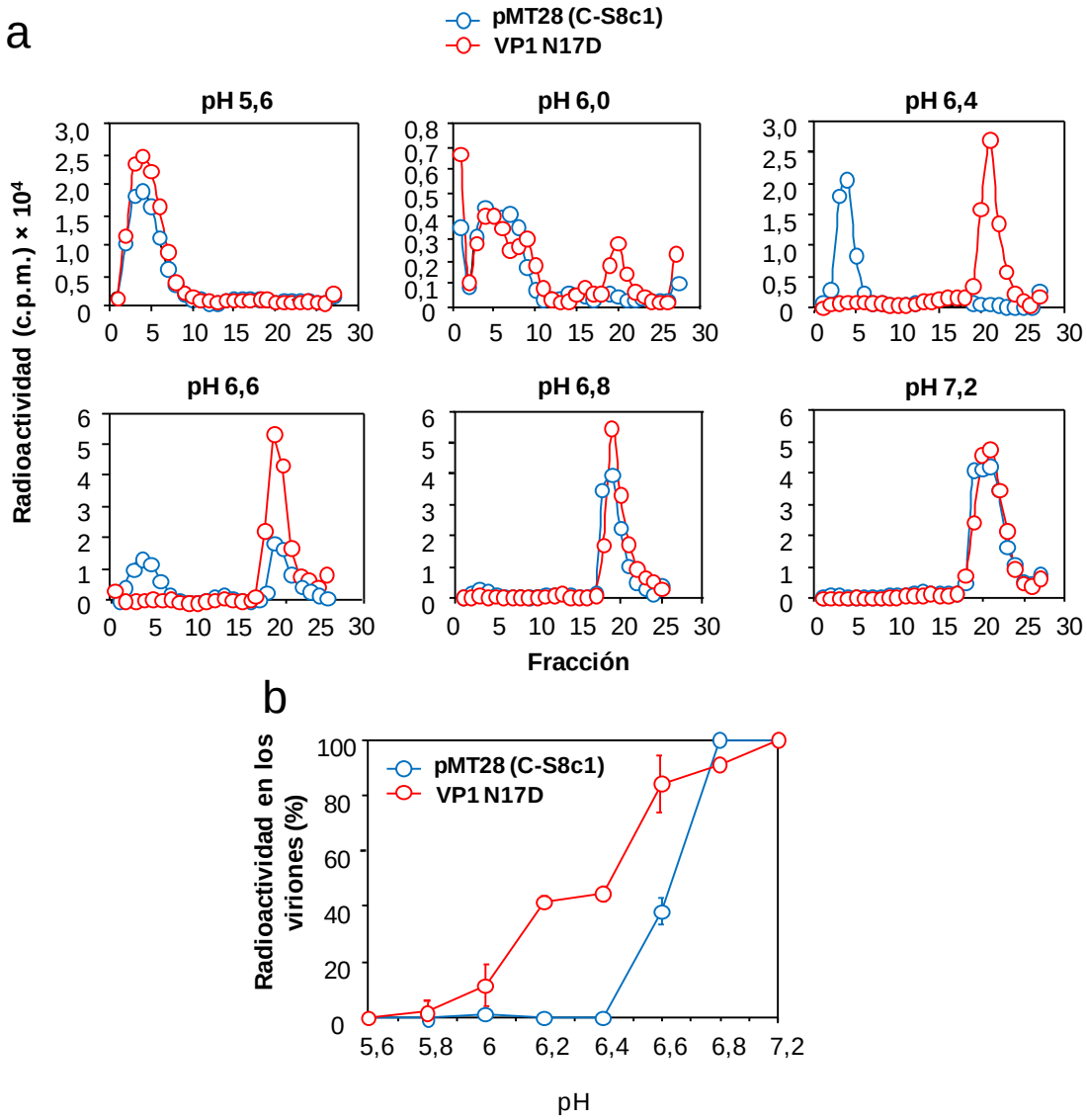

Figura 17. El tratamiento con pH ácido induce la disociación de los viriones de VFA. (a) Análisis del perfil de sedimentación de viriones de C-S8c1 (pMT28) y del mutante VP1 17D marcados radiativamente con ^{35}S, purificados (ver apartado 4.6.3), y posteriormente tratados con diferentes pH. Los picos localizados en las fracciones 0-10 corresponden a viriones no disociados (coeficiente de sedimentación de 140S) y los picos localizados en las fracciones 15-30 corresponden a los viriones disociados en subunidades pentaméricas (coeficiente de sedimentación de 12S). (b) Representación del porcentaje de viriones intactos (coeficiente de sedimentación de 140S) en función del pH del tampón, normalizado respecto a la cantidad de viriones intactos tras el tratamiento con pH 7,2 (considerado como el 100%).

5.2.2 El requerimiento de la acidificación endosomal no depende del receptor empleado por el VFA

El valor de $pH_{50}D$ para el virus C-S8c1 (pH de 6,6) es compatible con que la desencapsidación tenga lugar en los endosomas tempranos, puesto que el pH en su interior oscila entre 6,1 y 6,8 (Huotari y col., 2011; Jovic y col., 2010). Además, se ha observado que la expresión de una forma dominante negativa (DN) de la proteína Rab5

(implicada en el tráfico de membrana de los endosomas tempranos) inhibe la infección del VFA de serotipo O (Johns y col., 2009). Por este motivo, se estudió el efecto de la expresión de Rab5 DN en la infección de dos variantes del VFA que utilizan distintos receptores para ser internalizados en la célula: C-S8c1, cuya entrada es dependiente de integrinas α_v (Nuñez y col., 2007), y MARLS, que es capaz de entrar en la célula utilizando distintos receptores celulares (Baranowski y col., 2000; Baranowski y col., 1998). En ambos casos, la expresión de Rab5 DN redujo el número de células infectadas de forma similar (Fig. 18a), indicando que los aislados de VFA estudiados requieren esta proteína para dar lugar a una infección productiva.

A continuación, se determinó la sensibilidad a pH ácido de estos virus mediante ensayos de infectividad (apartado 4.9.2), observándose de nuevo un comportamiento similar en ambos casos (Fig. 18b). Los valores de $pH_{50}I$ determinados fueron de 6,56 para C-S8c1 y de 6,59 para MARLS. Como control de estos experimentos se incluyó un enterovirus bovino (EVB), otro picornavirus resistente a pH ácido (Ley y col., 2002), para el que no se observó bajada de infectividad alguna dentro del rango de pH analizado.

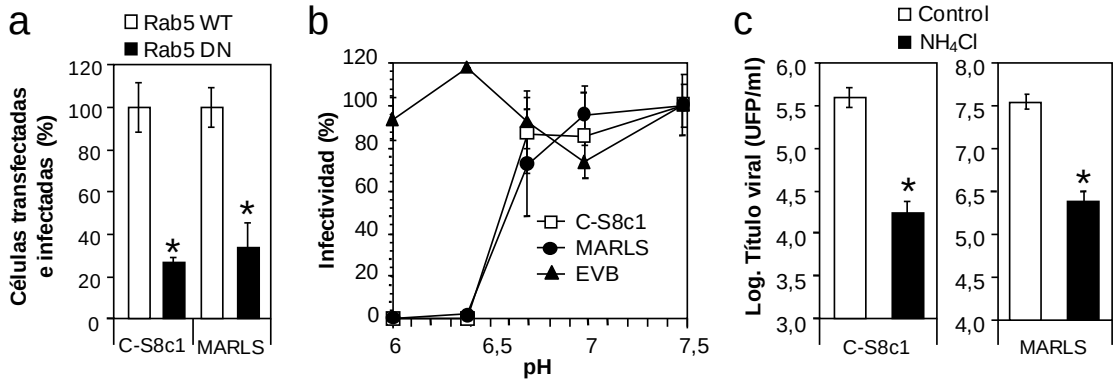

Figura 18. El requerimiento de la acidificación endosomal no depende del receptor de VFA. (a) El VFA requiere la proteína Rab5 para una infección productiva. Las células BHK-21 fueron electroporadas con el plásmido que codifica la forma WT o DN de la proteína Rab5 fusionada a GFP. A las 24 h, las células fueron infectadas con C-S8c1 o MARLS (m.d.i. de 1 UFP/célula). A las 7 h p.i. las células fueron fijadas y procesadas para inmunofluorescencia usando el anticuerpo 5C4. Como anticuerpo secundario se empleó un anticuerpo acoplado a AF 555 (n = 300 en 3 experimientos independientes). (b) Análisis de la inactivación de la infectividad viral inducida por pH ácido: determinación de los valores de $pH_{50}I$. Las mismas UFP (2-4 × 10^6 UFP) de cada virus fueron tratadas con tampones de diferentes pH y a continuación neutralizadas con un tampón Tris pH 7,6. La infectividad recuperada fue determinada mediante titulación en células BHK-21 (se expresa como porcentaje normalizado respecto al obtenido con un tampón pH 7,5). (c) Inhibición de la infección de C-S8c1 y MARLS con NH_4Cl. Monocapas de células BHK-21, tratadas o no con 25 mM NH_4Cl, fueron infectadas (m.d.i. de 0,5 UFP/célula) con los virus C-S8c1 o MARLS. El título viral se determinó 7 h p.i.

Finalmente, se analizó el efecto del tratamiento con NH_4Cl, que bloquea la acidificación de los compartimentos endosomales (Ohkuma y col., 1978), sobre la infección de C-S8c1 y MARLS. En ambos casos, el NH_4Cl inhibió la producción viral de manera similar, en torno a un orden de magnitud (Fig. 18c). Estos resultados confirman que tanto el requerimiento de acidificación endosomal, como la dependencia de la proteína Rab5 para la infección de VFA no se ven alterados por los cambios en la especificidad de receptor de MARLS.

5.2.3 El tratamiento con monensina y nigericina inhibe la infección de VFA

Los ionóforos monensina y nigericina se intercalan en las membranas celulares suprimiendo el gradiente de protones debido al intercambio de éstos por cationes monovalentes (Callaway y col., 1999; Parfenova y col., 1999), lo que inhibe la acidificación de los endosomas de forma similar a lo que sucede con el tratamiento con NH_4Cl (Marsh y col., 1982). Para analizar el efecto del tratamiento combinado con monensina y nigericina, células BHK-21, tratadas o no con estos fármacos, se infectaron con VFA y la producción viral se determinó a las 7 h p.i. En el análisis se incluyeron variantes de VFA con distintos valores de $pH_{50}I$: C-S8c1 (6,56), c2 (6,95) y m6 (6,11) (Martín-Acebes y col., 2010; Martín-Acebes y col., 2011c). En todos los casos, se observó una reducción significativa de la producción viral cuando las células se trataron con monensina y nigericina (Fig. 19a). Sin embargo, el porcentaje de inhibición fue diferente, siendo menor para el virus c2 que para C-S8c1 y m6. A su vez, se observó una correlación entre la inhibición por los ionóforos y el valor de $pH_{50}I$ de los virus (Fig. 19b), de manera que la inhibición era mayor cuanto mayor el requerimiento de acidificación endosomal ($pH_{50}I$ más ácido). Por tanto, estos resultados muestran una relación entre el valor de pH para la desencapsidación (estimado como el $pH_{50}I$) y la inhibición de la infección mediante el bloqueo de la acidificación endosomal con monensina y nigericina.

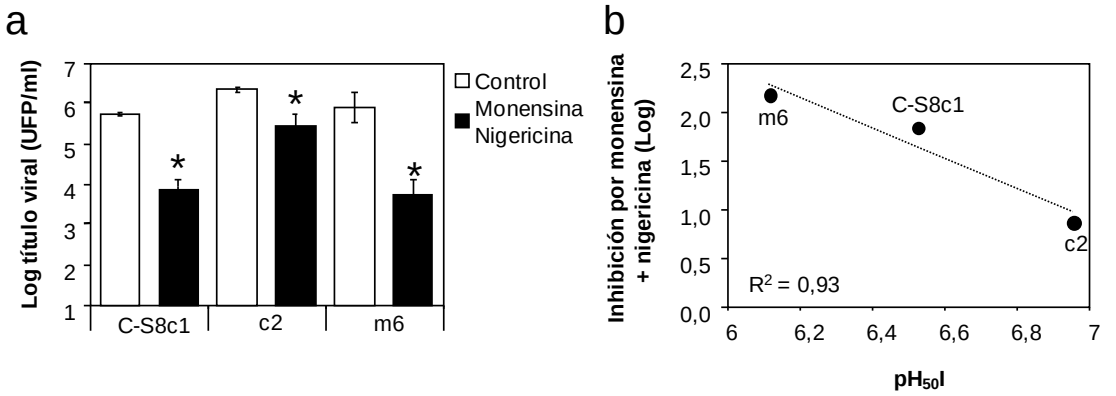

Figura 19. El tratamiento con monensina y nigericina inhibe la infección de VFA. (a) Células BHK-21 tratadas o no con monensina y nigericina (10µM de cada fármaco) fueron infectadas con distintos variantes de VFA (m.d.i. 0,5 de UFP/célula) y a las 7 h p.i. se determinó el título viral total. (b) Inhibición por monensina y nigericina obtenida en función de los valores de $pH_{50}I$ de cada virus. El coeficiente de correlación de Pearson (R^2) está indicado en la gráfica.

5.2.4 Relación entre el pH de desencapsidación de VFA y la función de las proteínas celulares Rab

La acidificación de los endosomas es un paso importante para su maduración (Huotari y col., 2011; Jovic y col., 2010). Con el objetivo de determinar si las variaciones en los valores de $pH_{50}I$ de los virus C-S8c1, c2 y m6 se asociaban a diferentes requerimientos endosomales, se comparó el efecto de la expresión de DN de distintas proteínas Rab, implicadas en la regulación del tráfico vesicular, en la infección de estos virus. La expresión de Rab5 DN, que bloquea el tráfico de los endosomas tempranos, inhibió la infección de los tres variantes de VFA analizados (Fig. 20a), siendo el porcentaje de inhibición mayor en el caso de m6 y menor en el caso de c2. También se observó una correlación directa entre el porcentaje de células infectadas que expresaban Rab5 DN y el valor de $pH_{50}I$, de nuevo seleccionado como una estimación del valor de pH de desencapsidación (Fig. 20b).

Por otro lado, la expresión de Rab7 DN, que bloquea el tráfico de los endosomas tempranos a los tardíos, no indujo una reducción significativa de la infección para ninguno de los virus estudiados (Fig. 20c). Sin embargo, al representar el porcentaje de células infectadas que expresaban Rab7 DN frente al valor de $pH_{50}I$ de cada virus, se observó una correlación inversa (Fig. 20d) entre el porcentaje de células infectadas con Rab7 DN y el valor de $pH_{50}I$ de los virus.

Cuando se expresó Rab11 DN, bloqueando así el tráfico de membrana de los endosomas tempranos a los endosomas de reciclaje, no se observó una reducción significativa de la infección para los virus analizados (Fig. 20e). En este caso también se

observó una correlación inversa entre el porcentaje de células infectadas que expresaban Rab11 DN y el valor de $pH_{50}I$ de los virus analizados (Fig. 20f). Como control, las células transfectadas se infectaron con VCML, cuya entrada es dependiente de la acidificación endosomal, pero independiente de la actividad de Rab5 y Rab7 (Di Simone y col., 1995; Quirin y col., 2008; Rojek y col., 2008), no observándose inhibición de la infección como resultado de la expresión de las proteínas Rab DN (Fig. 20a, c y e); confirmando así la especificidad de los resultados obtenidos con los variantes de VFA.

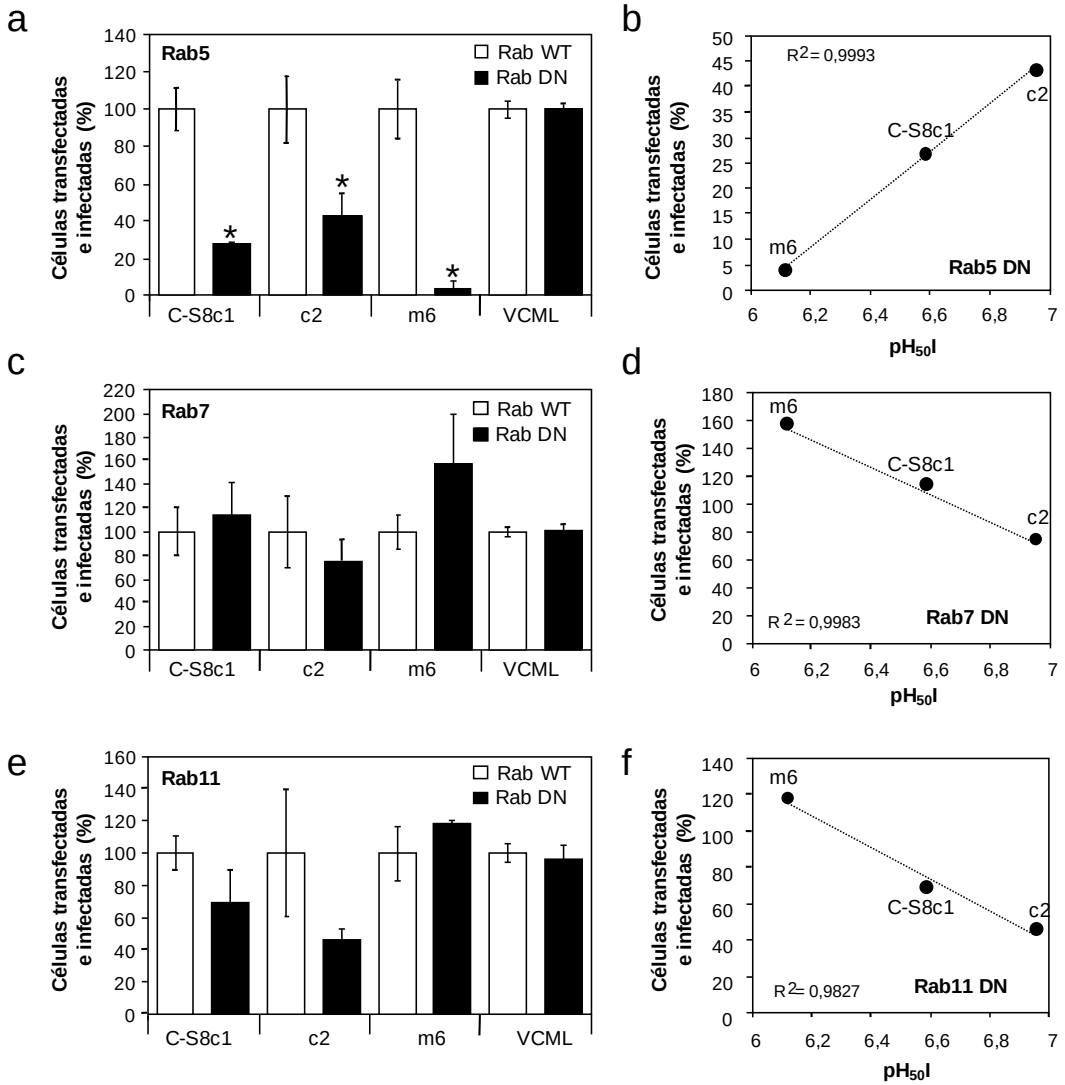

Figura 20. Relación entre el requerimiento de proteínas Rab y el valor de $pH_{50}I$ para la infección de VFA. Se transfectaron células BHK-21 mediante electroporación con plásmidos que codifican la forma WT o DN de las proteínas Rab5 (a), Rab7 (c), o Rab 11 (e) fusionada a GFP. A las 24 h p.t. las células fueron infectadas con C-S8c1, c3, m6 o VCML (m.d.i. de 1 UFP/célula). Las células fueron fijadas a las 7 ó 24 h p.i. en el caso de VFA o VCML, respectivamente, y procesadas para inmunofluorescencia usando el AcM 5C4 para detectar VFA o el 1.1.3 para VCML (n = 300, en 3 experimientos independientes). La media de los porcentajes de las células transfectadas con Rab5 DN (b), rab7 DN (d) o Rab11 DN (f) e infectadas se representa en función de los valores de $pH_{50}I$ de cada virus. El coeficiente de correlación de Pearson (R^2) está indicado en las gráficas.

Estos resultados sugieren que hay una relación entre el pH de desencapsidación (estimado como el valor de $pH_{50}I$) y el requerimiento de las proteínas Rab, de forma que cuanto más ácido es el valor de pH de desencapsidación, el virus depende en mayor medida de las proteínas Rab que controlan el tráfico hacia los endosomas tempranos (Rab5), y en menor medida de aquellas que controlan el tráfico que sale de los endosomas tempranos a los tardíos (Rab7), o a los de reciclaje (Rab11).

5.2.5 La modulación del pH de desencapsidación de VFA reduce la virulencia en el modelo de ratón lactante

Para analizar la virulencia de los variantes de VFA con distinto requerimiento de pH (C-S8c1, c2 y m6) se utilizaron ratones lactantes de 7 días de edad. Estos animales fueron inoculados intraperitonealmente con diferentes cantidades de UFP (desde 10^2 hasta 10^6). Tanto C-S8c1 como los mutantes c2 y m6 indujeron síntomas y muerte. Sin embargo, se encontraron diferencias significativas en el número de animales muertos entre los grupos inoculados con C-S8c1 y los inoculados con los mutantes (Tabla X).

Tabla X. Susceptibilidad a la infección de VFA en ratones lactantes inoculados con variantes de VFA con diferencias en los valores de $pH_{50}I$ y en el requerimiento de proteínas rab

	UFP inoculadas/ratón	Infectividad en ratón lactante	*P*-valor [a]
PBS	NA	0/10	NA
C-S8c1	10^4	11/11	NA
	10^3	9/10	NA
	10^2	7/10	NA
c2	10^6	9/10	NA
	10^4	7/10	0,0497*
	10^3	3/10	0,0062*
	10^2	1/10	0,0062*
m6	10^6	10/10	NA
	10^4	7/10	0,0497*
	10^3	7/10	0,5312
	10^2	2/10	0,0062*

[a] *P*-valor del test de la Chi^2 entre mutantes y C-S8c1. Los asteriscos (*) indican diferencias estadísticamente significativas.
NA, no aplicable.

Cuando los valores de dosis letal 50 (LD_{50}) (Muench, 1935) se compararon con las UFP/ml determinadas en células BHK-21 para cada *stock* viral, se observó una disminución en la infectividad en ratón lactante, de en torno a 2 veces y 10 veces para los mutantes m6 y c2, respectivamente, con respecto a la encontrada para C-S8c1 (Tabla XI).

Tabla XI. Infectividad en cultivo celular y virulencia en ratón lactante de distintos variantes de VFA

	Infectividad en células BHK-21 (UFP/ml)[a]	Virulencia en ratón lactante (LD_{50}/ml)[b]
C-S8c1	1×10^7	$\geq 10^7$
c2	1×10^7	5×10^5
m6	1×10^7	4×10^6

[a] Virus amplificado en células BHK-21.

[b] La LD_{50} fue determinada como se describe previamente (Muench, 1935).

Estos resultados indican que la modulación del pH de desencapsidación de VFA se asocia con la reducción de la virulencia *in vivo*.

5.3 Aislamiento y caracterización de mutantes de VFA resistentes a NH_4Cl a partir de muestras biológicas

5.3.1 Aislamiento de mutantes resistentes a NH_4Cl

En el laboratorio se habían aislado y caracterizado mutantes resistentes a NH_4Cl presentes en poblaciones de VFA C-S8c1 crecidas en cultivos celulares (Martín-Acebes y col., 2010). Con objeto de determinar si era posible aislar este tipo de mutantes de poblaciones de virus recuperados a partir de hospedadores naturales (ver apartado 4.8), se infectaron células BHK-21 con líquido vesicular (afta) procedente de cerdos infectados con C-S8c1 (apartado 4.3), a las que se añadió medio semisólido conteniendo NH_4Cl, tras 1h de disociación. Transcurridas 30 h de infección, las monocapas tratadas con NH_4Cl desarrollaron el 1,28 ± 0,93% (cerdo 5) y 0,15 ± 0,11% (cerdo 6) de las UFP detectadas en las monocapas no tratadas con NH_4Cl (Fig. 21). El porcentaje de UFP observado utilizando como control una población procedente de cultivos celulares de C-S8c1 fue de 0,14 ± 0,09% (Fig. 21). Por tanto, la frecuencia de selección de mutantes resistentes a NH_4Cl es similar en poblaciones de VFA crecidas tanto en cultivos celulares como en cerdo. A partir del líquido vesicular del cerdo 5 se aislaron cinco placas virales capaces de crecer en presencia de NH_4Cl (denominadas av1-5), mientras que del cerdo 6 se aisló una placa (av6). Todas ellas fueron amplificadas mediante un pase en células BHK-21 manteniendo el NH_4Cl.

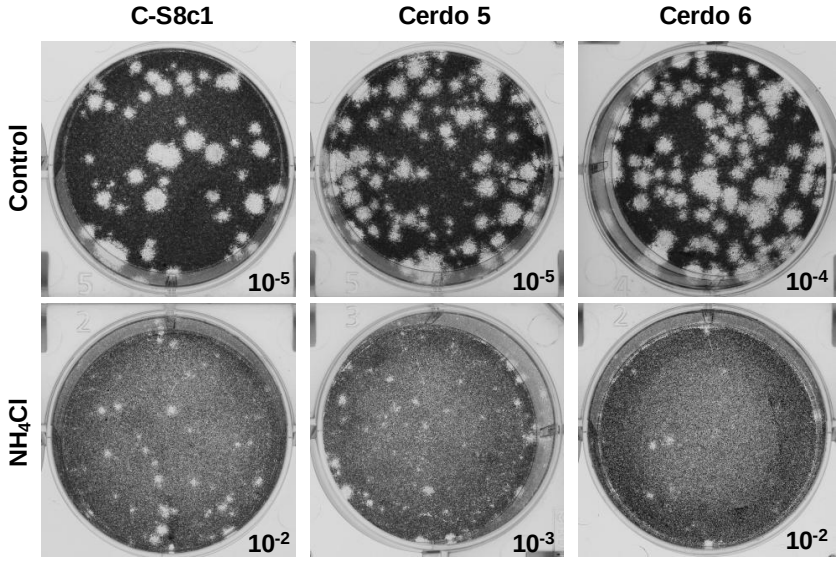

Figura 21. Placas de lisis obtenidas en presencia de NH_4Cl. Se realizaron diluciones seriadas de C-S8c1 procedentes de cultivos celulares o de los virus presentes en las lesiones vesiculares del cerdo 5 y cerdo 6, con las que se infectaron células BHK-21 en medio semisólido conteniendo o no (control) 25 mM NH_4Cl. Las células fueron fijadas y teñidas con cristal violeta 30 h p.i. La dilución del virus mostrada se indica en cada caso.

5.3.2 Análisis de las mutaciones en la cápsida seleccionadas en los virus resistentes a NH_4Cl

Para caracterizar los mutantes resistentes a NH_4Cl seleccionados como se describe en el apartado anterior, la región del RNA viral que codifica las proteínas de la cápsida fue secuenciada en los virus resistentes a NH_4Cl (av1, av2, av3, av4, av5 y av6), así como en las poblaciones virales presentes en las aftas empleadas para la selección de estos mutantes (Tabla XII). La región de la cápsida de los mutantes av1, av2, av3, av4 y av5 presentó una misma sustitución no sinónima responsable del cambio VP3 A116V. El mutante av6 también presentó una única sustitución no sinónima que originó el cambió en VP3 A25P. Estos cambios no se detectaron en los virus procedentes de las aftas originales.

Tabla XII. Sustituciones de nucleótido seleccionadas en clones de VFA resistentes a NH_4Cl obtenidas a partir de lesiones vesiculares de cerdos infectados con C-S8c1[a]

Región genómica	Virus							
	Cerdo5[b]	Cerdo6[b]	av1	av2	av3	av4	av5	av6
VP4								
VP2								
VP3			C2897T (A116V)	C2897T (A116V)	C2897T (A116V)	C2897T (A116V)	C2897T (A116V)	G2623C (A25P)
VP1								

[a] Se muestran las mutaciones encontradas respecto de la secuencia publicada por Toja y col., 1999. Las sustituciones de aminoácido a las que dieron lugar las mutaciones se indican en paréntesis.
[b] Muestras biológicas de las que se partió para aislar los virus indicados en la Tabla.

5.3.3 Localización espacial en la cápsida viral de las mutaciones seleccionadas en presencia de NH_4Cl

La estructura de la cápsida del aislado de VFA C-S8c1 ha sido resuelta mediante cristalografía de rayos X (Lea y col., 1994b), lo que permitió la localización espacial de los aminoácidos implicados en las mutaciones encontradas (Fig. 22). El cambio VP3 A25P se localizó en una estructura desordenada de la proteína (Fig. 22a), mientras que el cambio VP3 A116V lo hizó en el bucle que une la lámina β-D2 y la lámina β-E, en concreto, el residuo anterior al comienzo de la lámina β-E (Fig. 22a). La localización en las subunidades pentaméricas de la cápsida de los residuos implicados en las dos mutaciones encontradas se muestra en la Fig. 22b. La mutación VP3 A116V se sitúa cerca del borde del pentámero, mientras que la mutación VP3 A25P lo hace en una posición próxima al eje de simetría 5 de la cápsida, localizada en una zona interna de la proteína (Fig. 22c). Dado que el residuo VP3 116 se localiza cerca del borde interpentámerico (Fig. 22b), la sustitución A116V supone la introducción de un residuo más voluminoso, lo que podría generar perturbaciones estructurales. La posición VP3 116 se sitúa muy cerca de los residuos VP3 H140 y VP3 H143 (Fig. 23a), para los que se ha postulado una implicación en el desensamblaje de las cápsidas de VFA (Ellard y col., 1999; van Vlijmen y col., 1998). El reemplazamiento A116V se localiza cerca de otras sustituciones previamente descritas para otros mutantes de VFA resistentes a NH_4Cl: VP3 A118V y A123T (Martín-Acebes y col., 2010) (Fig. 23a), situadas todas en la lámina β-E de VP3 o en sus proximidades (Lea y col., 1994b) (Fig. 23b).

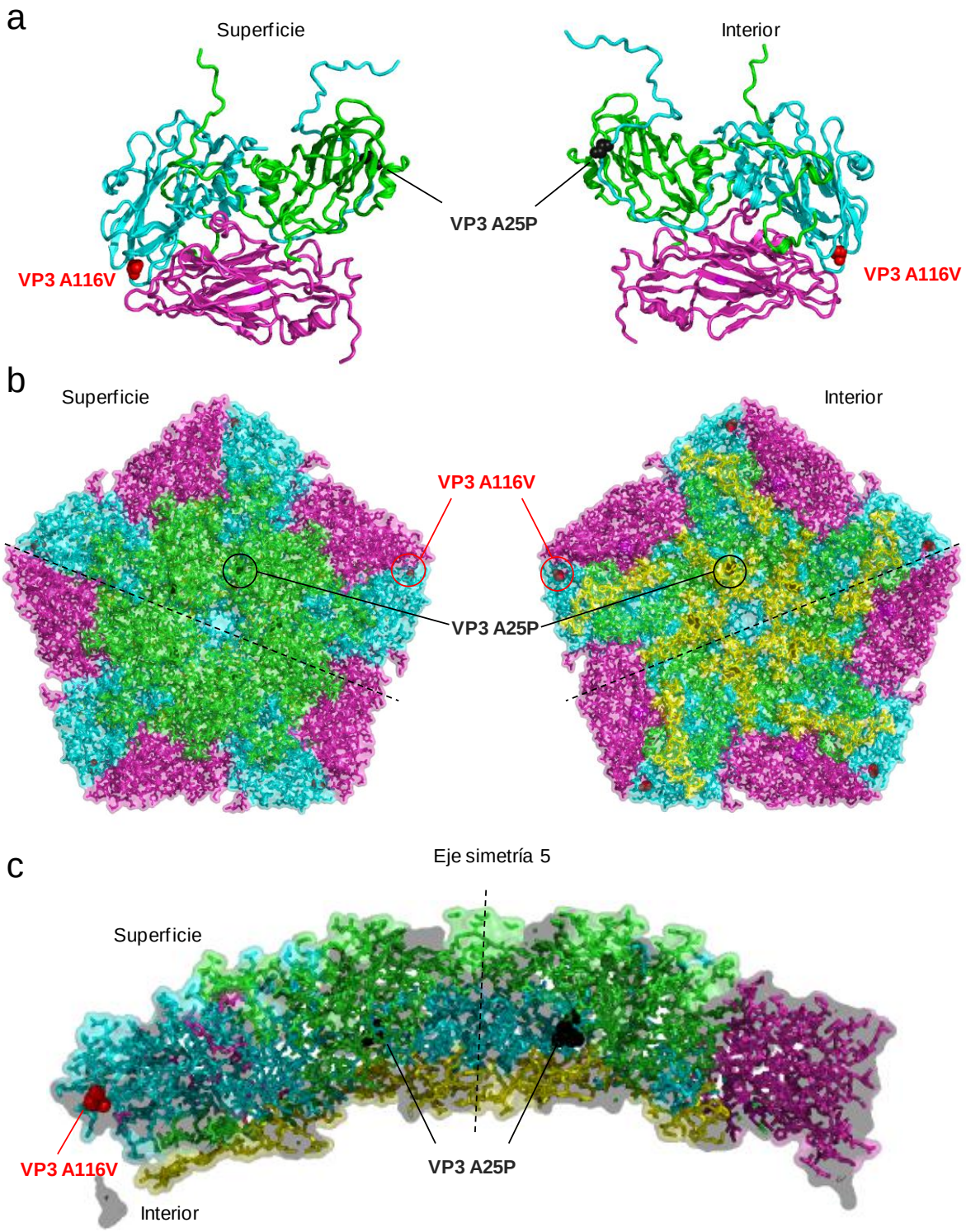

Figura 22. Localización espacial de los residuos mutados en la cápsida de los virus resistentes a NH_4Cl seleccionados a partir de lesiones vesiculares de cerdo. Ver apartado 4.29 (a) Vista de la superficie externa y la cara interna del protómero biológico de C-S8c1. La proteína VP4 no se enseña por simplicidad. Se indican los residuos VP3 A25 (esferas negras) y A116 (esferas rojas). (b) Vista de la superficie externa y la cara interna de la subunidad pentamérica de la cápsida. Se indican los residuos VP3 A25 y A116. La línea discontinua indica el corte transversal que se muestra detallado en (c). Código de colores de las proteínas: VP1 en verde; VP2 en magenta; VP3 en cian y VP4 en amarillo. La posición VP1 H151 no se muestra en el diagrama ya que está localizada en el bucle móvil G-H, cuya estructura no está determinada, debido a su flexibilidad, en el modelo de la cápsida de C-S8c1 (Lea y col., 1994b).

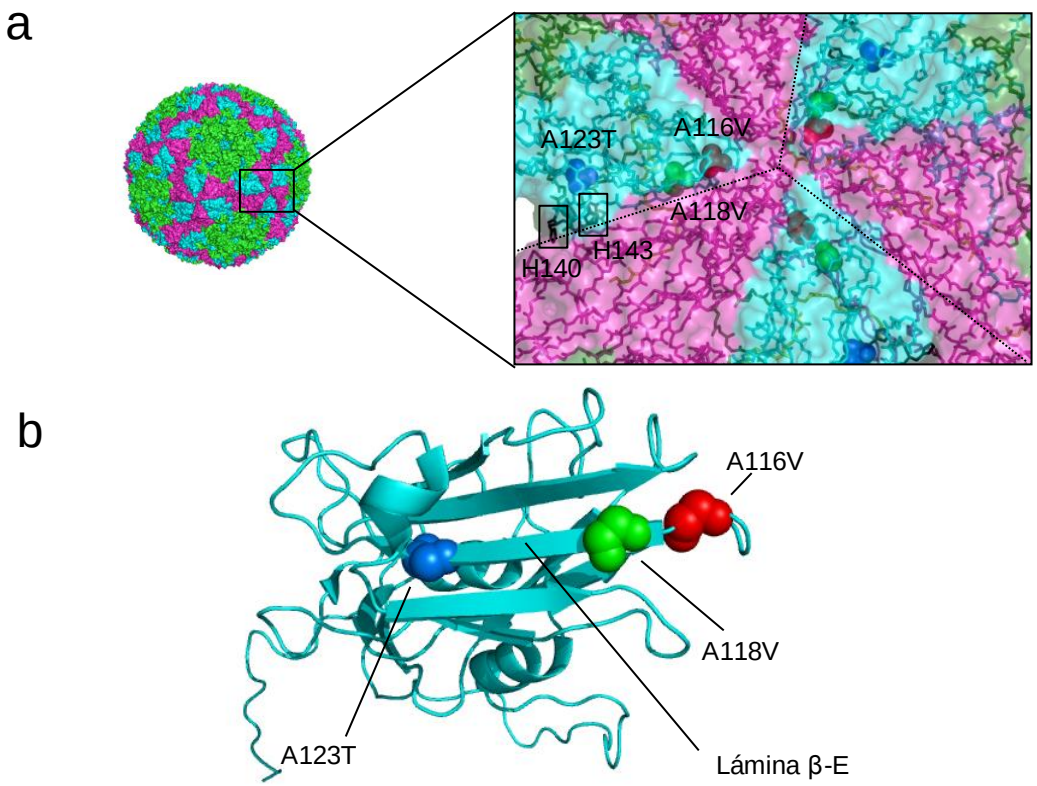

Figura 23. Comparación de la localización espacial de las distintas sustituciones de aminoácido encontradas en diferentes mutantes de VFA resistentes a NH_4Cl. Ver apartado 4.29. (a) Detalle de un eje de simetría de orden 3 mostrando el contacto entre tres pentámeros vecinos en el que se indica la posición VP3 A116V (esferas en rojo), VP3 A118V (esferas en verde), VP3 A123T (esferas en azul) y los residuos VP3 H140 y VP2 H143 (en negro). (b) Estructura de la proteína VP3. Se indican los residuos A116V, A118V y A123T con los mismos colores que en (a). Código de colores de las proteínas: VP1 en verde; VP2 en magenta y VP3 en cian.

5.3.4 La resistencia a NH_4Cl está relacionada con el incremento de la sensibilidad a pH ácido de las partículas de VFA

Para analizar la sensibilidad a NH_4Cl de los mutantes aislados a partir de lesiones vesiculares de cerdo, se seleccionaron los virus av1 y av6. Tras un pase adicional en presencia de NH_4Cl se confirmó que mantenían las mutaciones descritas anteriormente. Con los preparados virales obtenidos, se realizaron infecciones en presencia de NH_4Cl. En estos experimentos, se incluyeron como controles el virus C-S8c1 y el mutante c2, resistente a NH_4Cl (Martín-Acebes y col., 2010).

La producción viral de av1 y av6 fue inhibida en menor medida que la de C-S8c1, confirmando la resistencia a NH_4Cl de estos virus. Por otro lado, se observó una sensibilidad diferencial a NH_4Cl entre ellos, siendo los mutantes c2 y av1 los únicos que alcanzaron títulos similares tanto en presencia como en ausencia de NH_4Cl (Fig. 24a).

También se examinó la sensibilidad a pH ácido de estos virus (apartado 4.9.2), ya que se ha descrito para otros mutantes resistentes a NH_4Cl un aumento en la sensibilidad a pH ácido como mecanismo para permitir el desensamblaje de la cápsida en condiciones de acidificación endosomal reducida (Martín-Acebes y col., 2010). Ambos virus presentaron un incremento en la sensibilidad a pH ácido, aunque en estos experimentos se observó un comportamiento diferencial entre los mutantes (Fig. 24b), siendo av1 más sensible al tratamiento con pH ácido que av6. Los valores de $pH_{50}I$ obtenidos fueron 6,86 y 6,66 para av1 y av6, respectivamente, representando valores intermedios a los determinados para el virus C-S8c1 (6,56) y c2 (6,98).

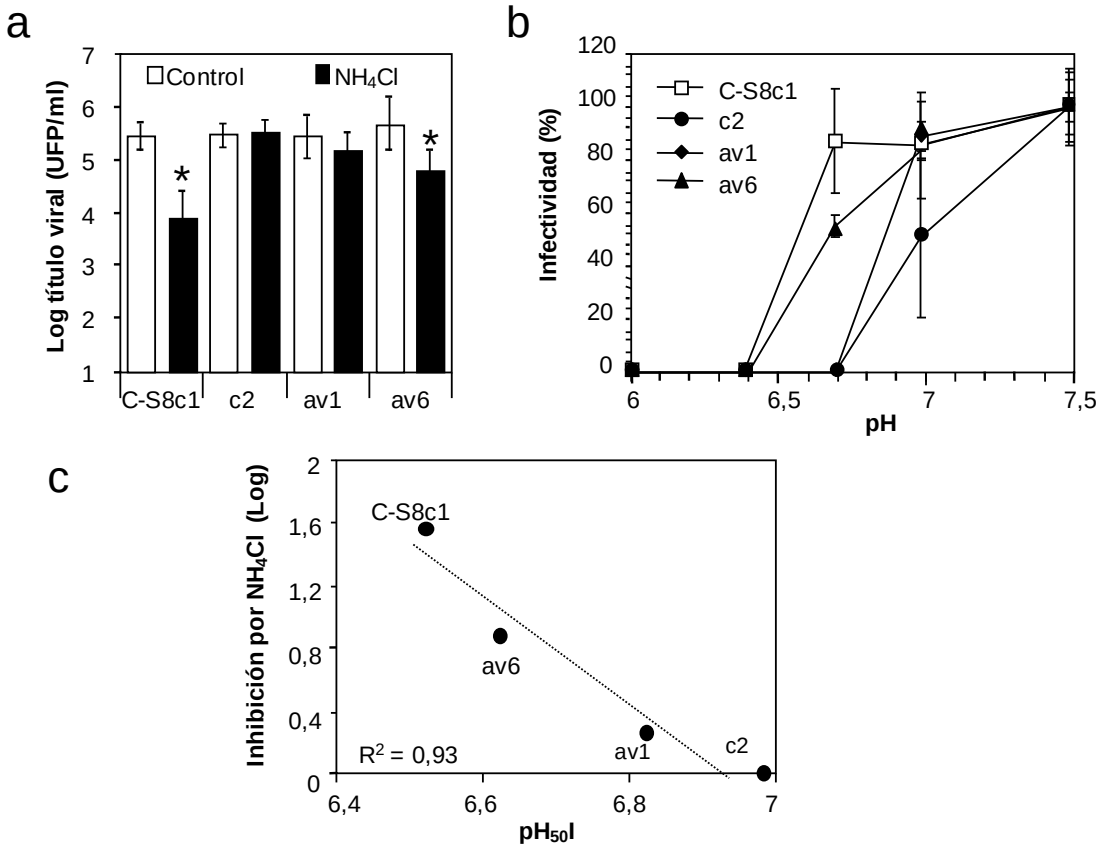

Figura 24. Correlación entre la resistencia a NH_4Cl y la sensibilidad a pH ácido de las partículas de VFA. (a) Sensibilidad de los mutantes de VFA al tratamiento con NH_4Cl. Monocapas de células BHK-21, tratadas o no con 25 mM NH_4Cl, fueron infectadas (m.d.i. de 0,5 UFP/célula) con los virus C-S8c1, c2, av1 y av6. El título viral se determinó 7 h p.i. (b) Incremento de la sensibilidad a pH ácido en los mutantes de VFA resistentes a NH_4Cl. Las mismas UFP de cada virus fueron tratadas con tampones de diferentes pH y a continuación neutralizadas con un tampón Tris pH 7,6. La infectividad recuperada fue determinada mediante titulación en células BHK-21 (se expresa como porcentaje normalizado sobre el obtenido con un tampón pH 7,5). (c) La inhibición de la producción viral debida al tratamiento con 25mM NH_4Cl obtenida con cada virus se representa en función de los valores de $pH_{50}I$ de cada virus. El coeficiente de correlación de Pearson (R^2) se indica en la gráfica.

Cuando se representaron los valores de inhibición del título viral por NH_4Cl frente a los valores de $pH_{50}I$ (como estimación del pH de desencapsidación) de cada virus estudiado, se observó una correlación entre ambas variables (Fig. 24c). Estos resultados apoyan la hipótesis de que la resistencia a la inhibición endosomal inducida por el tratamiento con NH_4Cl se asocia a un incremento en la sensibilidad a pH ácido de las partículas de VFA.

5.3.5 Efecto del tratamiento con monensina y nigericina en la producción viral de av1 y av6

Los experimentos realizados con los mutantes c2 y m6 indicaban la existencia de una relación entre el pH de desencapsidación y la inhibición de la infección debido al bloqueo de la acidificación endosomal inducido con monensina y nigericina (Fig. 19). Para determinar si los virus av1 y av6 también tenían una resistencia incrementada al tratamiento con monensina y nigericina, células BHK-21 tratadas o no (control) se infectaron con los virus C-S8c1, av1 o av6 determinándose el título viral (apartado 4.5.2) a las 7 h p.i. En todos los casos, el tratamiento con estos ionóforos provocó una reducción estadísticamente significativa de la producción viral (Fig. 25a). Sin embargo, al igual que lo observado previamente con los virus C-S8c1, c2 y m6 (Fig. 19b), se encontró una correlación entre el valor de inhibición por monensina y nigericina y el $pH_{50}I$ (Fig. 25b).

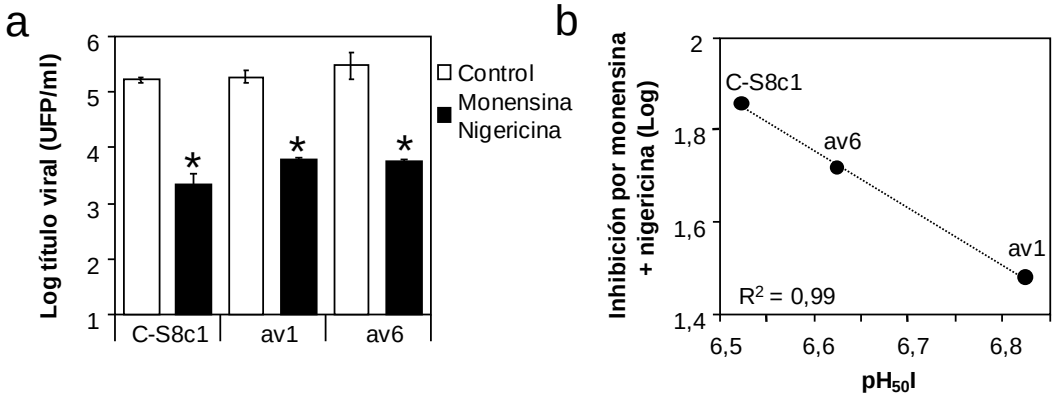

Figura 25. Efecto del tratamiento combinado con monensina y nigericina sobre la producción viral de av1 y av6. (a) Las células BHK-21 tratadas o no con 10 µM de monensina y 10 µM de nigericina fueron infectadas con C-S8c1, av1 o av6 (m.d.i. de 0,5 UFP/célula). A las 7 h p.i. se determinó el título viral total. (b) Representación de la inhibición por monensina y nigericina en función de los valores de $pH_{50}I$ de cada virus. El coeficiente de correlación de Pearson (R^2) se indica en la gráfica.

5.3.6 Confirmación de la resistencia a NH_4Cl del mutante av1

De los mutantes aislados a partir de lesiones vesiculares, el mutante av1 fue el único capaz de producir el mismo título viral en presencia y en ausencia de NH_4Cl (Fig. 24a).

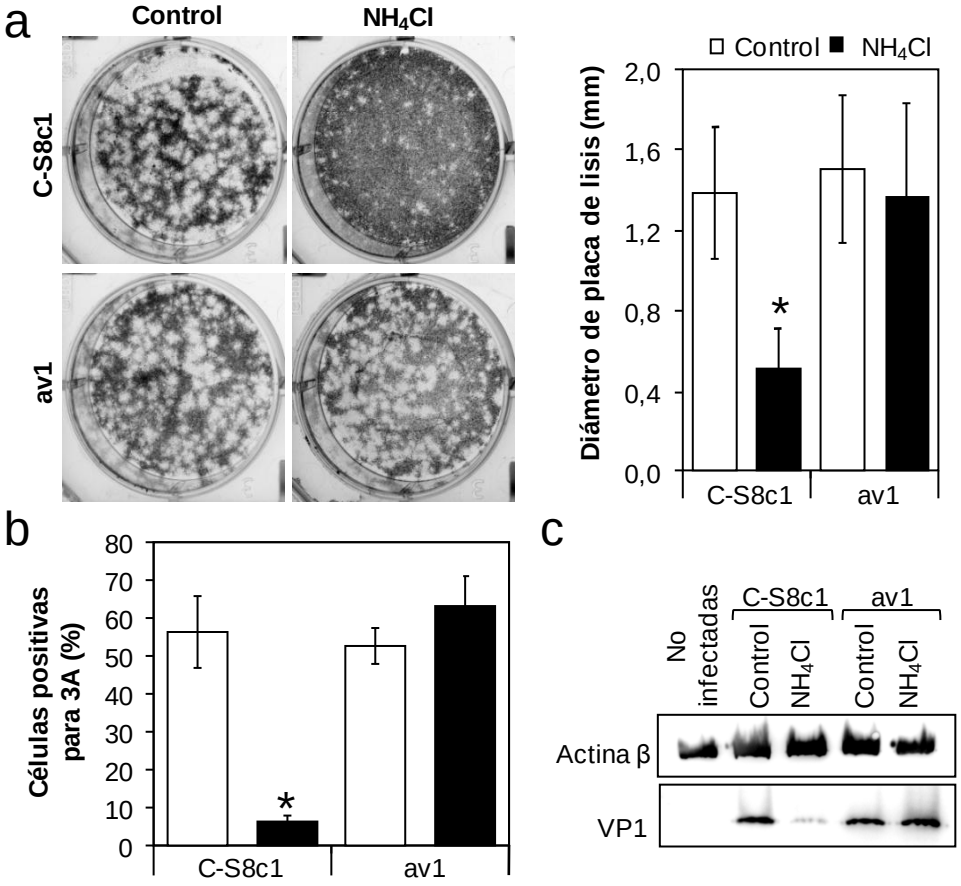

Figura 26. La infección con el mutante av1 es resistente al tratamiento con NH_4Cl. (a) Placas de lisis producidas por C-S8c1 y av1. Las células BHK-21 fueron infectadas con los virus indicados durante 30 h en medio semisólido conteniendo o no 25 mM NH_4Cl. La gráfica de la derecha representa el valor medio del diámetro de tamaño de las placas de lisis en cada situación (n = 20). (b) Células BHK-21 tratadas o no (control) con 25mM NH_4Cl fueron infectadas con los variantes de VFA C-S8c1 y av1 (m.d.i. 0.5 de UFP/célula), fijadas a las 7 h p.i. y procesadas para inmunofluorescencia usando el anticuerpo 163 para detectar la proteína 3A. El anticuerpo secundario utilizado estaba acoplado a AF 555. En la gráfica se muestra el porcentaje de células positivas para la fluorescencia de 3A, normalizado frente al valor obtenido en la situación control (n = 1000, en tres cubreobjetos diferentes). (c) El NH_4Cl no reduce la producción de la proteína VP1 en las células infectadas con el mutante av1. Células tratadas o no con 25 mM NH_4Cl e infectadas con C-S8c1 o av1 como en (a). La cantidad de proteína 7 h p.i. fue estimada mediante *Western blot* utilizando el anticuerpo SD6 que reconoce la proteína VP1. Los resultados obtenidos con un anticuerpo anti-β-acina, se muestran como control de carga.

La resistencia a NH_4Cl de este virus fue confirmada cuando se comparó el tamaño de las placas de lisis producidas en presencia de NH_4Cl (Fig. 26a), que fue similar al de las producidas en ausencia de NH_4Cl (1,36 ± 0,47 mm y 1,50 ± 0,37 mm,

respectivamente). Por el contrario, las placas de lisis producidas por C-S8c1 en presencia de NH_4Cl fueron significativamente menores que las producidas en ausencia del fármaco (0,51 ± 0,20 mm y 1,38 ± 0,33 mm, respectivamente, P = 0,001) (Fig. 26a). Además, se analizó el número de células infectadas en ausencia y presencia del fármaco, observándose que el virus av1 infectó un porcentaje de células similar en ambos casos, mientras que el virus C-S8c1 infectó un porcentaje de células significativamente menor en presencia de NH_4Cl (Fig. 26b).

5.3.7 Disección del papel funcional del cambio de aminoácido A116V encontrado en la proteína estructural VP3

Dado que el mutante av1 fue el más resistente a NH_4Cl, se evaluó el efecto de la mutación encontrada en él (VP3 A116V). Para ello, esta sustitución fue introducida en el clon infeccioso pMT28 (que contiene el cDNA correspondiente a la secuencia genómica completa del virus C-S8c1) de acuerdo a lo descrito en el apartado 4.25. El RNA viral fue sintetizado a partir del clon infeccioso mediante transcripción *in vitro* a partir del promotor de la RNA polimerasa del bacteriófago SP6 (apartado 4.27), y utilizado para transfectar células BHK-21 (apartado 4.12.3). El virus recuperado de esta transfección fue amplificado mediante un pase en esta línea celular y la secuencia consenso correspondiente a la región P1 de la poliproteína viral fue determinada. La mutación introducida se mantuvo en el virus recuperado, no detectándose cambios adicionales (datos no mostrados). Como se muestra en la Fig. 27a, el tamaño de placa del virus recuperado, denominado pMT28-VP3 116V, fue comparable al del virus C-S8c1 recuperado del clon infeccioso pMT28 (1,56 ± 0,57 mm y 1,33 ± 0,46 mm, respectivamente).

Por otra parte, la producción viral en función del tiempo mostró un ligero retraso para VP3 116V con respecto a C-S8c1, aunque a las 7 h pi el título viral fue similar para ambos virus (Fig. 27b); lo que indica que esta mutación no parece conferir una fuerte desventaja en la producción viral. La sustitución de nucleótido C2897T responsable del cambio VP3 116V fue estable tras diez pases seriados en ausencia de NH_4Cl (Fig. 27c).

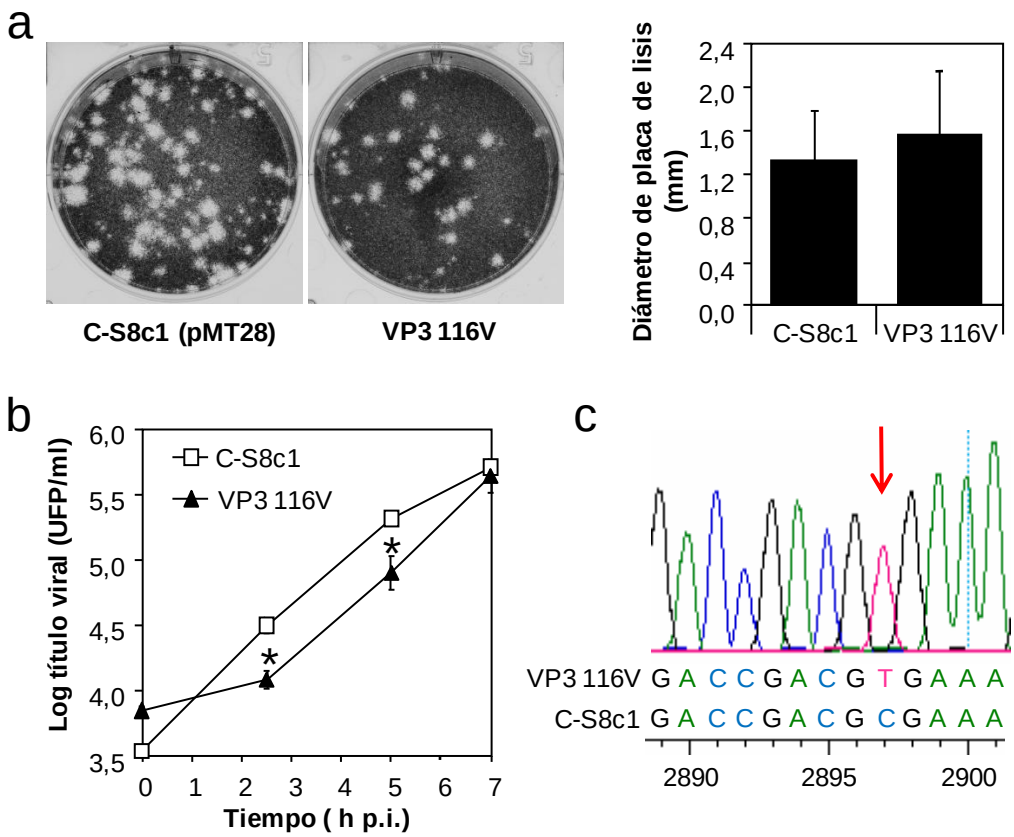

Figura 27. Fenotipo y estabilidad genética del virus recuperado a partir del clon infeccioso pMT28-VP3 116V. (a) Placas de lisis producidas por los virus recuperados de los clones infecciosos pMT28 y pMT28-VP3 116V. Las células BHK-21 fueron infectadas con los virus durante 24 h en medio semisólido. Posteriormente fueron fijadas y teñidas con cristal violeta. La gráfica de la derecha representa el valor medio del diámetro de tamaño de las placas de lisis recuperadas en cada caso (n = 20). (b) Células BHK-21 fueron infectadas con los virus recuperados de los clones infecciosos (m.d.i. de 0,5 UFP/célula). El título viral en el medio extracelular fue determinado a distintos tiempos p.i. (c) Estabilidad genética del cambio VP3 A116V. El virus recuperado de la transfección del RNA generado a partir del plásmido pMT28-VP3 116V fue sometido a 10 pases seriados en células BHK-21, secuenciándose el RNA viral extraído del último de los pases (apartado 4.21.11 y 4.22).

5.3.7.1 El cambio VP3 116V es suficiente para conferir resistencia a NH_4Cl

El estudio del efecto del tratamiento con NH_4Cl sobre la infección de los virus recuperados de los clones infecciosos pMT28 (C-S8c1) y pMT28 VP3 116V (VP3 116V), mostró que este compuesto inhibía el crecimiento de C-S8c1, no afectando al del virus VP3 116V (Fig. 28a). Estos resultados confirman que el cambio VP3 A116V es responsable del escape del mutante de VFA av1 a la inhibición de la acidificación endosomal inducida por NH_4Cl.

Posteriormente se analizó la sensibilidad a pH ácido del virus VP3 116V (Fig. 28b), que mostró una sensibilidad incrementada, con un valor de $pH_{50}I$ de 6.85 [muy similar al del virus resistente aislado de la placa (6,86, apartado 5.3.4)], mientras que en el caso del virus C-S8c1 recuperado del pMT28 el $pH_{50}I$ fue de 6,57 [muy similar al del

virus C-S8c1 (6,56, apartado 5.3.4)]. Estos resultados sugieren que el incremento en la sensibilidad a pH ácido de las partículas de VFA se debe al cambio VP3 A116V, lo que hace posible su escape a la inhibición por NH_4Cl.

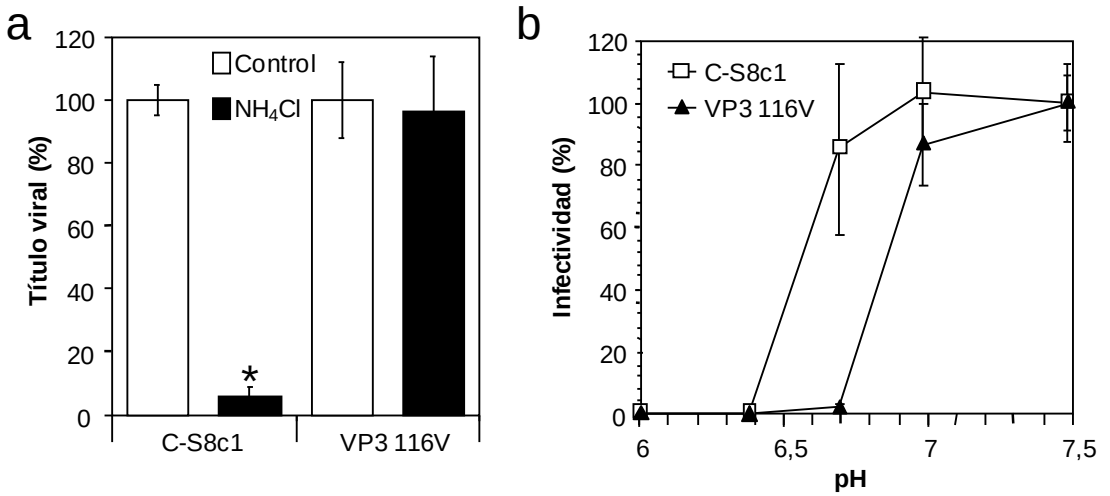

Figura 28. El cambio A116V en la proteína VP3 es responsable de la resistencia a NH_4Cl y del incremento a la sensibilidad a pH ácido. (a) Sensibilidad al tratamiento con NH_4Cl. Se infectaron células BHK-21 tratadas o no con 25 mM NH_4Cl (m.d.i. 0,5 de UFP/célula) y el título viral se determinó 7 h p.i. (b) Incremento de la sensibilidad a pH ácido del virus VP3 116V. Las mismas UFP del virus C-S8c1 y VP3 116V fueron tratadas con tampones de diferentes pH. La infectividad tras el tratamiento fue determinada mediante titulación en células BHK-21 (expresada como el porcentaje obtenido tras el tratamiento con tampón pH 7,5).

5.3.7.2 Estudio de la capacidad replicativa (*fitness*) del virus VP3 116V

Los virus recuperados de los clones infecciosos C-S8c1 y VP3 116V fueron empleados para realizar experimentos de competición en presencia o en ausencia de NH_4Cl. Para ello, células BHK-21, tratadas o no con NH_4Cl, se infectaron con una mezcla conteniendo la misma cantidad de UFP de cada virus. Los virus resultantes de esta infección se utilizaron para infectar de nuevo células BHK-21 tratadas o no con NH_4Cl, repitiéndose este proceso hasta 10 veces (apartado 4.10). Finalmente, se determinó el porcentaje aproximado de los genomas que estaban compitiendo en los pases 1, 2, 3, 4, 5, 7 y 10 (Fig. 29). En tres experimentos independientes se obtuvieron resultados similares. En ausencia del fármaco, la proporción del genoma del mutante VP3 116V fue disminuyendo progresivamente hasta llegar a niveles en torno al 13% en el pase 10. Por el contrario, en los experimentos en presencia de NH_4Cl el mutante VP3 116V ya fue dominante (99.2%) en el primer pase, manteniendo valores cercanos al 100% hasta el pase 10.

Por otra parte, se secuenció, en el pase 10, la región del RNA viral correspondiente a la cápsida completa del virus, no encontrándose ninguna mutación adicional a la descrita para el mutante VP3 116 V. Estos resultados indican que la sustitución de aminoácido VP3 A116V confiriere una ventaja selectiva en los pases seriados en presencia de NH_4Cl, mientras que en ausencia del fármaco reduce la capacidad replicativa (*fitness*) respecto al virus parental C-S8c1.

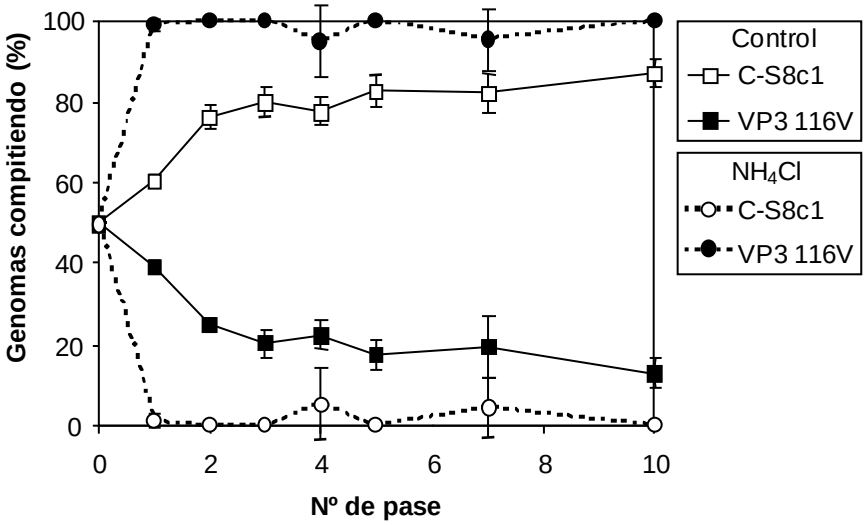

Figura 29. Estudio de la capacidad replicativa del virus VP3 116V. Se infectaron células BHK-21 con una mezcla de los virus recuperados de los clones infecciosos pMT28 (C-S8c1) o pMT28 VP3 116V (VP3 116V) [m.d.i. inicial de 0,1 ufp/célula (0,05 ufp/célula de cada virus)] en presencia o ausencia de 25 mM NH_4Cl. Cuando se observó efecto citopático completo se recogió el sobrenadante que fue utilizado para infectar nuevas monocapas de células. Estas infecciones seriadas se repitieron 10 veces. Se extrajó RNA de diferentes pases y el cDNA que codifica la proteína VP3 fue sintetizado y secuenciado. La proporción de los genomas que competían fue estimada a partir de los cromatogramas como el ratio del área integrada correspondiente a cada nucleótido en la posición de la mutación puntual (C2897T).

5.4 Efecto del AVP en la multiplicación de distintos virus con envoltura

El ácido valproico (AVP) es un ácido graso de cadena corta usado comúnmente para el tratamiento de desórdenes neurológicos (Bruni y col., 1979; Terbach y col., 2009). El mecanismo de acción del AVP no está claro, habiéndose propuesto distintos efectos sobre la célula entre los que destacan la inhibición de las deacetilasas de histonas (DACH) y la alteración del metabolismo de lípidos, incluyendo los fosfatidilinositoles (Shaltiel y col., 2004; Tokuoka y col., 2008; Venkataramani y col., 2010; Wittenburg y col., 2010; Xu y col., 2007). Por este último motivo se estudió el efecto de este fármaco sobre la infección de VFA y VEV, dos virus causantes de enfermedades vesiculares animales que durante esta Tesis Doctoral se ha visto que requieren la presencia de $PI(4,5)P_2$ de la membrana plasmática para internalizar.

5.4.1 Efecto del AVP en la viabilidad celular

Inicialmente se evaluó la toxicidad del AVP. Para ello, se determinó el valor de la concentración de AVP que producía la muerte del 50% (TC_{50}) de las células BHK-21 y Vero mediante tinción vital con azul Tripán.

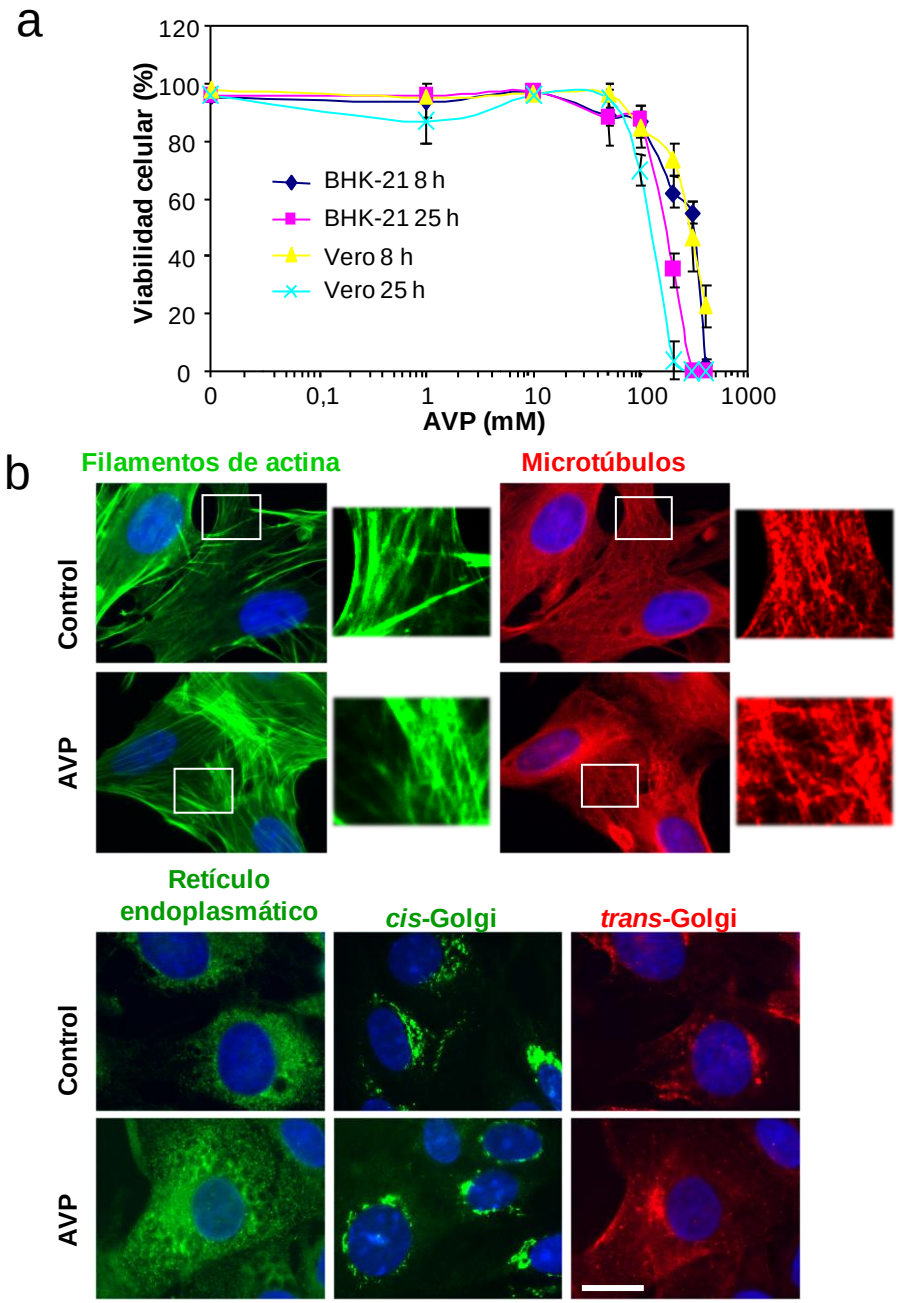

Figura 30. Efecto del AVP sobre la viabilidad celular. (a) Las células BHK-21 y Vero fueron tratadas con concentraciones crecientes de AVP durante 8 ó 25 h y la viabilidad celular fue determinada mediante tinción con azul Tripán. (b) Las células BHK-21 tratadas o no con 50 mM AVP durante 8 h fueron fijadas y procesadas para inmunofluorescencia. Para detectar los filamentos de actina se utilizó faloidina AF 488. El resto de las estrucuturas celulares se detectaron utilizando los siguientes anticuerpos: 196 (microtúbulos), 1D3 (retículo endoplásmico), 25H8 (*trans*-Golgi) y anti-caveolina (*cis*-Golgi). Los anticuerpos secundarios estaban acoplados a AF 488 o AF 555. Los núcleos teñidos con DAPI se muestran en azul. Barra: 20µm.

Tras un tratamiento de 8 h con el fármaco, el valor de TC_{50} fue de 244 mM para células BHK-21 y de 288 mM para células Vero. Cuando el tratamiento se mantuvo por un período de 25 h, estos valores fueron de 178 y 154 mM, respectivamente (Fig. 30a). Asimismo, se analizó mediante microscopía óptica de fluorescencia convencional la integridad de diferentes estructuras celulares como los microtúbulos, los filamentos de actina, el aparato de Golgi y el retículo endoplasmico, no observándose alteraciones en estas estructuras en las células tratadas con respecto a las células control (Fig. 30b).

5.4.2 El AVP no inhibe la entrada de VFA ni VEV

Se ha descrito que el AVP altera el metabolismo de lípidos, incluyendo el de los fosfolípidos (Shaltiel y col., 2004; Tokuoka y col., 2008; Xu y col., 2007). Durante la realización de esta Tesis doctoral, se había mostrado que la retirada del $PI(4,5)P_2$ de la membrana plasmática inhibe la entrada de VFA y VEV (apartado 5.1), por lo que se decidió estudiar el efecto del tratamiento con AVP (50 mM) sobre la distribución celular de este fosfolípido (Fig. 31a), no observándose diferencias entre las células control y las células tratadas. Por otro lado, también se analizó el efecto de este fármaco en la internalización de VFA y VEV (Fig. 31b). Para ello, se emplearon células BHK-21, tratadas o no con este fármaco, que fueron incubadas con los virus, analizándose por microscopia óptica de fluorescencia convencional la localización de las partículas virales (Fig. 31b).

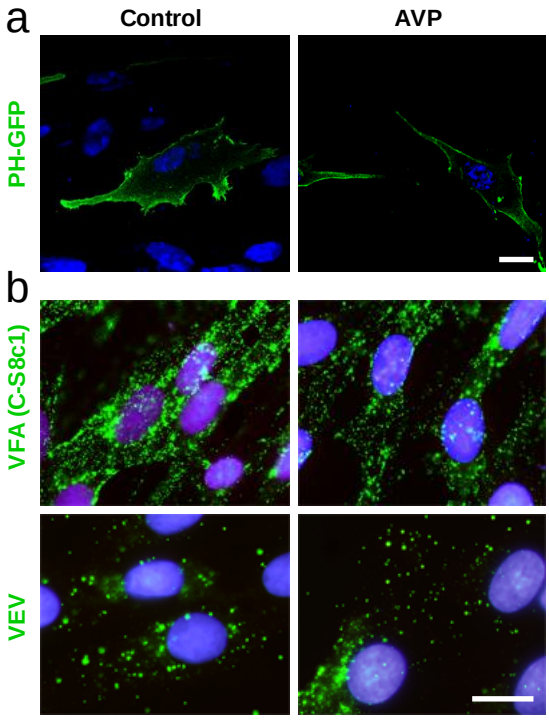

Figura 31. El AVP no inhibe la internalización de VFA ni de VEV. (a) El AVP no altera la distribución de $PI(4,5)P_2$ de la membrana plasmática. Las células BHK-21 fueron transfectadas con el plásmido PH-PLC-eGFP (PH-GFP) utilizando Lipofectamina Plus. A las 24 h p.t., las células fueron tratadas con AVP 50 mM durante 10 min, fijadas y procesadas para microscopía confocal. Los núcleos fueron teñidos con TO-PRO-3. Barra: 10 µm. (b) Efecto del tratamiento con AVP sobre la internalización de VFA y VEV. Las células BHK-21 tratadas o no con AVP como en (a) fueron infectadas con el virus correspondiente (m.d.i. de 70 UFP/célula) durante 25 min, fijadas y procesadas para inmunofluorescencia utilizando el anticuerpo primario 5C4 para detectar viriones de VFA y el anticuerpo I1 para los de VEV. El anticuerpo secundario estaba acoplado a AF 488. Los núcleos se tiñeron con DAPI. Barra: 10 µm.

Estos experimentos mostraron que el AVP no afecta significativamente la distribución del $PI(4,5)P_2$ de la membrana plasmática y, tampoco a la internalización de VFA ni de VEV, puesto que tanto las células control como las tratadas con AVP presentaron los viriones de VFA y VEV en su interior.

5.4.3 Efecto del AVP sobre la infección de otros virus

Tras un experimento preliminar que indicó que el AVP (50 mM) afectaba severamente la multiplicación de VEV, y no la de VFA, se analizó su efecto sobre la multiplicación de distintos virus con o sin envoltura en células BHK-21 y Vero (Fig. 32). En este experimento no se encontró una reducción significativa de la producción viral para ninguno de los virus sin envoltura analizados (VFA, EVB, VEMC y VREA).

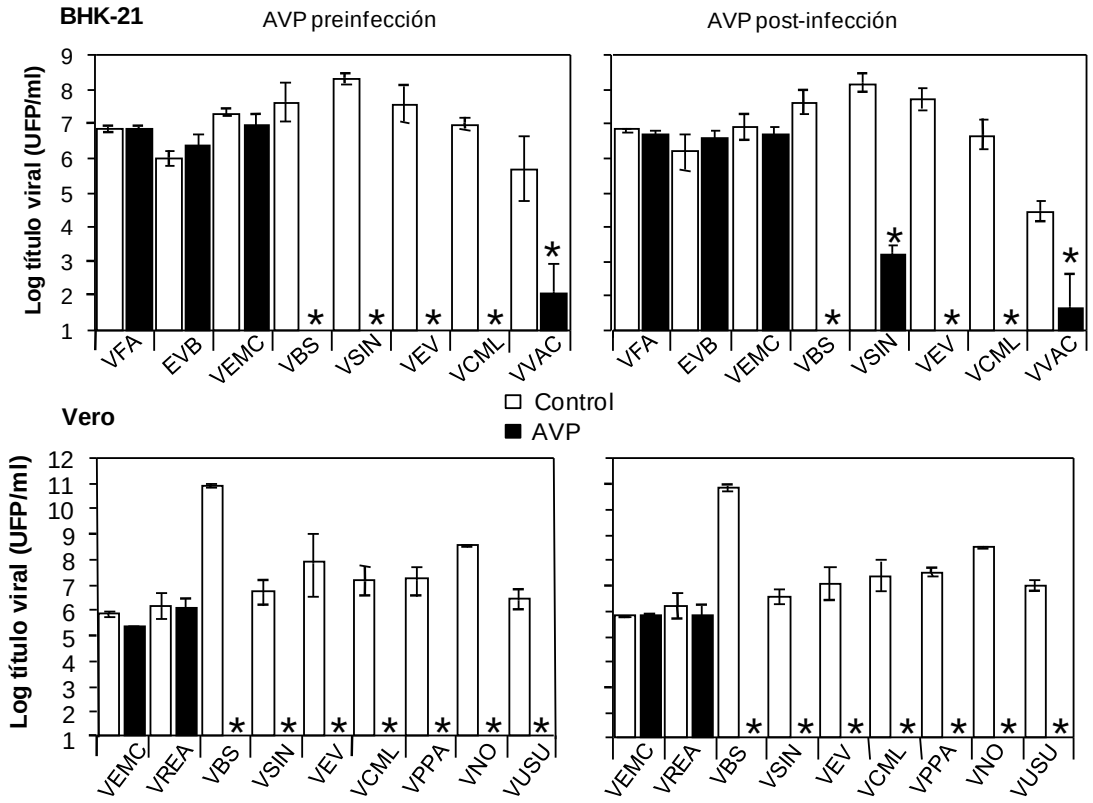

Figura 32. El AVP inhibe la producción viral de distintos virus con envoltura. Las células BHK-21 o Vero tratadas o no con 50 mM AVP, fueron infectadas con los virus indicados (m.d.i. de 0,5 UFP/célula) en medio líquido. El análisis preinfección corresponde a infecciones realizadas en presencia de AVP antes de la infección y durante ella. En el caso del análisis post-infección, el medio conteniendo AVP se añadió 2,5 h p.i y se mantuvo hasta el final de la infección.

Sin embargo, para los virus con envoltura se observó una inhibición total de la producción viral cuando el tratamiento con AVP se realizó antes de la infección y se mantuvo durante todo el proceso (VBS, VSIN, VEV, VCML, VPPA, VNO y VUSU), excepto en el caso de VVAC, cuya producción viral se vio reducida en torno a 4

órdenes de magnitud. Cuando se estudió el efecto del fármaco añadido 2,5 h p.i., se observaron inhibiciones similares (VBS, VEV, VCML, VPPA, VNO y VUSU), excepto para la infección de VSIN en células BHK-21. En este caso, la producción de VSIN se redujo en 4 órdenes de magnitud mientras que anteriormente la reducción fue total (7 órdenes de magnitud). El hecho de encontrar inhibiciones similares cuando el AVP se añdió 2,5 h p.i. o cuando se añadió pre-infección, sugiere que el efecto antiviral del AVP sobre la multiplicación de los virus con envoltura tendría lugar en etapas posteriores a la entrada viral.

5.4.4 La inhibición de las deacetilasas de histonas no afecta a la producción viral

La inhibición de las DACH es uno de los efectos asociados al AVP (Venkataramani y col., 2010; Wittenburg y col., 2010), habiéndose propuesto como un mecanismo para inducir reactivaciones (fases líticas) en infecciones virales latentes (Countryman y col., 2008; Ghosh y col., 2012; Lehrman y col., 2005; Lezin y col., 2007; Zhou y col., 2009). Para determinar si la inhibición de la producción viral de los distintos virus con envoltura estaba mediada por la inhibición de las DACH, se enpleó la tricostatina A (TSA), otro inhibidor de DACH (Fig. 33). El tratamiento con TSA provocó un incremento de los niveles de histonas acetiladas (Fig. 33a), pero no produjo un efecto significativo en la infección de los virus analizados (VFA, VSB, VSIN, VVAC, VCML, VPPA, VNO y VUSU) (Fig. 33b).

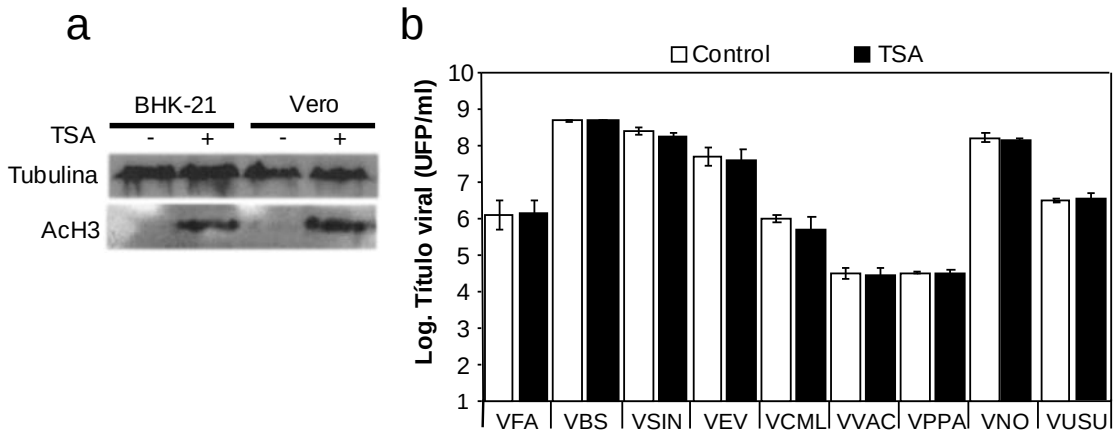

Figura 33. La inhibición de las deacetilasas de histonas no afecta la infección viral. (a) Las células BHK-21 y Vero fueron tratadas con 400 nM TSA durante 16 h, lisadas y procesadas para *Western blot*. Para analizar el efecto del fármaco se utilizó un anticuerpo frente a la histona 3 acetilada (AcH3). Los resultados obtenidos con un anticuerpo frente a tubulina βII se muetran como control de carga. (b) Las células BHK-21 o Vero tratadas o no con 400 nM TSA, fueron infectadas con los virus indicados (m.d.i. 0,5 de UFP/célula). El título viral fue determinado a las 7 ó 24 h p.i.

Estos resultados indican que la inhibición de las DACH no es la causa de la reducción de la producción viral provocada por el tratamiento con AVP.

5.4.5 La inhibición de VEV, VNO y VCML por el AVP es dependiente de dosis

A la vista de los resultados obtenidos tras el tratamiento con 50 mM AVP en la infección de los distintos virus con envoltura analizados (apartado 5.4.3), se determinó la concentración que inhibía el 50% de la producción viral (IC_{50}) para tres virus pertenecientes a diferentes familias virales: VEV (*Rhabdoviridae*), VNO (*Flaviviridae*) y VCML (*Arenaviridae*). Para los tres virus analizados se observó un efecto inhibitorio del AVP que fue dependiente de dosis, siendo los valores de IC_{50} de 0,6, 0,25 y 0,06 mM, respectivamente (Fig. 34a, c y e).

Para otros fármacos antivirales se ha descrito un efecto directo (viricida) sobre las partículas virales de virus con envoltura (Wolf y col., 2010). Para estudiar esta posibilidad, la misma cantidad de UFP de cada virus fue tratada con AVP, determinándose posteriormente su infectividad (Fig. 34b, d y f). En el caso de VEV y VCML no se encontraron diferencias significativas en la infectividad obtenida en las muestras tratadas con VPA con respecto a las muestras control (Fig. 34b y f). Sin embargo, en el caso de VNO se encontró una reducción de 2 órdenes de magnitud en la infectividad de las muestras tratadas por un periodo largo de tiempo (8 h) con respecto al control (Fig. 34d). Estos resultados indican que el AVP afecta de forma diferencial a las partículas virales de los virus estudiados, no inactivando a las de VEV y VCML, y haciéndolo, aunque a niveles bajos, con las de VNO. También sugieren que la reducción total del título viral provocada por el tratamiento con AVP está, principalmente, mediada por alteraciones intracelulares de las células infectadas.

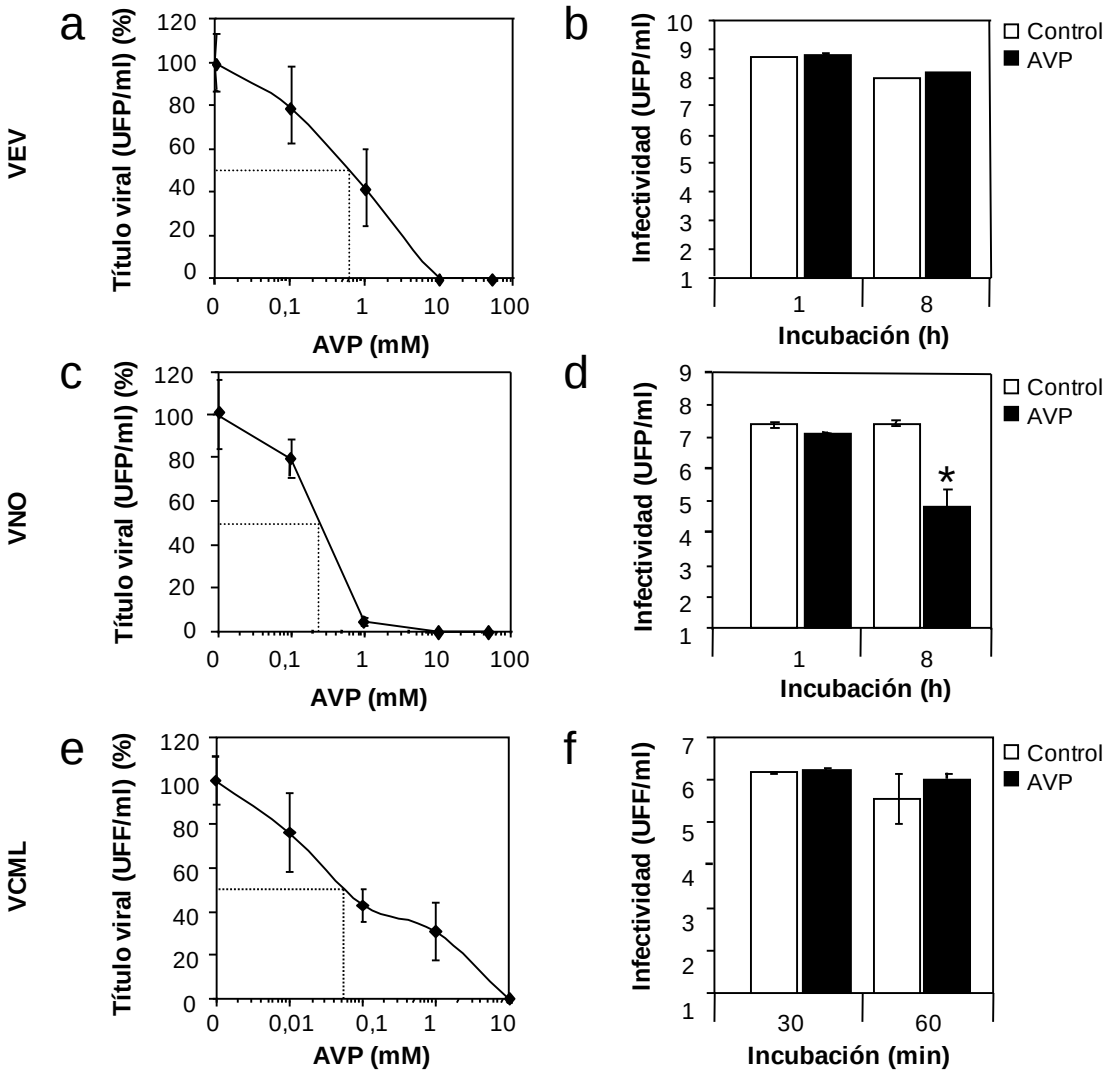

Figura 34. El AVP inhibe la producción viral de forma dependiente de dosis. (a) Las células BHK-21 se infectaron con VEV (m.d.i. de 0,5 UFP/célula) en presencia de diferentes concentraciones de AVP y el título viral fue determinado 7 h p.i. (b) Partículas de VEV incubadas con 50 mM AVP a 37º C durante 1 ó 8 h, tras lo que su infectividad fue determinada en células BHK-21. (c) Células Vero infectadas con VNO tal y como se describe en (a), posteriormente, el título viral fue determinado 24 h p.i. (d) Partículas virales de VNO incubadas con AVP como en (b) y su infectividad fue determinada en células Vero. (e) Células BHK-21 infectadas con VCML (m.d.i. de 0,01 UFF/célula) como se describe en (a); el título viral fue determinado a las 48 h p.i. (f) Partículas virales de VCML incubadas con 10 mM AVP a 37º C durante 30 ó 60 min, tras lo que su infectividad fue determinada.

5. 5 Caracterización del efecto del AVP en la infección de VEV

5.5.1 Efecto del AVP en la replicación de VEV

El tratamiento con AVP no inhibía la internalización de VEV (Fig. 31b) pero si bloqueaba la producción de este virus de forma dependiente de dosis (Fig. 34a). Para caracterizar los efectos producidos por este fármaco en pasos posteriores a la

internalización del virus, se llevaron a cabo experimentos en función del tiempo sobre la síntesis del RNA viral y la expresión de sus proteínas (Fig. 35), utilizando la concentración de AVP 50 mM, que inhibía completamente la producción de partículas infecciosas de VEV (Fig. 32). Como era de esperar, mientras que en las células control se detectó producción viral en el sobrenadante a tiempos cortos p.i., en las células tratadas con AVP no se detectó incluso después de 8,5 h p.i. (Fig. 35a). Cuando se realizó una inmunodetección de la glicoproteína G de VEV (G-VEV), se observó una reducción del porcentaje de células positivas a la fluorescencia de G-VEV en las células tratadas con respecto a las células control (Fig.35b). Mientras que en las células tratadas no se detectó un aumento significativo del número de células que expresaban G-VEV en función del tiempo, en las células control se observó un elevado incremento del porcentaje de células fluorescentes a partir de las 4,5 h p.i., tiempo en el que las células no tratadas estaban produciendo activamente virus (Fig. 35a). Este resultado sugiere que la progenie viral producida en las células control está siendo liberada al medio de infección pudiendo así infectar células vecinas, fenómeno que no ocurre en las células tratadas con AVP. Asimismo, el RNA viral se detectó a partir de las 4,5 h p.i. en las células control, mientras que en las células tratadas con AVP no se detectó hasta las 6,5 h p.i, siendo los niveles del RNA detectado menores que los observados en las células control (Fig. 35c).

Por otro lado, no se encontraron diferencias en el patrón de la distribución intracelular de la proteína G-VEV a lo largo de la infección (Fig. 35d). A las 2,5 h p.i. esta proteína se localizó de forma perinuclear, acumulándose en el aparato de Golgi. En las etapas más tardías de la infección (6,5 h p.i.) también se detectó en la periferia celular, donde los viriones sintetizados adquieren su envoltura. Cuando la proteína N de VEV procedente de células infectadas fue detectada mediante *Western blot*, se observó una reducción de la cantidad de ésta en las células tratadas con respecto a las células control (Fig. 35e).

Estos resultados indican que el AVP no bloquea la síntesis de RNA ni de proteínas, aunque se observa una menor detección de ambos en las células tratadas con AVP. Esto podría ser debido a que el AVP provoca que no haya rondas sucesivas de replicación o de infección de células vecinas, de forma que hay un menor número de células infectadas y por lo tanto menos cantidad de RNA y de proteínas.

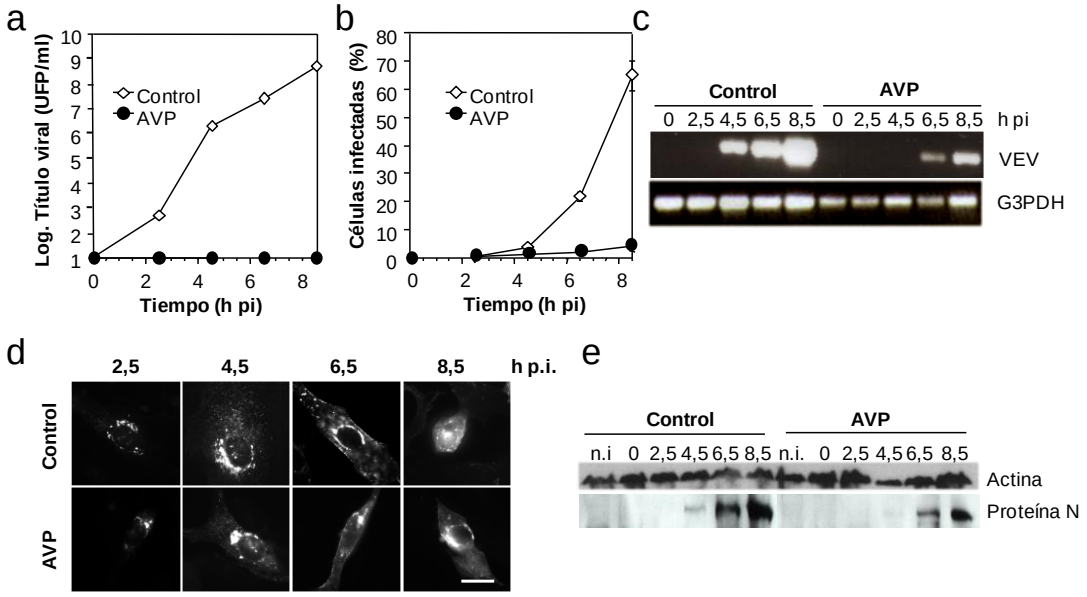

Figura 35. Efecto del AVP en la replicación de VEV. (a) Las células BHK-21 tratadas o no con 50 mM AVP se infectaron con VEV (m.d.i. de 0,5 UFP/célula). A los tiempos p.i. indicados se determinó el titulo viral en el sobrenadante. (b) Células BHK-21 crecidas en cubreobjetos infectadas como en (a) fueron fijadas y procesadas para inmunofluorescencia usando el anticuerpo I1 para detectar la proteína G-VEV. En la gráfica se muestra el porcentaje de células fluorescentes (infectadas) para cada tiempo. (c) El RNA viral total (intracelular y extracelular) procedente de cultivos infectados como en (a) fue extraído y amplificado por RT-PCR. La amplificación de G3PDH se utilizó como control interno del contenido de RNA celular. (d) Fotografías representativas de células infectadas positivas a G-VEV. Barra: 20 µm. (e) Detección de proteínas de VEV mediante *Western blot.* Las células BHK-21 fueron infectadas como en (a), lisadas y procesadas para *Western blot* usando un suero hiperinmune de cobaya frente a VEV Indiana. La migración de la banda que se muestra corresponde a la esperada para la proteína N de VEV. Los resultados obtenidos con un anticuerpo frente a β-actina se muestran como control de carga. Las células no infectadas se indican como n.i.

5.5.2 Efecto del AVP en la morfogénesis de VEV

En el caso del VEV, los nuevos viriones sintetizados adquieren su envoltura a partir de la membrana plasmática de la célula (Luan y col., 1995). Nuestros resultados indicaban que, a tiempos tardíos de infección, la proteína G-VEV se localizaba en la periferia celular de la misma manera en las células tratadas con AVP y en las no tratadas (Fig. 35d). Para analizar si el tratamiento con AVP estaba afectando a la formación de las partículas virales y a su liberación, se emplearon células BHK-21 que, tratadas o no con el fármaco, se infectaron con VEV y se procesaron para microscopía electrónica. Tanto en las células control, como en las tratadas con AVP, se observaron imágenes similares que correspondían al ensamblaje de las nuevas partículas de VEV (Zajac y col., 1970) (Fig. 36a). Cuando se cuantificó el número de partículas virales/µm de membrana, no se encontraron diferencias significativas entre las muestras control y las

tratadas con AVP (Tabla XIII). Tampoco se encontraron diferencias en la longitud y diámetro de las partículas virales que estaban gemando de la membrana plasmática. Para analizar si el AVP estaba afectando a la liberación de las partículas virales sintetizadas *de novo*, se procedió a purificar las partículas de VEV a partir de los sobrenadantes de cultivos tratados o no con AVP (apartado 4.6.1). Los preparados obtenidos fueron analizados mediante microscopía electrónica (Fig. 36a). En las muestras control se observaron partículas con forma de bala, correspondientes a viriones de VEV, con una frecuencia media de 31 ± 9,2 partículas/campo (20 campos). Por el contrario, en las muestras tratadas con AVP no se observó ninguna partícula similar a las encontradas para las muestras control, apreciándose agregados membranosos más pequeños (Fig. 36a). Por otra parte, cuando se determinaron las cantidades de RNA y de proteínas de VEV presentes en el medio extracelular (Fig. 36b), éstas fueron menores en las muestras tratadas con AVP que en las muestras control. Estos resultados indican que el AVP podría estar bloqueando el proceso de gemación de las partículas de VEV y/o alterando la composición de la envoltura de VEV, provocando que éstas sean menos estables en el medio de infección o durante el proceso de purificación.

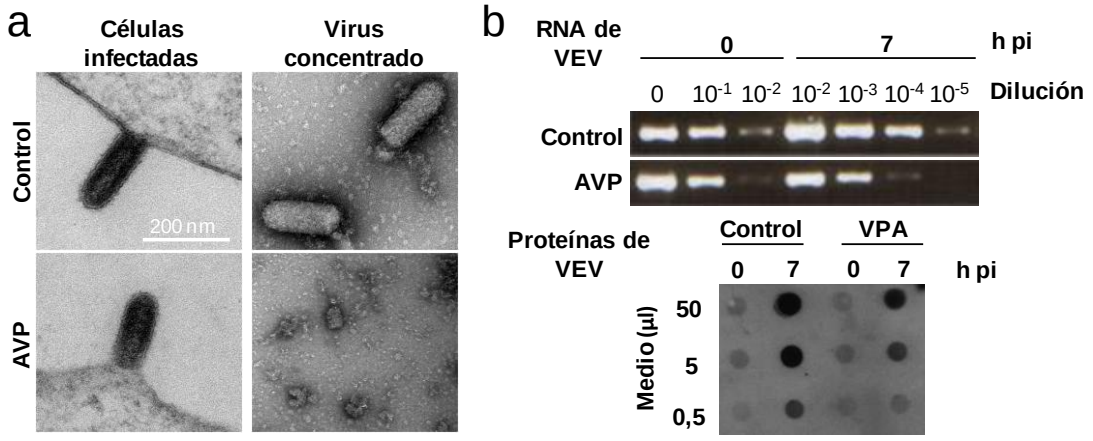

Figura 36. Efecto del AVP en la morfogénesis de las partículas de VEV. (a) Las células BHK-21 tratadas o no con 50 mM AVP fueron infectadas con VEV (m.d.i. de 70 UFP/célula). A las 7 h p.i. las células se fijaron y se procesaron para microscopía electrónica. Las partículas de VEV liberadas al medio se concentraron y se procesaron para microscopía electrónica. (b) Amplificación por RT-PCR del RNA de VEV y detección de las proteínas de VEV mediante *dot blot* del medio extracelular de las células infectadas como se describe en (a).

Tabla XIII. Efecto del tratamiento con AVP en la frecuencia de gemación de las partículas de VEV y en su tamaño

		Control	VPA	*P*
Frecuencia de gemación de partículas de VEV[a]		$3{,}67\times10^{-3}\pm0{,}0136$	$4{,}65\times10^{-3}\pm0{,}0178$	0,826
Tamaño de la partícula[b] (nm)	Longitud	160,61±35,57	144,61±38,00	0,088
	Diámetro	63,01±10,50	63,29±8,46	0,394

[a] La frecuencia de gemación de las partícuals de VEV se calculó como la media del número de partículas en gemación/µm de superficie celular analizada (n = 29 células).

[b] El tamaño medio de las partículas de VEV en proceso de gemación se determinó midiento 57 partículas virales en las células control y 24 partículas en las tratadas con AVP.

5.6 Caracterización del efecto del AVP en la infección de VNO

5.6.1 Efecto del AVP en la replicación de VNO

De la misma manera que para el VEV, se analizó la producción viral de VNO en función del tiempo. En estos experimentos se observó que mientras en las células control se detectaba producción viral en el medio de infección, no se recuperó virus en el caso de las células tratadas con 50 mM AVP, incluso tras 24 h p.i. (Fig. 37a). Asimismo, a diferencia de lo descrito para VEV, en el caso de VNO no se detectó expresión de proteínas virales ni del RNA viral en las células tratadas con AVP en ninguno de los tiempos analizados (Fig. 37b y c). Estos resultados indican que el AVP produce un bloqueo de la replicación y traducción del RNA viral de VNO.

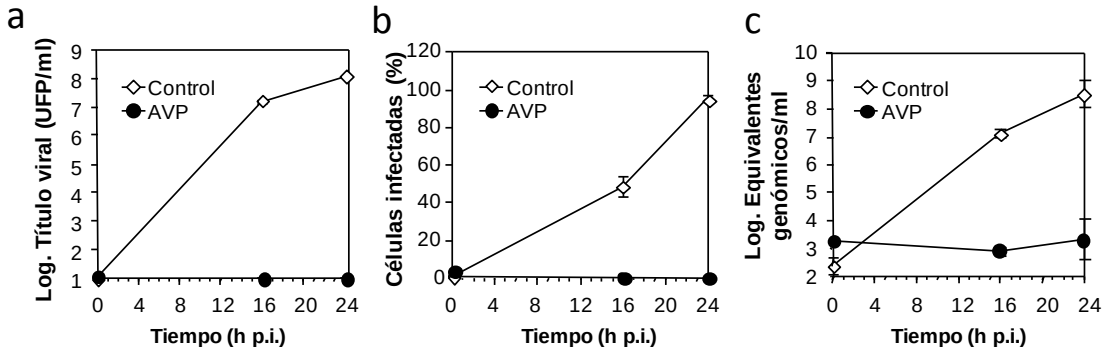

Figura 37. Efecto del AVP en la replicación de VNO. (a) Las células Vero tratadas o no con 50 mM AVP se infectaron con VNO (m.d.i. 0,5 de UFP/célula) y el título viral del medio extracelular se determinó a los tiempos p.i. indicados. (b) Las células Vero crecidas en cubreobjetos e infectadas como en (a) se fijaron a los tiempos p.i. indicados y se procesaron para inmunofluorescencia utilizando el anticuerpo 3.67G frente a la glicoproteína E de VNO. En la gráfica se representa el porcentaje de células fluorescentes (infectadas) para cada tiempo. (c) El RNA viral total (intracelular y extracelular) de células infectadas como en (a) fue extraído y amplificado mediante RT-PCR cuantitativa (ver apartado 4.24).

5.7 Caracterización del efecto del AVP en la infección de VCML

5.7.1 Efecto del AVP en la producción de VCML

Para determinar el efecto del AVP sobre la infección de VCML se utilizó una concentración de 10 mM de este fármaco, en lugar de 50 mM, debido a que los tiempos de infección con VCML eran más largos que con los virus empleados anteriormente. Esta concentración no provocó un efecto tóxico sobre las células tras 48 ó 72h de tratamiento, siendo los valores de TC_{50} de 100 mM y 30 mM, respectivamente (Fig. 38).

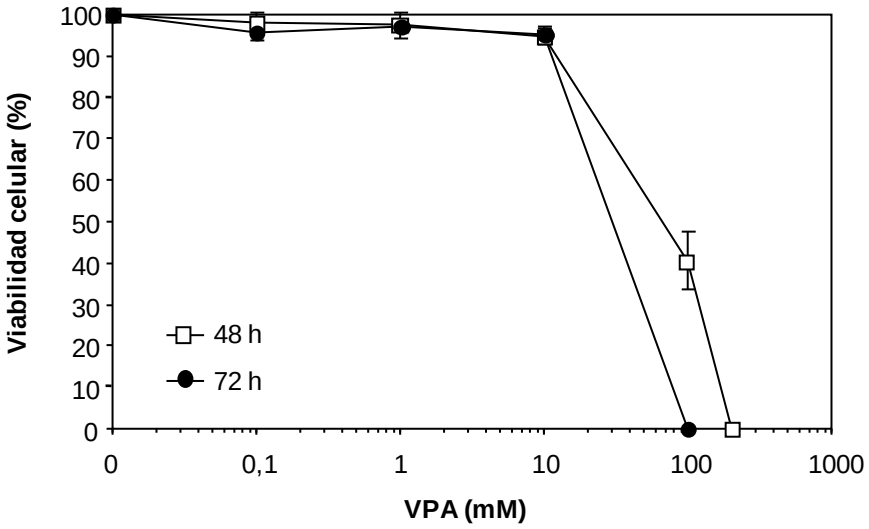

Figura 38. Efecto del AVP sobre la viabilidad de las células BHK-21. Las células BHK-21 fueron tratadas con concentraciones crecientes de AVP durante 48 o 72 h y la viabilidad celular fue determinada mediante tinción vital con azul Tripán.

A continuación, se analizó la producción viral en función del tiempo de r3-VCML-GFP, un VCML recombinante que expresa GFP. Para ello se infectaron células BHK-21 que se fijaron a distintos tiempos (Fig. 39a). A las 16 h p.i. se encontraron células positivas para GFP (células infectadas), cuyo número fue incrementándose en los tiempos posteriores, tanto en las células control como en las tratadas con AVP. Aunque la concentración de AVP utilizada no bloqueó la expresión de GFP, el porcentaje de células positivas para GFP fue menor que en las células control, observándose diferencias estadísticamente significativas a las 48 y 72 h p.i. (Fig. 39b). Estos resultados sugieren que la progenie viral de VCML de las células control estaba siendo liberada al medio e infectando nuevas células de manera más eficiente que la de las células tratadas con AVP. De forma compatible con esta hipótesis, el título viral observado en los sobrenadantes de cultivos infectados tratados con AVP fue significativamente menor a las 16, 24, 48 y 72 h p.i., siendo esta reducción de unos 3 a 5 órdenes de magnitud (Fig. 39c). Estos resultados fueron similares a los observados con

un aislado no modificado de VCML, que no expresa GFP (Fig. 39d). Como se describe en el apartado 5.4.5, el AVP no tiene ningún efecto directo sobre la infectividad de las partículas virales de VCML. Un análisis similar con las partículas del virus r3-VCML-GFP confirmó que el AVP tampoco tenía un efecto viricida para r3-VCML-GFP (datos no mostrados).

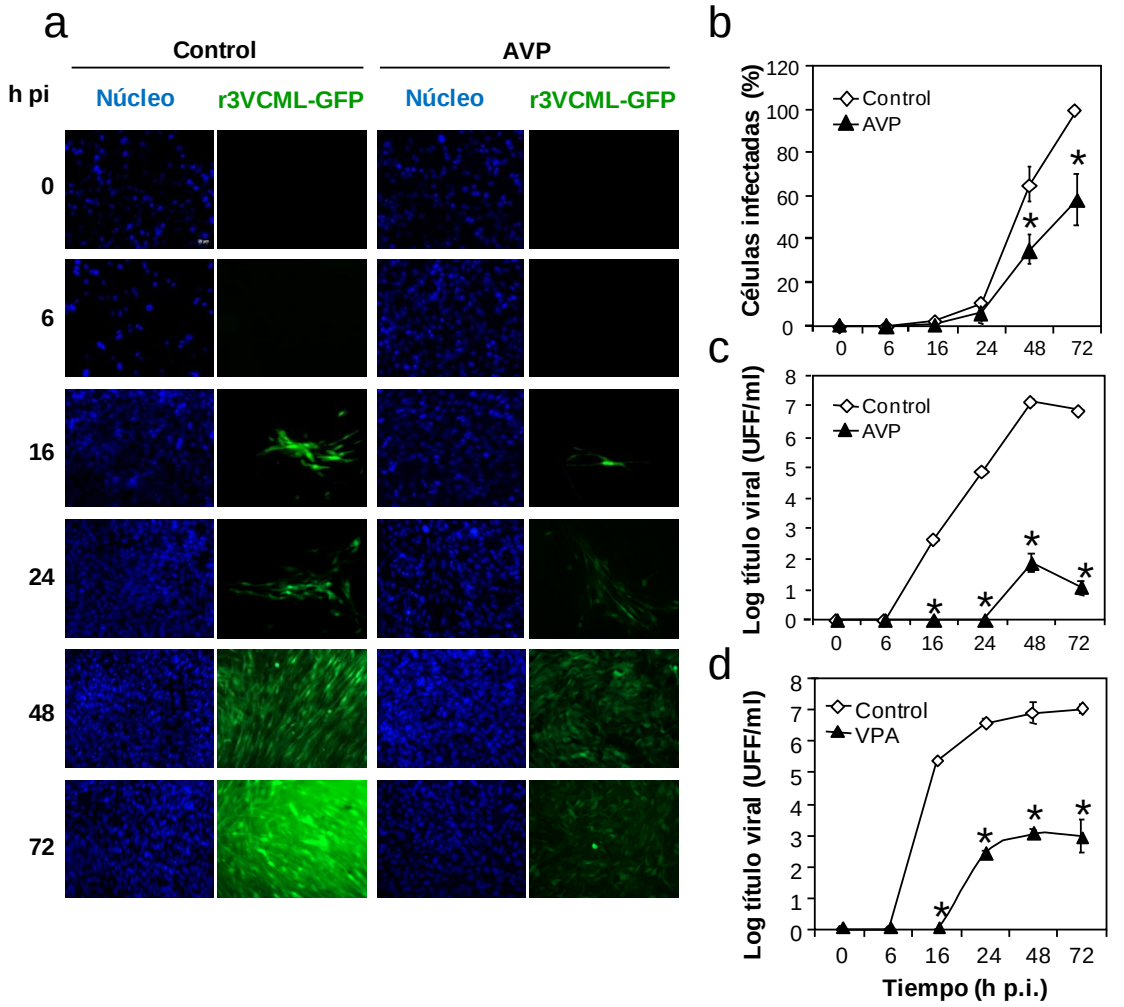

Figura 39. Efecto del AVP en la infección de VCML. (a) Las células BHK-21 crecidas sobre cubreobjetos se infectaron con r3-VCML-GFP (m.d.i. de 0,01 FFU/célula) conteniendo o no 10 mM AVP, se fijaron a los tiempos indicados y se prepararon para la observación en el microscopio. Los núcleos se tiñeron con DAPI. (b) Representación del porcentaje de células infectadas en (a). (c) A los tiempos p.i. indicados se determinó el título viral del medio extracelular en cultivos infectados como en (a). (d) El mismo experimento que en (c) fue realizado con el aislado VCML que no expresa GFP.

5.7.2 Efecto del AVP en la replicación de VCML

Para determinar los posibles efectos del AVP sobre la replicación de VCML, se realizó un análisis de la síntesis de RNA viral intracelular mediante *Northern blot*. En células BHK-21 infectadas con r3-VCML-GFP, se detectó el RNA de la proteína viral

NP a partir de las 16 h p.i., tanto en las células control como en las células tratadas con AVP, siendo los niveles de RNA detectados similares en ambos casos (Fig. 40a). Cuando se analizó la síntesis de RNA viral durante la infección del aislado VCML Arm (Fig. 40b), se obtuvieron resultados similares a los obtenidos para r3-VCML-GFP, lo que indica que el AVP no inhibe la replicación del RNA de VCML.

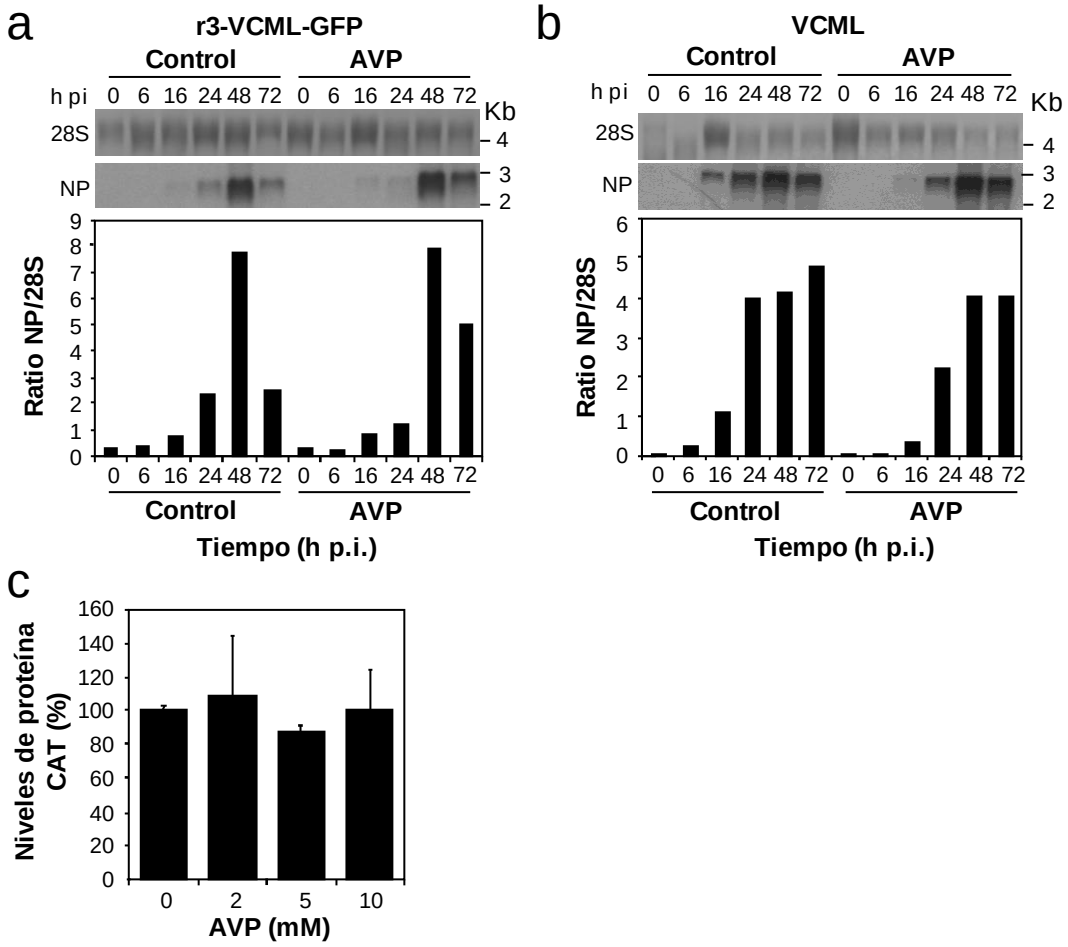

Figura 40. Efecto del AVP en la replicación de VCML. (a) Las células BHK-21 se infectaron con r3-VCML-GFP (m.d.i. de 0,01 UFF/célula) en medio líquido conteniendo o no 10 mM AVP. A los tiempos p.i. indicados se extrajo el RNA intracelular y los niveles de RNA viral de NP de VLCM se detectaron mediante *Northern blot.* En la gráfica se muestra la relación de la densidad de la banda obtenida frente a NP y el rRNA 28S. (b) Las células BHK-21 fueron infectadas con VCML y los niveles de RNA viral intracelular se detectaron como en (a). (c) Efecto del AVP sobre la replicación del minigenoma de VCML. Las células BHK-21 fueron transfectadas con los plásmidos Pol I MG-CAT, pCAGGS-NP y pCAGGS-L utilizando Lipofectamina 2000 y los niveles de proteína CAT fueron determinados a las 48 h p.t.

Estos experimentos se complementaron con un análisis de la replicación de RNA de VCML mediante un ensayo que empleaba un minigenoma de este virus (apartado 4.14). Este ensayo consistió en la contransfección de los plásmidos pCAGGS-NP, pCAGGS-L y pol I MG-CAT; de tal forma que la expresión del RNA del gen *reporter*

CAT, mediada por la polimerasa L de VCML, se detecta indirectamente mediante un ELISA frente a la proteína CAT. Mediante este sistema se estudió el efecto de distintas concentraciones de AVP sobre la replicación mediada por la proteína L, no observándose en ningún caso diferencias con el control (Fig. 40c). Estos resultados confirman que el efecto inhibitorio del AVP sobre la infección de VCML no se debe a una inhibición de la replicación del RNA viral.

5.7.3 El AVP inhibe la gemación mediada por la proteína Z de manera dependiente de dosis

Puesto que el AVP no inhibía la replicación del material genético de VCML (apartado anterior), se analizó si la actividad antiviral del fármaco estaba relacionada con el proceso de ensamblaje y la liberación de las partículas virales. Para determinar el efecto del AVP sobre la gemación de VCML se realizó un ensayo de gemación mediada por la proteína Z del virus, el cual está basado en la capacidad de la proteína Z de permitir la producción de VLP en ausencia de otros elementos virales (Pérez y col., 2003). Para ello, se transfectaron células 293T con el plásmido Z-Flag, que codifica la proteína Z fusionada a un epitopo Flag, que posteriormente se trataron con distintas concentraciones de AVP (apartado 4.15). A continuación, se procedió a detectar la proteína Z localizada en las VLP (medio extracelular) y la localizada en el interior celular, mediante *Western blot* (Fig. 41a).

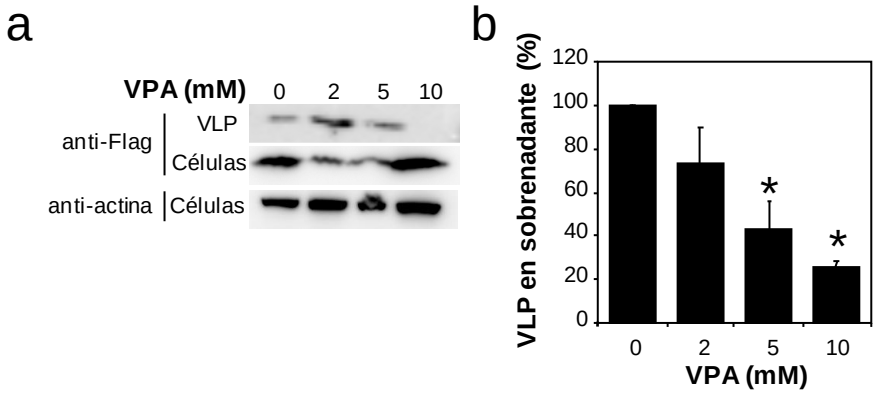

Figura 41. El AVP inhibe la gemación inducida por la proteína Z de manera dependiente de dosis. (a) Las células 293T fueron transfectadas con un plásmido que expresa una fusión de la proteína Z de VCML con el epítopo Flag. A las 16 h p.t. se añadió medio fresco conteniendo distintas concentraciones de AVP (0, 2, 5 o 10 mM) y tras 24 h se recogieron las VLP del medio extracelular y, por otro lado, los lisados celulares. La proteína Z recuperada se detectó mediante *Western blot* utilizando un anticuerpo que reconoce el epítopo Flag. Los resultados obtenidos con un anticuerpo frente a actina se muestran como control de carga. (b) Representación gráfica del porcentaje de VLP (proteína Z detectada en sobrenadante) normalizado frente al valor total de proteína Z.

Los niveles de proteína Z detectados en las VLP con respecto al total de proteína Z expresada fueron menores en los cultivos tratados con AVP (Fig. 41b). Esta reducción fue dependiente de dosis, indicando que el AVP inhibe la gemación mediada por la proteína Z.

5.7.4 El AVP reduce el número de partículas de VCML liberadas

Puesto que el AVP inhibía la gemación mediada por la proteína Z, se estudió si el tratamiento con este fármaco podría interferir en la liberación de las partículas virales. Para ello, se infectaron células BHK-21 con el aislado VCML Arm, que se trataron o no con AVP y se fijaron para microscopía electrónica. En ambos casos se observaron células con zonas ricas en vesículas de doble membrana características de las células infectadas (Fig. 42a), así como partículas de VCML localizadas en vesículas celulares (Fig. 42b). Cuando las partículas de VCML recuperadas del medio de infección (ver apartado 4.6.2) se analizaron mediante microscopía electrónica para determinar si el AVP producía algún efecto en la morfología y tamaño de éstas, no se encontraron diferencias significativas entre las muestras control y las tratadas (Fig. 42c y d). Sin embargo, cuando se cuantificó el número de partículas virales, se encontró una reducción estadísticamente significativa en las muestras tratadas con AVP (Fig. 42e), confirmando que el tratamiento con AVP produce una reducción de la liberación de las partículas de VCML.

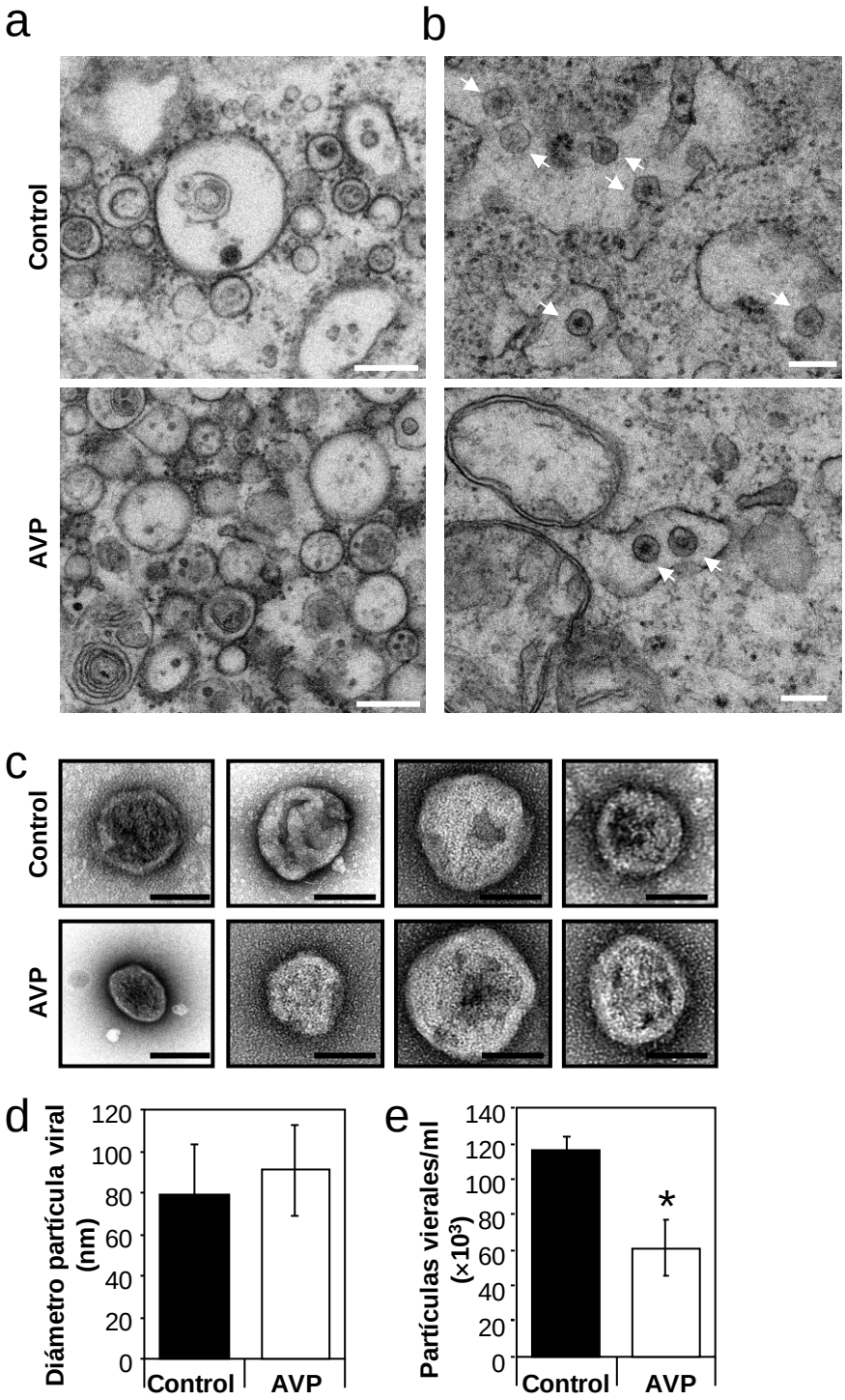

Figura 42. El AVP reduce la liberación de partículas de VCML. (a y b) Las células BHK-21 infectadas con VCML (m.d.i. de 1 UFP/célula) en medio líquido conteniendo o no 10 mM AVP se fijaron y procesaron para microscopía electrónica a las 24 h p.i. Barra: 200 nm. (a) El AVP no inhibe la capacidad de VCML de producir vesículas en células infectadas. (b) Partículas de VLCM en vesículas intracelulares. (c) Fotografías representativas de partículas virales de VCML purificadas a partir del medio extracelular de células infectadas como en (a). Barra: 50 nm. (d) Diámetro de las partículas virales recuperadas del medio extracelular (n = 20 partículas virales). (e) Cuantificación de partículas virales liberadas al medio extracelular. Las partículas virales producidas en células tratadas o no con AVP fueron purificadas, fijadas e incubadas con partículas de látex con una concentración conocida. A continuación, el número de partículas virales fue determinado mediante microscopía electrónica en dos purificaciones independientes (n = 20 campos por purificación).

Discusión

6. Discusión

6.1 Etapas tempranas en la infección de VFA

6.1.1 Importancia del PI(4,5)P_2 de la membrana plasmática en la internalización de VFA

El PI(4,5)P_2 es un fosfolípido localizado mayoritariamente en la cara interna de la membrana plasmática. Este lípido controla la actividad de un gran número de proteínas por medio de uniones espacio-temporales, lo que hace que tenga un papel muy importante en distintos procesos celulares, como son la generación de curvatura de membrana, la endocitosis, la exocitosis y la motilidad celular (Antonescu y col., 2011; De Matteis y col., 2004; Di Paolo y col., 2006; James y col., 2008b; Shewan y col., 2011; Zoncu y col., 2007). En el caso concreto de la endocitosis mediada por clatrina, se ha descrito que el PI(4,5)P_2 tiene un papel destacado debido a la unión con proteínas implicadas en el proceso de formación de la vesícula revestida de clatrina y a la inducción de la curvatura necesaria para dar lugar a la vesícula (para más detalles ver apartado 2.2.1). Una de estas proteínas es la dinamina, que se encarga de producir la escisión de la vesícula revestida de clatrina (Loerke y col., 2009; Takei y col., 1995; Takei y col., 2005).

En esta Tesis Doctoral se ha estudiado la implicación de la dinamina en la internalización del aislado de VFA C-S8c1 y de MARLS, un derivado de C-S8c1 que puede utilizar receptores diferentes a las integrinas (Baranowski y col., 2000). Además, se llevo a cabo un estudio comparativo con VEV, cuya ruta de entrada dependiente de clatrina está bien caracterizada (Cureton y col., 2009; Johannsdottir y col., 2009; Matlin y col., 1982; Simpson y col., 1969; Sun y col., 2005; Superti y col., 1987). La expresión de una forma dominante negativa de la dinamina inhibe tanto la internalización de los viriones como la producción de VFA (C-S8c1 y MARLS) y de VEV en células BHK-21 (Fig. 13). Estos resultados son compatibles con otros estudios que demuestran que proteínas que interaccionan con el PI(4,5)P_2, entre ellas la dinamina, son importantes para la entrada de diferentes virus (Abe y col., 2008; Aleksandrowicz y col., 2011; Ang y col., 2010; Chen y col., 2008; DeTulleo y col., 1998; Hernáez y col., 2010; Huang y col., 2011; Perry y col., 2010; Pizzato y col., 2007; Rahn y col., 2011).

Puesto que estos datos sugerían que el PI(4,5)P_2 podía tener un papel importante en los procesos de entrada viral, se analizó el requerimiento del PI(4,5)P_2 de la

membrana plasmática en la internalización de VFA y VEV. Para ello se emplearon tratamientos farmacológicos con ionomicina y 1-butanol, que afectan al metabolismo del $PI(4,5)P_2$ de la membrana plasmática (Boucrot y col., 2006; Zoncu y col., 2007). Mientras que la ionomicina provocó una alteración en la distribución de éste, el 1-butanol no lo hizo (Fig. 14a y 15a). Una posible explicación para estos resultados vendría dada porque la ionomicina provoca una retirada del $PI(4,5)P_2$ de la membrana plasmática (Zoncu y col., 2007), mientras que el 1-butanol sólo inhibe la síntesis de este fosfolípido (Boucrot y col., 2006). Los tratamientos con ionomicina y 1-butanol inhibieron la internalización de TF, ligando modelo de endocitosis mediada por clatrina (Miller y col., 1991), en células BHK-21, confirmando así que estos fármacos bloquean la endocitosis mediada por clatrina de este ligando en este tipo celular. Tanto el tratamiento con ionomicina como el tratamiento con 1-butanol inhibieron significativamente la internalización de los viriones de VFA (C-S8c1 y MARLS) y VEV (Fig. 14cy 15c). Asimismo, las inhibiciones obtenidas fueron similares cuando se utilizó un sistema inducible que produce la retirada del $PI(4,5)P_2$ en células BHK-21 (Fig. 16b). En conjunto, estos resultados indican que tanto VFA como VEV requieren la presencia de $PI(4,5)P_2$ en la membrana plasmática para poder ser internalizados, aunque el variante de VFA, MARLS, presenta un menor requerimiento que C-S8c1. Una posible explicación para esta diferencia es que MARLS es capaz de utilizar distintos receptores que C-S8c1 para entrar en las células (Baranowski y col., 2000), entre ellos HS, lo cual podría permitirle la utilización de rutas de entrada alternativas. De hecho, los variantes de VFA que usan HS como receptor entran en la célula siguiendo un mecanismo de endocitosis mediado por caveolas (O'Donnell y col., 2008), mientras que los variantes de VFA que usan integrinas como receptor siguen una ruta dependiente de clatrina (Berryman y col., 2005; Martín-Acebes y col., 2007; O'Donnell y col., 2005). De este modo, MARLS podría estar usando la vía de las caveolas para ser internalizado en la célula. Aunque el $PI(4,5)P_2$ es necesario para la formación de caveolas y vesículas revestidas de clatrina, los niveles de $PI(4,5)P_2$ son más constantes en las vesículas revestidas de clatrina que en las caveolas, lo que es posiblemente debido a las uniones del $PI(4,5)P_2$ con varias de las proteínas que están implicadas en el proceso de formación de la vesícula revestida de clatrina (Fujita y col., 2009). Esto podría explicar las diferencias de requerimiento de $PI(4,5)P_2$ encontradas entre C-S8c1 y MARLS.

6.1.2 Papel de la acidificación endosomal en la infección de distintos variantes de VFA

Los virus utilizan distintos mecanismos para asegurarse de que la cápsida se desensambla dentro de la célula hospedadora y en el compartimento celular adecuado, como por ejemplo el pH ácido de los compartimentos endosomales (Mackenzie y col., 2007; Marsh y col., 2006; Smith y col., 2004), reacciones de isomerización de puentes disulfuro en el retículo endoplásmico (Schelhaas y col., 2007) o una combinación de ambas estrategias (Jiang y col., 2009). El modelo aceptado para la desencapsidación de VFA está basado en la acidifcación endosomal, de forma que la cápsida sólo se desensambla dentro de los endosomas en un entorno ácido adecuado. Una vez que el VFA ha sido internalizado en la célula siguiendo la ruta de entrada mediada por clatrina (Berryman y col., 2005; Martín-Acebes y col., 2007; O'Donnell y col., 2005) se dirige hacia los endosomas tempranos de manera dependiente de Rab5 (Johns y col., 2009), donde posiblemente se produzca la liberación de su material genético, puesto que el valor de $pH_{50}D$ (6,6) corresponde con el pH del interior de los endosomas tempranos (6,8–6,1) (Huotari y col., 2011; Maxfield y col., 1987). De la misma manera, se ha sugerido que las variantes de VFA que utilizan HS como receptor también son transferidas hacia compartimentos endosomales (O'Donnell y col., 2009). A pesar de que los variantes de VFA C-S8c1 y MARLS utilizan distintos receptores para entrar en la célula, nuestros resultados muestran que los dos requieren la funcionalidad de la proteína Rab5 y presentan valores de $pH_{50}I$ similares. Además, cuando se bloqueó la acidificación endosomal con NH_4Cl la producción de ambos virus se inhibió de manera similar. Todos estos resultados indican que a pesar de sus diferencias en el receptor celular utilizado y en el requerimiento de $PI(4,5)P_2$ para ser internalizados dentro de la célula, los dos variantes de VFA siguen la misma ruta de tráfico vesicular para liberar su genoma.

En el laboratorio se habían descrito con anterioridad distintos mutantes de C-S8c1 con diferencias en sus requerimientos de acidificación endosomal (Martín-Acebes, 2009). Mientras que el virus m6 tiene una resistencia a pH ácido incrementada y es más sensible al tratamiento con NH_4Cl, el virus c2 tiene una sensibilidad a pH ácido incrementada siendo resistente al tratamiento con NH_4Cl. De esta manera, el virus parental (C-S8c1) representaría un fenotipo intermedio entre ambos mutantes. También, se había observado la existencia de una correlación entre el valor de $pH_{50}I$ y la inhibición producida por el tratamiento con NH_4Cl de estos mutantes, de forma tal que

cuanto más ácidos eran los valores de pH mayor era la inhibición producida por el tratamiento con NH_4Cl (Martín-Acebes, 2009). Como se muestra en la Fig. 19b, esta misma correlación se observó tras la inhibición de la acidificación endosomal producida por el tratamiento combinado con los ionóforos monensina y nigericina.

Entre los procesos que dan lugar a la maduración de los endosomas tempranos a endosomas tardíos se encuentran su acidificación progresiva y el intercambio de la proteína Rab5 presente en sus membranas por la proteína Rab7 (para más detalle ver el apartado 2.3.2). Utilizando los diferentes variantes de VFA con distintos valores de pH de desencapsidación (definido como el $pH_{50}I$), se decidió estudiar el efecto de la expresión de versiones dominantes negativas (DN) de las proteínas Rab5, Rab7 y Rab11 sobre la infección de los mismos (Fig. 20). Los resultados obtenidos indican que aunque sólo la expresión de Rab5 DN inhibió significativamente la producción viral de C-S8c1, c2 y m6, se encontró una correlación entre los valores de pH de desencapsidación de los virus y el requerimiento de las proteínas Rab, de manera que, cuanto más ácido es el valor de pH de desencapsidación, el virus depende en mayor medida de las proteínas Rab que controlan el tráfico hacia los endosomas tempranos (Rab5) (Fig. 20b), y en menor medida de aquellas que controlan el tráfico que sale de los endosomas tempranos hacia los tardíos (Rab7) o los de reciclaje (Rab11) (Fig. 20d y e). El valor del pH de desencapsidación del virus c2 (6,95) está cerca del pH que se empieza a encontrar en los endosomas tempranos (6,8), siendo posible que este proceso tenga lugar en la vesícula de endocitosis formada antes de fusionar con un endosoma temprano. Además, aunque el pH de desencapsidación de los virus C-S8c1 y m6 está en el rango de pH del interior de los endosomas tempranos (6,8–6,1) (Huotari y col., 2011; Maxfield y col., 1987), las diferencias en el requerimiento de proteínas Rab podrían ser debidas al proceso de maduración de los endosomas. Ésta es una maduración progresiva, de forma que el entorno proteico va modificándose y el pH del lumen va acidificándose (Huotari y col., 2011) (para más detalle ver apartado 2.3.2). Esto podría dar lugar a que en el momento de desencapsidación de cada virus los endosomas tempranos no estén en el mismo estadio de maduración, el cual se ve regulado mediante el contenido en GTPasas Rab. Por otro lado, estudios previos sugieren que el VFA podría ser parcialmente transportado a los endosomas tardíos y lisosomas para su degradación (Berryman y col., 2005; O'Donnell y col., 2005). En línea con esta posibilidad, cuando se inhibió el tráfico de los endosomas tempranos a los endosomas tardíos por la expresión de la proteína Rab7 DN, el virus m6, mostró una mayor eficiencia de infección que el virus c2, lo que

podría ser explicado por la acumulación del virus m6 en los endosomas tempranos en lugar de ser parcialmente transportado hasta los endosomas tardíos y lisosomas. Por otro lado, se ha sugerido que la desencapsidación de VFA podría no suceder exclusivamente en los endosomas tempranos ya que una pequeña proporción de virus podrían desencapsidar en los endosomas de reciclaje debido a los efectos de la expresión de Rab 11 DN (Johns y col., 2009). Esta hipótesis es compatible con lo que se ha observado para el virus c2, el cual es más sensible a la expresión de Rab11 DN (aunque las diferencias no son estadísitcamente significativas), lo que sugiere que la desencapsidación de c2 podría tener lugar en una población de endosomas tempranos más cercana a endosomas de reciclaje que los virus C-S8c1 y m6.

Aunque las diferencias encontradas en los valores de pH de desencapsidación entre el virus parental C-S8c1 y los mutantes c2 y m6, no dieron lugar a alteraciones de la infectividad en cultivos celulares (Martín-Acebes, 2009), si se encontraron diferencias en ensayos de infectividad *in vivo*. Los dos mutantes presentaron una infectividad en ratones lactantes disminuida con respecto a C-S8c1, siendo el virus c2 el menos infectivo (Tabla X). Estas diferencias encontradas entre el virus c2 y m6 podrían deberse a que los viriones de c2 son más lábiles, puesto que tienen una tendencia incrementada con respecto al m6 a disociarse (Martín-Acebes y col., 2010; Martín-Acebes y col., 2011c), lo que podría tener efectos negativos para su eficacia biológica *in vivo*. Mientras que, en principio, la extrema sensibilidad a pH ácido de VFA no parece estar selectivamente restringida en el ambiente tamponado en el que se crecen las lineas celulares, esto no es probablemente así en un contexto *in vivo*. La desencapsidacion de VFA probablemente se produce a un valor de pH óptimo, de manera tal que manipular éste puede producir una disminución del *fitness in vivo*. Esto puede ser debido a que la estabilidad de la cápsida es el resultado evolutivo de un balance muy fino entre estabilidad para proteger el genoma del medio ambiente y labilidad para permitir la salida del mismo en un entorno adecuado para la replicación.

En resumen, los cambios en la especificidad de receptor de VFA no causan alteraciones ni en el requerimiento de acidificación endosomal que da lugar a la desencapsidación ni en el requerimiento de la proteína Rab5. Sin embargo, las diferencias en los valores de pH de disociación correlacionan con una sensibilidad diferencial a la inhibición de la acidificación endosomal y a la dependencia de

distintas proteínas Rab, revelando una relación entre el requerimiento de las proteínas Rab y el pH de desencapsidación. A su vez, las variaciones del pH de desencapsidación de VFA producen una disminución de la virulencia *in vivo.*

6.2 Mutantes de VFA con diferentes grados de sensibilidad a pH ácido

El NH_4Cl se comporta como una base débil y en su forma no protonada difunde fácilmente a través de las membranas; sin embargo, en los compartimentos ácidos se protona y se acumula aumentando el pH de los mismos (Marsh y col., 1989). La capacidad de liberar el material genético a un valor de pH más alto (necesitando menor acidificación) es un mecanismo que se ha descrito en mutantes aislados en otros virus como el virus de la gripe (Daniels y col., 1985; Doms y col., 1985) o el VEV (Fredericksen y col., 1998). Resultados previos obtenidos en el laboratorio, habían mostrado que la frecuencia de aislamiento de mutantes de VFA resistentes a NH_4Cl en una población de C-S8c1 crecida en cultivos celulares, era muy elevada en comparación con la de otros mutantes como los resistentes a anticuerpos monoclonales (Martín-Acebes, 2009). Esto nos llevo a analizar si este tipo de variantes de VFA se encontraban presentes también en hospedadores naturales infectados con VFA. Para ello se analizó la frecuencia de selección de mutantes resistentes a NH_4Cl en poblaciones virales procedentes de lesiones vesiculares (aftas) de dos cerdos infectados con C-S8c1. En estas muestras los porcentajes de placas de lisis crecidas en presencia de NH_4Cl, respecto a las crecidas en ausencia del fármaco, fueron similares (0,15 ± 0,11% para el cerdo 6) a las encontradas en una población de C-S8c1 pasada en cultivo celular (0,14 ± 0,09%), e incluso superiores (1,28 ± 0,93% para el cerdo 5).

Mediante clonaje biológico se aislaron 6 mutantes resistentes a NH_4Cl (av1-av6) a partir de las muestras de líquido vesicular. El análisis de la secuencia de la región que codifica la cápsida de los mutantes de VFA resistentes a NH_4Cl estudiados reveló cambios de aminoácidos (Fig. 22) diferentes a los previamente descritos en mutantes resistentes a NH_4Cl (virus c1, c2 y c3) aislados a partir de cultivos celulares (Martín-Acebes y col., 2010). Una de estas mutaciones (VP3 A116V en el virus av1) se encontró muy cerca de las descritas para los virus c1 (VP3 A123T) y c2 (VP3 A118V) (Martín-Acebes y col., 2010), siendo en los tres casos cambios en residuos de Ala muy cercanos entre sí. Mientras que los mutantes previamente descritos c1 y c2 tenían cambios en las posiciones 123 y 118 de VP3, identificadas como invariantes entre aislados de los 7 serotipos de VFA (Carrillo y col., 2005), la posición 116 sólo está

conservada en los serotipos C, O y Asia 1. Tanto el residuo 116, como los residuos 118 y 123, se encuentran localizados cerca del borde interpentamérico, estando relativamente próximas a los residuos de His, predichos como sensores de pH, que se ha propuesto que desencadenan la desencapsidación de VFA (VP3 H140 y H143) (Curry y col., 1995; van Vlijmen y col., 1998). Los cambios VP3 A123T, A118V y A116V afectan residuos de Ala (que carece de cadena lateral) y suponen la introducción de aminoácidos con cadenas laterales cortas y no cargadas (Val y Thr), es decir más voluminosos, cerca de la interfase pentamérica. Esto podría generar perturbaciones estructurales que alterasen las interacciones interpentaméricas, esenciales para la estabilidad de la cápsida de VFA (Mateo y col., 2003). De hecho, para el mutante de la posición 118 se ha observado una tendencia incrementada al desensamblaje de la cápsida en subunidades pentaméricas incluso en ausencia de pH ácido (Martín-Acebes y col., 2010). A su vez, dada la cercanía de estas posiciones a los residuos de His potencialmente implicados en la desencapsidación de VFA, estos cambios podrían tener consecuencias sobre la función de estos residuos de His. Estos tres cambios se encuentran alineados en torno al mismo elemento estructural, la lámina β-E de VP3; lo que indica que ésta juega un papel importante en la estabilidad de la cápsida. Por otro lado, se han encontrado mutantes resistentes a NH_4Cl cuya sustitución de aminoácido no se encuentra en este elemento estructural de VP3, como son el mutante av6 (VP3 A25P) y el mutante previamente descrito c3 (VP2 D106G). La posición VP2 D106 está localizada cerca del borde interpentamérico, y la sustitución de aminoácido encontrada en el mutante c3 supone la interrupción de un puente salino entre este residuo y la H157 localizada en la misma proteína VP2, lo que podría suponer una reducción de la fuerza de unión interpentamérica, facilitando así el proceso de disociación (Martín-Acebes y col., 2010). En el caso del mecanismo molecular que media el incremento de la sensibilidad a pH ácido del mutante av6 (VP3 A25P), carecemos por el momento de una interpretación estructural.

Cuando se realizaron ensayos de competición entre los virus recuperados de los clones infecciosos pMT28 (C-S8c1) y pMT28-VP3 116V (resistente a NH_4Cl) se observó que en ausencia de NH_4Cl el virus parental (C-S8c1) tenía una mayor capacidad replicativa que el virus mutante, pero el virus VP3 116V se mantuvo en una proporción aproximada al 10% hasta en el pase 10 (Fig. 29). Estos resultados son compatibles con las elevadas frecuencias de aislamiento observadas para este tipo de

mutantes, que consiguen mantenerse en la población en frecuencias elevadas, sin ser extinguidas por el virus parental.

Los experimentos para determinar la sensibilidad a pH ácido de los viriones indicaron que el virus C-S8c1 mostraba valores de $pH_{50}I$ (6,56) muy similares a los descritos para VFA de serotipo A y para los previamente estimados para C-S8c1 (Curry y col., 1995; Martín-Acebes y col., 2010). El mutante av1, con la sustitución VP3 A116V y el correspondiente virus recuperado del clon infeccioso VP3 116V (ambos completamente resistentes al tratamiento con 25 mM NH_4Cl) presentaron valores de $pH_{50}I$ mayores (6,86), estando cercanos a los valores de $pH_{50}I$ descritos para el virus c2 (6,98). Por otro lado, el virus av6, que no escapó completamente al efecto inhibitorio del NH_4Cl, tuvo un valor de $pH_{50}I$ de 6,66. Esta gradación de sensibilidad a pH ácido de los mutantes correlaciona con el diferente grado de resistencia a NH_4Cl de cada mutante. Estos resultados confirman que el mecanismo de escape frente a la inhibición de la acidificación endosomal inducida por NH_4Cl se basa en un incremento de la sensibilidad a pH ácido de la cápsida de los mutantes, lo que permite la desencapsidación en los endosomas alcanizados por el NH_4Cl.

6.3 Efecto antiviral del ácido valproico

El ácido valproico (AVP) es un fármaco que tiene distintos efectos sobre la célula, entre los que se encuentra la alteración del metabolismo de lípidos, incluyendo los fosfatidilinositoles, y la inhibición de las DACH (Shaltiel y col., 2004; Tokuoka y col., 2008; Venkataramani y col., 2010; Wittenburg y col., 2010; Xu y col., 2007).

En esta Tesis Doctoral se ha observado un efecto antiviral del AVP sobre diferentes virus con envoltura que causan enfermedades veterinarias y humanas de importancia (Fig. 32). En cultivos celulares, el AVP inhibió completamente la producción de virus con envoltura de diferentes familias cuyo genoma consistía en RNA de polaridad positiva (VNO, VUSU, VBS y VSIN), de polaridad negativa (VEV), segmentado y de polaridad negativa (VCLM). También se observó inhibición con virus DNA, siendo ésta completa en el caso de VPPA y parcial en el de VVAC. En general, las inhibiciones observadas en células BHK-21 y Vero fueron similares, lo que sugiere que el mecanismo antiviral del AVP afecta pasos comunes en el metabolismo celular. Sin embargo, la inhibición diferencial de la producción de VSIN en BHK-21 y Vero cuando el fármaco se añadió 2.5 h pi indica que la inhibición producida por el AVP podría ser modulada por el tipo de célula infectada. Por el contrario, no se encontró

ninguna diferencia significativa en la producción viral en presencia del fármaco en los virus sin envoltura estudiados (VFA, EVB, VEMC y VREA), pertenecientes a la familia *Picornaviridae*.

Debido a los diferentes efectos que se le atribuyen al AVP, es complicado el análisis e interpretación de las inhibiciones observadas. Como ya se ha comentado, uno de los efectos del AVP es la inhibición de las DACH (Venkataramani y col., 2010), motivo por el cual se ha explorado la capacidad de este fármaco para disminuir el número de células latentemente infectadas con el VIH-1 (Lehrman y col., 2005), el virus linfotrópico humano T tipo 1 (Lezin y col., 2007) y el virus Epstein-Barr (Countryman y col., 2008; Zhou y col., 2009). El efecto antiviral observado sobre los virus con envoltura analizados en esta Tesis Doctoral no es atribuible a la inhibición de la actividad de las DACH puesto que la TSA, inhibidor de DACH, no produjo ningún efecto sobre la producción viral (Fig. 33). Por otro lado, como se ha comentado anteriormente, existen varios estudios que muestran que el AVP afecta a la composición de las membranas celulares (Shaltiel y col., 2004; Terbach y col., 2009; Tokuoka y col., 2008). La membrana lipídica de los virus con envoltura procede de las membranas de la célula hospedadora. De hecho, los flavivirus, como VNO y VUSU adquieren su envoltura a partir de las membranas del retículo endoplásmico (Welsch y col., 2009), mientras que otros virus, como VEV (Luan y col., 1995), VBS (Simons y col., 1984) y VCML lo hacen a partir de la membrana plasmática (Buchmeier, 2007; Murphy y col., 1975). Por tanto, el efecto inhibitorio del AVP sobre la producción de los virus con envoltura podría ser causado por alteraciones en la composición de las membranas celulares que afectasen de forma distinta a cada virus analizado. A continuación se discute el efecto antiviral del AVP sobre los tres virus modelo elegidos para un análisis más detallado: VEV, VNO y VCML.

6.3.1 Efecto del AVP sobre la infección de VEV

El AVP no indujo un bloqueo de la síntesis de RNA ni de proteínas de VEV, aunque sí se detectaron en menor cantidad que en su ausencia (Fig. 35c y e). Además, el porcentaje de células positivas para G-VEV(infectadas) aumentó en función del tiempo en el caso de las células control, pero no así en las células tratadas con AVP, sugiriendo que no se liberan partículas virales infecciosas que puedan infectar nuevas células desde las células inicialmente infectadas (Fig. 35b). Dado que el VEV adquiere su membrana lipídica a partir de la membrana plasmática celular (Luan y col., 1995) y que su

composición lipídica es muy similar a la membrana de la célula hospedadora (Kalvodova y col., 2009), el tratamiento con AVP podría dificultar el proceso de gemación del virus debido a la alteración de la composición de los lípidos de la membrana plasmática (Shaltiel y col., 2004; Tokuoka y col., 2008; Xu y col., 2007), lo que supondría un aumento del número de partículas virales en la membrana plasmática de las células tratadas. Por este motivo se decidió cuantificar el número de partículas virales de VEV/nm de membrana que estaban gemando, que resulto ser aproximadamente un 27% mayor en las células tratadas con AVP que en las células control; aunque estas diferencias no fueron significativas. A su vez, el tamaño de las partículas virales fue similar en ambos casos, lo que sugiere que el AVP no produce un efecto notable sobre el ensamblaje de las partículas de VEV, aunque podría estar teniendo algún efecto sobre el proceso de gemación del virus. Asimismo, se decidió purificar viriones de VEV a partir de sobrenadantes de células infectadas. En este caso, no se detectaron partículas virales en las células tratadas con AVP mientras que si se observaron en las muestras control (Fig. 36a). Sin embargo, si se detectó RNA viral y proteínas virales en el sobrenadante de las células infectadas con AVP, aunque en menor cantidad que en el control. En conjunto, los resultados sugieren que el AVP podría estar afectando al proceso de gemación del VEV, no permitiendo la liberación de la partícula viral al medio extracelular para poder infectar así a las células vecinas, o produciendo partículas más inestables que no soportan el proceso de purificación. De esta manera, estos resultados serían compatibles con un efecto inhibitorio del AVP mediado por alteraciones en el metabolismo lipídico.

6.3.2 Efecto del AVP sobre la infección de VNO

Las células infectadas con VNO sufren una gran remodelación de las membranas intracelulares para dar lugar a estructuras bien definidas donde se asocia el complejo de replicación viral. Estas membranas provienen mayoritariamente del retículo endoplásmico (Gillespie y col., 2010). Entre estas estructuras se encuentran las denominadas como los paquetes de vesículas (VP), donde tiene lugar la replicación viral (Gillespie y col., 2010; Mackenzie y col., 2001; Westaway y col., 1997). Los VP constituyen invaginaciones del retículo endoplásmico que están en contacto con el citoplasma a través de poros que contiene intermediarios replicativos (dsRNA) y viriones ensamblados que geman dentro del retículo endoplásmico (Gillespie y col., 2010; Martín-Acebes y col., 2011a). Al contrario que con VEV, en los *Flavivirus* la

replicación del RNA y el ensamblaje del virión se encuentran asociados en estas estructuras, de manera que la invaginación es necesaria para la replicación (Welsch y col., 2009). Se ha propuesto que el colesterol y los ácidos grasos tienen un papel importante en la inducción de estas estructuras membranosas importantes para la replicación de VNO (Heaton y col., 2011; Mackenzie y col., 2007; Martín-Acebes y col., 2011a). A diferencia de lo observado con el VEV, el AVP inhibió la síntesis de RNA y proteínas de VNO (Fig. 37). Esto podría explicarse porque el efecto del AVP sobe el metabolismo de lípidos provoque alteraciones en la composición de las VP, inhibiendo de este modo la replicación del RNA viral, la síntesis de proteínas y, consecuentemente la gemación de los viriones.

6.3.3 Efecto del AVP sobre la infección de VCML

En el caso de VCML, el efecto producido por el AVP fue similar al descrito para VEV. Este fármaco no inhibió la producción de proteínas ni la síntesis de RNA viral. Asimismo, el porcentaje de células positivas para GFP en los ensayos realizados con el virus r3 VCML-GFP fue mayor en el caso de las muestras control que en las muestras tratadas con AVP, lo que sugiere que las células inicialmente infectadas están liberando virus de forma más eficiente e infectando mayor número de células vecinas en ausencia de AVP, como se había observado para VEV. Esto explicaría la reducción encontrada en la cantidad de RNA viral detectado en las células tratadas, ya que el ensayo del minigenoma permite descartar que el AVP tenga algún efecto sobre la replicación del RNA viral.

La replicación de VCML se produce en el citoplasma de las células infectadas, mientras que el proceso de gemación del virus tiene lugar mayoritariamente en la membrana plasmática (Buchmeier, 2007). El proceso de gemación de los *Arenavirus* requiere la actividad de la proteína Z, que promueve la curvatura de la membrana para que pueda darse la gemación. En este sentido, la expresión aislada de la proteína Z puede producir la formación de VLP (Urata y col., 2011). La proteína Z debe miristoilarse para poder anclarse a la membrana plasmática, dónde interactúa con proteínas celulares que permiten que ésta pueda utilizar la maquinaria del complejo proteico denominado *endosomal sorting complex required for transport* (ESCRT) celular para poder salir de la célula (Urata y col., 2011). Nuestros resultados con VCML indicaron que el AVP inhibe de manera dosis dependiente la gemación mediada por la proteína Z (Fig. 41). Por otro lado, a pesar de que las partículas virales liberadas al

medio en ambos casos tenían una morfología y un tamaño similar, se observó un número significativamente menor de partículas virales en el caso de las células tratadas con AVP con respecto a las células control. Cabe destacar que está disminución fue aproximadamente del 50%, mientras que los títulos de la producción viral obtenida en presencia de la misma concentración de AVP fueron al menos dos órdenes de magnitud inferiores a los detectados en ausencia del fármaco. Esto podría indicar que el AVP está afectando tanto a la liberación de las partículas virales como a la infectividad de los viriones liberados. Todos estos resultados sugieren que, en este caso, el efecto antiviral del AVP podría estar mediado por una alteración en el proceso de gemación de VCML. Otros compuestos que inhiben este proceso han sido propuesto como potenciales antivirales (Urata y col., 2011).

6.3.4 El AVP como posible antiviral

Un método común de evaluar si un compuesto es un buen candidato como posible antiviral es calcular el índice de selectividad (SI), que relaciona la capacidad antiviral con la toxicidad de la molécula. Este valor viene definido por la relación entre el valor del TC_{50} y el IC_{50}, de forma que valores superiores a 100 se pueden considerar como indicador de un buen candidato antiviral (Li y col., 2005). Aunque las IC_{50} del AVP son relativamente altas (0,06 – 1 mM), el valor de SI para VEV es de 406, para VNO de 616 y para VCML de 1666. Estos datos junto con que el AVP es un fármaco comúnmente usado en desórdenes neurológicos (Bruni y col., 1979; Terbach y col., 2009), apoyan que el AVP podría ser usado como tratamiento antiviral para los virus estudiados. De hecho, en modelos animales la concentración de AVP en plasma correlaciona con las encontradas en cerebro (Ohdo y col., 1988; Pollack y col., 1985), lo que podría favorecer la inhibición de virus neurotrópicos como VNO o VCML.

El AVP se administra dependiendo de la masa corporal del paciente, siendo el rango terapéutico para el tratamiento de la epilepsia de 50-100 mg/l (en torno a 0,3-0,6 mM en plasma) (Cramer y col., 1986; Kanner, 2003). Esta concentración en plasma está próxima a los valores de IC_{50} determinados para VEV, VNO y VCML (0,6, 0,25 y 0,06 mM, respectivamente). Por otro lado, para considerar las posibles aplicaciones terapéuticas del AVP, se tiene que tener en cuenta su farmacocinética. Este fármaco es metabolizado de manera lineal, y tiene una vida media (en adultos que reciben monoterapia) que varía entre 12 ± 6 y 15 ± 2,5 h, aunque debido a la bajada de la concentración en suero, deberían administrarse dosis periódicas (Kanner, 2003).

Aunque los niveles normales del fármaco en plasma son compatibles con los valores de IC_{50}, las concentraciones que se encontrarían en las células donde tiene lugar el ciclo viral no están determinadas, lo que en conjunto hace que el diseño de experimentos en animales sea complicado. Por otro lado, también podría ser interesante estudiar el efecto de la denominada la "nueva generación" de AVP, que incluye compuestos con una vida media mayor y menor toxicidad (Bialer y col., 2007; Trojnar y col., 2004).

6.4 Alteración del metabolismo de lípidos como estrategia antiviral

A la vista de los resultados obtenidos durante esta Tesis Doctoral, que incluyen la identificación del $PI(4,5)P_2$ como factor necesario para la internalización de VFA y VEV, así como la descripción del efecto antiviral del AVP, parece interesante tener en cuenta la alteración del metabolismo de lípidos como posible estrategia antiviral. De hecho, determinados lípidos específicos son esenciales en procesos utilizados por distintos virus para su multiplicación, de forma que se pueden usar distintas estrategias para inhibir la infección de diferentes virus. Una primera aproximación para inhibir la multiplicación de virus con envoltura consiste en actuar sobre los lípidos de su envoltura empleando compuestos químicos o incluso anticuerpos (Moody y col., 2010). Este es el caso de un amplio rango de antivirales, algunos de los cuales, como el arbidol e inhibidores de la fusión de las membranas, han sido aprobados para ser utilizados en pacientes humanos (Boriskin y col., 2008; Lorizate y col., 2011; Teissier y col., 2011; Wolf y col., 2010).

Los virus pueden provocar alteraciones en el metabolismo de lípidos que originan modificaciones en la composición lipídica de las membranas celulares que favorece su multiplicación (Heaton y col., 2011). La inhibición de las enzimas implicadas en estos procesos constituye una estrategia antiviral alternativa (Munger y col., 2008), habiéndose descrito varios compuestos que actúan en distintos puntos del metabolismo de lípidos que tienen un efecto antiviral en cultivos celulares sobre diferentes virus. Ejemplos de estos compuestos son aquellos que alteran el metabolismo del colesterol (Bader y col., 2008; Brett y col., 2011; Giguere y col., 2004; Gilbert y col., 2005; Liu y col., 2009; Mihaila y col., 2009; Montoya y col., 2009; Poh y col., 2012), el metabolismo de ácidos grasos (Guinea y col., 1991; Heaton y col., 2010a; Huang y col., 2007; Martín-Acebes y col., 2011a; Munger y col., 2008; Perera y col., 2012; Rassmann y col., 2007; Yang y col., 2008) o el metabolismo de PI(4)P (Arita y col., 2011; Bianco y col., 2012; Hsu y col., 2010; Sasaki y col., 2011).

La alteración de vías metabólicas importantes para la homeostasis celular puede parecer una estrategia antiviral poco específica, ya que podrían originar efectos adversos en el hospedador. Sin embargo, hay que tener en cuenta que muchos de los compuestos antivirales que se usan actualmente actúan sobre rutas metabólicas importantes como la que regula el metabolismo de ácidos nucleicos (Andrei y col., 2008; De Clercq, 2009; Graci y col., 2006; Olschlager y col., 2011). Por otro lado, el uso de compuestos antivirales que actúan sobre factores celulares puede conllevar ventajas; ya que estos compuestos son *a priori* menos susceptibles de seleccionar resistencias virales que aquellos dirigidos frente a las proteínas del virus (Heaton y col., 2011). Además, se ha visto que compuestos que alteran el metabolismo de un lípido específico son capaces de inhibir virus de familias diferentes (referencias citadas anteriormente en el texto) constituyendo candidatos a antivirales de amplio espectro. Por ejemplo, las estatinas, que son compuestos que alteran el metabolismo del colesterol y que son comúnmente utilizados para el tratamiento de pacientes con enfermedades cardiovasculares, se han propuesto como una nueva aproximación antiviral (Giguere y col., 2004; Gilbert y col., 2005; Gower y col., 2001). De hecho, la lovastatina inhibe la infección en cultivos celulares y ratones del virus respiratorio sincitial (Gower y col., 2001). También cabe destacar las diferencias encontradas en el tratamiento de pacientes infectados con el virus de la hepatitis C con distintas estatinas (lovastatina, sinvastina, fluvastina), que van desde la ausencia de efecto hasta una reducción de la viremia (Bader y col., 2008; Harrison y col., 2010; Mihaila y col., 2009; Mihaila y col., 2011; Patel y col., 2011). En conjunto, la información acumulada en los últimos años apoya el potencial de compuestos que alteran el metabolismo de lípidos como antivirales (Bassendine y col., 2011; Heaton y col., 2011; Munger y col., 2008).

Conclusiones

7. Conclusiones

1. Las variantes de VFA C-S8c1 y MARLS requieren la función de la proteína dinamina para poder ser internalizados en la célula, lo que indica que este requerimiento es independiente del receptor celular utilizado por el virus.

2. Los tratamientos farmacológicos con ionomicina y 1-butanol, así como la retirada del $PI(4,5)P_2$ de la membrana plasmática mediante un sistema inducible, indican que el VFA C-S8c1 y el VEV requieren la presencia y síntesis de este lípido para ser internalizados en células BHK-21. El variante de VFA MARLS, que puede utilizar receptores diferentes a las integrinas, tiene un menor requerimiento de este fosfolípido que el virus parental C-S8c1.

3. De acuerdo a los resultados obtenidos con los distintos variantes de VFA utilizados (C-S8c1, MARLS) el requerimiento de acidificación endosomal y de la actividad de la proteína Rab5 en VFA es independiente del tipo de receptor utilizado por el virus.

4. Los estudios realizados con los virus C-S8c1, c2 y m6; que tienen diferente valor de pH de desencapsidación, indican que cuanato más ácido es el valor de pH de desencapasidación, mayor es el requerimiento de la actividad de la proteína Rab5. Los estudios en ratón lactante sugieren que las alteraciones en el valor de pH óptimo de desencapsidación provocan una disminución de la infectividad *in vivo*.

5. Las poblaciones virales encontradas en lesiones vesiculares de cerdos infectados con VFA C-S8c1 presentan una frecuencia alta de mutantes resistentes a NH_4Cl (0,14-1,28% de las UFP totales), habiéndose caracterizado mutantes con diferentes grados de resistencia a la inhibición de la acidificación endosomal inducida por esta droga. Estos mutantes muestran un incremento de la sensibilidad a pH ácido diferencial.

6. El cambio en la posición VP3 A116V de la cápsida, encontrado en uno de estos mutantes, es suficiente para incrementar la sensibilidad a pH ácido de C-S8c1 y de conferir resistencia a NH_4Cl. Este cambio se encuentra cerca de las sustituciones previamente encontradas en los virus resistentes a NH_4Cl c1 (VP3 A123T) y c2 (VP3 A118V), localizados todos en torno a la lámina β-E de VP3, lo que sugiere que este elemento estructural es importante en la estabilidad de la cápsida frente a pH ácido.

7. El AVP inhibe la producción de los distintos virus con envoltura analizados (VEV, VBS, VSIN, VNO, VUSU, VCML, VPPA, VVAC), pero no la de los virus sin envoltura (VFA, VEMC, RVE, EVB) estudiados.

8. El AVP reduce la liberación de partículas infecciosas de VEV y VCML sin afectar, en tanta medida, la síntesis de RNA y proteínas virales, lo que sugiere que el AVP afecta, fundamentalmente, a la gemación de estos virus.

9. El AVP bloquea completamente la síntesis de RNA y de proteínas de VNO, lo que indica que ese fármaco puede tener distintos efectos sobre el ciclo de multiplicación de diferentes virus.

Bibliografía

8. Bibliografía

Abe, N., Inoue, T., Galvez, T., Klein, L. y Meyer, T. (2008). Dissecting the role of PtdIns(4,5)P2 in endocytosis and recycling of the transferrin receptor. *J Cell Sci* **121**, 1488-1494.

Acharya, R., Fry, E., Stuart, D., Fox, G., Rowlands, D. y Brown, F. (1989). The three-dimensional structure of foot-and-mouth disease virus at 2.9 A resolution. *Nature* **337**, 709-716.

Adjobo-Hermans, M. J., Goedhart, J. y Gadella, T. W., Jr. (2008). Regulation of PLCbeta1a membrane anchoring by its substrate phosphatidylinositol (4,5)-bisphosphate. *J Cell Sci* **121**, 3770-3777.

Albertini, A. A., Schoehn, G., Weissenhorn, W. y Ruigrok, R. W. (2008). Structural aspects of rabies virus replication. *Cell Mol Life Sci* **65**, 282-294.

Alcalde, J., Egea, G. y Sandoval, I. V. (1994). gp74 a membrane glycoprotein of the cis-Golgi network that cycles through the endoplasmic reticulum and intermediate compartment. *J Cell Biol* **124**, 649-665.

Aleksandrowicz, P., Marzi, A., Biedenkopf, N., Beimforde, N., Becker, S., Hoenen, T., Feldmann, H. y Schnittler, H. J. (2011). Ebola virus enters host cells by macropinocytosis and clathrin-mediated endocytosis. *J Infect Dis* **204 Suppl 3**, S957-967.

Alvisi, G., Madan, V. y Bartenschlager, R. (2011). Hepatitis C virus and host cell lipids: an intimate connection. *RNA Biol* **8**, 258-269.

Andrei, G., De Clercq, E. y Snoeck, R. (2008). Novel inhibitors of human CMV. *Curr Opin Investig Drugs* **9**, 132-145.

Ang, F., Wong, A. P., Ng, M. M. y Chu, J. J. (2010). Small interference RNA profiling reveals the essential role of human membrane trafficking genes in mediating the infectious entry of dengue virus. *Virol J* **7**, 24.

Antonescu, C. N., Aguet, F., Danuser, G. y Schmid, S. L. (2011). Phosphatidylinositol-(4,5)-bisphosphate regulates clathrin-coated pit initiation, stabilization, and size. *Mol Biol Cell* **22**, 2588-2600.

Arendt, K. L., Royo, M., Fernandez-Monreal, M., Knafo, S., Petrok, C. N., Martens, J. R. y Esteban, J. A. (2010). PIP3 controls synaptic function by maintaining AMPA receptor clustering at the postsynaptic membrane. *Nat Neurosci* **13**, 36-44.

Arita, M., Kojima, H., Nagano, T., Okabe, T., Wakita, T. y Shimizu, H. (2011). Phosphatidylinositol 4-kinase III beta is a target of enviroxime-like compounds for antipoliovirus activity. *J Virol* **85**, 2364-2372.

Armas-Portela, R., Parrales, M. A., Albar, J. P., Martínez, A. C. y Ávila, J. (1999). Distribution and characteristics of betaII tubulin-enriched microtubules in interphase cells. *Exp Cell Res* **248**, 372-380.

Auperin, D. D., Compans, R. W. y Bishop, D. H. (1982). Nucleotide sequence conservation at the 3' termini of the virion RNA species of New World and Old World arenaviruses. *Virology* **121**, 200-203.

Auperin, D. D., Romanowski, V., Galinski, M. y Bishop, D. H. (1984). Sequencing studies of pichinde arenavirus S RNA indicate a novel coding strategy, an ambisense viral S RNA. *J Virol* **52**, 897-904.

Bader, T., Fazili, J., Madhoun, M., Aston, C., Hughes, D., Rizvi, S., Seres, K. y Hasan, M. (2008). Fluvastatin inhibits hepatitis C replication in humans. *Am J Gastroenterol* **103**, 1383-1389.

Baranowski, E., Ruiz-Jarabo, C. M. y Domingo, E. (2001). Evolution of cell recognition by viruses. *Science* **292**, 1102-1105.

Baranowski, E., Ruiz-Jarabo, C. M., Sevilla, N., Andreu, D., Beck, E. y Domingo, E. (2000). Cell recognition by foot-and-mouth disease virus that lacks the RGD integrin-binding motif: flexibility in aphthovirus receptor usage. *J Virol* **74**, 1641-1647.

Baranowski, E., Sevilla, N., Verdaguer, N., Ruiz-Jarabo, C. M., Beck, E. y Domingo, E. (1998). Multiple virulence determinants of foot-and-mouth disease virus in cell culture. *J Virol* **72**, 6362-6372.

Barbieri, M. A., Roberts, R. L., Mukhopadhyay, A. y Stahl, P. D. (1996). Rab5 regulates the dynamics of early endosome fusion. *Biocell* **20**, 331-338.

Bassendine, M. F., Sheridan, D. A., Felmlee, D. J., Bridge, S. H., Toms, G. L. y Neely, R. D. (2011). HCV and the hepatic lipid pathway as a potential treatment target. *J Hepatol* **55**, 1428-1440.

Bauer, M. y Pelkmans, L. (2006). A new paradigm for membrane-organizing and -shaping scaffolds. *FEBS Lett* **580**, 5559-5564.

Baxt, B. (1987). Effect of lysosomotropic compounds on early events in foot-and-mouth disease virus replication. *Virus Res* **7**, 257-271.

Baxt, B. y Becker, Y. (1990). The effect of peptides containing the arginine-glycine-aspartic acid sequence on the adsorption of foot-and-mouth disease virus to tissue culture cells. *Virus Genes* **4**, 73-83.

Baxt, B. y Mason, P. W. (1995). Foot-and-mouth disease virus undergoes restricted replication in macrophage cell cultures following Fc receptor-mediated adsorption. *Virology* **207**, 503-509.

Beasley, D. W. (2005). Recent advances in the molecular biology of west nile virus. *Curr Mol Med* **5**, 835-850.

Belsham, G. J. (1993). Distinctive features of foot-and-mouth disease virus, a member of the picornavirus family; aspects of virus protein synthesis, protein processing and structure. *Prog Biophys Mol Biol* **60**, 241-260.

Belsham, G. J., Abrams, C. C., King, A. M., Roosien, J. y Vlak, J. M. (1991). Myristoylation of foot-and-mouth disease virus capsid protein precursors is independent of other viral proteins and occurs in both mammalian and insect cells. *J Gen Virol* **72 (Pt 3)**, 747-751.

Belsham, G. J. y Brangwyn, J. K. (1990). A region of the 5' noncoding region of foot-and-mouth disease virus RNA directs efficient internal initiation of protein synthesis within cells: involvement with the role of L protease in translational control. *J Virol* **64**, 5389-5395.

Bernard, E., Solignat, M., Gay, B., Chazal, N., Higgs, S., Devaux, C. y Briant, L. (2010). Endocytosis of chikungunya virus into mammalian cells: role of clathrin and early endosomal compartments. *PLoS One* **5**, e11479.

Berryman, S., Clark, S., Monaghan, P. y Jackson, T. (2005). Early events in integrin alphavbeta6-mediated cell entry of foot-and-mouth disease virus. *J Virol* **79**, 8519-8534.

Bialer, M. y Yagen, B. (2007). Valproic Acid: second generation. *Neurotherapeutics* **4**, 130-137.

Bianco, A., Reghellin, V., Donnici, L., Fenu, S., Alvarez, R., Baruffa, C., Peri, F., Pagani, M., Abrignani, S., Neddermann, P. y De Francesco, R. (2012). Metabolism of phosphatidylinositol 4-kinase IIIalpha-dependent PI4P Is subverted by HCV and is targeted by a 4-anilino quinazoline with antiviral activity. *PLoS Pathog* **8**, e1002576.

Bienz, K., Egger, D. y Pasamontes, L. (1987). Association of polioviral proteins of the P2 genomic region with the viral replication complex and virus-induced membrane synthesis as visualized by electron microscopic immunocytochemistry and autoradiography. *Virology* **160**, 220-226.

Bigeriego, P., Rosas, M. F., Zamora, E., Martinez-Salas, E. y Sobrino, F. (1999). Heterotypic inhibition of foot-and-mouth disease virus infection by combinations of RNA transcripts corresponding to the 5' and 3' regions. *Antiviral Res* **44**, 133-141.

Blackham, S., Baillie, A., Al-Hababi, F., Remlinger, K., You, S., Hamatake, R. y McGarvey, M. J. (2010). Gene expression profiling indicates the roles of host oxidative stress, apoptosis, lipid metabolism, and intracellular transport genes in the replication of hepatitis C virus. *J Virol* **84**, 5404-5414.

Blasco, R. y Moss, B. (1992). Role of cell-associated enveloped vaccinia virus in cell-to-cell spread. *J Virol* **66**, 4170-4179.

Boriskin, Y. S., Leneva, I. A., Pecheur, E. I. y Polyak, S. J. (2008). Arbidol: a broad-spectrum antiviral compound that blocks viral fusion. *Curr Med Chem* **15**, 997-1005.

Borrow, P., Martinez-Sobrido, L. y de la Torre, J. C. (2010). Inhibition of the type I interferon antiviral response during arenavirus infection. *Viruses* **2**, 2443-2480.

Boucrot, E., Saffarian, S., Massol, R., Kirchhausen, T. y Ehrlich, M. (2006). Role of lipids and actin in the formation of clathrin-coated pits. *Exp Cell Res* **312**, 4036-4048.

Bradford, M. M. (1976). A rapid and sensitive method for the quantification of microgram quanties of protein utilizing the principle of protein-dye binding. *Anal Biochem* **72**, 248-254.

Brandenburg, B., Lee, L. Y., Lakadamyali, M., Rust, M. J., Zhuang, X. y Hogle, J. M. (2007). Imaging poliovirus entry in live cells. *PLoS Biol* **5**, e183.

Brett, S. J., Myles, P., Lim, W. S., Enstone, J. E., Bannister, B., Semple, M. G., Read, R. C., Taylor, B. L., McMenamin, J., Nicholson, K. G., Nguyen-Van-Tam, J. S. y Openshaw, P. J. (2011). Pre-admission statin use and in-hospital severity of 2009 pandemic influenza A(H1N1) disease. *PLoS One* **6**, e18120.

Brinton, M. A. (2002). The molecular biology of West Nile Virus: a new invader of the western hemisphere. *Annu Rev Microbiol* **56**, 371-402.

Brown, F. (1972). Structure-function relationships in foot-and-mouth disease virus. *Adv Exp Med Biol* **31**, 19-28.

Bruni, J. y Wilder, B. J. (1979). Valproic acid. Review of a new antiepileptic drug. *Arch Neurol* **36**, 393-398.

Bucci, C., Parton, R. G., Mather, I. H., Stunnenberg, H., Simons, K., Hoflack, B. y Zerial, M. (1992). The small GTPase rab5 functions as a regulatory factor in the early endocytic pathway. *Cell* **70**, 715-728.

Bucci, C., Thomsen, P., Nicoziani, P., McCarthy, J. y van Deurs, B. (2000). Rab7: a key to lysosome biogenesis. *Mol Biol Cell* **11**, 467-480.

Bucci, C., Wandinger-Ness, A., Lutcke, A., Chiariello, M., Bruni, C. B. y Zerial, M. (1994). Rab5a is a common component of the apical and basolateral endocytic machinery in polarized epithelial cells. *Proc Natl Acad Sci U S A* **91**, 5061-5065.

Buckley, A., Dawson, A., Moss, S. R., Hinsley, S. A., Bellamy, P. E. y Gould, E. A. (2003). Serological evidence of West Nile virus, Usutu virus and Sindbis virus infection of birds in the UK. *J Gen Virol* **84**, 2807-2817.

Buchmeier, M. J., C. J. Peters, J. C. de la Torre (2007). Arenaviridae: the viruses and their replication, 5th ed, vol. 2. Fields virology, Lippincott Williams & Wilkins, Philadelphia, PA.

.

Callaway, T. R. y Russell, J. B. (1999). Selection of a highly monensin-resistant Prevotella bryantii subpopulation with altered outer membrane characteristics. *Appl Environ Microbiol* **65**, 4753-4759.

Carneiro, F. A., Lapido-Loureiro, P. A., Cordo, S. M., Stauffer, F., Weissmuller, G., Bianconi, M. L., Juliano, M. A., Juliano, L., Bisch, P. M. y Da Poian, A. T. (2006). Probing the interaction between vesicular stomatitis virus and phosphatidylserine. *Eur Biophys J* **35**, 145-154.

Carrillo, C., Tulman, E. R., Delhon, G., Lu, Z., Carreno, A., Vagnozzi, A., Kutish, G. F. y Rock, D. L. (2005). Comparative genomics of foot-and-mouth disease virus. *J Virol* **79**, 6487-6504.

Carrillo, E. C., Giachetti, C. y Campos, R. (1985). Early steps in FMDV replication: further analysis on the effects of chloroquine. *Virology* **147**, 118-125.

Carrillo, E. C., Giachetti, C. y Campos, R. H. (1984). Effect of lysosomotropic agents on the foot-and-mouth disease virus replication. *Virology* **135**, 542-545.

Colpitts, T. M., Moore, A. C., Kolokoltsov, A. A. y Davey, R. A. (2007). Venezuelan equine encephalitis virus infection of mosquito cells requires acidification as well as mosquito homologs of the endocytic proteins Rab5 and Rab7. *Virology* **369**, 78-91.

Cornu, T. I. y de la Torre, J. C. (2001). RING finger Z protein of lymphocytic choriomeningitis virus (LCMV) inhibits transcription and RNA replication of an LCMV S-segment minigenome. *J Virol* **75**, 9415-9426.

Countryman, J. K., Gradoville, L. y Miller, G. (2008). Histone hyperacetylation occurs on promoters of lytic cycle regulatory genes in Epstein-Barr virus-infected cell lines which are refractory to disruption of latency by histone deacetylase inhibitors. *J Virol* **82**, 4706-4719.

Coyne, C. B., Shen, L., Turner, J. R. y Bergelson, J. M. (2007). Coxsackievirus entry across epithelial tight junctions requires occludin and the small GTPases Rab34 and Rab5. *Cell Host Microbe* **2**, 181-192.

Cramer, J. A., Mattson, R. H., Bennett, D. M. y Swick, C. T. (1986). Variable free and total valproic acid concentrations in sole- and multi-drug therapy. *Ther Drug Monit* **8**, 411-415.

Cremona, O., Di Paolo, G., Wenk, M. R., Luthi, A., Kim, W. T., Takei, K., Daniell, L., Nemoto, Y., Shears, S. B., Flavell, R. A., McCormick, D. A. y De Camilli, P. (1999). Essential role of phosphoinositide metabolism in synaptic vesicle recycling. *Cell* **99**, 179-188.

Cureton, D. K., Massol, R. H., Saffarian, S., Kirchhausen, T. L. y Whelan, S. P. (2009). Vesicular stomatitis virus enters cells through vesicles incompletely coated with clathrin that depend upon actin for internalization. *PLoS Pathog* **5**, e1000394.

Curry, S., Abrams, C. C., Fry, E., Crowther, J. C., Belsham, G. J., Stuart, D. I. y King, A. M. (1995). Viral RNA modulates the acid sensitivity of foot-and-mouth disease virus capsids. *J Virol* **69**, 430-438.

Curry, S., Fry, E., Blakemore, W., Abu-Ghazaleh, R., Jackson, T., King, A., Lea, S., Newman, J., Rowlands, D. y Stuart, D. (1996). Perturbations in the surface structure of A22 Iraq foot-and-mouth disease virus accompanying coupled changes in host cell specificity and antigenicity. *Structure* **4**, 135-145.

Curry, S., Fry, E., Blakemore, W., Abu-Ghazaleh, R., Jackson, T., King, A., Lea, S., Newman, J. y Stuart, D. (1997). Dissecting the roles of VP0 cleavage and RNA packaging in picornavirus capsid stabilization: the structure of empty capsids of foot-and-mouth disease virus. *J Virol* **71**, 9743-9752.

Chamberlain, L. H. (2004). Detergents as tools for the purification and classification of lipid rafts. *FEBS Lett* **559**, 1-5.

Chandran, K., Farsetta, D. L. y Nibert, M. L. (2002). Strategy for nonenveloped virus entry: a hydrophobic conformer of the reovirus membrane penetration protein micro 1 mediates membrane disruption. *J Virol* **76**, 9920-9933.

Charpentier, N., Dávila, M., Domingo, E. y Escarmis, C. (1996). Long-term, large-population passage of aphthovirus can generate and amplify defective noninterfering particles deleted in the leader protease gene. *Virology* **223**, 10-18.

Chen, C. y Zhuang, X. (2008). Epsin 1 is a cargo-specific adaptor for the clathrin-mediated endocytosis of the influenza virus. *Proc Natl Acad Sci U S A* **105**, 11790-11795.

Chinnapen, D. J., Chinnapen, H., Saslowsky, D. y Lencer, W. I. (2007). Rafting with cholera toxin: endocytosis and trafficking from plasma membrane to ER. *FEMS Microbiol Lett* **266**, 129-137.

Chu, J. J., Leong, P. W. y Ng, M. L. (2006). Analysis of the endocytic pathway mediating the infectious entry of mosquito-borne flavivirus West Nile into Aedes albopictus mosquito (C6/36) cells. *Virology* **349**, 463-475.

Chu, J. J. y Ng, M. L. (2004). Interaction of West Nile virus with alpha v beta 3 integrin mediates virus entry into cells. *J Biol Chem* **279**, 54533-54541.

Damke, H., Baba, T., Warnock, D. E. y Schmid, S. L. (1994). Induction of mutant dynamin specifically blocks endocytic coated vesicle formation. *J Cell Biol* **127**, 915-934.

Damm, E. M., Pelkmans, L., Kartenbeck, J., Mezzacasa, A., Kurzchalia, T. y Helenius, A. (2005). Clathrin- and caveolin-1-independent endocytosis: entry of simian virus 40 into cells devoid of caveolae. *J Cell Biol* **168**, 477-488.

Daniels, R. S., Downie, J. C., Hay, A. J., Knossow, M., Skehel, J. J., Wang, M. L. y Wiley, D. C. (1985). Fusion mutants of the influenza virus hemagglutinin glycoprotein. *Cell* **40**, 431-439.

Danthi, P., Tosteson, M., Li, Q. H. y Chow, M. (2003). Genome delivery and ion channel properties are altered in VP4 mutants of poliovirus. *J Virol* **77**, 5266-5274.

Davis, C. W., Nguyen, H. Y., Hanna, S. L., Sanchez, M. D., Doms, R. W. y Pierson, T. C. (2006). West Nile virus discriminates between DC-SIGN and DC-SIGNR for cellular attachment and infection. *J Virol* **80**, 1290-1301.

Davis, M. P., Bottley, G., Beales, L. P., Killington, R. A., Rowlands, D. J. y Tuthill, T. J. (2008). Recombinant VP4 of human rhinovirus induces permeability in model membranes. *J Virol* **82**, 4169-4174.

De Clercq, E. (2009). The history of antiretrovirals: key discoveries over the past 25 years. *Rev Med Virol* **19**, 287-299.

De Filette, M., Ulbert, S., Diamond, M. y Sanders, N. N. (2012). Recent progress in West Nile virus diagnosis and vaccination. *Vet Res* **43**, 16.

de la Torre, J. C., Dávila, M., Sobrino, F., Ortin, J. y Domingo, E. (1985). Establishment of cell lines persistently infected with foot-and-mouth disease virus. *Virology* **145**, 24-35.

de Los Santos, T., Díaz-San Segundo, F. y Grubman, M. J. (2007). Degradation of nuclear factor kappa B during foot-and-mouth disease virus infection. *J Virol* **81**, 12803-12815.

De Matteis, M. A. y Godi, A. (2004). PI-loting membrane traffic. *Nat Cell Biol* **6**, 487-492.

de Silva, A. M., Balch, W. E. y Helenius, A. (1990). Quality control in the endoplasmic reticulum: folding and misfolding of vesicular stomatitis virus G protein in cells and in vitro. *J Cell Biol* **111**, 857-866.

del Pozo, M. A., Balasubramanian, N., Alderson, N. B., Kiosses, W. B., Grande-Garcia, A., Anderson, R. G. y Schwartz, M. A. (2005). Phospho-caveolin-1 mediates integrin-regulated membrane domain internalization. *Nat Cell Biol* **7**, 901-908.

den Boon, J. A., Díaz, A. y Ahlquist, P. (2010). Cytoplasmic viral replication complexes. *Cell Host Microbe* **8**, 77-85.

DeTulleo, L. y Kirchhausen, T. (1998). The clathrin endocytic pathway in viral infection. *EMBO J* **17**, 4585-4593.

Devaney, M. A., Vakharia, V. N., Lloyd, R. E., Ehrenfeld, E. y Grubman, M. J. (1988). Leader protein of foot-and-mouth disease virus is required for cleavage of the p220 component of the cap-binding protein complex. *J Virol* **62**, 4407-4409.

Di Paolo, G. y De Camilli, P. (2006). Phosphoinositides in cell regulation and membrane dynamics. *Nature* **443**, 651-657.

Di Simone, C. y Buchmeier, M. J. (1995). Kinetics and pH dependence of acid-induced structural changes in the lymphocytic choriomeningitis virus glycoprotein complex. *Virology* **209**, 3-9.

Diamond, D. L., Syder, A. J., Jacobs, J. M., Sorensen, C. M., Walters, K. A., Proll, S. C., McDermott, J. E., Gritsenko, M. A., Zhang, Q., Zhao, R., Metz, T. O., Camp, D. G., 2nd, Waters, K. M., Smith, R. D., Rice, C. M. y Katze, M. G. (2011). Temporal proteome and lipidome profiles reveal hepatitis C virus-associated reprogramming of hepatocellular metabolism and bioenergetics. *PLoS Pathog* **6**, e1000719.

Díez, J., Davila, M., Escarmis, C., Mateu, M. G., Dominguez, J., Perez, J. J., Giralt, E., Melero, J. A. y Domingo, E. (1990). Unique amino acid substitutions in the capsid proteins of foot-and-mouth disease virus from a persistent infection in cell culture. *J Virol* **64**, 5519-5528.

Domingo, E., Baranowski, E., Escarmis, C. y Sobrino, F. (2002). Foot-and-mouth disease virus. *Comp Immunol Microbiol Infect Dis* **25**, 297-308.

Domingo, E., Escarmis, C., Baranowski, E., Ruiz-Jarabo, C. M., Carrillo, E., Nuñez, J. I. y Sobrino, F. (2003). Evolution of foot-and-mouth disease virus. *Virus Res* **91**, 47-63.

Domingo, E. y Holland, J. J. (1997). RNA virus mutations and fitness for survival. *Annu Rev Microbiol* **51**, 151-178.

Domingo, E., Martín, V., Perales, C., Grande-Perez, A., García-Arriaza, J. y Arias, A. (2006). Viruses as quasispecies: biological implications. *Curr Top Microbiol Immunol* **299**, 51-82.

Domingo, E., Mateu, M. G., Martínez, M. A., dopazo, J., Moya, A., Sobrino, F (1990). Genetic variability and antigenic diversity of Foot-and-mouth disease virus. *Applied virology research (F A Murphy, M H V Van Regenmortel, Eds)*.

Domingo, E., Verdaguer, N., Ochoa, W. F., Ruiz-Jarabo, C. M., Sevilla, N., Baranowski, E., Mateu, M. G. y Fita, I. (1999). Biochemical and structural studies with neutralizing antibodies raised against foot-and-mouth disease virus. *Virus Res* **62**, 169-175.

Doms, R. W., Helenius, A. y White, J. (1985). Membrane fusion activity of the influenza virus hemagglutinin. The low pH-induced conformational change. *J Biol Chem* **260**, 2973-2981.

DuBridge, R. B., Tang, P., Hsia, H. C., Leong, P. M., Miller, J. H. y Calos, M. P. (1987). Analysis of mutation in human cells by using an Epstein-Barr virus shuttle system. *Mol Cell Biol* **7**, 379-387.

Ellard, F. M., Drew, J., Blakemore, W. E., Stuart, D. I. y King, A. M. (1999). Evidence for the role of His-142 of protein 1C in the acid-induced disassembly of foot-and-mouth disease virus capsids. *J Gen Virol* **80 (Pt 8)**, 1911-1918.

Emonet, S. E., Urata, S. y de la Torre, J. C. (2011). Arenavirus reverse genetics: new approaches for the investigation of arenavirus biology and development of antiviral strategies. *Virology* **411**, 416-425.

Emonet, S. F., Garidou, L., McGavern, D. B. y de la Torre, J. C. (2009). Generation of recombinant lymphocytic choriomeningitis viruses with trisegmented genomes stably expressing two additional genes of interest. *Proc Natl Acad Sci U S A* **106**, 3473-3478.

Engel, S., Heger, T., Mancini, R., Herzog, F., Kartenbeck, J., Hayer, A. y Helenius, A. (2011). Role of endosomes in simian virus 40 entry and infection. *J Virol* **85**, 4198-4211.

Enjuanes, L., Carrascosa, A. L., Moreno, M. A. y Viñuela, E. (1976). Titration of African swine fever (ASF) virus. *J Gen Virol* **32**, 471-477.

Erlmann, P., Schmid, S., Horenkamp, F. A., Geyer, M., Pomorski, T. G. y Olayioye, M. A. (2009). DLC1 Activation Requires Lipid Interaction through a Polybasic Region Preceding the RhoGAP Domain. *Mol Biol Cell*.

Escarmis, C., Dávila, M., Charpentier, N., Bracho, A., Moya, A. y Domingo, E. (1996). Genetic lesions associated with Muller's ratchet in an RNA virus. *J Mol Biol* **264**, 255-267.

Escarmis, C., Toja, M., Medina, M. y Domingo, E. (1992). Modifications of the 5' untranslated region of foot-and-mouth disease virus after prolonged persistence in cell culture. *Virus Res* **26**, 113-125.

Eschli, B., Quirin, K., Wepf, A., Weber, J., Zinkernagel, R. y Hengartner, H. (2006). Identification of an N-terminal trimeric coiled-coil core within arenavirus glycoprotein 2 permits assignment to class I viral fusion proteins. *J Virol* **80**, 5897-5907.

Feng, Y., Press, B. y Wandinger-Ness, A. (1995). Rab 7: an important regulator of late endocytic membrane traffic. *J Cell Biol* **131**, 1435-1452.

Ferrer-Orta, C., Sierra, M., Agudo, R., de la Higuera, I., Arias, A., Pérez-Luque, R., Escarmis, C., Domingo, E. y Verdaguer, N. (2010). Structure of foot-and-mouth disease virus mutant polymerases with reduced sensitivity to ribavirin. *J Virol* **84**, 6188-6199.

FitzGerald, D. J., Padmanabhan, R., Pastan, I. y Willingham, M. C. (1983). Adenovirus-induced release of epidermal growth factor and pseudomonas toxin into the cytosol of KB cells during receptor-mediated endocytosis. *Cell* **32**, 607-617.

Fotin, A., Cheng, Y., Sliz, P., Grigorieff, N., Harrison, S. C., Kirchhausen, T. y Walz, T. (2004). Molecular model for a complete clathrin lattice from electron cryomicroscopy. *Nature* **432**, 573-579.

Fox, G., Parry, N. R., Barnett, P. V., McGinn, B., Rowlands, D. J. y Brown, F. (1989). The cell attachment site on foot-and-mouth disease virus includes the amino acid sequence RGD (arginine-glycine-aspartic acid). *J Gen Virol* **70 (Pt 3)**, 625-637.

Fredericksen, B. L. y Whitt, M. A. (1998). Attenuation of recombinant vesicular stomatitis viruses encoding mutant glycoproteins demonstrate a critical role for maintaining a high pH threshold for membrane fusion in viral fitness. *Virology* **240**, 349-358.

Fry, E. E., Lea, S. M., Jackson, T., Newman, J. W., Ellard, F. M., Blakemore, W. E., Abu-Ghazaleh, R., Samuel, A., King, A. M. y Stuart, D. I. (1999). The structure and function of a foot-and-mouth disease virus-oligosaccharide receptor complex. *Embo J* **18**, 543-554.

Fry, E. E., Newman, J. W., Curry, S., Najjam, S., Jackson, T., Blakemore, W., Lea, S. M., Miller, L., Burman, A., King, A. M. y Stuart, D. I. (2005). Structure of Foot-and-mouth disease virus serotype A10 61 alone and complexed with oligosaccharide receptor: receptor conservation in the face of antigenic variation. *J Gen Virol* **86**, 1909-1920.

Fujita, A., Cheng, J., Tauchi-Sato, K., Takenawa, T. y Fujimoto, T. (2009). A distinct pool of phosphatidylinositol 4,5-bisphosphate in caveolae revealed by a nanoscale labeling technique. *Proc Natl Acad Sci U S A* **106**, 9256-9261.

Ganges, L., Borrego, B., Fernández-Pacheco, P., Revilla, C., Fernández-Borges, N., Domínguez, J., Sobrino, F. y Rodríguez, F. (2011). DNA immunization of pigs with foot-and-mouth disease virus minigenes: from partial protection to disease exacerbation. *Virus Res* **157**, 121-125.

Gao, J., Takeuchi, H., Zhang, Z., Fujii, M., Kanematsu, T. y Hirata, M. (2009). Binding of phospholipase C-related but catalytically inactive protein to phosphatidylinositol 4,5-bisphosphate via the PH domain. *Cell Signal*.

García-Arriaza, J., Manrubia, S. C., Toja, M., Domingo, E. y Escarmis, C. (2004). Evolutionary transition toward defective RNAs that are infectious by complementation. *J Virol* **78**, 11678-11685.

García-Briones, M., Rosas, M. F., González-Magaldi, M., Martín-Acebes, M. A., Sobrino, F. y Armas-Portela, R. (2006). Differential distribution of non-structural proteins of foot-and-mouth disease virus in BHK-21 cells. *Virology* **349**, 409-421.

Gaudin, Y., Tuffereau, C., Durrer, P., Brunner, J., Flamand, A. y Ruigrok, R. (1999). Rabies virus-induced membrane fusion. *Mol Membr Biol* **16**, 21-31.

Gerges, N. Z., Brown, T. C., Correia, S. S. y Esteban, J. A. (2005). Analysis of Rab protein function in neurotransmitter receptor trafficking at hippocampal synapses. *Methods Enzymol* **403**, 153-166.

Ghosh, S. K., Perrine, S. P., Williams, R. M. y Faller, D. V. (2012). Histone deacetylase inhibitors are potent inducers of gene expression in latent EBV and sensitize lymphoma cells to nucleoside antiviral agents. *Blood* **119**, 1008-1017.

Giguere, J. F. y Tremblay, M. J. (2004). Statin compounds reduce human immunodeficiency virus type 1 replication by preventing the interaction between virion-associated host intercellular adhesion molecule 1 and its natural cell surface ligand LFA-1. *J Virol* **78**, 12062-12065.

Gilbert, C., Bergeron, M., Methot, S., Giguere, J. F. y Tremblay, M. J. (2005). Statins could be used to control replication of some viruses, including HIV-1. *Viral Immunol* **18**, 474-489.

Gillespie, L. K., Hoenen, A., Morgan, G. y Mackenzie, J. M. (2010). The endoplasmic reticulum provides the membrane platform for biogenesis of the flavivirus replication complex. *J Virol* **84**, 10438-10447.

Gorvel, J. P., Chavrier, P., Zerial, M. y Gruenberg, J. (1991). rab5 controls early endosome fusion in vitro. *Cell* **64**, 915-925.

Gower, T. L. y Graham, B. S. (2001). Antiviral activity of lovastatin against respiratory syncytial virus in vivo and in vitro. *Antimicrob Agents Chemother* **45**, 1231-1237.

Graci, J. D. y Cameron, C. E. (2006). Mechanisms of action of ribavirin against distinct viruses. *Rev Med Virol* **16**, 37-48.

Greber, U. F. y Fornerod, M. (2005). Nuclear import in viral infections. *Curr Top Microbiol Immunol* **285**, 109-138.

Green, E. G., Ramm, E., Riley, N. M., Spiro, D. J., Goldenring, J. R. y Wessling-Resnick, M. (1997). Rab11 is associated with transferrin-containing recycling compartments in K562 cells. *Biochem Biophys Res Commun* **239**, 612-616.

Grove, J. y Marsh, M. (2011). The cell biology of receptor-mediated virus entry. *J Cell Biol* **195**, 1071-1082.

Gruenberg, J. (2001). The endocytic pathway: a mosaic of domains. *Nat Rev Mol Cell Biol* **2**, 721-730.

Guinea, R. y Carrasco, L. (1991). Effects of fatty acids on lipid synthesis and viral RNA replication in poliovirus-infected cells. *Virology* **185**, 473-476.

Hackett, A. J., Schaffer, F. L. y Madin, S. H. (1967). The separation of infectious and autointerfering particles in vesicular stomatitis virus preparations. *Virology* **31**, 114-119.

Harbison, C. E., Lyi, S. M., Weichert, W. S. y Parrish, C. R. (2009). Early steps in cell infection by parvoviruses: host-specific differences in cell receptor binding but similar endosomal trafficking. *J Virol* **83**, 10504-10514.

Harrison, S. A., Rossaro, L., Hu, K. Q., Patel, K., Tillmann, H., Dhaliwal, S., Torres, D. M., Koury, K., Goteti, V. S., Noviello, S., Brass, C. A., Albrecht, J. K., McHutchison, J. G. y Sulkowski, M. S. (2010). Serum cholesterol and statin use predict virological response to peginterferon and ribavirin therapy. *Hepatology* **52**, 864-874.

Harrison, S. C. (2008). Viral membrane fusion. *Nat Struct Mol Biol* **15**, 690-698.

Haspot, F., Lavault, A., Sinzger, C., Laib Sampaio, K., Stierhof, Y. D., Pilet, P., Bressolette-Bodin, C. y Halary, F. (2012). Human cytomegalovirus entry into dendritic cells occurs via a macropinocytosis-like pathway in a pH-independent and cholesterol-dependent manner. *PLoS One* **7**, e34795.

Hayer, A., Stoeber, M., Ritz, D., Engel, S., Meyer, H. H. y Helenius, A. (2010). Caveolin-1 is ubiquitinated and targeted to intralumenal vesicles in endolysosomes for degradation. *J Cell Biol* **191**, 615-629.

Heaton, N. S., Perera, R., Berger, K. L., Khadka, S., Lacount, D. J., Kuhn, R. J. y Randall, G. (2010a). Dengue virus nonstructural protein 3 redistributes fatty acid synthase to sites of viral replication and increases cellular fatty acid synthesis. *Proc Natl Acad Sci U S A* **107**, 17345-17350.

Heaton, N. S. y Randall, G. (2010b). Dengue virus-induced autophagy regulates lipid metabolism. *Cell Host Microbe* **8**, 422-432.

Heaton, N. S. y Randall, G. (2011). Multifaceted roles for lipids in viral infection. *Trends Microbiol* **19**, 368-375.

Henley, J. R., Krueger, E. W., Oswald, B. J. y McNiven, M. A. (1998). Dynamin-mediated internalization of caveolae. *J Cell Biol* **141**, 85-99.

Henne, W. M., Boucrot, E., Meinecke, M., Evergren, E., Vallis, Y., Mittal, R. y McMahon, H. T. (2010). FCHo proteins are nucleators of clathrin-mediated endocytosis. *Science* **328**, 1281-1284.

Hernáez, B. y Alonso, C. (2010). Dynamin- and clathrin-dependent endocytosis in African swine fever virus entry. *J Virol* **84**, 2100-2109.

Hollidge, B. S., Nedelsky, N. B., Salzano, M. V., Fraser, J. W., Gonzalez-Scarano, F. y Soldan, S. S. (2012). Orthobunyavirus entry into neurons and other mammalian cells occurs via clathrin-mediated endocytosis and requires trafficking into early endosomes. *J Virol*.

Honing, S., Ricotta, D., Krauss, M., Spate, K., Spolaore, B., Motley, A., Robinson, M., Robinson, C., Haucke, V. y Owen, D. J. (2005). Phosphatidylinositol-(4,5)-bisphosphate regulates sorting signal recognition by the clathrin-associated adaptor complex AP2. *Mol Cell* **18**, 519-531.

Hsu, N. Y., Ilnytska, O., Belov, G., Santiana, M., Chen, Y. H., Takvorian, P. M., Pau, C., van der Schaar, H., Kaushik-Basu, N., Balla, T., Cameron, C. E., Ehrenfeld, E.,

van Kuppeveld, F. J. y Altan-Bonnet, N. (2010). Viral reorganization of the secretory pathway generates distinct organelles for RNA replication. *Cell* **141**, 799-811.

Huang, H., Chen, Y. y Ye, J. (2007). Inhibition of hepatitis C virus replication by peroxidation of arachidonate and restoration by vitamin E. *Proc Natl Acad Sci U S A* **104**, 18666-18670.

Huang, W. R., Wang, Y. C., Chi, P. I., Wang, L., Wang, C. Y., Lin, C. H. y Liu, H. J. (2011). Cell entry of avian reovirus follows a caveolin-1-mediated and dynamin-2-dependent endocytic pathway that requires activation of p38 mitogen-activated protein kinase (MAPK) and Src signaling pathways as well as microtubules and small GTPase Rab5 protein. *J Biol Chem* **286**, 30780-30794.

Huotari, J. y Helenius, A. (2011). Endosome maturation. *EMBO J* **30**, 3481-3500.

ICTV (2009). International Committee on Taxonomy of Viruses.

Igonet, S., Vaney, M. C., Vonhrein, C., Bricogne, G., Stura, E. A., Hengartner, H., Eschli, B. y Rey, F. A. (2011). X-ray structure of the arenavirus glycoprotein GP2 in its postfusion hairpin conformation. *Proc Natl Acad Sci U S A* **108**, 19967-19972.

Inoue, H., Nojima, H. y Okayama, H. (1990). High efficiency transformation of Escherichia coli with plasmids. *Gene* **96**, 23-28.

Jackson, T., Clark, S., Berryman, S., Burman, A., Cambier, S., Mu, D., Nishimura, S. y King, A. M. (2004). Integrin alphavbeta8 functions as a receptor for foot-and-mouth disease virus: role of the beta-chain cytodomain in integrin-mediated infection. *J Virol* **78**, 4533-4540.

Jackson, T., Ellard, F. M., Ghazaleh, R. A., Brookes, S. M., Blakemore, W. E., Corteyn, A. H., Stuart, D. I., Newman, J. W. y King, A. M. (1996). Efficient infection of cells in culture by type O foot-and-mouth disease virus requires binding to cell surface heparan sulfate. *J Virol* **70**, 5282-5287.

Jackson, T., Mould, A. P., Sheppard, D. y King, A. M. (2002). Integrin alphavbeta1 is a receptor for foot-and-mouth disease virus. *J Virol* **76**, 935-941.

Jackson, T., Sheppard, D., Denyer, M., Blakemore, W. y King, A. M. (2000). The epithelial integrin alphavbeta6 is a receptor for foot-and-mouth disease virus. *J Virol* **74**, 4949-4956.

Jacobson, K., Mouritsen, O. G. y Anderson, R. G. (2007). Lipid rafts: at a crossroad between cell biology and physics. *Nat Cell Biol* **9**, 7-14.

James, D. J., Khodthong, C., Kowalchyk, J. A. y Martin, T. F. (2008a). Phosphatidylinositol 4,5-bisphosphate regulates SNARE-dependent membrane fusion. *J Cell Biol* **182**, 355-366.

James, D. J., Khodthong, C., Kowalchyk, J. A. y Martín, T. F. (2008b). Phosphatidylinositol 4,5-bisphosphate regulates SNARE-dependent membrane fusion. *J Cell Biol* **182**, 355-366.

Jiang, M., Abend, J. R., Tsai, B. y Imperiale, M. J. (2009). Early events during BK virus entry and disassembly. *J Virol* **83**, 1350-1358.

Jiménez-Clavero, M. A., Escribano-Romero, E., Mansilla, C., Gómez, N., Córdoba, L., Roblas, N., Ponz, F., Ley, V. y Saiz, J. C. (2005). Survey of bovine enterovirus in biological and environmental samples by a highly sensitive real-time reverse transcription-PCR. *Appl Environ Microbiol* **71**, 3536-3543.

Johannsdottir, H. K., Mancini, R., Kartenbeck, J., Amato, L. y Helenius, A. (2009). Host cell factors and functions involved in vesicular stomatitis virus entry. *J Virol* **83**, 440-453.

Johns, H. L., Berryman, S., Monaghan, P., Belsham, G. J. y Jackson, T. (2009). A dominant-negative mutant of rab5 inhibits infection of cells by foot-and-mouth disease virus: implications for virus entry. *J Virol* **83**, 6247-6256.

Johnson, C. M., Chichili, G. R. y Rodgers, W. (2008). Compartmentalization of phosphatidylinositol 4,5-bisphosphate signaling evidenced using targeted phosphatases. *J Biol Chem* **283**, 29920-29928.

Jordens, I., Marsman, M., Kuijl, C. y Neefjes, J. (2005). Rab proteins, connecting transport and vesicle fusion. *Traffic* **6**, 1070-1077.

Jovic, M., Sharma, M., Rahajeng, J. y Caplan, S. (2010). The early endosome: a busy sorting station for proteins at the crossroads. *Histol Histopathol* **25**, 99-112.

Kalvodova, L., Sampaio, J. L., Cordo, S., Ejsing, C. S., Shevchenko, A. y Simons, K. (2009). The lipidomes of vesicular stomatitis virus, semliki forest virus, and the host plasma membrane analyzed by quantitative shotgun mass spectrometry. *J Virol* **83**, 7996-8003.

Kanner, A. M. (2003). The Pharmacology of Parenteral Valproate. *Epilepsy Curr* **3**, 109-111.

Kim, C. y Bergelson, J. M. (2012). Echovirus 7 entry into polarized intestinal epithelial cells requires clathrin and Rab7. *MBio* **3**.

Kirchhausen, T. y Harrison, S. C. (1981). Protein organization in clathrin trimers. *Cell* **23**, 755-761.

Knipe, T., Rieder, E., Baxt, B., Ward, G. y Mason, P. W. (1997). Characterization of synthetic foot-and-mouth disease virus provirions separates acid-mediated disassembly from infectivity. *J Virol* **71**, 2851-2856.

Knox, C., Moffat, K., Ali, S., Ryan, M. y Wileman, T. (2005). Foot-and-mouth disease virus replication sites form next to the nucleus and close to the Golgi apparatus, but exclude marker proteins associated with host membrane compartments. *J Gen Virol* **86**, 687-696.

Konecsni, T., Berka, U., Pickl-Herk, A., Bilek, G., Khan, A. G., Gajdzig, L., Fuchs, R. y Blaas, D. (2009). Low pH-triggered beta-propeller switch of the low-density lipoprotein receptor assists rhinovirus infection. *J Virol* **83**, 10922-10930.

Krishnan, M. N., Sukumaran, B., Pal, U., Agaisse, H., Murray, J. L., Hodge, T. W. y Fikrig, E. (2007). Rab 5 is required for the cellular entry of dengue and West Nile viruses. *J Virol* **81**, 4881-4885.

Kuhn, R., Luz, N. y Beck, E. (1990). Functional analysis of the internal translation initiation site of foot-and-mouth disease virus. *J Virol* **64**, 4625-4631.

Kunz, S. (2009). Receptor binding and cell entry of Old World arenaviruses reveal novel aspects of virus-host interaction. *Virology* **387**, 245-249.

Kwiatkowska, K. (2010). One lipid, multiple functions: how various pools of PI(4,5)P(2) are created in the plasma membrane. *Cell Mol Life Sci* **67**, 3927-3946.

Laemmli, U. K. (1970). Cleavage of structural proteins during the assembly of the head of bacteriophage T4. *Nature* **227**, 680-685.

Lakadamyali, M., Rust, M. J. y Zhuang, X. (2006). Ligands for clathrin-mediated endocytosis are differentially sorted into distinct populations of early endosomes. *Cell* **124**, 997-1009.

Lanciotti, R. S., Kerst, A. J., Nasci, R. S., Godsey, M. S., Mitchell, C. J., Savage, H. M., Komar, N., Panella, N. A., Allen, B. C., Volpe, K. E., Davis, B. S. y Roehrig, J. T. (2000). Rapid detection of west nile virus from human clinical specimens, field-collected mosquitoes, and avian samples by a TaqMan reverse transcriptase-PCR assay. *J Clin Microbiol* **38**, 4066-4071.

Lanciotti, R. S., Roehrig, J. T., Deubel, V., Smith, J., Parker, M., Steele, K., Crise, B., Volpe, K. E., Crabtree, M. B., Scherret, J. H., Hall, R. A., MacKenzie, J. S., Cropp, C. B., Panigrahy, B., Ostlund, E., Schmitt, B., Malkinson, M., Banet, C., Weissman, J., Komar, N., Savage, H. M., Stone, W., McNamara, T. y Gubler, D. J. (1999). Origin of the West Nile virus responsible for an outbreak of encephalitis in the northeastern United States. *Science* **286**, 2333-2337.

Le Blanc, I., Luyet, P. P., Pons, V., Ferguson, C., Emans, N., Petiot, A., Mayran, N., Demaurex, N., Faure, J., Sadoul, R., Parton, R. G. y Gruenberg, J. (2005). Endosome-to-cytosol transport of viral nucleocapsids. *Nat Cell Biol* **7**, 653-664.

Le, P. U. y Nabi, I. R. (2003). Distinct caveolae-mediated endocytic pathways target the Golgi apparatus and the endoplasmic reticulum. *J Cell Sci* **116**, 1059-1071.

Lea, S., Hernandez, J., Blakemore, W., Brocchi, E., Curry, S., Domingo, E., Fry, E., Abu-Ghazaleh, R., King, A., Newman, J. y et al. (1994a). The structure and antigenicity of a type C foot-and-mouth disease virus. *Structure* **2**, 123-139.

Lea, S., Hernández, J., Blakemore, W., Brocchi, E., Curry, S., Domingo, E., Fry, E., Abu-Ghazaleh, R., King, A., Newman, J. y et al. (1994b). The structure and antigenicity of a type C foot-and-mouth disease virus. *Structure* **2**, 123-139.

Lee, A. M., Pasquato, A. y Kunz, S. (2010). Novel approaches in anti-arenaviral drug development. *Virology* **411**, 163-169.

Lee, E., Hall, R. A. y Lobigs, M. (2004). Common E protein determinants for attenuation of glycosaminoglycan-binding variants of Japanese encephalitis and West Nile viruses. *J Virol* **78**, 8271-8280.

Lee, K. J., Novella, I. S., Teng, M. N., Oldstone, M. B. y de La Torre, J. C. (2000). NP and L proteins of lymphocytic choriomeningitis virus (LCMV) are sufficient for efficient transcription and replication of LCMV genomic RNA analogs. *J Virol* **74**, 3470-3477.

Lee, K. J., Pérez, M., Pinschewer, D. D. y de la Torre, J. C. (2002). Identification of the lymphocytic choriomeningitis virus (LCMV) proteins required to rescue LCMV RNA analogs into LCMV-like particles. *J Virol* **76**, 6393-6397.

Lefrancois, L. y Lyles, D. S. (1982). The interaction of antibody with the major surface glycoprotein of vesicular stomatitis virus. II. Monoclonal antibodies of nonneutralizing and cross-reactive epitopes of Indiana and New Jersey serotypes. *Virology* **121**, 168-174.

Lehrman, G., Hogue, I. B., Palmer, S., Jennings, C., Spina, C. A., Wiegand, A., Landay, A. L., Coombs, R. W., Richman, D. D., Mellors, J. W., Coffin, J. M., Bosch, R. J. y Margolis, D. M. (2005). Depletion of latent HIV-1 infection in vivo: a proof-of-concept study. *Lancet* **366**, 549-555.

Letchworth, G. J., Rodríguez, L. L. y Del cbarrera, J. (1999). Vesicular stomatitis. *Vet J* **157**, 239-260.

Ley, V., Higgins, J. y Fayer, R. (2002). Bovine enteroviruses as indicators of fecal contamination. *Appl Environ Microbiol* **68**, 3455-3461.

Lezin, A., Gillet, N., Olindo, S., Signate, A., Grandvaux, N., Verlaeten, O., Belrose, G., de Carvalho Bittencourt, M., Hiscott, J., Asquith, B., Burny, A., Smadja, D., Cesaire, R. y Willems, L. (2007). Histone deacetylase mediated transcriptional activation reduces proviral loads in HTLV-1 associated myelopathy/tropical spastic paraparesis patients. *Blood* **110**, 3722-3728.

Li, F., Browning, G. F., Studdert, M. J. y Crabb, B. S. (1996). Equine rhinovirus 1 is more closely related to foot-and-mouth disease virus than to other picornaviruses. *Proc Natl Acad Sci U S A* **93**, 990-995.

Li, S. Y., Chen, C., Zhang, H. Q., Guo, H. Y., Wang, H., Wang, L., Zhang, X., Hua, S. N., Yu, J., Xiao, P. G., Li, R. S. y Tan, X. (2005). Identification of natural compounds with antiviral activities against SARS-associated coronavirus. *Antiviral Res* **67**, 18-23.

Lichty, B. D., Power, A. T., Stojdl, D. F. y Bell, J. C. (2004). Vesicular stomatitis virus: re-inventing the bullet. *Trends Mol Med* **10**, 210-216.

Liu, Z., Guo, Z., Wang, G., Zhang, D., He, H., Li, G., Liu, Y., Higgins, D., Walsh, A., Shanahan-Prendergast, L. y Lu, J. (2009). Evaluation of the efficacy and safety of a statin/caffeine combination against H5N1, H3N2 and H1N1 virus infection in BALB/c mice. *Eur J Pharm Sci* **38**, 215-223.

Loerke, D., Mettlen, M., Yarar, D., Jaqaman, K., Jaqaman, H., Danuser, G. y Schmid, S. L. (2009). Cargo and dynamin regulate clathrin-coated pit maturation. *PLoS Biol* **7**, e57.

Lorizate, M. y Krausslich, H. G. (2011). Role of lipids in virus replication. *Cold Spring Harb Perspect Biol* **3**, a004820.

Lozach, P. Y., Huotari, J. y Helenius, A. (2011). Late-penetrating viruses. *Curr Opin Virol* **1**, 35-43.

Lozach, P. Y., Mancini, R., Bitto, D., Meier, R., Oestereich, L., Overby, A. K., Pettersson, R. F. y Helenius, A. (2010). Entry of bunyaviruses into mammalian cells. *Cell Host Microbe* **7**, 488-499.

Luan, P., Yang, L. y Glaser, M. (1995). Formation of membrane domains created during the budding of vesicular stomatitis virus. A model for selective lipid and protein sorting in biological membranes. *Biochemistry* **34**, 9874-9883.

Lukacs, G. L., Segal, G., Kartner, N., Grinstein, S. y Zhang, F. (1997). Constitutive internalization of cystic fibrosis transmembrane conductance regulator occurs via clathrin-dependent endocytosis and is regulated by protein phosphorylation. *Biochem J* **328 (Pt 2)**, 353-361.

Luo, M. (2012). Influenza virus entry. *Adv Exp Med Biol* **726**, 201-221.

Luria, S. E., and Burrous, J. W. (1957). Hybridization between Escherichia coli and Shigella. *J Bacteriology* **74**, 461-476.

Mackenzie, J. M., Khromykh, A. A. y Parton, R. G. (2007). Cholesterol manipulation by West Nile virus perturbs the cellular immune response. *Cell Host Microbe* **2**, 229-239.

Mackenzie, J. M., Khromykh, A. A. y Westaway, E. G. (2001). Stable expression of noncytopathic Kunjin replicons simulates both ultrastructural and biochemical characteristics observed during replication of Kunjin virus. *Virology* **279**, 161-172.

Marsh, M. y Helenius, A. (1989). Virus entry into animal cells. *Adv Virus Res* **36**, 107-151.

Marsh, M. y Helenius, A. (2006). Virus entry: open sesame. *Cell* **124**, 729-740.

Marsh, M., Wellsteed, J., Kern, H., Harms, E. y Helenius, A. (1982). Monensin inhibits Semliki Forest virus penetration into culture cells. *Proc Natl Acad Sci U S A* **79**, 5297-5301.

Marshansky, V. y Futai, M. (2008). The V-type H+-ATPase in vesicular trafficking: targeting, regulation and function. *Curr Opin Cell Biol* **20**, 415-426.

Martín-Acebes, M. A. (2009). Mecanismos de entrada y de organización del complejo de replicación del virus de la fiebre aftosa: estudio comparativo con el virus de la enfermedad del cerdo y el virus de la estomatitis vesicular. *Tesis Doctoral*.

Martín-Acebes, M. A., Blázquez, A. B., Jiménez de Oya, N., Escribano-Romero, E. y Saiz, J. C. (2011a). West Nile virus replication requires fatty acid synthesis but is independent on phosphatidylinositol-4-phosphate lipids. *PLoS One* **6**, e24970.

Martín-Acebes, M. A., González-Magaldi, M., Rosas, M. F., Borrego, B., Brocchi, E., Armas-Portela, R. y Sobrino, F. (2008). Subcellular distribution of swine vesicular disease virus proteins and alterations induced in infected cells: a comparative study with foot-and-mouth disease virus and vesicular stomatitis virus. *Virology* **374**, 432-443.

Martín-Acebes, M. A., González-Magaldi, M., Sandvig, K., Sobrino, F. y Armas-Portela, R. (2007). Productive entry of type C foot-and-mouth disease virus into susceptible cultured cells requires clathrin and is dependent on the presence of plasma membrane cholesterol. *Virology* **369**, 105-118.

Martín-Acebes, M. A., Rincón, V., Armas-Portela, R., Mateu, M. G. y Sobrino, F. (2010). A single amino acid substitution in the capsid of foot-and-mouth disease virus can increase acid lability and confer resistance to acid-dependent uncoating inhibition. *J Virol* **84**, 2902-2912.

Martín-Acebes, M. A. y Saiz, J. C. (2011b). A West Nile virus mutant with increased resistance to acid-induced inactivation. *J Gen Virol* **92**, 831-840.

Martín-Acebes, M. A., Vázquez-Calvo, A., Rincón, V., Mateu, M. G. y Sobrino, F. (2011c). A single amino acid substitution in the capsid of foot-and-mouth disease virus can increase acid resistance. *J Virol* **85**, 2733-2740.

Martín-Belmonte, F., Martínez-Menarguez, J. A., Aranda, J. F., Ballesta, J., de Marco, M. C. y Alonso, M. A. (2003). MAL regulates clathrin-mediated endocytosis at the apical surface of Madin-Darby canine kidney cells. *J Cell Biol* **163**, 155-164.

Martín, V., Grande-Pérez, A. y Domingo, E. (2008). No evidence of selection for mutational robustness during lethal mutagenesis of lymphocytic choriomeningitis virus. *Virology* **378**, 185-192.

Martínez, M. G., Forlenza, M. B. y Candurra, N. A. (2009). Involvement of cellular proteins in Junin arenavirus entry. *Biotechnol J* **4**, 866-870.

Mason, P. W., Baxt, B., Brown, F., Harber, J., Murdin, A. y Wimmer, E. (1993). Antibody-complexed foot-and-mouth disease virus, but not poliovirus, can infect normally insusceptible cells via the Fc receptor. *Virology* **192**, 568-577.

Mason, P. W., Rieder, E. y Baxt, B. (1994). RGD sequence of foot-and-mouth disease virus is essential for infecting cells via the natural receptor but can be bypassed by an antibody-dependent enhancement pathway. *Proc Natl Acad Sci U S A* **91**, 1932-1936.

Massol, R. H., Boll, W., Griffin, A. M. y Kirchhausen, T. (2006). A burst of auxilin recruitment determines the onset of clathrin-coated vesicle uncoating. *Proc Natl Acad Sci U S A* **103**, 10265-10270.

Mateo, R., Díaz, A., Baranowski, E. y Mateu, M. G. (2003). Complete alanine scanning of intersubunit interfaces in a foot-and-mouth disease virus capsid reveals critical contributions of many side chains to particle stability and viral function. *J Biol Chem* **278**, 41019-41027.

Mateo, R., Luna, E. y Mateu, M. G. (2007a). Thermostable variants are not generally represented in foot-and-mouth disease virus quasispecies. *J Gen Virol* **88**, 859-864.

Mateo, R. y Mateu, M. G. (2007b). Deterministic, compensatory mutational events in the capsid of foot-and-mouth disease virus in response to the introduction of mutations found in viruses from persistent infections. *J Virol* **81**, 1879-1887.

Mateu, M. G., Martínez, M. A., Capucci, L., Andreu, D., Giralt, E., Sobrino, F., Brocchi, E. y Domingo, E. (1990). A single amino acid substitution affects multiple overlapping epitopes in the major antigenic site of foot-and-mouth disease virus of serotype C. *J Gen Virol* **71 (Pt 3)**, 629-637.

Mateu, M. G., Valero, M. L., Andreu, D. y Domingo, E. (1996). Systematic replacement of amino acid residues within an Arg-Gly-Asp-containing loop of foot-and-mouth disease virus and effect on cell recognition. *J Biol Chem* **271**, 12814-12819.

Matlin, K. S., Reggio, H., Helenius, A. y Simons, K. (1982). Pathway of vesicular stomatitis virus entry leading to infection. *J Mol Biol* **156**, 609-631.

Maxfield, F. R. y Yamashiro, D. J. (1987). Endosome acidification and the pathways of receptor-mediated endocytosis. *Adv Exp Med Biol* **225**, 189-198.

Mayor, S. y Pagano, R. E. (2007). Pathways of clathrin-independent endocytosis. *Nat Rev Mol Cell Biol* **8**, 603-612.

McKenna, T. S., Lubroth, J., Rieder, E., Baxt, B. y Mason, P. W. (1995). Receptor binding site-deleted foot-and-mouth disease (FMD) virus protects cattle from FMD. *J Virol* **69**, 5787-5790.

McMahon, H. T. y Boucrot, E. (2011). Molecular mechanism and physiological functions of clathrin-mediated endocytosis. *Nat Rev Mol Cell Biol* **12**, 517-533.

Medigeshi, G. R., Hirsch, A. J., Streblow, D. N., Nikolich-Zugich, J. y Nelson, J. A. (2008). West Nile virus entry requires cholesterol-rich membrane microdomains and is independent of alphavbeta3 integrin. *J Virol* **82**, 5212-5219.

Mercer, J. y Helenius, A. (2009). Virus entry by macropinocytosis. *Nat Cell Biol* **11**, 510-520.

Mercer, J., Schelhaas, M. y Helenius, A. (2010). Virus entry by endocytosis. *Annu Rev Biochem* **79**, 803-833.

Meresse, S., Gorvel, J. P. y Chavrier, P. (1995). The rab7 GTPase resides on a vesicular compartment connected to lysosomes. *J Cell Sci* **108 (Pt 11)**, 3349-3358.

Mihaila, R., Nedelcu, L., Fratila, O., Rezi, E. C., Domnariu, C., Ciuca, R., Zaharie, A. V., Olteanu, A., Bera, L. y Deac, M. (2009). Lovastatin and fluvastatin reduce viremia and the pro-inflammatory cytokines in the patients with chronic hepatitis C. *Hepatogastroenterology* **56**, 1704-1709.

Mihaila, R. G., Nedelcu, L., Fratila, O., Retzler, L., Domnariu, C., Cipaian, R. C., Rezi, E. C., Beca, C. y Deac, M. (2011). Effects of simvastatin in patients with viral chronic hepatitis C. *Hepatogastroenterology* **58**, 1296-1300.

Miller, K., Shipman, M., Trowbridge, I. S. y Hopkins, C. R. (1991). Transferrin receptors promote the formation of clathrin lattices. *Cell* **65**, 621-632.

Miller, S. y Krijnse-Locker, J. (2008). Modification of intracellular membrane structures for virus replication. *Nat Rev Microbiol* **6**, 363-374.

Monaghan, P., Cook, H., Jackson, T., Ryan, M. y Wileman, T. (2004). The ultrastructure of the developing replication site in foot-and-mouth disease virus-infected BHK-38 cells. *J Gen Virol* **85**, 933-946.

Monaghan, P., Gold, S., Simpson, J., Zhang, Z., Weinreb, P. H., Violette, S. M., Alexandersen, S. y Jackson, T. (2005). The alpha(v)beta6 integrin receptor for Foot-and-mouth disease virus is expressed constitutively on the epithelial cells targeted in cattle. *J Gen Virol* **86**, 2769-2780.

Montoya, C. J., Jaimes, F., Higuita, E. A., Convers-Paez, S., Estrada, S., Gutierrez, F., Amariles, P., Giraldo, N., Penaloza, C. y Rugeles, M. T. (2009). Antiretroviral effect of lovastatin on HIV-1-infected individuals without highly active antiretroviral therapy (The LIVE study): a phase-II randomized clinical trial. *Trials* **10**, 41.

Moody, M. A., Liao, H. X., Alam, S. M., Scearce, R. M., Plonk, M. K., Kozink, D. M., Drinker, M. S., Zhang, R., Xia, S. M., Sutherland, L. L., Tomaras, G. D., Giles, I. P., Kappes, J. C., Ochsenbauer-Jambor, C., Edmonds, T. G., Soares, M., Barbero, G., Forthal, D. N., Landucci, G., Chang, C., King, S. W., Kavlie, A., Denny, T. N., Hwang, K. K., Chen, P. P., Thorpe, P. E., Montefiori, D. C. y Haynes, B. F. (2010). Anti-phospholipid human monoclonal antibodies inhibit CCR5-tropic HIV-1 and induce beta-chemokines. *J Exp Med* **207**, 763-776.

Muench, R. L. J. a. H. (1935). A simple method of estimating fifty percent endpoints. . *Am J Hyg* **27**, 493-497.

Mukhopadhyay, S., Kim, B. S., Chipman, P. R., Rossmann, M. G. y Kuhn, R. J. (2003). Structure of West Nile virus. *Science* **302**, 248.

Munger, J., Bennett, B. D., Parikh, A., Feng, X. J., McArdle, J., Rabitz, H. A., Shenk, T. y Rabinowitz, J. D. (2008). Systems-level metabolic flux profiling identifies fatty acid synthesis as a target for antiviral therapy. *Nat Biotechnol* **26**, 1179-1186.

Murphy, F. A. y Whitfield, S. G. (1975). Morphology and morphogenesis of arenaviruses. *Bull World Health Organ* **52**, 409-419.

Nabi, I. R. y Le, P. U. (2003). Caveolae/raft-dependent endocytosis. *J Cell Biol* **161**, 673-677.

Neff, S., Sa-Carvalho, D., Rieder, E., Mason, P. W., Blystone, S. D., Brown, E. J. y Baxt, B. (1998). Foot-and-mouth disease virus virulent for cattle utilizes the integrin alpha(v)beta3 as its receptor. *J Virol* **72**, 3587-3594.

Neuman, B. W., Adair, B. D., Burns, J. W., Milligan, R. A., Buchmeier, M. J. y Yeager, M. (2005). Complementarity in the supramolecular design of arenaviruses and retroviruses revealed by electron cryomicroscopy and image analysis. *J Virol* **79**, 3822-3830.

Newman, J. F., Rowlands, D. J. y Brown, F. (1973). A physico-chemical sub-grouping of the mammalian picornaviruses. *J Gen Virol* **18**, 171-180.

Novella, I. S., Presloid, J. B., Zhou, T., Smith-Tsurkan, S. D., Ebendick-Corpus, B. E., Dutta, R. N., Lust, K. L. y Wilke, C. O. (2010). Genomic evolution of vesicular stomatitis virus strains with differences in adaptability. *J Virol* **84**, 4960-4968.

Nuñez, J. I., Baranowski, E., Molina, N., Ruiz-Jarabo, C. M., Sánchez, C., Domingo, E. y Sobrino, F. (2001). A single amino acid substitution in nonstructural protein 3A can mediate adaptation of foot-and-mouth disease virus to the guinea pig. *J Virol* **75**, 3977-3983.

Nuñez, J. I., Blanco, E., Hernández, T., Gómez-Tejedor, C., Martín, M. J., Dopazo, J. y Sobrino, F. (1998). A RT-PCR assay for the differential diagnosis of vesicular viral diseases of swine. *J Virol Methods* **72**, 227-235.

Nuñez, J. I., Molina, N., Baranowski, E., Domingo, E., Clark, S., Burman, A., Berryman, S., Jackson, T. y Sobrino, F. (2007). Guinea pig-adapted foot-and-mouth disease virus with altered receptor recognition can productively infect a natural host. *J Virol* **81**, 8497-8506.

O'Donnell, V., Larocco, M. y Baxt, B. (2008). Heparan sulfate-binding foot-and-mouth disease virus enters cells via caveola-mediated endocytosis. *J Virol* **82**, 9075-9085.

O'Donnell, V., LaRocco, M., Duque, H. y Baxt, B. (2005). Analysis of foot-and-mouth disease virus internalization events in cultured cells. *J Virol* **79**, 8506-8518.

O'Donnell, V., Pacheco, J. M., Gregg, D. y Baxt, B. (2009). Analysis of foot-and-mouth disease virus integrin receptor expression in tissues from naive and infected cattle. *J Comp Pathol* **141**, 98-112.

Oda, K., Fujiwara, T. y Ikehara, Y. (1990). Brefeldin A arrests the intracellular transport of viral envelope proteins in primary cultured rat hepatocytes and HepG2 cells. *Biochem J* **265**, 161-167.

Oh, P., McIntosh, D. P. y Schnitzer, J. E. (1998). Dynamin at the neck of caveolae mediates their budding to form transport vesicles by GTP-driven fission from the plasma membrane of endothelium. *J Cell Biol* **141**, 101-114.

Ohdo, S., Nakano, S. y Ogawa, N. (1988). Chronopharmacological study of sodium valproate in mice: dose-concentration-response relationship. *Jpn J Pharmacol* **47**, 11-19.

Ohkuma, S. y Poole, B. (1978). Fluorescence probe measurement of the intralysosomal pH in living cells and the perturbation of pH by various agents. *Proc Natl Acad Sci U S A* **75**, 3327-3331.

Ohno, H., Stewart, J., Fournier, M. C., Bosshart, H., Rhee, I., Miyatake, S., Saito, T., Gallusser, A., Kirchhausen, T. y Bonifacino, J. S. (1995). Interaction of tyrosine-based sorting signals with clathrin-associated proteins. *Science* **269**, 1872-1875.

Olschlager, S., Neyts, J. y Gunther, S. (2011). Depletion of GTP pool is not the predominant mechanism by which ribavirin exerts its antiviral effect on Lassa virus. *Antiviral Res* **91**, 89-93.

Ongvarrasopone, C., Saejia, P., Chanasakulniyom, M. y Panyim, S. (2011). Inhibition of Taura syndrome virus replication in Litopenaeus vannamei through silencing the LvRab7 gene using double-stranded RNA. *Arch Virol* **156**, 1117-1123.

Ortiz-Riano, E., Cheng, B. Y., de la Torre, J. C. y Martínez-Sobrido, L. (2011). The C-Terminal Region of Lymphocytic Choriomeningitis Virus Nucleoprotein Contains Distinct and Segregable Functional Domains Involved in NP-Z Interaction and Counteraction of the Type I Interferon Response. *J Virol* **85**, 13038-13048.

Parfenova, H., Haffner, J. y Leffler, C. W. (1999). Phosphorylation-dependent stimulation of prostanoid synthesis by nigericin in cerebral endothelial cells. *Am J Physiol* **277**, C728-738.

Parry, N., Fox, G., Rowlands, D., Brown, F., Fry, E., Acharya, R., Logan, D. y Stuart, D. (1990). Structural and serological evidence for a novel mechanism of antigenic variation in foot-and-mouth disease virus. *Nature* **347**, 569-572.

Parton, R. G. y Howes, M. T. (2010). Revisiting caveolin trafficking: the end of the caveosome. *J Cell Biol* **191**, 439-441.

Parton, R. G. y Simons, K. (2007). The multiple faces of caveolae. *Nat Rev Mol Cell Biol* **8**, 185-194.

Pasqual, G., Rojek, J. M., Masin, M., Chatton, J. Y. y Kunz, S. (2011). Old world arenaviruses enter the host cell via the multivesicular body and depend on the endosomal sorting complex required for transport. *PLoS Pathog* **7**, e1002232.

Patel, K., Lim, S. G., Cheng, C. W., Lawitz, E., Tillmann, H. L., Chopra, N., Altmeyer, R., Randle, J. C. y McHutchison, J. G. (2011). Open-label phase 1b pilot study to assess the antiviral efficacy of simvastatin combined with sertraline in chronic hepatitis C patients. *Antivir Ther* **16**, 1341-1346.

Pearse, B. M. (1976). Clathrin: a unique protein associated with intracellular transfer of membrane by coated vesicles. *Proc Natl Acad Sci U S A* **73**, 1255-1259.

Pelkmans, L., Burli, T., Zerial, M. y Helenius, A. (2004). Caveolin-stabilized membrane domains as multifunctional transport and sorting devices in endocytic membrane traffic. *Cell* **118**, 767-780.

Pelkmans, L. y Helenius, A. (2003). Insider information: what viruses tell us about endocytosis. *Curr Opin Cell Biol* **15**, 414-422.

Pelkmans, L., Kartenbeck, J. y Helenius, A. (2001). Caveolar endocytosis of simian virus 40 reveals a new two-step vesicular-transport pathway to the ER. *Nat Cell Biol* **3**, 473-483.

Pelkmans, L., Puntener, D. y Helenius, A. (2002). Local actin polymerization and dynamin recruitment in SV40-induced internalization of caveolae. *Science* **296**, 535-539.

Pelkmans, L. y Zerial, M. (2005). Kinase-regulated quantal assemblies and kiss-and-run recycling of caveolae. *Nature* **436**, 128-133.

Pereira, H. G. (1981). *Virus disease of food animals*. London: Academic Press.

Perera, R., Riley, C., Isaac, G., Hopf-Jannasch, A. S., Moore, R. J., Weitz, K. W., Pasa-Tolic, L., Metz, T. O., Adamec, J. y Kuhn, R. J. (2012). Dengue virus infection perturbs lipid homeostasis in infected mosquito cells. *PLoS Pathog* **8**, e1002584.

Pérez, M., Craven, R. C. y de la Torre, J. C. (2003). The small RING finger protein Z drives arenavirus budding: implications for antiviral strategies. *Proc Natl Acad Sci U S A* **100**, 12978-12983.

Perry, J. W. y Wobus, C. E. (2010). Endocytosis of murine norovirus 1 into murine macrophages is dependent on dynamin II and cholesterol. *J Virol* **84**, 6163-6176.

Pierschbacher, M. D. y Ruoslahti, E. (1984a). Cell attachment activity of fibronectin can be duplicated by small synthetic fragments of the molecule. *Nature* **309**, 30-33.

Pierschbacher, M. D. y Ruoslahti, E. (1984b). Variants of the cell recognition site of fibronectin that retain attachment-promoting activity. *Proc Natl Acad Sci U S A* **81**, 5985-5988.

Pietiainen, V., Marjomaki, V., Upla, P., Pelkmans, L., Helenius, A. y Hyypia, T. (2004). Echovirus 1 endocytosis into caveosomes requires lipid rafts, dynamin II, and signaling events. *Mol Biol Cell* **15**, 4911-4925.

Pizzato, M., Helander, A., Popova, E., Calistri, A., Zamborlini, A., Palu, G. y Gottlinger, H. G. (2007). Dynamin 2 is required for the enhancement of HIV-1 infectivity by Nef. *Proc Natl Acad Sci U S A* **104**, 6812-6817.

Plemper, R. K. (2011). Cell Entry of Enveloped Viruses. *Curr Opin Virol* **1**, 92-100.

Poh, M. K., Shui, G., Xie, X., Shi, P. Y., Wenk, M. R. y Gu, F. (2012). U18666A, an intra-cellular cholesterol transport inhibitor, inhibits dengue virus entry and replication. *Antiviral Res* **93**, 191-198.

Pollack, G. M. y Shen, D. D. (1985). A timed intravenous pentylenetetrazol infusion seizure model for quantitating the anticonvulsant effect of valproic acid in the rat. *J Pharmacol Methods* **13**, 135-146.

Porter, A. G. (1993). Picornavirus nonstructural proteins: emerging roles in virus replication and inhibition of host cell functions. *J Virol* **67**, 6917-6921.

Poteryaev, D., Datta, S., Ackema, K., Zerial, M. y Spang, A. (2010). Identification of the switch in early-to-late endosome transition. *Cell* **141**, 497-508.

Poteryaev, D., Datta, S., Ackema, K., Zerial, M. y Spang, A. (2011). Identification of the switch in early-to-late endosome transition. *Cell* **141**, 497-508.

Prchla, E., Kuechler, E., Blaas, D. y Fuchs, R. (1994). Uncoating of human rhinovirus serotype 2 from late endosomes. *J Virol* **68**, 3713-3723.

Prchla, E., Plank, C., Wagner, E., Blaas, D. y Fuchs, R. (1995). Virus-mediated release of endosomal content in vitro: different behavior of adenovirus and rhinovirus serotype 2. *J Cell Biol* **131**, 111-123.

Press, B., Feng, Y., Hoflack, B. y Wandinger-Ness, A. (1998). Mutant Rab7 causes the accumulation of cathepsin D and cation-independent mannose 6-phosphate receptor in an early endocytic compartment. *J Cell Biol* **140**, 1075-1089.

Puri, A., Paternostre, M. y Blumenthal, R. (2002). Lipids in viral fusion. *Methods Mol Biol* **199**, 61-81.

Querbes, W., O'Hara, B. A., Williams, G. y Atwood, W. J. (2006). Invasion of host cells by JC virus identifies a novel role for caveolae in endosomal sorting of noncaveolar ligands. *J Virol* **80**, 9402-9413.

Quirin, K., Eschli, B., Scheu, I., Poort, L., Kartenbeck, J. y Helenius, A. (2008). Lymphocytic choriomeningitis virus uses a novel endocytic pathway for infectious entry via late endosomes. *Virology* **378**, 21-33.

Rahn, E., Petermann, P., Hsu, M. J., Rixon, F. J. y Knebel-Morsdorf, D. (2011). Entry pathways of herpes simplex virus type 1 into human keratinocytes are dynamin- and cholesterol-dependent. *PLoS One* **6**, e25464.

Rassmann, A., Henke, A., Jarasch, N., Lottspeich, F., Saluz, H. P. y Munder, T. (2007). The human fatty acid synthase: a new therapeutic target for coxsackievirus B3-induced diseases? *Antiviral Res* **76**, 150-158.

Reeves, V. L., Thomas, C. M. y Smart, E. J. (2012). Lipid rafts, caveolae and GPI-linked proteins. *Adv Exp Med Biol* **729**, 3-13.

Reider, A., Barker, S. L., Mishra, S. K., Im, Y. J., Maldonado-Baez, L., Hurley, J. H., Traub, L. M. y Wendland, B. (2009). Syp1 is a conserved endocytic adaptor that contains domains involved in cargo selection and membrane tubulation. *EMBO J* **28**, 3103-3116.

Ren, M., Xu, G., Zeng, J., De Lemos-Chiarandini, C., Adesnik, M. y Sabatini, D. D. (1998). Hydrolysis of GTP on rab11 is required for the direct delivery of transferrin from the pericentriolar recycling compartment to the cell surface but not from sorting endosomes. *Proc Natl Acad Sci U S A* **95**, 6187-6192.

Renau, J., and Megías, L. (1998). "Manual de Técnicas de Microscopía Electrónica (M.E.T). Aplicaciones Biológicas".

Rhim JS, S. K. (1967). Cytophatic and plaque assay of rubella virus in a line of African green monkey kiency cells. *Proc Soc Exp Biol Med* **125**, 602-606.

Rink, J., Ghigo, E., Kalaidzidis, Y. y Zerial, M. (2005). Rab conversion as a mechanism of progression from early to late endosomes. *Cell* **122**, 735-749.

Robinson, M. S. (2004). Adaptable adaptors for coated vesicles. *Trends Cell Biol* **14**, 167-174.

Roche, S., Albertini, A. A., Lepault, J., Bressanelli, S. y Gaudin, Y. (2008). Structures of vesicular stomatitis virus glycoprotein: membrane fusion revisited. *Cell Mol Life Sci* **65**, 1716-1728.

Roche, S., Bressanelli, S., Rey, F. A. y Gaudin, Y. (2006). Crystal structure of the low-pH form of the vesicular stomatitis virus glycoprotein G. *Science* **313**, 187-191.

Roche, S., Rey, F. A., Gaudin, Y. y Bressanelli, S. (2007). Structure of the prefusion form of the vesicular stomatitis virus glycoprotein G. *Science* **315**, 843-848.

Rodal, S. K., Skretting, G., Garred, O., Vilhardt, F., van Deurs, B. y Sandvig, K. (1999). Extraction of cholesterol with methyl-beta-cyclodextrin perturbs formation of clathrin-coated endocytic vesicles. *Mol Biol Cell* **10**, 961-974.

Rodgers, M. A., Saghatelian, A. y Yang, P. L. (2009). Identification of an overabundant cholesterol precursor in hepatitis B virus replicating cells by untargeted lipid metabolite profiling. *J Am Chem Soc* **131**, 5030-5031.

Rodrigo, W. W., de la Torre, J. C. y Martínez-Sobrido, L. (2011). Use of single-cycle infectious lymphocytic choriomeningitis virus to study hemorrhagic fever arenaviruses. *J Virol* **85**, 1684-1695.

Rodríguez, L. L. (2002). Emergence and re-emergence of vesicular stomatitis in the United States. *Virus Res* **85**, 211-219.

Rojek, J. M., Pérez, M. y Kunz, S. (2008). Cellular entry of lymphocytic choriomeningitis virus. *J Virol* **82**, 1505-1517.

Rollason, R., Korolchuk, V., Hamilton, C., Schu, P. y Banting, G. (2007). Clathrin-mediated endocytosis of a lipid-raft-associated protein is mediated through a dual tyrosine motif. *J Cell Sci* **120**, 3850-3858.

Rosas, M. F., Vieira, Y. A., Postigo, R., Martín-Acebes, M. A., Armas-Portela, R., Martínez-Salas, E. y Sobrino, F. (2008). Susceptibility to viral infection is enhanced by stable expression of 3A or 3AB proteins from foot-and-mouth disease virus. *Virology* **380**, 34-45.

Roth, S. L. y Whittaker, G. R. (2011). Promotion of vesicular stomatitis virus fusion by the endosome-specific phospholipid bis(monoacylglycero)phosphate (BMP). *FEBS Lett* **585**, 865-869.

Rothberg, K. G., Heuser, J. E., Donzell, W. C., Ying, Y. S., Glenney, J. R. y Anderson, R. G. (1992). Caveolin, a protein component of caveolae membrane coats. *Cell* **68**, 673-682.

Ruiz-Sáenz, J., Goez, Y., Tabares, W. y López-Herrera, A. (2009). Cellular receptors for foot and mouth disease virus. *Intervirology* **52**, 201-212.

Ryan, M. D., King, A. M. y Thomas, G. P. (1991). Cleavage of foot-and-mouth disease virus polyprotein is mediated by residues located within a 19 amino acid sequence. *J Gen Virol* **72 (Pt 11)**, 2727-2732.

Saiz, M., Gomez, S., Martinez-Salas, E. y Sobrino, F. (2001). Deletion or substitution of the aphthovirus 3' NCR abrogates infectivity and virus replication. *J Gen Virol* **82**, 93-101.

Saiz, M., Nunez, J. I., Jimenez-Clavero, M. A., Baranowski, E. y Sobrino, F. (2002). Foot-and-mouth disease virus: biology and prospects for disease control. *Microbes Infect* **4**, 1183-1192.

Salvato, M., Shimomaye, E., Southern, P. y Oldstone, M. B. (1988). Virus-lymphocyte interactions. IV. Molecular characterization of LCMV Armstrong (CTL+) small genomic segment and that of its variant, Clone 13 (CTL-). *Virology* **164**, 517-522.

Sasaki, J., Ishikawa, K., Arita, M. y Taniguchi, K. (2011). ACBD3-mediated recruitment of PI4KB to picornavirus RNA replication sites. *EMBO J* **31**, 754-766.

Schelhaas, M., Malmstrom, J., Pelkmans, L., Haugstetter, J., Ellgaard, L., Grunewald, K. y Helenius, A. (2007). Simian Virus 40 depends on ER protein folding and quality control factors for entry into host cells. *Cell* **131**, 516-529.

Schlegel, R., Tralka, T. S., Willingham, M. C. y Pastan, I. (1983). Inhibition of VSV binding and infectivity by phosphatidylserine: is phosphatidylserine a VSV-binding site? *Cell* **32**, 639-646.

Schmid, E. M. y McMahon, H. T. (2007). Integrating molecular and network biology to decode endocytosis. *Nature* **448**, 883-888.

Schmid, S. L. y Frolov, V. A. (2011). Dynamin: functional design of a membrane fission catalyst. *Annu Rev Cell Dev Biol* **27**, 79-105.

Schober, D., Kronenberger, P., Prchla, E., Blaas, D. y Fuchs, R. (1998). Major and minor receptor group human rhinoviruses penetrate from endosomes by different mechanisms. *J Virol* **72**, 1354-1364.

Shaltiel, G., Shamir, A., Shapiro, J., Ding, D., Dalton, E., Bialer, M., Harwood, A. J., Belmaker, R. H., Greenberg, M. L. y Agam, G. (2004). Valproate decreases inositol biosynthesis. *Biol Psychiatry* **56**, 868-874.

Shewan, A., Eastburn, D. J. y Mostov, K. (2011). Phosphoinositides in cell architecture. *Cold Spring Harb Perspect Biol* **3**, a004796.

Sieczkarski, S. B. y Whittaker, G. R. (2003). Differential requirements of Rab5 and Rab7 for endocytosis of influenza and other enveloped viruses. *Traffic* **4**, 333-343.

Sierra, M., Airaksinen, A., González-López, C., Agudo, R., Arias, A. y Domingo, E. (2007). Foot-and-mouth disease virus mutant with decreased sensitivity to ribavirin: implications for error catastrophe. *J Virol* **81**, 2012-2024.

Silverstein, S. C., Steinman, R. M. y Cohn, Z. A. (1977). Endocytosis. *Annu Rev Biochem* **46**, 669-722.

Simons, K. y Warren, G. (1984). Semliki Forest virus: a probe for membrane traffic in the animal cell. *Adv Protein Chem* **36**, 79-132.

Simpson, R. W., Hauser, R. E. y Dales, S. (1969). Viropexis of vesicular stomatitis virus by L cells. *Virology* **37**, 285-290.

Smith, A. E. y Helenius, A. (2004). How viruses enter animal cells. *Science* **304**, 237-242.

Sobrino, F., Dávila, M., Ortín, J. y Domingo, E. (1983). Multiple genetic variants arise in the course of replication of foot-and-mouth disease virus in cell culture. *Virology* **128**, 310-318.

Sobrino, F., Saiz, M., Jimenez-Clavero, M. A., Nunez, J. I., Rosas, M. F., Baranowski, E. y Ley, V. (2001). Foot-and-mouth disease virus: a long known virus, but a current threat. *Vet Res* **32**, 1-30.

Stapleford, K. A. y Miller, D. J. (2010). Role of cellular lipids in positive-sense RNA virus replication complex assembly and function. *Viruses* **2**, 1055-1068.

Stein, M. P., Feng, Y., Cooper, K. L., Welford, A. M. y Wandinger-Ness, A. (2003). Human VPS34 and p150 are Rab7 interacting partners. *Traffic* **4**, 754-771.

Stenmark, H. (2009). Rab GTPases as coordinators of vesicle traffic. *Nat Rev Mol Cell Biol* **10**, 513-525.

Stoddart, A., Dykstra, M. L., Brown, B. K., Song, W., Pierce, S. K. y Brodsky, F. M. (2002). Lipid rafts unite signaling cascades with clathrin to regulate BCR internalization. *Immunity* **17**, 451-462.

Stoker, M. y Macpherson, I. (1964). Syrian Hamster Fibroblast Cell Line Bhk21 And Its Derivatives. *Nature* **203**, 1355-1357.

Sullivan, B. M., Emonet, S. F., Welch, M. J., Lee, A. M., Campbell, K. P., de la Torre, J. C. y Oldstone, M. B. (2011). Point mutation in the glycoprotein of lymphocytic choriomeningitis virus is necessary for receptor binding, dendritic cell infection, and long-term persistence. *Proc Natl Acad Sci U S A* **108**, 2969-2974.

Sun, X., Yau, V. K., Briggs, B. J. y Whittaker, G. R. (2005). Role of clathrin-mediated endocytosis during vesicular stomatitis virus entry into host cells. *Virology* **338**, 53-60.

Superti, F., Seganti, L., Ruggeri, F. M., Tinari, A., Donelli, G. y Orsi, N. (1987). Entry pathway of vesicular stomatitis virus into different host cells. *J Gen Virol* **68 (Pt 2)**, 387-399.

Swanson, J. A. (2008). Shaping cups into phagosomes and macropinosomes. *Nat Rev Mol Cell Biol* **9**, 639-649.

Szentpetery, Z., Balla, A., Kim, Y. J., Lemmon, M. A. y Balla, T. (2009). Live cell imaging with protein domains capable of recognizing phosphatidylinositol 4,5-bisphosphate; a comparative study. *BMC Cell Biol* **10**, 67.

Taboga, O., Tami, C., Carrillo, E., Nuñez, J. I., Rodríguez, A., Saiz, J. C., Blanco, E., Valero, M. L., Roig, X., Camarero, J. A., Andreu, D., Mateu, M. G., Giralt, E., Domingo, E., Sobrino, F. y Palma, E. L. (1997). A large-scale evaluation of peptide vaccines against foot-and-mouth disease: lack of solid protection in cattle and isolation of escape mutants. *J Virol* **71**, 2606-2614.

Takada, Y., Ye, X. y Simon, S. (2007). The integrins. *Genome Biol* **8**, 215.

Takei, K., McPherson, P. S., Schmid, S. L. y De Camilli, P. (1995). Tubular membrane invaginations coated by dynamin rings are induced by GTP-gamma S in nerve terminals. *Nature* **374**, 186-190.

Takei, K., Yoshida, Y. y Yamada, H. (2005). Regulatory mechanisms of dynamin-dependent endocytosis. *J Biochem* **137**, 243-247.

Targett-Adams, P., Boulant, S., Douglas, M. W. y McLauchlan, J. (2010). Lipid metabolism and HCV infection. *Viruses* **2**, 1195-1217.

Teissier, E. y Pecheur, E. I. (2007). Lipids as modulators of membrane fusion mediated by viral fusion proteins. *Eur Biophys J* **36**, 887-899.

Teissier, E., Zandomeneghi, G., Loquet, A., Lavillette, D., Lavergne, J. P., Montserret, R., Cosset, F. L., Bockmann, A., Meier, B. H., Penin, F. y Pecheur, E. I. (2011). Mechanism of inhibition of enveloped virus membrane fusion by the antiviral drug arbidol. *PLoS One* **6**, e15874.

Terbach, N. y Williams, R. S. (2009). Structure-function studies for the panacea, valproic acid. *Biochem Soc Trans* **37**, 1126-1132.

Thorley, J. A., McKeating, J. A. y Rappoport, J. Z. (2010). Mechanisms of viral entry: sneaking in the front door. *Protoplasma* **244**, 15-24.

Toja, M., Escarmis, C. y Domingo, E. (1999). Genomic nucleotide sequence of a foot-and-mouth disease virus clone and its persistent derivatives. Implications for the evolution of viral quasispecies during a persistent infection. *Virus Res* **64**, 161-171.

Tokuoka, S. M., Saiardi, A. y Nurrish, S. J. (2008). The mood stabilizer valproate inhibits both inositol- and diacylglycerol-signaling pathways in Caenorhabditis elegans. *Mol Biol Cell* **19**, 2241-2250.

Trojnar, M. K., Wierzchowska-Cioch, E., Krzyzanowski, M., Jargiello, M. y Czuczwar, S. J. (2004). New generation of valproic acid. *Pol J Pharmacol* **56**, 283-288.

Tsai, B. (2007). Penetration of nonenveloped viruses into the cytoplasm. *Annu Rev Cell Dev Biol* **23**, 23-43.

Ullrich, O., Reinsch, S., Urbe, S., Zerial, M. y Parton, R. G. (1996). Rab11 regulates recycling through the pericentriolar recycling endosome. *J Cell Biol* **135**, 913-924.

Ungewickell, E. y Branton, D. (1981). Assembly units of clathrin coats. *Nature* **289**, 420-422.

Urata, S. y de la Torre, J. C. (2011). Arenavirus budding. *Adv Virol* **2011**, 180326.

Urata, S., Ngo, N. y de la Torre, J. C. (2012). The PI3K/Akt pathway contributes to arenavirus budding. *J Virol* **86**, 4578-4585.

van Vlijmen, H. W., Curry, S., Schaefer, M. y Karplus, M. (1998). Titration calculations of foot-and-mouth disease virus capsids and their stabilities as a function of pH. *J Mol Biol* **275**, 295-308.

Varnai, P., Thyagarajan, B., Rohacs, T. y Balla, T. (2006). Rapidly inducible changes in phosphatidylinositol 4,5-bisphosphate levels influence multiple regulatory functions of the lipid in intact living cells. *J Cell Biol* **175**, 377-382.

Vela, E. M., Colpitts, T. M., Zhang, L., Davey, R. A. y Aronson, J. F. (2008). Pichinde virus is trafficked through a dynamin 2 endocytic pathway that is dependent on cellular Rab5- and Rab7-mediated endosomes. *Arch Virol* **153**, 1391-1396.

Venkataramani, V., Rossner, C., Iffland, L., Schweyer, S., Tamboli, I. Y., Walter, J., Wirths, O. y Bayer, T. A. (2010). Histone deacetylase inhibitor valproic acid inhibits cancer cell proliferation via down-regulation of the alzheimer amyloid precursor protein. *J Biol Chem* **285**, 10678-10689.

Ventoso, I., Sanz, M. A., Molina, S., Berlanga, J. J., Carrasco, L. y Esteban, M. (2006). Translational resistance of late alphavirus mRNA to eIF2alpha phosphorylation: a strategy to overcome the antiviral effect of protein kinase PKR. *Genes Dev* **20**, 87-100.

Vicinanza, M., D'Angelo, G., Di Campli, A. y De Matteis, M. A. (2008). Function and dysfunction of the PI system in membrane trafficking. *EMBO J* **27**, 2457-2470.

Vidricaire, G. y Tremblay, M. J. (2005). Rab5 and Rab7, but not ARF6, govern the early events of HIV-1 infection in polarized human placental cells. *J Immunol* **175**, 6517-6530.

Vitelli, R., Santillo, M., Lattero, D., Chiariello, M., Bifulco, M., Bruni, C. B. y Bucci, C. (1997). Role of the small GTPase Rab7 in the late endocytic pathway. *J Biol Chem* **272**, 4391-4397.

Vonderheit, A. y Helenius, A. (2005). Rab7 associates with early endosomes to mediate sorting and transport of Semliki forest virus to late endosomes. *PLoS Biol* **3**, e233.

Welsch, S., Miller, S., Romero-Brey, I., Merz, A., Bleck, C. K., Walther, P., Fuller, S. D., Antony, C., Krijnse-Locker, J. y Bartenschlager, R. (2009). Composition and three-dimensional architecture of the dengue virus replication and assembly sites. *Cell Host Microbe* **5**, 365-375.

Welling, P. A. y Weisz, O. A. (2010). Sorting it out in endosomes: an emerging concept in renal epithelial cell transport regulation. *Physiology (Bethesda)* **25**, 280-292.

Westaway, E. G., Mackenzie, J. M., Kenney, M. T., Jones, M. K. y Khromykh, A. A. (1997). Ultrastructure of Kunjin virus-infected cells: colocalization of NS1 and NS3 with double-stranded RNA, and of NS2B with NS3, in virus-induced membrane structures. *J Virol* **71**, 6650-6661.

Whittaker, G. R. y Helenius, A. (1998). Nuclear import and export of viruses and virus genomes. *Virology* **246**, 1-23.

Wilcke, M., Johannes, L., Galli, T., Mayau, V., Goud, B. y Salamero, J. (2000). Rab11 regulates the compartmentalization of early endosomes required for efficient transport from early endosomes to the trans-golgi network. *J Cell Biol* **151**, 1207-1220.

Wilson, S. M. y Clegg, J. C. (1991). Sequence analysis of the S RNA of the African arenavirus Mopeia: an unusual secondary structure feature in the intergenic region. *Virology* **180**, 543-552.

Wittenburg, L. A., Bisson, L., Rose, B. J., Korch, C. y Thamm, D. H. (2010). The histone deacetylase inhibitor valproic acid sensitizes human and canine osteosarcoma to doxorubicin. *Cancer Chemother Pharmacol*.

Wolf, M. C., Freiberg, A. N., Zhang, T., Akyol-Ataman, Z., Grock, A., Hong, P. W., Li, J., Watson, N. F., Fang, A. Q., Aguilar, H. C., Porotto, M., Honko, A. N., Damoiseaux, R., Miller, J. P., Woodson, S. E., Chantasirivisal, S., Fontanes, V., Negrete, O. A., Krogstad, P., Dasgupta, A., Moscona, A., Hensley, L. E., Whelan, S. P., Faull, K. F., Holbrook, M. R., Jung, M. E. y Lee, B. (2010). A broad-spectrum antiviral targeting entry of enveloped viruses. *Proc Natl Acad Sci U S A* **107**, 3157-3162.

Xu, X., Muller-Taubenberger, A., Adley, K. E., Pawolleck, N., Lee, V. W., Wiedemann, C., Sihra, T. S., Maniak, M., Jin, T. y Williams, R. S. (2007). Attenuation of

phospholipid signaling provides a novel mechanism for the action of valproic acid. *Eukaryot Cell* **6**, 899-906.

Yang, W., Hood, B. L., Chadwick, S. L., Liu, S., Watkins, S. C., Luo, G., Conrads, T. P. y Wang, T. (2008). Fatty acid synthase is up-regulated during hepatitis C virus infection and regulates hepatitis C virus entry and production. *Hepatology* **48**, 1396-1403.

Yang, Z. (2002). Small GTPases: versatile signaling switches in plants. *Plant Cell* **14 Suppl**, S375-388.

Zaitseva, E., Yang, S. T., Melikov, K., Pourmal, S. y Chernomordik, L. V. (2010). Dengue virus ensures its fusion in late endosomes using compartment-specific lipids. *PLoS Pathog* **6**, e1001131.

Zajac, B. A. y Hummeler, K. (1970). Morphogenesis of the nucleoprotein of vesicular stomatitis virus. *J Virol* **6**, 243-252.

Zhao, Q., Pacheco, J. M. y Mason, P. W. (2003). Evaluation of genetically engineered derivatives of a Chinese strain of foot-and-mouth disease virus reveals a novel cell-binding site which functions in cell culture and in animals. *J Virol* **77**, 3269-3280.

Zheng, J., Cahill, S. M., Lemmon, M. A., Fushman, D., Schlessinger, J. y Cowburn, D. (1996). Identification of the binding site for acidic phospholipids on the pH domain of dynamin: implications for stimulation of GTPase activity. *J Mol Biol* **255**, 14-21.

Zhou, J., Snyder, A. R. y Lieberman, P. M. (2009). Epstein-Barr virus episome stability is coupled to a delay in replication timing. *J Virol* **83**, 2154-2162.

Zoncu, R., Perera, R. M., Sebastian, R., Nakatsu, F., Chen, H., Balla, T., Ayala, G., Toomre, D. y De Camilli, P. V. (2007). Loss of endocytic clathrin-coated pits upon acute depletion of phosphatidylinositol 4,5-bisphosphate. *Proc Natl Acad Sci U S A* **104**, 3793-3798.

Anexos

JOURNAL OF VIROLOGY, May 2009, p. 4216–4226 Vol. 83, No. 9
0022-538X/09/$08.00+0 doi:10.1128/JVI.02436-08

Internalization of Swine Vesicular Disease Virus into Cultured Cells: a Comparative Study with Foot-and-Mouth Disease Virus▽†

Miguel A. Martín-Acebes,[1] Mónica González-Magaldi,[1] Angela Vázquez-Calvo,[1] Rosario Armas-Portela,[1,2] and Francisco Sobrino[1,3]*

Centro de Biología Molecular Severo Ochoa (CSIC-UAM), Cantoblanco, Madrid, Spain[1]; Departamento de Biología, Facultad de Ciencias, Universidad Autónoma de Madrid (UAM), Cantoblanco, Madrid, Spain[2]; and Centro de Investigación en Sanidad Animal, INIA, Valdeolmos, Madrid, Spain[3]

Received 26 November 2008/Accepted 8 February 2009

We performed a comparative analysis of the internalization mechanisms used by three viruses causing important vesicular diseases in animals. Swine vesicular disease virus (SVDV) internalization was inhibited by treatments that affected clathrin-mediated endocytosis and required traffic through an endosomal compartment. SVDV particles were found in clathrin-coated pits by electron microscopy and colocalized with markers of early endosomes by confocal microscopy. SVDV infectivity was significantly inhibited by drugs that raised endosomal pH. When compared to foot-and-mouth disease virus (FMDV), which uses clathrin-mediated endocytosis, the early step of SVDV was dependent on the integrity of microtubules. SVDV-productive endocytosis was more sensitive to plasma membrane cholesterol extraction than that of FMDV, and differential cell signaling requirements for virus infection were also found. Vesicular stomatitis virus, a model virus internalized by clathrin-mediated endocytosis, was included as a control of drug treatments. These results suggest that different clathrin-mediated routes are responsible for the internalization of these viruses.

The ways in which viruses are internalized into host cells to initiate a productive infection are varied. Viruses gaining entry via endocytosis hijack components of different pathways used by the cell to internalize ligands such as nutrients and signaling molecules. The best-characterized route is classical clathrin-mediated endocytosis, in which ligands are internalized in clathrin-coated pits (CCPs) and subsequently sorted into early endosomes that can mature into late endosomes and lysosomes (71). Distinct CCP subpopulations, defined by using different, specific adaptor proteins, have recently been reported (7). Other non-clathrin-mediated endocytosis routes, dependent on plasma membrane cholesterol-enriched microdomains called lipid-rafts, have been also characterized (50). These lipid-rafts are enriched in glycosylphosphatidylinositol-anchored proteins and, when containing caveolin-1, this pathway is commonly referred as caveola-mediated endocytosis. In addition, viruses using alternative entry pathways that do not correspond to clathrin or lipid-raft/caveola-mediated endocytosis have been reported (11, 50, 77).

Virus infection is a reproducible and easily measurable event, so viruses can act as useful endocytic tracers (65). In fact, much of the information about caveolae-mediated endocytosis has been obtained from the study of virus entry and infection (63). Recent reports show that closely related viruses can enter into the cell via different pathways, whereas viruses of different families can exploit similar mechanisms, highlighting the importance of understanding the cell biology of virus entry (19). Comparative studies of the internalization of different viruses have revealed differential dependence on dynamin, an endocytosis-associated protein (24), as well as the differential involvement of Rab5 and Rab7 GTPases in intracellular virus trafficking and infection (76). Other studies comparing ligands for caveola-mediated endocytosis, such as that seen with viruses and cholera toxin, have uncovered diversity in caveola-mediated endocytosis routes (64, 66). In the present study, we have analyzed the internalization pathway of swine vesicular disease virus (SVDV), and we have performed a comparative analysis with foot-and-mouth disease virus (FMDV) and vesicular stomatitis virus (VSV). SVDV is a porcine pathogen and a member of the *Picornaviridae* family; it is included into the *Enterovirus* genus and is closely related to the human pathogen coxsackievirus B5 (CVB5) (91). FMDV is a typical species of the *Aphthovirus* genus within the *Picornaviridae* family (80), and VSV is a member of the genus *Vesiculovirus* of the family *Rhabdoviridae* (70). Despite the marked differences exhibited by the three viruses at the taxonomical level and in their requirements to organize replication complexes, these viruses share similar growth kinetics on IBRS-2 cells, and the vesicular lesions and clinical signs of the disease they produce in natural hosts are so similar as to require a differential diagnosis (2, 51).

SVDV and FMDV virions are composed of an icosahedral capsid of about 26 nm in diameter, built up with 60 copies of each of the four structural proteins (VP1 to VP4). The capsid contains a single-stranded RNA molecule of positive polarity that constitutes the viral genome (27, 82, 87). VSV is a negative-stranded RNA virus whose virions are much more complex and enveloped by lipid bilayers (70).

SVDV can infect cultured cells using heparan sulfate (HS) proteoglycans as surface receptors, via the coxsackievirus-and-adenovirus receptor (CAR), and some isolates retain the ability to bind human decay-accelerating factor (DAF) (26, 34).

* Corresponding author. Mailing address: CBMSO, UAM, Cantoblanco 28049, Madrid, Spain. Phone: 34-91-1964493. Fax: 34-91-1964420. E-mail: fsobrino@cbm.uam.es.

† Dedicated to the memory of Rosario Armas-Portela.

▽ Published ahead of print on 18 February 2009.

After attachment to the cell, SVDV particles undergo receptor-induced conformational alterations that expose the N-terminal portion of VP1 that is internal within the capsid (33); this interaction with CAR is responsible for the conformational capsid rearrangements in related coxsackieviruses (55). Internalization through different endocytic pathways has been reported among the SVDV-related coxsackieviruses. Thus, a clathrin-dependent mechanism is exploited by a CVB3 strain that only uses CAR as a cell receptor (18), and a caveola-mediated, dynamin-independent route that shares common features with macropinocytosis has been reported for another CVB3 strain that uses both DAF and CAR as cell receptors (15, 16). Also, a CVB3 variant entering through HS has been shown to be internalized in a pH-dependent way (90), whereas a CVB4 strain interacting with DAF and CAR is endocytosed via a lipid-raft-dependent mechanism (85).

In contrast, FMDV binds different α_v integrins as surface receptors, specifically $\alpha_v\beta_8$ in IBRS-2 cells, the cell line used in the present study (12), and it is internalized following the clathrin endocytic route (8, 52, 61). Early work suggested phosphatidylserine as the VSV cell receptor (72), but recent observations do not support this hypothesis (13). However, it is well established that VSV is internalized through clathrin-mediated endocytosis and has become a model virus internalized through this route (36, 52, 54, 84).

Our results indicate that SVDV is internalized into the cell by a mechanism which can be inhibited by treatments that affect clathrin-mediated endocytosis and also requires traffic through an endosomal compartment for penetration. Supporting this hypothesis, SVDV particles were found in CCPs in electron microscopy studies, colocalized with markers of early endosomes by confocal microscopy, and SVDV infectivity could be significantly inhibited by drugs that raise endosomal pH. The early step of SVDV and VSV infection—but not that of FMDV—was dependent on the integrity of microtubules, and SVDV-productive endocytosis was more sensitive to plasma membrane cholesterol extraction than those of FMDV and VSV. Taken together, these results suggest that different endosomal routes are responsible for the internalization of these viruses into different populations of early endosomes.

MATERIALS AND METHODS

Cells and viruses. IBRS-2 cells (22) and BHK-21 cells (ATCC) were maintained in Dulbecco modified Eagle medium (DMEM) (Gibco-BRL) supplemented with 5% fetal calf serum (Sigma), L-glutamine (2 mM), penicillin (100 U/ml), and streptomycin (100 μg/ml). SVDV SPA/1/'93 isolate was grown on IBRS-2 cells. Type C FMDV C-S8c1 (81) and VSV Indiana serotype viral stocks were prepared by amplification in BHK-21 cells. Type C FMDV C-S8c1 isolate entered cells using αv integrins, but not HS (6, 53, 59). Nucleotide sequencing confirmed the absence of mutations responsible for HS binding acquisition (6) in the viral stock used in the present study, which was unable to infect CHO cells that do not express integrin receptors for FMDV but are susceptible to infection by FMDV mutants that bind HS (6; data not shown).

Antibodies and reagents. The following antibodies against viral proteins were used: monoclonal antibody (MAb) I1 anti-VSV G protein (47), MAb 2H12 against VP1 SVDV (9), rabbit polyclonal antiserum against VP1 SVDV (33), and MAb 5C4 against FMDV antigenic site D (45). MAb against EEA1, rabbit polyclonal antiserum against caveolin-1, and a phospho-specific MAb against Tyr^{14}-phosphorylated caveolin-1 were from BD Transduction Labs. MAbs against tubulin (DM1A) and β-actin (AC-15) were from Sigma. A rabbit polyclonal anti-βII tubulin antiserum (4) and MAb 25H8 to the *cis*-Golgi marker protein gp74 (1) were also used. Alexa Fluor 488-conjugated phalloidin; Alexa Fluor 488-conjugated transferrin (TF); Alexa Fluor 488-, 594-, or 555-labeled goat anti-mouse immunoglobulin G (IgG); and Alexa Fluor 488- or 594-labeled goat anti-rabbit IgG were purchased from Invitrogen. Anti-mouse and anti-rabbit horseradish peroxidase-coupled IgG secondary antibodies were from GE Healthcare.

Bisindolmaleymide I (Bis), cytochalasin D (Cyt D), concanamycin A, filipin III, genistein, methyl-β-cyclodextrin (MβCD), α-cyclodextrin (αCD), lovastatin, nocodazole, wortmannin, chlorpromazine (Cpmz), and sodium orthovanadate (OV) were from Sigma. PP2 in solution was purchased from Calbiochem. Sucrose and ammonium chloride (NH_4Cl) were from Merck. Bis, Cyt D, concanamycin A, filipin, Geneticin, lovastatin, nocodazole, wortmannin, and dynasore were dissolved in dimethyl sulfoxide. OV and NH_4Cl were dissolved in water. Cpmz, sucrose, MβCD, and αCD were directly prepared in DMEM.

Drug treatments. Preinfection analyses were performed in the presence of drugs before infection (pretreatment) and during the whole infection period (except for sucrose, concanamycin A, MβCD, and αCD), while for postinfection analyses the drug was added 3 h postinfection. Monolayers of IBRS-2 cells grown on tissue culture plates were extensively washed with DMEM and pretreated for 30 min with Bis (5 μM), Cyt D (1 μM), filipin (1 μg/ml), concanamycin A (1,000 nM), dynasore (80 μM), genistein (100 μM), MβCD (10 mM), αCD (10 mM), nocodazole (40 μM), wortmannin (200 nM), Cpmz (30 μM), OV (1 mM), or sucrose (0.45 M) or for 1 h in the case of NH_4Cl (25 or 50 mM in 25 mM HEPES [pH 7.4]), PP2 (10 μM), lovastatin (5 μM), or nystatin (25 μg/ml). For sucrose and concanamycin A treatment, the drug was maintained only during pretreatment and the first infection hour or TF internalization period. MβCD and αCD were only present during 30 min preinfection. The rest of the drugs were maintained throughout the infection to avoid cellular recovery. To evaluate the effect of the treatments on virus replication (postinfection), all of the drugs were added 3 h postinfection and maintained during the rest of infection, except MβCD, sucrose and concanamycin A, which were removed 0.5 and 1.5 h after their addition, respectively. Control cells were incubated in parallel with the same volume of drug solvent.

Infections and virus titrations. Triplicate wells of IBRS-2 cells pretreated or not with the drugs were infected with VSV, SVDV, or FMDV using a multiplicity of infection (MOI) of 0.5 PFU/cell in experiments measuring the productive virus infection or an MOI of 100 PFU/cell in experiments tracking virus entry by immunofluorescence or to determine caveolin-1 phosphorylation. After the first infection hour, the viral inoculum was removed, and fresh medium containing 5% fetal calf serum was added (this time point was considered 1 h postinfection). For dynasore treatment, infections were performed in medium without serum since this drug binds to serum proteins, losing activity (49). Seven hours later, cells were subjected to three freeze-thaw cycles, and the total (intracellular and medium-released) virus yield was determined by plaque assay (in BHK-21 cells for VSV and FMDV or in IBRS-2 cells for SVDV), as described previously (81). Infected monolayers were also fixed and processed for immunofluorescence to determine the number of infected cells (51). Experiments in which the first hour of infection was carried out on ice to allow virus adsorption, but not internalization, are indicated in the figure legends.

TEM. Transmission electron microscopy (TEM) was performed as described previously (51). IBRS-2 cells grown on 100-mm tissue culture plates were incubated with VSV (MOI of 300) or SVDV (MOI of 63) for 1 h on ice and subsequently transferred to 37°C for 5 min. Cells were washed with phosphate-buffered saline (PBS) and fixed for 30 min at 37°C in 2% glutaraldehyde in 0.1 M sodium cacodylate buffer (pH 7.4) supplemented with 5 mM $CaCl_2$, postfixed in 1% osmium tetroxide plus 1% potassium ferrocianure for 1 h at 4°C, and treated with 0.15% tanic acid in phosphate buffer (pH 7.4) for 1 min. Samples were stained with 2% uranyl acetate for 1 h at room temperature, dehydrated in ethanol according to standard protocols, and embedded in TAAB 812 resin (TAAB Laboratories). Samples were examined with a JEOL JEM-1010 electron microscope operating at 80 kV, and images were acquired by using a digital camera Bioscan792 (Gatan).

Immunofluorescence and confocal microscopy. Cells grown on glass coverslips were washed with PBS, fixed in 4% paraformaldehyde for 15 min at room temperature (or methanol fixed for Golgi staining), blocked, and permeabilized with PBTG buffer (0.1% Triton X-100, 1% bovine serum albumin [BSA], and 1 M glycine in PBS) for 15 min at room temperature. Samples were incubated with primary antibodies diluted in 1% BSA in PBS for 1 h at room temperature, washed with PBS, and incubated with secondary antibodies 30 min at room temperature. After washing with PBS, nuclei were stained with 1 μg of DAPI (4′,6′-diamidino-2-phenylindole; Invitrogen)/ml or by using To-Pro-3 (Invitrogen) in the case of confocal microscopy, and the samples were mounted in Fluoromount G (Southern Biotech). To determine the number of infected cells, three coverslips per treatment were examined, counting at least 300 cells per coverslip.

Samples were observed by using an Olympus BX61 epifluorescence microscope coupled to a digital camera DP70 and acquired by using Olympus DP controller software. Confocal laser scanning microscopy was performed with an Axiovert S100 TV microscope (Zeiss) coupled to a confocal Radiance 2000 system (Bio-Rad) using Lasersharp2000 5.2 software (Bio-Rad) for image acquisition. Sequential laser scanning for different laser lines was performed to avoid false colocalization. Images were processed using Adobe Photoshop 7.0.1 (Adobe Systems, Inc.).

For quantification of colocalization, the percentage of EEA1-positive structures (red) containing SVDV (green) was calculated by counting the number of EEA1-positive structures containing yellow pixels, divided by the total number of EEA1 spots in at least three different cells for each time. The same process was performed for SVDV colocalization with TF.

TF internalization assays. Cells grown on coverslips were incubated for 15 min with 10 μg of TF-Alexa Fluor 488/ml in DMEM containing 0.5% BSA. To evaluate the effect of sucrose and Cpmz in TF endocytosis, the cells were washed with 200 mM acetic acid and 200 mM NaCl and sequentially with 150 mM NaCl, 20 mM HEPES (pH 7.4), 10 mM glucose, 5 mM KCl, 1 mM $MgCl_2$, and 1 mM $CaCl_2$ to eliminate extracellular TF (48) prior to fixation. Aldehyde fluorescence was quenched by incubating cells 15 min with 1 M glycine in PBS. Images of TF in cells treated or not with the drugs were acquired using the same exposure time and detector sensitivity.

AO vital staining. Acridine orange (AO) vital staining (52) was used to qualitatively evaluate the effects of NH_4Cl treatment on acidic organelles. Cells treated as described above were incubated in fresh medium, containing or not NH_4Cl, and 5 μg of AO/ml at 37°C for 10 min, washed three times with the same medium without AO, and observed under a fluorescence microscope. AO fluorescence is red when it protonates and accumulates into acidic organelles.

Filipin staining. Detection of cellular cholesterol by filipin staining was performed as previously reported (39). Briefly, cells treated or not with MβCD were fixed on ice and incubated with 125 μg of filipin/ml in PBS at room temperature, washed twice with PBS, and mounted in Fluoromount G. Images of cells treated or not with MβCD were acquired using the same exposure time and detector sensitivity. The fluorescence intensity of filipin staining in control and MβCD-treated cells was quantified with ImageJ software (http://rsbweb.nih.gov/ij/).

Western blot. IBRS-2 cells grown on 35-mm tissue culture plates were scraped on ice into NP-40 lysis buffer (10 mM EGTA, 2.5 mM $MgCl_2$, 1% NP-40, 20 mM HEPES [pH 7.4]) and sonicated. Protein concentration was determined by Bradford method, and equal amounts of protein mixed with Laemmli sample buffer were boiled, separated by sodium dodecyl sulfate-polyacrylamide gel electrophoresis, and transferred onto a nitrocellulose membrane. The membrane was blocked, and proteins were detected by incubation with primary antibodies and with horseradish peroxidase-coupled secondary antibodies using a chemiluminescence kit (Perkin-Elmer) as previously described (28).

Data analysis. To probe statistical significance of the data, one-way analysis of the variance was performed with statistical package SPSS 13.0 (SPSS, Inc.) for Windows. For multiple comparisons, Bonferroni's correction was applied. The data are presented as means ± the standard deviations, and statistically significant differences between control treatments and drug treatments are indicated in the figures by one or two asterisks (corresponding to $P < 0.05$ or $P < 0.005$, respectively).

RESULTS

SVDV is internalized through clathrin-mediated endocytosis. To test the role of CCPs in SVDV endocytosis, cells were treated with a hypertonic medium containing 0.45 M sucrose. This treatment has been shown to inhibit CCP assembly (30) and to reduce infection by viruses that use clathrin-mediated endocytosis (8, 38). Sucrose treatment reduced the ability of IBRS-2 cells to internalize TF (Fig. 1A), a ligand known to utilize clathrin-mediated endocytosis (29, 56). Cpmz interferes with plasma membrane CCP formation (88) and inhibits virus infection that uses clathrin mediated-endocytosis, including VSV and FMDV (36–38, 60, 61, 84). Treatment with Cpmz reduced TF internalization (Fig. 1B). As estimated by confocal microscopy, sucrose and Cpmz reduced internalization of SVDV into the cells but did not impair virus binding (Fig. 1C), since fluorescence corresponding to virions is observed at the

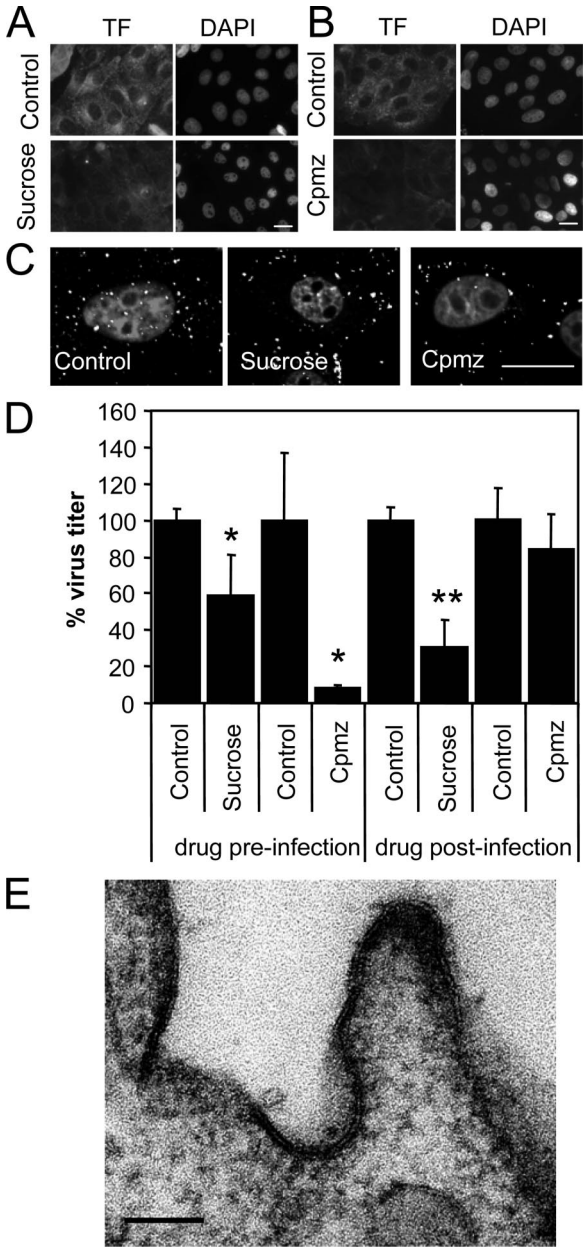

FIG. 1. Role of clathrin for SVDV endocytosis in IBRS-2 cells. (A) Hypertonic medium inhibits TF endocytosis. Cells pretreated 30 min with sucrose were incubated 15 min with Alexa Fluor 488-labeled TF maintaining the sucrose, acid washed to eliminate extracellular TF, and fixed. (B) Cpmz inhibits TF endocytosis. Cells pretreated 30 min with chlorpromazine were incubated as for panel A with fluorescent TF. (C) Sucrose and Cpmz inhibit internalization of SVDV. Confocal sections of IBRS-2 cells were pretreated with sucrose or Cpmz and incubated with SVDV (MOI of 100) for 25 min at 37°C. SVDV was detected by immunofluorescence staining with rabbit polyclonal antiserum against VP1 and a secondary antibody labeled with Alexa Fluor 488. Nuclei were stained with To-Pro-3. (D) Effect of sucrose and Cpmz treatment on SVDV infection determined by plaque assay. (E) TEM of SVDV-infected cells. IBRS-2 cells were incubated with SVDV (MOI of 300) for 1 h on ice prior to incubation for 5 min at 37°C, fixed, and processed for electron microscopy. White bars (A to C), 20 μm; black bar (E), 100 nm. Statistically significant differences between control and drug treatments are indicated by one asterisk ($P < 0.05$) or two asterisks ($P < 0.005$).

plasma membrane. Preinfection treatment with sucrose reduced SVDV (40%) virus production (Fig. 1D). In this assay, sucrose was not present during the postinfection period; therefore, the effect observed is likely due to inhibition of entry. However, when sucrose was added 3 h postinfection, a virus titer reduction was also observed, indicating that hypertonic medium affects also virus replication. Preinfection treatment with Cpmz caused a marked inhibition of SVDV yield (Fig. 1D). When Cpmz was added postinfection, reduction in SVDV infection was not statistically significant. These results confirm that the drug was affecting an early step of SVDV infection cycle. Attempts to use more specific inhibitors such as dominant-negative Eps15, dynamin II, or Rab5 resulted in very low levels of transfection of IBRS-2 cells that impaired the analyses.

SVDV particle location during the internalization process was studied by means of TEM. Electrodense, spherical virus-like particles ~26 nm in diameter, corresponding to SVDV virions, were located in the CCPs (ca. 84% of the particles undergoing endocytosis), and a representative example is shown in Fig. 1E. These particles were not found in mock-infected cells. The lack of antibodies suitable for gold-labeling impaired detection by TEM immunostaining of viral capsid proteins in these particles. Taken together, these results support a clathrin-mediated endocytosis for SVDV internalization.

Infection of SVDV requires transit through acidic endosomes. After internalization, viruses release their genetic material penetrating into the host cell cytoplasm and leading to a productive infection. A common uncoating mechanism used by viruses entering trough CCP-mediated endocytosis depends on endosomal acidification (50, 58, 66). Pretreatment with NH_4Cl resulted in a neutralization of intralumenal pH within acidic organelles, as estimated by the lack of detection of red spots corresponding to acidic organelles labeled by AO vital staining (Fig. 2A). As reported earlier (52, 54), preinfection treatment with NH_4Cl significantly reduced VSV and to a lower extent FMDV titers, as well as the percentage of infected cells (Fig. 2B). This compound also reduced SVDV infection in a dose-dependent manner. Postinfection addition of NH_4Cl had no effect on virus infection (data not shown), suggesting that a transit through an acidic compartment is required for the productive entry of these three viruses. Indeed, pretreatment with concanamycin A, a potent and specific inhibitor of the vacuolar ATPase (25), reduced SVDV infection (Fig. 2C); this was not observed when this drug was added postinfection (data not shown; for a comparison of the effects of concanamycin A in FMDV and VSV infection, see reference 52). These results led us to study SVDV infection by confocal microscopy. At very early times postinfection (5 min) most of the virus was not internalized yet and appeared attached to the cell membrane. After 15 min, virus was observed inside the cell, and the viral fluorescence colocalized (16.6% ± 2%) with that of early endosomes positive for EEA1 (Fig. 2D, circles). The percentage of early endosomes containing SVDV was reduced with the infection progress (45 min), indicating particle translocation to a different cell compartment (Fig. 2E). SVDV particles also colocalized with TF (18% ± 6%) (Fig. 2F, circles), and endosomes loaded with SVDV could be observed close to microtubules (Fig. 2F, arrowheads). Often, these microtubule-associated endosomes were negative for TF. Taken together, these results suggest that SVDV-productive infection requires transit through acidic endosomes for penetration.

Differential cytoskeleton requirements for intracellular sorting of SVDV, VSV, and FMDV. A pre-early endosome sorting that begins at the CCP, segregating cargo into two different early endosome populations has been recently described (43). One population corresponds to static and not microtubule-associated endosomes, while in the other the endosomes are dynamic and highly mobile along microtublules containing ligands that are directed preferentially to late endosomes/lysosomes. The proximity of SVDV particles to microtubules observed at early infection times (Fig. 2F) prompted us to study the requirement of intact microtubules for virus infection. When added preinfection (Fig. 3A), the microtubule-disrupting agent nocodazole reduced VSV and SVDV infection by 60%, while, as reported (8), it did not affect FMDV infection. When nocodazole was added postinfection, SVDV titers were not reduced, suggesting that microtubules play an important role at an early infection stage. Conversely, VSV infection was reduced at a level similar to that when the drug was added postinfection, indicating that VSV can be affected by microtubule disruption at later infection stages; this is likely due to the dependence on an intact secretory pathway for VSV infection progress (21, 51, 68). In fact, microtubule depolymerization induced by nocodazole (Fig. 3B) also caused Golgi fragmentation as estimated by immunostaining of the *cis*-Golgi marker gp74, which was dispersed in nocodazole treated cells.

Disruption of actin cytoskeleton with Cyt D (which was maintained throughout the assay to avoid cellular recovery) did not induce any significant effect on VSV, SVDV, or FMDV infection (Fig. 3C). As expected, this compound resulted in actin depolymerization (Fig. 3D). These results indicate a dependence on microtubule integrity for SVDV but not for FMDV internalization. On the other hand, disruption of actin cytoskeleton does not affect the infection of any of these three viruses.

Dynamin and differential signaling events are required for SVDV, VSV, and FMDV infection. Dynamin is a GTPase involved in several types of endocytosis, including the clathrin-mediated pathway. Preinfection treatment with dynasore, a cell-permeable inhibitor of dynamin function (42, 49), inhibited the virus yield recovered upon infection of SVDV and FMDV (Fig. 4A). When added postinfection, dynasore did not inhibit SVDV and FMDV infection, indicating the requirement for dynamin is present at an early step of infection. As previously reported (36), dynasore inhibited VSV infection when added preinfection. Our results show that when added postinfection dynasore also inhibited virus growth, possibly due to effects on intracellular vesicle traffic dependent on dynamin, as vesicle formation from the Golgi (31, 40). The requirement for an intact secretory pathway in VSV infection has been reported (21, 51, 68).

Internalization and intracellular trafficking are governed by complex signaling events, including a galaxy of cellular kinases and phosphatases (65). We next addressed the effect of different inhibitors on the infection of the viruses studied. Bis, an inhibitor of protein kinase C (PKC) (66), did not inhibit significantly virus entry or infection (Fig. 4B). On the other hand,

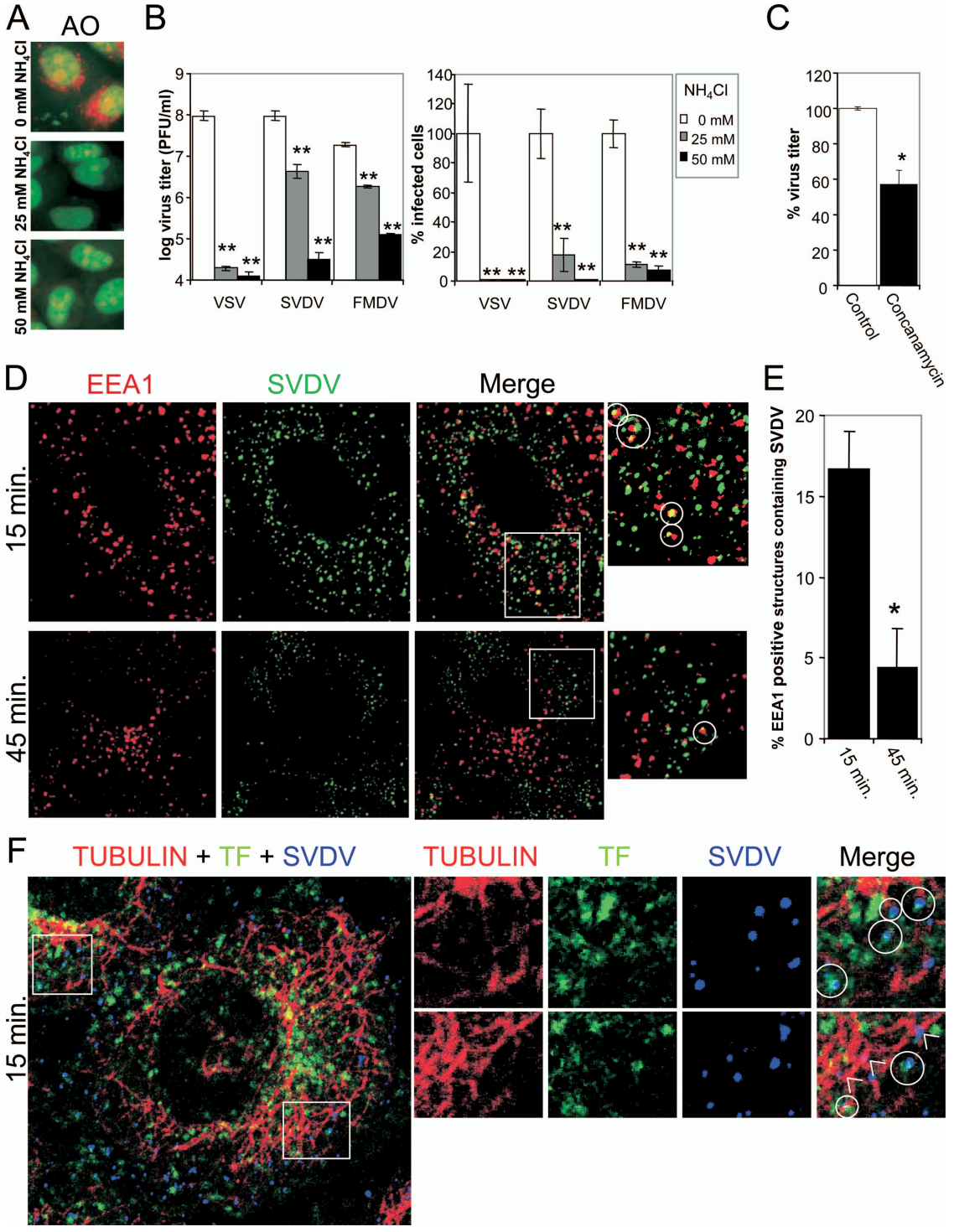

FIG. 2. Dependence on acidic endosomes for virus penetration. (A) Evaluation of treatment with increasing NH_4Cl concentrations on acidic intracellular compartments by AO vital staining. AO stains in red acidic organelles and nuclei in green. (B) Effects of pretreatment with different concentrations of NH_4Cl (0, 25, or 50 mM) on virus infection analyzed by plaque assay and by determination of the percentage of infected cells in immunofluorescence studies using I1, 2H12, and 5C4 antibodies to detect VSV, SVDV, and FMDV, respectively. Appropriate secondary antibodies coupled to Alexa Fluor 488 were used for detection of virus-specific antibodies. (C) Effects of pretreatment with concanamycin A on SVDV infection studied by plaque assay. (D) Colocalization assay of SVDV with the early endosomes marker EEA1. Cells were infected with SVDV (MOI of 100) for 1 h on ice and then transferred to 37°C 15 or 45 min, fixed, and processed for immunofluorescence using a mouse MAb to stain EEA1 (red) and a rabbit polyclonal antiserum to detect SVDV VP1 (green). Colocalization is shown in yellow (circles). Anti-mouse IgG secondary antibodies labeled with Alexa Fluor 594 and anti-rabbit IgG Alexa Fluor 488-coupled secondary antibodies were used to detect primary antibodies. (E) Quantification of colocalization between EEA1 and SVDV. (F) Colocalization assays of SVDV with TF and microtubules. Cells were infected as in panel D in combination with TF for 1 h on ice, transferred to 37°C 15 min, fixed, and processed for immunofluorescence using a rabbit polyclonal antiserum against SVDV VP1 and a mouse MAb against tubulin. Anti-mouse Alexa Fluor 555-labeled and anti-rabbit Alexa Fluor 647-labeled secondary antibodies were used. Alexa Fluor 488-labeled TF is shown in green, tubulin is shown in red, and SVDV is shown in blue. Colocalization between blue and green appears in aqua (circles) in the merged image. Arrowheads point to SVDV loaded endosomes in close association with microtubules. Statistically significant differences between control and drug treatments are indicated by one asterisk ($P < 0.05$) or two asterisks ($P < 0.005$).

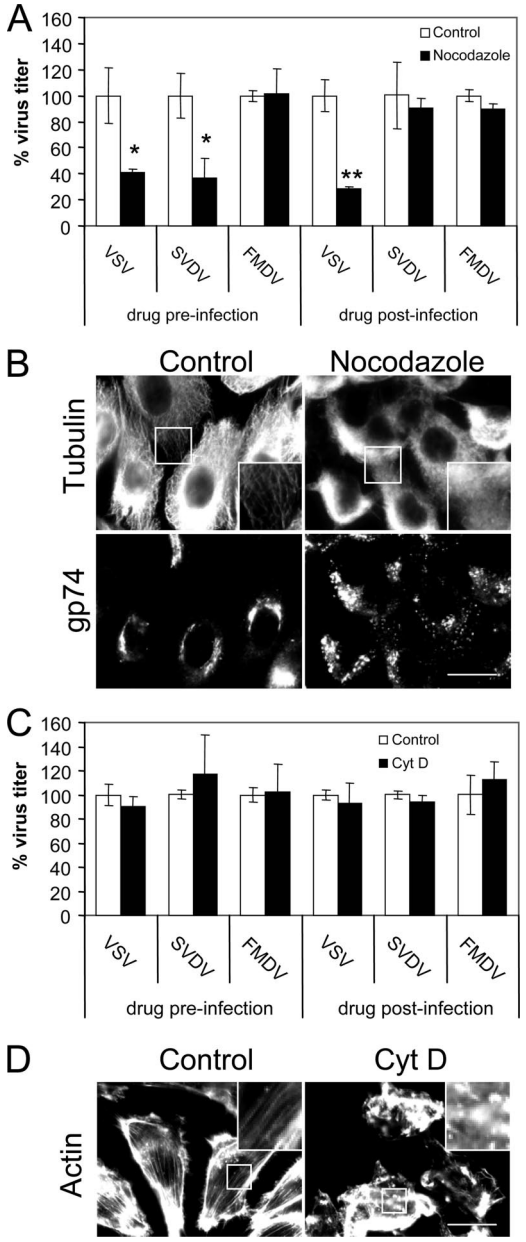

FIG. 3. Differential cytoskeleton requirements for intracellular sorting of viruses. (A) Effects of nocodazole on VSV, SVDV, and FMDV infection studied by plaque assay. (B) Evaluation of nocodazole treatment on microtubule and Golgi integrity. Cells treated or not with nocodazole were fixed and processed for immunofluorescence using rabbit polyclonal antiserum against tubulin and MAb 25H8 against *cis*-Golgi protein gp74. Anti-rabbit Alexa Fluor 488-coupled and anti-mouse Alexa Fluor 594-coupled secondary antibodies were used. Bar, 20 μm. (C) Effects of Cyt D on virus infection studied by plaque assay. (D) Evaluation of Cyt D treatment on actin cytoskeleton integrity. Cells treated or not with Cyt D were fixed and processed for immunofluorescence using Alexa Fluor 488-labeled phalloidin to stain the cellular actin. Bar, 20 μm. Statistically significant differences between control and drug treatments are indicated by one asterisk ($P < 0.05$) or two asterisks ($P < 0.005$).

inhibition of SVDV infection by the tyrosine phosphatase inhibitor OV (66) was higher for SVDV than for FMDV and VSV when OV was added preinfection (Fig. 4C). However, OV also inhibited SVDV replication when added postinfection, supporting the possibility that the differential dependence on tyrosine phosphates was mainly due to postinternalization events. In the case of VSV and FMDV, OV only reduced virus infection when added preinfection, indicating that this drug affected virus entry of these two viruses. The nonspecific tyrosine kinase inhibitor genistein (15, 66) inhibited infection of VSV and SVDV, but not of FMDV, when added pre- and postinfection (Fig. 4D) This indicates that the inhibitory effect of this drug may be related to inhibition of virus replication rather than virus entry. The specific inhibitor of SRC-family tyrosine kinases PP2 (15), inhibited VSV, SVDV, and FMDV when added preinfection but not postinfection, suggesting that SRC kinases were involved at an early infection step (Fig. 5E).

Inhibition of phosphatidylinositol 3-kinases with wortmannin prevents or delays ligand transfer from early to late endosomes (14). Preinfection treatment with wortmannin neither inhibited VSV and FMDV infection, as reported (8, 45), nor did it affect SVDV yields in IBRS-2 cells (Fig. 4F). This lack of effect was also observed when the drug was added postinfection. SVDV growth kinetics in the presence of wortmannin was also analyzed by plaque assay, revealing no delay in virus multiplication (data not shown). These results indicate that while dynamin is required for SVDV, VSV, and FMDV infection, differences exist in the signaling events that mediate the entry of these three viruses.

Differential cholesterol requirement for VSV, SVDV, and FMDV internalization. Cholesterol is important for lipid-raft and caveola function and has also been implicated in clathrin-mediated endocytosis (69, 83). Plasma membrane cholesterol depletion induced by MβCD inhibits lipid-raft/caveola-dependent virus infection (66) and can also affect infection of viruses using clathrin-mediated endocytosis (52, 79, 86). In addition, cholesterol plays an important role for the endosomal penetration of different viruses (20, 32). To evaluate the role of cholesterol in the early infection steps of the viruses compared, we treated IBRS-2 cells with MβCD. As estimated by filipin staining, this drug extracted cholesterol from plasma membrane (40% ± 19% reduction in filipin staining intensity), leaving the intracellular cholesterol content intact (no reduction of filipin staining) (Fig. 5A). Treatment with αCD, a cyclodextrin that does not significantly extract cholesterol from plasma membrane (74), did not reduce filipin staining intensity.

Preinfection treatment with MβCD differentially affected virus infection (Fig. 5B). Although the VSV yield was not significantly modified, the SVDV and FMDV titers were reduced 80 and 25%, respectively, and these results correlated with the percentage of infected cells. When the drug was added postinfection, no effect was observed, confirming that MβCD affected an early step of infection (Fig. 5B). Preinfection treatment with αCD did not have any significant effect on VSV, SVDV, and FMDV infection (Fig. 5C), supporting that the inhibitory effect of MβCD was due to cholesterol depletion and not to other effects derived from the addition of a cyclodextrin.

As MβCD can inhibit virus infection through caveolae, we investigated the ability of these viruses to induce caveolin-1 phosphorylation on Tyr 14, an essential event reported for CVB3 caveola-mediated endocytosis (15) and caveola internalization (23). None of the virus tested induced caveolin-1 phos-

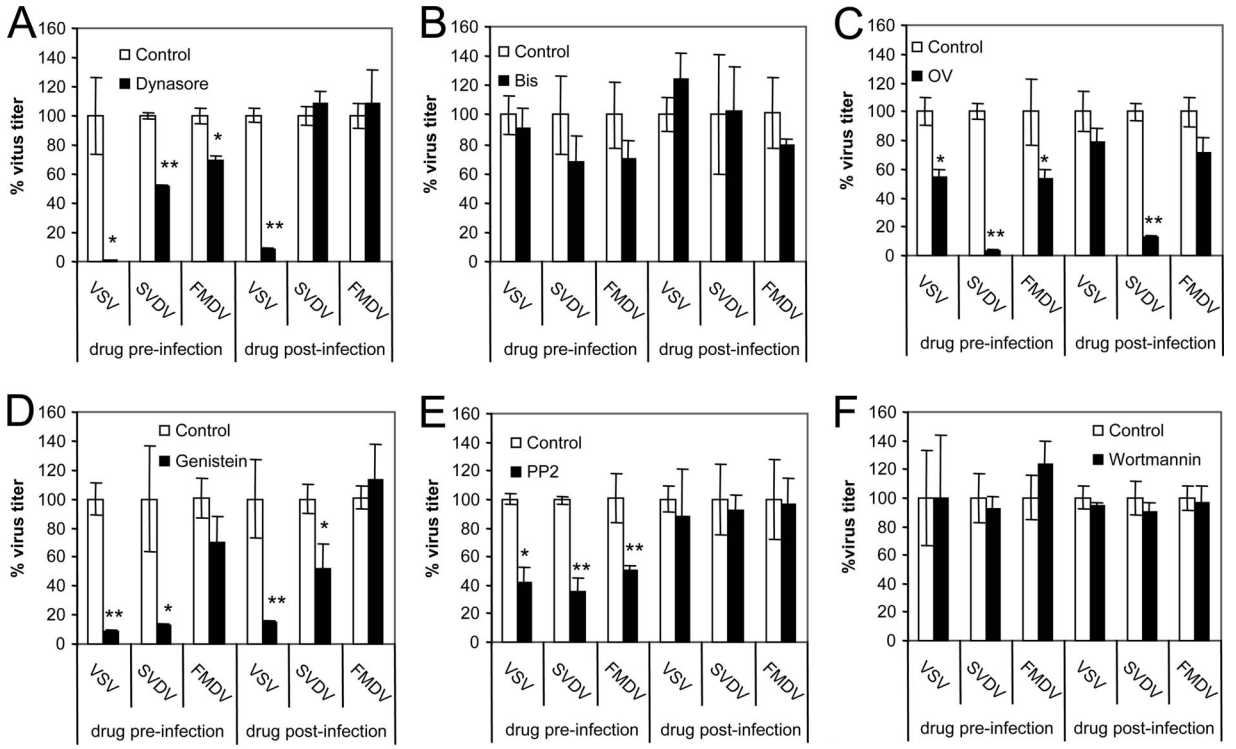

FIG. 4. Dynamin and cell signaling requirements for virus infection. The effects of dynasore (A), Bis (B), OV (C), genistein (D), PP2 (E), and wortmannin (F) on VSV, SVDV, and FMDV infection were studied by plaque assay. The following treatments induced measurable reported effects: dynasore, inhibition of TF internalization (49); wortmannin, endosomal vacuolation (46); and OV, tyrosine phosphorylation (73). Statistically significant differences between control and drug treatments are indicated by one asterisk ($P < 0.05$) or two asterisks ($P < 0.005$).

phorylation (Fig. 5D). The only positive signal was obtained in IBRS-2 cells treated with the tyrosine phosphatase inhibitor OV, whose addition results in caveolin-1 phosphorylation (73), used here as a control of the antibody used for detection of phosphorylated caveolin-1. In addition, treatment with nystatin, filipin, or lovastatin, which impair lipid-raft/caveola-mediated endocytosis (15, 85), did not inhibit SVDV or, as reported (52), VSV and FMDV infection (data not shown). These findings suggest that the role of cholesterol in SVDV and FMDV internalization is independent of caveolae.

DISCUSSION

In this study we have attempted a sequential and comparative analysis of the entry events of three important animal viruses by using drugs inhibiting different components of cell machinery involved in viral entry. A summary of the effects on SVDV, FMDV, and VSV entry of the drugs tested for all three viruses is shown in Table 1. Our results indicate that the SVDV isolate used here, which binds CAR but not DAF (34) and is able to interact with HS (26), is internalized through dynamin-dependent, clathrin-mediated endocytosis and transported to early endosomes, as indicated by its colocalization with EEA1 and TF. Infection requires endosomal acidification, as revealed by the inhibitory effect of NH_4Cl and concanamycin A. Interestingly, infection inhibition by concanamycin A was different from that observed for NH_4Cl. Previous work using FMDV indicated that NH_4Cl block of endosomal acidification caused a higher reduction of virus infection than concanamycin A treatment (52). This may be explained by the different conditions of NH_4Cl and concanamycin treatments; while NH_4Cl was present throughout the infection, concanamycin was removed after the first infection hour. However, the effect of concanamycin A, in contrast to that observed for NH_4Cl, is not readily reversible (57, 62). Another differential factor is that NH_4Cl blockage of endosomal acidification is produced by neutralization of endosomal pH, whereas concanamycin inhibits the proton flux into the endosome but does not neutralize remaining acid pH within the endosomes.

Macropinocytosis has been implicated in coxsackievirus entry (16). Our results indicate that SVDV, FMDV, and VSV infections depend on dynamin but not on PKC function (Fig. 4B) and actin cytoskeleton integrity (Fig. 3C), two of the important features of macropinocytosis (3, 16), suggesting that this route is not exploited by any of the viruses studied.

Interestingly, comparison of the SVDV internalization events to those of VSV and FMDV suggests diversity in the endosomal pathways that can be exploited by these three animal viruses that use clathrin to enter cells. It has been recently reported that FMDV mutants using HS as a receptor can be internalized via caveolae in contrast to FMDV isolates interacting with integrins, whose internalization is dependent on clathrin (60). The C-S8c1 isolate used in this study does not bind HS (6), ruling out this possibility (see Materials and Methods).

Differential endocytosis requirements included sensitivity to plasma membrane cholesterol depletion with MβCD, which

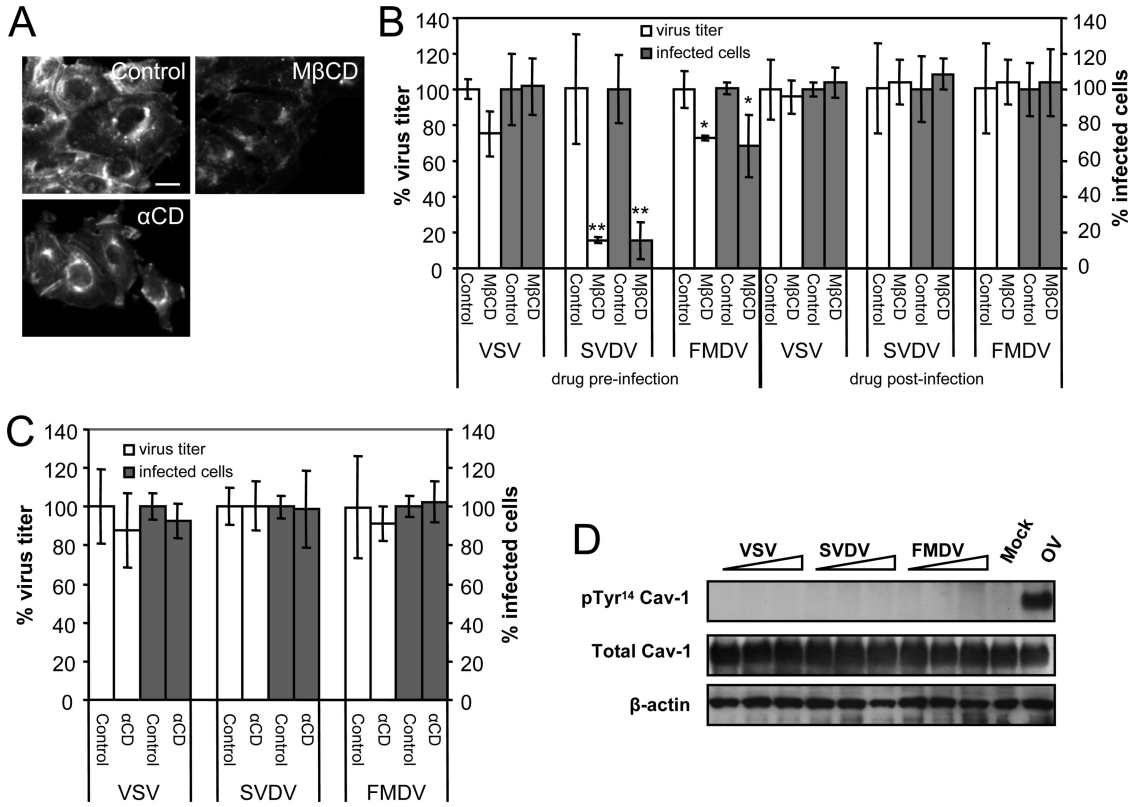

FIG. 5. Differential requirements for cholesterol in virus infection. (A) Effects of MβCD and αCD on cellular cholesterol content of IBRS-2 cells studied by filipin staining. Bar, 20 μm. (B) Effect of cholesterol depletion by MβCD on virus infection evaluated by plaque assay and the percentage of infected cells in immunofluorescence studies using I1, 2H12, and 5C4 antibodies to detect VSV, SVDV, and FMDV, respectively, and appropriate secondary antibodies coupled to Alexa Fluor 488. (C) Effects of treatment with αCD on virus infection. (D) VSV, SVDV, and FMDV infections do not induce caveolin-1 phosphorylation on Tyr14. IBRS-2 cells were infected (MOI of 100) for 1 h on ice and then incubated for 15, 30, or 60 min at 37°C; lysed; and processed for Western blotting using MAb anti-Tyr^{14} phosphorylated caveolin-1, and polyclonal serum to caveolin-1 to detect total caveolin-1. An extract of IBRS-2 cells treated with 1 mM OV 60 min was included as a control of MAb anti-Tyr^{14} phosphorylated caveolin-1. Results obtained with β-actin are also shown as a control for protein loading. Statistically significant differences between control and drug treatments are indicated by one asterisk ($P < 0.05$) or two asterisks ($P < 0.005$).

TABLE 1. Summary of effects on SVDV, FMDV, and VSV entry of the drugs tested[a]

Cellular target	Drug	Virus[b]		
		SVDV	FMDV	VSV
Dynamin	Dynasore	+	+	+PI
Endosomal pH	NH_4Cl	+	+	+
Microtubules	Nocodazole	+	−	+PI
Actin microfilaments	Cyt D	−	−	−
Cell signaling machinery	OV	+PI	+	+
	Genistein	+PI	−	+PI
	PP2	+	+	+
	Bis	−	−	−
	Wortmannin	−	−	−
Cholesterol	MβCD	+	+	−
	Filipin	−	−	−
	Lovastatin	−	−	−
	Nystatin	−	−	−

[a] Only drugs for which results with the three viruses compared were obtained are included.

[b] +, Statistically significant inhibitory effect of the drug on virus infection only when added preinfection; +PI, the drug also had a statistically significant inhibitory effect when added postinfection; −, no statistically significant effect when added pre- or postinfection.

was higher for SVDV than for FMDV and not significant in the case of VSV. This SVDV and FMDV cholesterol requirement was independent of caveolin-1 phosphorylation, and more specific drugs affecting the caveolin pathway (nystatin, filipin, and lovastatin) did not affect virus infection, suggesting that the cholesterol requirement observed is not related to caveola function. These results could be explained by an altered location of virus receptors on plasma membrane microdomains in MβCD-treated cells (52). Supporting this hypothesis, CAR has been shown to be associated to lipid-rafts distinct from those containing caveolin-1 and glycosylphosphatidylinositol-anchored proteins (5), and infection by type 2 adenovirus, a virus internalized by clathrin-mediated endocytosis that uses CAR as a cellular receptor, is inhibited by MβCD (32). However, we cannot exclude that the different cholesterol requirements of the three viruses studied could be due to distinct endosomal escape mechanisms resulting in viral penetration, since cholesterol can play a key role in endosomal escape of different viruses, and this can be affected by cholesterol extraction with MβCD (20, 32).

Because CCPs were first associated with VSV endocytosis in a process named viropexis (78), the role of clathrin and asso-

ciated proteins in viral infection has been widely investigated. Internalization of ligands by clathrin CCPs has been proposed to rely on different signaling events (89). Indeed, genistein, a tyrosine kinase inhibitor, can differentially affect clathrin-mediated internalization of ligands (44). The differences found in our experiments in the sensitivity of the viruses studied to OV (phosphatase inhibitor) and genistein (kinase inhibitor) support this notion of signaling diversity. The ability of these two molecules producing opposite effects on Tyr phosphorylation to inhibit viral infection has been also reported for echovirus (66). These observations may be explained because the signaling events driving ligand internalization are very complex and requires both regulated phosphorylation and dephosphorylation of cellular components.

Different populations of CCPs with specific adaptor proteins have been identified (35, 41, 67). Lakadamyali et al. (43) showed by means of live cell imaging that ligands for clathrin-mediated endocytosis can be sorted, in a process that begins at CCP, into two populations of early endosomes that show different microtubule-mediated mobility. Our results, obtained from the effect of different drugs on viral infection, support this specialized cargo sorting into distinct endosome populations. Treatment with nocodazole showed that SVDV may be internalized to dynamic endosomes in contrast to FMDV. VSV dependence on microtubules for intracellular sorting has been previously described (46), suggesting that it is sorted into the dynamic endosome population, although it may infect from early and late endosomes (46, 76). Since TF traffics through early and recycling endosomes but not to late endosomes (43), the observation of SVDV particles close to microtubules but not associated to TF (Fig. 2F) suggests that SVDV can be sorted to a different cell compartment in a microtubule-dependent way. These results could be explained by the possibility of SVDV and VSV (but not FMDV) being transported to late endosomes/lysosomes for productive infection. However, this possibility was ruled out because of the lack of inhibition by wortmannin, a drug that inhibits early to late endosome transport, and by Bis, an inhibitor of PKC function that has been implicated in early to late endosome viral transport (8, 10, 17, 75).

Taken together, these results indicate that SVDV and VSV are sorted to a distinct population of early endosomes different from FMDV. This pre-early endosome sorting process may begin at plasma membrane CCP as reported for other ligands (43), thus segregating cargo into different CCP populations as a mechanism to reduce competition between diverse endocytic cargo (67). A better understanding of this emerging complexity will aid in the design of new antiviral compounds targeting the clathrin-mediated endocytosis machinery of host cells.

ACKNOWLEDGMENTS

We thank V. Ley and M. A. Jiménez-Clavero for providing SVDV isolate SPA/1/'93 and with serum to SVDV VP1, M. Dávila and E. Domingo for VSV Indiana isolate and MAb I1, I. Sandoval for MAb 25H8, E. Brocchi for MAb 2H12, and M. T. Rejas for advice in the TEM studies. Dynasore was synthesized by H. E. Pelish and was kindly provided by T. Kirchhausen.

This study was supported by Spanish grants from CICYT (Bio2008-04487-C03-01) and MEC (CSD2006-0007) and by the Fundación Severo Ochoa.

REFERENCES

1. **Alcalde, J., G. Egea, and I. V. Sandoval.** 1994. gp74 a membrane glycoprotein of the cis-Golgi network that cycles through the endoplasmic reticulum and intermediate compartment. J. Cell Biol. **124:**649–665.
2. **Alexandersen, S., and N. Mowat.** 2005. Foot-and-mouth disease: host range and pathogenesis. Curr. Top. Microbiol. Immunol. **288:**9–42.
3. **Amstutz, B., M. Gastaldelli, S. Kalin, N. Imelli, K. Boucke, E. Wandeler, J. Mercer, S. Hemmi, and U. F. Greber.** 2008. Subversion of CtBP1-controlled macropinocytosis by human adenovirus serotype 3. EMBO J. **27:**956–964.
4. **Armas-Portela, R., M. A. Parrales, J. P. Albar, A. C. Martinez, and J. Avila.** 1999. Distribution and characteristics of betaII tubulin-enriched microtubules in interphase cells. Exp. Cell Res. **248:**372–380.
5. **Ashbourne Excoffon, K. J., T. Moninger, and J. Zabner.** 2003. The coxsackie B virus and adenovirus receptor resides in a distinct membrane microdomain. J. Virol. **77:**2559–2567.
6. **Baranowski, E., N. Sevilla, N. Verdaguer, C. M. Ruiz-Jarabo, E. Beck, and E. Domingo.** 1998. Multiple virulence determinants of foot-and-mouth disease virus in cell culture. J. Virol. **72:**6362–6372.
7. **Benmerah, A., and C. Lamaze.** 2007. Clathrin-coated pits: vive la difference? Traffic **8:**970–982.
8. **Berryman, S., S. Clark, P. Monaghan, and T. Jackson.** 2005. Early events in integrin αvβ6-mediated cell entry of foot-and-mouth disease virus. J. Virol. **79:**8519–8534.
9. **Borrego, B., E. Carra, J. A. Garcia-Ranea, and E. Brocchi.** 2002. Characterization of neutralization sites on the circulating variant of swine vesicular disease virus (SVDV): a new site is shared by SVDV and the related coxsackie B5 virus. J. Gen. Virol. **83:**35–44.
10. **Brabec, M., D. Blaas, and R. Fuchs.** 2006. Wortmannin delays transfer of human rhinovirus serotype 2 to late endocytic compartments. Biochem. Biophys. Res. Commun. **348:**741–749.
11. **Brandenburg, B., L. Y. Lee, M. Lakadamyali, M. J. Rust, X. Zhuang, and J. M. Hogle.** 2007. Imaging poliovirus entry in live cells. PLoS Biol. **5:**e183.
12. **Burman, A., S. Clark, N. G. Abrescia, E. E. Fry, D. I. Stuart, and T. Jackson.** 2006. Specificity of the VP1 GH loop of foot-and-mouth disease virus for αv integrins. J. Virol. **80:**9798–9810.
13. **Coil, D. A., and A. D. Miller.** 2004. Phosphatidylserine is not the cell surface receptor for vesicular stomatitis virus. J. Virol. **78:**10920–10926.
14. **Corvera, S.** 2001. Phosphatidylinositol 3-kinase and the control of endosome dynamics: new players defined by structural motifs. Traffic **2:**859–866.
15. **Coyne, C. B., and J. M. Bergelson.** 2006. Virus-induced Abl and Fyn kinase signals permit coxsackievirus entry through epithelial tight junctions. Cell **124:**119–131.
16. **Coyne, C. B., L. Shen, J. R. Turner, and J. M. Bergelson.** 2007. Coxsackievirus entry across epithelial tight junctions requires occludin and the small GTPases Rab34 and Rab5. Cell Host Microbe **2:**181–192.
17. **Chu, J. J., P. W. Leong, and M. L. Ng.** 2006. Analysis of the endocytic pathway mediating the infectious entry of mosquito-borne flavivirus West Nile into *Aedes albopictus* mosquito (C6/36) cells. Virology **349:**463–475.
18. **Chung, S. K., J. Y. Kim, I. B. Kim, S. I. Park, K. H. Paek, and J. H. Nam.** 2005. Internalization and trafficking mechanisms of coxsackievirus B3 in HeLa cells. Virology **333:**31–40.
19. **Damm, E. M., and L. Pelkmans.** 2006. Systems biology of virus entry in mammalian cells. Cell Microbiol. **8:**1219–1227.
20. **Danthi, P., and M. Chow.** 2004. Cholesterol removal by methyl-beta-cyclodextrin inhibits poliovirus entry. J. Virol. **78:**33–41.
21. **Das, S. C., D. Nayak, Y. Zhou, and A. K. Pattnaik.** 2006. Visualization of intracellular transport of vesicular stomatitis virus nucleocapsids in living cells. J. Virol. **80:**6368–6377.
22. **De Castro, M. P.** 1964. Behaviour of the foot-and-mouth disease virus in cell cultures: susceptibility of the IB-RS-2 cell line. Arq. Inst. Biol. Sao Paulo **31:**63–78.
23. **del Pozo, M. A., N. Balasubramanian, N. B. Alderson, W. B. Kiosses, A. Grande-Garcia, R. G. Anderson, and M. A. Schwartz.** 2005. Phospho-caveolin-1 mediates integrin-regulated membrane domain internalization. Nat. Cell Biol. **7:**901–908.
24. **DeTulleo, L., and T. Kirchhausen.** 1998. The clathrin endocytic pathway in viral infection. EMBO J. **17:**4585–4593.
25. **Drose, S., and K. Altendorf.** 1997. Bafilomycins and concanamycins as inhibitors of V-ATPases and P-ATPases. J. Exp. Biol. **200:**1–8.
26. **Escribano-Romero, E., M. A. Jimenez-Clavero, P. Gomes, J. A. Garcia-Ranea, and V. Ley.** 2004. Heparan sulphate mediates swine vesicular disease virus attachment to the host cell. J. Gen. Virol. **85:**653–663.
27. **Fry, E. E., N. J. Knowles, J. W. Newman, G. Wilsden, Z. Rao, A. M. King, and D. I. Stuart.** 2003. Crystal structure of Swine vesicular disease virus and implications for host adaptation. J. Virol. **77:**5475–5486.
28. **Garcia-Briones, M., M. F. Rosas, M. Gonzalez-Magaldi, M. A. Martin-Acebes, F. Sobrino, and R. Armas-Portela.** 2006. Differential distribution of nonstructural proteins of foot-and-mouth disease virus in BHK-21 cells. Virology **349:**409–421.
29. **Hanover, J. A., M. C. Willingham, and I. Pastan.** 1984. Kinetics of transit of

transferrin and epidermal growth factor through clathrin-coated membranes. Cell **39:**283–293.
30. **Heuser, J. E., and R. G. Anderson.** 1989. Hypertonic media inhibit receptor-mediated endocytosis by blocking clathrin-coated pit formation. J. Cell Biol. **108:**389–400.
31. **Hinshaw, J. E.** 2000. Dynamin and its role in membrane fission. Annu. Rev. Cell Dev. Biol. **16:**483–519.
32. **Imelli, N., O. Meier, K. Boucke, S. Hemmi, and U. F. Greber.** 2004. Cholesterol is required for endocytosis and endosomal escape of adenovirus type 2. J. Virol. **78:**3089–3098.
33. **Jimenez-Clavero, M. A., E. Escribano-Romero, A. J. Douglas, and V. Ley.** 2001. The N-terminal region of the VP1 protein of swine vesicular disease virus contains a neutralization site that arises upon cell attachment and is involved in viral entry. J. Virol. **75:**1044–1047.
34. **Jimenez-Clavero, M. A., E. Escribano-Romero, V. Ley, and O. B. Spiller.** 2005. More recent swine vesicular disease virus isolates retain binding to coxsackie-adenovirus receptor, but have lost the ability to bind human decay-accelerating factor (CD55). J. Gen. Virol. **86:**1369–1377.
35. **Johannessen, L. E., N. M. Pedersen, K. W. Pedersen, I. H. Madshus, and E. Stang.** 2006. Activation of the epidermal growth factor (EGF) receptor induces formation of EGF receptor- and Grb2-containing clathrin-coated pits. Mol. Cell. Biol. **26:**389–401.
36. **Johannsdottir, H. K., R. Mancini, J. Kartenbeck, L. Amato, and A. Helenius.** 2008. Host cell factors and functions involved in vesicular stomatitis virus entry. J. Virol. **83:**440–453.
37. **Joki-Korpela, P., V. Marjomaki, C. Krogerus, J. Heino, and T. Hyypia.** 2001. Entry of human parechovirus 1. J. Virol. **75:**1958–1967.
38. **Kee, S. H., E. J. Cho, J. W. Song, K. S. Park, L. J. Baek, and K. J. Song.** 2004. Effects of endocytosis inhibitory drugs on rubella virus entry into VeroE6 cells. Microbiol. Immunol. **48:**823–829.
39. **Keller, P., and K. Simons.** 1998. Cholesterol is required for surface transport of influenza virus hemagglutinin. J. Cell Biol. **140:**1357–1367.
40. **Kessels, M. M., J. Dong, W. Leibig, P. Westermann, and B. Qualmann.** 2006. Complexes of syndapin II with dynamin II promote vesicle formation at the trans-Golgi network. J. Cell Sci. **119:**1504–1516.
41. **Keyel, P. A., S. K. Mishra, R. Roth, J. E. Heuser, S. C. Watkins, and L. M. Traub.** 2006. A single common portal for clathrin-mediated endocytosis of distinct cargo governed by cargo-selective adaptors. Mol. Biol. Cell **17:**4300–4317.
42. **Kirchhausen, T., E. Macia, and H. E. Pelish.** 2008. Use of dynasore, the small molecule inhibitor of dynamin, in the regulation of endocytosis. Methods Enzymol. **438:**77–93.
43. **Lakadamyali, M., M. J. Rust, and X. Zhuang.** 2006. Ligands for clathrin-mediated endocytosis are differentially sorted into distinct populations of early endosomes. Cell **124:**997–1009.
44. **Lamaze, C., T. Baba, T. E. Redelmeier, and S. L. Schmid.** 1993. Recruitment of epidermal growth factor and transferrin receptors into coated pits in vitro: differing biochemical requirements. Mol. Biol. Cell **4:**715–727.
45. **Lea, S., J. Hernandez, W. Blakemore, E. Brocchi, S. Curry, E. Domingo, E. Fry, R. Abu-Ghazaleh, A. King, J. Newman, et al.** 1994. The structure and antigenicity of a type C foot-and-mouth disease virus. Structure **2:**123–139.
46. **Le Blanc, I., P. P. Luyet, V. Pons, C. Ferguson, N. Emans, A. Petiot, N. Mayran, N. Demaurex, J. Faure, R. Sadoul, R. G. Parton, and J. Gruenberg.** 2005. Endosome-to-cytosol transport of viral nucleocapsids. Nat. Cell Biol. **7:**653–664.
47. **Lefrancois, L., and D. S. Lyles.** 1982. The interaction of antibody with the major surface glycoprotein of vesicular stomatitis virus. II. Monoclonal antibodies of nonneutralizing and cross-reactive epitopes of Indiana and New Jersey serotypes. Virology **121:**168–174.
48. **Lukacs, G. L., G. Segal, N. Kartner, S. Grinstein, and F. Zhang.** 1997. Constitutive internalization of cystic fibrosis transmembrane conductance regulator occurs via clathrin-dependent endocytosis and is regulated by protein phosphorylation. Biochem. J. **328**(Pt. 2)**:**353–361.
49. **Macia, E., M. Ehrlich, R. Massol, E. Boucrot, C. Brunner, and T. Kirchhausen.** 2006. Dynasore, a cell-permeable inhibitor of dynamin. Dev. Cell **10:**839–850.
50. **Marsh, M., and A. Helenius.** 2006. Virus entry: open sesame. Cell **124:**729–740.
51. **Martin-Acebes, M. A., M. Gonzalez-Magaldi, M. F. Rosas, B. Borrego, E. Brocchi, R. Armas-Portela, and F. Sobrino.** 2008. Subcellular distribution of swine vesicular disease virus proteins and alterations induced in infected cells: a comparative study with foot-and-mouth disease virus and vesicular stomatitis virus. Virology **374:**432–443.
52. **Martin-Acebes, M. A., M. Gonzalez-Magaldi, K. Sandvig, F. Sobrino, and R. Armas-Portela.** 2007. Productive entry of type C foot-and-mouth disease virus into susceptible cultured cells requires clathrin and is dependent on the presence of plasma membrane cholesterol. Virology **369:**105–118.
53. **Mateu, M. G., M. L. Valero, D. Andreu, and E. Domingo.** 1996. Systematic replacement of amino acid residues within an Arg-Gly-Asp-containing loop of foot-and-mouth disease virus and effect on cell recognition. J. Biol. Chem. **271:**12814–12819.
54. **Matlin, K. S., H. Reggio, A. Helenius, and K. Simons.** 1982. Pathway of vesicular stomatitis virus entry leading to infection. J. Mol. Biol. **156:**609–631.
55. **Milstone, A. M., J. Petrella, M. D. Sanchez, M. Mahmud, J. C. Whitbeck, and J. M. Bergelson.** 2005. Interaction with coxsackievirus and adenovirus receptor, but not with decay-accelerating factor (DAF), induces A-particle formation in a DAF-binding coxsackievirus B3 isolate. J. Virol. **79:**655–660.
56. **Miller, K., M. Shipman, I. S. Trowbridge, and C. R. Hopkins.** 1991. Transferrin receptors promote the formation of clathrin lattices. Cell **65:**621–632.
57. **Muroi, M., N. Shiragami, and A. Takatsuki.** 1994. Destruxin B, a specific and readily reversible inhibitor of vacuolar-type H(+)-translocating ATPase. Biochem. Biophys. Res. Commun. **205:**1358–1365.
58. **Norkin, L. C., H. A. Anderson, S. A. Wolfrom, and A. Oppenheim.** 2002. Caveolar endocytosis of simian virus 40 is followed by brefeldin A-sensitive transport to the endoplasmic reticulum, where the virus disassembles. J. Virol. **76:**5156–5166.
59. **Nunez, J. I., N. Molina, E. Baranowski, E. Domingo, S. Clark, A. Burman, S. Berryman, T. Jackson, and F. Sobrino.** 2007. Guinea pig-adapted foot-and-mouth disease virus with altered receptor recognition can productively infect a natural host. J. Virol. **81:**8497–8506.
60. **O'Donnell, V., M. Larocco, and B. Baxt.** 2008. Heparan sulfate-binding foot-and-mouth disease virus enters cells via caveola-mediated endocytosis. J. Virol. **82:**9075–9085.
61. **O'Donnell, V., M. LaRocco, H. Duque, and B. Baxt.** 2005. Analysis of foot-and-mouth disease virus internalization events in cultured cells. J. Virol. **79:**8506–8518.
62. **Ohkuma, S., and B. Poole.** 1978. Fluorescence probe measurement of the intralysosomal pH in living cells and the perturbation of pH by various agents. Proc. Natl. Acad. Sci. USA **75:**3327–3331.
63. **Pelkmans, L.** 2005. Secrets of caveolae- and lipid raft-mediated endocytosis revealed by mammalian viruses. Biochim. Biophys. Acta **1746:**295–304.
64. **Pelkmans, L., T. Burli, M. Zerial, and A. Helenius.** 2004. Caveolin-stabilized membrane domains as multifunctional transport and sorting devices in endocytic membrane traffic. Cell **118:**767–780.
65. **Pelkmans, L., E. Fava, H. Grabner, M. Hannus, B. Habermann, E. Krausz, and M. Zerial.** 2005. Genome-wide analysis of human kinases in clathrin- and caveolae/raft-mediated endocytosis. Nature **436:**78–86.
66. **Pietiainen, V., V. Marjomaki, P. Upla, L. Pelkmans, A. Helenius, and T. Hyypia.** 2004. Echovirus 1 endocytosis into caveosomes requires lipid rafts, dynamin II, and signaling events. Mol. Biol. Cell **15:**4911–4925.
67. **Puthenveedu, M. A., and M. von Zastrow.** 2006. Cargo regulates clathrin-coated pit dynamics. Cell **127:**113–124.
68. **Rindler, M. J., I. E. Ivanov, H. Plesken, E. Rodriguez-Boulan, and D. D. Sabatini.** 1984. Viral glycoproteins destined for apical or basolateral plasma membrane domains traverse the same Golgi apparatus during their intracellular transport in doubly infected Madin-Darby canine kidney cells. J. Cell Biol. **98:**1304–1319.
69. **Rodal, S. K., G. Skretting, O. Garred, F. Vilhardt, B. van Deurs, and K. Sandvig.** 1999. Extraction of cholesterol with methyl-beta-cyclodextrin perturbs formation of clathrin-coated endocytic vesicles. Mol. Biol. Cell **10:**961–974.
70. **Rose, J. K., and M. A. Whitt.** 2001. *Rhabdoviridae*: the viruses and their replication, p. 1221–1224. *In* D. M. Knipe and P. M. Howley (ed.), Fields virology, 4th ed. Lippincott-Raven Publishers, Philadelphia, PA.
71. **Roth, M. G.** 2006. Clathrin-mediated endocytosis before fluorescent proteins. Nat. Rev. Mol. Cell. Biol. **7:**63–68.
72. **Schlegel, R., T. S. Tralka, M. C. Willingham, and I. Pastan.** 1983. Inhibition of VSV binding and infectivity by phosphatidylserine: is phosphatidylserine a VSV-binding site? Cell **32:**639–646.
73. **Shin, J., H. Jo, and H. Park.** 2006. Caveolin-1 is transiently dephosphorylated by shear stress-activated protein tyrosine phosphatase mu. Biochem. Biophys. Res. Commun. **339:**737–741.
74. **Shvartsman, D. E., O. Gutman, A. Tietz, and Y. I. Henis.** 2006. Cyclodextrins but not compactin inhibit the lateral diffusion of membrane proteins independent of cholesterol. Traffic **7:**917–926.
75. **Sieczkarski, S. B., H. A. Brown, and G. R. Whittaker.** 2003. Role of protein kinase C βII in influenza virus entry via late endosomes. J. Virol. **77:**460–469.
76. **Sieczkarski, S. B., and G. R. Whittaker.** 2003. Differential requirements of Rab5 and Rab7 for endocytosis of influenza and other enveloped viruses. Traffic **4:**333–343.
77. **Sieczkarski, S. B., and G. R. Whittaker.** 2002. Dissecting virus entry via endocytosis. J. Gen. Virol. **83:**1535–1545.
78. **Simpson, R. W., R. E. Hauser, and S. Dales.** 1969. Viropexis of vesicular stomatitis virus by L cells. Virology **37:**285–290.
79. **Snyers, L., H. Zwickl, and D. Blaas.** 2003. Human rhinovirus type 2 is internalized by clathrin-mediated endocytosis. J. Virol. **77:**5360–5369.
80. **Sobrino, F., and E. Domingo (ed.).** 2004. Foot-and-mouth disease: current perspectives. Horizon Bioscience, Norfolk, United Kingdom.
81. **Sobrino, F., M. Davila, J. Ortin, and E. Domingo.** 1983. Multiple genetic variants arise in the course of replication of foot-and-mouth disease virus in cell culture. Virology **128:**310–318.
82. **Sobrino, F., M. Saiz, M. A. Jimenez-Clavero, J. I. Nunez, M. F. Rosas, E.**

Baranowski, and V. Ley. 2001. Foot-and-mouth disease virus: a long known virus, but a current threat. Vet. Res. **32:**1–30.
83. **Subtil, A., I. Gaidarov, K. Kobylarz, M. A. Lampson, J. H. Keen, and T. E. McGraw.** 1999. Acute cholesterol depletion inhibits clathrin-coated pit budding. Proc. Natl. Acad. Sci. USA **96:**6775–6780.
84. **Sun, X., V. K. Yau, B. J. Briggs, and G. R. Whittaker.** 2005. Role of clathrin-mediated endocytosis during vesicular stomatitis virus entry into host cells. Virology **338:**53–60.
85. **Triantafilou, K., and M. Triantafilou.** 2004. Lipid-raft-dependent coxsackievirus B4 internalization and rapid targeting to the Golgi. Virology **326:** 6–19.
86. **Vela, E. M., L. Zhang, T. M. Colpitts, R. A. Davey, and J. F. Aronson.** 2007. Arenavirus entry occurs through a cholesterol-dependent, non-caveolar, clathrin-mediated endocytic mechanism. Virology **369:**1–11.
87. **Verdaguer, N., M. A. Jimenez-Clavero, I. Fita, and V. Ley.** 2003. Structure of swine vesicular disease virus: mapping of changes occurring during adaptation of human coxsackie B5 virus to infect swine. J. Virol. **77:**9780–9789.
88. **Wang, L. H., K. G. Rothberg, and R. G. Anderson.** 1993. Mis-assembly of clathrin lattices on endosomes reveals a regulatory switch for coated pit formation. J. Cell Biol. **123:**1107–1117.
89. **Warren, R. A., F. A. Green, P. E. Stenberg, and C. A. Enns.** 1998. Distinct saturable pathways for the endocytosis of different tyrosine motifs. J. Biol. Chem. **273:**17056–17063.
90. **Zautner, A. E., B. Jahn, E. Hammerschmidt, P. Wutzler, and M. Schmidtke.** 2006. N- and 6-O-sulfated heparan sulfates mediate internalization of coxsackievirus B3 variant PD into CHO-K1 cells. J. Virol. **80:**6629–6636.
91. **Zhang, G., D. T. Haydon, N. J. Knowles, and J. W. McCauley.** 1999. Molecular evolution of swine vesicular disease virus. J. Gen. Virol. **80**(Pt. 3)**:**639–651.

JOURNAL OF VIROLOGY, Feb. 2011, p. 1267–1274 Vol. 85, No. 3
0022-538X/11/$12.00 doi:10.1128/JVI.01717-10

Inhibition of Enveloped Virus Infection of Cultured Cells by Valproic Acid▽†

Ángela Vázquez-Calvo,[1] Juan-Carlos Saiz,[2] Francisco Sobrino,[1,3]* and Miguel A. Martín-Acebes[2]

Centro de Biología Molecular Severo Ochoa (UAM-CSIC), Cantoblanco, Madrid, Spain[1]; Departamento de Biotecnología, Instituto Nacional de Investigación y Tecnología Agraria y Alimentaria, Madrid, Spain[2]; and Centro de Investigación en Sanidad Animal, Instituto Nacional de Investigación y Tecnología Agraria y Alimentaria, Valdeolmos, Madrid, Spain[3]

Received 13 August 2010/Accepted 12 November 2010

Valproic acid (VPA) is a short-chain fatty acid commonly used for treatment of neurological disorders. As VPA can interfere with cellular lipid metabolism, its effect on the infection of cultured cells by viruses of seven viral families relevant to human and animal health, including eight enveloped and four nonenveloped viruses, was analyzed. VPA drastically inhibited multiplication of all the enveloped viruses tested, including the zoonotic lymphocytic choriomeningitis virus and West Nile virus (WNV), while it did not affect infection by the nonenveloped viruses assayed. VPA reduced vesicular stomatitis virus infection yield without causing a major blockage of either viral RNA or protein synthesis. In contrast, VPA drastically abolished WNV RNA and protein synthesis, indicating that this drug can interfere the viral cycle at different steps of enveloped virus infection. Thus, VPA can contribute to an understanding of the crucial steps of viral maturation and to the development of future strategies against infections associated with enveloped viruses.

Conventional antiviral agents can interfere successfully with viral components but often lead to development of drug resistance in virus populations evolving under selective pressures (9, 14). One of the approaches to circumvent this limitation is the identification of antivirals targeted against cellular functions required for the virus to complete its viral cycle, thus reducing the potential of viruses to escape from drug effects (26, 35, 44). Indeed, some long-used drugs commonly administered by clinicians to treat human disorders, such as lithium or statins, have been proposed as new antiviral agent candidates (3, 18, 20) as part of drug repositioning (finding of new applications to licensed drugs) in drug development. Massive screenings have also revealed the potential antiviral effect of multiple clinical compounds, supporting this kind of approach (17).

Valproic acid ([VPA] 2-propylpentanoic acid) is a branched short-chain fatty acid commonly used for treatment of neurological disorders (6, 52). The proposed cellular targets of VPA are diverse, including (i) interruption of γ-amino butyric acid (GABA) signaling, (ii) inhibition of histone deacetylases (HDAC), (iii) modulation of sodium channel activity, (iv) inhibition of glycogen synthase kinase 3, and (v) disruption of membrane lipid metabolism, including that of phosphatidylinositol (48, 53, 54, 57, 59).

As intracellular parasites, many viruses hijack cellular membranes from host cells for virus replication and/or virion assembly, and alterations in the membrane lipid environment can interfere with these processes (22, 43). This prompted us to examine the effect of VPA on the infectivity of different viruses relevant to human and animal health, such as the flaviviruses West Nile virus (WNV) and Usutu virus (USUV), the arenavirus lymphocytic choriomeningitis virus (LCMV), the rhabdovirus vesicular stomatitis virus (VSV), the togaviruses Semliki forest virus (SFV) and Sindbis virus (SINV), the asfivirus African swine fever virus (ASFV), the poxvirus vaccinia virus (VACV), and the picornaviruses foot-and-mouth disease virus (FMDV), encephalomyocarditis virus (EMCV), bovine enterovirus (BEV), and equine rhinitis A virus (ERAV). We observed that VPA caused a drastic reduction of the yield of all enveloped viruses (WNV, USUV, VSV, SFV, SINV, LCMV, VACV, and ASFV) but did not affect the nonenveloped viruses FMDV, EMCV, BEV, and ERAV. We further analyzed the effect of VPA on enveloped virus infections. For this purpose, two viruses, VSV and WNV, whose infectious cycle are well characterized (1, 5, 13, 19, 28, 30, 33, 36, 46) were used. Our results indicate that VPA reduced the yield of these two viruses by more than 7 orders of magnitude; however, while both WNV RNA and protein synthesis were drastically abolished, no major blockage of VSV RNA and protein synthesis was observed, indicating that VPA can interfere at different steps of enveloped virus infection. These results make VPA an interesting drug for understanding the crucial steps of viral maturation and for developing future strategies against infectious diseases associated with enveloped viruses.

MATERIALS AND METHODS

Cells, viruses, antibodies, and reagents. BHK-21 cells (ATCC) and Vero cells (ATCC) were maintained in Dulbecco's modified Eagle's medium (DMEM) (Gibco-BRL, Invitrogen, Carlsbad, CA) supplemented with 5% fetal calf serum (FCS) (Sigma, St. Louis, MO), L-glutamine (2 mM), penicillin (100 U/ml), and streptomycin (100 μg/ml). Type C FMDV C-S8c1 (50), BEV (23), EMCV (47), SFV and SINV (55), VSV Indiana (40), LCMV (37), and Western Reserve VACV (4) viral stocks were grown in BHK-21 cells. USUV (7), WNV (10), ERAV (32), and ASFV strain BA71V (15) stocks were amplified in Vero cells. Antibodies against WNV E glycoprotein from Chemicon (Temecula, CA), acetylated histone H3 (AcH3) from Upstate (Lake Placid, NY), and tubulin (2) were used. The remaining antibodies and stains used have been previously described (38). Valproic acid sodium salt, VPA (Sigma), was directly dissolved in DMEM.

* Corresponding author. Mailing address: Centro de Biología Molecular Severo Ochoa, Nicolás Cabrera 1, UAM, 28049 Madrid, Spain. Phone: 34 91 196 4493. Fax: 34 91 196 4420. E-mail: fsobrino@cbm.uam.es.

† Dedicated to the memory of Rosario Armas-Portela.

▽ Published ahead of print on 24 November 2010.

The effect of VPA in cultured cells was analyzed by trypan blue exclusion (51). Trichostatin A (TSA) (Cell Signaling Technology, Danvers, MA) was prepared in ethanol as a 4 mM stock solution.

Infections and virus titrations. Confluent monolayers (grown in six-well plates) of BHK-21 or Vero cells were extensively washed with DMEM and left untreated or were pretreated with VPA for 10 min. Cells were infected with the different viruses at the selected multiplicity of infection (MOI), defined as the number of PFU/cell. After the first infection hour (or 1.5 h for LCMV) in the presence or absence of VPA, the viral inoculum was removed, the cell monolayer was washed twice with DMEM, and fresh medium containing 5% FCS and VPA was added; this time point was considered 0 h postinfection (p.i.). Seven hours (for FMDV, EMCV, BEV, VSV, SFV, SINV, and VACV) or 24 h (for ERAV, LCMV, WNV, USUV, and ASFV) later infected plates were frozen. To test the effect of the p.i. addition of VPA, the drug was added and maintained from 2.5 h p.i. To analyze the effect of TSA, BHK-21 cells were left untreated or were pretreated with 400 nM TSA for 16 h, as described by the manufacturer. At this time, cells were infected with FMDV, VSV, SFV, SINV, LCMV, or VACV, as described previously, and TSA was maintained throughout the infection period (total TSA treatment of 24 h). For WNV, USUV, and ASFV, Vero cells were treated at the time of infection with 400 nM TSA, and infections were allow to proceed for 24 h. For virus titration, unless otherwise stated, infected plates were subjected to three freeze-thaw cycles, and the total (intracellular and medium-released) virus yield was determined by plaque assay in BHK-21 or Vero cells as described previously (15, 47, 50). Briefly, after the first hour of infection, viral inoculum was removed, and medium containing 0.5% agar, 1% FCS, and DEAE-dextran (0.045 mg/ml) was added. For LCMV, after 1.5 h of infection, the viral inoculum was removed, and medium containing 0.3% agar, 1% FCS, and DEAE-dextran (0.045 mg/ml) was added. For WNV and USUV, after inoculum removal, infections were allowed to proceed in semisolid medium containing 1% low-melting-point agarose and 2% FCS. Plates were incubated at 37°C for 24 h (FMDV, EMCV, and VSV), 48 h (BEV, ERAV, SFV, and SINV), 72 h (VACV, WNV, and USUV) or 1 week (LCMV and ASFV). At this time point, cells were fixed in 4% formaldehyde for 15 min at room temperature and stained with 3% crystal violet in 2% formaldehyde.

Detection of viral RNA and proteins and concentration of viral particles. VSV particles were sedimented from VSV-infected BHK-21 cell medium as described previously (21). For VSV, total (intracellular and extracellular) RNA and extracellular RNA were extracted using Tri-Reagent (Sigma). Samples were 10-fold serially diluted in water, and VSV cDNA was synthesized and amplified by reverse transcription-PCR (RT-PCR) (41). Glyceraldehyde-3-phosphate-dehydrogenase (G3PDH) RNA amplification was used as an internal control for cellular RNA content (16). PCR products were analyzed by agarose gel electrophoresis (2%) and ethidium bromide staining. For WNV, viral RNA was extracted using a NucleoSpin viral RNA isolation kit (Macherey-Nagel, Düren, Germany) and quantified by quantitative RT-PCR as genomic equivalents to the number of PFU/ml by comparison with RNA extracted from titrated samples (27). For VSV protein detection by dot blot, infection medium samples were loaded onto a nitrocellulose membrane, which was blocked, incubated with a guinea pig hyperimmune serum against VSV Indiana and then with horseradish-peroxidase (HRP)-labeled goat anti-guinea pig IgG, and subsequently developed using an ECL kit (Amersham). These antibodies were also used for Western blot detection (38).

TEM and immunofluorescence. Transmission electron microscopy (TEM) and immunofluorescence were performed as previously described (38). To determine the number of infected cells in immunofluorescence assays, three coverslips per time point were examined, and at least 500 cells were counted. The number of viral particles attached to the cell surface/nm was scored using the NeuronJ plug-in (39) of ImageJ software (http://rsbweb.nih.gov/ij/). For negative staining, VSV virions were concentrated from infection medium (21) and fixed with 1% glutaraldehyde. Samples were adsorbed for 3 min to copper grids coated with collodion-carbon and ionized. Grids were negatively stained with 2% uranyl acetate and air dried.

Data analysis. One-way analysis of variance was performed with the statistical package SPSS, version 17.0 (SPSS, Inc., Chicago, IL) for Windows. For multiple comparisons, Bonferroni's correction was applied. Data are presented as means ± standard deviations. Differences were considered statistically significant at a P value of <0.05.

RESULTS

Effect of VPA on viral infection. We first evaluated the viability of BHK-21 and Vero cells treated with the drug (Fig. 1A). The 50% toxic concentration (TC_{50}) was 244 and 280 mM after 8 h of treatment and 178 and 154 mM after 25 h of treatment for BHK-21 and Vero cells, respectively. Microtubules, actin microfilaments, the Golgi complex, and the endoplasmic reticulum architecture were not altered by VPA treatment (Fig. 1B). Next, the effect of treatment with VPA on the viral yield of four nonenveloped and eight enveloped viruses was analyzed (Fig. 2). No statistically significant reduction in the virus yield postinfection was found for any of the nonenveloped viruses. Conversely, complete inhibition, ranging from 6 to 10 orders of magnitude, was observed in the virus yield from infections with the enveloped viruses when VPA was added before infection and maintained throughout the assay, except for VACV, whose yield, albeit reduced by about 4 logs, was not completely inhibited. For the viruses tested on the two cell lines used in this study, the inhibitions observed were similar, regardless of whether VPA was added before infection or postinfection (p.i.), with the only exception being SINV infection of BHK-21 cells, in which p.i. addition of VPA resulted in a reduction of viral titer by 4 orders of magnitude

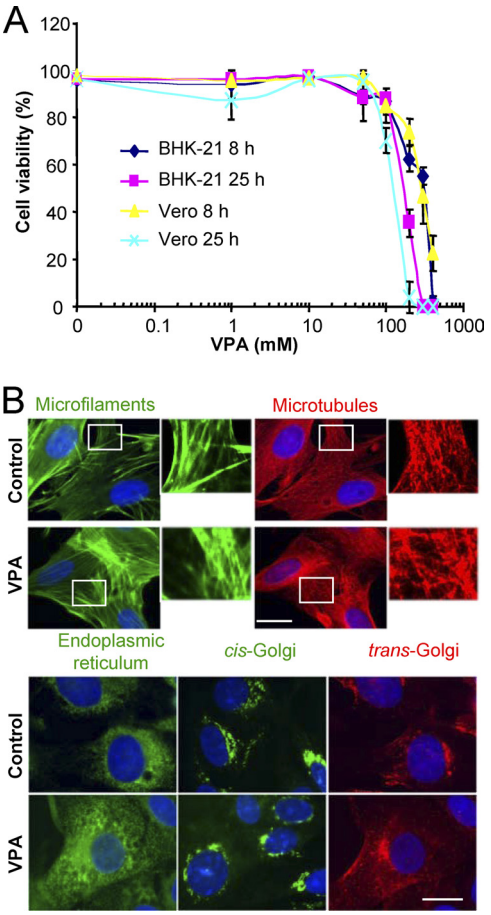

FIG. 1. Effect of VPA on cell viability. (A) BHK-21 and Vero cells were incubated for 8 or 25 h in the presence of increasing concentrations of VPA and then analyzed for cell viability by trypan blue assay. (B) BHK-21 cells, either untreated or treated for 8 h with 50 mM VPA, were fixed and processed for immunofluorescence using antibodies against marker proteins from different cell structures. DAPI (4′,6′-diamidino-2-phenylindole) was used to stain cell nuclei (blue). Scale bar, 20 μm.

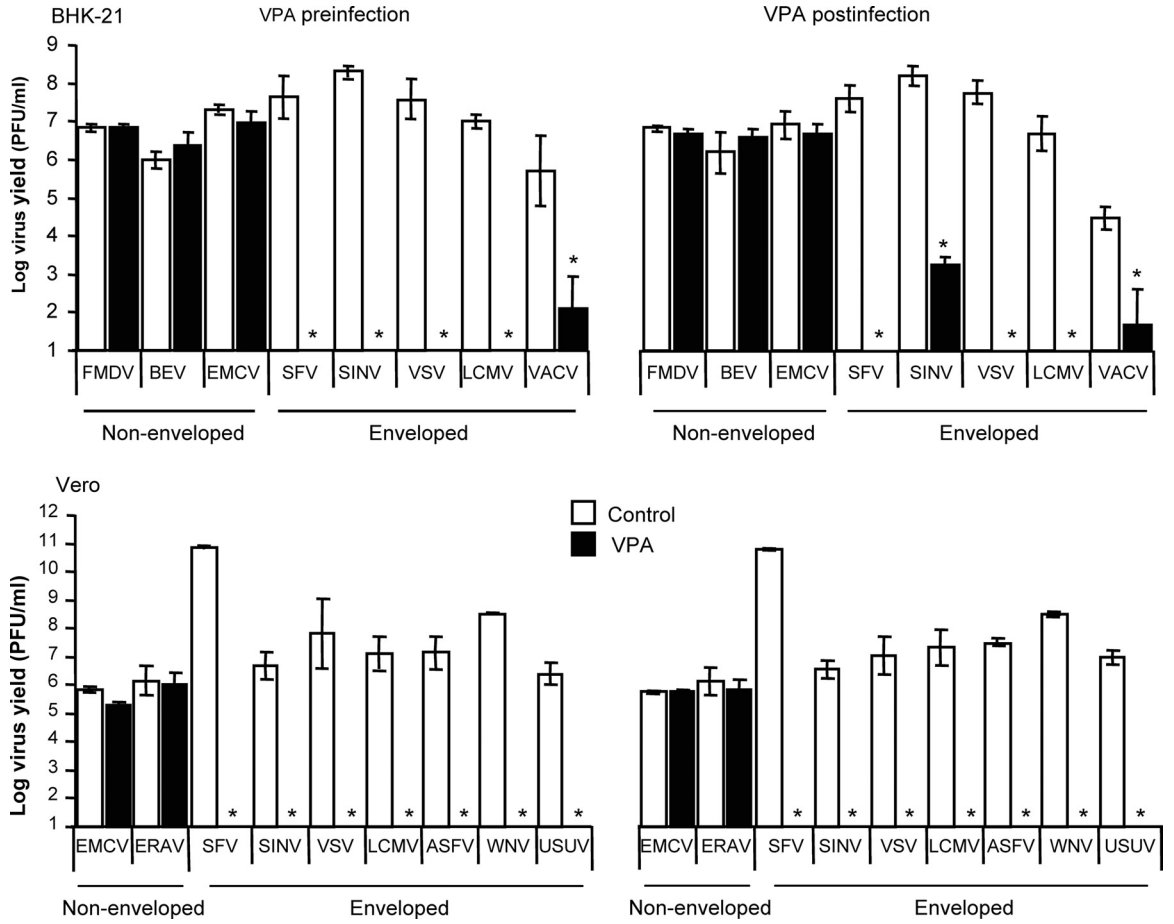

FIG. 2. Effect of VPA on virus yield. BHK-21 or Vero cell monolayers, either untreated or treated with 50 mM VPA, were infected with the indicated viruses (MOI of 0.5 PFU/cell), as described in Materials and Methods. Preinfection analysis corresponds to infections performed in the presence of drug before infection (pretreatment) and throughout the infection time. In the case of postinfection analyses, VPA was added at 2.5 h pi and maintained throughout the infection time. Statistically significant differences between control and VPA-treated cells are indicated by an asterisk ($P \leq 0.05$).

instead of the complete suppression (over 7 orders of magnitude) observed on Vero cells. Overall, these results indicate that VPA affects mainly postentry steps in the multiplication of the enveloped viruses analyzed in the present study.

Inhibition of histone deacetylases does not affect viral infection. Inhibition of histone deacetylases is one of the effects of VPA on cells (54, 57), which has been proposed to have an antiviral effect on latent infections (11, 29, 31, 61). To address the implication of this mechanism on the inhibition observed in this study, the effect of TSA—another HDAC inhibitor (8)—on the infection of FMDV, SFV, SINV, VSV, VACV, LCMV, ASFV, WNV, and USUV was tested. As expected, treatment with TSA resulted in an increase in the levels of the acetylated histone AcH3 (Fig. 3A). However, TSA did not significantly affect infection of the viruses tested (Fig. 3B), supporting the idea that this mechanism does not play a major role on the antiviral effect exerted by VPA.

VPA inhibits viral infection in a dose-dependent manner without drastically inactivating viral particles. From the analysis of the effect of VPA on viral growth, 50% inhibitory concentrations (IC_{50}s) of 0.6 and 0.25 mM were determined for VSV and WNV, respectively (Fig. 4A and C). To asses a possible direct effect of VPA on the infectivity of viral particles, as described for other antiviral drugs directed against enveloped viruses (58), equal numbers of PFU were treated with VPA, and the infectivity levels of the samples were determined by plaque assay after incubation at 37°C for up to 8 h (Fig. 4B and D). While no statistically significant differences were found in the VSV titers observed in control and VPA-treated samples (Fig. 4B), a reduction of 2 orders of magnitude was observed for WNV (Fig. 4D). These results indicate that VPA, although differentially affecting VSV and WNV viral particles, does not produce a major effect on the infectivity of the viral particles, and they suggest that VPA inhibition of viral yield is mainly mediated by intracellular alterations of infected cells.

Effect of VPA on viral replication. A concentration of 50 mM VPA that completely abolished viral production (Fig. 2) was used to perform a time course analysis of VSV and WNV virus production, protein expression, and RNA synthesis (Fig. 5). As expected, while infectious virus was recovered shortly after infection in control cells, no infectious virus was detected in VPA-treated cells infected with either VSV or WNV up to 8.5 and 24 h p.i., respectively (Fig. 5A and D). Upon WNV infection, fluorescence against WNV E protein and viral RNA, the

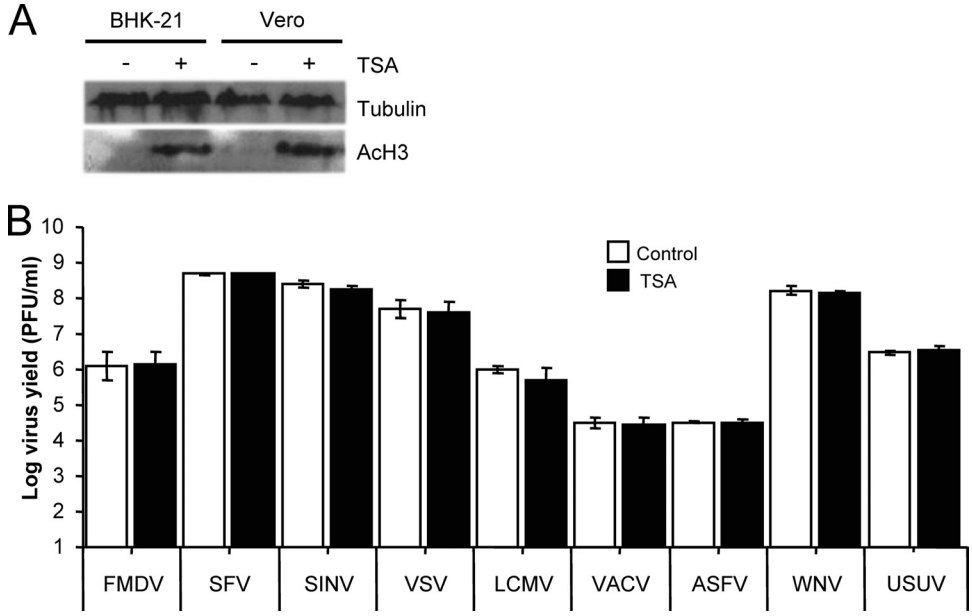

FIG. 3. Inhibition of histone deacetylases does not affect viral infection. (A) Western blot analysis of acetylated histone H3 (AcH3) in BHK-21 and Vero cells after TSA treatment. Results obtained with an anti-β-tubulin antibody are shown as a control for protein loading. (B) BHK-21 or Vero cell monolayers, either untreated or treated with 400 nM TSA, were infected with FMDV, SFV, SINV, VSV, LCMV, VACV, ASFV, WNV, or USUV (MOI of 0.5 PFU/cell). Virus yield was determined by plaque assay as described in Materials and Methods.

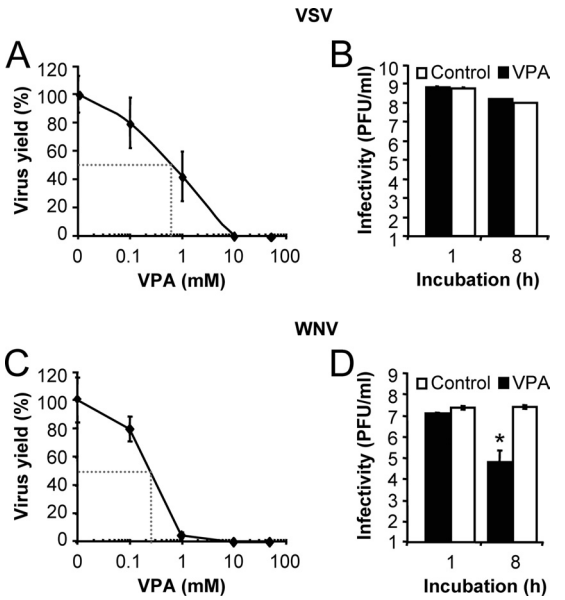

FIG. 4. VPA inhibits VSV and WNV infection in a dose-dependent manner, but VPA treatment does not inactivates VSV particles even though it reduces the infectivity of WNV particles. (A) BHK-21 cells were infected with VSV (MOI of 0.5 PFU/cell) in the presence of different concentrations of VPA, and the total virus yield was determined by plaque assay. Dotted lines correspond to IC_{50}s. (B) VSV particles were incubated with 50 mM VPA at 37°C for 1 h or 8 h, and virus titer was determined by plaque assay. (C) Vero cells were infected with WNV as described in panel A. Dotted lines correspond to IC_{50}s. (D) WNV particles were incubated with VPA as described in panel B, and infectivity was determined by plaque assay. Statistically significant differences between control and VPA-treated cells are indicated by an asterisk ($P \leq 0.05$).

latter being amplified in control cells from 16 h p.i, was not detected in VPA-treated cells at any time point (Fig. 5B and C). In contrast, a reduced percentage of cells positive for fluorescence against the VSV G glycoprotein (VSV-G) was found in VSV-infected cells treated with VPA, and only control cells, not VPA-treated cells, showed a marked increase in the percentage of fluorescent cells from 4.5 h p.i., a time at which untreated cells were actively producing new viruses (Fig. 5D and E). These results suggest that VSV progeny from control cells but not from VPA-treated cells was released to the infection medium and infected neighbor cells. Likewise, in total RNA (intracellular and extracellular) from control VSV-infected cells, viral RNA was already detected at 4.5 h p.i while in VPA-treated VSV-infected cells, viral RNA detection was delayed until 6.5 h. p.i., and the levels were lower than those observed in nontreated control cells (Fig. 5F). On the other hand, no differences were found in the intracellular distribution pattern of VSV-G protein between control cells and those treated with VPA that were positive for VSV-G staining (Fig. 5G). VSV-G protein was observed perinuclearly at 2.5 h p.i., indicating its accumulation in the Golgi complex; at later infection stages (6.5 h p.i.) this protein was observed at the cell periphery, where newly synthesized virions acquire their envelope. When the VSV proteins were detected in infected cells by Western blotting using a polyclonal VSV serum, a reduction of about 10-fold was noticed in the amount of protein N found in VPA-treated cells relative to that of control infected cells (Fig. 5H). Whether the differences observed in VSV RNA and protein detection are due to a reduction in their synthesis in VPA-treated cells and/or to the increasing number of infected control cells remains to be determined. Thus, even though no infective viruses are released from either WNV- or VSV-infected cells, VPA intracellular effects on the infectivity of both

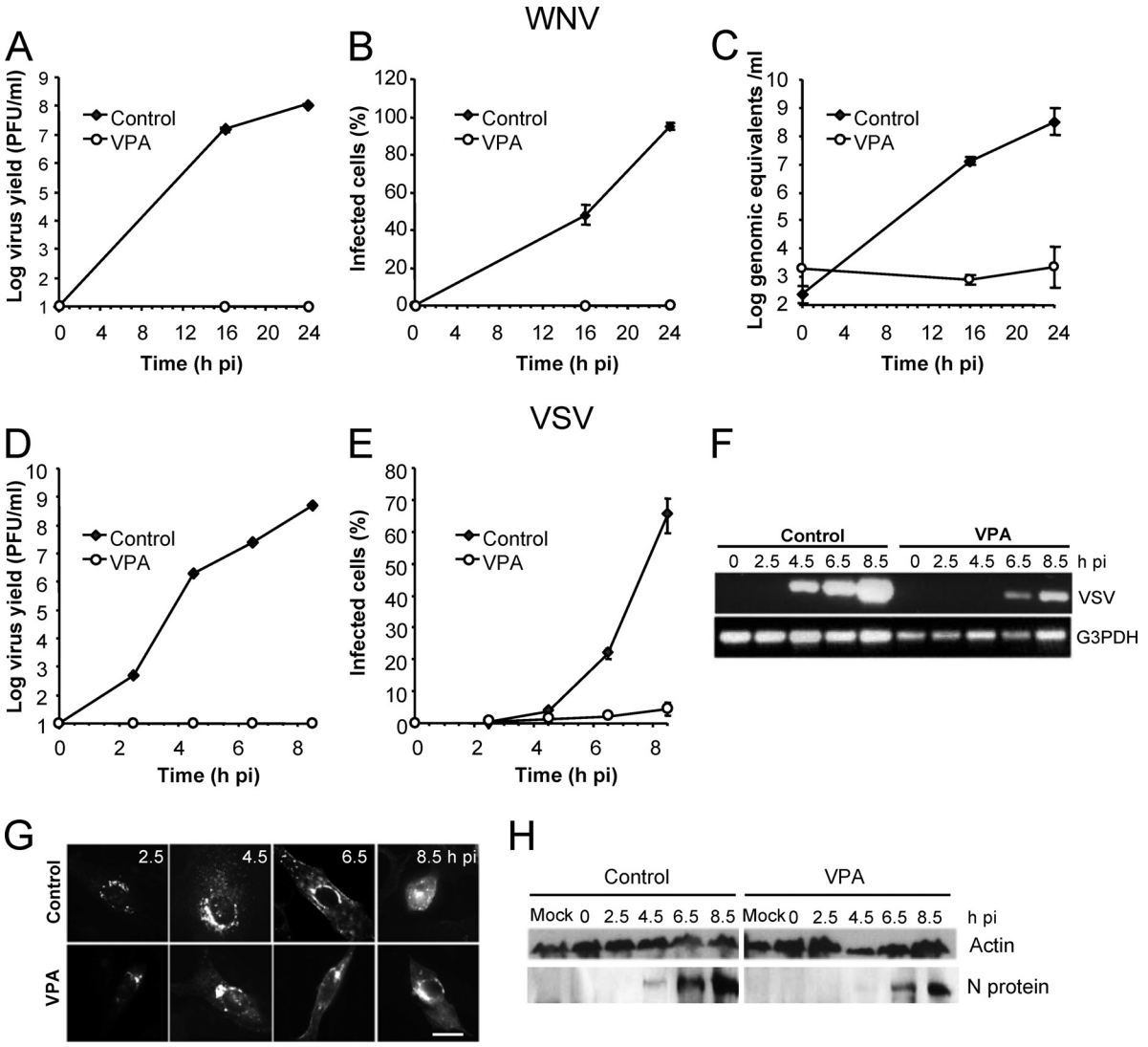

FIG. 5. Effect of VPA on VSV and WNV infection. (A) Vero cells, either untreated or treated with 50 mM VPA, were infected with WNV (MOI of 0.5 PFU/cell), and the virus titer in the extracellular medium was determined by plaque assay. (B) Cells infected as described in panel A were fixed at different times p.i. and processed for immunofluorescence using a MAb against WNV-E glycoprotein. For each time point, the percentage of fluorescent cells (infected cells) is shown. (C) Total viral RNA (intracellular and extracellular) from samples infected with WNV as described in panel A was extracted at different times p.i. and amplified by quantitative RT-PCR as described in Materials and Methods. (D) BHK-21 cells were infected with VSV, and the virus titer in the extracellular medium was determined as in panel A. (E) Cells infected with VSV and processed as described in panel B using MAb I1 against VSV-G protein. (F) Detection of VSV RNA by RT-PCR. BHK-21 cell monolayers were infected with VSV as in panel A. Total viral RNA was amplified by RT-PCR. G3PDH amplification was used as an internal control for cellular RNA content. (G) Representative micrographs of VSV-G-positive cells infected and immunostained as described in panel E. Scale bar, 20 μm. (H) Detection of VSV proteins by Western blotting. BHK-21 cell monolayers were infected with VSV as in panel A. For each time point, cells were lysed and processed for Western blotting using a guinea pig hyperimmune serum against VSV Indiana. The migration of the band shown corresponded to that expected for VSV N protein. Results obtained with an anti-β-actin antibody are shown as a control for protein loading.

viruses seem to differ. Taken together, these results indicate that while in some viruses, such as WNV, VPA can produce a drastic blockage of replication and translation of viral RNA, in other viruses (VSV) this reduction is less severe.

Effect of VPA on VSV morphogenesis. Since in VPA-treated cells infected by VSV, G protein was observed at the cell periphery, where newly synthesized virions acquire their envelope, we further analyzed whether VPA treatment interfered with viral particle formation and egress. To this purpose, BHK-21 cells, treated or not with this drug, were infected with VSV, fixed, and processed for TEM. In both cases, similar images corresponding to newly assembled VSV particles (60) could be observed (Fig. 6A). When the number of viral particles/μm of membrane was quantified, no significant differences between control and VPA-treated cells were found (Table 1). Similarly, no significant differences in the lengths and diameters of the budding VSV particles were found between VPA-treated and untreated infected cells, indicating that VPA does

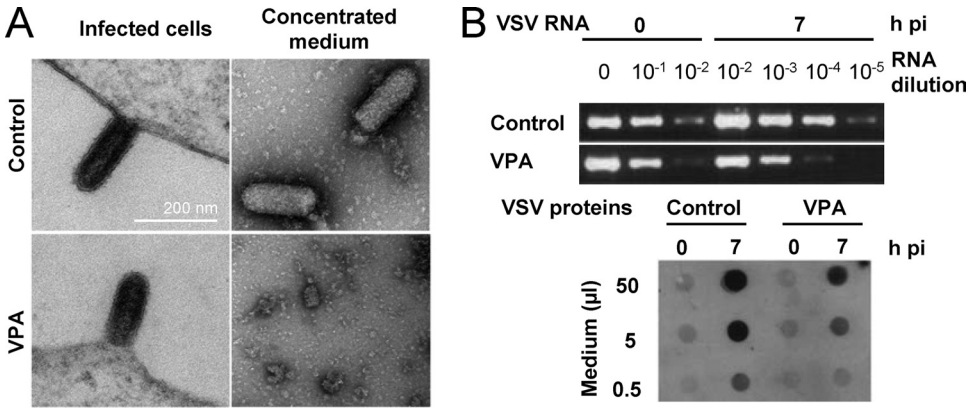

FIG. 6. Effect of VPA on VSV particle morphogenesis. (A) BHK-21 cells, either untreated or treated with 50 mM VPA, were infected with VSV (MOI of 70 PFU/cell). Cells were fixed and processed for TEM at 7 h p.i. (left panels). VSV particles released to infection medium were concentrated and processed for TEM (right panels). Scale bar, 200 nm. (B) VSV RNA amplification by RT-PCR and dot blot detection of VSV proteins in extracellular medium of infected cells described in panel A.

not cause a major blockage of intracellular VSV particle formation. To analyze whether the *de novo* synthesized viral particles were actually released from VPA-treated cells, medium from infected cultures, treated or not with VPA, was sedimented under conditions used for VSV purification. In control infections, bullet-shaped particles corresponding to VSV virions were observed by TEM in resuspended pellets (an average of 31 ± 9.2 particles/field in 20 random fields). None particles of this type were found in the 20 random fields from VPA-treated infected cells (Fig. 6A), suggesting that VPA treatment could either block virion budding or alter VSV composition, producing virions with a highly reduced stability in the infection medium and/or during the sedimentation process. As shown in Fig. 6B, the latter possibility seems to be favored since VSV RNA and proteins were detected in the extracellular medium of infection at levels only about 10-fold lower than those found in control infected cells.

DISCUSSION

In this study we describe the antiviral effect of VPA on different enveloped viruses causing human and veterinary diseases, including important zoonoses such as those caused by WNV and LCMV. Thus, cell culture infection of enveloped viruses whose genomes consist of RNA of positive polarity (WNV, USUV, SFV, and SINV), negative polarity (VSV), and segmented and negative polarity (LCMV), as well as of DNA (ASFV), was completely inhibited by VPA and that of the DNA virus VACV was severely reduced. In general, the inhibitions observed in BHK-21 and Vero cells were similar, suggesting that the alterations produced by VPA that mediate its antiviral activity affect common steps of mammalian cell metabolism. However, the differential inhibition of SINV multiplication in BHK-21 and Vero cells when VPA was added after virus entry indicates that the inhibition by VPA may also be modulated by the cell type infected. In contrast, no significant inhibitory effect was observed for nonenveloped viruses such as FMDV, EMCV, BEV, and ERAV.

As noted in the introduction, different effects have been described for VPA, which complicates the analysis and interpretation of the inhibitions observed. One such effect is the inhibition of histone deacetylases, which has been proposed to favor depletion of cells latently infected with human immunodeficiency virus (29), human T-cell leukemia virus type-1 (31), and Epstein-Barr virus (11, 61). The lack of effect of the drug TSA, which inhibits deacetylation of histones, on the infections of the viruses studied indicates that this mechanism does not play a major role in the observed antiviral effect of VPA. On the other hand, a number of studies have shown that VPA affects the lipid composition of cellular membranes (48, 52, 53, 59). Viruses acquire their lipid envelope from membranes of host cells. For instance, flaviviruses, such as WNV and USUV, acquire their envelope from intracellular membranes such as those from the endoplasmic reticulum (56), while in other viruses, such as VSV and SFV, the lipid composition of the

TABLE 1. Effect of VPA treatment on the frequency and size of VSV budding particles in infected cells

Parameter	Value for the group		*P*
	Control cells	VPA-treated cells	
Frequency of VSV budding[a]	$3.67 \times 10^{-3} \pm 0.0136$	$4.65 \times 10^{-3} \pm 0.0178$	0.826
Avg particle size (nm)[b]			
Length	160.61 ± 35.57	144.61 ± 38.00	0.088
Diam	63.01 ± 10.50	63.29 ± 8.46	0.394

[a] Average number of budding viral particles/μm of cell surface (number of cell surfaces scored, 29).
[b] Average size of budding VSV particles was determined by measuring 57 particles from control cells and 24 particles from VPA-treated cells.

virus particles strongly resembles that of the plasma membrane of the cells used for virus growth (24). Therefore, the inhibitory effect of VPA on enveloped virus multiplication described here could be due to alterations in cellular membrane composition that would result in impairment of infectious particle production. Indeed, targeting plasma membrane anionic phospholipids has been revealed as a promising new antiviral strategy (49). Our results indicate that VPA completely blocks WNV RNA and protein synthesis; whether this effect is associated with alterations of endomembranes that could impair viral RNA translation and/or replication or other cell effects of VPA remains to be determined. Conversely, VPA did not cause a major blockage of VSV RNA and protein synthesis as cells positive for VSV-G protein were detected in immunofluorescence studies (Fig. 5E and G), and only a limited (about 10-fold) reduction was observed in the amount of viral RNA and proteins in infected cells. In these experiments, the increase in the percentage of VSV-positive cells noticed in control monolayers was not observed in cells treated with VPA (Fig. 5E), indicating that in the latter no infectious particles are released from initially infected cells. Since VSV and other enveloped viral particles acquire their envelope from the plasma membrane (34), VPA treatment could impair this process due to alterations in the plasma membrane lipid composition (48, 53, 59). However, comparable frequencies of budding particles similar in size and length to those observed in control cells were found in VPA-treated cells, suggesting that VPA does not severely impair VSV particle assembly. Nevertheless, when we attempted to concentrate VSV virions from infected cells, virion-like particles were not detected in purified supernatants from VPA-treated cells. The detection of VSV RNA and viral proteins in the extracellular medium of infection, at levels only 10-fold lower than those found in control infected cells, suggests that, rather than blocking virion budding, VPA treatment alters VSV composition so as to leave extracellular particles with a highly reduced stability. Overall, our results indicate that at least two different mechanisms are involved in the inhibition exerted by VPA on VSV and WNV cell culture infection, and they point out that further experiments are required to characterize these mechanisms and to extend these studies to other viruses inhibited by this drug.

The present results raise the possibility of the therapeutic antiviral potential of VPA, a widely used drug for nervous disorders, including chronic treatments. Although the use of a known drug that affects the nervous system as an antiviral would require determining possible side effects, it could also favor inhibition of neurotropic viruses such as WNV. Indeed, in animal models VPA concentration in plasma positively correlates with that found in the brain (42, 45). VPA doses usually administered to humans are dependent on the body mass, with a therapeutic range for epilepsy treatment of 50 to 100 mg/liter (about 0.3 to 0.6 mM) in plasma (12, 25). These plasma concentrations are very close to the IC_{50}s determined in our work for VSV and WNV (0.6 and 0.25, respectively), supporting a potential antiviral effect *in vivo*. For hypothetical therapeutic applications, VPA pharmacokinetics should also be considered. This drug is metabolized by linear kinetics and its half-life (in adults receiving monotherapy) ranges between 12 ± 6 and 15 ± 2.5 h, although due to the relatively rapid decrease in serum concentrations of VPA, periodic doses should be administered (25). Experiments in animal models are now being designed to assess whether VPA can interfere viral infection *in vivo*.

In summary, VPA is a potent inhibitor of virus multiplication in cultured cells of the enveloped viruses analyzed here, including viruses of the *Flaviviridae* and *Arenaviridae* families, which comprise a number of important human pathogens responsible for diseases such as yellow fever, dengue fever, hepatitis C, and hemorrhagic fevers. Even if further studies with a wider range of virus families are required to address the antiviral spectrum of VPA, our results indicate that VPA may help shed light on the crucial steps of envelope virus maturation and that it might be a potential candidate for development as an antiviral drug either alone or as coadjuvant in combined therapies.

ACKNOWLEDGMENTS

We thank E. Domingo, J. Ortín, E. Tabarés, M. A. Martínez, F. Gavilanes, A. Rodríguez, M. Sáiz, I. Ventoso, L. Carrasco, C. A Hartley, A. L. Carrascosa, I. V. Sandoval, E. Blanco, and M. T. Rejas for providing us with viruses, reagents, and scientific advice.

This work was supported by grants BIO2008-0447-C03-01, CSD2006-0007, SAF2008-04232, FIS-PI071310, FAU2008-0006, and NADIR-UE-228394 and by an institutional grant from the Fundación Ramón Areces.

REFERENCES

1. **Albertini, A. A., G. Schoehn, W. Weissenhorn, and R. W. Ruigrok.** 2008. Structural aspects of rabies virus replication. Cell Mol. Life Sci. **65:**282–294.
2. **Armas-Portela, R., M. A. Parrales, J. P. Albar, A. C. Martinez, and J. Avila.** 1999. Distribution and characteristics of betaII tubulin-enriched microtubules in interphase cells. Exp. Cell Res. **248:**372–380.
3. **Asenjo, A., J. C. Gonzalez-Armas, and N. Villanueva.** 2008. Phosphorylation of human respiratory syncytial virus P protein at serine 54 regulates viral uncoating. Virology **380:**26–33.
4. **Blasco, R., and B. Moss.** 1992. Role of cell-associated enveloped vaccinia virus in cell-to-cell spread. J. Virol. **66:**4170–4179.
5. **Brinton, M. A.** 2002. The molecular biology of West Nile Virus: a new invader of the western hemisphere. Annu. Rev. Microbiol. **56:**371–402.
6. **Bruni, J., and B. J. Wilder.** 1979. Valproic acid. Review of a new antiepileptic drug. Arch. Neurol. **36:**393–398.
7. **Buckley, A., et al.** 2003. Serological evidence of West Nile virus, Usutu virus and Sindbis virus infection of birds in the UK. J. Gen. Virol. **84:**2807–2817.
8. **Codd, R., N. Braich, J. Liu, C. Z. Soe, and A. A. Pakchung.** 2009. Zn(II)-dependent histone deacetylase inhibitors: suberoylanilide hydroxamic acid and trichostatin A. Int. J. Biochem. Cell Biol. **41:**736–739.
9. **Colman, P. M.** 2009. New antivirals and drug resistance. Annu. Rev. Biochem. **78:**95–118.
10. **Cordoba, L., E. Escribano-Romero, A. Garmendia, and J. C. Saiz.** 2007. Pregnancy increases the risk of mortality in West Nile virus-infected mice. J. Gen. Virol. **88:**476–480.
11. **Countryman, J. K., L. Gradoville, and G. Miller.** 2008. Histone hyperacetylation occurs on promoters of lytic cycle regulatory genes in Epstein-Barr virus-infected cell lines which are refractory to disruption of latency by histone deacetylase inhibitors. J. Virol. **82:**4706–4719.
12. **Cramer, J. A., R. H. Mattson, D. M. Bennett, and C. T. Swick.** 1986. Variable free and total valproic acid concentrations in sole- and multi-drug therapy. Ther. Drug Monit. **8:**411–415.
13. **de Silva, A. M., W. E. Balch, and A. Helenius.** 1990. Quality control in the endoplasmic reticulum: folding and misfolding of vesicular stomatitis virus G protein in cells and in vitro. J. Cell Biol. **111:**857–866.
14. **Domingo, E., and J. Gomez.** 2007. Quasispecies and its impact on viral hepatitis. Virus Res. **127:**131–150.
15. **Enjuanes, L., A. L. Carrascosa, M. A. Moreno, and E. Vinuela.** 1976. Titration of African swine fever (ASF) virus. J. Gen. Virol. **32:**471–477.
16. **Garcia-Briones, M. M., et al.** 2004. Immunogenicity and T cell recognition in swine of foot-and-mouth disease virus polymerase 3D. Virology **322:**264–275.
17. **Gastaminza, P., C. Whitten-Bauer, and F. V. Chisari.** 2010. Unbiased probing of the entire hepatitis C virus life cycle identifies clinical compounds that target multiple aspects of the infection. Proc. Natl. Acad. Sci. U. S. A. **107:**291–296.
18. **Gilbert, C., M. Bergeron, S. Methot, J. F. Giguere, and M. J. Tremblay.** 2005. Statins could be used to control replication of some viruses, including HIV-1. Viral Immunol. **18:**474–489.

19. **Gillespie, L. K., A. Hoenen, G. Morgan, and J. M. Mackenzie.** 2010. The endoplasmic reticulum provides the membrane platform for biogenesis of the flavivirus replication complex. J. Virol. **84:**10438–10447.
20. **Gower, T. L., and B. S. Graham.** 2001. Antiviral activity of lovastatin against respiratory syncytial virus in vivo and in vitro. Antimicrob. Agents Chemother. **45:**1231–1237.
21. **Hackett, A. J., F. L. Schaffer, and S. H. Madin.** 1967. The separation of infectious and autointerfering particles in vesicular stomatitis virus preparations. Virology **31:**114–119.
22. **Hsu, N. Y., et al.** 2010. Viral reorganization of the secretory pathway generates distinct organelles for RNA replication. Cell **141:**799–811.
23. **Jimenez-Clavero, M. A., et al.** 2005. Survey of bovine enterovirus in biological and environmental samples by a highly sensitive real-time reverse transcription-PCR. Appl. Environ. Microbiol. **71:**3536–3543.
24. **Kalvodova, L., et al.** 2009. The lipidomes of vesicular stomatitis virus, Semliki forest virus, and the host plasma membrane analyzed by quantitative shotgun mass spectrometry. J. Virol. **83:**7996–8003.
25. **Kanner, A. M.** 2003. The pharmacology of parenteral valproate. Epilepsy Curr. **3:**109–111.
26. **Khattab, M. A.** 2009. Targeting host factors: a novel rationale for the management of hepatitis C virus. World J. Gastroenterol. **15:**3472–3479.
27. **Lanciotti, R. S., et al.** 2000. Rapid detection of West Nile virus from human clinical specimens, field-collected mosquitoes, and avian samples by a TaqMan reverse transcriptase-PCR assay. J. Clin. Microbiol. **38:**4066–4071.
28. **Le Blanc, I., et al.** 2005. Endosome-to-cytosol transport of viral nucleocapsids. Nat. Cell Biol. **7:**653–664.
29. **Lehrman, G., et al.** 2005. Depletion of latent HIV-1 infection in vivo: a proof-of-concept study. Lancet **366:**549–555.
30. **Letchworth, G. J., L. L. Rodriguez, and J. Del Cbarrera.** 1999. Vesicular stomatitis. Vet. J. **157:**239–260.
31. **Lezin, A., et al.** 2007. Histone deacetylase mediated transcriptional activation reduces proviral loads in HTLV-1 associated myelopathy/tropical spastic paraparesis patients. Blood **110:**3722–3728.
32. **Li, F., G. F. Browning, M. J. Studdert, and B. S. Crabb.** 1996. Equine rhinovirus 1 is more closely related to foot-and-mouth disease virus than to other picornaviruses. Proc. Natl. Acad. Sci. U. S. A. **93:**990–995.
33. **Lichty, B. D., A. T. Power, D. F. Stojdl, and J. C. Bell.** 2004. Vesicular stomatitis virus: re-inventing the bullet. Trends Mol. Med. **10:**210–216.
34. **Luan, P., L. Yang, and M. Glaser.** 1995. Formation of membrane domains created during the budding of vesicular stomatitis virus. A model for selective lipid and protein sorting in biological membranes. Biochemistry **34:** 9874–9883.
35. **Ludwig, S.** 2009. Targeting cell signalling pathways to fight the flu: towards a paradigm change in anti-influenza therapy. J. Antimicrob. Chemother. **64:**1–4.
36. **Mackenzie, J. M., and E. G. Westaway.** 2001. Assembly and maturation of the flavivirus Kunjin virus appear to occur in the rough endoplasmic reticulum and along the secretory pathway, respectively. J. Virol. **75:**10787–10799.
37. **Martin, V., A. Grande-Perez, and E. Domingo.** 2008. No evidence of selection for mutational robustness during lethal mutagenesis of lymphocytic choriomeningitis virus. Virology **378:**185–192.
38. **Martin-Acebes, M. A., et al.** 2008. Subcellular distribution of swine vesicular disease virus proteins and alterations induced in infected cells: a comparative study with foot-and-mouth disease virus and vesicular stomatitis virus. Virology **374:**432–443.
39. **Meijering, E., et al.** 2004. Design and validation of a tool for neurite tracing and analysis in fluorescence microscopy images. Cytometry A **58:**167–176.
40. **Novella, I. S., et al.** 1996. Large-population passages of vesicular stomatitis virus in interferon-treated cells select variants of only limited resistance. J. Virol. **70:**6414–6417.
41. **Nunez, J. I., et al.** 1998. A RT-PCR assay for the differential diagnosis of vesicular viral diseases of swine. J. Virol. Methods **72:**227–235.
42. **Ohdo, S., S. Nakano, and N. Ogawa.** 1988. Chronopharmacological study of sodium valproate in mice: dose-concentration-response relationship. Jpn. J. Pharmacol. **47:**11–19.
43. **Ono, A., S. D. Ablan, S. J. Lockett, K. Nagashima, and E. O. Freed.** 2004. Phosphatidylinositol (4,5) bisphosphate regulates HIV-1 Gag targeting to the plasma membrane. Proc. Natl. Acad. Sci. U. S. A. **101:**14889–14894.
44. **Pereira, A. A., and I. M. Jacobson.** 2009. New and experimental therapies for HCV. Nat. Rev. Gastroenterol. Hepatol. **6:**403–411.
45. **Pollack, G. M., and D. D. Shen.** 1985. A timed intravenous pentylenetetrazol infusion seizure model for quantitating the anticonvulsant effect of valproic acid in the rat. J. Pharmacol. Methods **13:**135–146.
46. **Rodriguez, L. L.** 2002. Emergence and re-emergence of vesicular stomatitis in the United States. Virus Res. **85:**211–219.
47. **Rosas, M. F., et al.** 2008. Susceptibility to viral infection is enhanced by stable expression of 3A or 3AB proteins from foot-and-mouth disease virus. Virology **380:**34–45.
48. **Shaltiel, G., et al.** 2004. Valproate decreases inositol biosynthesis. Biol. Psychiatry **56:**868–874.
49. **Soares, M. M., S. W. King, and P. E. Thorpe.** 2008. Targeting inside-out phosphatidylserine as a therapeutic strategy for viral diseases. Nat. Med. **14:**1357–1362.
50. **Sobrino, F., M. Davila, J. Ortin, and E. Domingo.** 1983. Multiple genetic variants arise in the course of replication of foot-and-mouth disease virus in cell culture. Virology **128:**310–318.
51. **Strober, W.** 2001. Trypan blue exclusion test of cell viability. Curr. Protoc. Immunol. **Appendix 3:**Appendix 3B.
52. **Terbach, N., and R. S. Williams.** 2009. Structure-function studies for the panacea, valproic acid. Biochem. Soc. Trans. **37:**1126–1132.
53. **Tokuoka, S. M., A. Saiardi, and S. J. Nurrish.** 2008. The mood stabilizer valproate inhibits both inositol- and diacylglycerol-signaling pathways in *Caenorhabditis elegans*. Mol. Biol. Cell **19:**2241–2250.
54. **Venkataramani, V., et al.** 2010. Histone deacetylase inhibitor valproic acid inhibits cancer cell proliferation via down-regulation of the Alzheimer amyloid precursor protein. J. Biol. Chem. **285:**10678–10689.
55. **Ventoso, I., et al.** 2006. Translational resistance of late alphavirus mRNA to eIF2α phosphorylation: a strategy to overcome the antiviral effect of protein kinase PKR. Genes Dev. **20:**87–100.
56. **Welsch, S., et al.** 2009. Composition and three-dimensional architecture of the dengue virus replication and assembly sites. Cell Host Microbe **5:**365–375.
57. **Wittenburg, L. A., L. Bisson, B. J. Rose, C. Korch, and D. H. Thamm.** 2010. The histone deacetylase inhibitor valproic acid sensitizes human and canine osteosarcoma to doxorubicin. Cancer Chemother. Pharmacol. doi:10.1007/s00280-010-1287-z.
58. **Wolf, M. C., et al.** 2010. A broad-spectrum antiviral targeting entry of enveloped viruses. Proc. Natl. Acad. Sci. U. S. A. **107:**3157–3162.
59. **Xu, X., et al.** 2007. Attenuation of phospholipid signaling provides a novel mechanism for the action of valproic acid. Eukaryot. Cell **6:**899–906.
60. **Zajac, B. A., and K. Hummeler.** 1970. Morphogenesis of the nucleoprotein of vesicular stomatitis virus. J. Virol. **6:**243–252.
61. **Zhou, J., A. R. Snyder, and P. M. Lieberman.** 2009. Epstein-Barr virus episome stability is coupled to a delay in replication timing. J. Virol. **83:** 2154–2162.

JOURNAL OF VIROLOGY, Mar. 2011, p. 2733–2740 Vol. 85, No. 6
0022-538X/11/$12.00 doi:10.1128/JVI.02245-10

A Single Amino Acid Substitution in the Capsid of Foot-and-Mouth Disease Virus Can Increase Acid Resistance▽†

Miguel A. Martín-Acebes,[1]‡ Ángela Vázquez-Calvo,[1] Verónica Rincón,[1] Mauricio G. Mateu,[1] and Francisco Sobrino[1,2]*

Centro de Biología Molecular Severo Ochoa (CSIC-UAM), Cantoblanco 28049, Madrid, Spain,[1] and Centro de Investigación en Sanidad Animal, INIA, Valdeolmos, 28130 Madrid, Spain[2]

Received 26 October 2010/Accepted 14 December 2010

Foot-and-mouth disease virus (FMDV) particles lose infectivity due to their disassembly at pH values slightly below neutrality. This acid-dependent disassembly process is required for viral RNA release inside endosomes. To study the molecular determinants of viral resistance to acid-induced disassembly, six FMDV variants with increased resistance to acid inactivation were isolated. Infection by these mutants was more sensitive to drugs that raise the endosomal pH (NH_4Cl and concanamycin A) than was infection by the parental C-S8c1 virus, confirming that the increase in acid resistance is related to a lower pH requirement for productive uncoating. Amino acid replacement N17D at the N terminus of VP1 capsid protein was found in all six mutants. This single substitution was shown to be responsible for increased acid resistance when introduced into an infectious FMDV clone. The increased resistance of this mutant against acid-induced inactivation was shown to be due to its increased resistance against capsid dissociation into pentameric subunits. Interestingly, the N17D mutation was located close to but not at the interpentamer interfaces. The mutants described here extend the panel of FMDV variants exhibiting different pH sensitivities and illustrate the adaptive flexibility of viral quasispecies to pH variations.

Foot-and-mouth disease virus (FMDV) is the causative agent of a highly contagious disease of cloven-hoofed animals (23) that poses important restrictions for international trading (11, 45, 49, 51). FMDV is the type species of the *Aphthovirus* genus within the family *Picornaviridae* (20). Its genome is composed of a single RNA molecule of positive polarity and about 8.5 kb in length. Like other RNA viruses, FMDV populations consist of complex and dynamic distributions of variants termed quasispecies (17) and exhibit a high potential for variation and adaptation, reflected in seven serotypes and multiple antigenic variants (18, 50).

FMDV RNA is protected by a capsid that comprises 60 copies of each of the four structural proteins (VP1 to VP4) arranged in an icosahedral lattice of 12 pentameric subunits, which constitute intermediates of capsid assembly and disassembly (56). After attachment to the host cell using a variety of receptors, such as different $\alpha_v\beta$ integrins, heparan sulfate glycosaminoglycans (for some tissue culture-adapted variants), or other not-well-characterized molecules (2, 3, 5, 25–28, 46), FMDV particles are internalized by endocytosis mediated by clathrin (for viruses using integrin receptor) or caveolae (in the case of variants using heparan sulfate). In both cases, FMDV particles are delivered to early endosomes for capsid disassembly and viral genome release (7, 29, 33, 43, 44).

FMDV particles display extreme acid lability, being inactivated at pH values slightly below neutrality (12, 35, 41, 55). The pH sensitivity of FMDV is required for capsid disassembly triggered by acidification inside endosomes, allowing release of the RNA genome within infected cells (4, 9, 10). An acid-labile capsid is not a general feature of picornaviruses; in fact, it is only shared by other aphthoviruses, cardiovirus, and rhinovirus (41). Histidine residues located close to the interpentameric interface act as pH sensors, triggering FMDV capsid dissociation after their protonation at the acidic pH inside the endosome and the establishment of electrostatic repulsions between capsid subunits (1, 12, 19, 55). Capsid disassembly of FMDV into pentameric intermediates is accomplished with the release of the internal VP4 protein. Since VP4 is a highly hydrophobic and myristoylated protein, its exposure could facilitate endosomal membrane permeabilization and viral RNA release from the endosome (6, 14, 15, 30).

Although the role of endosomal acidification was related to FMDV uncoating more than 20 years ago (4, 9, 10), the molecular determinants that mediate FMDV uncoating at acidic pH have not been fully elucidated. The isolation and characterization of mutants displaying alterations in the uncoating mechanism should provide a useful tool for the study of this process. Along this line, FMDV variants with increased acid lability have been previously characterized (35); an FMDV variant with increased resistance to acid inactivation was also isolated (54), although the molecular basis for this phenotype was not elucidated. In the present study, we have addressed the study of the molecular determinants associated with viral resistance to acid inactivation as an approach to provide a deeper insight into the structural bases for FMDV uncoating. To this end, six FMDV variants with increased resistance to acid inactivation were isolated. Infection by these mutants displayed increased sensitivity to drugs that raise endosomal pH, con-

* Corresponding author. Mailing address: CBMSO, UAM, Cantoblanco 28049, Madrid, Spain. Phone: 34-91-1964493. Fax: 34-91-1964420. E-mail: fsobrino@cbm.uam.es.

† Dedicated to the memory of Rosario Armas-Portela.

‡ Present address: Departamento de Biotecnología. Instituto Nacional de Investigación y Tecnología Agraria y Alimentaria, 28040 Madrid, Spain.

▽ Published ahead of print on 22 December 2010.

TABLE 1. Mutations found in the capsid coding regions of FMDV mutants with increased resistance to acid induced inactivation selected after two serial acid treatments

Genomic region	Mutation(s) found in viral population[a]						
	m1	m2	m3	m4	m5	m6	C-S8c1
VP4							
VP2	T1996C **F34L**						
VP3	A2576T* **D9V**	A2576T* **D9V**	A2576T* **D9V**	A2576T* **D9V**	A2576T* **D9V** G3000A		
	T3117C	T3117C	T3117C	T3117C	T3117C	T3117C	T3117C
VP1	A3256G **N17D**	A3256G **N17D** C3750T	A3256G **N17D**	A3256G **N17D**	A3256G **N17D** C3390*	A3256G **N17D**	

[a] The nucleotide position in the C-S8c1 genome (52) and the substitution found are indicated. For nonsynonymous substitutions, amino acid replacements are indicated in boldface. *, nucleotide mixture at this position between mutant and base in C-S8c1. See the text for details.

firming that the increase in acid resistance was related to a lower pH requirement for productive uncoating within host cells. A single amino acid substitution located at the N terminus of VP1 protein, common in all mutants isolated, was found to be responsible for the increased resistance to acid inactivation, which correlated with an increased resistance to acid-induced dissociation into pentameric subunits. These results extend the range of pH sensitivities of FMDV mutants (35) and illustrate the adaptive flexibility of viral quasispecies to environmental changes, in this case related to pH variations.

MATERIALS AND METHODS

Cells, viruses, infections, and virus titrations. The origin and culture procedures for BHK-21 cells have been described (32, 33). C-S8c1 is a biological clone of a type C FMDV isolate (48). c2 is a FMDV variant with increased resistance to endosomal acidification blockage (35). Procedures for infections and virus titration in semisolid agar medium were as described previously (33–35, 48).

Radioactive labeling and purification of virions. A previously published procedure (37, 39) was followed. Briefly, FMDV virions (C-S8c1 and mutants) were metabolically labeled with [^{35}S]methionine (EasyTag Express protein labeling mix; Perkin-Elmer) during infection of BHK-21 cells. The total virus produced was centrifuged through a cushion of 20% sucrose in TNE buffer (10 mM Tris-HCl [pH 7.5], 0.1 M NaCl, 1 mM EDTA) in an AH-625 rotor (Sorvall) at 25,000 rpm for 2.5 h at 4°C. The viral pellet was resuspended in TNE buffer and centrifuged in 7.5 to 30% sucrose density gradients in the same buffer at 37,000 rpm for 1 h at 4°C in an SW40 rotor (Beckman). The fractions containing full virions (sedimentation coefficient, 140S) were pooled and extensively dialyzed against phosphate-buffered saline (PBS). The integrity of virions was analyzed in 7.5 to 45% sucrose density gradients at 18,000 rpm for 18 h at 4°C in an SW40 rotor (Beckman Instruments).

Acid-induced inactivation assays. A modification of a previously reported procedure was followed (30, 35). Briefly, equal amounts (10 μl containing ~10^6 PFU) of the virus tested were mixed with 300 μl of PBS solutions (50 mM $NaPO_4$ and 140 mM NaCl) of different pHs for 30 min at room temperature. The solution was neutralized by adding 100 μl of 1 M Tris (pH 7.6), and the remaining PFU counts in each sample were determined by plaque assay on BHK-21 cells. The number of PFU developed was determined and is expressed as the percentage of infectivity compared to that obtained using PBS at pH 7.4 or 7.6.

Acid-induced disassembly assays. Aliquots (100 μl) of ^{35}S-labeled purified virions were mixed with 300 μl of PBS solutions (50 mM $NaPO_4$ and 140 mM NaCl) of different pHs (i.e., pH 5.6 to 7.2) for 30 min at room temperature. The solution was neutralized by adding 100 μl of 1 M Tris (pH 7.6). Subsequently, the solution was loaded in 7.5 to 45% sucrose density gradients and centrifuged at 4°C in an SW40 rotor (Beckman Instruments) at 18,000 rpm for 18 h. The gradients were fractionated in 0.5-ml aliquots, and the radioactivity was determined by using a liquid scintillation counter. Values were expressed as a percentage of the amount of full virions (sedimentation coefficient, 140S) obtained at different pHs, relative to the amount obtained at pH 7.2.

Thermal inactivation assays. A previously published procedure was followed (37). Briefly, equal amounts of infectious virions (~10^7 PFU) were incubated at 42 or 50°C during 0, 30, 60, or 120 min. At these times, virus samples were frozen, and the remaining virus titer was determined by plaque assay.

Endosomal acidification blockage. Inhibition of endosomal acidification with NH_4Cl was performed as described previously (4, 33). Briefly, cells were treated for 1 h prior to infection with 25 mM NH_4Cl in culture medium supplemented with 25 mM HEPES at pH 7.4, and the drug was maintained throughout the rest of the assay. Alternatively, cells were pretreated with 1 μM concanamicin A (ConA) 30 min prior to infection, and the drug was only maintained during the first infection hour (7, 33). Control samples were treated in parallel with the same amount of drug solvent (dimethyl sulfoxide).

Viral RNA extraction, cDNA synthesis, and DNA sequencing. Viral RNA was extracted from supernatants of infected cell cultures by using TRI reagent (Sigma). cDNA synthesis by reverse transcription, amplification by PCR, and DNA sequencing have been previously described (35). DNA sequences were confirmed by at least two independent sequencing reactions. Nucleotide positions correspond to those of the FMDV C-S8c1 isolate (52).

Infectious clone manipulation, *in vitro* transcription, and transfection of BHK-21 cells. Plasmid pMT28 (21), which contains the full-length cDNA of FMDV C-S8c1, was used to construct plasmid pMT28-VP1 N17D bearing the nucleotide substitution A3256G found in the capsid coding region of the six FMDV mutants with increased resistance to acid induced inactivation (Table) 1. To this end, cDNA obtained from reverse transcription of RNA extracted from virus m6 was digested with SfiI and AvrII (New England Biolabs), and the resultant fragment purified by agarose gel electrophoresis was ligated into pMT28 vector digested with the same restriction endonucleases using T4 DNA ligase (Promega). Amplification of plasmid DNA was performed in *Escherichia coli* DH5α. Nucleotide sequences of infectious DNA clones were confirmed by DNA sequencing as described above. Transcription of viral RNA from infectious clones and transfection of cells with *in vitro*-synthesized viral RNA was performed as reported elsewhere (35).

Competition experiments. A modification of a previously published procedure (40) was followed. Briefly, a mixture containing equal amounts of each pair of competing viruses derived from infectious clones—initial multiplicity of infection (MOI) of 0.1 (0.05 for each virus)—was treated with pH 7.6 or pH 6.0 buffers, neutralized, and used to infect a 35-mm-diameter tissue culture dish. When a complete cytopathic effect was observed, the viruses were harvested. Viral suspensions (50 μl) were incubated at pH 7.6 or 6.0, neutralized, and used to infect fresh cell monolayers. These cycles of pH treatment, infection, and harvest were repeated up to four times in triplicate. Viral RNA was extracted, and the cDNA encoding VP1 protein was synthesized and sequenced. The proportions of the competing genomes were estimated from the chromatograms as a ratio of the integrated areas of each nucleotide under each peak of mutated position (40).

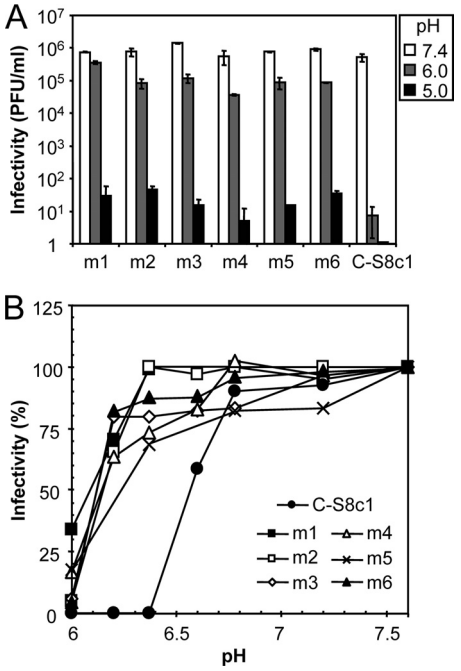

FIG. 1. Resistance to acid-induced inactivation of FMDV mutants selected after pH 6 treatment. (A) Equal PFU amounts of the different viruses were treated with acid buffers (pH 6.0 and 5.0) or pH 7.4 as a control. The samples were then neutralized and plated on BHK-21 monolayers. (B) Acid sensitivity profiles of FMDV mutants selected after pH 6 treatment. Infectivity was calculated from experiments performed as in panel A as the percentage of PFU recovered at each different pH relative to that obtained at pH 7.5.

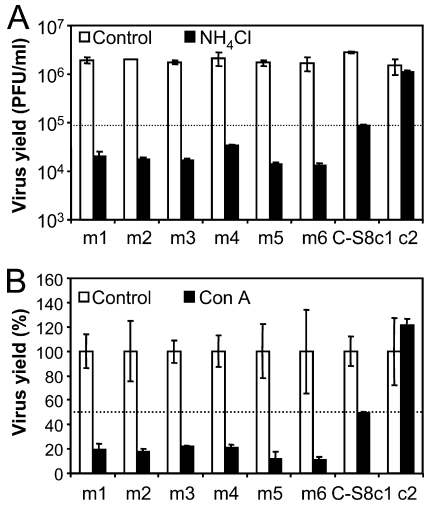

FIG. 2. Sensitivity to endosomal acidification blockage of FMDV mutants resistant to acid pH inactivation. (A) Sensitivity to NH_4Cl treatment. Monolayers of BHK-21 cells treated or not treated with 25 mM NH_4Cl were infected with the mutants and the parental virus C-S8c1 (MOI of 0.5). FMDV mutant c2 with increased resistance to endosomal acidification blockage (35) was also included. Virus yield was determined 8 h postinfection. (B) Sensitivity to ConA treatment. Monolayers treated or not with ConA (1 μM) were infected as described for panel A.

Molecular graphics. The atomic coordinates of FMDV C-S8c1 (31) and the programs RasMol (47) and Pymol (DeLano Scientific, Inc.) were used to locate the mutated amino acid residues on the capsid structure (35).

RESULTS

Isolation of FMDV mutants with increased resistance to acid inactivation. Infectious FMDV mutants with increased acid resistance were isolated by biological cloning after acid treatment. About 10^6 PFU of C-S8c1 were incubated 30 min at room temperature in PBS at pH 6.0 or 7.4 (control) and then neutralized. These samples were used to infect BHK-21 cell monolayers in semisolid agar medium. After 48 h, cells infected with samples treated at pH 6.0 showed approximately $0.0029 \pm 0.0005\%$ (selection frequency of 2.9×10^{-5}) of the number of plaques observed in control cells. The viruses recovered from six lysis plaques were amplified by infection in liquid medium (first passage) and subjected to a second treatment with pH 6.0 and subsequent amplification in liquid medium.

The viral populations obtained, termed mutants m1 to m6, were used for further experiments. The six mutants analyzed showed a decreased acid sensitivity compared to that of the parental virus C-S8c1 (Fig. 1A). Thus, relative to the drastic loss of infectivity observed (about 5 orders of magnitude) upon pH 6.0 treatment of C-S8c1, mutants m2 to m6 showed an infectivity reduction of only about 1 order of magnitude, which was even lower for mutant m1. When incubation was performed at pH 5.0, an infectivity reduction of about 5 orders of magnitude was observed for mutants m1 to m6, whereas no C-S8c1 PFU were recovered (Fig. 1A), confirming the increased resistance of these mutants to acid-induced inactivation of infectivity.

A detailed analysis of the sensitivity to pH values from 6 to 7.5 (Fig. 1B) confirmed that mutants m1 to m6 displayed inactivation profiles that are shifted to lower pH values relative to that exhibited by C-S8c1. When pH_{50} values (defined as the pH value leading to a 50% loss of infectivity [35]) were calculated, viruses m1 to m6 displayed very similar values (6.07, 6.15, 6.11, 6.15, 6.22, and 6.11, respectively). In the case of C-S8c1 the pH_{50} value was 6.58, as previously reported (35).

Increased acid sensitivity correlates with higher sensitivity to endosomal acidification blockage. FMDV uncoating leading to productive infection is triggered by acidification inside endosomes where viral particles are delivered (4, 7, 29, 33). Thus, infection by FMDV particles with increased acid lability displays higher resistance to the endosomal acidification blockage induced by different drugs such as NH_4Cl and ConA (35). These drugs were used to study whether an opposite effect was observed with the acid-resistant mutants. Compared to C-S8c1, mutants m1 to m6 showed, as expected, an increased sensitivity to NH_4Cl (Fig. 2A) and ConA treatment (Fig. 2B). In these experiments, mutant c2, which encodes a capsid with increased acid lability that confers resistance to endosomal acidification inhibition (35), was included as a control. These results indicate that the higher resistance to acid inactivation shown by these mutants is related to an increased sensitivity to drugs that raise the endosomal pH.

Analysis of mutations in the capsid-coding regions of acid-resistant FMDV mutants. To identify the genotypic changes responsible for the increased resistance to acid inactivation, the complete capsid coding regions of mutants m1 to m6 and

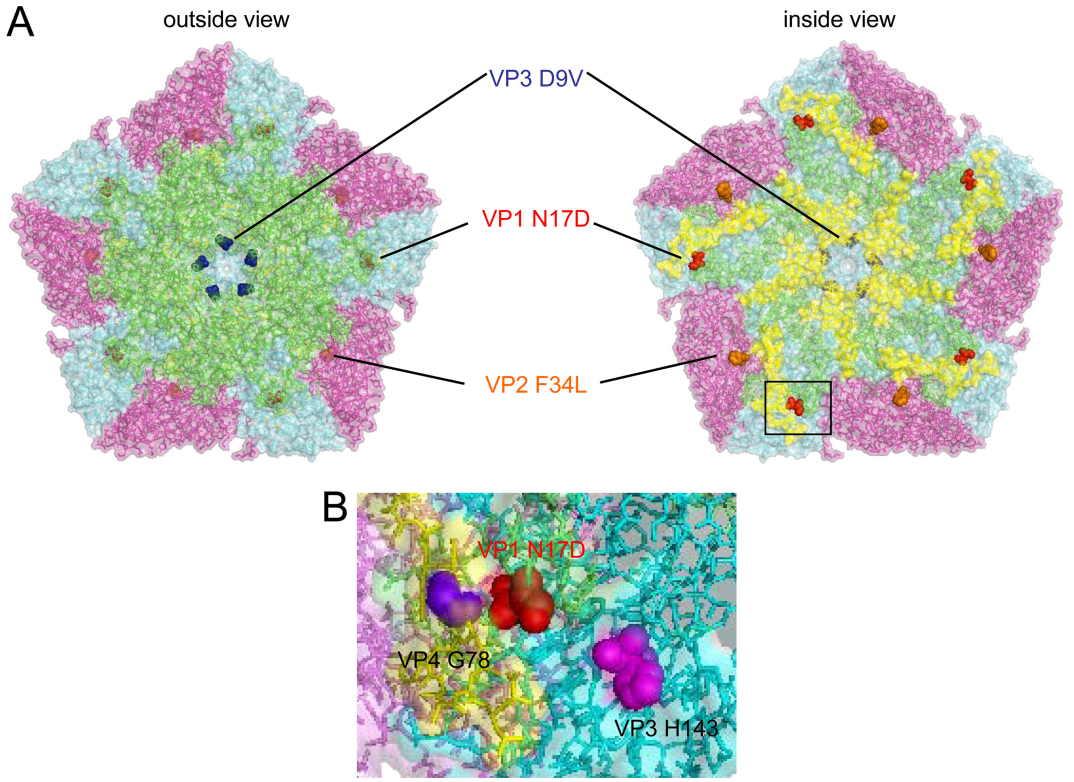

FIG. 3. Location on the structure of the C-S8c1 capsid (31) of amino acid residues found to be substituted in FMDV mutants with increased resistance to acid inactivation. (A) Outside and inside schematic views of a pentameric subunit in the capsid are shown. VP1 is green, VP2 is magenta, VP3 is cyan, and VP4 is yellow. (B) Close-up view of the region boxed in panel A showing relevant neighbor amino acids to the VP1 N17D position (red). VP4 G78 establishes a hydrogen bond with N17 which should be disrupted upon N17D amino acid replacement, and VP3 H143 is implicated on an acid pH-sensing mechanism for FMDV uncoating. See the text for details.

of the parental population C-S8c1 were sequenced and compared. Nucleotide and amino acid replacements found in viruses selected after two cycles of acid treatment and selection are shown in Table 1. Remarkably, all mutants showed a common nucleotide substitution A3256G leading to amino acid replacement VP1 N17D. Viruses m1 to m5 displayed also various degrees of nucleotide mixture at position 2576 between A (the nucleotide present in C-S8c1 sequence) and T (leading to amino acid replacement VP3 D9V); the A/T % values were as follows: m1, 53/47; m2, 28/72; m3, 68/32; m4, 78/21; and m5, 81/19. Virus m1 also exhibited an additional dominant nonsynonymous nucleotide substitution T1996C responsible for VP2 F34L amino acid replacement. The rest of the nucleotide substitutions found were synonymous.

The nucleotide substitution leading to replacement VP1 N17D was shown already imposed in all six viral progenies from cells infected with the virus recovered after the first cycle of acid treatment and selection (first passage). Such imposition was not observed for substitutions responsible for replacements VP2 F34L in virus m1 (present at ca. 60%) and VP3 D9V, for which only traces (lower than 5%) were detected in viruses m1 to m5.

None of the amino acid replacements selected involved invariant residues in the FMDV capsid (8). Replacement VP1 N17D found in viruses m1 to m6 affected a residue located at the N terminus of VP1 protein, within an internal region of the capsid, not far from the interpentamer interfaces (Fig. 3A). This amino acid replacement produced a disruption of a hydrogen bond between VP1 N17 and VP4 G78 and was located close to VP3 H143, which has been implicated in acid-induced capsid disassembly (1, 19, 55) (Fig. 3B). Residue VP3 9 was located at the outer surface of the capsid close to the capsid pore (5-fold symmetry axis), and residue VP2 34 was located at the internal surface of the capsid. Taken together, these results suggest that an internal capsid amino acid replacement (VP1 N17D) was responsible for the acid-resistant phenotype of viruses m1 to m6.

Amino acid substitution VP1 N17D confers increased resistance to acid-induced inactivation of FMDV. To test whether amino acid replacement VP1 N17D is sufficient to confer resistance to acid induced inactivation, a plasmid carrying the mutation responsible for this replacement was derived from the infectious clone pMT28, which encodes the complete genomic sequence of FMDV C-S8c1. The consensus nucleotide sequence of the capsid-coding region of the virus derived from the modified infectious clone (mutant VP1 17D) was determined and compared to that of the virus derived from the nonmutated, parental infectious clone pMT28 (C-S8c1). The only nonsynonymous nucleotide replacement found was that leading to replacement VP1 N17D (data not shown). Viruses derived from the mutated and the parental infectious clones were tested in acid-induced inactivation assays (Fig. 4). A significant increase in the acid resistance was observed for mutant VP1 N17D compared to C-S8c1. Virus VP1 N17D displayed a

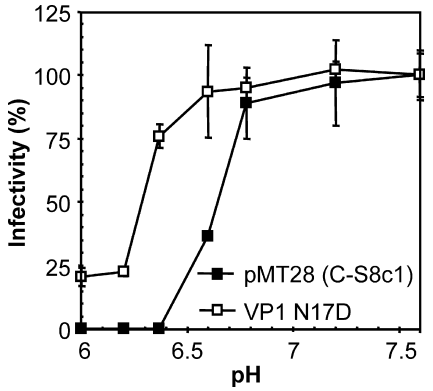

FIG. 4. The single amino acid substitution N17D in VP1 is responsible for increased acid resistance in FMDV mutants. Acid sensitivity of viruses C-S8c1 (derived from infectious clone pMT28) or VP1 D17 (a derivative carrying the mutation responsible for replacement VP1 N17D). Equal PFU amounts of the different viruses were treated with acid buffers, and samples were neutralized and plated. Infectivity was calculated as the percentage of PFU recovered in BHK-21 cells relative to the obtained at pH 7.6.

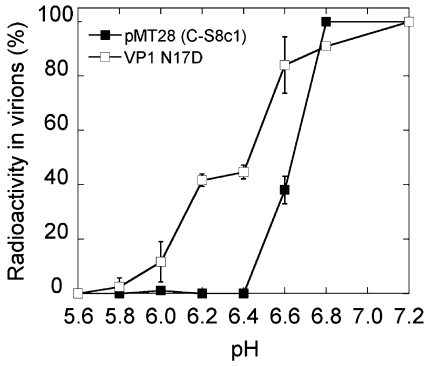

FIG. 5. pH-induced disassembly of FMDV virions. The remaining percentage of intact virions (sedimentation coefficient, 140S) is represented as a function of the pH of the buffer, relative to the amount of intact virion at a pH of 7.2 (taken as 100%). Mutant virions (VP1 N17D, □) and the nonmutated control virions (pMT28 [C-S8c1], ■) were radioactively labeled, purified, and assayed in parallel as described in Materials and Methods. The average values and error bars corresponding to two independent measurements are indicated. Dissociation of the virus was correlated with an increase in the amount of pentameric capsid subunits (sedimentation coefficient, 12S) (39).

pH_{50} value of 6.25 (very close to the pH_{50} values for viruses m2 to m6), whereas the pH_{50} value determined for C-S8c1 virus derived from the parental infectious clone was 6.62. These results confirm that amino acid replacement VP1 N17D is responsible for the increased resistance to acid inactivation phenotype.

The increased resistance of mutant VP1 N17D against acid-induced inactivation is due to its increased resistance against capsid dissociation. To investigate whether the increased resistance of mutant VP1 N17D to biological inactivation is related to an impaired dissociation into subunits, virions of C-S8c1 and the VP1 N17D mutant were radiolabeled and purified through sucrose gradients. Similar amount of virions (sedimentation coefficient, 140S) were obtained in both cases. The viruses were then incubated at different pHs for a defined amount of time and subjected to analytical sedimentation analysis to determine the amount of intact virions remaining after the treatment. The results (Fig. 5) show that the VP1 N17D mutant virion is substantially more resistant than the parental C-S8c1 virion to acid-induced dissociation of the capsid into pentameric subunits. Their respective pH_{50} values for dissociation (about 6.3 and 6.6, respectively) were very similar to their pH_{50} values for inactivation of infectivity (see above), and their dissociation and inactivation curves overlapped to a large extent. Thus, the increased resistance of mutant VP1 N17D to acid-induced inactivation is due to its increased resistance to capsid dissociation into pentameric subunits.

Biological fitness of an acid-resistant FMDV virion. Viruses recovered from infectious clones were tested in competition experiments performed at different pHs (7.6 and 6.0). Equal PFU amounts of C-S8c1 and VP1 N17D viruses were mixed (initial MOIs of 0.1 [0.05 for each virus]), incubated at pH 7.6 (control) or 6.0, and used to infect BHK-21 cells. Viruses recovered from these infections were harvested, incubated again at pH 7.6 or 6.0, and further passaged. Approximate percentages of competing genomes during the four serial passages analyzed were determined (Fig. 6). In three independent experiments performed at pH 7.6, a similar proportion of the competing genomes (ca. 50%) was observed along the four passages. Conversely, in each of the three independent experiments performed at pH 6.0, mutant VP1 N17D was already dominant in the first passage (ca. 90%), and its proportion progressively increased during passages up to values close to 100%. These results show that replacement VP1 N17D, responsible for increased resistance to acid inactivation, confers a selective advantage in serial passages after incubation at low pH (6.0), whereas it did not drastically alter viral fitness when incubations were performed at a neutral pH. (pH 7.6).

Amino acid substitution VP1 N17D also confers increased resistance to heat inactivation of FMDV. To continue the characterization of the physicochemical alterations caused by replacement VP1 N17D, the effect of high temperature on the infectivity of C-S8c1 and VP1 17D viruses was analyzed. Rel-

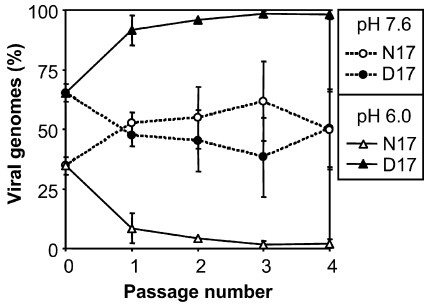

FIG. 6. Competition experiments between viruses C-S8c1 (N17) or VP1 D17 (D17) during serial passages of a virus mixture, in which viruses were incubated at pH 7.6 or pH 6.0 prior to each infection. An initial MOI of 0.1 (0.05 for each virus) was used for the each infection. Approximate percentages of competing genomes during serial passages are represented. Passage 0 denotes the initial mixture of viruses. The proportions of A (in VP1 N17) and G (in VP1 D17) at position 3256 were determined by nucleotide sequencing as described in Materials and Methods. The average proportions of viral genomes found in three independent competition experiments are represented.

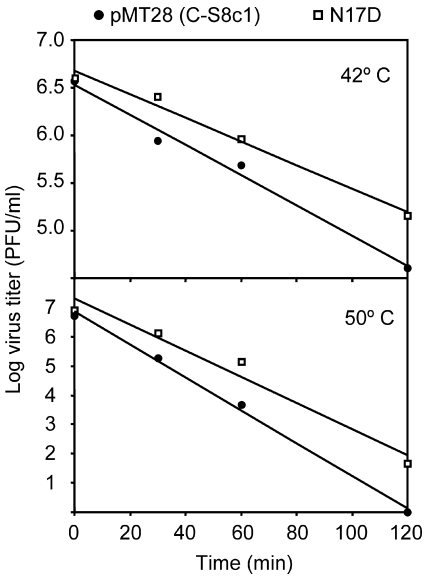

FIG. 7. The single amino acid replacement N17D in VP1 increases FMDV resistance to thermal inactivation. Equal PFU amounts of the different viruses were incubated at 42 or 50°C, and the remaining infectivity in viral samples was determined by plaque assay. Each point corresponds to the average of three independent experiments.

ative to C-S8c1, a moderate increase in resistance to virus inactivation at 42 or 50°C was observed for mutant VP1 N17D (Fig. 7). The t_{50} values (calculated as the time in minutes value leading to a 50% loss of infectivity) derived from these data were 20 min for C-S8c1 and 41 min for VP1 17D at 42°C and 17.7 min for C-S8c1 and 24.7 min for VP1 17D at 50°C. These experiments confirmed that amino acid substitution VP1 N17D also confers some increase in the resistance of FMDV to thermal inactivation.

DISCUSSION

A few FMDV mutants with altered acid sensitivity have been described. We recently showed that mutations in structural proteins can reduce FMDV stability at acidic pH (35). An FMDV mutant with increased resistance against acid inactivation has also been described (54) but not fully characterized. In addition, the rational introduction of a charge reversal mutation in the FMDV capsid led to impaired dissociation of the nucleic acid-free capsid under acidic conditions (19). In the present study, type C FMDV mutants (named m1 to m6) with increased resistance to acid-induced inactivation were isolated from a viral population after *in vitro* incubation at pH 6.0. The selection frequency of these mutants—2.9×10^{-5}—was similar to that reported for FMDV monoclonal antibody resistant mutants (36), but it was 4 orders of magnitude lower than that reported for FMDV mutants with increased capsid lability selected by NH_4Cl treatment ($\sim 10^{-1}$) (35). This lower frequency of acid-resistant mutants could in principle be due to a fitness loss related to modifications of the acid-dependent uncoating mechanism, as suggested by the small plaque phenotype reported for type A acid resistant FMDVs (54). However, viruses m1 to m6 displayed plaque size and growth kinetics similar to those of the C-S8c1 parental virus (data not shown). All mutants with increased resistance to acid inactivation isolated in the present study carried a common nucleotide substitution responsible for amino acid replacement VP1 N17D. Introduction of this replacement into an infectious clone was sufficient to confer an increase in the resistance to acid-induced inactivation in the viruses recovered. Replacement in mutant VP1 N17D also conferred a selective advantage relative to the parental C-S8c1 virus in mixed-serial infections in which viruses were incubated at pH 6.0 prior to infection. When this experiment was performed at pH 7.6, no alteration in the proportion of the parental and the mutant residues was observed. This result indicates that the relatively low mutant frequency of acid-resistant variants in FMDV populations may not be due to a substantially reduced biological fitness.

Amino acid replacement VP1 N17D is located at the N terminus of VP1 on the inner surface of FMDV capsid. This is a nearly isosteric replacement (since the amide and carboxylate groups have similar volumes and geometries) but introduces an additional negative charge per capsid protomer (60 additional charges in the virion). No positively charged groups suitable to form a short-range coulombic interaction with this newly introduced negatively charged carboxylate are close enough in the capsid structure. In addition, residue 17 in VP1 is relatively close to the interpentameric interface, but it neither forms part of the interpentamer or interprotomer interfaces nor establishes any short-range interpentameric or interprotomeric interaction that could result in capsid stabilization. The amide group in VP1 N17 only establishes a hydrogen bond with the main chain oxygen of VP4 G78 residue of the same protomer that would disappear upon VP1 N17D mutation, which could destabilize the interaction between VP1 and the C terminus of VP4 within the same protomer. In natural FMDV empty particles, which display an increased resistance to acid disassembly compared to virions (12), both the N terminus of VP1 and the C terminus of VP4 are more disordered than in the corresponding virions (13). In the case of type A acid-resistant FMDV, this mutant displayed four amino acid replacements (54), one of which was also located at the N terminus of VP1, but the role of each of these mutations in the acid-resistant phenotype was not determined. Conformational rearrangements in the N terminus of VP1 have been recently implicated on the uncoating mechanism of equine rhinitis A virus (ERAV) (53), an *Aphthovirus* that shares physicochemical properties with FMDV such as buoyant density and acid lability (41, 42). As described for FMDV (see the introduction), ERAV is internalized within host cell following a clathrin-dependent pathway, and its uncoating is supposed to occur within early endosomes (22), where low pH should trigger capsid disassembly into pentameric subunits via a transient 80S intermediate particle which has lost the genomic RNA (53). However, besides similarities between ERAV and FMDV, this uncoating intermediate has not yet been described for FMDV.

An alternative, nonexclusive model for explaining acid resistance in mutant VP1 N17D is based on the fact that residue 17 of VP1 is located only about 10 Å from the interpentamer interface and about 15 and 8 Å, respectively, from H140 and H143 in VP3 of the same protomer. In FMDV, conserved histidines at these positions (equivalent to residues 141 and 144 in type O or 142 and 145 in type A) may provide a pH-dependent switch for capsid dissociation in the acidic environ-

ment of the endosome; the protonated histidines could establish an electrostatic repulsion with the dipole of an alpha helix in the neighboring pentamer, facilitating capsid dissociation (1, 19, 55). The introduction of an additional negative charge in mutant VP1 N17D could partially neutralize the positive charge of the protonated H143, reducing the interpentamer repulsion at acidic pH and leading to increased resistance against acid-induced dissociation into pentamers, as observed here.

Along this line, it is interesting that the N17D mutation also led to a somewhat increased resistance against thermal inactivation of the FMDV virion at neutral pH. A previously engineered neutral-to-charged A65H substitution in VP2 at the interpentameric interfaces in the FMDV capsid led to a similar, moderate increase in resistance against thermal inactivation at neutral pH (39). However, while mutants with a substantially shifted pH-dependent stability (35, 54; the present study) can be readily isolated from FMDV populations, mutants with a highly increased stability against thermal inactivation do not appear to be generally present in FMDV quasispecies (38). In addition, whereas acid inactivation of the FMDV virion is directly caused by dissociation of the capsid into pentameric subunits (19; the present study), its thermal inactivation at moderate temperatures appears to be due to a conformational change without capsid dissociation, with dissociation occurring only at much longer incubation times (39). Thus, the mechanisms for the increased resistance against acid inactivation or thermal inactivation of mutant N17D and other FMDV mutants may be quite different.

The additional amino acid replacement VP2 F34L found in mutant m1 (but not in m2 to m6) is located at an internal capsid position. Mutant m1 showed slightly higher resistance to acid inactivation than those of the rest of mutants isolated (Fig. 1A), suggesting that this replacement could be responsible for its slightly increased acid resistance. For ERAV, conformational rearrangements in the N terminus of VP2 have been also described in the uncoating intermediate (53).

Five of the six mutants (m1 to m5) displayed an additional nucleotide mixture at position 2576 responsible for amino acid replacement VP3 D9V. This position has been involved in interprotomer interactions and a salt bridge with VP1 K109 (40), which should be disrupted upon substitution. Amino acid replacements at this position have been also described in viruses recovered from persistent cell culture infections (16, 24, 52). The proportion of the nucleotide substitution leading to VP3 D9V was increased after a second acid treatment (data not shown), suggesting that this additional replacement could be related to an increase in acid resistance. However, virus m6, which lacks VP3 D9V substitution (Table 1), showed a degree of resistance to acid inactivation similar to that of mutants m2 to m5, which carried this mutation at different proportions (Fig. 1). Even when further experiments are required to determine the biological effect of replacement VP3 D9V, an alternative possibility is that this mutation might compensate for some detrimental effect of the replacement VP1 N17D. Indeed, the selection of compensatory mutations in response to amino acid replacements that alter FMDV capsid stability has been previously documented (40).

Enhanced resistance to acid inactivation correlated with an increase in the sensitivity of these mutants to drugs that raise endosomal pH, such as NH_4Cl and ConA. This effect is opposite to that previously shown for mutants with increased capsid lability that were resistant to these drugs (35). These observations confirm that resistance to *in vitro* acid inactivation is related to a lower pH requirement for productive uncoating within host cells. In this way, the acid-resistant mutants described here extend the spectrum of FMDV variants, including pH_{50} values ranging from 6.95 for mutant c2 (35) to 6.07 for mutant m1. These results further illustrate the adaptive flexibility of viral quasispecies to external changes, in this case alterations associated with pH variations.

ACKNOWLEDGMENTS

We thank E. Domingo and C. Escarmís for infectious clone pMT28.

Work at the F.S. laboratory was supported by grants from Ministerio de Ciencia e Innovación (MICINN) BIO2008-0447-C03-01 and CSD2006-0007; work at the M.G.M. laboratory was supported by grants from MICINN (BIO2009-10092) and Comunidad de Madrid (S-2009/MAT/1467). An institutional grant from Fundación Ramón Areces is also acknowledged.

REFERENCES

1. **Acharya, R., et al.** 1989. The three-dimensional structure of foot-and-mouth disease virus at 2.9 Å resolution. Nature **337:**709–716.
2. **Baranowski, E., et al.** 2000. Cell recognition by foot-and-mouth disease virus that lacks the RGD integrin-binding motif: flexibility in aphthovirus receptor usage. J. Virol. **74:**1641–1647.
3. **Baranowski, E., et al.** 1998. Multiple virulence determinants of foot-and-mouth disease virus in cell culture. J. Virol. **72:**6362–6372.
4. **Baxt, B.** 1987. Effect of lysosomotropic compounds on early events in foot-and-mouth disease virus replication. Virus Res. **7:**257–271.
5. **Baxt, B., and Y. Becker.** 1990. The effect of peptides containing the arginine-glycine-aspartic acid sequence on the adsorption of foot-and-mouth disease virus to tissue culture cells. Virus Genes **4:**73–83.
6. **Belsham, G. J., C. C. Abrams, A. M. King, J. Roosien, and J. M. Vlak.** 1991. Myristoylation of foot-and-mouth disease virus capsid protein precursors is independent of other viral proteins and occurs in both mammalian and insect cells. J. Gen. Virol. **72**(Pt. 3)**:**747–751.
7. **Berryman, S., S. Clark, P. Monaghan, and T. Jackson.** 2005. Early events in integrin αvβ6-mediated cell entry of foot-and-mouth disease virus. J. Virol. **79:**8519–8534.
8. **Carrillo, C., et al.** 2005. Comparative genomics of foot-and-mouth disease virus. J. Virol. **79:**6487–6504.
9. **Carrillo, E. C., C. Giachetti, and R. Campos.** 1985. Early steps in FMDV replication: further analysis on the effects of chloroquine. Virology **147:**118–125.
10. **Carrillo, E. C., C. Giachetti, and R. H. Campos.** 1984. Effect of lysosomotropic agents on the foot-and-mouth disease virus replication. Virology **135:**542–545.
11. **Cottam, E. M., et al.** 2008. Transmission pathways of foot-and-mouth disease virus in the United Kingdom in 2007. PLoS Pathog. **4:**e1000050.
12. **Curry, S., et al.** 1995. Viral RNA modulates the acid sensitivity of foot-and-mouth disease virus capsids. J. Virol. **69:**430–438.
13. **Curry, S., et al.** 1997. Dissecting the roles of VP0 cleavage and RNA packaging in picornavirus capsid stabilization: the structure of empty capsids of foot-and-mouth disease virus. J. Virol. **71:**9743–9752.
14. **Danthi, P., M. Tosteson, Q. H. Li, and M. Chow.** 2003. Genome delivery and ion channel properties are altered in VP4 mutants of poliovirus. J. Virol. **77:**5266–5274.
15. **Davis, M. P., et al.** 2008. Recombinant VP4 of human rhinovirus induces permeability in model membranes. J. Virol. **82:**4169–4174.
16. **Díez, J., et al.** 1990. Unique amino acid substitutions in the capsid proteins of foot-and-mouth disease virus from a persistent infection in cell culture. J. Virol. **64:**5519–5528.
17. **Domingo, E., et al.** 2006. Viruses as quasispecies: biological implications. Curr. Top. Microbiol. Immunol. **299:**51–82.
18. **Domingo, E., et al.** 1990. Genetic variability and antigenic diversity of foot-and-mouth disease virus, p. 233–266. *In* F. A. Murphy and M. H. V. Van Regenmortel (ed.), Applied virology research, vol. 2. Plenum Publishing Corp., New York, NY.
19. **Ellard, F. M., J. Drew, W. E. Blakemore, D. I. Stuart, and A. M. King.** 1999. Evidence for the role of His-142 of protein 1C in the acid-induced disassembly of foot-and-mouth disease virus capsids. J. Gen. Virol. **80**(Pt. 8)**:**1911–1918.
20. **Fauquet, C., et al (ed.).** 2005. Virus taxonomy. Eighth Report of the Inter-

national Committee on Taxonomy of Viruses. Elsevier Academic Press, Inc., San Diego, CA.
21. **García-Arriaza, J., S. C. Manrubia, M. Toja, E. Domingo, and C. Escarmís.** 2004. Evolutionary transition toward defective RNAs that are infectious by complementation. J. Virol. **78:**11678–11685.
22. **Groppelli, E., T. J. Tuthill, and D. J. Rowlands.** 2010. Cell entry of the aphthovirus equine rhinitis A virus is dependent on endosome acidification. J. Virol. **84:**65235–65240.
23. **Grubman, M. J., and B. Baxt.** 2004. Foot-and-mouth disease. Clin. Microbiol. Rev. **17:**465–493.
24. **Herrera, M., A. Grande-Pérez, C. Perales, and E. Domingo.** 2008. Persistence of foot-and-mouth disease virus in cell culture revisited: implications for contingency in evolution. J. Gen. Virol. **89:**232–244.
25. **Jackson, T., et al.** 2004. Integrin alphavbeta8 functions as a receptor for foot-and-mouth disease virus: role of the beta-chain cytodomain in integrin-mediated infection. J. Virol. **78:**4533–4540.
26. **Jackson, T., et al.** 1996. Efficient infection of cells in culture by type O foot-and-mouth disease virus requires binding to cell surface heparan sulfate. J. Virol. **70:**5282–5287.
27. **Jackson, T., A. P. Mould, D. Sheppard, and A. M. King.** 2002. Integrin αvβ1 is a receptor for foot-and-mouth disease virus. J. Virol. **76:**935–941.
28. **Jackson, T., D. Sheppard, M. Denyer, W. Blakemore, and A. M. King.** 2000. The epithelial integrin αvβ6 is a receptor for foot-and-mouth disease virus. J. Virol. **74:**4949–4956.
29. **Johns, H. L., S. Berryman, P. Monaghan, G. J. Belsham, and T. Jackson.** 2009. A dominant-negative mutant of rab5 inhibits infection of cells by foot-and-mouth disease virus: implications for virus entry. J. Virol. **83:**6247–6256.
30. **Knipe, T., E. Rieder, B. Baxt, G. Ward, and P. W. Mason.** 1997. Characterization of synthetic foot-and-mouth disease virus provirions separates acid-mediated disassembly from infectivity. J. Virol. **71:**2851–2856.
31. **Lea, S., et al.** 1994. The structure and antigenicity of a type C foot-and-mouth disease virus. Structure **2:**123–139.
32. **Martín-Acebes, M. A., et al.** 2008. Subcellular distribution of swine vesicular disease virus proteins and alterations induced in infected cells: a comparative study with foot-and-mouth disease virus and vesicular stomatitis virus. Virology **374:**432–443.
33. **Martín-Acebes, M. A., M. González-Magaldi, K. Sandvig, F. Sobrino, and R. Armas-Portela.** 2007. Productive entry of type C foot-and-mouth disease virus into susceptible cultured cells requires clathrin and is dependent on the presence of plasma membrane cholesterol. Virology **369:**105–118.
34. **Martín-Acebes, M. A., M. González-Magaldi, A. Vázquez-Calvo, R. Armas-Portela, and F. Sobrino.** 2009. Internalization of swine vesicular disease virus into cultured cells: a comparative study with foot-and-mouth disease virus. J. Virol. **83:**4216–4226.
35. **Martín-Acebes, M. A., V. Rincón, R. Armas-Portela, M. G. Mateu, and F. Sobrino.** 2010. A single amino acid substitution in the capsid of foot-and-mouth disease virus can increase acid lability and confer resistance to acid-dependent uncoating inhibition. J. Virol. **84:**2902–2912.
36. **Martinez, M. A., et al.** 1991. Fitness alteration of foot-and-mouth disease virus mutants: measurement of adaptability of viral quasispecies. J. Virol. **65:**3954–3957.
37. **Mateo, R., A. Diaz, E. Baranowski, and M. G. Mateu.** 2003. Complete alanine scanning of intersubunit interfaces in a foot-and-mouth disease virus capsid reveals critical contributions of many side chains to particle stability and viral function. J. Biol. Chem. **278:**41019–41027.
38. **Mateo, R., E. Luna, and M. G. Mateu.** 2007. Thermostable variants are not generally represented in foot-and-mouth disease virus quasispecies. J. Gen. Virol. **88:**859–864.
39. **Mateo, R., E. Luna, V. Rincon, and M. G. Mateu.** 2008. Engineering viable foot-and-mouth disease viruses with increased thermostability as a step in the development of improved vaccines. J. Virol. **82:**12232–12240.
40. **Mateo, R., and M. G. Mateu.** 2007. Deterministic, compensatory mutational events in the capsid of foot-and-mouth disease virus in response to the introduction of mutations found in viruses from persistent infections. J. Virol. **81:**1879–1887.
41. **Newman, J. F., D. J. Rowlands, and F. Brown.** 1973. A physico-chemical sub-grouping of the mammalian picornaviruses. J. Gen. Virol. **18:**171–180.
42. **Newman, J. F., et al.** 1977. Physicochemical characterization of two serologically unrelated equine rhinoviruses. Intervirology **8:**145–154.
43. **O'Donnell, V., M. Larocco, and B. Baxt.** 2008. Heparan sulfate-binding foot-and-mouth disease virus enters cells via caveola-mediated endocytosis. J. Virol. **82:**9075–9085.
44. **O'Donnell, V., M. LaRocco, H. Duque, and B. Baxt.** 2005. Analysis of foot-and-mouth disease virus internalization events in cultured cells. J. Virol. **79:**8506–8518.
45. **Pluimers, F. H., A. M. Akkerman, P. van der Wal, A. Dekker, and A. Bianchi.** 2002. Lessons from the foot and mouth disease outbreak in the Netherlands in 2001. Rev. Sci. Tech. **21:**711–721.
46. **Sá-Carvalho, D., et al.** 1997. Tissue culture adaptation of foot-and-mouth disease virus selects viruses that bind to heparin and are attenuated in cattle. J. Virol. **71:**5115–5123.
47. **Sayle, R. A., and E. J. Milner-White.** 1995. RASMOL: biomolecular graphics for all. Trends Biochem. Sci. **20:**374.
48. **Sobrino, F., M. Dávila, J. Ortín, and E. Domingo.** 1983. Multiple genetic variants arise in the course of replication of foot-and-mouth disease virus in cell culture. Virology **128:**310–318.
49. **Sobrino, F., and E. Domingo.** 2001. Foot-and-mouth disease in Europe: FMD is economically the most important disease of farm animals, and its re-emergence in Europe is likely to have consequences that go beyond severe alterations of livestock production and trade. EMBO Rep. **2:**459–461.
50. **Sobrino, F., et al.** 2001. Foot-and-mouth disease virus: a long known virus, but a current threat. Vet. Res. **32:**1–30.
51. **Thompson, D., et al.** 2002. Economic costs of the foot and mouth disease outbreak in the United Kingdom in 2001. Rev. Sci. Tech. **21:**675–687.
52. **Toja, M., C. Escarmis, and E. Domingo.** 1999. Genomic nucleotide sequence of a foot-and-mouth disease virus clone and its persistent derivatives. Implications for the evolution of viral quasispecies during a persistent infection. Virus Res. **64:**161–171.
53. **Tuthill, T. J., et al.** 2009. Equine rhinitis A virus and its low pH empty particle: clues toward an aphthovirus entry mechanism? PLoS Pathog. **5:**e1000620.
54. **Twomey, T., et al.** 1995. Characterization of an acid-resistant mutant of foot-and-mouth disease virus. Virology **206:**69–75.
55. **van Vlijmen, H. W., S. Curry, M. Schaefer, and M. Karplus.** 1998. Titration calculations of foot-and-mouth disease virus capsids and their stabilities as a function of pH. J. Mol. Biol. **275:**295–308.
56. **Vasquez, C., C. D. Denoya, J. L. La Torre, and E. L. Palma.** 1979. Structure of foot-and-mouth disease virus capsid. Virology **97:**195–200.

Vaccine 29 (2011) 9655–9662

Contents lists available at SciVerse ScienceDirect

Vaccine

journal homepage: www.elsevier.com/locate/vaccine

Foot-and-mouth disease virus particles inactivated with binary ethylenimine are efficiently internalized into cultured cells

Miguel A. Martín-Acebes[a,1], Ángela Vázquez-Calvo[a], Mónica González-Magaldi[a], Francisco Sobrino[a,b,*]

[a] Centro de Biología Molecular "Severo Ochoa" (CSIC-UAM), Cantoblanco 28049, Madrid, Spain
[b] Centro de Investigación en Sanidad Animal, INIA, Valdeolmos, 28130 Madrid, Spain

ARTICLE INFO

Article history:
Received 15 June 2011
Received in revised form 7 October 2011
Accepted 13 October 2011
Available online 24 October 2011

Keywords:
FMDV
Binary ethylenimide
Inactivated vaccine
Endocytosis
Endosomes
Integrin

ABSTRACT

Conventional foot-and-mouth disease (FMD) vaccines are produced from virus grown in cell culture that is chemically inactivated by using binary ethylenimide (BEI). Here, we show that BEI treatment preserves both the architecture of FMDV particles, as inactivated viral particles showed by electron microscopy characteristics similar to those of infectious virions, as well as the general features of infectious virus internalization. Binding of inactivated particles to BHK-21 cells was blocked by preincubation with either a FMDV-specific monoclonal antibody or a synthetic peptide spanning the integrin-binding viral motif Arg-Gly-Asp (RGD). In addition, these particles were internalized into cultured cells through endocytosis, being directed to early endosomes, as indicated by their colocalization with the marker protein Rab5. When purified BEI-inactivated virions were labelled and their interaction with live cultured cells analyzed by time-lapse fluorescence microscopy, a major subpopulation of virus particles, about 80%, was shown to undergo internalization into a static endosome population, insensitive to the microtubule depolymerization exerted by nocodazole, while the remaining subpopulation (about 20%) was dynamic and sensitive to this drug. Thus, BEI-inactivated particles provide an interesting tool to study early steps in FMDV–cell interactions enabling a distinction between FMDV internalization and productive infection. Possible implications for FMDV immune response elicited following vaccine administration are discussed.

1. Introduction

Foot-and-mouth disease virus (FMDV) is the aetiological agent of a highly contagious disease of cloven-hoofed animals [1,2]. As FMDV hosts include important livestock species (i.e. sheeps, goats, cattle and swine) disease outbreaks cause large economic losses derived from reductions in dairy and meat industries, slaughter policies and restrictions for national and international trading [3–6]. These factors make FMD to be included within the list of diseases notifiable to the World Organisation for Animal Health (former OIE). At present, vaccination is the best tool for disease control together with culling programs and animal movement restrictions in and from infected areas. Considerable effort has been paid on the design of novel vaccines including approaches such as engineered attenuated viruses [7,8], recombinant DNA immunization [9,10] or peptide subunits [11,12]. However vaccines based on chemical inactivation of viral preparations produced in cultured cells remain as the only strategy approved by the OIE. Binary ethylenimide (BEI) has progressively displaced other virus inactivants such as formaldehyde for vaccine production [13,14]. While the mechanism of FMDV inactivation by BEI remains to be known in detail, it seems to imply modification (alkylation) of viral RNA preserving the antigenic structure of the viral capsid [15]. Immune responses derived from BEI-inactivated vaccines showed a good correlation between induction of neutralizing antibodies and the protection they confer [2,16]; however, the molecular mechanisms underlying this protection have not been studied in depth. Little is known on the role in protection of crossreactive CD8+ T cell responses mediated by MHC class I, recently reported to be induced upon FMDV infection or vaccination [17]. The contribution of CTL responses to protection is suggested by the observation of protected animals showing low neutralizing antibody levels [18].

The internalization of viral particles is important for the presentation of antigenic peptides to T cells as well as to trigger innate immunity [18,19]. Cell entry of FMDV has been proven to be dependent on the usage of cellular receptors, followed by

* Corresponding author at: Centro de Biología Molecular "Severo Ochoa" (CSIC-UAM), Cantoblanco 28049, Madrid, Spain. Tel.: +34 91 1964493; fax: +34 91 1964420.
E-mail address: fsobrino@cbm.uam.es (F. Sobrino).
[1] Present address: Departamento de Biotecnología, Instituto Nacional de Investigación y Tecnología Agraria y Alimentaria (INIA), 28040 Madrid, Spain.

0264-410X/$ – see front matter © 2011 Elsevier Ltd. All rights reserved.
doi:10.1016/j.vaccine.2011.10.031

internalization via endocytosis and its delivery to endosomal compartments [20–22]. Field FMDV isolates attach to several molecules of the integrin family as a receptor via the binding of a Arg-Gly-Asp (RGD) triplet exposed on the viral capsid [23,24]. In addition, tissue culture adapted FMDV variants can expand its receptor spectrum and are able to bind alternative receptors such as heparan sulfate glycosaminoglycans or other not well characterized molecules [25–27].

To gain information on the cell interactions of inactivated FMDV we determined the ability of BEI-inactivated viral particles to enter into cultured cells. By electron microscopy particles with similar characteristics to those of infectious virions were found in BEI-inactivated viral samples. Binding of these particles was blocked by preincubation with a FMDV-specific monoclonal antibody, and inactivated particles were internalized into cultured cells through endocytosis in an integrin-dependent pathway. Thus, BEI-inactivated particles provide a new tool to study the early steps in FMDV–host cell interaction. Possible implications for FMDV immune response following vaccine administration are also discussed.

2. Materials and methods

2.1. Cells and viruses

The origin and culture procedures for BHK-21, CHO and IBRS-2 cells have been extensively described, as well as procedures for infections and virus titration in semisolid agar medium [21,28]. C-S8c1 is a biological clone of a type C FMDV isolated from a naturally infected pig in Spain [29]. FMDV MARLS is a monoclonal antibody (MAb)-resistant mutant selected with MAb SD6 from a population of highly tissue culture passaged C-S8c1 [26]. Encephalomyocarditis virus (EMCV) [30] was also used as control for the specificity of the internalization assay.

2.2. Viral inactivation

Chemical inactivation of FMDV and EMCV with BEI was performed following the standard protocol for vaccine preparation [13]. BEI was prepared from a 0.01 M solution of 2-bromethylamine hydrobromide (BEA) (Merck) in 0.7% NaOH. After the addition of 0.05 ml/l of β-naftol, the solution was incubated at 37 °C until a colour shift from violet to orange (indicative of the complete conversion from BEA to BEI) was observed. Then, the solution was filtered through a 0.22 μm filter and added to the viral suspension at a final concentration of 3%. Viral suspensions were incubated for 24 h at 37 °C with gently rocking and residual BEI was hydrolyzed with 2% of 1 M Na_2SO_3. The efficacy of viral inactivation was confirmed by the absence of cytophatic effect after three blind passages in monolayers of BHK-21 cells. The amount of inactivated virus was estimated from the viral titer of the sample prior to inactivation.

2.3. Virion purification and electron microscopy

Virion purification was performed by sucrose gradient centrifugation [31]. Inactivated virus samples were centrifuged through a cushion of 20% sucrose in TNE buffer [10 mM Tris–HCl (pH 7.5), 0.1 M NaCl, 1 mM EDTA] in an AH-625 rotor (Sorvall) at 25,000 rpm, 2.5 h, 4 °C. The viral pellet was resuspended in TNE and centrifuged in 7.5–30% sucrose density gradients in the same buffer at 37,000 rpm, 1 h at 4 °C in a SW40 rotor (Beckman). Relative amounts of viral protein and RNA were determined by UV-spectrophotometry using a Nanodrop equipment. A drop from the fraction corresponding to virion peak (sedimentation coefficient of 140 s) was adsorbed to the ionized face of an electron microscopy copper grid and viral particles were fixed in 2% glutaraldehyde and negatively stained with 2% uranyl acetate [32]. Samples were observed using a Jeol JEM-1010 electron microscope operating at 80 kV and images were acquired using a digital camera Bioscan792 (Gatan).

2.4. Inhibition of viral cell binding

The ability of BEI-inactivated FMDV particles to bind cells was investigated by two different approaches. (i) Infectious virus (10^7 plaque forming units (PFU), corresponding to a MOI of 100 PFU/cell), or the equivalent amount of inactivated virus were preincubated with MAbs SD6 or irrelevant MAb I1 against vesicular stomatitis virus G protein (supernatant from hybridoma cultures diluted 1:10 in culture medium) for 1.5 h at room temperature (RT) prior to addition to cell monolayers [33]. After 25 min of incubation at 37 °C, cells were fixed and immunostained [31]. (ii) Cells were preincubated with RGD-containing peptide SARGDLAHLTTTHAR (positions 139–153 of VP1 in C-S8c1) diluted in phosphate-buffered saline (PBS) completed with Ca^{2+} and Mg^{2+} at a final peptide concentration of 1 mM, for 30 min at 37 °C. Then cells were washed and incubated with the amounts of infective or inactivated virus used in (i) diluted in complete PBS for 25 min at 37 °C [31]. Cells were finally fixed and immunostained.

2.5. Drug treatments

Inhibition of clathrin-mediated endocytosis was performed by sucrose treatment [20,21]. Cells grown on coverslips were extensively washed with culture medium and pre-treated or not for 30 min with sucrose (0.45 M). Infectious virus (10^7 PFU, corresponding to a MOI of 100 PFU/cell), or the equivalent amount of inactivated virus were incubated 25 min with the cells in the presence or in the absence of sucrose, fixed and processed for immunofluorescence. Microtubule depolymerization was performed using 40 μm nocodazole (Sigma) [28].

2.6. Immunofluorescence microscopy

Procedures for immunofluorescence staining of FMDV particles have been described [21,31]. Samples were observed with an Axioskop (Zeiss) epifluorescence microscope coupled to a digital monochrome camera Coolsnap FX (Roper Scientific). Confocal laser scanning microscopy was performed with an Axiovert S100 TV microscope (Zeiss) coupled to a confocal Radiance 2000 system (Bio-Rad). Images were processed using ImageJ (http://rsbweb.nih.gov/ij/) and Adobe Photoshop CS2 (Adobe, Inc.).

2.7. Transfections

Plasmid encoding a wt form of Rab 5 fused to green fluorescent protein (GFP) [34] was transfected using Lipofectamine Plus (Invitrogen) as described by the manufacturer.

2.8. Fluorescent labelling of BEI-inactivated virions and time-lapse fluorescence microscopy

Fractions containing the peak of inactivated virions after sucrose gradient sedimentation (Section 2.3) were pooled and dialyzed against PBS. Inactivated virions were incubated with amine reactive dye Alexa Fluor 555 succinimidyl ester (Invitrogen) following manufacturers instructions for protein labelling. Dye excess was eliminated from samples by extensive dialysis. Cells were grown on glass bottom tissue culture plates and experiments were carried out in medium without phenol red. Fluorescently labelled inactivated particles were adsorbed to cell monolayers for 1 h on ice. Non-bound particles were eliminated by washing and samples

were transferred to the microscope incubator previously warmed at 37 °C. Images (5 different planes along *Z* axis at intervals of 15 s for 20 min) were acquired using an inverted Axiovert200 microscope (Zeiss) coupled to a digital camera C9100-02 (Hamamatsu). Humidity, CO_2 and temperature (37 °C) were controlled using the In Vivo Cell Observer system (Zeiss). Trajectory and speed analysis of fluorescent particles were carried out automatically using Track Object tool of Metamorph 6.2r6 (Universal Imaging). After automated object tracking, it was revised and manually corrected if necessary.

3. Results

3.1. Inactivated FMDV can be internalized into cultured cells

To study how BEI affected FMDV particles, a stock of FMDV C-S8c1, produced in BHK-21 cells, was inactivated by BEI treatment and subjected to ultracentrifugation in a sucrose gradient under the standard conditions for purification of FMDV virions [31]. A single peak corresponding to protein (280 nm) and nucleic acid (260 nm) was observed by UV spectrophotometry of gradient fractions (Fig. S1A). The corresponding fractions contained spherical particles of around 30 nm in diameter, as revealed by electron microscopy (Fig. S1B). The observation that BEI inactivation preserved virion architecture prompted us to study the ability of these particles to be internalized into cultured cells, which, for the FMDV isolate C-S8c1 studied, is mediated by integrin recognition [35,36]. Inactivated FMDV was incubated with BHK-21 cells for 5 or 25 min. Cells were fixed and immunostained using MAb 5C4, which recognizes the discontinuous antigenic site D on FMDV capsid [37]. When these samples were observed by confocal microscopy after 5 min of incubation, FMDV antigen was detected mainly at cell periphery, being its distribution perinuclear after 25 min (Fig. 1A). Confirming the specificity of the assay, no fluorescence was observed either in mock-incubated cells or in cells incubated with BEI-treated EMCV, a picornavirus belonging to the cardiovirus genus (Fig. S2). Orthogonal sections of cells incubated 25 min with inactivated FMDV were performed from a series of optical sections across *Z* axis. In these sections, fluorescent spots were located inside the cell (Fig. 1B). Similar results were obtained for IBRS-2 cells incubated with BEI-inactivated FMDV (Fig. S3). These results indicate that BEI-inactivated FMDV retains its ability to be internalized by host cells.

3.2. Internalization of inactivated FMDV is dependent on integrins as cellular receptors

BEI-inactivation of FMDV does not affect the antigenicity of the G-H loop on VP1 protein (antigenic site A) [38], where the RGD motif that mediates FMDV attachment to cellular integrins is located [23,24]. The implication of VP1 G-H loop for cell entry of the BEI-inactivated FMDV was tested by using neutralizing MAb SD6, which recognizes an epitope located within the G-H loop [37]. Infectious or inactivated FMDV particles were preincubated with MAb SD6 and then added to cultured cells (Fig. 2). Immunofluorescence staining revealed that preincubation with MAb SD6 inhibited adsorption of infectious as well as BEI-inactivated FMDV particles. When the viruses were preincubated with the control irrelevant MAb I1 [39] specific fluorescence was detected, confirming the specificity of the inhibition exerted by MAb SD6. The antigenic preservation of the epitope recognized by MAb SD6 in BEI-inactivated FMDV suggested that these particles might be using integrins as cellular receptor for attachment and internalization. To test this possibility, BHK-21 cells were first incubated with synthetic peptides containing the RGD motif in VP1 and then with infectious or BEI-inactivated FMDV. In these experiments, MARLS, a derivative of C-S8c1 that is internalized using cellular receptors different from integrins [25,26] was included to probe the specificity of the inhibition of RGD-dependent entry of FMDV. Fluorescence to capsid proteins, revealed with MAb 5C4, could be detected only in those cells incubated with MARLS (Fig. 3A). When these viruses were tested in CHO cells, which lack expression of the integrin receptors used by FMDV [40], fluorescence to viral antigen was detected again only in cells incubated with MARLS (Fig. 3B). Taken together, these results indicate that, as described for infectious FMDV C-S8c1, BEI-inactivated C-S8c1 uses integrins as cellular receptors for attachment and internalization into cultured cells and that this interaction is mediated by residues located within G-H loop of VP1 capsid protein.

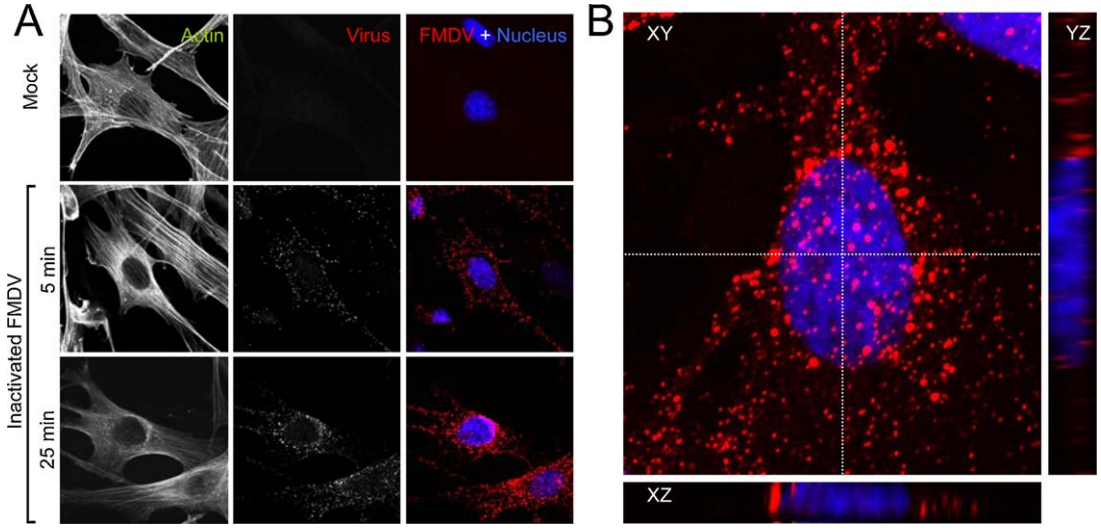

Fig. 1. BEI-inactivated FMDV antigens are internalized by cells. (A) BHK-21 cells were incubated with inactivated FMDV (10^7 PFU prior to inactivation, quantity equivalent at a MOI of 100) for 5 or 25 min at 37 °C, fixed and processed for immunofluorescence using MAb 5C4 and a secondary antibody coupled to Alexa Fluor 555. Actin staining using phalloidin coupled to Alexa Fluor 488 reveals cell shape. Cell nuclei were stained using To-Pro 3. Confocal images correspond to single optical sections at the middle plane level of the cell. (B) Maximum intensity projection of a series of planes through *Z* axis of cell incubated with inactivated FMDV (25 min) and processed for immunofluorescence as in (A). Dashed lines indicate the position of orthogonal sections (XZ and YZ) displayed.

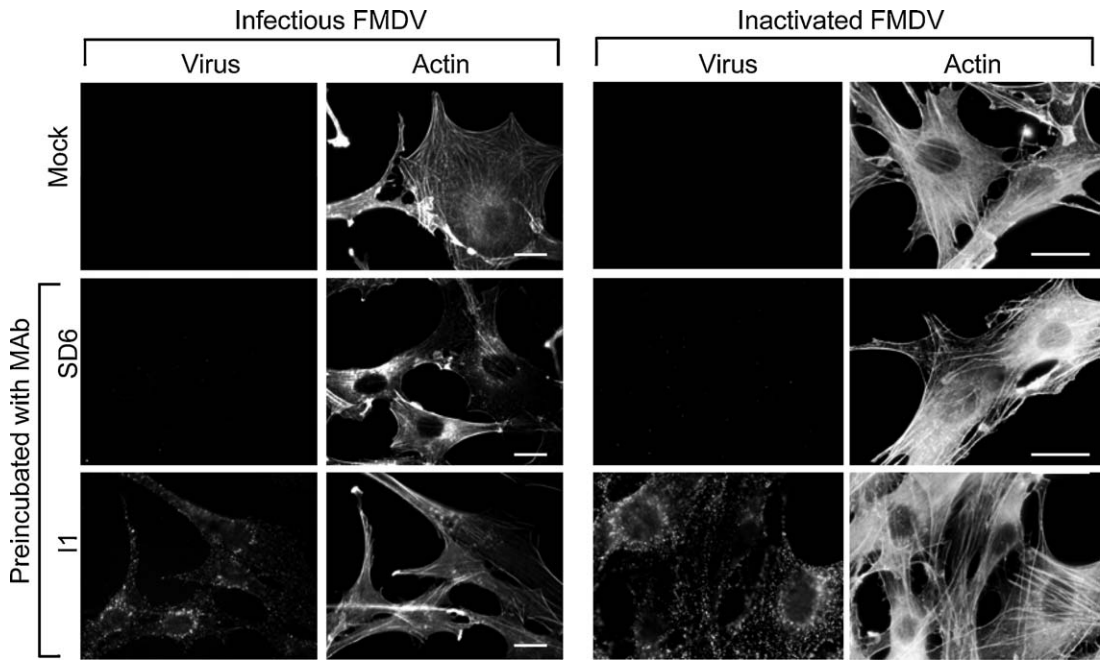

Fig. 2. Inhibition of inactivated FMDV cell binding by preincubation with neutralizing MAb SD6. Infectious or BEI-inactivated FMDV were preincubated with neutralizing MAb SD6 or the irrelevant MAb I1 as control. Samples were incubated with BHK-21 cells (as in Fig. 1, equivalent to a MOI of 100) for 25 min, fixed and processed for immunofluorescence using MAb 5C4 and a secondary antibody labelled with Alexa Fluor 555. Actin staining using phalloidin coupled to Alexa Fluor 488 reveals cell shape. Scale bars: 20 μm.

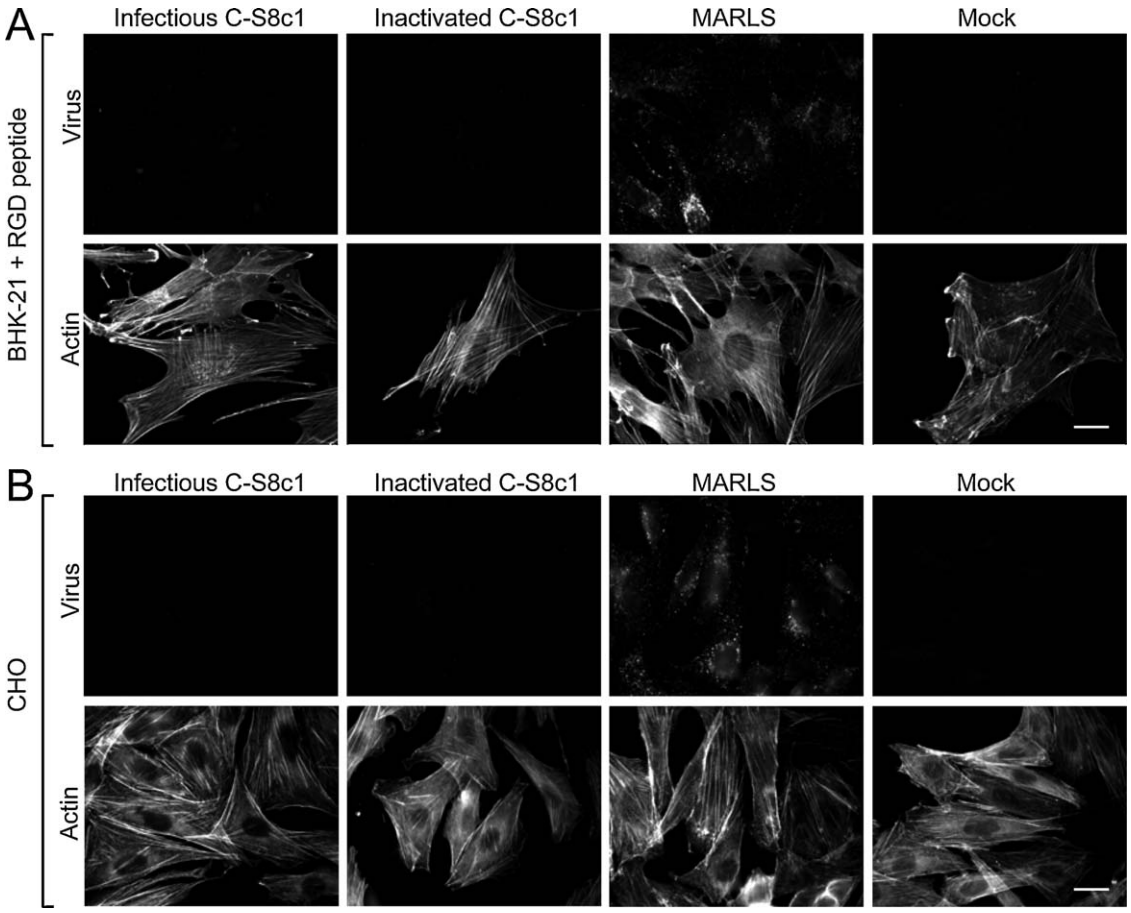

Fig. 3. Inactivated FMDV uses integrins as a receptor for cell entry. (A) Preincubation with RGD peptides inhibits inactivated FMDV cell binding. BHK-21 cells were preincubated with synthetic peptides and next incubated with infectious or inactivated viruses for 25 min (as in Fig. 1, equivalent to a MOI of 100). Cells were fixed and processed for immunofluorescence using MAb 5C4 and a secondary antibody labelled with Alexa Fluor 555. (B) Inactivated FMDV does not bind CHO cells. CHO cells were incubated with the different viruses, fixed and processed for immunofluorescence as in (A). Actin staining using phalloidin coupled to Alexa Fluor 488 reveals cell shape. Scale bars: 20 μm.

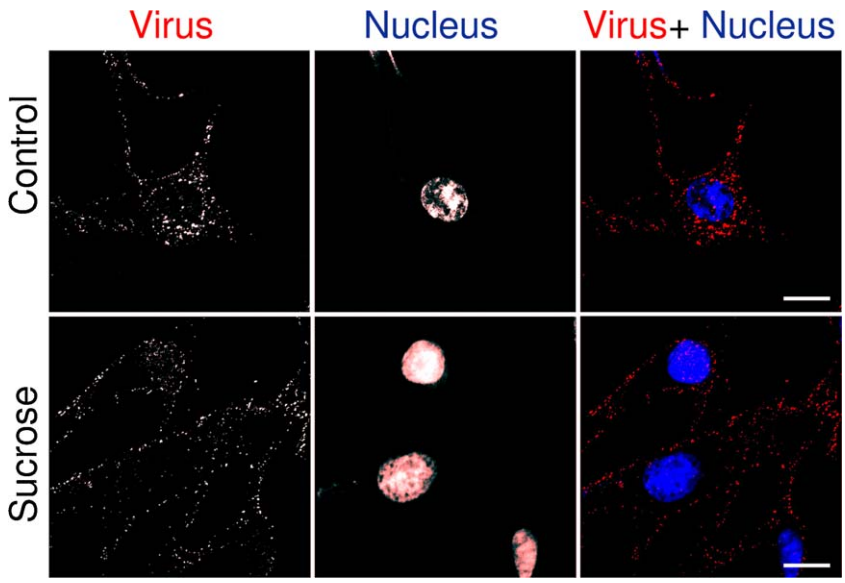

Fig. 4. Hypertonic medium inhibits internalization of inactivated FMDV. BHK-21 cells treated or not with 0.45 M sucrose were incubated with inactivated FMDV (as in Fig. 1, equivalent to a MOI of 100) for 25 min and processed for immunofluorescence using MAb 5C4 and a secondary antibody labelled with Alexa Fluor 555. Cell nuclei were stained with To-Pro 3. Confocal images correspond to a single optical section at the middle plane level of the cell. Scale bars: 20 μm.

3.3. Internalization of inactivated FMDV is inhibited by hypertonic medium

Hypertonic medium decreases the number of clathrin coated pits at the plasma membrane and reduces entry and infection of FMDV variants that use integrins as cellular receptors [20,21]. Cells treated or not with sucrose were incubated with BEI-inactivated FMDV and the location of viral antigens was revealed by immunofluorescence and confocal microscopy (Fig. 4). Control cells displayed an immunostaining pattern in which viral fluorescence mainly accumulated at the perinuclear region, as reported for infectious C-S8c1 [21]. In contrast, viral fluorescence was located at the cellular periphery in sucrose-treated cells, indicating that incubation with hypertonic medium inhibits internalization of BEI-inactivated FMDV.

3.4. Inactivated FMDV particles are sorted to early endosomes

It has been reported that FMDV particles are sorted to endosomal compartments after internalization [20,22,31]. To analyze whether BEI-inactivated FMDV particles followed this route, BHK-21 cells were transfected with a plasmid encoding the GFP-fused GTPase Rab5, a marker of early endosomes implicated in FMDV infection [41]. Transfected cells were incubated with inactivated FMDV and examined by confocal microscopy. Colocalization of inactivated FMDV with Rab5 was observed (Fig. 5), showing that inactivated particles of FMDV were directed to early endosomes.

3.5. Analysis of the interaction of inactivated FMDV with cultured cells by live fluorescence microscopy

A number of reports have shown the ability to track single virus particles by fluorescence microscopy after labelling with amino reactive dyes [42–44]. Following this approach, purified BEI-inactivated virions were labelled using an amine reactive dye (Alexa Fluor 555 succinimidyl ester), and their interaction with live cultured cells was analyzed by time-lapse fluorescence microscopy. After adsorption of fluorescent FMDV particles on ice, samples were transferred to the microscope chamber and incubated at 37 °C. A representative time-lapse experiment is shown in Movie S1. Remarkably, two distinct populations could be distinguished among fluorescent viral particles: one nearly static and the other displaying long and rapid displacements. Members of each of these populations are indicated in Fig. 6A. Particle speed along time was measured applying a single particle tracking algorithm, and maximum speed distribution was plotted as a histogram (Fig. 6B)

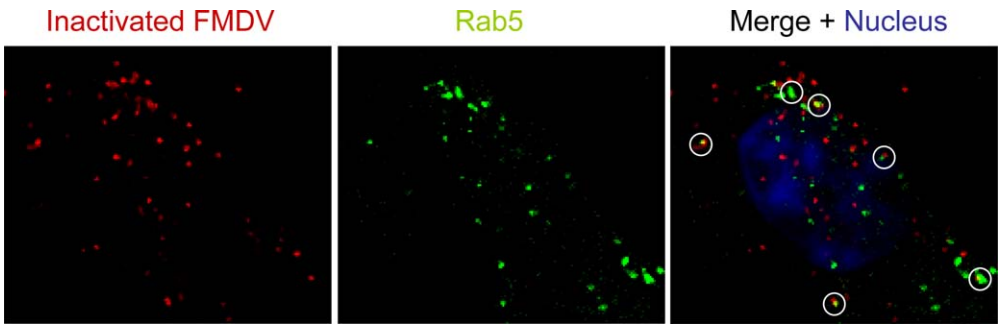

Fig. 5. Inactivated FMDV particles are sorted to early endosomes. BHK-21 cells transfected 24 h with a plasmid encoding Rab5 fused to GFP (green) were incubated with inactivated FMDV (as in Fig. 1, equivalent to MOI of 100) for 10 min, fixed and processed for immunofluorescence and confocal microscopy using MAb 5C4 and a secondary antibody labelled with Alexa Fluor 555 (red). Cell nucleus was stained with To-Pro 3 (blue). (For interpretation of the references to color in this figure caption, the reader is referred to the web version of the article.)

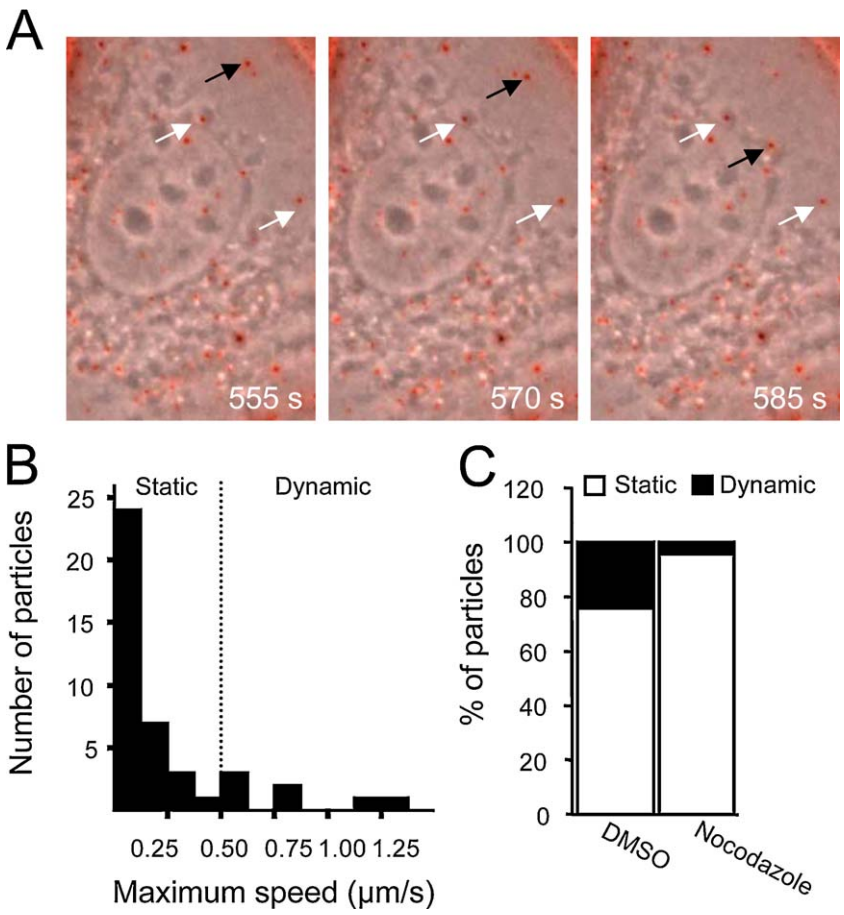

Fig. 6. Time-lapse microscopy analysis of labelled inactivated FMDV. (A) Selected time-lapse microscopy images from a cell incubated with fluorescently labelled BEI-inactivated FMDV (red) (see Section 2 for details). Black arrows indicate highly mobile spots while white arrows point to static spots. (B) Histogram summarizing the distribution of maximum speeds of the 42 fluorescent particles analyzed by single particle tracking. (C) Reduction on the proportion of dynamic spots upon nocodazole treatment. (For interpretation of the references to color in this figure caption, the reader is referred to the web version of the article.)

and individualized plots of the speed of each of the particles analyzed along time are shown in Fig. S4. Particles showing a speed of 0.5 μm/s or lower were considered as static while particles with higher speeds were considered as dynamic [45]. Based on this classification, about 80% of virus particles fell within static group while the remaining particles could be considered as dynamic. High speed movements of viral particles after uptake, could rely on the internalization on endosomes that are subjected to transport mediated by microtubules [46,47]. To test this hypothesis, live fluorescence microscopy experiments were carried out in the presence or in the absence of the microtubule depolymerizing agent nocodazole (Fig. 6C). These experiments showed a statistically significant reduction in the proportion of dynamic particles (ANOVA *P*-value 0.034), suggesting the involvement of microtubules in the rapid movements of these particles. These results illustrate the potential for the study of virus cell interaction of the use of BEI-inactivated FMDV in combination with fluorescent labels and time-lapse microscopy.

4. Discussion

Vaccines based on BEI inactivation play a key role in FMD control and BEI has replaced other less efficient inactivants, such as formaldehyde, in vaccine production [14,48]. By means of sucrose sedimentation and electron microscopy analyses, viral particles were observed in BEI-inactivated FMDV samples, indicating that BEI preserved virion architecture, which is consistent with the antigenic preservation of BEI-treated FMDVs [38,49]. Inactivated particles were efficiently internalized by cultured cells, maintaining the general features described for the integrin-dependent internalization of the infectious C-S8c1 FMDV used in these experiments [21,28]. Thus, binding and internalization of inactivated particles was shown to be dependent on residues encompassed in the VP1 G-H loop of FMDV capsid and on the use of cellular integrins as viral receptors. Internalization was also inhibited by hypertonic medium, suggesting that it was dependent on clathrin-mediated endocytosis, and inactivated viral particles were directed to early endosomes. These results are consistent with those previously reported for infectious FMDV [20,21,28,31,41], confirming that BEI treatment renders inactivated virus particles that reproduce the attachment and internalization of infectious FMDV.

The results obtained enabled us to perform time-lapse fluorescence microscopy studies on the internalization of FMDV using BEI-inactivated particles as a model for virus entry. Live fluorescence microscopy showed two distinct behaviours within viral particles. One major population (about 80%) displayed slow movements in contrast to a minority of particles (about 20%) that underwent rapid microtubule-mediated movements, since proportion of the latter population could be reduced by nocodazole treatment. These two different populations of particles undergoing internalization have been reported for other viral models such as dengue virus as well as for cellular ligands [45,46]. The observation that the majority of FMDV particles did not display microtubule-mediated motility was consistent with the lack of effect of nocodazole treatment on FMDV infection [20,28]. Ligands destined for degradation are preferentially targeted to the

small population of dynamic early endosomes (which rapidly undergoes microtubule-mediated maturation towards late endosomes/lysosomes), whereas recycling ligands as transferrin are non-selectively targeted to all early endosomes and being enriched in the larger population of static, slowly maturing early endosomes [46]. As the major proportion of internalized FMDV particles was sorted to the static endosome population, this should imply that only a small fraction of inactivated FMDV particles easily reaches late endosomal compartments. Indeed, colocalization of infectious FMDV particles with the recycling ligand transferrin, but not with lysosomes has been reported [20,22]. In this way, the ability of BEI-inactivated FMDV to gain entry into cultured cells through a pathway similar to that of infectious virions, provides an interesting tool to study FMDV–cell interactions in the absence of translation and replication of viral RNA.

Studies performed with infectious FMDV have shown that viral particles can be internalized into diverse types of antigen presenting cells using RGD-independent receptors, such as heparan sulfate or Fc receptors, the latter after viral binding with specific antibodies [50–52]. In addition, and regarding the analysis of inactivated FMDV–cell interactions, the limited evidence available suggests that inactivated FMDV can be also internalized by dendritic cells in a receptor specific pathway [51,53]. Our results indicate that viral particles included within BEI-inactivated suspensions used for vaccine formulation, could be also internalized (via an RGD-dependent pathway) by cells that express integrins susceptible to be used as FMDV receptors. This scenario opens new possibilities for understanding the modulation of the immune response elicited by conventional FMDV vaccines. Thus, internalization of inactivated virus by susceptible cells could diminish the amount of viral immunogen able to interact with immune cells and establish a protective immune response. On the other hand, internalization of inactivated virus could trigger immune innate response mechanisms as those based on viral sensors located along the endocytic pathway [54]. This potential innate response should localize at specific tissues susceptible for FMDV infection, thus generating an antiviral state that could help to prevent FMDV infection and spread, since innate immune response may play an important role in FMDV protection [55,56]. In addition, internalization of BEI-inactivated particles to early endosomes could allow antigen processing and epitope presentation by pathways other than that mediated by the MHC class II [57]. Such possibility could contribute to explain previous reports on the induction of CD8+ T cell responses in pigs and cattle vaccinated with BEI-inactivated vaccines [58–60]. Along this line, the small proportion of inactivated viral particles sorted to the dynamic early endosome population revealed by time lapse microscopy (about 20%) could also be relevant for immune response they ellicit, as these endosomes are supposed to rapid maturate to late endosomes/lysosomes and could modulate antigen presentation either by promoting antigen processing or by favouring antigen degradation.

The findings here presented indicate that BEI-inactivated FMDV particles used for vaccine formulation can be internalized in an integrin-dependent pathway to early endosomal compartments. Modulation of the interaction of these particles with different host cells may open new possibilities for vaccine optimization. On the other hand, BEI-inactivated particles provide an interesting tool to study the early steps of FMDV–cell interactions enabling separation between FMDV internalization and productive infection.

Acknowledgements

We thank E. Domingo for FMDV MARLS and MAb SD6, E. Brocchi for MAb 5C4, M. Sáiz for CHO cell line, J. A. Esteban for plasmid encoding Rab5, and M. T. Rejas for her assistance with electron microscopy. This work was supported by Spanish grants BIO2008-0447-C03-01, CSD2006-0007 and by an institutional grant from Fundación Ramón Areces.

Appendix A. Supplementary data

Supplementary data associated with this article can be found, in the online version, at doi:10.1016/j.vaccine.2011.10.031.

References

[1] Grubman MJ, Baxt B. Foot-and-mouth disease. Clin Microbiol Rev 2004;17(April (2)):465–93.
[2] Saiz M, Nunez JI, Jimenez-Clavero MA, Baranowski E, Sobrino F. Foot-and-mouth disease virus: biology and prospects for disease control. Microbes Infect/Institut Pasteur 2002;4(September (11)):1183–92.
[3] Cottam EM, Wadsworth J, Shaw AE, Rowlands RJ, Goatley L, Maan S, et al. Transmission pathways of foot-and-mouth disease virus in the United Kingdom in 2007. PLoS Pathog 2008;4(April (4)):e1000050.
[4] Pluimers FH, Akkerman AM, van der Wal P, Dekker A, Bianchi A. Lessons from the foot and mouth disease outbreak in The Netherlands in 2001. Revue scientifique et technique (International Office of Epizootics) 2002;21(December (3)):711–21.
[5] Sobrino F, Domingo E. Foot-and-mouth disease in Europe, FMD is economically the most important disease of farm animals. Its re-emergence in Europe is likely to have consequences that go beyond severe alterations of livestock production and trade. EMBO Rep 2001;2(June (6)):459–61.
[6] Thompson D, Muriel P, Russell D, Osborne P, Bromley A, Rowland M, et al. Economic costs of the foot and mouth disease outbreak in the United Kingdom in 2001. Revue scientifique et technique (International Office of Epizootics) 2002;21(December (3)):675–87.
[7] Chinsangaram J, Mason PW, Grubman MJ. Protection of swine by live and inactivated vaccines prepared from a leader proteinase-deficient serotype A12 foot-and-mouth disease virus. Vaccine 1998;16(October (16)):1516–22.
[8] Mason PW, Piccone ME, McKenna TS, Chinsangaram J, Grubman MJ. Evaluation of a live-attenuated foot-and-mouth disease virus as a vaccine candidate. Virology 1997;227(January (1)):96–102.
[9] Niborski V, Li Y, Brennan F, Lane M, Torche AM, Remond M, et al. Efficacy of particle-based DNA delivery for vaccination of sheep against FMDV. Vaccine 2006;24(November (49–50)):7204–13.
[10] Wong HT, Cheng SC, Chan EW, Sheng ZT, Yan WY, Zheng ZX, et al. Plasmids encoding foot-and-mouth disease virus VP1 epitopes elicited immune responses in mice and swine and protected swine against viral infection. Virology 2000;278(December (1)):27–35.
[11] Cubillos C, de la Torre BG, Jakab A, Clementi G, Borras E, Barcena J, et al. Enhanced mucosal immunoglobulin A response and solid protection against foot-and-mouth disease virus challenge induced by a novel dendrimeric peptide. J Virol 2008;82(July (14)):7223–30.
[12] Taboga O, Tami C, Carrillo E, Nuñez JI, Rodríguez A, Sáiz JC, et al. A large-scale evaluation of peptide vaccines against foot-and-mouth disease: lack of solid protection in cattle and isolation of escape mutants. J Virol 1997;71(April (4)):2606–14.
[13] Bahnemann HG. Binary ethylenimine as an inactivant for foot-and-mouth disease virus and its application for vaccine production. Arch Virol 1975;47(1):47–56.
[14] Barteling SJ. Modern inactivated foot-and-mouth disease (FMD) vaccines: historical background and key elements in production and use. In: Sobrino F, Domingo E, editors. Foot and mouth disease: current perspectives. Norfolk: Horizon Bioscience; 2004.
[15] Brown F. Inactivation of viruses by aziridines. Vaccine 2001;20(November (3–4)):322–7.
[16] Barnett PV, Statham RJ, Vosloo W, Haydon DT. Foot-and-mouth disease vaccine potency testing: determination and statistical validation of a model using a serological approach. Vaccine 2003;21(July (23)):3240–8.
[17] Guzman E, Taylor G, Charleston B, Ellis SA. Induction of a cross-reactive CD8(+) T cell response following foot-and-mouth disease virus vaccination. J Virol 2010;84(December (23)):12375–84.
[18] McCullough KC, Sobrino F. Immunology of foot-and-mouth disease. In: Sobrino F, Domingo E, editors. Foot and mouth disease: current perspectives. Norfolk: Horizon Bioscience; 2004.
[19] Isaacson MK, Juckem LK, Compton T. Virus entry and innate immune activation. Curr Top Microbiol Immunol 2008;325:85–100.
[20] Berryman S, Clark S, Monaghan P, Jackson T. Early events in integrin alphavbeta6-mediated cell entry of foot-and-mouth disease virus. J Virol 2005;79(July (13)):8519–34.
[21] Martín-Acebes MA, González-Magaldi M, Sandvig K, Sobrino F, Armas-Portela R. Productive entry of type C foot-and-mouth disease virus into susceptible cultured cells requires clathrin and is dependent on the presence of plasma membrane cholesterol. Virology 2007;369(December (1)):105–18.
[22] O'Donnell V, LaRocco M, Duque H, Baxt B. Analysis of foot-and-mouth disease virus internalization events in cultured cells. J Virol 2005;79(July (13)):8506–18.

[23] Baxt B, Becker Y. The effect of peptides containing the arginine-glycine-aspartic acid sequence on the adsorption of foot-and-mouth disease virus to tissue culture cells. Virus Genes 1990;4(June (1)):73–83.
[24] Burman A, Clark S, Abrescia NG, Fry EE, Stuart DI, Jackson T. Specificity of the VP1 GH loop of foot-and-mouth disease virus for alphav integrins. J Virol 2006;80(October (19)):9798–810.
[25] Baranowski E, Ruiz-Jarabo CM, Sevilla N, Andreu D, Beck E, Domingo E. Cell recognition by foot-and-mouth disease virus that lacks the RGD integrin-binding motif: flexibility in aphthovirus receptor usage. J Virol 2000;74(February (4)):1641–7.
[26] Baranowski E, Sevilla N, Verdaguer N, Ruiz-Jarabo CM, Beck E, Domingo E. Multiple virulence determinants of foot-and-mouth disease virus in cell culture. J Virol 1998;72(August (8)):6362–72.
[27] Sá-Carvalho D, Rieder E, Baxt B, Rodarte R, Tanuri A, Mason PW. Tissue culture adaptation of foot-and-mouth disease virus selects viruses that bind to heparin and are attenuated in cattle. J Virol 1997;71(July (7)):5115–23.
[28] Martín-Acebes MA, González-Magaldi M, Vázquez-Calvo A, Armas-Portela R, Sobrino F. Internalization of swine vesicular disease virus into cultured cells: a comparative study with foot-and-mouth disease virus. J Virol 2009;83(May (9)):4216–26.
[29] Sobrino F, Dávila M, Ortín J, Domingo E. Multiple genetic variants arise in the course of replication of foot-and-mouth disease virus in cell culture. Virology 1983;128(July (2)):310–8.
[30] Rosas MF, Vieira YA, Postigo R, Martin-Acebes MA, Armas-Portela R, Martinez-Salas E, et al. Susceptibility to viral infection is enhanced by stable expression of 3A or 3AB proteins from foot-and-mouth disease virus. Virology 2008;380(October (1)):34–45.
[31] Martín-Acebes MA, Rincón V, Armas-Portela R, Mateu MG, Sobrino F. A single amino acid substitution in the capsid of foot-and-mouth disease virus can increase acid lability and confer resistance to acid-dependent uncoating inhibition. J Virol 2010;84(March (6)):2902–12.
[32] García-Arriaza J, Manrubia SC, Toja M, Domingo E, Escarmís C. Evolutionary transition toward defective RNAs that are infectious by complementation. J Virol 2004;78(November (21)):11678–85.
[33] Martin-Acebes MA, Herrera M, Armas-Portela R, Domingo E, Sobrino F. Cell density-dependent expression of viral antigens during persistence of foot-and-mouth disease virus in cell culture. Virology 2010;403(July (1)):47–55.
[34] Brown TC, Tran IC, Backos DS, Esteban JA. NMDA receptor-dependent activation of the small GTPase Rab5 drives the removal of synaptic AMPA receptors during hippocampal LTD. Neuron 2005;45(January (1)):81–94.
[35] Mateu MG, Valero ML, Andreu D, Domingo E. Systematic replacement of amino acid residues within an Arg-Gly-Asp-containing loop of foot-and-mouth disease virus and effect on cell recognition. J Biol Chem 1996;271(May (22)):12814–9.
[36] Nuñez JI, Molina N, Baranowski E, Domingo E, Clark S, Burman A, et al. Guinea pig-adapted foot-and-mouth disease virus with altered receptor recognition can productively infect a natural host. J Virol 2007;81(August (16)):8497–506.
[37] Lea S, Hernandez J, Blakemore W, Brocchi E, Curry S, Domingo E, et al. The structure and antigenicity of a type C foot-and-mouth disease virus. Structure 1994;2(February (2)):123–39.
[38] Patil PK, Suryanarayana V, Bist P, Bayry J, Natarajan C. Integrity of GH-loop of foot-and-mouth disease virus during virus inactivation: detection by epitope specific antibodies. Vaccine 2002;20(January (7–8)):1163–8.
[39] Lefrancois L, Lyles DS. The interaction of antibody with the major surface glycoprotein of vesicular stomatitis virus. II. Monoclonal antibodies of non-neutralizing and cross-reactive epitopes of Indiana and New Jersey serotypes. Virology 1982;121(August (1)):168–74.
[40] Gutierrez-Rivas M, Pulido MR, Baranowski E, Sobrino F, Sáiz M. Tolerance to mutations in the foot-and-mouth disease virus integrin-binding RGD region is different in cultured cells and in vivo and depends on the capsid sequence context. J Gen Virol 2008;89(October (Pt 10)):2531–9.
[41] Johns HL, Berryman S, Monaghan P, Belsham GJ, Jackson T. A dominant-negative mutant of rab5 inhibits infection of cells by foot-and-mouth disease virus: implications for virus entry. J Virol 2009;83(June (12)):6247–56.
[42] Brandenburg B, Lee LY, Lakadamyali M, Rust MJ, Zhuang X, Hogle JM. Imaging Poliovirus Entry in Live Cells. PLoS Biol 2007;5(July (7)):e183.
[43] Pelkmans L, Kartenbeck J, Helenius A. Caveolar endocytosis of simian virus 40 reveals a new two-step vesicular-transport pathway to the ER. Nat Cell Biol 2001;3(May (5)):473–83.
[44] Pietiäinen V, Marjomäki V, Upla P, Pelkmans L, Helenius A, Hyypiä T. Echovirus 1 endocytosis into caveosomes requires lipid rafts, dynamin II, and signaling events. Mol Biol Cell 2004;15(November (11)):4911–25.
[45] van der Schaar HM, Rust MJ, Waarts BL, van der Ende-Metselaar H, Kuhn RJ, Wilschut J, et al. Characterization of the early events in dengue virus cell entry by biochemical assays and single-virus tracking. J Virol 2007;81(November (21)):12019–28.
[46] Lakadamyali M, Rust MJ, Zhuang X. Ligands for clathrin-mediated endocytosis are differentially sorted into distinct populations of early endosomes. Cell 2006;124(March (5)):997–1009.
[47] Vonderheit A, Helenius A. Rab7 associates with early endosomes to mediate sorting and transport of Semliki forest virus to late endosomes. PLoS Biol 2005;3(July (7)):e233.
[48] Doel TR. FMD vaccines. Virus Res 2003;91(January (1)):81–99.
[49] Aarthi D, Ananda Rao K, Robinson R, Srinivasan VA. Validation of binary ethylenimine (BEI) used as an inactivant for foot and mouth disease tissue culture vaccine. Biologicals 2004;32(September (3)):153–6.
[50] Baxt B, Mason PW. Foot-and-mouth disease virus undergoes restricted replication in macrophage cell cultures following Fc receptor-mediated adsorption. Virology 1995;207(March (2)):503–9.
[51] Harwood LJ, Gerber H, Sobrino F, Summerfield A, McCullough KC. Dendritic cell internalization of foot-and-mouth disease virus: influence of heparan sulfate binding on virus uptake and induction of the immune response. J Virol 2008;82(July (13)):6379–94.
[52] Robinson L, Windsor M, McLaughlin K, Hope J, Jackson T, Charleston B. Foot-and-mouth disease virus exhibits an altered tropism in the presence of specific immunoglobulins, enabling productive infection and killing of dendritic cells. J Virol 2011;85(March (5)):2212–23.
[53] Jin H, Xiao C, Zhao G, Du X, Yu Y, Kang Y, et al. Induction of immature dendritic cell apoptosis by foot and mouth disease virus is an integrin receptor mediated event before viral infection. J Cell Biochem 2007;102(November (4)):980–91.
[54] Kawai T, Akira S. Toll-like receptor and RIG-I-like receptor signaling. Ann N Y Acad Sci 2008;1143(November):1–20.
[55] Summerfield A, Guzylack-Piriou L, Harwood L, McCullough KC. Innate immune responses against foot-and-mouth disease virus: current understanding and future directions. Vet Immunol Immunopathol 2009;128(March (1–3)):205–10.
[56] Grubman MJ, Moraes MP, Diaz-San Segundo F, Pena L, de los Santos T. Evading the host immune response: how foot-and-mouth disease virus has become an effective pathogen. FEMS Immunol Med Microbiol 2008;53(June (1)): 8–17.
[57] Burgdorf S, Kurts C. Endocytosis mechanisms and the cell biology of antigen presentation. Curr Opin Immunol 2008;20(February (1)):89–95.
[58] Saiz JC, Rodriguez A, Gonzalez M, Alonso F, Sobrino F. Heterotypic lymphoproliferative response in pigs vaccinated with foot-and-mouth disease virus, Involvement of isolated capsid proteins. J Gen Virol 1992;73(October (Pt 10)):2601–7.
[59] Garcia-Valcarcel M, Doel T, Collen T, Ryan M, Parkhouse RM. Recognition of foot-and-mouth disease virus and its capsid protein VP1 by bovine peripheral T lymphocytes. J Gen Virol 1996;77(April (Pt 4)):727–35.
[60] Guzman E, Taylor G, Charleston B, Skinner MA, Ellis SA. An MHC-restricted CD8+ T-cell response is induced in cattle by foot-and-mouth disease virus (FMDV) infection and also following vaccination with inactivated FMDV. J Gen Virol 2008;89(March (Pt 3)):667–75.

Virus Research 167 (2012) 125–137

Contents lists available at SciVerse ScienceDirect

Virus Research

journal homepage: www.elsevier.com/locate/virusres

Review

Acid-dependent viral entry

Ángela Vázquez-Calvo[a], Juan-Carlos Saiz[b], Kenneth C. McCullough[c], Francisco Sobrino[a,*], Miguel A. Martín-Acebes[a]

[a] Centro de Biología Molecular "Severo Ochoa" (CSIC-UAM), Cantoblanco, 28049 Madrid, Spain
[b] Departamento de Biotecnología. Instituto Nacional de Investigación y Tecnología Agraria y Alimentaria (INIA), 28040 Madrid, Spain
[c] Institute of Virology and Immunoprophylaxis, CH-3147 Mittelhäusern, Switzerland

ARTICLE INFO

Article history:
Received 7 March 2012
Received in revised form 28 May 2012
Accepted 29 May 2012
Available online 7 June 2012

Keywords:
Viral internalisation
Acidic pH
Endosome
Uncoating
Membrane fusion

ABSTRACT

Virus infection of host cells requires that entry into the cell results in efficient genome release leading to translation and replication. These initial steps revolving around the entry and genomic release processes are crucial for viral progeny generation. Despite the variety of receptors used by viruses to initiate entry, evidence from both enveloped and non-enveloped viral infections is highlighting the important role played by intracellular acidic compartments in the entry of many viruses. These compartments provide connecting nodes within the endocytic network, presenting multiple viral internalization pathways. Endosomal compartments employing an internal acidic pH can trigger molecular mechanisms leading to disassembly of viral particles, thus providing appropriate genome delivery. Accordingly, viruses have evolved to select optimal intracellular conditions for promoting efficient genome release, leading to propagation of the infectious agent. This review will address the implications of cellular compartment involvement in virus infectious processes, and the roles played by the viruses' own machinery, including pH sensing mechanisms and the methodologies applied for studying acid-dependent viral entry into host cells.

Contents

* Corresponding author. Tel.: +34 91 1964493; fax: +34 91 1964420.
E-mail addresses: avazquez@cbm.uam.es (Á. Vázquez-Calvo), jcsaiz@inia.es (J.-C. Saiz), kmc.projects1@gmail.com (K.C. McCullough), fsobrino@cbm.uam.es (F. Sobrino), mamartin@cbm.uam.es (M.A. Martín-Acebes).

0168-1702/$ – see front matter © 2012 Elsevier B.V. All rights reserved.
http://dx.doi.org/10.1016/j.virusres.2012.05.024

1. Introduction

Cells use a broad spectrum of mechanisms for internalizing substances in their environment (Benmerah and Lamaze, 2007; Conner and Schmid, 2003a; Mayor and Pagano, 2007; Sandvig and van Deurs, 2005). With viral infection being reproducible and readily measurable, viruses have become useful probes for the analysis of endocytic routes (Pelkmans, 2005; Pelkmans et al., 2005; Pelkmans and Helenius, 2003). Initially, two different routes for virus entry were distinguished, based on the morphology of the cellular vesicular structures into which the viruses were internalized. These structures are known as clathrin-coated vesicles and non-clathrin dependent vesicles (Marsh and Helenius, 1989). Indeed, our current knowledge of endocytic routes groups them as clathrin-dependent and clathrin-independent endocytosis; the latter includes micropinocytosis, macropinocytosis, phagocytosis and caveolae-dependent endocytosis (Brandenburg and Zhuang, 2007; Damm and Pelkmans, 2006; Gruenberg, 2009; Marsh and Helenius, 2006; Mercer et al., 2010a,b; Sieczkarski and Whittaker, 2005; Thorley et al., 2010; Tsai, 2007). The form taken by the endocytic process is dependent on the cellular machinery involved, and the type of material to be internalised. While micropinocytosis tends to involve relatively non-particulate material such as macromolecules, the other processes have all been linked to the uptake of different viruses. Phagocytosis is a rather loosely applied term, often referring to uptake of large particles and immune complexes. Nevertheless, it has much in common with macropinocytosis in terms of the signalling cascades and intracellular events which follow internalisation.

Recent studies on the routes and mechanisms of viral entry have demonstrated that the different endocytic processes cannot be regarded in isolation. It is now know that there are a number of interconnections among endocytic components and routes, observable as complex networks of internalisation pathways rather than simplistic "linear" routes. The present review will focus on showing how the growing evidence of the roles played by intracellular endocytic compartments is demonstrating the diversity of the processes and interactions involved. In particular, the importance of the low pH associated with maturing endosomes, and the connecting nodes within the endocytic network of multiple internalisation pathways, are of major importance in determining the outcome of virus entry into the host cell. Not only will the pH of the endocytic pathways relate to the success of the replicative cycle for many viruses, it will also determine the outcome of processing by cells of the innate immune system.

2. General concepts in viral entry

As a first requisite for infection, the virus must interact with the surface of the host cell in a process commonly referred as attachment. One general element therein is the ability of certain molecules and structures on the virus particle surface to act as ligands for particular cell receptors, which in turn gives rise to cell and host tropisms (Baranowski et al., 2001). The majority of viruses use specific cellular proteins as receptors, but viruses can also use lipids and sugars to this end. Examples of viruses in the latter category are vesicular stomatitis virus, which may interact directly with phosphatidylserine (Schlegel et al., 1983), and polyomaviruses, which attach to gangliosides (lipids with attached sugars) (Low et al., 2006; Magaldi et al., 2012; Tsai et al., 2003; Tsai and Qian, 2010).

When viral surface molecules bind to their cellular receptors, akin to the natural ligand binding, the receptor is modulated to initiate a cascade of events involving transposition of the receptor, and therefore the virus interacting with it. This is often regulated by kinase and phosphatase activities associated with that receptor. The consequence is activation of particular endocytic pathways associated with ligation of that receptor, promoting internalisation of the virus-receptor complex (Coyne et al., 2007a; Liberali et al., 2008; Pelkmans et al., 2005). There is quite some diversity in both receptor–ligand interaction and endocytic processing, as witnessed by the reports over 200 known cellular kinases involved in endocytosis mechanisms (Pelkmans et al., 2005).

A key point for viral entry, essential for successful virus infection and replication, is the release of viral genomic material at the appropriate site within the host cell. This process is important to enable both genome replication and synthesis of the encoded viral proteins, necessary for both replication and viral particle assembly (maturation). Although enveloped and non-enveloped viruses can share similar mechanisms of internalisation, one may already observe major differences between them. Enveloped viruses can release their genome either naked or associated with nucleocapsid components, via the fusion of viral envelope with a cellular membrane (Harrison, 2008b). This process can occur at the plasma membrane or inside endocytic compartments. In the case of non-enveloped virus, their lack of a viral envelope requires that membrane penetration be mediated through perturbation of the membrane structure, as witnessed with the formation of pores due to ion channel activities (Tsai, 2007), or disruption of endocytic vesicle membranes through modification of the membrane structure or adsorption of protons through the proton sponge effect. Despite such differences among enveloped and non-enveloped viruses, and important component is the role played by low pH inside endocytic compartments.

3. Endocytic pathways and low pH compartments

Virus entry, and involvement of the acidifying endosomal system therein, is dependent not only on the virus, but also on the cell receptor and signalling pathways involved (examples of viruses entering through different pathways, but having in common requirements for acidifying processes leading to initiation of their replicative cycle, are shown in Table 1). The characteristics of this relationship will also vary dependent on the cell type. For example, virus infection of an epithelial cell via clathrin mediated endocytosis may perfectly suit the virus. Therein, the endocytic pathway would acidify in a manner favouring virus uncoating and genome release into the cytosol before the maturing endosomes would become too degradative. In contrast, activated macrophages may present a less favourable intracellular environment for a virus, even when using the same endocytic processes as the epithelial cell; an activated macrophage can present a more rapidly acidifying endosomal pathway, and therefore maturing endosomes, particularly when linked to clathrin-mediated endocytosis. Such characteristics of different cell types is important when considering not only how a virus evolved to survive, but also how evolution developed a powerful acidifying endosomal system for

Table 1
Examples of receptors and entry mechanisms used by viruses dependent on acid pH for infection.

Virus	Receptor	Entry route[a]	References
Adenoviridae			
Adenovirus 2	Coxsackievirus and adenovirus receptor (CAR), $\alpha_v$integrins	Clathrin pits and macropinocytosis	Meier et al. (2002)
Adenovirus 3	CD46, $\alpha_v$integrins	Macropinocytosis	Amstutz et al. (2008)
Adenovirus 5	CAR, $\alpha_v$integrins	Clathrin pits	Chardonnet and Dales (1970) and Gastaldelli et al. (2008)
Rhabdoviridae			
Vesicular stomatitis virus	Phosphatidylserine	Clathrin pits	Johannsdottir et al. (2009), Matlin et al. (1982), Simpson et al. (1969), and Sun et al. (2005)
Orthomyxoviridae			
Influenza virus	Sialic acid	Clathrin pits	Chen and Zhuang (2008) and Matlin et al. (1981)
		Non-clathrin, non-caveolin	Sieczkarski and Whittaker (2002b)
Arenaviridae			
Lymphocytic choriomeningitis virus	α-distroglycan	Non-clathrin, non-caveolin[b]	Borrow and Oldstone (1994), Quirin et al. (2008), and Rojek et al. (2008a)
		Clathrin pits	Quirin et al. (2008)
Lassa fever virus	α-distroglycan	Clathrin pits	Vela et al. (2007)
		Non-clathrin, non-caveolin[b]	Rojek et al. (2008b)
Junin virus	Transferrin receptor	Clathrin pits	Martínez et al. (2007)
Picornaviridae			
Human rhinovirus 2	Low density lipoprotein receptor	Non-clathrin	Bayer et al. (2001)
		Clathrin pits	Snyers et al. (2003)
Foot-and-mouth disease virus	Integrins $\alpha_v\beta_1$, $\alpha_v\beta_3$, $\alpha_v\beta_6$ $\alpha_v\beta_8$	Clathrin pits	Berryman et al. (2005), Martin-Acebes et al. (2007), and O'Donnell et al. (2005)
	Heparan sulfate (cell culture adapted virus)	Caveolae	O'Donnell et al. (2008)
Flaviviridae			
Dengue virus		Clathrin pits	Acosta et al. (2008), Krishnan et al. (2007), and Mosso et al. (2008)
West Nile virus	Integrin $\alpha_v\beta_3$	Clathrin pits	Chu and Ng (2004a,b) and Krishnan et al. (2007)
	Non integrin $\alpha_v\beta_3$	Lipid rafts	Medigeshi et al. (2008)
Togaviridae			
Semliki Forest virus	MHC I	Clathrin pits	Helenius et al. (1980)

[a] Non-clathrin, non-caveolin is used in a wide sense, and refers to endocytic pathways independent of clathrin and caveolin. Lipid rafts refers to internalisation routes in which these plasma membrane microdomains have been implied, but caveolin function has not been proven.
[b] Dynamin independent.

innate immune defence cells. Certainly, a number of viruses evolved a preference for infecting epithelial cells; their interaction with macrophages can lead to abortive infection and destruction of the infectious threat. Despite this, there are viruses which evolved to survive in degradative innate defence cells such as macrophages and dendritic cells – generally termed monocytotropic viruses, even though dendritic cells are not always derived from monocytes. Moreover, some viruses targeting macrophages and dendritic cells can have an obligate requirement for infection therein. An example is seen with African swine fever virus (ASFV) (McCullough et al., 1999), which actually requires an efficient acidifying endosomal system in the macrophage to initiate its replicative cycle (Natale and McCullough, 1998). Indeed, these conditions are met in the macrophages, but not in the more endocytically quiescent monocytes (Basta et al., 2010, 1999; McCullough et al., 1993).

Consequently, it is important to compare the different endocytic pathways with respect to how viruses have evolved in different directions related to their requirements for low pH. It is also important to appreciate this in terms of the cells targeted by the virus for infection, compared with how the host seeks to defend itself against the virus. Certainly, not all viruses evolved to require the acidifying endosomal system for initiating their replicative cycle. Moreover, certain viruses can use alternative pathways, or directly penetrate the cell via the plasma membrane. Considering the apparently fine line between initiation of virus replication and degradation by acidifying cellular processes, this review will focus on such pathways. Information will be summarised, demonstrating how virus entry can lead to relocation of the virus inside acidic compartments leading to initiation of virus replication as opposed to its degradation by the cell (Fig. 1).

3.1. Clathrin-mediated endocytosis

3.1.1. The importance of clathrin-dependency

Considering the number of viruses with which clathrin-dependent entry has been associated (Mercer et al., 2010b) gives the impression that this is the dominant form for virus entry. Clathrin-mediated endocytosis (Fig. 1A and B) is the most widely characterized virus entry route, but this may have influenced the number of reports in this area. Studies on virus interaction with cells are now showing that a wide variety of viruses are more diverse in terms of the mechanisms employed. Consequently, it is important to remember that while clathrin-mediated endocytic processes remain a major contributor to infection by many viruses, these cellular processes are not exclusive in this context.

Clathrin-dependent virus entry was first described from electron microscopy observations of comb-like coats on the cytoplasmic face of plasma membrane invaginations – bristle-coated pits, now also referred to as clathrin-coated pits, or just coated pits – associated with the formation of intracellular vesicles (Roth and

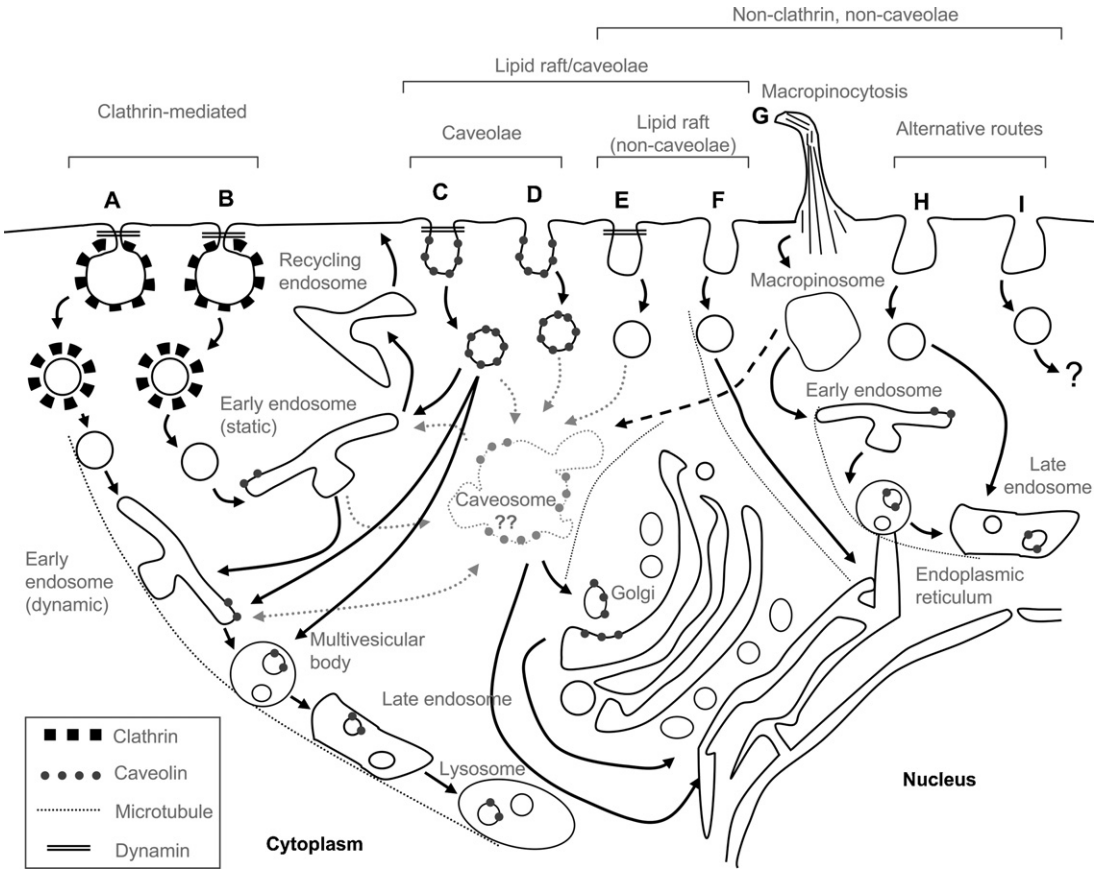

Fig. 1. Internalisation pathways exploited by viruses and their connections with acidic pH organelles (based on (Marsh and Helenius, 2006)). (A) Clathrin-mediated endocytosis associated with microtubule trafficking through dynamic early endosomes and the maturing endosomal system. (B) Clathrin-mediated endocytosis and delivery into static endosomes. (C) Caveolae-dependent endocytosis associated with dynamin activity. (D) Caveolae-dependent endocytosis independent of dynamin. (E) Lipid raft-mediated endocytosis independent of caveolin, but dependent on dynamin activity. (F) Lipid raft-mediated endocytosis independent of caveolin and dynamin. (G) Macropinocytosis. (H) Alternative routes for internalisation into late endosomes, bypassing early endosomes. (I) Alternative endocytic routes that are not characterised by the other known pathways. The caveosome is included in the scheme, although recent reports suggest that it may constitute a specialisation of the late endosomal compartment and/or multivesicular bodies rather than an independent organelle. For a detailed description see text.

Porter, 1964). A protein component termed clathrin was associated with these structures (Pearse, 1976), forming a cage-or net-like structure, hence the term "clathrin cages". The first description of a role for clathrin-coated vesicular endocytosis being associated with viral entry came from electron microscopy studies on vesicular stomatitis virus (VSV) internalisation, a process initially termed viropexis (Simpson et al., 1969). Clathrin interacts through a multi-protein adaptor complex with the cytoplasmic tail of ligand receptors (Keyel et al., 2006; Kirchhausen, 1999; Owen et al., 2004; Sorkin, 2004). Importantly, clathrin-mediated endocytosis is not a single process; the wide variety of adaptor molecules present in the cells offers a certain diversity in the clathrin endocytic route (Benmerah and Lamaze, 2007; Lakadamyali et al., 2006; Leonard et al., 2008; Puthenveedu and von Zastrow, 2006). This in turn is consistent with different requirements for the cell signalling and cytoskeletal components associated with clathrin-mediated endocytosis (Martin-Acebes et al., 2009). Nevertheless, there are core elements typifying this form of endocytosis. The involvement of the clathrin cages distinguishes clathrin-dependent endocytosis from the other endocytic mechanisms. A second characteristic is the role of the large GTPase dynamin in clathrin-coated pit scission from plasma membrane to form the endocytic vesicle (Hinshaw, 2000; Macia et al., 2006; Mercer et al., 2010b; van der Bliek and Meyerowitz, 1991). Unlike clathrin, dynamin is also associated with certain type of clathrin-independent endocytosis, but there are also particular endocytic processes independent of dynamin (see below).

3.1.2. Linking with acidifying structures

Following internalisation, vesicles arising from clathrin-dependent endocytosis lose their clathrin coat and fuse with early endosomes. These are the principal intracellular organelles for controlling and promoting the acidification of vesicular structures arising from endocytosis (not just clathrin-dependent). Using a variety of ligands, including influenza virus, two distinct vesicular populations arising from coated pits have been described (Lakadamyali et al., 2006). A "dynamic population" (Fig. 1A) is associated with internalising ligands mainly destined for degradation. This population employs endosomes maturing into late endosomes and lysosomes, as well as the additional interaction with existing late endosomes and lysosomes. The endosomal structures associated with this route are highly mobile on microtubules. A second more "static population" (Fig. 1B), directs internalised ligands into recycling endosomes, from where receptors may be recycled to the plasma membrane. As with the "dynamic population", the "static" compartment can also direct endocytosed material into an endosomal system of gradually acidifying pH. As the pH continues to decrease, and the endosomal/lysosomal enzymes become active, the risk of virus degradation increases. This may well explain why some viruses capable of efficient replication in epithelial cells display an abortive infection in dendritic cells and macrophages, these latter cells possessing an endosomal system more efficient at promoting destruction of the virus infectious capacity. One example of this is foot-and-mouth disease virus (FMDV), which is highly efficient at replicating in epithelial cells. Although FMDV can survive

for a period of time in dendritic cells and macrophages, albeit at a low infectious level, the infection is abortive with the ultimate destruction of the infectious threat (Harwood et al., 2008; Rigden et al., 2002; Summerfield et al., 2009).

Considering the large variety of viruses employing clathrin-dependent endocytosis for entry into the host cell (Mercer et al., 2010b), the critical step is how the virus escapes the endosomal system at the auspicious moment to ensure efficient replication. Despite the use of a similar entry process, endosomal escape mechanisms vary dependent on the virus. In addition, certain viruses can employ novel interconnections between the clathrin-dependent route and other endocytic routes. This is the case bovine papillomavirus and JC virus. Although they are internalised by a clathrin-dependent route, these viruses are directed from early endosomes into the caveolae route (see section 3.2.1) (Laniosz et al., 2008; Querbes et al., 2006). This presents an intriguing communication between acid and neutral pH organelles, demonstrating that virus uncoating may only require acidification at a particular point. It is also important to remember that a number of viruses are perfectly adapted to initiating their replicative cycle without requirement for an acidifying pH.

3.2. Lipid raft mediated endocytosis and the role of caveolae

In addition to the important role played by clathrin in the entry of a variety of viruses into the host cell, it is important to consider the mechanisms underlying cell membrane modulation during endocytosis. The plasma membrane does not present a continuous or homogeneous composition. It contains lipid microdomains termed lipid rafts (Simons and Ikonen, 1997), initially characterised as portions of plasma membrane insoluble in non-ionic detergents at low temperatures (4 °C) (Chamberlain, 2004). These domains are characterised by their high content of cholesterol, glycosphingolipids and glycophosphatidylinositol (GPI), as well as anchored proteins such as GPI-anchored, myristoylated and palmitoylated proteins, and transmembrane proteins (Jacobson et al., 2007). Lipid rafts are also present on intracellular membranes (Rajendran and Simons, 2005), but do not constitute a specific endocytic route per se.

Lipid rafts have been associated with various endocytic mechanisms, which internalise these membrane regions (Chinnapen et al., 2006; Martín-Belmonte et al., 2003; Rollason et al., 2007; Stoddart et al., 2002); they have also been associated with the entry of a number of viruses (Mercer et al., 2010b; Pelkmans, 2005; Thorley et al., 2010). Endocytic mechanisms most frequently related to lipid raft activity are clathrin-independent (Fig. 1C–F). While caveolin-dependent lipid raft mediated endocytosis has been characterised, other routes independent of caveolin (and clathrin) exist (Nichols, 2003). Accordingly, lipid raft dependent modes of entry cannot be related to one particular form of endocytosis. It is likely that internalisation of lipid rafts, and a virus which has interacted with a receptor therein, will be dependent on the receptor activity and the composition of the lipid rafts; this in turn relates to the relative roles played by dynamin and the different small GTPases (Cdc42, Arf6, RhoA) (Mayor and Pagano, 2007). Indeed, it has been proposed that the different mechanisms of lipid raft uptake are variants of a diverse endocytic process involving lipid rafts and caveolae (Marsh and Helenius, 2006; Nabi and Le, 2003).

3.2.1. Caveolae-mediated endocytosis

Caveolae were first described as flask-shaped plasma membrane invaginations (Palade, 1953), in which the name refers to its cave-like appearance (Yamada, 1955). Caveolae can be considered to provide a specialisation among lipid rafts, characterised by the presence of caveolin-1 protein (Parton and Simons, 2007; Rothberg et al., 1992). Caveolae formation involves caveolin-1 oligomerisation, and its association with cholesterol-enriched microdomains (Bauer and Pelkmans, 2006; Nichols, 2003). Caveolin oligomers assembly at the Golgi complex, rather than de novo at the plasma membrane (Tagawa et al., 2005), suggesting a pre-formed caveolae model cycling between the Golgi complex and plasma membrane, regulated by cellular kinases (Coyne and Bergelson, 2006; Pelkmans and Zerial, 2005; Shajahan et al., 2004).

Caveolin-dependent endocytosis requires formation of the caveolar vesicle, and fission of the caveolae from the plasma membrane. The latter may be dependent on the large GTPase dynamin (Fig. 1C) (del Pozo et al., 2005; Henley et al., 1998; Oh et al., 1998; Pelkmans et al., 2002; Pietiäinen et al., 2004), showing commonality with clathrin-dependent processes. In addition, caveolar uptake can be dynamin-independent, with which the small GTPases Arf6 and Cdc42 are employed for the vesicular fission process (Mayor and Pagano, 2007; Welling and Weisz, 2010). For example, internalisation of Coxsackievirus B3 (CVB3) in caveolae proceeds in a dynamin-independent manner (Fig. 1D) (Coyne and Bergelson, 2006).

Endocytosis via caveolae can deliver viruses to an intracellular organelle characterised 10 years ago as the caveosome (Pelkmans et al., 2001). In contrast to endosomes, the caveosome was associated to a neutral pH (Pelkmans et al., 2004, 2001, 2002). However, the concept of caveosomes as truly independent organelles is now changing; recent evidence is describing the caveosome as a specialisation of late endosomal compartments, modified by caveolin accumulation and awaiting degradation (Hayer et al., 2010; Parton and Howes, 2010). Supporting this view is the work on SV40 entry, a virus model for caveolae-mediated endocytosis and transport to caveosomes, wherein the virus enters an endosomal pathway prior to its transport to the ER (Engel et al., 2011). This implies connections and communications between caveolae and other organelles (see Fig. 1), which may be mediated by particular endosomal compartments. Certainly, the reported fusion of caveolae with early endosomes (Pelkmans et al., 2004) would relate to more recent findings (Botos et al., 2008; Hayer et al., 2010). A number of viruses internalised through caveolae have now been described as being directed into the endosomal route (O'Donnell et al., 2008; Pelkmans et al., 2004; Smith et al., 2008). Such evidence is implying that viruses entering cells through a neutral pH pathway would still transit acid organelles. However, further work is required to understand the functional role of caveosomes, and how they relate to other organelles, particularly those of the acidifying endosomal pathway.

3.2.2. Lipid raft-dependent endocytosis independent of caveolae

Internalisation via lipid rafts can also occur independently of caveolin (Fig. 1E–F). For example, Echovirus 1 is internalised in a dynamin-dependent manner, being visualised in vesicles lacking caveolin prior to transfer into caveolin-enriched organelles (Fig. 1E) (Marsh and Helenius, 2006; Pietiainen et al., 2004). Recent findings have also described a route independent of dynamin, sharing characteristics with macropinocytosis. Therein, the virus is transported into caveolin-containing organelles that constitute a type of multivesicular bodies (Karjalainen et al., 2008, 2011). Likewise, SV40 can be internalised in cells that do not express caveolin, by means of a lipid-dependent, dynamin-independent pathway (Fig. 1F) to reach the endoplasmic reticulum (Damm et al., 2005).

Endocytic pathways independent of both clathrin and caveolin appear to be more reliant on the small GTPases Cdc41 and Arf6 (Mayor and Pagano, 2007; Welling and Weisz, 2010). This may relate to processes involving flotillin-1 (Glebov et al., 2006; Mercer et al., 2010b), which is found associated with lipid rafts and endocytosis distinct from clathrin-coated pits and caveolin-1 positive caveolae (Conner and Schmid, 2003b). Although flotillin-1 can be found in morphologically defined caveolae, it is

also expressed by cells lacking caveolin. Moreover, flotillin-1 can be found in acidic organelles including lysosomes and other endosomal structures. The relationship between flotillin-dependent and caveolin-dependent endocytosis is still open. Nevertheless, flotillin-1 is associated with a form of clathrin-independent endocytosis employing structures morphologically indistinguishable from caveolae, and sharing features known for caveolar endocytosis. However, connections between acid organelles and these caveolin-independent, lipid raft-dependent endocytic routes remain to be elucidated.

3.3. Additional endocytic routes employed by different cell types

3.3.1. Macropinocytosis

With macropinocytosis (Fig. 1G), the cargo is internalised into vesicular structures formed by plasma membrane protrusions termed "ruffles" (Mercer and Helenius, 2009; Swanson, 2008). The vesicles – termed macropinosomes – are formed in a dynamin-independent process requiring actin polymerization and activation of Rac and Rho GTPases (Mayor and Pagano, 2007; Pelkmans and Helenius, 2003; Swanson, 2008). Viruses internalised through macropinosomes can be directed to interact with neutral pH organelles such as caveosomes, or acidic compartments such as endosomes (Coyne et al., 2007b; Chang et al., 2010; Imelli et al., 2004; Karjalainen et al., 2008; Laliberte and Moss, 2009; Mercer and Helenius, 2008; Mercer et al., 2010a; Saeed et al., 2010; Sieczkarski and Whittaker, 2002a) (Fig. 1). The entry routes for CVB3 and echovirus 1 referred to above combine characteristics of both macropinocytosis and caveolae/lipid raft-mediated endocytosis, combining the F and G pathways shown in Fig. 1. An important characteristic of macropinocytosis is its role in dendritic cells, whereby it appears to be a major endocytic route in immature cells for initiating antigen-processing pathways. Monocytotropic viruses which have evolved to infect such cells may well have circumvented this pathway, or commandeered the process to promote initiation of their replicative cycle.

An interesting example of a virus using a macropinocytic route is vaccinia virus (Schmidt et al., 2012), although it is important to note that vaccinia virus entry can be dependent on the virus strain and host cell type (Bengali et al., 2009; Chang et al., 2010; Whitbeck et al., 2009). The outer envelope of extracellular virions (EVs) is acquired from the host cell plasma membrane. Within the cell, mature virions (MVs) lack this outer envelope, but are still infectious. When MVs interact with host cells, they trigger the formation of blebs at the host cell surface to gain entry (Mercer and Helenius, 2008). The presence of phosphatidylserine in the MV viral envelope has been proposed as a key factor in the process, to inducing a form of autophagy termed apoptotic mimicry (Mercer and Helenius, 2008). This may be a variable phenomenon, considering that other studies do not support this hypothesis (Laliberte and Moss, 2009). Certainly, MVs of a different strain induced another form of macropinocytosis, also dependent on the phosphatidylserine content of the viral envelope, but based on the formation of filopodia in the host cell (Mercer et al., 2010a). Moreover, EVs are also internalised by a macropinocytic route, but disruption of the outer envelope within the endocytic compartment is necessary for fusion of the inner membrane with the vesicular membrane promoting cytosolic release (Schmidt et al., 2011).

3.3.2. Other alternative routes

There are several endocytic routes that do not fit under the categories described above (Fig. 1H and I). These routes have been referred to as non-clathrin, non-caveolae processes (Sieczkarski and Whittaker, 2002a); strictly, this term should also include macropinocytosis as well as the caveolin-independent, lipid raft-mediated endocytosis. While these can involve non-acidic compartments, there are examples of alternative endocytic route leading into acidic compartments. One example is seen with lymphocytic choriomeningitis virus. Internalisation is independent of both clathrin and lipid rafts, with the virus being transported into late endosomes, bypassing early endosomes (Quirin et al., 2008; Rojek et al., 2008a). In other cases, such as in influenza virus, internalisation can occur through alternative pathways to the clathrin-mediated route. These also bring the virus into late endosomal compartments where acid-induced membrane fusion takes place (Lakadamyali et al., 2003; Rust et al., 2004).

4. Acidification of endocytosed material

Internalisation of virus via clathrin-coated pits often results in a relatively rapid acidification process, in which a gradual reduction of the internal vesicular pH due to interaction with early endosomes is noted. This can contrast with endocytosis into macropinosomes or caveolar vesicles. Nevertheless, macropinosomes and caveolae vesicles can also be acidified, when the endocytic processing involves interaction with early endosomes. Indeed, most endocytic routes employable by viruses – clathrin-dependent and -independent; caveolin-dependent and -independent; and dynamin-dependent and -independent – all have the potential for acidification when interaction and fusion with early endosomes is implicated (Welling and Weisz, 2010).

When endocytosis leads to an acidifying process, the internalised vesicular structures will often fuse with early endosomes, employing docking-type interactions involving the early endosomal antigen-1 (EEA1) with Soluble N-Ethylmaleimide-Sensitive Factor Attachment Protein Receptor (SNARE) proteins such as syntaxin-6 or syntaxin-13, along with small GTPases such as Rab5 (Duman and Forte, 2003; Galvis et al., 2009; Mills et al., 2001; Simonsen et al., 1999; Stenmark, 2009). The interaction of the SNARE proteins and small GTPases regulate the processes, being necessary for ensuring the appropriate membrane fusion. This interaction of endosomal structures with endocytic vesicles provides the endosomal enzymes, as well as promoting the acidification mechanism reliant on vacuolar H^+-ATPases (Jefferies et al., 2008). As a result of these activities, the pH inside such endocytic compartments progressively acidifies through the 6.5 of early endosomes to the 5.5–5.0 associated with late endosomes/lysosomes (Yamashiro and Maxfield, 1984), this can be enhanced by additional interactions with existing late endosomal and lysosomal structures. Acidification requires the vacuolar H^+-ATPases pumping protons into the vesicular lumen (Marshansky and Futai, 2008; Yamashiro et al., 1983). By such means, the appropriate pH level is provided for initiating the virus replicative cycle – also referred to as "uncoating" – with different viruses requiring particular pH values, and therefore particular cellular organelles, as exemplified in Table 2.

5. Virus trafficking through the endosomal system

5.1. Endosomal pH triggering relating to delivery of viral genomes

As seen from the above overview of the diversity of endocytic processes available, viruses have evolved different strategies for delivering their genetic material into the appropriate compartments of host cells, to ensure the establishment of infection. From the first element in the process leading to intracellular localisation – the mode of virus entry or penetration into the host cell – diversity is observed. Variation is seen with the cell receptor ligation employed by the virus, whether intracellular deposition involves early and late endosomes, the role of endoplasmic reticulum (ER), or the requirement for the cell nucleus.

Table 2
Examples of pH values for membrane fusion or uncoating of different viruses dependent on acid pH for infection.

Virus	Membrane fusion or uncoating		References
	pH	Cellular organelle	
Rhabdoviridae			
Vesicular stomatitis virus	6.2	Multivesicular bodies/late endosomes	Carneiro et al. (2001), Le Blanc et al. (2005), and White et al. (1981)
Orthomyxoviridae			
Influenza virus	5.5	Late endosomes	Doms et al. (1986) and Lakadamyali et al. (2006)
Arenaviridae			
Junin virus	<5.5	Late endosomes	York and Nunberg (2006)
Picornaviridae			
Foot-and-mouth disease virus	6.6	Early endosomes	Berryman et al. (2005), Curry et al. (1995), Johns et al. (2009), Martin-Acebes et al. (2007), Martin-Acebes et al. (2010), and O'Donnell et al., 2005
Flaviviridae			
Dengue virus	5.8–6.4	Late endosomes	van der Schaar et al. (2008) and Zaitseva et al. (2010)
West Nile virus	6.3	Early endosomes?/late endosomes	Chu and Ng (2004a), Krishnan et al. (2007), Martin-Acebes and Saiz (2011), and Moesker et al., 2010
Tick-borne encephalitis virus	5.5	Not determined	Corver et al. (2000)
Togaviridae			
Semliki Forest virus	<6.2	Late endosomes	Kielian et al. (1984) and Vonderheit and Helenius (2005)

Conformational rearrangements of the virus capsid structure can be initiated by the interaction with the cell surface receptor. Yet, for a wide variety of viruses, it is the acidifying pH of the endosomal system which is ultimately the determining factor for promoting release of genomic material into the cytosol (Le Blanc et al., 2005; Marsh and Helenius, 2006; Pelkmans and Helenius, 2003; Smith and Helenius, 2004).

The overall outcome of this fine strategy ensures that the virus only releases its genome inside the host cell. Regardless of the receptor employed, the virus takes advantage of its internalisation by the cell into endosomal compartments. This will often occur whether the virus enters via clathrin-mediated uptake leading directly into the acidifying endosomal system, or via clathrin-independent pathways such as macropinocytosis or caveolar uptake with which endosomal fusion is required for the acidification to ensue. This notion is supported by recent studies on certain viruses for which entry was supposed to be independent of pH. For example, SV40 employs a caveolar endocytosis, in which its genome release requires disulfide bond isomerisation reactions (Schelhaas et al., 2007). These processes are associated with cellular machinery located in the ER, employed by the cell for protein folding. Such observations demonstrate the importance of the ER with its neutral pH for initiating the replicative cycle of certain viruses. Nevertheless, SV40 can employ acidic compartments prior to delivery into the ER (Engel et al., 2011). Another member of the *Polyomaviridae*, BK virus, also employs a combination of acidifying and non-acidifying strategies for initiating infection (Jiang et al., 2009). BK virus initially enters into an acidic endosomal environment, triggering conformational changes in the capsid. Thereafter, the virus is delivered into another cellular compartment for disulphide isomerization leading to cleavage of the capsid VP1 protein.

5.2. Viral genome delivery from endosomal compartments

5.2.1. Enveloped viruses

For cytosolic deposition of their genome (free as with positive-strand RNA viruses, or retained within a polymerase complex as with negative strand viruses), enveloped viruses employ fusion of their envelope with cellular vesicular membranes through the action of virion surface proteins (Harrison, 2008b; Plemper, 2011). With viruses such as measles virus and respiratory syncytial virus these viral proteins are termed fusion proteins, which undergo conformational changes due to the action of cellular proteases, to effect the fusion from within the internalised vesicular structure (Plemper, 2011; Smith et al., 2009). Fusion proteins of viruses such as rabies virus may arise through reversible conformational alterations of surface proteins (G protein) involved in binding to the cell (Gaudin et al., 1999).

Related to the latter are viruses such as myxoviruses and influenza virus, which employ cellular proteases to modify the interaction of their surface glycoproteins (haemagglutinin) with the receptor (Luo, 2012); this also occurs on the lumen side of the endocytic vesicle into which the virus has been internalised. Influenza virus haemagglutinin is a trimeric glycoprotein that is present in the viral envelope, containing a fusion peptide (Cross et al., 2009), the receptor binding site, a metastable structural motif, and the transmembrane domain. After recognition of the host cell receptor molecule (terminal α-sialic acid), influenza virus particles are endocytosed by different mechanisms including the clathrin-mediate route (Lakadamyali et al., 2003, 2006; Sieczkarski and Whittaker, 2002b). Upon interaction of the endocytic vesicle with endosomes, the acidifying pH induces important conformational changes in the haemagglutinin (Bullough et al., 1994; Jiang et al., 2010), attracting this to the vesicular membrane for insertion of the fusion peptide therein. This results in juxtaposition of the two membranes, and formation of a fusion pore for facilitating release of the viral genome (Harrison, 2008b; Luo, 2012). The outcome of these fusion events is the "inversion" of the viral envelope fused with the endocytic vesicular membrane, or the formation of a pore through the two membranes, such that the virion internal contents are delivered to the cytosol.

With such negative strand viruses as mentioned above, the resultant delivery is for their nucleocapsid complex carrying the viral genome, due to the requirement of the latter for the polymerase complex contained within the nucleocapsid. The activity

of these fusion proteins, as well as the cellular proteases assisting cytosolic entry, is dependent on the pH of the endosomal vesicles in which the virus is to be found; as this pH decreases in line with the maturation of the endosomal pathway, the fusion activity becomes active, and therefore the release of the virus nucleocapsid complex (Gaudin et al., 1999; Luo, 2012; Plemper, 2011; Smith et al., 2009). Indeed, for HIV it has been described that fusion at the plasma membrane does not proceed from lipid mixing without forming a fusion pore, as is induced inside the endosomal structures (de la Vega et al., 2011). In addition to reduced pH, there is increasing evidence that particular enveloped viruses require cofactors to trigger membrane fusion. Implicated examples are anionic lipid-rich areas on late endosomal/lysosomal membranes (Zaitseva et al., 2010) and internal vesicles of multivesicular bodies (Roth and Whittaker, 2011), as well as lysobisphosphatidic acid (Le Blanc et al., 2005) or the presence of cholesterol in the target membranes (Ahn et al., 2002; Moesker et al., 2010; Umashankar et al., 2008). Intriguingly, the release of the rhabdovirus vesicular stomatitis virus genome into the cytosol appears to involve a two-step process. The first step involves fusion of the viral envelope with the internal membranes of a multivesicular endosome; the second step is a back-fusion of internal vesicles with the endosome-limiting membrane (Le Blanc et al., 2005).

Selecting specific lipids for membrane fusion has been proposed as a novel mechanism for timing fusion events, to promote efficient delivery of viral genomic material to the appropriate sites for genome translation and ultimately the generation of progeny virus (Zaitseva et al., 2010). Cellular proteins can be also implicated in the entry of enveloped viruses. This has been observed with influenza virus and certain arenaviruses, whereby entry involves components of the pathway associated with ubiquitin and endosomal sorting complex required for transport (ESCRT) (Khor et al., 2003; Pasqual et al., 2011).

5.2.2. Non-enveloped viruses

Viruses lacking a lipid envelope must also delivery their genomes from within endocytic vesicles; clearly they employ different mechanisms to enveloped viruses. One process often observed is based on virion particle alteration and exposition of hydrophobic residues (Tsai, 2007); conformational changes in the viral receptor induced by acidifying pH can also assist these processes (Konecsni et al., 2009). Such pH-dependent cytosolic penetration by viruses can result from disruption of endosomal structures wherein the viral particles were internalised, promoting release into the cytoplasm of not only the virus but also the endosomal content. In contrast, non-enveloped viruses can enter the cytosol through the formation of pores in endosomal membranes (Chandran et al., 2002; Danthi et al., 2003; FitzGerald et al., 1983; Knipe et al., 1997; Prchla et al., 1994, 1995; Schober et al., 1998).

Both endocytic vesicle membrane disruption and pore-formation have been reported for rhinoviruses, thus providing a well-documented model for non-enveloped virus uncoating (Brabec et al., 2005; Schober et al., 1998). Therein, a major intermediary is the formation of ion channels by endosomal pH-dependent alterations of viral structural proteins, as witnessed with human rhinovirus type 2 (HRV2) (Fuchs and Blaas, 2010). This can be mimicked by interacting the virus with the plasma membrane followed by low pH treatment, resulting in virus entry and replication independent of endosomal activity (Brabec et al., 2003). It is hypothesised that the ion channel formation involves exposure of the virion VP4 myristoylated protein together with N-terminal sequences of the VP1; five VP4 molecules together with five VP1 N-termini, which can insert into the endocytic vesicle membrane. This leads to pore formation and viral genome translocation into the cytosol (Fuchs and Blaas, 2010). A similar dependency on ion channel formation through action of VP4 and VP1 N-termini has been shown for poliovirus (Tosteson and Chow, 1997).

Nevertheless, the ion channel formation reported for HRV2 and poliovirus may also lead to destabilisation of the endocytic vesicle membrane, resulting in cytosolic release without the need for pore formations. Moreover, two viruses within a single group can behave differently, although the reported observations may actually reflect two processes operative with both viruses, but only observed with one under particular circumstances. Contrasting with HRV2, the cumulative evidence for HRV type 14 (HRV14) shows accumulation of subviral particles in the cytosol and reduced numbers of endosomes; this is indicative of endosomal rupture (Fuchs and Blaas, 2010). The mechanisms by which such viruses destabilise endocytic vesicle membranes still require clarification, but weakening of the vesicular membrane by modifying its structure or increasing vesicular swelling beyond the retaining capacity of the membrane are strong candidates. Membrane destabilisation may be related to the activity known for cationic amino acids, particularly in a polycationic form, following interaction with protons pumped into the endosomal lumen by the vacuolar H^+-ATPase pump (Meade and Dowdy, 2007). Protonation of such polycationic peptides, and indeed lipopeptides, leads to destabilisation of the endosomal membranes and release of the virus into the cytosol.

5.2.3. Current knowledge on viral genome delivery

Overall, the current knowledge is showing that different viruses possess a variety of mechanisms for promoting escape from the acidifying endosomal compartment. This circumvents degradation of the virus, while ensuring initiation of the viral replicative cycle. Different endosomal escape processes introduce into the cytosol either the virus nucleocapsid structure or its free genome. Alternatively, the viral material may be delivered into another cellular compartment, such as the caveosome or ER, which completes the uncoating process. Whichever process is employed, the end product renders the genome available for translation and replication.

In addition to acidic pH, endosomal vesicles maintain a positive potential (10–20 mV) on the internal face of their membranes, due to the action of their vacuolar H^+-ATPase and Na^+/K^+-ATPase. It is becoming clear that not only endosomal acidification, but also the degrees of membrane polarisation and depolarisation are important for a number of viruses to escape the endosomal maturation pathway (leading ultimately to the degradative lysosomal structures) (Berka et al., 2009; Markosyan et al., 2007). Nevertheless, an important element therein is the capacity of a virus to sense the acidifying pH, leading into the processes for cytosolic release and initiation of the virus replicative cycle.

6. Acidic pH sensing mechanisms

Evolution has provided viruses with sensing mechanisms to detect pH variations within acidifying vesicles, and trigger reactions promoting cytosolic release. As mentioned above, viral proteins can be conformationally altered by the pH changes, and action of endosomal enzymes, leading to the fusion of endocytic vesicle membranes with viral membranes, or the generation of ion channels. The outcome will be cytosolic delivery of the genome via the formation of pores in the vesicle membrane or membrane disruption. Viruses can also employ particular amino acids in their structure as pH sensing mechanisms, for example amino acids such as histidine (His) with ionisable side chains (Thurlkill et al., 2006). His residues in proteins display a pK_a about 6.4, which implies that at pH values found inside early endosomes and multivesicular bodies (MVB), relatively small shifts in pH will modify the average cationic charge of the His. This behaviour makes His residues important pH sensors in proteins (Kampmann et al., 2006;

Srivastava et al., 2007; Thurlkill et al., 2006). Moreover, the imidazole ring of the His side chain in solvent-exposed His residues on viral particles protonates within the pH range (6.5–5.0) of endosomal compartments. The introduced cationic charges inside the viral proteins can trigger conformational rearrangements, which may lead to membrane fusion or nucleic acid uncoating. With Tick-borne encephalitis virus (Fritz et al., 2008; Harrison, 2008a) and Semliki Forest virus (Qin et al., 2009), a single His residue in the appropriate location may prove sufficient.

Non-enveloped viruses also exploit pH sensing mechanisms. With FMDV, two His residues were identified as critical pH sensors for uncoating (Ellard et al., 1999; van Vlijmen et al., 1998). Mutations close to these residues altered the efficiency of uncoating, either increasing (Martin-Acebes et al., 2010) or lowering its pH requirement (Martin-Acebes et al., 2011).

7. Methods for the study of acid-dependent viral entry

Evidence for acid dependent penetration can be obtained through a wide variety of cell biological, genetic and structural techniques. All these approaches can be combined with in vitro fusion/uncoating assays, which allow recreation of environmental conditions inside endosomal compartments. Initial evidence for acid-dependent initiation of virus replicative cycles was obtained using drugs impairing endosomal acidification: lysosomotropic compounds including weak bases such as NH_4Cl, ionophores such as monesin (Marsh and Helenius, 1989; Marsh et al., 1982), and vacuolar-ATPases inhibitors such as bafilomycin and concanamycin (Huss and Wieczorek, 2009). Addition of these compounds to cultured cells results in impairment of endosomal acidification. This in turn impedes membrane fusion or perturbation, interfering with acid-dependent virus uncoating and productive infection. The problem with analysing virus progeny in these experiments is that weak bases and ionophores affect all acidic cell compartments, potentially interfering with steps other than virus entry (Marsh and Helenius, 1989). Moreover, any metabolic inhibitor against endosomal activities may lead to an eventual shutdown in membrane recycling, or even collapse of the vesicular and microtubule networks, resulting in a loss of all endocytic and exocytic processes.

Cell biological approaches offer many advantages, and certainly circumvent the shortcomings associated with metabolic inhibitors. In this context, application of RNAi knock-down, such as delivery of siRNA, is proving to be a useful strategy for studying the entry routes for a number of viruses. For instance, siRNA application has lead to the identification of cellular kinases involved in viral entry (Pelkmans et al., 2005). Advances in understanding virus entry processes have gained from applying cell fractionation of endosomal compartments and detection of viral particles inside these fractions, together with specific endosomal/lysosomal markers. Colocalisation analyses of endocytosed viral particles together with endosomal markers (for example, EEA1, Rab5 or transferrin for early endosomes; LAMP1 and Rab7 for late endosomes/lysosomes) provide a powerful tool for determining viral transit through acidic compartments. Using fluorescently labelled viral particles and in vivo imaging techniques such as time-lapse microscopy, direct observation of virus-endosomal interactions have been forthcoming: influenza virus or dengue virus fusion (Brandenburg and Zhuang, 2007; Lakadamyali et al., 2006; van der Schaar et al., 2008); endosome maturation and Rab5/7 conversion during Semliki Forest virus entry (Vonderheit and Helenius, 2005); entry of HIV into acidic endosomes (Jha et al., 2011). Expression of dominant negative forms of Rab GTPases has also helped define the roles of these proteins during virus uncoating cycle, as well as the involvement of endosomal populations in viral entry (Sieczkarski and Whittaker, 2003).

Genetic approaches have also provided information on acid-dependent viral entry. Classical genetic strategy implies the isolation of mutant viruses with altered acid phenotype. These mutants can be selected by applying selective pressures, such as inhibitors of endosomal acidification (Guirakhoo et al., 1993; Martin-Acebes et al., 2010). Mutants with increased acid resistance can be selected by exposure of virus populations to acidic conditions (Guirakhoo et al., 1993; Martin-Acebes and Saiz, 2011; Martin-Acebes et al., 2011). Sequencing and characterisation of the mutants provides information about the amino acid residues involved in acid-dependent conformational rearrangements of viral particles or structural proteins. Reverse genetics approaches have also been applied, engineering viruses carrying designed mutations. For instance, His residues on tick-borne encephalitis virus were mutated, allowing the identification of His residues as pH sensors (Fritz et al., 2008).

Structural approaches provide an interesting tool for studying acid-dependent virus entry. The structure of several fusion proteins under particular pH conditions has been resolved, providing information on pre-fusion and post-fusion conformations and the conformational rearrangements that are acid-induced (Bressanelli et al., 2004; Bullough et al., 1994; Igonet et al., 2011; Modis et al., 2004; Roche et al., 2006; Wilson et al., 1981). With non-enveloped viruses, comparing the structure of acid-induced uncoating intermediates with native capsids identified molecular rearrangements orchestrated through the acid pH exposure (Garriga et al., 2012; Nam et al., 2011).

8. Conclusions

Regardless of the receptor and the internalisation pathway used, a wide variety of viruses take advantage of intracellular low pH compartments to establish a productive infection. The study of viral internalisation pathways has revealed the existence of a complex crosstalk between endocytic pathways. Since viruses exploit cellular machinery for their internalisation, this new information is not only useful for virologists, but is also important in cell biology. Viruses from different families, including enveloped and non-enveloped viruses, can traffic through different endocytic pathways to reach endosomal compartments where acid pH triggers their penetration. Although alternative internalisation pathways have been described, including endocytic routes independent of acidifying pH, it is clear that intracellular compartments characterised by a low pH are important connecting nodes within the network of viral internalisation pathways. Considering pH-dependence as a common feature shared among many viruses, there is potential therapeutic application for inhibiting pH-dependent virus penetration. This inhibition might be achieved by targeting either cellular or viral factors involved in the penetration reactions. Such an antiviral approach may prove more generically advantageous compared with blocking a specific internalisation pathway, which may be restricted to only one type of virus, or even subtype.

Acknowledgments

Work supported by grants BIO2011-2435, CSD2006-0007, RTA2011-00036, NADIR-UE-228394, and by an institutional grant from Fundación Ramón Areces for AV-C, J-CS, FS, MAM-A; PANFLUVAC (EU-FP6, 044115), NANOVACC (Swiss National Science Foundation, 310000-1198828) and Replixcel (EU_FP7 Marie Curie IAAP Action, 251420) for KMC. MAM-A is the recipient of a JAE-Doc fellowship from CSIC.

References

Acosta, E.G., Castilla, V., Damonte, E.B., 2008. Functional entry of dengue virus into *Aedes albopictus* mosquito cells is dependent on clathrin-mediated endocytosis. Journal of General Virology 89 (Pt 2), 474–484.

Ahn, A., Gibbons, D.L., Kielian, M., 2002. The fusion peptide of Semliki Forest virus associates with sterol-rich membrane domains. Journal of Virology 76 (7), 3267–3275.

Amstutz, B., Gastaldelli, M., Kalin, S., Imelli, N., Boucke, K., Wandeler, E., Mercer, J., Hemmi, S., Greber, U.F., 2008. Subversion of CtBP1-controlled macropinocytosis by human adenovirus serotype 3. EMBO Journal 27 (7), 956–969.

Baranowski, E., Ruiz-Jarabo, C.M., Domingo, E., 2001. Evolution of cell recognition by viruses. Science 292 (5519), 1102–1105.

Basta, S., Gerber, H., Schaub, A., Summerfield, A., McCullough, K.C., 2010. Cellular processes essential for African swine fever virus to infect and replicate in primary macrophages. Veterinary Microbiology 140 (1–2), 9–17.

Basta, S., Knoetig, S.M., Spagnuolo-Weaver, M., Allan, G., McCullough, K.C., 1999. Modulation of monocytic cell activity and virus susceptibility during differentiation into macrophages. Journal of Immunology 162 (7), 3961–3969.

Bauer, M., Pelkmans, L., 2006. A new paradigm for membrane-organizing and -shaping scaffolds. FEBS Letters 580 (23), 5559–5564.

Bayer, N., Schober, D., Huttinger, M., Blaas, D., Fuchs, R., 2001. Inhibition of clathrin-dependent endocytosis has multiple effects on human rhinovirus serotype 2 cell entry. Journal of Biological Chemistry 276 (6), 3952–3962.

Bengali, Z., Townsley, A.C., Moss, B., 2009. Vaccinia virus strain differences in cell attachment and entry. Virology 389 (1–2), 132–140.

Benmerah, A., Lamaze, C., 2007. Clathrin-coated pits: vive la difference? Traffic 8 (8), 970–982.

Berka, U., Khan, A., Blaas, D., Fuchs, R., 2009. Human rhinovirus type 2 uncoating at the plasma membrane is not affected by a pH gradient but is affected by the membrane potential. Journal of Virology 83 (8), 3778–3787.

Berryman, S., Clark, S., Monaghan, P., Jackson, T., 2005. Early events in integrin alphavbeta6-mediated cell entry of foot-and-mouth disease virus. Journal of Virology 79 (13), 8519–8534.

Borrow, P., Oldstone, M.B., 1994. Mechanism of lymphocytic choriomeningitis virus entry into cells. Virology 198 (1), 1–9.

Botos, E., Klumperman, J., Oorschot, V., Igyarto, B., Magyar, A., Olah, M., Kiss, A.L., 2008. Caveolin-1 is transported to multi-vesicular bodies after albumin-induced endocytosis of caveolae in HepG2 cells. Journal of Cell and Molecular Medicine 12 (5A), 1632–1639.

Brabec, M., Baravalle, G., Blaas, D., Fuchs, R., 2003. Conformational changes, plasma membrane penetration, and infection by human rhinovirus type 2: role of receptors and low pH. Journal of Virology 77 (9), 5370–5377.

Brabec, M., Schober, D., Wagner, E., Bayer, N., Murphy, R.F., Blaas, D., Fuchs, R., 2005. Opening of size-selective pores in endosomes during human rhinovirus serotype 2 in vivo uncoating monitored by single-organelle flow analysis. Journal of Virology 79 (2), 1008–1016.

Brandenburg, B., Zhuang, X., 2007. Virus trafficking—learning from single-virus tracking. Nature Review and Microbiology 5 (3), 197–208.

Bressanelli, S., Stiasny, K., Allison, S.L., Stura, E.A., Duquerroy, S., Lescar, J., Heinz, F.X., Rey, F.A., 2004. Structure of a flavivirus envelope glycoprotein in its low-pH-induced membrane fusion conformation. EMBO Journal 23 (4), 728–738.

Bullough, P.A., Hughson, F.M., Skehel, J.J., Wiley, D.C., 1994. Structure of influenza haemagglutinin at the pH of membrane fusion. Nature 371 (6492), 37–43.

Carneiro, F.A., Ferradosa, A.S., Da Poian, A.T., 2001. Low pH-induced conformational changes in vesicular stomatitis virus glycoprotein involve dramatic structure reorganization. Journal of Biological Chemistry 276 (1), 62–67.

Conner, S.D., Schmid, S.L., 2003a. Differential requirements for AP-2 in clathrin-mediated endocytosis. Journal of Cell Biology 162 (5), 773–779.

Conner, S.D., Schmid, S.L., 2003b. Regulated portals of entry into the cell. Nature 422 (6927), 37–44.

Corver, J., Ortiz, A., Allison, S.L., Schalich, J., Heinz, F.X., Wilschut, J., 2000. Membrane fusion activity of tick-borne encephalitis virus and recombinant subviral particles in a liposomal model system. Virology 269 (1), 37–46.

Coyne, C.B., Bergelson, J.M., 2006. Virus-induced Abl and Fyn kinase signals permit coxsackievirus entry through epithelial tight junctions. Cell 124 (1), 119–131.

Coyne, C.B., Kim, K.S., Bergelson, J.M., 2007a. Poliovirus entry into human brain microvascular cells requires receptor-induced activation of SHP-2. EMBO Journal 26 (17), 4016–4028.

Coyne, C.B., Shen, L., Turner, J.R., Bergelson, J.M., 2007b. Coxsackievirus entry across epithelial tight junctions requires occludin and the small GTPases Rab34 and Rab5. Cell Host Microbe 2 (3), 181–192.

Cross, K.J., Langley, W.A., Russell, R.J., Skehel, J.J., Steinhauer, D.A., 2009. Composition and functions of the influenza fusion peptide. Protein and Peptide Letters 16 (7), 766–778.

Curry, S., Abrams, C.C., Fry, E., Crowther, J.C., Belsham, G.J., Stuart, D.I., King, A.M., 1995. Viral RNA modulates the acid sensitivity of foot-and-mouth disease virus capsids. Journal of Virology 69 (1), 430–438.

Chamberlain, L.H., 2004. Detergents as tools for the purification and classification of lipid rafts. FEBS Letters 559 (1–3), 1–5.

Chandran, K., Farsetta, D.L., Nibert, M.L., 2002. Strategy for nonenveloped virus entry: a hydrophobic conformer of the reovirus membrane penetration protein micro 1 mediates membrane disruption. Journal of Virology 76 (19), 9920–9933.

Chang, S.J., Chang, Y.X., Izmailyan, R., Tang, Y.L., Chang, W., 2010. Vaccinia virus A25 and A26 proteins are fusion suppressors for mature virions and determine strain-specific virus entry pathways into HeLa, CHO-K1, and L cells. Journal of Virology 84 (17), 8422–8432.

Chardonnet, Y., Dales, S., 1970. Early events in the interaction of adenoviruses with HeLa cells. I. Penetration of type 5 and intracellular release of the DNA genome. Virology 40 (3), 462–477.

Chen, C., Zhuang, X., 2008. Epsin 1 is a cargo-specific adaptor for the clathrin-mediated endocytosis of the influenza virus. Proceedings of the National Academy of Sciences of the United States of America 105 (33), 11790–11795.

Chinnapen, D.J., Chinnapen, H., Saslowsky, D., Lencer, W.I., 2006. Rafting with cholera toxin: endocytosis and trafficking from plasma membrane to ER. FEMS Microbiology Letters 266 (2), 129–137.

Chu, J.J., Ng, M.L., 2004a. Infectious entry of West Nile virus occurs through a clathrin-mediated endocytic pathway. Journal of Virology 78 (19), 10543–10555.

Chu, J.J., Ng, M.L., 2004b. Interaction of West Nile virus with alpha v beta 3 integrin mediates virus entry into cells. Journal of Biological Chemistry 279 (52), 54533–54541.

Damm, E.M., Pelkmans, L., 2006. Systems biology of virus entry in mammalian cells. Cellular Microbiology 8 (8), 1219–1227.

Damm, E.M., Pelkmans, L., Kartenbeck, J., Mezzacasa, A., Kurzchalia, T., Helenius, A., 2005. Clathrin- and caveolin-1-independent endocytosis: entry of simian virus 40 into cells devoid of caveolae. Journal of Cell Biology 168 (3), 477–488.

Danthi, P., Tosteson, M., Li, Q.H., Chow, M., 2003. Genome delivery and ion channel properties are altered in VP4 mutants of poliovirus. Journal of Virology 77 (9), 5266–5274.

de la Vega, M., Marin, M., Kondo, N., Miyauchi, K., Kim, Y., Epand, R.F., Epand, R.M., Melikyan, G.B., 2011. Inhibition of HIV-1 endocytosis allows lipid mixing at the plasma membrane, but not complete fusion. Retrovirology 8 (1), 99.

del Pozo, M.A., Balasubramanian, N., Alderson, N.B., Kiosses, W.B., Grande-García, A., Anderson, R.G., Schwartz, M.A., 2005. Phospho-caveolin-1 mediates integrin-regulated membrane domain internalization. Nature Cell Biology 7 (9), 901–908.

Doms, R.W., Gething, M.J., Henneberry, J., White, J., Helenius, A., 1986. Variant influenza virus hemagglutinin that induces fusion at elevated pH. Journal of Virology 57 (2), 603–613.

Duman, J.G., Forte, J.G., 2003. What is the role of SNARE proteins in membrane fusion? American Journal of Physiology: Cell Physiology 285 (2), C237–C249.

Ellard, F.M., Drew, J., Blakemore, W.E., Stuart, D.I., King, A.M., 1999. Evidence for the role of His-142 of protein 1C in the acid-induced disassembly of foot-and-mouth disease virus capsids. Journal of General Virology 80 (Pt 8), 1911–1918.

Engel, S., Heger, T., Mancini, R., Herzog, F., Kartenbeck, J., Hayer, A., Helenius, A., 2011. The role of endosomes in SV40 entry and infection. Journal of Virology.

FitzGerald, D.J., Padmanabhan, R., Pastan, I., Willingham, M.C., 1983. Adenovirus-induced release of epidermal growth factor and pseudomonas toxin into the cytosol of KB cells during receptor-mediated endocytosis. Cell 32 (2), 607–617.

Fritz, R., Stiasny, K., Heinz, F.X., 2008. Identification of specific histidines as pH sensors in flavivirus membrane fusion. Journal of Cell Biology 183 (2), 353–361.

Fuchs, R., Blaas, D., 2010. Uncoating of human rhinoviruses. Reviews in Medical Virology 20 (5), 281–297.

Galvis, A., Balmaceda, V., Giambini, H., Conde, A., Villasana, Z., Fornes, M.W., Barbieri, M.A., 2009. Inhibition of early endosome fusion by Rab5-binding defective Ras interference 1 mutants. Archives of Biochemistry and Biophysics 482 (1–2), 83–95.

Garriga, D., Pickl-Herk, A., Luque, D., Wruss, J., Caston, J.R., Blaas, D., Verdaguer, N., 2012. Insights into minor group rhinovirus uncoating: the X-ray structure of the HRV2 empty capsid. PLoS Pathogens 8 (1), e1002473.

Gastaldelli, M., Imelli, N., Boucke, K., Amstutz, B., Meier, O., Greber, U.F., 2008. Infectious adenovirus type 2 transport through early but not late endosomes. Traffic 9 (12), 2265–2278.

Gaudin, Y., Tuffereau, C., Durrer, P., Brunner, J., Flamand, A., Ruigrok, R., 1999. Rabies virus-induced membrane fusion. Molecular Membrane Biology 16 (1), 21–31.

Glebov, O.O., Bright, N.A., Nichols, B.J., 2006. Flotillin-1 defines a clathrin-independent endocytic pathway in mammalian cells. Nature Cell Biology 8 (1), 46–54.

Gruenberg, J., 2009. Viruses and endosome membrane dynamics. Current Opinion in Cell Biology 21 (4), 582–588.

Guirakhoo, F., Hunt, A.R., Lewis, J.G., Roehrig, J.T., 1993. Selection and partial characterization of dengue 2 virus mutants that induce fusion at elevated pH. Virology 194 (1), 219–223.

Harrison, S.C., 2008a. The pH sensor for flavivirus membrane fusion. Journal of Cell Biology 183 (2), 177–179.

Harrison, S.C., 2008b. Viral membrane fusion. Nature Structural Molecular Biology 15 (7), 690–698.

Harwood, L.J., Gerber, H., Sobrino, F., Summerfield, A., McCullough, K.C., 2008. Dendritic cell internalization of foot-and-mouth disease virus: influence of heparan sulfate binding on virus uptake and induction of the immune response. Journal of Virology 82 (13), 6379–6394.

Hayer, A., Stoeber, M., Ritz, D., Engel, S., Meyer, H.H., Helenius, A., 2010. Caveolin-1 is ubiquitinated and targeted to intralumenal vesicles in endolysosomes for degradation. Journal of Cell Biology 191 (3), 615–629.

Helenius, A., Kartenbeck, J., Simons, K., Fries, E., 1980. On the entry of Semliki forest virus into BHK-21 cells. Journal of Cell Biology 84 (2), 404–420.

Henley, J.R., Krueger, E.W., Oswald, B.J., McNiven, M.A., 1998. Dynamin-mediated internalization of caveolae. Journal of Cell Biology 141 (1), 85–99.

Hinshaw, J.E., 2000. Dynamin and its role in membrane fission. Annual Review of Cell and Developmental Biology 16, 483–519.

Huss, M., Wieczorek, H., 2009. Inhibitors of V-ATPases: old and new players. Journal of Experimental Biology 212 (Pt 3), 341–346.
Igonet, S., Vaney, M.C., Vonhrein, C., Bricogne, G., Stura, E.A., Hengartner, H., Eschli, B., Rey, F.A., 2011. X-ray structure of the arenavirus glycoprotein GP2 in its post-fusion hairpin conformation. Proceedings of the National Academy of Sciences of the United States of America 108 (50), 19967–19972.
Imelli, N., Meier, O., Boucke, K., Hemmi, S., Greber, U.F., 2004. Cholesterol is required for endocytosis and endosomal escape of adenovirus type 2. Journal of Virology 78 (6), 3089–3098.
Jacobson, K., Mouritsen, O.G., Anderson, R.G., 2007. Lipid rafts: at a crossroad between cell biology and physics. Nature Cell Biology 9 (1), 7–14.
Jefferies, K.C., Cipriano, D.J., Forgac, M., 2008. Function, structure and regulation of the vacuolar (H+)-ATPases. Archives of Biochemistry and Biophysics 476 (1), 33–42.
Jha, N.K., Latinovic, O., Martin, E., Novitskiy, G., Marin, M., Miyauchi, K., Naughton, J., Young, J.A., Melikyan, G.B., 2011. Imaging single retrovirus entry through alternative receptor isoforms and intermediates of virus-endosome fusion. PLoS Pathogens 7 (1), e1001260.
Jiang, M., Abend, J.R., Tsai, B., Imperiale, M.J., 2009. Early events during BK virus entry and disassembly. Journal of Virology 83 (3), 1350–1358.
Jiang, S., Li, R., Du, L., Liu, S., 2010. Roles of the hemagglutinin of influenza A virus in viral entry and development of antiviral therapeutics and vaccines. Protein Cell 1 (4), 342–354.
Johannsdottir, H.K., Mancini, R., Kartenbeck, J., Amato, L., Helenius, A., 2009. Host cell factors and functions involved in vesicular stomatitis virus entry. Journal of Virology 83 (1), 440–453.
Johns, H.L., Berryman, S., Monaghan, P., Belsham, G.J., Jackson, T., 2009. A dominant-negative mutant of rab5 inhibits infection of cells by foot-and-mouth disease virus: implications for virus entry. Journal of Virology 83 (12), 6247–6256.
Kampmann, T., Mueller, D.S., Mark, A.E., Young, P.R., Kobe, B., 2006. The role of histidine residues in low-pH-mediated viral membrane fusion. Structure 14 (10), 1481–1487.
Karjalainen, M., Kakkonen, E., Upla, P., Paloranta, H., Kankaanpaa, P., Liberali, P., Renkema, G.H., Hyypia, T., Heino, J., Marjomaki, V., 2008. A Raft-derived, Pak1-regulated entry participates in alpha2beta1 integrin-dependent sorting to caveosomes. Molecular Biology of the Cell 19 (7), 2857–2869.
Karjalainen, M., Rintanen, N., Lehkonen, M., Kallio, K., Maki, A., Hellstrom, K., Siljamaki, V., Upla, P., Marjomaki, V., 2011. Echovirus 1 infection depends on biogenesis of novel multivesicular bodies. Cellular Microbiology 13 (12), 1975–1995.
Keyel, P.A., Mishra, S.K., Roth, R., Heuser, J.E., Watkins, S.C., Traub, L.M., 2006. A single common portal for clathrin-mediated endocytosis of distinct cargo governed by cargo-selective adaptors. Molecular Biology of the Cell 17 (10), 4300–4317.
Khor, R., McElroy, L.J., Whittaker, G.R., 2003. The ubiquitin-vacuolar protein sorting system is selectively required during entry of influenza virus into host cells. Traffic 4 (12), 857–868.
Kielian, M.C., Keranen, S., Kaariainen, L., Helenius, A., 1984. Membrane fusion mutants of Semliki Forest virus. Journal of Cell Biology 98 (1), 139–145.
Kirchhausen, T., 1999. Adaptors for clathrin-mediated traffic. Annual Review of Cell and Developmental Biology 15, 705–732.
Knipe, T., Rieder, E., Baxt, B., Ward, G., Mason, P.W., 1997. Characterization of synthetic foot-and-mouth disease virus provirions separates acid-mediated disassembly from infectivity. Journal of Virology 71 (4), 2851–2856.
Konecsni, T., Berka, U., Pickl-Herk, A., Bilek, G., Khan, A.G., Gajdzig, L., Fuchs, R., Blaas, D., 2009. Low pH-triggered beta-propeller switch of the low-density lipoprotein receptor assists rhinovirus infection. Journal of Virology 83 (21), 10922–10930.
Krishnan, M.N., Sukumaran, B., Pal, U., Agaisse, H., Murray, J.L., Hodge, T.W., Fikrig, E., 2007. Rab 5 is required for the cellular entry of dengue and West Nile viruses. Journal of Virology 81 (9), 4881–4885.
Lakadamyali, M., Rust, M.J., Babcock, H.P., Zhuang, X., 2003. Visualizing infection of individual influenza viruses. Proceedings of the National Academy of Sciences of the United States of America 100 (16), 9280–9285.
Lakadamyali, M., Rust, M.J., Zhuang, X., 2006. Ligands for clathrin-mediated endocytosis are differentially sorted into distinct populations of early endosomes. Cell 124 (5), 997–1009.
Laliberte, J.P., Moss, B., 2009. Appraising the apoptotic mimicry model and the role of phospholipids for poxvirus entry. Proceedings of the National Academy of Sciences of the United States of America 106 (41), 17517–17521.
Laniosz, V., Holthusen, K.A., Meneses, P.I., 2008. Bovine papillomavirus type 1: from clathrin to caveolin. Journal of Virology 82 (13), 6288–6298.
Le Blanc, I., Luyet, P.P., Pons, V., Ferguson, C., Emans, N., Petiot, A., Mayran, N., Demaurex, N., Faure, J., Sadoul, R., Parton, R.G., Gruenberg, J., 2005. Endosome-to-cytosol transport of viral nucleocapsids. Nature Cell Biology 7 (7), 653–664.
Leonard, D., Hayakawa, A., Lawe, D., Lambright, D., Bellve, K.D., Standley, C., Lifshitz, L.M., Fogarty, K.E., Corvera, S., 2008. Sorting of EGF and transferrin at the plasma membrane and by cargo-specific signaling to EEA1-enriched endosomes. Journal of Cell Science 121 (Pt 20), 3445–3458.
Liberali, P., Ramo, P., Pelkmans, L., 2008. Protein kinases: starting a molecular systems view of endocytosis. Annual Review of Cell and Developmental Biology 24, 501–523.
Low, J.A., Magnuson, B., Tsai, B., Imperiale, M.J., 2006. Identification of gangliosides GD1b and GT1b as receptors for BK virus. Journal of Virology 80 (3), 1361–1366.
Luo, M., 2012. Influenza virus entry. Advances in Experimental Medicine and Biology 726, 201–221.
Macia, E., Ehrlich, M., Massol, R., Boucrot, E., Brunner, C., Kirchhausen, T., 2006. Dynasore, a cell-permeable inhibitor of dynamin. Developmental Cell 10 (6), 839–850.
Magaldi, T.G., Buch, M.H., Murata, H., Erickson, K.D., Neu, U., Garcea, R.L., Peden, K., Stehle, T., Dimaio, D., 2012. Mutations in the GM1 binding site of SV40 VP1 alter receptor usage and cell tropism. Journal of Virology 86 (13), 7028–7042.
Markosyan, R.M., Kielian, M., Cohen, F.S., 2007. Fusion induced by a class II viral fusion protein, semliki forest virus E1, is dependent on the voltage of the target cell. Journal of Virology 81 (20), 11218–11225.
Marsh, M., Helenius, A., 1989. Virus entry into animal cells. Advances in Virus Research 36, 107–151.
Marsh, M., Helenius, A., 2006. Virus entry: open sesame. Cell 124 (4), 729–740.
Marsh, M., Wellsteed, J., Kern, H., Harms, E., Helenius, A., 1982. Monensin inhibits Semliki Forest virus penetration into culture cells. Proceedings of the National Academy of Sciences of the United States of America 79 (17), 5297–5301.
Marshansky, V., Futai, M., 2008. The V-type H+-ATPase in vesicular trafficking: targeting, regulation and function. Current Opinion in Cell Biology 20 (4), 415–426.
Martin-Acebes, M.A., Gonzalez-Magaldi, M., Sandvig, K., Sobrino, F., Armas-Portela, R., 2007. Productive entry of type C foot-and-mouth disease virus into susceptible cultured cells requires clathrin and is dependent on the presence of plasma membrane cholesterol. Virology 369 (1), 105–118.
Martin-Acebes, M.A., Gonzalez-Magaldi, M., Vazquez-Calvo, A., Armas-Portela, R., Sobrino, F., 2009. Internalization of swine vesicular disease virus into cultured cells: a comparative study with foot-and-mouth disease virus. Journal of Virology 83 (9), 4216–4226.
Martin-Acebes, M.A., Rincon, V., Armas-Portela, R., Mateu, M.G., Sobrino, F., 2010. A single amino acid substitution in the capsid of foot-and-mouth disease virus can increase acid lability and confer resistance to acid-dependent uncoating inhibition. Journal of Virology 84 (6), 2902–2912.
Martin-Acebes, M.A., Saiz, J.C., 2011. A West Nile virus mutant with increased resistance to acid-induced inactivation. Journal of General Virology 92 (Pt 4), 831–840.
Martin-Acebes, M.A., Vazquez-Calvo, A., Rincon, V., Mateu, M.G., Sobrino, F., 2011. A single amino acid substitution in the capsid of foot-and-mouth disease virus can increase acid resistance. Journal of Virology 85 (6), 2733–2740.
Martín-Belmonte, F., Martínez-Menárguez, J.A., Aranda, J.F., Ballesta, J., de Marco, M.C., Alonso, M.A., 2003. MAL regulates clathrin-mediated endocytosis at the apical surface of Madin-Darby canine kidney cells. Journal of Cell Biology 163 (1), 155–164.
Martínez, M.G., Cordo, S.M., Candurra, N.A., 2007. Characterization of Junin arenavirus cell entry. Journal of General Virology 88 (Pt 6), 1776–1784.
Matlin, K.S., Reggio, H., Helenius, A., Simons, K., 1981. Infectious entry pathway of influenza virus in a canine kidney cell line. Journal of Cell Biology 91 (3 Pt 1), 601–613.
Matlin, K.S., Reggio, H., Helenius, A., Simons, K., 1982. Pathway of vesicular stomatitis virus entry leading to infection. Journal of Molecular Biology 156 (3), 609–631.
Mayor, S., Pagano, R.E., 2007. Pathways of clathrin-independent endocytosis. Nature Review: Molecular Cell Biology 8 (8), 603–612.
McCullough, K.C., Basta, S., Knotig, S., Gerber, H., Schaffner, R., Kim, Y.B., Saalmuller, A., Summerfield, A., 1999. Intermediate stages in monocyte-macrophage differentiation modulate phenotype and susceptibility to virus infection. Immunology 98 (2), 203–212.
McCullough, K.C., Schaffner, R., Fraefel, W., Kihm, U., 1993. The relative density of CD44-positive porcine monocytic cell populations varies between isolations and upon culture and influences susceptibility to infection by African swine fever virus. Immunology Letters 37 (1), 83–90.
Meade, B.R., Dowdy, S.F., 2007. Exogenous siRNA delivery using peptide transduction domains/cell penetrating peptides. Advanced Drug Delivery Reviews 59 (2–3), 134–140.
Medigeshi, G.R., Hirsch, A.J., Streblow, D.N., Nikolich-Zugich, J., Nelson, J.A., 2008. West Nile virus entry requires cholesterol-rich membrane microdomains and is independent of alphavbeta3 integrin. Journal of Virology 82 (11), 5212–5219.
Meier, O., Boucke, K., Hammer, S.V., Keller, S., Stidwill, R.P., Hemmi, S., Greber, U.F., 2002. Adenovirus triggers macropinocytosis and endosomal leakage together with its clathrin-mediated uptake. Journal of Cell Biology 158 (6), 1119–1131.
Mercer, J., Helenius, A., 2008. Vaccinia virus uses macropinocytosis and apoptotic mimicry to enter host cells. Science 320 (5875), 531–535.
Mercer, J., Helenius, A., 2009. Virus entry by macropinocytosis. Nature Cell Biology 11 (5), 510–520.
Mercer, J., Knebel, S., Schmidt, F.I., Crouse, J., Burkard, C., Helenius, A., 2010a. Vaccinia virus strains use distinct forms of macropinocytosis for host-cell entry. Proceedings of the National Academy of Sciences of the United States of America 107 (20), 9346–9351.
Mercer, J., Schelhaas, M., Helenius, A., 2010b. Virus entry by endocytosis. Annual Review of Biochemistry 79, 803–833.
Mills, I.G., Urbe, S., Clague, M.J., 2001. Relationships between EEA1 binding partners and their role in endosome fusion. Journal of Cell Science 114 (Pt 10), 1959–1965.
Modis, Y., Ogata, S., Clements, D., Harrison, S.C., 2004. Structure of the dengue virus envelope protein after membrane fusion. Nature 427 (6972), 313–319.
Moesker, B., Rodenhuis-Zybert, I.A., Meijerhof, T., Wilschut, J., Smit, J.M., 2010. Characterization of the functional requirements of West Nile virus membrane fusion. Journal of General Virology 91 (Pt 2), 389–393.
Mosso, C., Galvan-Mendoza, I.J., Ludert, J.E., del Angel, R.M., 2008. Endocytic pathway followed by dengue virus to infect the mosquito cell line C6/36 HT. Virology 378 (1), 193–199.

Nabi, I.R., Le, P.U., 2003. Caveolae/raft-dependent endocytosis. Journal of Cell Biology 161 (4), 673–677.
Nam, H.J., Gurda, B.L., McKenna, R., Potter, M., Byrne, B., Salganik, M., Muzyczka, N., Agbandje-McKenna, M., 2011. Structural studies of adeno-associated virus serotype 8 capsid transitions associated with endosomal trafficking. Journal of Virology 85 (22), 11791–11799.
Natale, V.A., McCullough, K.C., 1998. Macrophage cytoplasmic vesicle pH gradients and vacuolar H+-ATPase activities relative to virus infection. Journal of Leukocyte Biology 64 (3), 302–310.
Nichols, B., 2003. Caveosomes and endocytosis of lipid rafts. Journal of Cell Science 116 (Pt 23), 4707–4714.
O'Donnell, V., Larocco, M., Baxt, B., 2008. Heparan sulfate-binding foot-and-mouth disease virus enters cells via caveola-mediated endocytosis. Journal of Virology 82 (18), 9075–9085.
O'Donnell, V., LaRocco, M., Duque, H., Baxt, B., 2005. Analysis of foot-and-mouth disease virus internalization events in cultured cells. Journal of Virology 79 (13), 8506–8518.
Oh, P., McIntosh, D.P., Schnitzer, J.E., 1998. Dynamin at the neck of caveolae mediates their budding to form transport vesicles by GTP-driven fission from the plasma membrane of endothelium. Journal of Cell Biology 141 (1), 101–114.
Owen, D.J., Collins, B.M., Evans, P.R., 2004. Adaptors for clathrin coats: structure and function. Annual Review of Cell and Developmental Biology 20, 153–191.
Palade, G.E., 1953. Fine structure of blood capillaries. Journal of Applied Physics 24, 1424.
Parton, R.G., Howes, M.T., 2010. Revisiting caveolin trafficking: the end of the caveosome. Journal of Cell Biology 191 (3), 439–441.
Parton, R.G., Simons, K., 2007. The multiple faces of caveolae. Nature Review: Molecular and Cellular Biology 8 (3), 185–194.
Pasqual, G., Rojek, J.M., Masin, M., Chatton, J.Y., Kunz, S., 2011. Old world arenaviruses enter the host cell via the multivesicular body and depend on the endosomal sorting complex required for transport. PLoS Pathogens 7 (9), e1002232.
Pearse, B.M., 1976. Clathrin: a unique protein associated with intracellular transfer of membrane by coated vesicles. Proceedings of the National Academy of Sciences of the United States of America 73 (4), 1255–1259.
Pelkmans, L., 2005. Secrets of caveolae- and lipid raft-mediated endocytosis revealed by mammalian viruses. Biochimica Et Biophysica Acta 1746 (3), 295–304.
Pelkmans, L., Burli, T., Zerial, M., Helenius, A., 2004. Caveolin-stabilized membrane domains as multifunctional transport and sorting devices in endocytic membrane traffic. Cell 118 (6), 767–780.
Pelkmans, L., Fava, E., Grabner, H., Hannus, M., Habermann, B., Krausz, E., Zerial, M., 2005. Genome-wide analysis of human kinases in clathrin- and caveolae/raft-mediated endocytosis. Nature 436 (7047), 78–86.
Pelkmans, L., Helenius, A., 2003. Insider information: what viruses tell us about endocytosis. Current Opinion in Cell Biology 15 (4), 414–422.
Pelkmans, L., Kartenbeck, J., Helenius, A., 2001. Caveolar endocytosis of simian virus 40 reveals a new two-step vesicular-transport pathway to the ER. Nature Cell Biology 3 (5), 473–483.
Pelkmans, L., Puntener, D., Helenius, A., 2002. Local actin polymerization and dynamin recruitment in SV40-induced internalization of caveolae. Science 296 (5567), 535–539.
Pelkmans, L., Zerial, M., 2005. Kinase-regulated quantal assemblies and kiss-and-run recycling of caveolae. Nature 436 (7047), 128–133.
Pietiainen, V., Marjomaki, V., Upla, P., Pelkmans, L., Helenius, A., Hyypia, T., 2004. Echovirus 1 endocytosis into caveosomes requires lipid rafts, dynamin II, and signaling events. Molecular Biology of the Cell 15 (11), 4911–4925.
Pietiäinen, V., Marjomäki, V., Upla, P., Pelkmans, L., Helenius, A., Hyypiä, T., 2004. Echovirus 1 endocytosis into caveosomes requires lipid rafts, dynamin II, and signaling events. Molecular Biology of the Cell 15 (11), 4911–4925.
Plemper, R.K., 2011. Cell entry of enveloped viruses. Current Opinion in Virology 1 (2), 92–100.
Prchla, E., Kuechler, E., Blaas, D., Fuchs, R., 1994. Uncoating of human rhinovirus serotype 2 from late endosomes. Journal of Virology 68 (6), 3713–3723.
Prchla, E., Plank, C., Wagner, E., Blaas, D., Fuchs, R., 1995. Virus-mediated release of endosomal content in vitro: different behavior of adenovirus and rhinovirus serotype 2. Journal of Cell Biology 131 (1), 111–123.
Puthenveedu, M.A., von Zastrow, M., 2006. Cargo regulates clathrin-coated pit dynamics. Cell 127 (1), 113–124.
Qin, Z.L., Zheng, Y., Kielian, M., 2009. Role of conserved histidine residues in the low-pH dependence of the Semliki Forest virus fusion protein. Journal of Virology 83 (9), 4670–4677.
Querbes, W., O'Hara, B.A., Williams, G., Atwood, W.J., 2006. Invasion of host cells by JC virus identifies a novel role for caveolae in endosomal sorting of noncaveolar ligands. Journal of Virology 80 (19), 9402–9413.
Quirin, K., Eschli, B., Scheu, I., Poort, L., Kartenbeck, J., Helenius, A., 2008. Lymphocytic choriomeningitis virus uses a novel endocytic pathway for infectious entry via late endosomes. Virology 378 (1), 21–33.
Rajendran, L., Simons, K., 2005. Lipid rafts and membrane dynamics. Journal of Cell Science 118 (Pt 6), 1099–1102.
Rigden, R.C., Carrasco, C.P., Summerfield, A., KC, M.C., 2002. Macrophage phagocytosis of foot-and-mouth disease virus may create infectious carriers. Immunology 106 (4), 537–548.
Roche, S., Bressanelli, S., Rey, F.A., Gaudin, Y., 2006. Crystal structure of the low-pH form of the vesicular stomatitis virus glycoprotein G. Science 313 (5784), 187–191.
Rojek, J.M., Pérez, M., Kunz, S., 2008a. Cellular entry of lymphocytic choriomeningitis virus. Journal of Virology 82 (3), 1505–1517.
Rojek, J.M., Sánchez, A.B., Nguyen, N.T., de la Torre, J.C., Kunz, S., 2008b. Different mechanisms of cell entry by human-pathogenic Old World and New World arenaviruses. Journal of Virology 82 (15), 7677–7687.
Rollason, R., Korolchuk, V., Hamilton, C., Schu, P., Banting, G., 2007. Clathrin-mediated endocytosis of a lipid-raft-associated protein is mediated through a dual tyrosine motif. Journal of Cell Science 120 (Pt 21), 3850–3858.
Roth, S.L., Whittaker, G.R., 2011. Promotion of vesicular stomatitis virus fusion by the endosome-specific phospholipid bis(monoacylglycero)phosphate (BMP). FEBS Letters.
Roth, T.F., Porter, K.R., 1964. Yolk Protein Uptake in the Oocyte of the Mosquito Aedes Aegypti. L. Journal of Cell Biology 20, 313–332.
Rothberg, K.G., Heuser, J.E., Donzell, W.C., Ying, Y.S., Glenney, J.R., Anderson, R.G., 1992. Caveolin, a protein component of caveolae membrane coats. Cell 68 (4), 673–682.
Rust, M.J., Lakadamyali, M., Zhang, F., Zhuang, X., 2004. Assembly of endocytic machinery around individual influenza viruses during viral entry. Nature Structural Molecular Biology 11 (6), 567–573.
Saeed, M.F., Kolokoltsov, A.A., Albrecht, T., Davey, R.A., 2010. Cellular entry of ebola virus involves uptake by a macropinocytosis-like mechanism and subsequent trafficking through early and late endosomes. PLoS Pathogens 6. (9).
Sandvig, K., van Deurs, B., 2005. Delivery into cells: lessons learned from plant and bacterial toxins. Gene Therapy 12 (11), 865–872.
Schelhaas, M., Malmstrom, J., Pelkmans, L., Haugstetter, J., Ellgaard, L., Grunewald, K., Helenius, A., 2007. Simian Virus 40 depends on ER protein folding and quality control factors for entry into host cells. Cell 131 (3), 516–529.
Schlegel, R., Tralka, T.S., Willingham, M.C., Pastan, I., 1983. Inhibition of VSV binding and infectivity by phosphatidylserine: is phosphatidylserine a VSV-binding site? Cell 32 (2), 639–646.
Schmidt, F.I., Bleck, C.K., Helenius, A., Mercer, J., 2011. Vaccinia extracellular virions enter cells by macropinocytosis and acid-activated membrane rupture. EMBO Journal 30 (17), 3647–3661.
Schmidt, F.I., Bleck, C.K., Mercer, J., 2012. Poxvirus host cell entry. Current Opinion in Virology 2 (1), 20–27.
Schober, D., Kronenberger, P., Prchla, E., Blaas, D., Fuchs, R., 1998. Major and minor receptor group human rhinoviruses penetrate from endosomes by different mechanisms. Journal of Virology 72 (2), 1354–1364.
Shajahan, A.N., Timblin, B.K., Sandoval, R., Tiruppathi, C., Malik, A.B., Minshall, R.D., 2004. Role of Src-induced dynamin-2 phosphorylation in caveolae-mediated endocytosis in endothelial cells. Journal of Biological Chemistry 279 (19), 20392–20400.
Sieczkarski, S.B., Whittaker, G.R., 2002a. Dissecting virus entry via endocytosis. Journal of General Virology 83 (Pt 7), 1535–1545.
Sieczkarski, S.B., Whittaker, G.R., 2002b. Influenza virus can enter and infect cells in the absence of clathrin-mediated endocytosis. Journal of Virology 76 (20), 10455–10464.
Sieczkarski, S.B., Whittaker, G.R., 2003. Differential requirements of Rab5 and Rab7 for endocytosis of influenza and other enveloped viruses. Traffic 4 (5), 333–343.
Sieczkarski, S.B., Whittaker, G.R., 2005. Viral entry. Current Topics in Microbiology and Immunology 285, 1–23.
Simons, K., Ikonen, E., 1997. Functional rafts in cell membranes. Nature 387 (6633), 569–572.
Simonsen, A., Gaullier, J.M., D'Arrigo, A., Stenmark, H., 1999. The Rab5 effector EEA1 interacts directly with syntaxin-6. Journal of Biological Chemistry 274 (41), 28857–28860.
Simpson, R.W., Hauser, R.E., Dales, S., 1969. Viropexis of vesicular stomatitis virus by L cells. Virology 37 (2), 285–290.
Smith, A.E., Helenius, A., 2004. How viruses enter animal cells. Science 304 (5668), 237–242.
Smith, E.C., Popa, A., Chang, A., Masante, C., Dutch, R.E., 2009. Viral entry mechanisms: the increasing diversity of paramyxovirus entry. FEBS Journal 276 (24), 7217–7227.
Smith, J.L., Campos, S.K., Wandinger-Ness, A., Ozbun, M.A., 2008. Caveolin-1-dependent infectious entry of human papillomavirus type 31 in human keratinocytes proceeds to the endosomal pathway for pH-dependent uncoating. Journal of Virology 82 (19), 9505–9512.
Snyers, L., Zwickl, H., Blaas, D., 2003. Human rhinovirus type 2 is internalized by clathrin-mediated endocytosis. Journal of Virology 77 (9), 5360–5369.
Sorkin, A., 2004. Cargo recognition during clathrin-mediated endocytosis: a team effort. Current Opinion in Cell Biology 16 (4), 392–399.
Srivastava, J., Barber, D.L., Jacobson, M.P., 2007. Intracellular pH sensors: design principles and functional significance. Physiology (Bethesda) 22, 30–39.
Stenmark, H., 2009. Rab GTPases as coordinators of vesicle traffic. Nature Review: Molecular Cell Biology 10 (8), 513–525.
Stoddart, A., Dykstra, M.L., Brown, B.K., Song, W., Pierce, S.K., Brodsky, F.M., 2002. Lipid rafts unite signaling cascades with clathrin to regulate BCR internalization. Immunity 17 (4), 451–462.
Summerfield, A., Guzylack-Piriou, L., Harwood, L., McCullough, K.C., 2009. Innate immune responses against foot-and-mouth disease virus: current understanding and future directions. Veterinary Immunology and Immunopathology 128 (1–3), 205–210.
Sun, X., Yau, V.K., Briggs, B.J., Whittaker, G.R., 2005. Role of clathrin-mediated endocytosis during vesicular stomatitis virus entry into host cells. Virology 338 (1), 53–60.
Swanson, J.A., 2008. Shaping cups into phagosomes and macropinosomes. Nature Review: Molecular Cell Biology 9 (8), 639–649.

Tagawa, A., Mezzacasa, A., Hayer, A., Longatti, A., Pelkmans, L., Helenius, A., 2005. Assembly and trafficking of caveolar domains in the cell: caveolae as stable, cargo-triggered, vesicular transporters. Journal of Cell Biology 170 (5), 769–779.
Thorley, J.A., McKeating, J.A., Rappoport, J.Z., 2010. Mechanisms of viral entry: sneaking in the front door. Protoplasma 244 (1–4), 15–24.
Thurlkill, R.L., Grimsley, G.R., Scholtz, J.M., Pace, C.N., 2006. pK values of the ionizable groups of proteins. Protein Science 15 (5), 1214–1218.
Tosteson, M.T., Chow, M., 1997. Characterization of the ion channels formed by poliovirus in planar lipid membranes. Journal of Virology 71 (1), 507–511.
Tsai, B., 2007. Penetration of nonenveloped viruses into the cytoplasm. Annual Review of Cell and Developmental Biology 23, 23–43.
Tsai, B., Gilbert, J.M., Stehle, T., Lencer, W., Benjamin, T.L., Rapoport, T.A., 2003. Gangliosides are receptors for murine polyoma virus and SV40. EMBO Journal 22 (17), 4346–4355.
Tsai, B., Qian, M., 2010. Cellular entry of polyomaviruses. Current Topics in Microbiology and Immunology 343, 177–194.
Umashankar, M., Sanchez-San Martin, C., Liao, M., Reilly, B., Guo, A., Taylor, G., Kielian, M., 2008. Differential cholesterol binding by class II fusion proteins determines membrane fusion properties. Journal of Virology 82 (18), 9245–9253.
van der Bliek, A.M., Meyerowitz, E.M., 1991. Dynamin-like protein encoded by the *Drosophila shibire* gene associated with vesicular traffic. Nature 351 (6325), 411–414.
van der Schaar, H.M., Rust, M.J., Chen, C., van der Ende-Metselaar, H., Wilschut, J., Zhuang, X., Smit, J.M., 2008. Dissecting the cell entry pathway of dengue virus by single-particle tracking in living cells. PLoS Pathogens 4 (12), e1000244.
van Vlijmen, H.W., Curry, S., Schaefer, M., Karplus, M., 1998. Titration calculations of foot-and-mouth disease virus capsids and their stabilities as a function of pH. Journal of Molecular Biology 275 (2), 295–308.
Vela, E.M., Zhang, L., Colpitts, T.M., Davey, R.A., Aronson, J.F., 2007. Arenavirus entry occurs through a cholesterol-dependent, non-caveolar, clathrin-mediated endocytic mechanism. Virology 369 (1), 1–11.
Vonderheit, A., Helenius, A., 2005. Rab7 associates with early endosomes to mediate sorting and transport of Semliki forest virus to late endosomes. PLoS Biology 3 (7), e233.
Welling, P.A., Weisz, O.A., 2010. Sorting it out in endosomes: an emerging concept in renal epithelial cell transport regulation. Physiology (Bethesda) 25 (5), 280–292.
Whitbeck, J.C., Foo, C.H., Ponce de Leon, M., Eisenberg, R.J., Cohen, G.H., 2009. Vaccinia virus exhibits cell-type-dependent entry characteristics. Virology 385 (2), 383–391.
White, J., Matlin, K., Helenius, A., 1981. Cell fusion by Semliki Forest, influenza, and vesicular stomatitis viruses. Journal of Cell Biology 89 (3), 674–679.
Wilson, I.A., Skehel, J.J., Wiley, D.C., 1981. Structure of the haemagglutinin membrane glycoprotein of influenza virus at 3 A resolution. Nature 289 (5796), 366–373.
Yamada, E., 1955. The fine structure of the gall bladder epithelium of the mouse. Journal of Biophysical and Biochemical Cytology 1 (5), 445–458.
Yamashiro, D.J., Fluss, S.R., Maxfield, F.R., 1983. Acidification of endocytic vesicles by an ATP-dependent proton pump. Journal of Cell Biology 97 (3), 929–934.
Yamashiro, D.J., Maxfield, F.R., 1984. Acidification of endocytic compartments and the intracellular pathways of ligands and receptors. Journal of Cellular Biochemistry 26 (4), 231–246.
York, J., Nunberg, J.H., 2006. Role of the stable signal peptide of Junin arenavirus envelope glycoprotein in pH-dependent membrane fusion. Journal of Virology 80 (15), 7775–7780.
Zaitseva, E., Yang, S.T., Melikov, K., Pourmal, S., Chernomordik, L.V., 2010. Dengue virus ensures its fusion in late endosomes using compartment-specific lipids. PLoS Pathogens 6 (10), e1001131.

Journal of General Virology (2012), **93**, 000–000 DOI 10.1099/vir.0.045419-0

Short Communication

Modulation of foot-and-mouth disease virus pH threshold for uncoating correlates with differential sensitivity to inhibition of cellular Rab GTPases and decreases infectivity *in vivo*

Ángela Vázquez-Calvo,[1] Flavia Caridi,[1] Miguel Rodriguez-Pulido,[1] Belén Borrego,[2] Margarita Sáiz,[1] Francisco Sobrino[1,2] and Miguel A. Martín-Acebes[1]

[1]Centro de Biología Molecular 'Severo Ochoa' (UAM/CSIC), Cantoblanco, Madrid, Spain

[2]Centro de Investigación en Sanidad Animal, INIA, Valdeolmos, Madrid, Spain

Correspondence
Francisco Sobrino
fsobrino@cbm.uam.es

Received 18 June 2012
Accepted 6 August 2012

The role of cellular Rab GTPases that govern traffic between different endosome populations was analysed on foot-and-mouth disease virus (FMDV) infection. Changes of viral receptor specificity did not alter Rab5 requirement for infection. However, a correlation between uncoating pH and requirement of Rab5 for infection was observed. A mutant FMDV with less acidic uncoating pH threshold was less sensitive to inhibition of Rab5, whereas another mutant with more acidic requirements was more sensitive to inhibition of Rab5. On the contrary, opposed correlations between uncoating pH and dependence of Rab function were observed upon expression of dominant-negative forms of Rab7 or 11. Modulation of uncoating pH also reduced FMDV virulence in suckling mice. These results are consistent with FMDV uncoating inside early endosomes and indicate that displacements from optimum pH for uncoating reduce viral fitness *in vivo*.

Foot-and-mouth disease virus (FMDV), the aetiological agent of an important disease of cloven-hoofed animals, is the type species of the genus *Aphthovirus* within the family *Picornaviridae* (Grubman & Baxt, 2004; Sáiz *et al.*, 2002). FMDV infects cells by binding to different $\alpha_v\beta$ integrins although tissue culture-adapted variants can also use heparan sulfate glycosaminoglycans (HS) or other uncharacterized receptors (Ruiz-Sáenz *et al.*, 2009). FMDV isolates using integrins undergo clathrin-mediated endocytosis to gain entry into early endosomes (EE) (Berryman *et al.*, 2005; Jackson *et al.*, 1996; Martín-Acebes *et al.*, 2007; O'Donnell *et al.*, 2005), while variants that bind HS are internalized through caveolae and transferred to EE (O'Donnell *et al.*, 2008). Following similar principles shared by a wide variety of viruses, penetration of FMDV is triggered by acidic pH inside endosomal compartments (Vázquez-Calvo *et al.*, 2012). The current model suggests that uncoating should mainly take place inside EE, since FMDV particles disassemble at pH values around 6.5 (Curry *et al.*, 1995; Knipe *et al.*, 1997; Martín-Acebes *et al.*, 2010, 2011), which is consistent with pH values inside EE, 6.1–6.8 (Huotari & Helenius, 2011; Jovic *et al.*, 2010). Supporting this hypothesis, expression of a dominant-negative (DN) form of Rab5 GTPase (a small GTPase that governs traffic of EE) inhibited infection by type O FMDV (Johns *et al.*, 2009).

The effect of the expression of a DN Rab5 GTPase was tested on the infection of FMDV C-S8c1, a plaque-purified derivative of a type C field FMDV isolate (Sobrino *et al.*, 1983), whose entry route is integrin-dependent (Núñez *et al.*, 2007). The requirement of Rab5 by C-S8c1 was compared to that of MARLS, a derivative that uses non-integrin receptors (Baranowski *et al.*, 1998, 2000). To this end, BHK-21 cells (ATCC) were transfected with plasmids encoding wild-type (WT) or DN forms of Rab5 fused to green fluorescent protein (GFP) (Gerges *et al.*, 2005) by electroporation using a Gene Pulser XCell (Bio-Rad). Twenty-four hours post-electroporation, cells were infected at an m.o.i. of 1 p.f.u. cell^{-1}, fixed 7 h later, processed for immunofluorescence (Martín-Acebes *et al.*, 2009) and the number of infected cells expressing GFP was scored (Fig. 1a). In accordance with the results reported for type O FMDV (Johns *et al.*, 2009), expression of DN Rab5 reduced the infection by C-S8c1 significantly. The extent of this inhibition was similar to that displayed by MARLS. As FMDV capsid disassembles at acid pH losing infectivity, acid sensitivity profiles of C-S8c1 and MARLS were determined by incubation with buffers of different pH values, as reported (Martín-Acebes *et al.*, 2010, 2011) (Fig. 1b). This assay has revealed a good association between

A supplementary figure is available with the online version of this paper.

pH_{50} values, defined as the pH values leading to a 50 % loss of infectivity, and those of corresponding pH_{50} values determined for capsid disassembly (Martín-Acebes *et al.*, 2011). The pH_{50} for C-S8c1 infectivity was 6.56, very close to previously reported value of 6.58 (Martín-Acebes *et al.*, 2010, 2011), and 6.59 for MARLS, confirming that involvement of acidic pH, as well as the dependence on Rab5 GTPase for FMDV uncoating, is not affected by the changes in receptor specificity shown by MARLS.

Acidification is an important step in endosome maturation (Huotari & Helenius, 2011; Jovic *et al.*, 2010). In this way, variations of the pH threshold for FMDV uncoating could lead to differences in endosomal requirements. To test this hypothesis, the involvement of Rab GTPases on virus infectivity was compared for C-S8c1 and two of its derivatives: one mutant with less acidic requirement for capsid disassembly termed c2 − pH_{50} of 6.95 (Martín-Acebes *et al.*, 2010), and another mutant with more acidic requirement termed m6 − pH_{50} of 6.11 (Martín-Acebes *et al.*, 2011). Expression of either WT or DN fusion Rab proteins was confirmed by fluorescence microscopy and Western blotting (Fig. S1, available in JGV Online). Expression of DN Rab5 inhibited infection by C-S8c1 and by the two mutants (Fig. 2a), although differences in the extent of inhibition were noticed, being higher for m6 and lower for c2. A direct correlation between the percentage of infected cells expressing DN Rab5 and pH_{50} (selected as an estimation of pH for disassembly) was found (Fig. 2b), highlighting that uncoating pH was directly related to Rab5 function. On the other hand, the expression of DN Rab7 (Gerges *et al.*, 2005), a GTPase involved in traffic from EE to late endosomes (LE) (Poteryaev *et al.*, 2010), did not induce a significant reduction of infection by any of the viruses tested (Fig. 2c), which was consistent with previous results with type O FMDV (Johns *et al.*, 2009). However, when the percentage of infected cells expressing DN Rab7 was plotted against pH_{50} values of the viruses, an inverse correlation was found (Fig. 2d), in contrast to the direct correlation obtained for Rab5. The effect of the expression of DN Rab11 (Gerges *et al.*, 2005), a GTPase involved in traffic from EE to recycling endosomes (RE) (Schwartz *et al.*, 2007) was also analysed (Fig. 2e). As described for type O FMDV (Johns *et al.*, 2009), no statistically significant inhibition of viral infection was noticed. However, an inverse correlation between the percentage of infected cells expressing DN Rab11 and pH_{50} values of the viruses was found again (Fig. 2f). Transfected cells were alternatively infected with lymphocytic choriomeninigitis virus (LCMV) (Martín *et al.*, 2008), whose acid-dependent mechanism of entry is independent of Rab5 or Rab7 activity (Di Simone & Buchmeier, 1995; Quirin *et al.*, 2008). No inhibition of LCMV infection was derived from expression of DN forms of these GTPases (Fig. 2a, c and e), confirming the specificity of the results obtained for FMDV. Mutants c2 and m6 only differ in two (c2) and one amino acid (m6) relative to the parental virus C-S8c1, and these mutations that are located at structural proteins, modulate capsid disassembly, whilst they do not affect viral multiplication in cultured cells (Martín-Acebes *et al.*, 2010, 2011). Thus, the differences observed between these viruses upon expression of DN Rabs are probably related to differences on entry and uncoating (processes in which the capsid plays major roles) rather than on other aspects of the virus life cycle, such as replication. Therefore, the analysis of the correlations between Rab5 and Rab7/11 and viral pH_{50} values uncover an opposite relationship between uncoating pH and the requirement of Rab proteins controlling entry

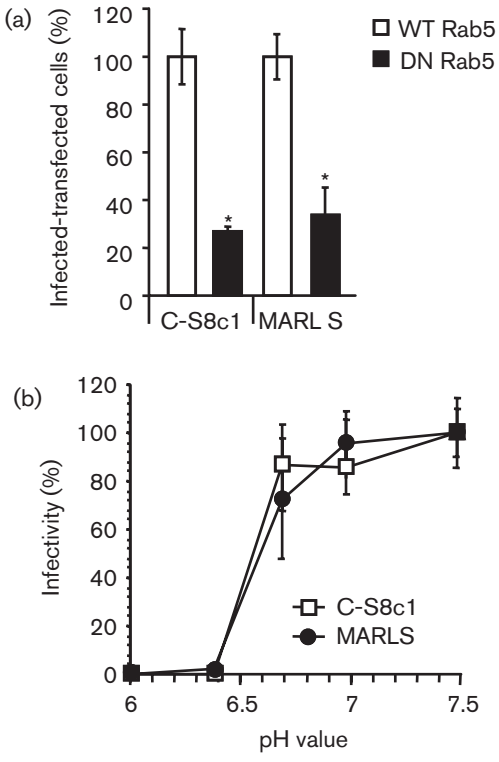

Fig. 1. Requirements of Rab5 and pH for FMDV infection are independent of receptor usage. (a) BHK-21 cells were transfected by eletroporation with plasmids encoding WT or DN Rab5 fused to GFP. Transfected monolayers were infected (m.o.i. of 1 p.f.u. $cell^{-1}$) with C-S8c1 or MARLS at 24 h post-electroporation. Infected cells were fixed and processed for immunofluorescence (7 h post-infection) using antibody 5C4 (Lea *et al.*, 1994) and a secondary antibody coupled with Alexa Fluor 555 (Invitrogen) as described previously (Martín-Acebes *et al.*, 2007). The bars represent mean percentage of transfected and infected cells ± SD normalized to the level of infection of cells expressing the WT Rab protein. At least 300 transfected cells expressing GFP fusion proteins were scored in each case in three independent experiments. (b) Acid sensitivity profiles of C-S8c1 and MARLS. Equal amounts of the different viruses were treated with acid buffers at different pH values for 30 min, neutralized and plated as described previously (Martín-Acebes *et al.*, 2010, 2011). Infectivity was calculated as the percentage of p.f.u. recovered relative to that obtained at pH 7.5.

into EE (Rab5) and those controlling exit from EE either to LE (Rab7) or to RE (Rab11).

These results obtained with mutant viruses are consistent with an FMDV uncoating that mainly takes place inside EE. Endosomal maturation and its consequent acidification are gradual processes regulated by Rab5 to Rab7 conversion (Huotari & Helenius, 2011; Poteryaev *et al.*, 2010). According to this, mutant m6, which is more dependent on lower pH for infection, exhibited greater inhibition by DN Rab5 because its pH_{50} (6.1) is close to the lower end of the EE pH gradient. On the other hand, mutant c2 that is less dependent on lower pH for infection was less inhibited by the DN Rab5. However, the infection of parental C-S8c1 and both mutant viruses was not significantly reduced by expression of the DN Rab7 and Rab11, indicating that the uncoating process probably does not occur in LE or RE as shown previously for type O FMDV (Johns *et al.*, 2009). Interestingly, mutant virus m6, that requires lower pH for disassembly, exhibited better infection compared with the c2 mutant, when function of Rab7 or Rab11 was inhibited. This phenomenon may be explained because once the trafficking from early to medium to late endosome is shut off by DN Rab7, mutant m6 accumulates in the early to medium endosomes rather than being partially transported through late endosome to lysosomes for degradation, as it has been previously suggested (Berryman *et al.*, 2005; O'Donnell *et al.*, 2005). As a result, the infectivity for m6 was higher in DN Rab7-transfected cells. Regarding the involvement of Rab11 in FMDV infection, it has been suggested that uncoating may not be exclusive to EE and that a small amount of infection could occur from within the RE due to the effect of DN Rab11 expression (Johns *et al.*, 2009). This hypothesis is compatible with the inhibition of the c2 virus observed in this study, which was more sensitive to the expression of the DN form of this GTPase (although the differences were not significant), suggesting that uncoating of the c2 virus could take place in a population of EE more close to RE than C-S8c1 and m6 viruses.

To address whether uncoating differences, leading to different requirements of Rab GTPases in cultured cells, affected infectivity *in vivo*, the virulence of FMDV variants differing in uncoating pH (C-S8c1, c2 and m6) was assayed in suckling mice, as described previously (Baranowski *et al.*, 2003; Gutiérrez-Rivas *et al.*, 2008). Viral stock dilutions were inoculated intraperitoneally and dead animals were scored up to 9 days after inoculation to estimate LD_{50} values (Table 1). When LD_{50} values were compared with

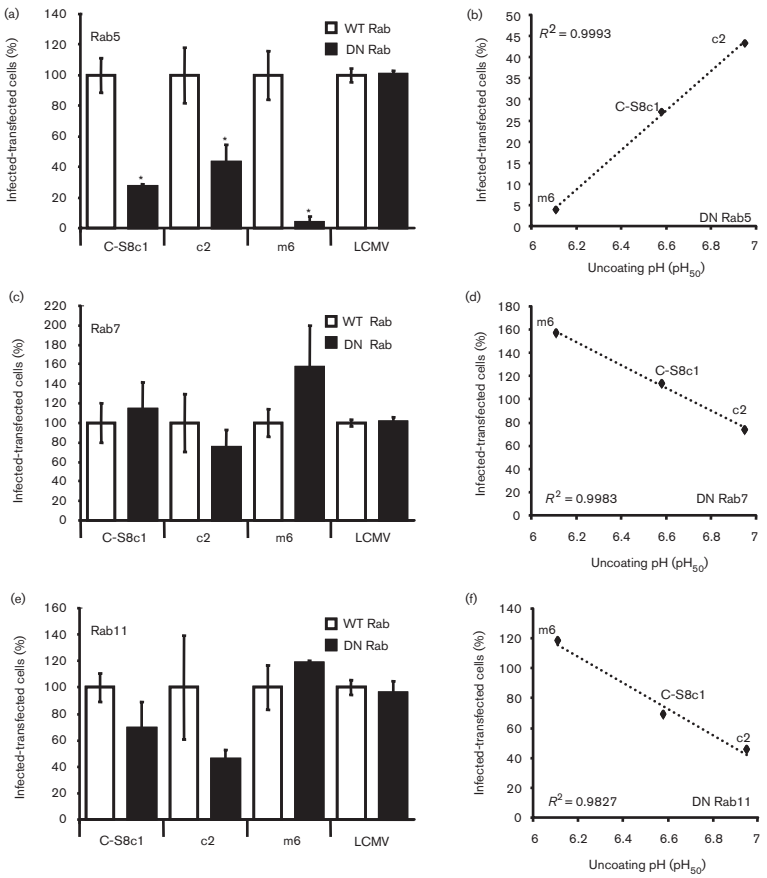

Fig. 2. Relationship between Rab requirements and uncoating pH for FMDV infection. BHK-21 cells were transfected by electroporation with plasmids encoding WT or DN Rab5 (a), Rab7 (c) or Rab11 (e) fused to GFP and infected with FMDV variants C-S8c1, c2 or m6 or LCMV (m.o.i. of 1 p.f.u. $cell^{-1}$) as a control. Cells were fixed (7 or 24 h post-infection for FMDV and LCMV, respectively) and stained by immunofluorescence (Martín-Acebes *et al.*, 2007) using antibody 5C4 (Lea *et al.*, 1994) to detect FMDV-infected cells or antibody 1.1.3 to detect LCMV (Urata *et al.*, 2011). Alexa Fluor 555 secondary antibodies were used in both cases. The bars represent mean percentage of transfected and infected cells ± SD normalized to the level of infection of cells expressing the WT Rab protein. At least 300 transfected cells expressing GFP fusion proteins were scored in each case in three independent experiments. Statistically significant differences between cells transfected with WT or DN Rabs are indicated by one asterisk (ANOVA $P \leqslant 0.05$). The mean percentage of cells transfected with DN Rab5 (b), DN Rab7 (d) or DN Rab11 (f) and infected with FMDV variants C-S8c1, c2 or m6 was plotted against the uncoating pH (estimated by pH_{50} value) for each of the FMDV variants analysed. Pearson's correlation coefficients (R^2) are indicated in the graphs.

the p.f.u. ml^{-1} determined for the viral stocks used, a decrease in mouse infectivity, relative to that of C-S8c1, of about twofold and tenfold was observed for mutants m6 and c2, respectively. The presence of nucleotide replacements described for c2−C2903T (VP3 A118V) and A3346G (VP1 N47D) (Martín-Acebes *et al.*, 2010), and m6, A3256G (VP1 N17D) (Martín-Acebes *et al.*, 2011) was confirmed by nucleotide sequencing of RNA from dead mice homogenates (two animals per mutant), indicating that revertant viruses had not been selected in dead mice (data not shown). No additional mutations in the capsid of viruses recovered from dead animals were found, indicating that compensatory mutations were not selected in dead animals. This lack of reversion was consistent with previous results obtained from infections performed in cultured cells, in which these mutations were maintained after six passages in absence of the selective pressure applied to isolate mutants c2 and m6 (Martín-Acebes *et al.*, 2010, 2011). The difference in virulence between c2 and m6 indicates that the alteration of uncoating pH of FMDV exhibited by mutant viruses carries a reduction of viral fitness *in vivo*, although it had no noticeable effects on cultured cells (Martín-Acebes *et al.*, 2010, 2011). The higher reduction of the virulence exhibited by the c2 virus could also be related to differences on particle stability that can affect infection *in vivo*, since particles from this mutant display an increased tendency to dissociation not observed for the m6 virus (Martín-Acebes *et al.*, 2010, 2011).

In summary, we have studied the relationships between receptor specificity, uncoating pH and Rab requirements for FMDV infectivity. Changes of receptor specificity of FMDV did not alter either uncoating pH or Rab5 requirement. However, modulation of uncoating pH correlated with differential sensitivity of infection to inhibition of different Rab GTPases function, and also reduced virulence in suckling mice. These results reveal a relationship between dependence on Rab GTPases and uncoating pH of FMDV, and are consistent with the current model of uncoating mainly occurring inside EE.

Acknowledgements

This work was supported by Spanish grants BIO2008-0447-C03-01 and BIO2011-24351, and by an institutional grant from Fundación Ramón Areces and by the ICTS program from the Spanish Ministry of Science and Innovation. M. A. M. A. is the recipient of JAE-Doc fellowship from CSIC. We thank E. Brocchi for antibody 5C4, J. C. de la Torre for antibody 1.1.3, E. Domingo for FMDV MARLS and LCMV, J.A. Esteban for plasmid constructs encoding Rab proteins and N. de la Losa for advice with animal experimentation.

References

Baranowski, E., Sevilla, N., Verdaguer, N., Ruiz-Jarabo, C. M., Beck, E. & Domingo, E. (1998). Multiple virulence determinants of foot-and-mouth disease virus in cell culture. *J Virol* **72**, 6362–6372.

Baranowski, E., Ruiz-Jarabo, C. M., Sevilla, N., Andreu, D., Beck, E. & Domingo, E. (2000). Cell recognition by foot-and-mouth disease virus that lacks the RGD integrin-binding motif: flexibility in aphthovirus receptor usage. *J Virol* **74**, 1641–1647.

Baranowski, E., Molina, N., Núñez, J. I., Sobrino, F. & Sáiz, M. (2003). Recovery of infectious foot-and-mouth disease virus from suckling mice after direct inoculation with in vitro-transcribed RNA. *J Virol* **77**, 11290–11295.

Berryman, S., Clark, S., Monaghan, P. & Jackson, T. (2005). Early events in integrin $\alpha v\beta 6$-mediated cell entry of foot-and-mouth disease virus. *J Virol* **79**, 8519–8534.

Curry, S., Abrams, C. C., Fry, E., Crowther, J. C., Belsham, G. J., Stuart, D. I. & King, A. M. (1995). Viral RNA modulates the acid sensitivity of foot-and-mouth disease virus capsids. *J Virol* **69**, 430–438.

Di Simone, C. & Buchmeier, M. J. (1995). Kinetics and pH dependence of acid-induced structural changes in the lymphocytic choriomeningitis virus glycoprotein complex. *Virology* **209**, 3–9.

Gerges, N. Z., Brown, T. C., Correia, S. S. & Esteban, J. A. (2005). Analysis of Rab protein function in neurotransmitter receptor trafficking at hippocampal synapses. *Methods Enzymol* **403**, 153–166.

Grubman, M. J. & Baxt, B. (2004). Foot-and-mouth disease. *Clin Microbiol Rev* **17**, 465–493.

Gutiérrez-Rivas, M., Pulido, M. R., Baranowski, E., Sobrino, F. & Sáiz, M. (2008). Tolerance to mutations in the foot-and-mouth disease virus integrin-binding RGD region is different in cultured cells and in vivo and depends on the capsid sequence context. *J Gen Virol* **89**, 2531–2539.

Table 1. Infectivity in cell culture and virulence in suckling mice of FMDVs

These experiments were approved by the Committee on the Ethics of Animal Experiments of INIA (permit number: CBS 2008/016).

Virus*	Infectivity in BHK-21 cells (p.f.u. ml^{-1})†	Virulence in suckling mice (LD_{50} ml^{-1})‡
C-S8c1	1×10^7	$>10^7$
c2	1×10^7	5×10^5
m6	1×10^7	4×10^6

*Virus stock prepared in BHK-21 cells.

†Viral titres recovered upon infection of BHK-21 cells with the corresponding virus stock.

‡Different dilutions of the corresponding viral stock were inoculated intraperitoneally (in a group of ten mice each) and LD_{50} values were determined as described previously (Muench, 1935).

Huotari, J. & Helenius, A. (2011). Endosome maturation. *EMBO J* **30**, 3481–3500.

Jackson, T., Ellard, F. M., Ghazaleh, R. A., Brookes, S. M., Blakemore, W. E., Corteyn, A. H., Stuart, D. I., Newman, J. W. & King, A. M. (1996). Efficient infection of cells in culture by type O foot-and-mouth disease virus requires binding to cell surface heparan sulfate. *J Virol* **70**, 5282–5287.

Johns, H. L., Berryman, S., Monaghan, P., Belsham, G. J. & Jackson, T. (2009). A dominant-negative mutant of rab5 inhibits infection of cells by foot-and-mouth disease virus: implications for virus entry. *J Virol* **83**, 6247–6256.

Jovic, M., Sharma, M., Rahajeng, J. & Caplan, S. (2010). The early endosome: a busy sorting station for proteins at the crossroads. *Histol Histopathol* **25**, 99–112.

Knipe, T., Rieder, E., Baxt, B., Ward, G. & Mason, P. W. (1997). Characterization of synthetic foot-and-mouth disease virus provirions separates acid-mediated disassembly from infectivity. *J Virol* **71**, 2851–2856.

Lea, S., Hernández, J., Blakemore, W., Brocchi, E., Curry, S., Domingo, E., Fry, E., Abu-Ghazaleh, R., King, A. & other authors (1994). The structure and antigenicity of a type C foot-and-mouth disease virus. *Structure* **2**, 123–139.

Martín, V., Grande-Pérez, A. & Domingo, E. (2008). No evidence of selection for mutational robustness during lethal mutagenesis of lymphocytic choriomeningitis virus. *Virology* **378**, 185–192.

Martín-Acebes, M. A., González-Magaldi, M., Sandvig, K., Sobrino, F. & Armas-Portela, R. (2007). Productive entry of type C foot-and-mouth disease virus into susceptible cultured cells requires clathrin and is dependent on the presence of plasma membrane cholesterol. *Virology* **369**, 105–118.

Martín-Acebes, M. A., González-Magaldi, M., Rosas, M. F., Borrego, B., Brocchi, E., Armas-Portela, R. & Sobrino, F. (2008). Subcellular distribution of swine vesicular disease virus proteins and alterations induced in infected cells: a comparative study with foot-and-mouth disease virus and vesicular stomatitis virus. *Virology* **374**, 432–443.

Martín-Acebes, M. A., González-Magaldi, M., Vázquez-Calvo, A., Armas-Portela, R. & Sobrino, F. (2009). Internalization of swine vesicular disease virus into cultured cells: a comparative study with foot-and-mouth disease virus. *J Virol* **83**, 4216–4226.

Martín-Acebes, M. A., Rincón, V., Armas-Portela, R., Mateu, M. G. & Sobrino, F. (2010). A single amino acid substitution in the capsid of foot-and-mouth disease virus can increase acid lability and confer resistance to acid-dependent uncoating inhibition. *J Virol* **84**, 2902–2912.

Martín-Acebes, M. A., Vázquez-Calvo, A., Rincón, V., Mateu, M. G. & Sobrino, F. (2011). A single amino acid substitution in the capsid of foot-and-mouth disease virus can increase acid resistance. *J Virol* **85**, 2733–2740.

Muench, R. L. J. H. (1935). A simple method of estimating fifty percent endpoints. *Am J Hyg* **27**, 493–497.

Núñez, J. I., Molina, N., Baranowski, E., Domingo, E., Clark, S., Burman, A., Berryman, S., Jackson, T. & Sobrino, F. (2007). Guinea pig-adapted foot-and-mouth disease virus with altered receptor recognition can productively infect a natural host. *J Virol* **81**, 8497–8506.

O'Donnell, V., LaRocco, M., Duque, H. & Baxt, B. (2005). Analysis of foot-and-mouth disease virus internalization events in cultured cells. *J Virol* **79**, 8506–8518.

O'Donnell, V., Larocco, M. & Baxt, B. (2008). Heparan sulfate-binding foot-and-mouth disease virus enters cells via caveola-mediated endocytosis. *J Virol* **82**, 9075–9085.

Poteryaev, D., Datta, S., Ackema, K., Zerial, M. & Spang, A. (2010). Identification of the switch in early-to-late endosome transition. *Cell* **141**, 497–508.

Quirin, K., Eschli, B., Scheu, I., Poort, L., Kartenbeck, J. & Helenius, A. (2008). Lymphocytic choriomeningitis virus uses a novel endocytic pathway for infectious entry via late endosomes. *Virology* **378**, 21–33.

Ruiz-Sáenz, J., Goez, Y., Tabares, W. & López-Herrera, A. (2009). Cellular receptors for foot and mouth disease virus. *Intervirology* **52**, 201–212.

Sáiz, M., Núñez, J. I., Jimenez-Clavero, M. A., Baranowski, E. & Sobrino, F. (2002). Foot-and-mouth disease virus: biology and prospects for disease control. *Microbes Infect* **4**, 1183–1192.

Schwartz, S. L., Cao, C., Pylypenko, O., Rak, A. & Wandinger-Ness, A. (2007). Rab GTPases at a glance. *J Cell Sci* **120**, 3905–3910.

Sobrino, F., Dávila, M., Ortín, J. & Domingo, E. (1983). Multiple genetic variants arise in the course of replication of foot-and-mouth disease virus in cell culture. *Virology* **128**, 310–318.

Urata, S., Yun, N., Pasquato, A., Paessler, S., Kunz, S. & de la Torre, J. C. (2011). Antiviral activity of a small-molecule inhibitor of arenavirus glycoprotein processing by the cellular site 1 protease. *J Virol* **85**, 795–803.

Vázquez-Calvo, A., Saiz, J. C., McCullough, K. C., Sobrino, F. & Martín-Acebes, M. A. (2012). Acid-dependent viral entry. *Virus Res* **167**, 125–137.

Plasma Membrane Phosphatidylinositol 4,5 Bisphosphate is Required for Internalization of Foot-and-mouth Disease Virus and Vesicular Stomatitis Virus

Short title: $PI(4,5)P_2$ in FMDV and VSV entry

Ángela Vázquez-Calvo[1], Francisco Sobrino[1,2,*] and Miguel A. Martín-Acebes[1]

[1]Centro de Biología Molecular "Severo Ochoa" (UAM/CSIC), Cantoblanco, Madrid (Spain); [2] Centro de Investigación en Sanidad Animal, INIA, Valdeolmos, Madrid (Spain)

*Corresponding author: Francisco Sobrino. Centro de Biología Molecular Severo Ochoa, Nicolás Cabrera 1, UAM, 28049 Madrid, Spain. Phone: 34-91 196 4493; fax: 34-91 196 4420; email: fsobrino@cbm.uam.es

Abstract Word count: 182

Text word count: 2453

Abstract

Phosphatidylinositol-4,5-bisphosphate, PI(4,5)P_2, is a phospholipid which plays important roles in clathrin-mediated endocytosis. To investigate the possible role of this lipid on viral entry, two viruses important for animal health were selected: the enveloped vesicular stomatitis virus (VSV) − which uses a well characterized clathrin mediated endocytic route − and two different variants of the non-enveloped foot-and-mouth disease virus (FMDV) with distinct receptor specificities. The expression of a dominant negative dynamin, an effector protein of PI(4,5)P_2, inhibited the internalization and infection of VSV and both FMDV isolates. Depletion of PI(4,5)P_2 from plasma membrane using ionomycin or an inducible system, and inhibition of its *de novo* synthesis with 1-butanol revealed that VSV as well as FMDV C-S8c1, which uses integrins as receptor, displayed a high dependence on PI(4,5)P_2 for internalization. Interestingly FMDV MARLS variant that uses receptors other than integrins for cell entry was less sensitive to PI(4,5)P_2 depletion, suggesting the involvement of endocytic routes other than the clathrin-mediated on its entry. These results highlight the role of PI(4,5)P_2 on viral entry and point to modulation of this molecule as a potential antiviral strategy.

Introduction

Phosphatidylinositols (PIs) and their phosphorylated derivatives are low abundant lipids in cellular membranes (< 10 % of total phospholipids) that have been revealed as key membrane components, particularly for membrane traffic [1]. One of these lipids, phosphatidyilinositol-4,5-bisphosphate ($PI(4,5)P_2$), which is mostly localized in the internal hemimembrane of the plasma membrane, participates in regulation of a variety of cellular processes such as generation of membrane curvature, fission of endosomes, exocytosis and binding to different effectors of clathrin-dependent endocytosis as well as at actin regulator proteins [1,2,3,4]. In this way, depletion of $PI(4,5)P_2$ from plasma membrane has been shown to inhibit clathrin-mediated endocytosis [2,3,4,5,6,7]. In this endocytic route clathrin-coated pits (CCPs) are assembled at the plasma membrane from cytosolic coat proteins. Upon capture of transmembrane receptor molecules CCPs invaginate to maturate into clathrin-coated vesicles (CCVs) [8]. Recent reports have shown that synthesis of $PI(4,5)P_2$ is the major determinant of $PI(4,5)P_2$ availability for CCP initiation and nucleation by contributing to progression beyond the endocytosis checkpoint and stabilization of nascent CCPs [2,3,4,5,6,9,10]. Although late states of CCP maturation to CCV do not require the synthesis of $PI(4,5)P_2$, the presence of this lipid is necessary to bind proteins involved in CCV scission [2,11]. As the other PIs, $PI(4,5)P_2$ carries out these regulatory functions by binding to different effector proteins through well characterized domains [1]. It is suggested that $PI(4,5)P_2$ levels regulate CCP assembly, whereas localized turnovers of this phospholipid can control multiple stages in CCV formation [2,12]

Proteins interacting with PIs (e.g Rab proteins, dynamin) have been involved in the entry of multiple viruses [13,14,15,16,17,18,19] thus pointing the importance of specific PIs in several steps for viral progression. However, a direct involvement of PIs,

and specifically of $PI(4,5)P_2$, in viral entry has been poorly evaluated, and the evidence for this is limited to the Human immunodeficiency virus type-1 (HIV-1) entry [20]. Indeed, HIV-1 binding to the plasma membrane through Env-gp120 actives PI4P5K I_α protein, increasing the production of $PI(4,5)P_2$. In addition, $PI(4,5)P_2$ is required for late steps of HIV-1 and HIV-2 infection to promote the localization of Gag protein on plasma membrane during viral assembly [21,22].

In the present study, we addressed the role of $PI(4,5)P_2$ on the internalization of non-enveloped as well as of enveloped viruses. For this purpose, two important pathogens for animal health, causing indistinguishable diseases, were selected: foot-and-mouth disease virus (FMDV) and vesicular stomatitis virus (VSV). FMDV is a small, non-enveloped virus responsible for a highly contagious disease affecting cloven-hoofed animals [23]. FMDV initiates infection of cultured cells via different α_v integrins [24,25,26,27], although receptors different from integrins can be used by FMDV variants selected upon passages in cultured cells [28,29]. FMDV isolates that recognize integrins as cellular receptor utilize CCPs to enter cultured cells [30,31,32], while FMDV variants using heparan sulphate (HS) proteoglycans as receptor instead of integrins are internalized via caveolae [33]. To compare the $PI(4,5)P_2$ requirements derived from the use of different cellular receptors, two different FMDV isolates were included in the study: C-S8c1 that is dependent on integrins for infection [34] and MARLS, a C-S8c1 derivative that has acquired the ability to enter cultured cells using HS and other not well characterized receptor(s) [28,35]. On the other hand, VSV is an enveloped virus that has become a widely used system for the study of the clathrin-mediated endocytosis of viruses [36,37,38,39].

Our results showed that dynamin − a $PI(4,5)P_2$ effector − was a common requirement for infection of VSV and the two FMDVs analyzed. In contrast, while

endocytosis of both FMDV C-S8c1 and VSV was highly dependent on plasma membrane PI(4,5)P_2, that of FMDV MARLS showed a lower dependence on this phospholipid. These results highlight the role of PI(4,5)P_2 on viral entry and show the potential of the depletion of PI(4,5)P_2 from plasma membrane as a novel antiviral strategy.

Results and discussion

Functional requirement of dynamin for FMDV and VSV infection

PI(4,5)P_2 is involved in several cellular events as a result of its binding to different partners [1,4,40,41,42,43,44]. One of these proteins is the GTPase dynamin that works in endocytosis as a regulatory molecule and as a component of the fission machinery [45]. This prompted us to analyze the effect of the expression of a dominant negative (DN) form of dynamin (Dyn K44A) [46] on the entry of two FMDV isolates with different receptor specificities (C-S8c1 and MARLS) and VSV. BHK-21 cells were transfected, incubated with the viruses and the percentage of cells with internalized viral particles was estimated by confocal microscopy as described [31,47]. While similar percentages of cells that internalized virus were observed in control cells infected with VSV (76%), C-S8c1 (74%) and MARLS (79%), these values were significantly reduced in cells expressing DN dynamin (9%, 12% and 11%, respectively), indicating that all viruses tested required dynamin for cell entry (Fig. 1A). In addition, expression of DN dynamin significantly reduced the percentage of transfected-infected cells for C-S8c1, MARLS and VSV (Fig.1B), indicating the functional requirement of this PI(4,5)P_2-interacting protein for the infection of the three viruses tested.

Effect of depletion of $PI(4,5)P_2$ on FMDV and VSV internalization

It has been documented that ionomycin treatment reduces the levels of $PI(4,5)P_2$ by activation of phospholipase C [4]. BHK-21 cells were transfected with a reporter plasmid (PH-PLC-eGFP) [48] that expresses a fusion protein that binds this phospholipid and allows its detection by fluorescence microscopy [43]. Under control conditions, fluorescence was concentrated at the plasma membrane. However, in cells treated with ionomycin, a cytoplasmic distribution of the reporter for $PI(4,5)P_2$ was observed. This result confirmed that ionomycin treatment induced a depletion of $PI(4,5)P_2$ from plasma membrane, which resulted in a cytoplasmic relocation of the fluorescent reporter protein (Fig. 2A). The effect of this drug on clathrin-mediated endocytosis was further analyzed by using fluorescent transferrin (TF), a marker of clathrin-mediated endocytosis [49]. In contrast to non treated cells, those treated with ionomycin displayed a reduction in TF internalization (Fig. 2B). As these results supported the conclusion that ionomycin treatment affected clathrin-mediated endocytosis, the effect of ionomycin was tested on virus internalization. Thus, BHK-21 cells were treated with ionomycin, incubated with the viruses and the proportion of cells that internalized viral particles was determined by immunofluorescence and confocal microscopy. As expected, ionomycin treatment inhibited (reduction by 90%) the internalization of VSV particles (Fig. 2C), whose entry through clathrin-mediated endocytosis is well characterized [36,37,38,39], and a similar reduction was observed for FMDV C-S8c1 that enters into the cells via CCPs [31]. However, the inhibition was lower for FMDV MARLS (only a reduction about 40%), which has the ability to use cellular receptors other than integrins. These results highlight that depletion of $PI(4,5)P_2$ from plasma membrane inhibits endocytosis of viruses that use CCV, and reveal that the

different internalization pathway followed by C-S8c1 and MARLS FMDV variants can modulate PI(4,5)P2 requirement.

Effect of inhibition of PI(4,5)P_2 synthesis on FMDV and VSV internalization

Rather than causing PI(4,5)P_2 depletion from plasma membrane, as described for ionomycin, primary alcohols, like 1-butanol, promote phospholipase D (PLD) to generate phosphatidylalcohols instead of phosphatidic acid (PA), leading to a lower activation of phosphatidylinositol 4-phosphate 5-kinase (PI4P5K) and consequently inhibiting PI(4,5)P_2 synthesis and CCP assembly [5]. On the other hand, this effect does not occur in the presence of secondary alcohols such as 2-butanol [5]. Treatment with either 1.5% 1-butanol or 2-butanol did not affect the distribution pattern observed for the PI(4,5)P_2 reporter (Fig. 3A), confirming that none of these alcohols produced a significant depletion of PI(4,5)P2 from plasma membrane. However, treatment with 1-butanol reduced the ability of BHK-21 cells to internalize TF, indicating a requirement for *de novo* synthesis of PI(4,5)P_2 of clathrin-mediated endocytosis (Fig. 3B). As expected, treatment with 2-butanol did not result in reduction of TF internalization, confirming the specificity of the inhibition of clathrin-mediated endocytosis by 1-butanol. Regarding viral entry, treatment with 1-butanol reduced by 90% the internalization of C-S8c1 and VSV. Conversely, it only reduced MARLS internalization by 50%, suggesting that the different receptor used by MARLS and C-S8c1 for cell entry can modulate the requirement of PI(4,5)P2 synthesis. The specificity of this inhibition was confirmed as treatment with 2-butanol resulted in a limited reduction by 10% in the internalization of each of the three viruses analyzed (Fig. 3C). These results indicate that FMDV and VSV require synthesis of PI(4,5)P_2 at the plasma membrane

for internalization, and again suggest differences between MARLS and C-S8c1 internalization pathways.

Effect of induced depletion of PI(4,5)P_2 from the plasma membrane on FMDV and VSV internalization

To confirm the results obtained with pharmacological inhibitors, the effect of PI(4,5)P_2- targeted depletion with an inducible system [44] was analyzed. The approach used, which has been proven to be highly specific [4,50,51], is based on the conditional recruitment to plasma membrane of an inositol 5-phosphatase (fused to red fluorescent protein – RFP -) by its rapamycin-induced heterodimerization with a membrane-targeted, rapamycin-binding domain of mTOR fused to the cyan fluorescent protein (CFP) [44]. In this way, only when rapamycin is added to the culture medium, both fusion proteins interact and the phosphatase is recruited to plasma membrane causing a targeted depletion of PI(4,5)P_2. First, we evaluated that this system induced the depletion of PI(4,5)P_2 from the plasma membrane when rapamycin was added to BHK-21 cells (Fig. 4). To this end, cells were cotransfected for 24 h with plasmids encoding phosphatase (mRFP-FKBP-dom5ptase), membrane anchored rapamycin-binding domain (PM-FRB-CFP) and PH-PLC-eGFP (to detect PI(4,5)P_2). Then, cells were treated with rapamycin for 10 min to induce the depletion of PI(4,5)P_2 from plasma membrane. As expected, when rapamycin was added the fluorescence of PI(4,5)P_2 reporter protein was relocated from plasma membrane to the cytoplasm (Fig. 4). Next, cells cotransfected with plasmids mRFP-FKBP-dom5ptase and PM-FRB-CFP, were treated with rapamycin to induce the PI(4,5)P_2 depletion, and then incubated with the viruses (Fig. S1). About 89% of the cells expressing both plasmids in the absence of rapamycin were able to internalize C-S8c1 (Table 1). However, when rapamycin was

added, only 12% of cotransfected cells were shown to internalize C-S8c1 particles. Addition of rapamycin similarly reduced the number of cells internalizing VSV or C-S8c1 particles (from 89% in control cells to 12% in rapamycin-treated cells for C-S8c1, and from 88% in control cells to 15% in rapamycin-treated cells for VSV). On the other hand, targeted depletion of $PI(4,5)P_2$ only slightly reduced the percentage of cells internalizing MARLS (from 83% in control cells to 76% in rapamycin treated cells) (Table 1). Rapamycin alone had no effect on viral internalization of any of the three virus tested, since treatment with rapamycin of untransfected cells or cells only transfected with one plasmid did not reduce the percentages of cells that internalized the viral particles (data not shown). Overall, these results support those previously obtained with pharmacological treatments, indicating e that internalization of FMDV C-S8c1 and VSV strongly depends on plasma membrane $PI(4,5)P_2$ phospholipids, while MARLS internalization is less sensitive to $PI(4,5)P_2$ depletion. These differences could be explained by the usage of an alternative dynamin-dependent endocytic pathway, such as caveolae, for MARLS internalization, since caveolae-mediated endocytosis can rely on dynamin function [52] and is less sensitive to $PI(4,5)P_2$ depletion than clathrin-mediated endocytosis [53]. In fact, as commented in the introduction, MARLS could utilize HS binding to gain entry into cells through caveolae.

The results presented in this study highlight the involvement of $PI(4,5)P_{2,}$ on viral entry of either enveloped and non-enveloped viruses and show the potential of the depletion of $PI(4,5)P_2$ from plasma membrane as a novel antiviral strategy.

Materials and Methods

Cells and viruses

BHK-21 cells (ATCC) were grown in Dulbecco's modified Eagle's medium (DMEM) supplemented with 5% fetal calf serum (FCS), L-glutamine (2 mM), penicillin (100 U/ml), and streptomycin (100 µg/ml). FMDV isolate C-S8c1 is a derivative of a type C field virus isolated in Santa Pau (Spain, 1970) by triple plaque purification [54]. MARLS virus is a monoclonal antibody (MAb)-resistant mutant isolated with MAb SD6, which recognizes the G-H loop of capsid protein VP1 [55], from C-S8c1 virus after 213 passages on BHK-21 cells [35]. Mutations in MARLS virus compared to parental C-S8c1 have described previously [28]. VSV Indiana [56] was also used. The sequence of the capsid proteins of C-S8c1 and MARLS stocks used in this work was confirmed by RT-PCR amplification of viral RNA and sequencing of the amplicons obtained as described [57].

Antibodies and reagents

FMDV VP1 and VSV glycoprotein (G) protein were detected using MAb 5C4 [58] and I1 [59], respectively. Goat anti-mouse IgG labelled with Alexa Fluor (AF) 555 or 647 were from Molecular Probes. Transferrin (TF) conjugated to AF 488 was from Invitrogen. Ionomycin (Sigma) and rapamicyn (Calbiochem) were prepared in DMSO as 1.4 mM and 1.1 mM stock solutions, respectively. 1-butanol and 2-butanol were from Merck.

Drug treatments

BHK-21 cells grown on coverslips were washed twice with DMEM and incubated with ionomycin (5 µM) for 30 min, or with 1.5% 1-butanol or 2-butanol for 5 min. Control cells were incubated in the same conditions in DMEM containing the

solvent concentration used for each drug. The drug was maintained during the virus internalization time.

Plasmids and transfections

The following plasmids were used in this study: PH-PLC-eGFP [43], PM-FRB-CFP, mRFP-FKBP-dom5ptase [44], eGFP (Clontech) and eGFP-Dyn K44A [46]. BHK-21 cells were transfected using Lipofectamine Plus (Invitrogen) as described by the manufacturer or electroparated with the corresponding plasmid using Gene Pulser XCell^{TM} (Bio Rad).

Immunofluorescence

Immunofluorescence was performed as described previously [60]. For confocal microscopy; a LSM510 META Inverted (Zeiss) confocal laser scanning microscope coupled to an Axiovert200 (Zeiss) inverted microscope (objective Plan-Apochromat 63x/AN 1.4) was used. Images were acquired using Zeiss LSM510 4.2 Sp2 software. The percentage of cells which internalized viral particles was determined by observation of Z-stacks (scan zoom 1 ×, step size 0.4 μm) ($n \geq 100$) of cells using confocal microscopy [61]. For conventional fluorescence microscopy an Axioskop (Zeiss) fluorescence microscope coupled to a Coolsnap FX monochrome camera Roper Scientific was used and were acquired using RS Image software (Roper Scientific). To determine the number of infected cells, more than 150 cells expressing GFP were analyzed and the experiment was carried out three independent times. The images were processed using Adobe Photoshop 7.0 (Adobe System Inc.).

Data analysis

Analysis of variance (ANOVA) using *F* Fischer-Snedecor distribution was performed with statistical package SPSS v.17.0 (SPSS Inc) for Windows. Data are presented as means ± standard deviations (SD). Chi-square test was performed with statistical package Graph Pad Prism. Statistically significant differences are denoted in the figures by one asterisk for a *P* value of <0.05.

Acknowledgments

We wish to thank, E. Domingo for MARLS and VSV, and J.A Esteban, M. A. Alonso and T. Balla for plasmid constructs.

References

1. De Matteis MA, Godi A (2004) PI-loting membrane traffic. Nat Cell Biol 6: 487-492.
2. Antonescu CN, Aguet F, Danuser G, Schmid SL (2011) Phosphatidylinositol-(4,5)-bisphosphate regulates clathrin-coated pit initiation, stabilization, and size. Mol Biol Cell 22: 2588-2600.
3. James DJ, Khodthong C, Kowalchyk JA, Martin TF (2008) Phosphatidylinositol 4,5-bisphosphate regulates SNARE-dependent membrane fusion. J Cell Biol 182: 355-366.
4. Zoncu R, Perera RM, Sebastian R, Nakatsu F, Chen H, et al. (2007) Loss of endocytic clathrin-coated pits upon acute depletion of phosphatidylinositol 4,5-bisphosphate. Proc Natl Acad Sci U S A 104: 3793-3798.
5. Boucrot E, Saffarian S, Massol R, Kirchhausen T, Ehrlich M (2006) Role of lipids and actin in the formation of clathrin-coated pits. Exp Cell Res 312: 4036-4048.
6. Haucke V (2005) Phosphoinositide regulation of clathrin-mediated endocytosis. Biochem Soc Trans 33: 1285-1289.
7. Richard JP, Leikina E, Langen R, Henne WM, Popova M, et al. (2011) Intracellular curvature generating proteins in cell-to-cell fusion. Biochem J.
8. McMahon HT, Boucrot E (2011) Molecular mechanism and physiological functions of clathrin-mediated endocytosis. Nat Rev Mol Cell Biol 12: 517-533.
9. Henne WM, Boucrot E, Meinecke M, Evergren E, Vallis Y, et al. (2010) FCHo proteins are nucleators of clathrin-mediated endocytosis. Science 328: 1281-1284.
10. Jackson LP, Kelly BT, McCoy AJ, Gaffry T, James LC, et al. (2010) A large-scale conformational change couples membrane recruitment to cargo binding in the AP2 clathrin adaptor complex. Cell 141: 1220-1229.
11. Bethoney KA, King MC, Hinshaw JE, Ostap EM, Lemmon MA (2009) A possible effector role for the pleckstrin homology (PH) domain of dynamin. Proc Natl Acad Sci U S A 106: 13359-13364.

12. Wenk MR, Pellegrini L, Klenchin VA, Di Paolo G, Chang S, et al. (2001) PIP kinase Igamma is the major PI(4,5)P(2) synthesizing enzyme at the synapse. Neuron 32: 79-88.
13. Chaudhry A, Das SR, Jameel S, George A, Bal V, et al. (2008) HIV-1 Nef induces a Rab11-dependent routing of endocytosed immune costimulatory proteins CD80 and CD86 to the Golgi. Traffic 9: 1925-1935.
14. Chu H, Wang JJ, Spearman P (2009) Human immunodeficiency virus type-1 gag and host vesicular trafficking pathways. Curr Top Microbiol Immunol 339: 67-84.
15. Eisfeld AJ, Kawakami E, Watanabe T, Neumann G, Kawaoka Y (2011) RAB11A is essential for transport of the influenza virus genome to the plasma membrane. J Virol 85: 6117-6126.
16. Johns HL, Berryman S, Monaghan P, Belsham GJ, Jackson T (2009) A dominant-negative mutant of rab5 inhibits infection of cells by foot-and-mouth disease virus: implications for virus entry. J Virol 83: 6247-6256.
17. Krishnan MN, Sukumaran B, Pal U, Agaisse H, Murray JL, et al. (2007) Rab 5 is required for the cellular entry of dengue and West Nile viruses. J Virol 81: 4881-4885.
18. Vidricaire G, Tremblay MJ (2005) Rab5 and Rab7, but not ARF6, govern the early events of HIV-1 infection in polarized human placental cells. J Immunol 175: 6517-6530.
19. Vonderheit A, Helenius A (2005) Rab7 associates with early endosomes to mediate sorting and transport of Semliki forest virus to late endosomes. PLoS Biol 3: e233.
20. Barrero-Villar M, Barroso-Gonzalez J, Cabrero JR, Gordon-Alonso M, Alvarez-Losada S, et al. (2008) PI4P5-kinase Ialpha is required for efficient HIV-1 entry and infection of T cells. J Immunol 181: 6882-6888.
21. Chukkapalli V, Hogue IB, Boyko V, Hu WS, Ono A (2008) Interaction between the human immunodeficiency virus type 1 Gag matrix domain and phosphatidylinositol-(4,5)-bisphosphate is essential for efficient gag membrane binding. J Virol 82: 2405-2417.
22. Legendre-Guillemin V, Wasiak S, Hussain NK, Angers A, McPherson PS (2004) ENTH/ANTH proteins and clathrin-mediated membrane budding. J Cell Sci 117: 9-18.
23. Sobrino F, Saiz M, Jimenez-Clavero MA, Nunez JI, Rosas MF, et al. (2001) Foot-and-mouth disease virus: a long known virus, but a current threat. Vet Res 32: 1-30.
24. Berinstein A, Roivainen M, Hovi T, Mason PW, Baxt B (1995) Antibodies to the vitronectin receptor (integrin alpha V beta 3) inhibit binding and infection of foot-and-mouth disease virus to cultured cells. J Virol 69: 2664-2666.
25. Jackson T, Blakemore W, Newman JW, Knowles NJ, Mould AP, et al. (2000) Foot-and-mouth disease virus is a ligand for the high-affinity binding conformation of integrin alpha5beta1: influence of the leucine residue within the RGDL motif on selectivity of integrin binding. J Gen Virol 81: 1383-1391.
26. Jackson T, Clark S, Berryman S, Burman A, Cambier S, et al. (2004) Integrin alphavbeta8 functions as a receptor for foot-and-mouth disease virus: role of the beta-chain cytodomain in integrin-mediated infection. J Virol 78: 4533-4540.
27. Jackson T, Mould AP, Sheppard D, King AM (2002) Integrin alphavbeta1 is a receptor for foot-and-mouth disease virus. J Virol 76: 935-941.

28. Baranowski E, Ruiz-Jarabo CM, Sevilla N, Andreu D, Beck E, et al. (2000) Cell recognition by foot-and-mouth disease virus that lacks the RGD integrin-binding motif: flexibility in aphthovirus receptor usage. J Virol 74: 1641-1647.
29. Jackson T, Ellard FM, Ghazaleh RA, Brookes SM, Blakemore WE, et al. (1996) Efficient infection of cells in culture by type O foot-and-mouth disease virus requires binding to cell surface heparan sulfate. J Virol 70: 5282-5287.
30. Berryman S, Clark S, Monaghan P, Jackson T (2005) Early events in integrin alphavbeta6-mediated cell entry of foot-and-mouth disease virus. J Virol 79: 8519-8534.
31. Martin-Acebes MA, Gonzalez-Magaldi M, Sandvig K, Sobrino F, Armas-Portela R (2007) Productive entry of type C foot-and-mouth disease virus into susceptible cultured cells requires clathrin and is dependent on the presence of plasma membrane cholesterol. Virology 369: 105-118.
32. O'Donnell V, LaRocco M, Duque H, Baxt B (2005) Analysis of foot-and-mouth disease virus internalization events in cultured cells. J Virol 79: 8506-8518.
33. O'Donnell V, Larocco M, Baxt B (2008) Heparan sulfate-binding foot-and-mouth disease virus enters cells via caveola-mediated endocytosis. J Virol 82: 9075-9085.
34. Nunez JI, Molina N, Baranowski E, Domingo E, Clark S, et al. (2007) Guinea pig-adapted foot-and-mouth disease virus with altered receptor recognition can productively infect a natural host. J Virol 81: 8497-8506.
35. Baranowski E, Sevilla N, Verdaguer N, Ruiz-Jarabo CM, Beck E, et al. (1998) Multiple virulence determinants of foot-and-mouth disease virus in cell culture. J Virol 72: 6362-6372.
36. Cureton DK, Massol RH, Saffarian S, Kirchhausen TL, Whelan SP (2009) Vesicular stomatitis virus enters cells through vesicles incompletely coated with clathrin that depend upon actin for internalization. PLoS Pathog 5: e1000394.
37. Johannsdottir HK, Mancini R, Kartenbeck J, Amato L, Helenius A (2009) Host cell factors and functions involved in vesicular stomatitis virus entry. J Virol 83: 440-453.
38. Matlin KS, Reggio H, Helenius A, Simons K (1982) Pathway of vesicular stomatitis virus entry leading to infection. J Mol Biol 156: 609-631.
39. Sun X, Yau VK, Briggs BJ, Whittaker GR (2005) Role of clathrin-mediated endocytosis during vesicular stomatitis virus entry into host cells. Virology 338: 53-60.
40. Abe N, Inoue T, Galvez T, Klein L, Meyer T (2008) Dissecting the role of PtdIns(4,5)P2 in endocytosis and recycling of the transferrin receptor. J Cell Sci 121: 1488-1494.
41. Erlmann P, Schmid S, Horenkamp FA, Geyer M, Pomorski TG, et al. (2009) DLC1 Activation Requires Lipid Interaction through a Polybasic Region Preceding the RhoGAP Domain. Mol Biol Cell.
42. Johnson CM, Chichili GR, Rodgers W (2008) Compartmentalization of phosphatidylinositol 4,5-bisphosphate signaling evidenced using targeted phosphatases. J Biol Chem 283: 29920-29928.
43. Szentpetery Z, Balla A, Kim YJ, Lemmon MA, Balla T (2009) Live cell imaging with protein domains capable of recognizing phosphatidylinositol 4,5-bisphosphate; a comparative study. BMC Cell Biol 10: 67.
44. Varnai P, Thyagarajan B, Rohacs T, Balla T (2006) Rapidly inducible changes in phosphatidylinositol 4,5-bisphosphate levels influence multiple regulatory functions of the lipid in intact living cells. J Cell Biol 175: 377-382.

45. Loerke D, Mettlen M, Yarar D, Jaqaman K, Jaqaman H, et al. (2009) Cargo and dynamin regulate clathrin-coated pit maturation. PLoS Biol 7: e57.
46. Martin-Belmonte F, Martinez-Menarguez JA, Aranda JF, Ballesta J, de Marco MC, et al. (2003) MAL regulates clathrin-mediated endocytosis at the apical surface of Madin-Darby canine kidney cells. J Cell Biol 163: 155-164.
47. Martin-Acebes MA, Herrera M, Armas-Portela R, Domingo E, Sobrino F (2010) Cell density-dependent expression of viral antigens during persistence of foot-and-mouth disease virus in cell culture. Virology 403: 47-55.
48. Arendt KL, Royo M, Fernandez-Monreal M, Knafo S, Petrok CN, et al. (2010) PIP3 controls synaptic function by maintaining AMPA receptor clustering at the postsynaptic membrane. Nat Neurosci 13: 36-44.
49. Sandvig K, Olsnes S, Petersen OW, van Deurs B (1987) Acidification of the cytosol inhibits endocytosis from coated pits. J Cell Biol 105: 679-689.
50. Adjobo-Hermans MJ, Goedhart J, Gadella TW, Jr. (2008) Regulation of PLCbeta1a membrane anchoring by its substrate phosphatidylinositol (4,5)-bisphosphate. J Cell Sci 121: 3770-3777.
51. Suh BC, Inoue T, Meyer T, Hille B (2006) Rapid chemically induced changes of PtdIns(4,5)P2 gate KCNQ ion channels. Science 314: 1454-1457.
52. Mercer J, Schelhaas M, Helenius A (2010) Virus entry by endocytosis. Annu Rev Biochem 79: 803-833.
53. Fujita A, Cheng J, Tauchi-Sato K, Takenawa T, Fujimoto T (2009) A distinct pool of phosphatidylinositol 4,5-bisphosphate in caveolae revealed by a nanoscale labeling technique. Proc Natl Acad Sci U S A 106: 9256-9261.
54. Sobrino F, Davila M, Ortin J, Domingo E (1983) Multiple genetic variants arise in the course of replication of foot-and-mouth disease virus in cell culture. Virology 128: 310-318.
55. Mateu MG, Martinez MA, Capucci L, Andreu D, Giralt E, et al. (1990) A single amino acid substitution affects multiple overlapping epitopes in the major antigenic site of foot-and-mouth disease virus of serotype C. J Gen Virol 71 (Pt 3): 629-637.
56. Novella IS, Cilnis M, Elena SF, Kohn J, Moya A, et al. (1996) Large-population passages of vesicular stomatitis virus in interferon-treated cells select variants of only limited resistance. J Virol 70: 6414-6417.
57. Nunez JI, Baranowski E, Molina N, Ruiz-Jarabo CM, Sanchez C, et al. (2001) A single amino acid substitution in nonstructural protein 3A can mediate adaptation of foot-and-mouth disease virus to the guinea pig. J Virol 75: 3977-3983.
58. Mateu MG, Rocha E, Vicente O, Vayreda F, Navalpotro C, et al. (1987) Reactivity with monoclonal antibodies of viruses from an episode of foot-and-mouth disease. Virus Res 8: 261-274.
59. Lefrancois L, Lyles DS (1982) The interaction of antibody with the major surface glycoprotein of vesicular stomatitis virus. II. Monoclonal antibodies of nonneutralizing and cross-reactive epitopes of Indiana and New Jersey serotypes. Virology 121: 168-174.
60. Martin-Acebes MA, Gonzalez-Magaldi M, Vazquez-Calvo A, Armas-Portela R, Sobrino F (2009) Internalization of swine vesicular disease virus into cultured cells: a comparative study with foot-and-mouth disease virus. J Virol 83: 4216-4226.

61. Gastaldelli M, Imelli N, Boucke K, Amstutz B, Meier O, et al. (2008) Infectious adenovirus type 2 transport through early but not late endosomes. Traffic 9: 2265-2278.

Figure legends

Figure. 1. Functional requirement for dynamin of FMDV and VSV infection. (A) BHK-21 cells transfected with eGFP or fused to a DN version of dynamin (eGFP-Dyn K44A) and 24 h latter were incubated with the different FMDV variants (C-S8c1 and MARLS) or VSV (MOI of 70 PFU/cell) for 25 min and processed for immunofluorescence. The percentage of cells that showed internalized virus is indicated (100 transfected cells were examined in each case). Transfected cells are indicated by an asterisk. Nuclei were stained using ToPro-3. Bar: 10 µm. (B) BHK-21 cells were electroporated with a plasmid encoding eGFP as control, or eGFP-Dyn K44A. At 24h post-electroporation, monolayers were infected with the corresponding viruses (MOI of 1 PFU/cell). Cells were fixed and processed for immunofluorescence at 7 h post-infection. Bars represent the mean percentage of transfected and infected cells ± SD, normalized to the level of infection of cells expressing the eGFP. Statistically significant differences between control and cells treated are indicated by an asterisk (ANOVA $P \leq 0.05$).

Figure. 2. Effect of PI(4,5)P_2 depletion by ionomycin on FMDV and VSV internalization. (A) Visualization of PI(4,5)P_2 depletion from plasma membrane. BHK-21 cells transfected (24 h) with PH-PLC-eGFP, encoding a reporter protein for PI(4,5)P_2 fused to GFP, were treated or not with 5µM ionomycin 30 min and then fixed and observed by confocal microscopy. Nuclei were stained using ToPro-3. Bar 10µm. (B) Treatment with ionomycin inhibits clathrin-mediated endocytosis. BHK-21 cells, treated with ionomycin as in (A), were incubated with Alexa Fluor 488-labelled TF for 5 min in the presence of the drug and extracellular TF was eliminated by acid wash as

described [31]. Cells were fixed and nuclei were stained using DAPI. Bar: 10 µm. (C) Inhibition of the ability of cells to internalize FMDV and VSV upon ionomycin treatment. Cells treated with ionomycin as in (A) were incubated with the different FMDV variants (C-S8c1 and MARLS) or with VSV (MOI of 70 PFU/cell) for 25 min in the presence of ionomycin. Cells were fixed and processed for immunofluorescence to stain viral particles as described in Materials and Methods. Bars represent the mean percentage of cells with internalized virions ± SD, normalized to the level of cells with internalized virions in control samples. At least 500 cells per coverslip were scored for each case (3 coverslips). Asterisks denote statistically significant differences (ANOVA $P \leq 0.05$).

Figure. 3. Effect of blocking *de novo* synthesis of PI(4,5)P_2 with 1-butanol on FMDV and VSV internalization. (A) BHK-21 cells transfected (24h) with PH-PLC-eGFP were treated or not with 1.5% 1-butanol or 2-butanol for 5 min and then fixed and observed by confocal microscopy. Nuclei were stained using ToPro-3. Bar 10µm. (B) Treatment with 1-butanol inhibits clathrin-dependent endocytosis. BHK-21 cells were treated as in (A) were incubated with fluorescent TF and processed as described in the legend of Fig. 1. Bar: 10 µm. (C) Reduction of the ability of cells to internalize FMDV and VSV upon 1-butanol treatment. Cells treated as in (A) were incubated with the different FMDV variants (C-S8c1 and MARLS) or VSV (MOI of 70 PFU/cell) for 25 min in the presence of the drugs. Bars represent the mean percentage of cells with internalized virions ± SD, normalized to the level of cells with internalized virions in control samples. At least 500 cells per coverslip were scored for each case (3 coverslips). Asterisks denote statistically significant differences (ANOVA $P \leq 0.05$).

Figure. 4. Depletion of PI(4,5)P_2 from plasma membrane after rapamycin-induced membrane targeting of an inositol 5-phosphatase. BHK-21 cells were cotransfected with PM-FRB-CFP (blue), mRFP-FKBP-dom5ptase (red) and PH-PLC-eGFP (green) plasmids using Lipofectamine Plus. At 24 h post-transfection, cells were treated with 10 nM rapamycin (10 min) to induce the depletion of PI(4,5)P_2 from plasma membrane. Then cells were fixed and observed by confocal microscopy. A representative example of a co-transfected cell is shown. See text for details regarding the inducible system for PI(4,5)P_2 depletion. DIC images are also shown. Bar: 10 µm.

TABLE 1. Inducible depletion of PI(4,5)P_2 from plasma membrane inhibits internalization of FMDV and VSV.

		% Cells with internalized virions	% Cells without internalized virions	P-value
CS8-c1	Control	89	11	0.0001*
	Rapamycin	12	88	
MARLS	Control	83	17	0.2202
	Rapamycin	76	24	
VSV	Control	88	12	0.0001*
	Rapamycin	15	85	

Number of cotransfected cells scored: 100

* Statistically significant difference.

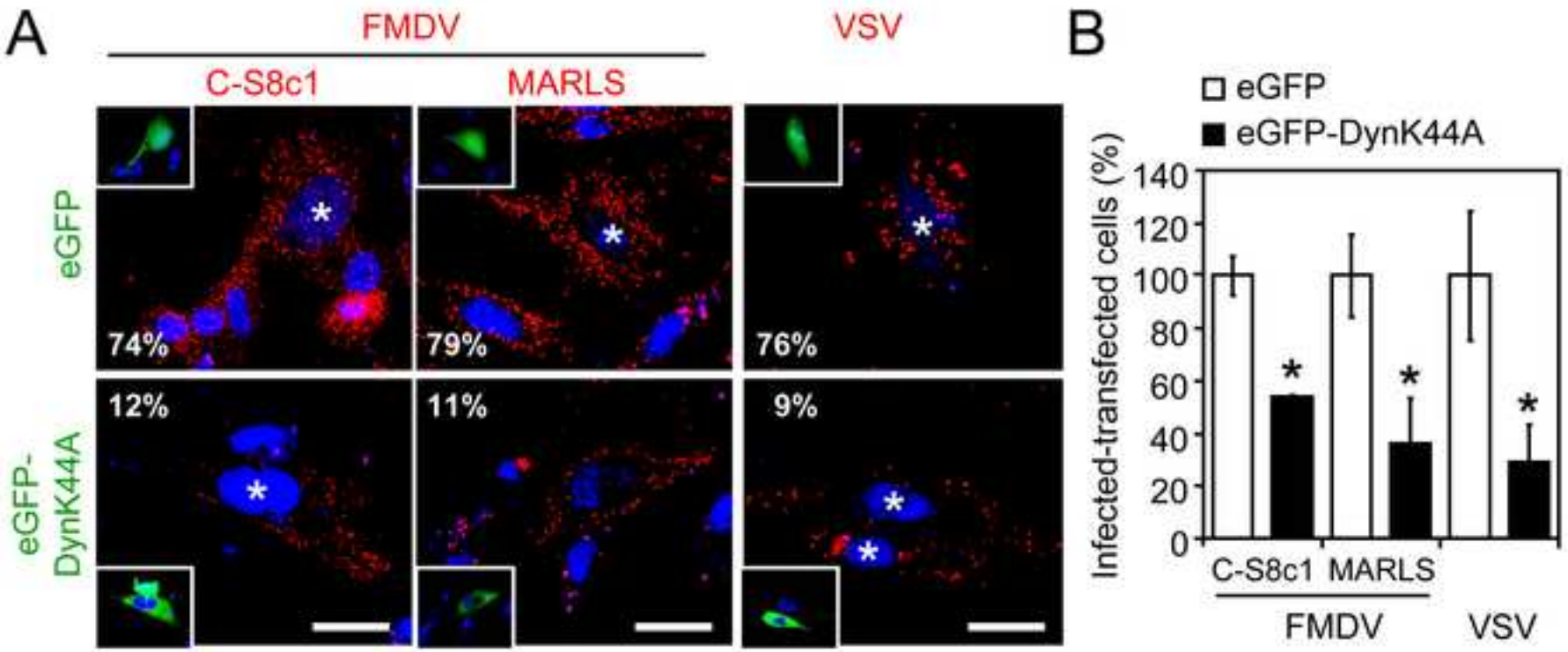
A
FMDV
VSV
C-S8c1
MARLS
eGFP
eGFP-DynK44A
74%
79%
76%
12%
11%
9%
B
eGFP
eGFP-DynK44A
Infected-transfected cells (%)
140
120
100
80
60
40
20
0
C-S8c1
MARLS
FMDV
VSV

Fig. 1

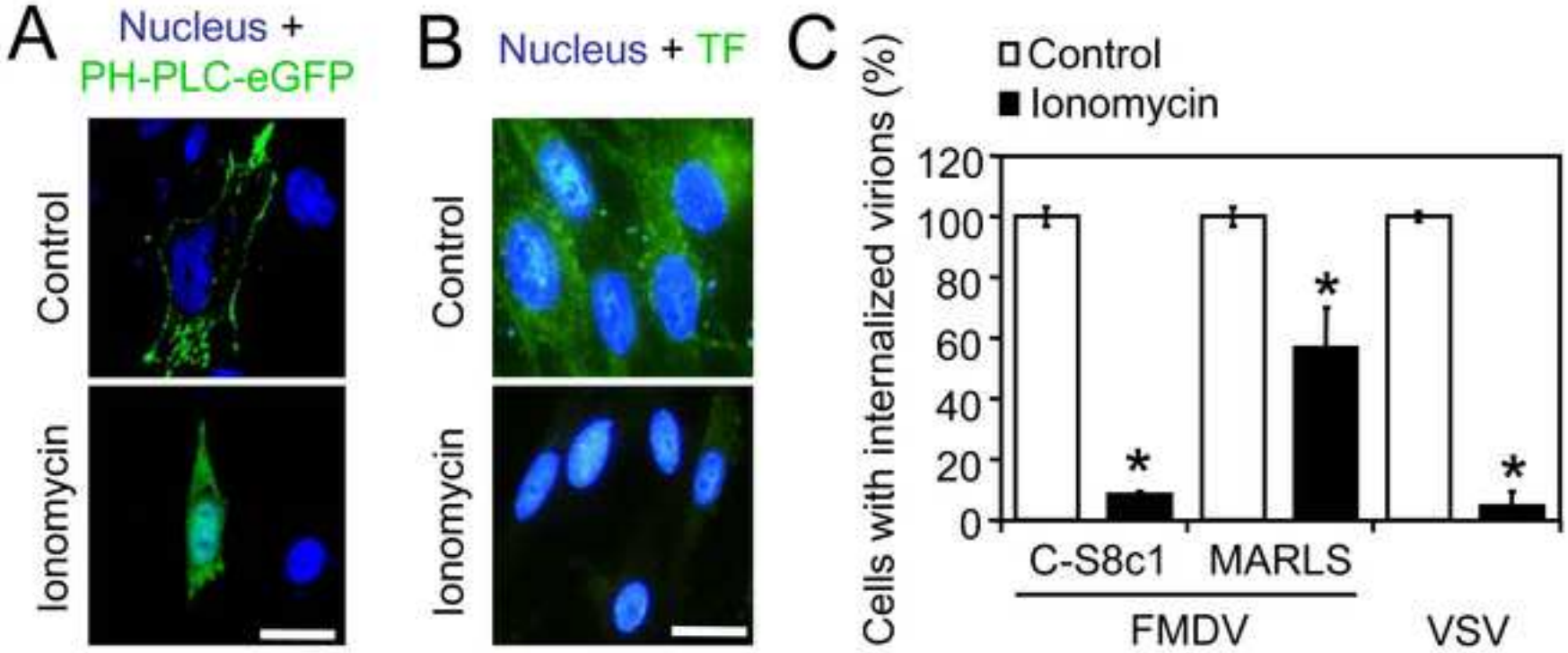
A
Nucleus +
PH-PLC-eGFP
Control
Ionomycin
B
Nucleus + TF
Control
Ionomycin
C
Control
Ionomycin
Cells with internalized virions (%)
120
100
80
60
40
20
0
*
*
*
C-S8c1
MARLS
FMDV
VSV

Fig. 2

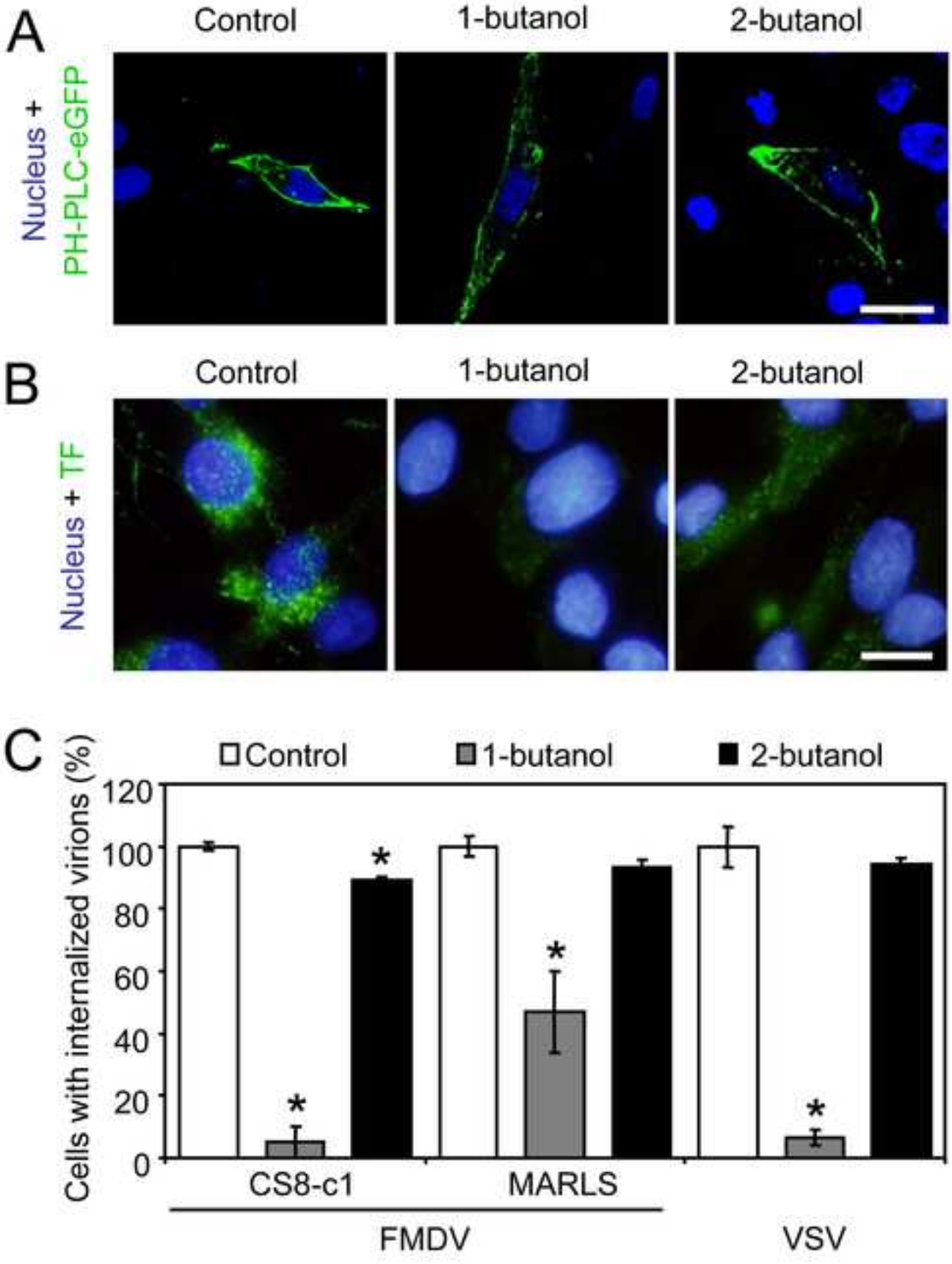
A
Control
1-butanol
2-butanol
Nucleus +
PH-PLC-eGFP
B
Control
1-butanol
2-butanol
Nucleus + TF
C
Control
1-butanol
2-butanol
Cells with internalized virions (%)
120
100
80
60
40
20
0
*
*
*
*
CS8-c1
MARLS
FMDV
VSV

Fig. 3

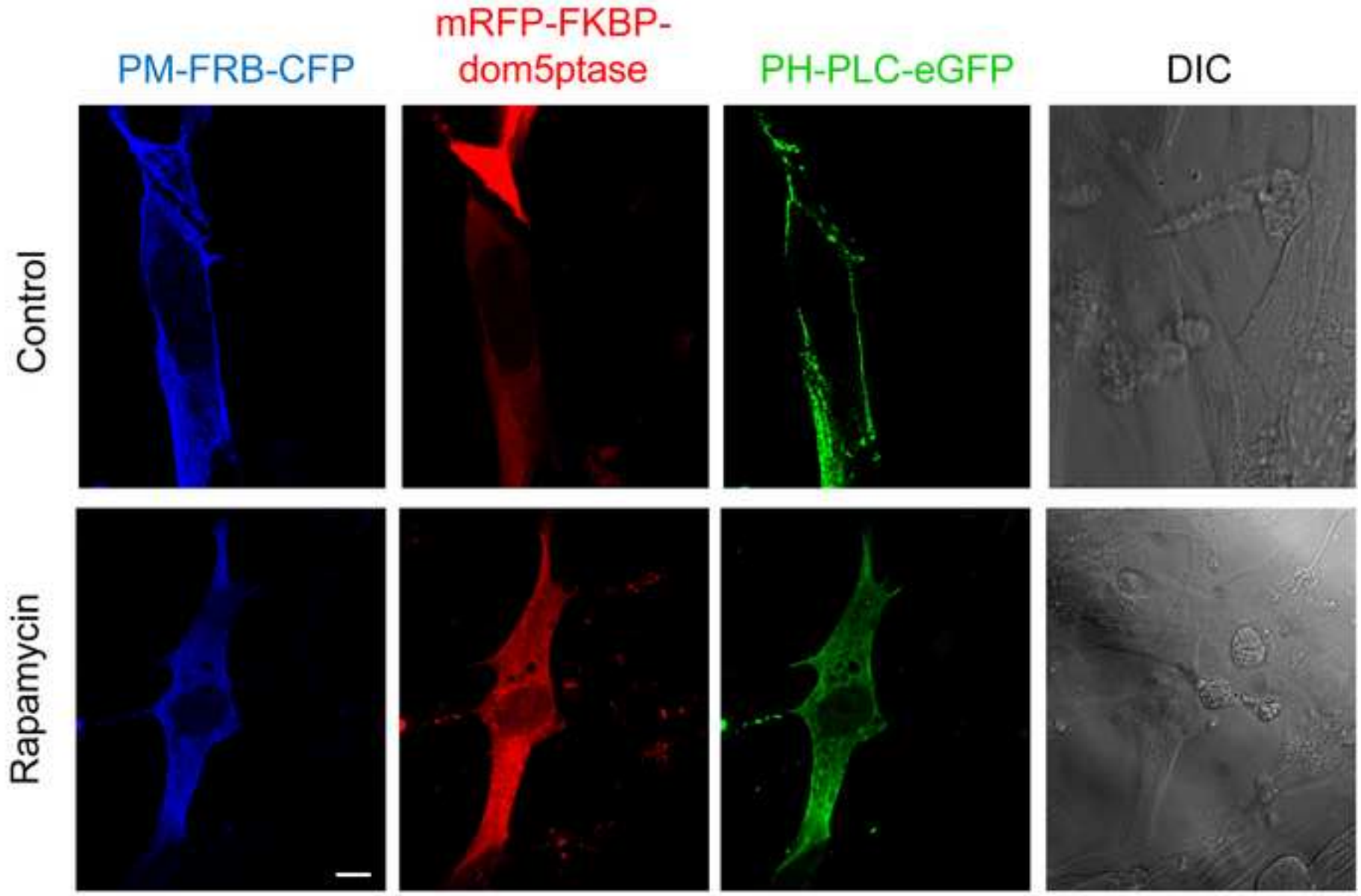
PM-FRB-CFP
mRFP-FKBP-dom5ptase
PH-PLC-eGFP
DIC
Control
Rapamycin

Fig. 4